

**THE GEOCHEMISTRY OF SOME COMMON WESTERN CAPE SOILS (SOUTH AFRICA)  
WITH EMPHASIS ON TOXIC AND ESSENTIAL ELEMENTS**

by

**Hendrik Schloemann**

Thesis Presented for the Degree of  
**DOCTOR OF PHILOSOPHY**  
in the Department of Geological Sciences

**UNIVERSITY OF CAPE TOWN**

December, 1994

The copyright of this thesis vests in the author. No quotation from it or information derived from it is to be published without full acknowledgement of the source. The thesis is to be used for private study or non-commercial research purposes only.

Published by the University of Cape Town (UCT) in terms of the non-exclusive license granted to UCT by the author.

## ABSTRACT

Knowledge about the abundance and behaviour of elements in soils has important implications in the fields of soil science, environmental health, botany and agriculture. This study investigates the geochemistry of forty-one elements, many of which are relevant to plant, animal or human health, in some common Western Cape soils (South Africa). The sampled soils are underlain by granite, sands of granitic origin, argillaceous and arenaceous sediments of the Malmesbury Group, ferruginized materials or coastal sands. Samples were taken from different soil horizons and slope positions. For some of the underlying materials it was impossible to find sampling sites which were characterised by uncultivated, common soil types and samples had to be taken from cultivated soils.

The particle size distributions and the chemical compositions of the soil samples are reported in detail. This includes data for Li, Be, F, Na, Mg, Al, Si, P, S, Cl, K, Ca, Ti, V, Cr, Mn, Fe, Co, Ni, Cu, Zn, Ga, Ge, As, Se, Br, Rb, Sr, Y, Zr, Nb, Mo, Cd, Sn, Sb, I, W, Pb, Bi, Th and U. A Principal Component Analysis was successfully applied to reduce the number of particle size classes, while minimising the loss of variance. Other parameters determined were the  $\text{NH}_4\text{NO}_3$  extractable concentrations of numerous elements, pH(KCl) values, proportions of organic matter and conductivities of the water-suspended soils. Mineralogical data are purely qualitative and were only determined for selected samples.

A comparison of several leaching techniques showed that extraction with 1 M  $\text{NH}_4\text{NO}_3$  is suitable to (a) quantify the proportion of an element which is "readily mobilised" and (b) assess the environmental risk associated with contaminated soils. The 1 M  $\text{NH}_4\text{NO}_3$  matrix, however, results in relatively high detection limits if the analyses are performed using Inductively Coupled Plasma Mass Spectrometry. Many of the investigated elements, therefore, had extractable concentrations mainly below the detection limit.

The underlying geological material is the most important factor in determining the chemical composition of the investigated soils. Fluvial and aeolian input of relatively fresh detritus, hill slope processes and pedogenic processes such as eluviation, illuviation, colluviation, formation of secondary soil minerals, accumulation of organic matter, leaching and adsorption account for most of the chemical variance not explained by the underlying materials.

Most trace metals have higher concentrations in soil horizons with higher proportions of clay minerals. Phosphorus, S, V, Fe, As, Se and Cr are typically enriched in soils with high proportions of Fe-oxides. The elements Mg, P, S, K, Ca and Mn and the  $\text{NH}_4\text{NO}_3$  extractable fractions of P and Ca often show increasing concentrations from the subsoil to the relatively organic-rich topsoil. The lateral change of the concentrations of Na, S, Cl, Br, I and  $\text{NH}_4\text{NO}_3$  extractable Na, Mg, P, S, K, Ca, Zn and Ti in the landscape is commonly governed by (a) the retention of water and dissolved solids by fines and organic matter, and (b) the evaporation of water from the soils in the lower slope positions.

The results imply that the soil of a granite-derived toposequence was subjected to gravitational transport (average gradient 75 ‰). The continuous weathering, leaching and eluviation of the soil during transport caused the concentrations of most major and trace elements to decrease with increasing distance from the granite. The continuous loss of Na, Al, K and Ca and relatively fine particles resulted in high concentrations of Si and high

proportions of coarse sand in the most leached soil at the lowermost slope position. Leachates from the granite above the toposequence infiltrated the soil and adsorption and(or) precipitation of dissolved elements resulted in high concentrations of S, V, As, Se, Br, Th and U. It is hypothesised that the transportation of Fe-oxide concretions by gravity and their subsequent breakdown due to reducing conditions at the footslope is a potential source of trace elements for the underlying subsoil and the ground water. More research is required to provide supporting evidence for this hypothesis. Chemical changes from the exposed granite to the upper limit of the soil cover of the toposequence indicate a major loss of the more soluble elements during the very early stages of weathering (losses in percent: Na: 72, Ca: 63, K: 61, Si: 55 and Mn: 44).

The results for the soils associated with the sediments of the Malmesbury Group show that the elements Li, Be, Mg, Al, S, K, Ca, Ti, Mn, Ni, Cu, Zn, Rb, Sr, Y, Nb, Sn, U and 1 M  $\text{NH}_4\text{NO}_3$  extractable K, Ca and Ba may have both increasing and decreasing concentrations down a toposequence. It was suggested that colluviation down the toposequence associated with schist resulted in admixture of weathering products from the underlying rock into the topsoil and caused increasing concentrations down the slope. The decrease of the concentrations of the same elements down the toposequence associated with phyllite may be the result of continuous eluviation during gravitational transport. Many of the elements listed above are important nutrients. More research should be directed in order to investigate in more detail why eluviation of finer particles and removal of nutrients from the topsoil predominates in the toposequence associated with phyllite while admixture of finer particles and nutrients from the underlying material into the topsoil predominates in the toposequence associated with schist.

The tendency of elements to become leached from the coastal sand-derived soil is  $\text{Rb} > \text{K} > \text{Na} > \text{P} > \text{Al} > \text{Mg} > \text{Sr} = \text{Ca}$ . It is concluded that large proportions of the Ca, Mg and P released from their primary host minerals are retained by organic matter. Abrupt lateral geochemical changes coincide with changing proportions of organic matter. The results for the coastal sand-derived soils also indicate that the occurrence of shallow and reducing ground waters can cause acidification of the overlying soil.

Basic statistics of the elemental concentrations are tabulated separately for soils underlain by different geological materials. Most of the presented mean concentrations are probably best possible estimates of the true background concentrations because only the results for V, Cr, Sn and Cd gave reason to speculate about soil pollution.

Pedogenic processes alone adequately account for high concentrations of As and Se. High concentrations F, Sb and 1 M  $\text{NH}_4\text{NO}_3$  extractable V are not indicative of soil pollution. The natural maximum concentrations of F, As, Se, Sb and extractable V exceed recommended maximum levels for the assessment of polluted soils. It is concluded that recommended maximum concentrations can only be considered as guidelines, and not as absolute limits.

A comparison of the mean elemental concentrations with levels reported in the literature indicates that the investigated soils generally have high As, Br and W concentrations. The concentrations of Li, Na, Mg, Mn, Co, Ni, Cu and Zn are relatively low. Further research is necessary to confirm these results and to investigate whether the anomalous concentrations affect plant, animal or human health.

Hopefully this work will form the basis for more comprehensive knowledge about the geochemistry of South African soils.

## DECLARATION

I hereby

- (a) grant the University of Cape Town free licence to reproduce this thesis in whole or in part, for the purpose of research;
- (b) declare that:
  - (i) this thesis is my own unaided work, both in concept and execution, and that apart from the normal guidance from my supervisor, I have received no assistance, except as stated in the acknowledgements.
  - (ii) neither the substance nor any part of this thesis has been submitted in the past, or is being, or is to be submitted for a degree in this University or any other university.

H. Schloemann

November 1994

## ACKNOWLEDGEMENTS

A note of thanks must go towards the following persons and organisations, without whom this project would have been impossible.

Prof. James Willis (Department of Geological Sciences; UCT) for his invaluable supervision over the period.

Mr G.R. Thompson (Department of Agriculture and Water Supply; Elsenburg), Mr A.B. Low (Kirstenbosch Botanical Gardens; Cape Town), Mr J.J.N. Lambrechts (Department of Soil Science; University of Stellenbosch), Dr R.M. Cowling and Dr W.D. Stock (both Botany Department; UCT) for their help with defining and planning the project in its initial phase.

Mr A.B. Oosthuizen (Institute for Soil, Climate and Water; Elsenburg) for his essential help with the classification of the sampled soil profiles.

The Foundation for Research Development for a bursary.

The Institute for Soil, Climate and Water in Pretoria for a supplementary bursary.

Dr John Rogers and Mathew Smith (both Department of Geological Sciences; UCT) for making the settling column and the sedigraph available, and for assisting where help was needed.

Dave Hill (previously Department of Geological Sciences; UCT) for giving me help with the computer systems.

Ms Rebecca Tharme (Freshwater Research Unit; UCT), Mr Lewis McCaffrey, Dr Kevin Faure, Dr Ruth Lanyon, Prof. Martin Fey (all Department of Geological Sciences; UCT) and Mr Peter Holmes (Environmental and Geographical Sciences; UCT) for their constructive criticism.

## TABLE OF CONTENT

<b>ABSTRACT</b> .....	<b>i</b>
<b>DECLARATION</b> .....	<b>iii</b>
<b>ACKNOWLEDGEMENTS</b> .....	<b>iv</b>
<b>TABLE OF CONTENT</b> .....	<b>v</b>
<b>DEFINITIONS OF TERMS AND ABBREVIATIONS AS USED IN THIS THESIS</b> .....	<b>xi</b>
<b>LIST OF TABLES</b> .....	<b>xii</b>
<b>LIST OF FIGURES</b> .....	<b>xiv</b>
 <b>CHAPTER 1.</b>	
<b>INTRODUCTION</b> .....	<b>1</b>
1.1. AIMS OF THE STUDY .....	<b>1</b>
1.2. RATIONALE FOR THE STRUCTURE OF THIS THESIS .....	<b>3</b>
1.3. LOCATION .....	<b>4</b>
1.4. HISTORY .....	<b>4</b>
1.5. GEOLOGY .....	<b>6</b>
1.6. SOILS AND GEOMORPHOLOGY .....	<b>6</b>
1.7. CLIMATE .....	<b>7</b>
1.8. INDIGENOUS VEGETATION .....	<b>7</b>
1.9. PREVIOUS WORK .....	<b>8</b>
 <b>CHAPTER 2.</b>	
<b>METHODS OF INVESTIGATION</b> .....	<b>11</b>
2.1. INTRODUCTION .....	<b>11</b>
2.2. FIELD SAMPLING .....	<b>11</b>
2.3. SOIL DESCRIPTION AND CLASSIFICATION .....	<b>17</b>
2.4. WHOLE-SOIL ANALYSIS .....	<b>17</b>
2.4.1. X-Ray Fluorescence Spectrometry .....	<b>19</b>
2.4.1.1. <i>Sample preparation for the analysis of major and minor elements</i> .....	<b>19</b>
2.4.1.2. <i>Sample preparation for the analysis of trace elements</i> .....	<b>20</b>
2.4.1.3. <i>Mass absorption coefficients</i> .....	<b>20</b>

2.4.1.4. <i>Lower limit of detection and errors</i> .....	20
2.4.1.5. <i>Analytical difficulties experienced</i> .....	23
2.4.2. Inductively Coupled Plasma Mass Spectrometry .....	24
2.5. ANALYSIS OF EXTRACTABLE ELEMENT PORTIONS .....	26
2.5.1. Selection of an appropriate leaching method .....	26
2.5.1.1. <i>Finding a suitable way of preparation of samples for the extraction</i> ...	27
2.5.1.2. <i>Selection of a suitable extraction method</i> .....	30
2.5.2. Analysis of leachates .....	33
2.5.2.1. <i>Inductively Coupled Plasma Mass Spectrometry</i> .....	34
2.5.2.2. <i>Inductively Coupled Plasma Atomic Emission Spectrometry</i> .....	38
2.6. MINERALOGICAL ANALYSIS .....	40
2.7. PARTICLE SIZE DISTRIBUTION, pH(KCl), ORGANIC MATTER AND CONDUCTIVITY OF WATER-SUSPENDED SOIL .....	40
2.8. APPLYING THE RESULTS OF A PRINCIPAL COMPONENT ANALYSIS TO DEFINE THE PARTICLE SIZE CLASSES USED IN THIS THESIS .....	44

### CHAPTER 3.

<b>MINERALOGY</b> .....	47
3.1. INTRODUCTION .....	47
3.2. RESULTS .....	47
3.3. DISCUSSION .....	52

### CHAPTER 4.

<b>GRANITE-DERIVED SOILS</b> .....	54
4.1. INTRODUCTION .....	54
4.2. ANALYTICAL RESULTS - AN OVERVIEW .....	55
4.3. PARTICLE SIZE DISTRIBUTIONS AND FIELD OBSERVATIONS .	61
4.4. MAJOR SOIL COMPONENTS .....	65
4.5. FACTORS WHICH DETERMINE THE LATERAL AND VERTICAL CHANGES OF THE CONCENTRATIONS .....	66
4.5.1. Loss and gain of elements during soil formation .....	68
4.5.2. Group-I: Li, P <sub>2</sub> O <sub>5</sub> , TiO <sub>2</sub> , V, Fe <sub>2</sub> O <sub>3</sub> , Zn, Zr and Sn .....	70
4.5.3. Group-II: SiO <sub>2</sub> , Cr, Mn, Co, Ni, Cu, Sr, Mo and W .....	73
4.5.4. Group-III: Depletion of Be, F, Na <sub>2</sub> O, Al <sub>2</sub> O <sub>3</sub> , K <sub>2</sub> O, CaO, Rb, Y, Nb, Pb, Th and U during soil formation .....	74
4.5.5. Group-IV: Accumulation of S, As, Se and Br in the soil .....	77
4.5.6. Group-V: 1 M NH <sub>4</sub> NO <sub>3</sub> extractable element fractions .....	78
4.5.7. Elements which were not assigned to groups: Mg, Cl, Ge, I and Bi ..	80
4.6. SUMMARY .....	81

## CHAPTER 5.

<b>SOILS ASSOCIATED WITH UNCONSOLIDATED SANDS OF GRANITIC ORIGIN</b> .....	84
5.1. INTRODUCTION .....	84
5.2. ANALYTICAL RESULTS - AN OVERVIEW .....	86
5.3. PARTICLE SIZE DISTRIBUTIONS AND FIELD OBSERVATIONS .	90
5.4. MAJOR SOIL COMPONENTS .....	93
5.5. FACTORS WHICH DETERMINE THE LATERAL CHANGES OF THE CONCENTRATIONS .....	94
5.5.1. Group-I (topsoil): Detrital input of Na <sub>2</sub> O, MgO, Al <sub>2</sub> O <sub>3</sub> , K <sub>2</sub> O, CaO, TiO <sub>2</sub> , Mn, Co, Zn, Rb, Sr, Th, U and 1 M NH <sub>4</sub> NO <sub>3</sub> extractable Co and Ba .	94
5.5.2. Group-II (topsoil): Detrital input of Y, Zr, Nb and Sn .....	94
5.5.3. Group-III (topsoil): Association of P <sub>2</sub> O <sub>5</sub> , V, Fe <sub>2</sub> O <sub>3</sub> , As, and Pb with Fe-oxides .....	96
5.5.4. Group-IV (topsoil): Retention of S, Cl, Br, I and 1 M NH <sub>4</sub> NO <sub>3</sub> extractable Na, Mg, S, K, Ca and Zn .....	96
5.5.5. Group-V (subsoil): Detrital input of Al <sub>2</sub> O <sub>3</sub> , P <sub>2</sub> O <sub>5</sub> , TiO <sub>2</sub> , V, Cr, Fe <sub>2</sub> O <sub>3</sub> , Ni, Zn, As, Rb, Y, Nb, Sn, Pb, Th, U and 1 M NH <sub>4</sub> NO <sub>3</sub> extractable Ba and Tl .....	96
5.5.6. Group-VI (subsoil): Similar behaviour of F, MgO, S, K <sub>2</sub> O, CaO, Br, Sr and 1 M NH <sub>4</sub> NO <sub>3</sub> extractable B, Mg, K, Ca, Cr, Ni, Pb and organic matter	98
5.5.7. Group-VII (subsoil): Na <sub>2</sub> O, Cl, Mn, W and 1 M NH <sub>4</sub> NO <sub>3</sub> extractable Na, S and Zn .....	99
5.6. VERTICAL CHANGES OF THE CONCENTRATIONS .....	100
5.7. SUMMARY .....	101

## CHAPTER 6.

<b>SOILS ASSOCIATED WITH SEDIMENTS OF THE MALMESBURY GROUP</b>	104
6.1. INTRODUCTION .....	104
6.2. ANALYTICAL RESULTS - AN OVERVIEW .....	107
6.3. PARTICLE SIZE DISTRIBUTIONS AND FIELD OBSERVATIONS	111
6.3.1. Soil associated with schist .....	111
6.3.2. Soil associated with phyllite .....	113
6.3.3. Soil associated with sandstone .....	113
6.4. MAJOR SOIL COMPONENTS .....	113
6.5. FACTORS WHICH DETERMINE THE SOIL CHEMISTRY .....	114
6.5.1. Effect of underlying rock-type on soil chemistry .....	114
6.5.2. Effect of agro-chemicals and sampling procedure on the analytical results .....	116
6.5.3. Lateral change of the concentrations down the topsoil .....	117

6.5.4.	Lateral change of the concentrations down the subsoil of the toposequence on schist . . . . .	121
6.5.5.	Lateral change of the concentrations down the subsoil of the toposequence on phyllite . . . . .	123
6.5.6.	Vertical changes of the concentrations . . . . .	125
6.6.	SUMMARY . . . . .	125

## CHAPTER 7.

<b>SOILS ASSOCIATED WITH FERRUGINIZED MATERIALS . . . . .</b>	<b>129</b>
7.1. INTRODUCTION . . . . .	129
7.2. ANALYTICAL RESULTS - AN OVERVIEW . . . . .	131
7.3. PARTICLE SIZE DISTRIBUTIONS AND FIELD OBSERVATIONS	135
7.4. MAJOR SOIL COMPONENTS . . . . .	136
7.5. FACTORS WHICH DETERMINE THE LATERAL CHANGES OF THE CONCENTRATIONS . . . . .	137
7.5.1. Group-I (top- and subsoil): Association of $P_2O_5$ , V, Cr, $Fe_2O_3$ , As, Se, Pb, Th and 1 M $NH_4NO_3$ extractable Mg and Co with Fe-oxide concretions . . . . .	137
7.5.2. Group-II (subsoil): Lateral eluviation of $Na_2O$ , MgO, $K_2O$ , CaO, Mn, Ni, Cu, Zn, Rb, Sr, Y, W and 1 M $NH_4NO_3$ extractable Na, K and Ca .	139
7.5.3. Group-III (topsoil): Be, $Na_2O$ , $K_2O$ , Mn, Cu, Zn, Rb, Sr, Sb and 1 M $NH_4NO_3$ extractable Mg . . . . .	139
7.5.4. Group-IV (subsoil): S, Cl, Br, I and 1 M $NH_4NO_3$ extractable Al, S, Fe and Tl concentrations controlled by retention and evaporation of soil water . . . . .	140
7.5.5. Group-V (topsoil): S, Cl, W and 1 M $NH_4NO_3$ extractable Na, P, S, K, Co, Zn and Tl . . . . .	140
7.5.6. Other elements ( $SiO_2$ , Zr and 1 M $NH_4NO_3$ extractable Fe, Ni, Zn and Ba) . . . . .	140
7.6. VERTICAL CHANGES OF THE CONCENTRATIONS . . . . .	141
7.7. SUMMARY . . . . .	143

## CHAPTER 8.

<b>COASTAL SAND-DERIVED SOILS . . . . .</b>	<b>145</b>
8.1. INTRODUCTION . . . . .	145
8.2. ANALYTICAL RESULTS - AN OVERVIEW . . . . .	147
8.3. MAJOR SOIL COMPONENTS . . . . .	151
8.4. FACTORS WHICH DETERMINE THE LATERAL CHANGES OF THE CONCENTRATIONS . . . . .	151
8.4.1. Group-I: $Na_2O$ , MgO, $Al_2O_3$ , $P_2O_5$ , $K_2O$ , CaO, Zn, Rb, Sr, Y, Nb and Pb concentrations controlled by aeolian and colluvial input of detritus .	152

8.4.2.	Relative loss of Na, Mg, Al, P, K, Ca, Rb and Sr during soil weathering .....	154
8.4.3.	Group-II: Association of Fe <sub>2</sub> O <sub>3</sub> , Ni, Mo and W in Fe-oxides and heavy minerals .....	155
8.4.4.	Group-III: Total S, Cl, Br and 1 M NH <sub>4</sub> NO <sub>3</sub> extractable Na, Mg, Al, P, S, K, Ca, Fe and Ba concentrations controlled by the retention ability .	158
8.4.5.	Elements which were not assigned to groups (Li, Ti, V, Cr, Mn, As, Zr, Sb and U) .....	160
8.4.6.	Particularly rapid lateral change of some soil properties .....	160
8.4.7.	Control of ground water and calcium carbonate on soil pH .....	162
8.5.	VERTICAL CHANGES OF THE CONCENTRATIONS .....	164
8.6.	SUMMARY .....	165

## CHAPTER 9.

<b>SUMMARY AND EXTENDED DISCUSSION OF INDIVIDUAL ELEMENTS AND SOIL FORMING FACTORS .....</b>		<b>167</b>
9.1.	INTRODUCTION .....	167
9.2.	LITHIUM .....	167
9.3.	BERYLLIUM .....	172
9.3.1.	Total Be concentrations .....	173
9.3.2.	1 M NH <sub>4</sub> NO <sub>3</sub> extractable concentrations of Be .....	173
9.4.	FLUORINE .....	175
9.5.	SODIUM .....	176
9.5.1.	Total Na <sub>2</sub> O concentrations .....	176
9.5.2.	1 M NH <sub>4</sub> NO <sub>3</sub> extractable concentrations of Na .....	176
9.6.	MAGNESIUM .....	177
9.7.	ALUMINIUM .....	179
9.8.	PHOSPHORUS .....	179
9.9.	SULFUR .....	181
9.10.	CHLORINE .....	181
9.11.	POTASSIUM .....	183
9.12.	CALCIUM .....	184
9.13.	VANADIUM .....	186
9.13.1.	Total V concentrations .....	186
9.13.2.	1 M NH <sub>4</sub> NO <sub>3</sub> extractable concentrations of V .....	187
9.14.	CHROMIUM .....	188
9.14.1.	Total Cr concentrations .....	188
9.14.2.	1 M NH <sub>4</sub> NO <sub>3</sub> extractable concentrations of Cr .....	189
9.15.	MANGANESE .....	190
9.16.	COBALT .....	191
9.16.1.	Total Co concentrations .....	192
9.16.2.	1 M NH <sub>4</sub> NO <sub>3</sub> extractable concentrations of Co .....	192

9.17.	NICKEL, COPPER AND ZINC .....	193
9.17.1.	Total Ni, Cu and Zn concentrations .....	194
9.17.2.	1 M NH <sub>4</sub> NO <sub>3</sub> extractable concentrations of Ni, Cu and Zn .....	195
9.18.	GALLIUM .....	196
9.19.	GERMANIUM .....	196
9.20.	ARSENIC .....	196
9.20.1.	Total As concentrations .....	197
9.20.2.	1 M NH <sub>4</sub> NO <sub>3</sub> extractable concentrations of As .....	198
9.21.	SELENIUM .....	198
9.22.	BROMINE AND IODINE .....	200
9.23.	MOLYBDENUM .....	202
9.24.	CADMIUM .....	202
9.25.	TIN .....	203
9.26.	ANTIMONY .....	205
9.27.	BARIUM .....	206
9.28.	TUNGSTEN .....	208
9.29.	THALLIUM .....	209
9.30.	LEAD .....	210
9.31.	THORIUM AND URANIUM .....	211
9.32.	TIME .....	214
9.33.	PARENT MATERIAL .....	215
9.34.	TOPOGRAPHY .....	218
9.35.	CLIMATE, BIOTA AND MAN .....	219
 <b>CHAPTER 10.</b>		
<b>CONCLUSIONS AND RECOMMENDATIONS FOR FUTURE RESEARCH ..</b>		<b>221</b>
10.1.	CONCLUSIONS .....	221
10.2.	RECOMMENDATIONS FOR FUTURE RESEARCH .....	223
<b>REFERENCES CITED .....</b>		<b>227</b>
<b>APPENDIX-I:</b>	<b>Description and classification of individual soil profiles .....</b>	<b>241</b>
<b>APPENDIX-II:</b>	<b>Method for extraction of elements with ammonium nitrate ..</b>	<b>287</b>
<b>APPENDIX-III:</b>	<b>Elemental concentrations, pH values, conductivities of the water-suspended soils and particle size distributions .....</b>	<b>288</b>

## DEFINITIONS OF TERMS AND ABBREVIATIONS AS USED IN THIS THESIS

**Eluviation:** Removal of soil material in suspension or solution from a part or from the whole of the soil profile.

**Extractable portion:** The portion of an element which can be extracted with 1 M  $\text{NH}_4\text{NO}_3$ . The  $\text{NH}_4\text{NO}_3$  extractable portion is regarded as being "readily mobilised" and is, therefore, of particular environmental relevance (NAW, 1993). The steps that were involved in selecting an appropriate method for extraction are discussed in section 2.5.1. The method for the extraction is given in Appendix-II. The units of the concentrations given in the text are ppm or ppb in air-dried soil.

**Fine clay:** Particles smaller than 0.5  $\mu\text{m}$ . The division of the particle size classes is based on the results of a Principal Component Analysis (section 2.8).

**Fines:** This particle size fraction includes the finer part of the silt fraction and the coarser part of the clay fraction. The unification into one particle size class is based on a Principal Component Analysis (section 2.8).

**ICP-MS:** Inductively Coupled Plasma Mass Spectrometry.

**ICP-AES:** Inductively Coupled Plasma Atomic Emission Spectrometry.

**Illuviation:** The downward movement and deposition of material which has been removed from the upper soil horizons by percolating water.

**Kaolinite:** All minerals of the kaolinite-group (d-spacing = 7 Å). No distinction was made between dickite, nacrite and metahalloysite.

**LLD:** Lower limit of detection; the lowest detectable concentration of an element for a specific analytical method.

**LOP:** Loss on pretreatment. The sample preparation for the particle size analyses included the removal of carbonates, soluble salts and organic matter. The corresponding weight loss is referred to as LOP. The suitability of the LOP as a measure for the proportion of organic matter is discussed in section 2.7.

**Mud:** A particle size fraction that includes silt and clay (particles smaller than 53  $\mu\text{m}$ ).

**Non-extractable portion:** Difference between total concentration and extractable concentration. It is assumed that the non-extractable portion of an element is hosted mostly by relatively insoluble minerals and organic matter.

**Real loss(gain):** Changes in the concentration of a particular element from a less to a more weathered sample may be due to loss(gain) of other elements, especially major elements. The real loss(gain) of an element was calculated from concentrations which were corrected for this effect. The calculations involved in this correction are discussed in Chapter 4.

**Sesquioxides:** Iron, aluminium and manganese oxides in soils.

**Soil form:** The soil classification system for South Africa is based on seventy-three soil forms, each of them defined by a different sequence of horizons. The definition of individual soil forms is given in Soil Classification: A Taxonomic System for South Africa (Soil Classification Working Group, 1991).

**Subsoil:** The lower soil horizons. In this thesis B-, C- and G-horizons.

**Throughflow:** Lateral subsurface soil-water movement (Kirkby, 1969).

**Toposequence:** A number of different soil types occurring down the length of a slope. Each soil type has properties attributable to its slope position (Figure 2.1).

**Topsoil:** The upper soil horizons. In this thesis A- and E-horizons because these horizons were occasionally sampled as a composite.

**USGO:** Unconsolidated sands north-east of Darling. It has been suggested (Van Niekerk, 1967) and is confirmed in this thesis, that the sands are partly of granitic origin, hence USGO (Unconsolidated Sands of Granitic Oorigin). Figure 5.1 shows the occurrence of the USGO.

**XRD:** X-Ray Diffractometry.

**XRFS:** X-Ray Fluorescence Spectrometry.

## LIST OF TABLES

- Table 1.1:** Past and projected population growth of the metropolitan Cape Town (including Stellenbosch, Paarl, Somerset West and Atlantis) after Bridgeman *et al.* (1992).
- Table 2.1:** Analyses of trace elements. Tabulation of the criteria used when deciding if XRFS or ICP-MS results should be used for the data set.
- Table 2.2:** Quality control for XRFS analyses. Certified and determined concentrations of trace elements for some of the standards used to set up the calibration curves.
- Table 2.3:** Lower limits of detection and estimate of errors for XRFS analyses.
- Table 2.4:** Lower limits of detection and the estimate of errors for the analyses of trace elements using ICP-MS.
- Table 2.5:** Experiments to find a suitable method for sample preparation prior to leaching. Powdered and -2 mm sieved soil samples were leached with 1 M  $\text{NH}_4\text{NO}_3$ . The ratios of [concentration in extract of powdered sample] over [concentration in extract of sieved sample] are tabulated.
- Table 2.6:** Comparison of possible soil treatments prior to leaching.
- Table 2.7:** Determination of 1 M  $\text{NH}_4\text{NO}_3$  extractable element concentrations. Tabulation of the criteria used when deciding if ICP-AES or ICP-MS results should be used for the data set.
- Table 2.8:** ICP-MS instrumental settings.
- Table 2.9:** Determination of 1 M  $\text{NH}_4\text{NO}_3$  extractable element concentrations using ICP-MS. The achieved LLDs are compared with the highest acceptable LLDs for the assessment of polluted soils, as recommended by the NAW (1993).
- Table 2.10:** ICP-AES instrumental settings.
- Table 2.11:** Tabulation of LLDs and calibration ranges for the analyses of the 1 M  $\text{NH}_4\text{NO}_3$  extractable element fractions using ICP-AES.
- Table 2.12:** Suitability of the loss on pretreatment as a measure for the proportion of organic matter.
- Table 2.13:** Variables (size classes) used for the Principal Component Analysis of the particle size distributions and their loadings on the different principal components.
- Table 2.14:** Combination of particle size classes according to the results of a Principal Component Analysis.
- Table 4.1:** Basic statistics of the major elements in the granite-derived soils.
- Table 4.2:** Basic statistics summarising the pH(KCl) values, the conductivities of the water-suspended soil samples and the percentages of various particle size fractions and organic matter for the granite-derived soils.
- Table 4.3:** Basic statistics of the trace elements in the granite-derived soils.
- Table 4.4:** Basic statistics of the 1 M  $\text{NH}_4\text{NO}_3$  extractable element concentrations for the granite-derived soils.

- Table 4.5:** Enrichment factors from (a) the granite to the subsoil with abundant Fe-oxide concretions, (b) the composite samples of the topsoil to the samples of the organic-rich top 15 cm of the topsoil and (c) the topsoil to the fine textured subsoil at the bottom of the toposequence.
- Table 4.6:** Whole-rock analyses of the slightly weathered granite which forms the parent material of the Klipberg toposequence.
- Table 5.1:** Basic statistics of the major elements in the soils associated with the unconsolidated sands of granitic origin.
- Table 5.2:** Basic statistics summarising the pH(KCl) values, the conductivities of the water-suspended soil samples and the percentages of various particle size fractions and organic matter for the soils associated with the unconsolidated sands of granitic origin.
- Table 5.3:** Basic statistics of the trace elements in the soils associated with the unconsolidated sands of granitic origin.
- Table 5.4:** Basic statistics of the 1 M  $\text{NH}_4\text{NO}_3$  extractable element concentrations for the soils associated with the unconsolidated sands of granitic origin.
- Table 6.1:** Basic statistics of the major elements in the soils associated with the sediments of the Malmesbury Group.
- Table 6.2:** Basic statistics summarising the pH(KCl) values, the conductivities of the water-suspended soil samples and the percentages of various particle size fractions and organic matter for the soils associated with the sediments of the Malmesbury Group.
- Table 6.3:** Basic statistics of the trace elements in the soils associated with the sediments of the Malmesbury Group.
- Table 6.4:** Basic statistics of the 1 M  $\text{NH}_4\text{NO}_3$  extractable element concentrations for the soils associated with the sediments of the Malmesbury Group.
- Table 6.5:** High concentrations of S, I and the 1 M  $\text{NH}_4\text{NO}_3$  extractable portions of some elements in the subsoil at the midslope position of the toposequence associated with the phyllite of the Malmesbury Group.
- Table 7.1:** Basic statistics of the major elements in the soils associated with the ferruginized materials.
- Table 7.2:** Basic statistics summarising the pH(KCl) values, the conductivities of the water-suspended soil samples and the percentages of various particle size fractions and organic matter for the soils associated with the ferruginized materials.
- Table 7.3:** Basic statistics of the trace elements in the soils associated with the ferruginized materials.
- Table 7.4:** Basic statistics of the 1 M  $\text{NH}_4\text{NO}_3$  extractable element concentrations for the soils associated with the ferruginized materials.
- Table 8.1:** Basic statistics of the major elements in the coastal sand-derived soils.
- Table 8.2:** Basic statistics summarising the percentages of mud and organic matter, the pH(KCl) values and the conductivities of the water-suspended soil samples for the coastal sand-derived soils.
- Table 8.3:** Basic statistics of the trace elements in the coastal sand-derived soils.

- Table 8.4:** Basic statistics of the 1 M  $\text{NH}_4\text{NO}_3$  extractable element concentrations for the coastal sand-derived soils.
- Table 8.5:** The  $\text{Rb}/\text{Al}_2\text{O}_3$  ratios and the concentrations of  $\text{CaO}$ ,  $\text{Sr}$ ,  $\text{MgO}$ ,  $\text{Al}_2\text{O}_3$ ,  $\text{P}_2\text{O}_5$ ,  $\text{Na}_2\text{O}$ ,  $\text{K}_2\text{O}$  and  $\text{Rb}$  in the freshest and in a strongly weathered sample of the coastal sand-derived soils. The ratios of [concentration in weathered sample] over [concentration in fresh sample] were calculated to quantify the tendency of a particular element to become depleted during soil weathering.
- Table 8.6:** Vertical changes of the concentrations in the coastal sand-derived soils.
- Table 9.1:** Comparison of concentrations in underlying materials and soil groups with concentrations reported in the literature.
- Table 9.2:** Concentrations of ammonium nitrate extractable element fractions that should not be exceeded in the soil (Prüß et al., 1991). A concentration that is higher than the recommended maximum concentration can limit the functioning of the soil.
- Table App-1:** Code system used in Appendix-I.
- Table App-2:** Concentrations of major elements in percent.
- Table App-3:** Concentrations of trace elements in ppm.
- Table App-4:** Concentrations of 1 M  $\text{NH}_4\text{NO}_3$  extractable element fractions in ppm. Analyses using ICP-AES.
- Table App-5:** Concentrations of 1 M  $\text{NH}_4\text{NO}_3$  extractable element fractions in ppb. Analyses using ICP-MS.
- Table App-6:** The  $\text{pH}(\text{KCl})$  values, the conductivities of the water-suspended soils in  $\mu\text{S cm}^{-1}$  and the proportions of gravel, sand, mud, LOP, silt and clay in weight percent of the total sample. The weight percentages of the particle size classes unified according to a Principal Component Analysis are given on the right side of the table.
- Table App-7:** The proportions of individual phi units for the -2 mm sieved soil fraction as determined with the sedigraph and the settling column. The proportions are expressed in weight percent of the entire sample.

## LIST OF FIGURES

- Figure 1.1:** The location of the field area and its major features.
- Figure 1.2:** Simplified map of the major rock types in the field area.
- Figure 2.1:** Simplified profile through a toposequence.
- Figure 2.2:** The approximate positions of the sampling sites.
- Figure 2.3:** A photograph of Pit 36 exemplifies a typical pit and the nature of the field work.
- Figure 2.4:** Schematic soil profile illustrating the major soil horizons which were sampled (master horizons).
- Figure 3.1:** Stacked XRD patterns of a subset of samples taken from the soils associated with the coastal sands and the unconsolidated sands of granitic origin.

- Figure 3.2:** Stacked XRD patterns of a subset of granite-derived soils.
- Figure 3.3:** Stacked XRD patterns of a subset of samples taken from the soils associated with the schists of the Malmesbury Group.
- Figure 3.4:** Stacked XRD patterns of a subset of samples taken from the soils associated with the feldspathic sandstone and phyllite of the Malmesbury Group.
- Figure 3.5:** Stacked XRD patterns of a subset of samples taken from the soils associated with the ferruginized materials.
- Figure 4.1:** Simplified section through the granite-derived toposequence.
- Figure 4.2:** A photograph showing the view from the uppermost pit down the granite-derived toposequence.
- Figure 4.3:** Particle size distributions of the samples taken from the granitic toposequence at Klipberg.
- Figure 4.4:** Change of the  $Al_2O_3$ ,  $SiO_2$  and Zr concentrations from the exposed granite down the topsoil.
- Figure 4.5:** The concentrations of As, S, Br and Se from the granite to the topsoil of Pit 30 and further to the subsoils of Pits 31, 32 and 33. The graphs show the strong accumulation of Group-IV elements in the soil.
- Figure 4.6:** Real loss and gain of elements from the granite to the uppermost part of the toposequence.
- Figure 4.7:** The concentrations of the  $NH_4NO_3$  extractable portions of K, Na, Mg, Ca, Ba, Al and the pH(KCl) values from the granite down the topsoil of the toposequence in ppm.
- Figure 4.8:** Interpretative diagram of the granite-derived toposequence (Klipberg).
- Figure 5.1:** Simplified map of the sampling sites in the soils associated with the unconsolidated sands of granitic origin.
- Figure 5.2:** Simplified section through the sampling sites in the soils associated with unconsolidated sands of granitic origin.
- Figure 5.3:** Particle size distributions of the top- and subsoils from the slightly higher lying areas near the Darling granite exposure towards the floodplain.
- Figure 5.4:** Particle size frequency curves of the sand fraction. The soils associated with the unconsolidated sands of granitic origin show a shift from a bimodal to a unimodal particle size distribution. This shift demonstrates the change from a partly colluvial and partly fluvial(aeolian) underlying material to an exclusively fluvial(aeolian) underlying material in the floodplain.
- Figure 5.5:** Horizontal changes of the concentrations of selected elements in the topsoils associated with the USGO.
- Figure 5.6:** Horizontal changes of the concentrations of selected parameters in the subsoils associated with the USGO.
- Figure 5.7:** Interpretative diagram of the soils associated with the unconsolidated sands of granitic origin.
- Figure 6.1:** Simplified sections through the sampling sites in the soils associated with the sediments of the Malmesbury Group.

- Figure 6.2:** A photograph showing the view from the midslope (Pit 37) down the toposequence on schist of the Malmesbury Group.
- Figure 6.3:** A photograph showing the view from the top (Pit 40) towards the footslope of the toposequence on phyllite of the Malmesbury Group.
- Figure 6.4:** Particle size distributions of the soils associated with the sediments of the Malmesbury Group.
- Figure 6.5:** Lateral change of the elemental concentrations and the pH(KCl) values down the topsoil of the toposequences associated with the sediments of the Malmesbury Group.
- Figure 6.6:** Lateral change of the elemental concentrations and the pH(KCl) values down the subsoil of the toposequences associated with the sediments of the Malmesbury Group.
- Figure 6.7:** Interpretative diagram of the toposequences associated with schist and phyllite of the Malmesbury Group.
- Figure 7.1:** Simplified sections through the sampling sites in the soils associated with the ferruginized materials.
- Figure 7.2:** A photograph showing the view from the footslope (Pit 45) towards the higher slope positions of the toposequence associated with the ferruginized materials.
- Figure 7.3:** Particle size distributions of the toposequence associated with the ferruginized materials.
- Figure 7.4:** Lateral change of the concentrations down the top- and the subsoil of the toposequence associated with the ferruginized materials.
- Figure 7.5:** The similar vertical change of the Na<sub>2</sub>O, K<sub>2</sub>O and sand percentages in Pits 46 and 47.
- Figure 7.6:** Interpretative diagram of the toposequence associated with the ferruginized materials.
- Figure 8.1:** Simplified section through the sampling sites in the soils derived from the coastal sands.
- Figure 8.2:** A photograph showing the view from the coastal dunes at Pit 4 towards Rondeberg.
- Figure 8.3:** Particle size distributions of three A-horizons which derived from the wind-deposited coastal sands.
- Figure 8.4:** Lateral variation of the Al<sub>2</sub>O<sub>3</sub>, K<sub>2</sub>O and Rb concentrations and the Rb/Al<sub>2</sub>O<sub>3</sub> ratios in the topsoil along the sampling line.
- Figure 8.5:** Lateral trend of the Fe<sub>2</sub>O<sub>3</sub>, W, Zr and Al<sub>2</sub>O<sub>3</sub> concentrations in the topsoil along the sampling line.
- Figure 8.6:** The covariance of Fe<sub>2</sub>O<sub>3</sub>, Ni, Mo, W and medium sand in the coastal sand-derived soils.
- Figure 8.7:** The 1 M NH<sub>4</sub>NO<sub>3</sub> extractable concentrations of Fe versus the total Fe concentration and the proportion of organic matter for the coastal sand-derived topsoils. Samples with higher concentrations of extractable Fe generally have lower total Fe concentrations and higher proportions of organic matter.
- Figure 8.8:** Similar lateral trends of organic matter, mud, conductivity of water-suspended soil and 1 M NH<sub>4</sub>NO<sub>3</sub> extractable concentrations of Ca and Fe in the topsoil. The lateral trend demonstrated by extractable Ca and Fe is typical for total Br, Cl, S and extractable Mg, Ba, S, Na, P, Fe, Al, Ca.
- Figure 8.9:** Conceptual diagram summarising the processes which caused the rapid lateral change of some soil properties and low pH values.

- Figure 9.1:** Fluorine versus  $\text{Al}_2\text{O}_3$  in soil samples, showing that high F concentrations occur mainly in subsoils with high  $\text{Al}_2\text{O}_3$  concentrations.
- Figure 9.2:**  $\text{NH}_4\text{NO}_3$  extractable versus non-extractable Mg for the soils associated with the sediments of the Malmesbury Group and the granite.
- Figure 9.3:**  $\text{NH}_4\text{NO}_3$  extractable S versus non-extractable S for all soils.
- Figure 9.4:** Correlation of the conductivity of the water-suspended soil and the chlorine concentration.
- Figure 9.5:**  $\text{NH}_4\text{NO}_3$  extractable K versus non-extractable K for the topsoils of the granite-derived toposequence.
- Figure 9.6:** The (weak) covariance of  $\text{NH}_4\text{NO}_3$  extractable Ca and non-extractable Ca in the soils associated with the sediments of the Malmesbury Group.
- Figure 9.7:** The (weak) covariance of organic matter and CaO in the topsoils.
- Figure 9.8:** The correlation of V and  $\text{Fe}_2\text{O}_3$  in the soil.
- Figure 9.9:** The correlation of Cr and  $\text{Fe}_2\text{O}_3$  in the soil.
- Figure 9.10:** The correlation of Co and  $\text{Fe}_2\text{O}_3$  in the soil.
- Figure 9.11:** Covariance of Ni and  $\text{Al}_2\text{O}_3$  in Pit 44.
- Figure 9.12:** The (weak) correlation of  $\text{Fe}_2\text{O}_3$  and Se in the soils.
- Figure 9.13:** The plots of bromine and iodine versus mud show that higher proportions of mud (> 40 %) are a condition for higher levels of Br and I in the investigated soils.
- Figure 9.14:** Tin versus  $\text{Al}_2\text{O}_3$  for rock and soil samples.
- Figure 9.15:** The loss of  $\text{K}_2\text{O}$  and  $\text{NH}_4\text{NO}_3$  extractable Ba down the granite-derived toposequence.
- Figure 9.16:** [ $\text{Al}_2\text{O}_3 + \text{Fe}_2\text{O}_3$ ] versus  $\text{NH}_4\text{NO}_3$  extractable Ba for rock and soil samples.
- Figure 9.17:** [ $\text{Fe}_2\text{O}_3 + \text{Al}_2\text{O}_3$ ] versus Pb for all soil samples.
- Figure 9.18:** Thorium versus U for all soil samples.
- Figure 9.19:** The (weak) correlation of U and  $\text{Al}_2\text{O}_3$  in the investigated soils.
- Figure 9.20:** Principal Component Analysis of the chemical composition of soils and parent rocks.

# CHAPTER 1.

## INTRODUCTION

---

"Malmesbury and its wheatlands do not lure the tourist, or even the Cape Town motorist, as do Paarl and Worcester and the towns among the trees and the mountains. Yet this Malmesbury district is my favourite and there are parts where I could draw a map of the farms from memory. Malmesbury has such contrasts within its boundaries." That is how Lawrence G. Green (1949) describes the central part of the area studied in this thesis, colloquially called the Swartland. "It was not the black soil that gave the district its name", he goes on. "It was the dark, notorious and aggressive shrub, the *renosterbos*."

Since his times the Swartland has been exposed to increasing agricultural development. The area is witness to the rapid environmental change in South Africa and very little of its original character and indigenous vegetation is left. However, with careful observation of the landscape I discovered places still showing the beauty that Lawrence G. Green wrote about.

### 1.1. AIMS OF THE STUDY

**Importance of soils:** The functions of soil are diverse and important. Soil is the habitat of micro- and macro-organisms. These include agricultural and indigenous plants covering the soil and organisms living in the soil. The ability of soil to retain water is the reason why soil is an important factor in the cycling of water. More recently, the importance of soils to function as a buffer for pollutants with regard to the ground water and plants has received much attention (Blume, 1992). Also more recently, and especially in the urban environment, functional soil was identified as being essential for the development of recreational areas (e.g. forests, parks).

**Present usage of the soils in the study area:** The south-western Cape is South Africa's most valuable producer of agricultural commodities, both in terms of Rand output per person and in terms of total yield (Walton *et al.*, 1984). The flat terrain of the field area between the Cape Fold Belt and the coastline forms a very productive part of the Western Cape. The dominant agricultural product is cereal (Walton *et al.*, 1984). Industrial developments are rare and restricted to the larger towns.

**Future:** The population of the Cape Town metropolitan area, including Stellenbosch, Paarl, Somerset West and Atlantis, is at present 3.3 million and is predicted to increase by 50 % within the next 15 years (Table 1.1; Bridgeman *et al.*

1992). It can thus be predicted that (a) the agricultural pressure on the soil in the study area will further increase and (b) the southern part of the field area will be the location for future housing and(or) industrial developments.

**Lack of information on the geochemistry of Western Cape soils:**

Knowledge about the soils in the study area would generally help to identify, control and minimise the misuse and pollution of Western Cape soils. A definite need for more information on the distribution of health-related elements in the soils of the study area was identified when consulting with

local soil and medical scientists. Existing information is difficult to gather because it is restricted to unpublished theses and reports compiled for agricultural purposes. Two M.Sc. theses submitted to the University of Stellenbosch deal with the soils of the study area (Merryweather, 1965; Van Niekerk, 1967). The main aim of their work was to classify and map the soils in the Wellington-Malmesbury and Darling areas. The chemistry of the soils was only investigated to help with the soil classification and to assess the agricultural potential of the soils. Hartmann (1969) investigated the chemical heterogeneity of some soils in the Western Cape. Some of his results are discussed in section 2.2. A number of honours theses, investigating the geochemistry of various weathering profiles on sediments of the Malmesbury Group and granites close to the study area, were submitted to the Department of Geological Sciences (University of Cape Town). These include Martin (1973), Dent (1973), Brunke (1973), Smith (1972), Lawless (1972) and Topping (1972). The aim of the projects was to determine and understand the vertical change of the elemental concentrations from the rock to the soil. Lateral changes of the concentrations were not determined. Apart from the major elements only a few trace elements were investigated in these studies. It is clear that the information available on trace elements in Western Cape soils is incomplete and covers only a small proportion of the elements which are presently considered relevant to health.

**The aims of this study:** Considering what is outlined above the following aims were defined for this study.

- i. To further the understanding of the factors and processes governing the spatial distribution in soils of elements relevant to health. Elements less relevant to health

**Table 1.1:** Past and projected population growth of the metropolitan Cape Town (including Stellenbosch, Paarl, Somerset West and Atlantis) after Bridgeman *et al.* (1992).

Cape Town metropolitan population in millions	
1980	1.92
1985	2.39
1990	2.93
1995	3.43
2000	3.96
2005	4.33
2010	4.80

(e.g. SiO<sub>2</sub> and Zr) were investigated in order to facilitate the interpretation of the results for the health-relevant elements (e.g. Li and Sb). While most other studies are restricted to the vertical changes of the concentrations in individual soil profiles this study attempts to explain both the vertical and the lateral chemical variation. In addition to the total elemental concentrations the extractable concentrations of the elements were determined because this fraction may be leached into the ground water or taken up by plants, animals and humans.

- ii. To provide background values for the different soil groups and elements under investigation. Such background values are essential for the identification and assessment of soil pollution. Most countries in the northern hemisphere encounter great difficulty in obtaining true natural background values because of earlier diffuse soil contamination (Bundesverband Deutscher Geologen, 1990; Nriagu and Pacyna, 1988).
- iii. To produce a geochemical data base for the study area for the use of scientists in the fields of soil science, environmental health, agriculture and botany.

## 1.2. RATIONALE FOR THE STRUCTURE OF THIS THESIS

The discussion of the geochemical results is divided into two main parts. The first main part consists of Chapters 4 to 8. Each of these chapters deals with a group of soils associated with a particular underlying material (rock-type). These chapters are of interest to the reader who needs geochemical information for a specific soil group. The elements examined in Chapters 4 to 8 are grouped in order to facilitate their discussion. The basis of the grouping is the lateral trend of the elemental concentrations, presuming that elemental concentrations which have the same lateral trend are controlled chiefly by the same factor(s). The lateral trends of the concentrations in the top- and the subsoil are examined separately. The results show that the factor(s) which control the distribution of a particular element in the topsoil may differ from the factor(s) which control the distribution of the same element in the subsoil. One element can, therefore, belong to more than one group and may be discussed in more than one section in each chapter. The advantages of this structure are:

- (a) repetition is avoided in the presentation of the results because the lateral change of the concentrations can easily be summarised for the whole group of elements.
- (b) less well understood elements (e.g. Li) appear together with better understood elements (e.g. Fe) which show the same lateral trend. This makes it easier to explain the results for the less well understood elements.

The second main part of the discussion consists of Chapter 9 which provides a summary and extended discussion of most of the elements under investigation. This chapter is helpful if the reader needs specific information about individual elements.

### 1.3. LOCATION

The study area is situated in the south-west of South Africa and is depicted on sheet Cape Town 3318 (1 : 250 000). Most of the area belongs to the administrative district of Malmesbury and is bounded by the towns of Hopefield, Piketberg, Paarl and Cape Town (Figure 1.1).

The territory ranges from the Cape Fold Belt orographic line in the east to the Atlantic Ocean in the west and forms part of the Coastal Foreland as defined by Wellington (1955). The Coastal Foreland is colloquially divided into "Swartland" and "Sandveld" (Figure 1.1).

### 1.4. HISTORY

The region has possibly the longest record of human habitation of all Mediterranean climate regions (Boucher, 1987). Human populations became established in the middle Pleistocene and are referred to as the stone-age Acheulian culture. Animal husbandry was practised at the Cape for more than a thousand years prior to the arrival of Europeans in 1487 (Deacon, 1983). Sheep remains at Die Kelders near Hermanus date to between 1500 and 2000 years ago (Schweitzer, 1974).

The earliest written record about the Cape is by the mariner, Bartholomew Diaz, who in 1487 - 1488 landed at several points along the coast and recorded seeing people with cattle who practised veld-burning (Axelson, 1973). In 1652 Jan van Riebeck established the first formal settlement of Europeans in the Cape. The settlement served as a refreshment station for the ships of the Dutch East India Company and was the nucleus for the colonization of southern Africa. Jan van Riebeck estimated the number of Khoi, a tribe of herders, living in the coastal foreland between Table Bay and Berg River at 17000 - 18000 people (Boucher, 1987). In search of cattle he engaged Jan Wintervogel in 1655 to lead the first expedition towards the lower Berg River (Walton *et al.*, 1984). Barrow (1806) remarked that by 1797 the Swartland was extensively cultivated and he considered it to be the most populous part of the country. As a result of these historic events the study area has been exposed to the longest period of European farming on the sub-continent (Boucher, 1987).

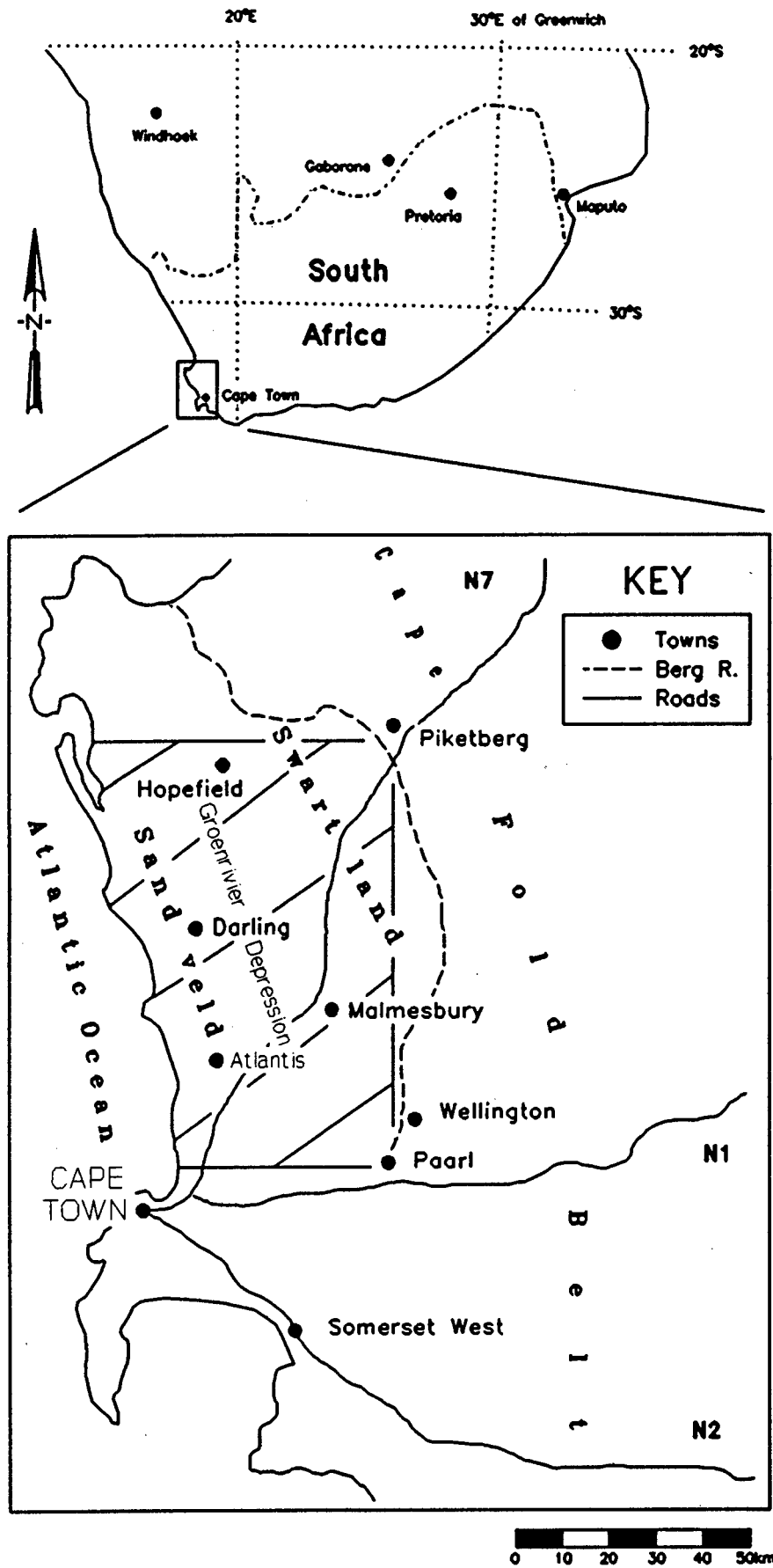
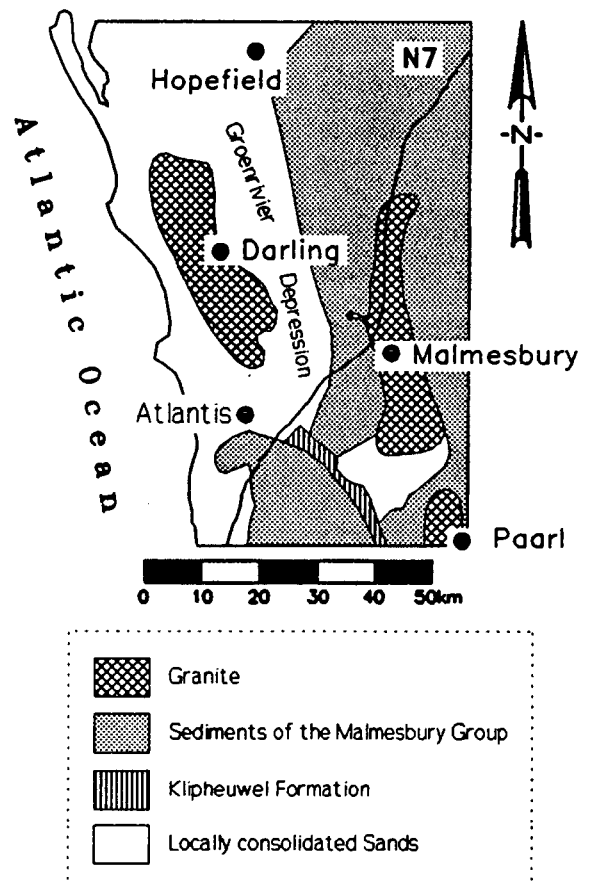


Figure 1.1: The location of the field area and its major features.

## 1.5. GEOLOGY

The major geological units in the area of interest are the sediments of the Malmesbury Group (Precambrian) with greywackes, schists, phyllites and quartzitic sandstones, the Cape Granites (pre-Ordovician) and the Klipheuwel Formation (Cambrian) with sandstones, conglomerates, greywackes and shales.

The Tertiary and the Quaternary are represented by locally consolidated sands of marine origin and aeolian/alluvial/colluvial deposits (Theron, 1991). None of these have any great thicknesses. They were, however, of importance to the present study because they overlie older materials of different lithology and formed the parent material to some of the investigated soils. Large bodies of sand, deposited on the outer margin of the coastal platform by former high sea levels, were partly reworked in subsequent times to form extensive coastal dune fields. Figure 1.2 shows the distribution of the above described rocks and sediments in the field area.



**Figure 1.2:** Simplified map of the major rock types in the field area, modified after Theron (1991).

## 1.6. SOILS AND GEOMORPHOLOGY

Lambrechts (1979) described the terrain as a smoothly undulating coastal plain with a maximum elevation of less than 200 m. The surface is, however, broken by a number of smooth, rounded granite batholiths.

A number of factors have contributed to the evolution of the soils found in the field area. The most important being the climatic changes throughout the Cenozoic, the geomorphological history and the different geological parent materials. Transgressions and regressions during the Cenozoic caused changes of the stream erosion base level.

The resulting dissection and stripping of older soils remodelled earlier erosion surfaces. In this way new parent materials were provided(exposed) for the ongoing formation of soils. Hence the soils of the region are both old and young and they are products of dynamic changes (Lambrechts, 1983).

The controls of soil formation discussed above resulted in a coherent pattern of soils in the landscape. Red apedal soils are found where the preweathered, ferruginized materials were preserved and not covered by younger materials. Residual and duplex soils are found on the planation surfaces. These soils are associated with granites, sediments of the Malmesbury Group and unconsolidated sediments of younger age. The soils of the lowest and youngest land forms in the landscape are podsollic or calcareous. These soils derived from windblown sands and partly consolidated sediments of Cenozoic age and various origins. A more complete review of the soils in the study area is given by Lambrechts (1979 and 1983) and Schloms *et al.* (1983).

## 1.7. CLIMATE

The climate in the study area is mediterranean. Most of the area receives an average annual precipitation of 300-400 mm. Depending mainly on the topography, values of up to 1000 mm are possible (Weather Bureau, 1980). Most of the precipitation occurs during winter. The Berg River and its tributaries form the most important drainage system in the area. The Berg River's estuary is the only one in the area which is permanently open to the sea.

Due to the moderating effect of the sea, the temperatures vary least along the coast. Further inland more extreme minimum and maximum temperatures are encountered. In Darling the temperatures range from 11.1 to 37.6° C for February and from 3.5 to 27.4° C for August. Walton *et al.* (1984) give average temperatures of 20.1 to 22.5° C for January and 12.6 to 15° C for July. Frost is rare in the Coastal Foreland. The area is known for its strong winds. The month with the strongest winds is January. These winds come most commonly from southerly to south-easterly directions and frequently reach velocities of 8-13.8 m/s. The most frequent wind direction in July is northerly to north-westerly (Boucher, 1987).

## 1.8. INDIGENOUS VEGETATION

The distribution of the different plant communities is most closely related to the geology. Other major controls of the vegetation are the soil types, the soil base status, topography and precipitation. The latter factors are partly pre-determined by the geology. The following classification of the indigenous vegetation is based on an east-

west vegetation type transect through the field area (Cowling, 1992; Campbell, 1985). The vegetation types can be divided into two major associations, the fynbos group and the non-fynbos group.

The eastern part of the field area is extensively used for agricultural purposes. The remains of the indigenous vegetation were classified to be renoster shrubland and belong to the non-fynbos group. The relatively high base status of the soils in this area is inherited from the underlying sediments of the Malmesbury Group and is required by the renoster shrubland.

Further west, in the Darling area, the soils are underlain by granite. The granitic soils also have a high base status and support renoster shrublands and thicket (both non-fynbos). The indigenous vegetation on the acid and calcareous sands east and west of the granites belongs mainly to the restioid and proteoid fynbos series. A table with the species and the genera associated with the above mentioned vegetation series is given in Cowling (1992).

## 1.9. PREVIOUS WORK

**Western Cape:** A broad outline of the distribution and nature of the different soil types occurring in the Western Cape and a discussion of the processes that affected their formation is given in Lambrechts (1983), Schloms *et al.* (1983) and Lambrechts (1979). Some detailed soil mapping, covering parts of the field area, was conducted by Van Niekerk (1967) and Merryweather (1965). The information available on the geochemistry of Western Cape soils was reviewed in section 1.1. It was concluded that the previous work is incomplete and covers only a small proportion of the elements presently considered relevant to health.

**Information for individual elements:** The number of significant international publications dealing with the abundance, distribution and behaviour of the 41 investigated elements in soils is too high to be reviewed in detail here. The most important information is summarised in high quality textbooks: Alloway (1993), Blume (1992), Swaine (1990), Scheffer and Schachtschabel (1989), Fiedler and Rösler (1987), Adriano (1986), Kabata-Pendias and Pendias (1985), Davies (1980), Wedepohl (1969-1978) and Vinogradov (1959). The relevance of individual elements for plants, animals and humans is discussed in Merian (1984) and Mertz (1981). Nriagu and Pacyna (1988) quantify the worldwide emissions of trace metals into soils. A publication by the German Association of Geologists (Bundesverband Deutscher Geologen, 1990) reviews the highest acceptable concentrations of toxic elements in soils, as published and used in different European countries. Important interactions between organic matter and certain metal ions are discussed in Stevenson (1982). Sorption of metals by humic acid was researched by Kerndorf and Schnitzer (1980).

**Best possible background concentrations and concentrations in soils exposed to increased emissions of heavy metals:** To establish best possible background concentrations of trace elements in Western Cape soils is one of the aims of this study. Similar studies were undertaken to determine such concentrations for European soils. Ruppert (1987) summarised and published the concentrations of Cr, Mn, Fe, Co, Ni, Cu, Zn, Cd and Pb in 3000 soil samples from Bavaria. Hoffmann *et al.* (1981) and Häni *et al.* (1981) conducted similar research for other parts of Germany and Switzerland, respectively. Brüne and Ellinghaus (1982) and Van Driel and Smilde (1981) established heavy metal concentrations in German and Dutch arable soils. They found that concentrations were mostly below the recommended maximum concentrations. A gradual pollution of Dutch river sediments, however, was proven by Van Driel and Smilde. Lux (1981) investigated arable soils and plants in the close vicinity of industrial areas and found high concentrations of heavy metals which greatly exceeded recommended maximum concentrations. It was noted that concentrations can vary substantially over short distances and time periods.

**Weathering:** Bühmann and Kirsten (1991) studied the mineralogy and the major element geochemistry of five weathering profiles on South African granites. Gibbsite-kaolinite-quartz-hematite associations were established for the highly weathered profiles while feldspar-quartz-mica-kaolinite associations dominated the less weathered profiles. Nesbitt and Young (1989) demonstrated that the changes of the bulk compositions of weathering profiles follow simple trends that are largely unaffected by climatic conditions: alkali and alkaline earth elements are leached from the profile in preference to elements such as Ti,  $Fe^{3+}$  and Al. Mineralogical changes were perceived to be much more complex. Minarik *et al.* (1983) studied the weathering profile of a granite and found that  $SiO_2$ ,  $Al_2O_3$ ,  $Fe_2O_3$  and  $H_2O$  are relatively enriched in the residuum of the weathered granite. The behaviour of the investigated trace elements was not uniform. Kesel and Spicer (1985) investigated soils on alluvial fans in Costa Rica. The age of the subsurfaces were determined to range from 100 to approximately 65000 years. The results showed that with time  $Al_2O_3$  and  $Fe_2O_3$  concentrations increased while  $SiO_2$  decreased. Primary minerals were completely altered to clay minerals. In the oldest soils kaolinite was altered to gibbsite.

**Parent Material:** Jenny (1941) stated that the parent material is one of five soil forming factors. Stephen (1952) studied soils derived from different igneous parent rocks and emphasised the importance of the parent rock in determining the mineralogical composition of the overlying soils. Moura and Kroonenberg (1988) investigated the geochemistry and mineralogy of soil profiles on four different parent materials in Colombia. They concluded that, in spite of intensive weathering and soil formation under tropical conditions, geochemical signatures of the parent materials can survive. Litaor *et al.* (1989) investigated a lithosequence in the northeastern Samaria steppe (Israel). A Factor Analysis was used to show that different quantities of clay, salt

and calcium carbonate were the main controls of the physical and chemical differences between the soils. Different quantities of clay, salt and calcium carbonate were related to different parent materials. The effect of parent material on soils derived from granite and andesite in the Western Transvaal (South Africa) was studied by Bruce and Beukes (1992). They found that soils derived from different parent materials have different concentrations of extractable P, Ca and Mg. The importance of the parent material as a soil forming factor in the field area was pointed out by Talbot (1947), Lambrechts (1979) and Schloms *et al.* (1983).

**Toposequences:** Geochemical studies down toposequences are very scarce. Glazovskaya (1968) suggested that lateral migration of elements links soils of elevations, slopes and depressions into a single geochemical whole. The author described some regularities of migration and differentiation of elements in essentially different climates. Nyamapfene (1986), Purves (1976) and Conacher (1975) recognised throughflow and sheet floods as important in transporting solubles and clay particles down toposequences. A comparison of two slope sequences on moraines in Wyoming showed that the older soils contain more clay minerals and free sesquioxides (Swanson, 1985). The author suggested that the soil undergoes weathering throughout its slow movement down slope as a result of creep. The close relationship between hillslope creep and soil morphology was stressed. Munnik *et al.* (1992) sampled 64 soil profiles along nine hillslopes in a South African granite landscape. Soil creep and deposition of material at the footslope was suggested. The proportions of coarse sand increase down the toposequences while the proportions of clay decrease. The possibility of pedoturbation and admixture of colluvium with materials weathered from the nearby saprolite was discussed.

**Slope processes:** Slope processes proved to be an important factor in determining the geochemical changes down the toposequences sampled for this thesis. Selby (1982) and Statham (1977) give a good understanding of the different forms of slope processes occurring along a toposequence. Schumm (1967) and Williams (1974) quantified rates of surficial rock creep. Ploey and Moeyersons (1975) showed that relatively slow movement of particles induced by runoff is particularly effective on slopes covered with granite gneiss or sandy materials.

# CHAPTER 2.

## METHODS OF INVESTIGATION

---

### 2.1. INTRODUCTION

Representative field sampling and the analyses of approximately 90 parameters per sample formed a very time consuming and important part of this study. The methods and techniques used are explained and discussed below.

### 2.2. FIELD SAMPLING

The number of soil types occurring in the study area is high and the distribution of the soil types is typically non-contiguous (Schloms *et al.*, 1983; Hartmann, 1969). This variability is a function of time, climate, different geological parent materials, topography and biotic factors, as well as different soil forming processes such as ferrallization, plinthite formation, podzolisation, eluviation and illuviation (Lambrechts, 1983).

**Ascertaining the chemical variance with a low number of samples:** Only 106 soil samples were collected because the analytical procedures required for this study were time intensive and expensive. Chemically similar soils were grouped together. Samples were taken from each soil group in an attempt to ensure that they are sufficiently representative of the chemical variability within the study area. A decision had to be made whether the grouping should be based on soil forms or the underlying geological materials. Soil forms are defined in Soil Classification: A Taxonomic System For South Africa (Soil Classification Working Group, 1991; see also page xi). The decision was critical because one soil form can include soils from more than one parent material and many soil forms may occur on the same underlying material. The following paragraphs will clarify why preference was given to a sampling strategy based on the underlying geological material.

**Preliminary analyses for trace elements:** Preliminary field trips were undertaken in order to gather information needed to decide which sampling strategy was most suitable for the present study. This included the collection of 25 preliminary samples from different soil forms and underlying materials. The preliminary version of the Soil Association Map of the Western Cape (Ellis *et al.*, 1979) was used to locate specific soil

types. The samples were analysed for Ni, Cu, Zn, As, Se, Br, Rb, Sr, Zr, Nb, Mo, W, Pb, Th, and U.

**Distinct chemical differences between soils associated with different underlying materials:** The soil samples were grouped according to the underlying material: coastal sands, unconsolidated sands of granitic origin, granite, sediments of the Malmesbury Group and ferruginized materials. A Discriminant Function Analysis, a Principal Component Analysis and a Cluster Analysis (SAS Institute Inc., 1988) demonstrated that the underlying material is the dominating factor in determining the chemical composition of the soils. This was substantiated by an Analysis of Variance (SAS Institute Inc., 1988) which showed significant differences between some of the five soil groups for 12 of the 15 trace elements under investigation (95 % confidence level). These findings are in agreement with Moura and Kroonenberg (1988) who found that the parent material is the most important criteria in determining the geochemical differences between soils in the Araracuara area (Columbia).

**Chemical differences between soil forms:** Hartmann (1969) analysed 96 soil samples (Ap-horizons) from three different, but closely related, soil forms of the Stellenbosch area for extractable Na, K, Ca, Mg, N, P, Cu, Mn, B, Zn and Fe. Additionally, he determined the particle size distribution, pH, moisture equivalents, bulk densities, organic matter and the electrical resistance of the soil pastes. An Analysis of Variance was applied to examine the data set. Only two of the 11 elements (free iron and nitrogen), the particle size distribution and the bulk density were significantly different (95 % confidence level) between some of the three soil forms. It is, therefore, assumed that the chemical differences between the soil forms under investigation were not highly significant, indicating that the criteria which define a soil form (particle size distribution, colour, presence and succession of horizons, organic matter and others) can only partly account for the geochemistry of the soils.

It was concluded that a sampling strategy based on the underlying material would be more suitable for the present study than a sampling strategy based on soil forms.

Mr J.J.N. Lambrechts (Department of Soil Science, University of Stellenbosch; pers. comm., 1990) suggested grouping the soils of the study area according to the underlying material as listed below:

- (a) deep sandy soils, derived from recent coastal sands.
  - (b) duplex soils of the flat terrains, associated with unconsolidated sands of (partly) granitic origin.
  - (c) soils associated with ferruginized materials of Miocene to Pliocene age.
  - (d) soils of the undulating, hilly terrain associated with granitic rocks.
  - (e) soils of the rolling terrain associated with sediments of the Malmesbury Group.
- Soil samples were taken from type localities representative for the listed soil groups.

**Location and selection of sampling sites:** Down-slope successions of distinctive soil types formed on the different underlying materials (Schloms *et al.*, 1983). Such a

succession includes a soil type occupying the highest topographic position, one or more soil types covering the intermediate slope positions and a soil type occupying the lowest topographic position. Each soil type has properties attributable to its slope position. Soil sequences of that kind are referred to as toposequences (Figure 2.1). Extensive field trips were undertaken to locate toposequences which are representative of all soils underlain by the same geological material. Preference was given to toposequences which were sited in areas covered with indigenous vegetation and not subjected to fertilisation or other anthropogenic activities. This was done to obtain the best possible background values for the elements under investigation. The realisation that it was generally difficult, and for some underlying materials impossible, to find such sampling sites was an important result of the field sampling. Record was kept of where the above listed conditions were not met (Appendix-I). For most soil groups it was possible to collect at least a few samples which are probably almost unspoiled by contamination. This allowed the comparison of cultivated and uncultivated soils (section 6.5.2.). Figure 2.2 depicts the approximate positions of the sampling sites in the field area. The coordinates of each individual pit are given in Appendix-I.

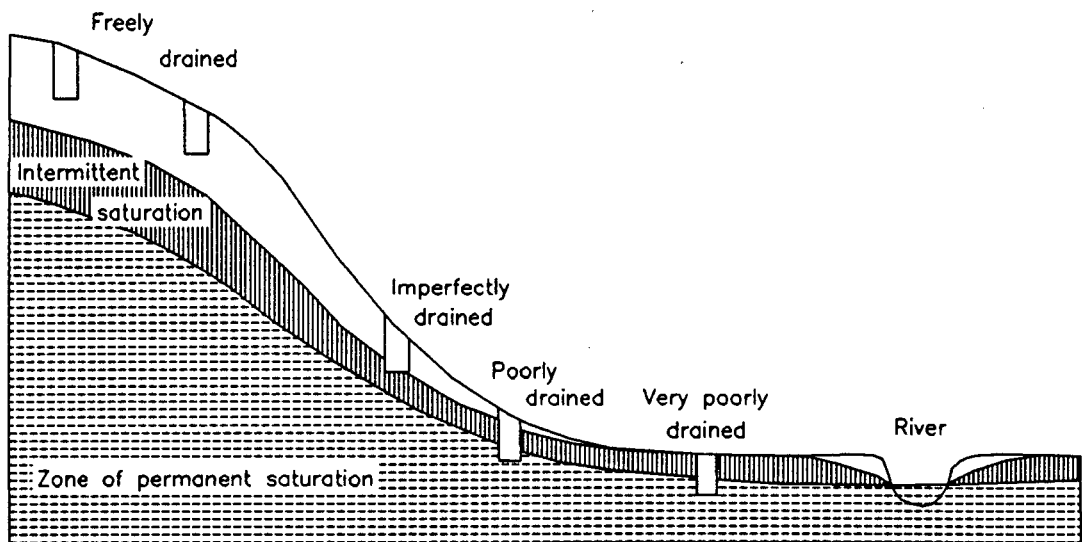


**Figure 2.1:** Simplified profile through a toposequence.

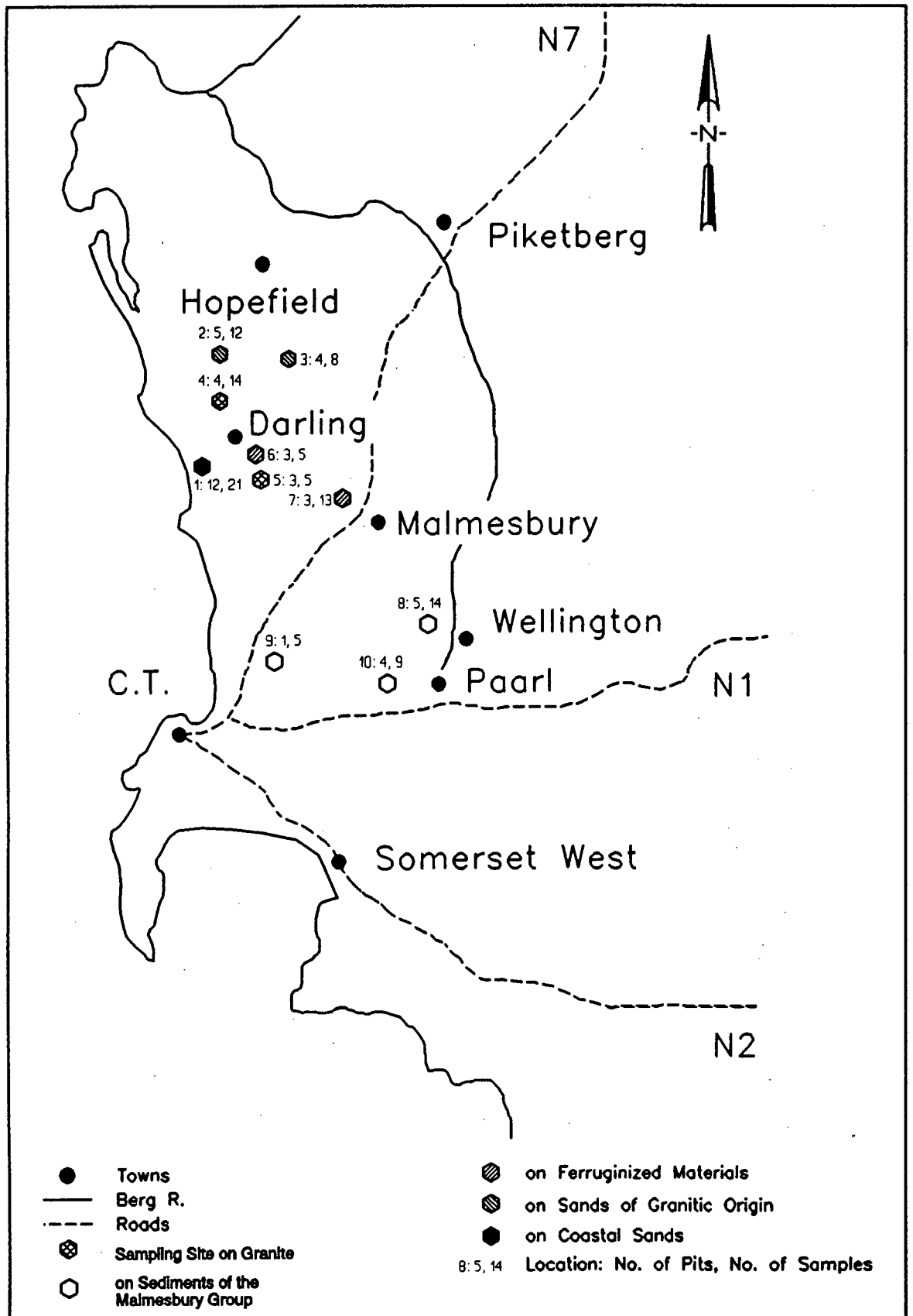


**Figure 2.2:** The approximate positions of the sampling sites. It is important to note that the positions of the sampling sites (pits) are more spread out than indicated by the symbols.

**Sample collection and labelling:** An auger was used to verify the expected vertical succession of soil horizons before the pits were dug. Spades, shovels and picks were used to excavate the soil. The depth of the pits varied between 50 and 300 cm. This variation was due to the depth of rock and the thicknesses of the different soil horizons. The photograph of Pit 36 exemplifies a typical pit and the nature of the field work (Figure 2.3). Several pits were dug along the selected toposequences and all recognisable horizons down to and including the B or G-horizon were sampled (e.g. samples 2, 3 and 4 in Figure 2.4). Due to the possibly uneven distribution of elements within a horizon, soil from the whole vertical range of a horizon was, where possible, included when collecting the samples. However, only the top of lowest horizon was sampled (sample 4 or 5 in Figure 2.4). If the A-horizon was thicker than 30 cm, an additional sample was taken from the top 15 cm of the A-horizon (sample 1 in Figure 2.4). Where possible, C-horizons (sample 5 in Figure 2.4), saprolites and underlying rocks were sampled. The samples were labelled as follows: the pit number, followed by one or two letters indicating the soil horizon and, if applicable, followed by a number indicating the subhorizon. "AE" refers to a composite sample of A- and the E- horizon. "Top" refers to a sample of the top 15 cm of a soil profile. The names and the origin of the samples are given in Appendix-I.



**Figure 2.3:** A photograph of Pit 36 exemplifies a typical pit and the nature of the field work.

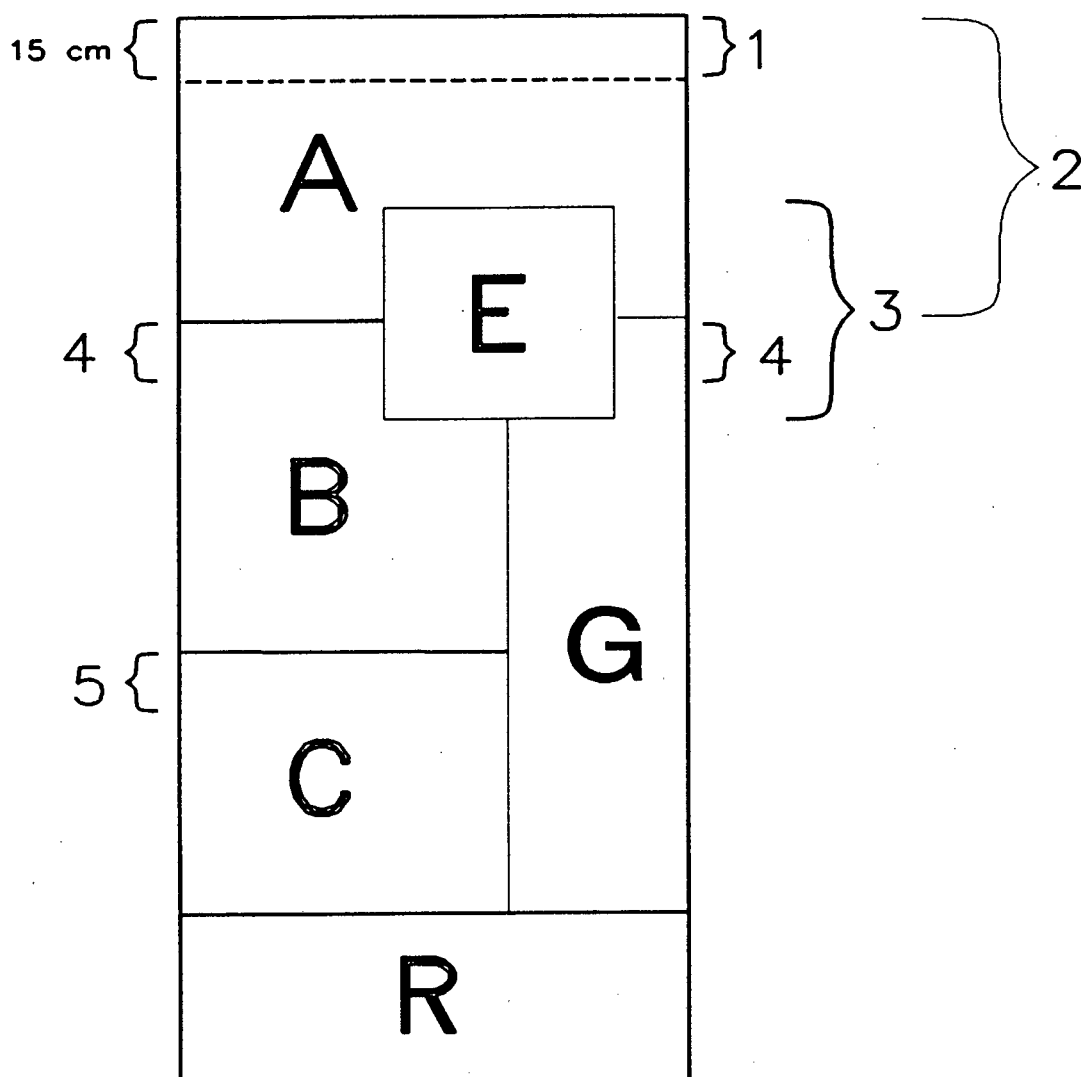


**Figure 2.4:** Schematic soil profile illustrating the major soil horizons (master horizons) that were sampled (after Soil Classification Working Group, 1991). The numbered brackets indicate the vertical range of a soil horizon which was sampled.

- A** = The horizon adjacent to the soil surface and consisting of mineral particles mixed with organic matter.
- E** = A leached horizon (if present) having a lower content of organic matter and(or) clay and(or) sesquioxides than the underlying horizon. This is usually reflected by a relative accumulation of quartz and(or) other resistant minerals as well as lighter colours.
- B** = This horizon is characterised by a concentration of clay, sesquioxides and(or) organic matter.
- G** = A grey, green or blue horizon that has been or is subject to intense reduction as a result of prolonged saturation with water (gleying).
- C** = A horizon consisting of unconsolidated material (including weathered rock) which does not show the properties of the other horizons.
- R** = Bedrock.

To avoid contamination, samples were, where possible, taken with plastic spades and stored in three-litre plastic containers. The possibility of contamination from digging implements when the soil was too hard to be sampled with plastic spades is discussed in section 6.5.2. Prior to the sampling two plastic containers were leached with hydrochloric acid to test for possible contaminants. The leachate was analysed for Mn, Co, Ni, Cu, Zn, Cd and Pb. None of the mentioned elements showed values higher than 10 ppb. Hence no significant contamination was to be expected from the sample containers.

In total 106 samples were collected from 44 pits. This included 6 soil samples that were taken from the field but not analysed. Each sample was split into two subsamples, one to be the sample for analysis and the other a sample for reference purposes. Each subsample consisted of approximately 2.5 kg soil.

### **2.3. SOIL DESCRIPTION AND CLASSIFICATION**

The sampled soil profiles were described and classified by Mr AB Oosthuizen (Institute for Soil, Climate and Water, Elsenburg) and the author using Soil Classification: A Taxonomic System For South Africa (Soil Classification Working Group, 1991). Soil profile description forms, compiled by the Institute for Soil, Climate and Water (Elsenburg), were used to collect the information needed for the classification of the soil profiles. The forms hold the following information: date, pit number, land-use, underlying material, slope position, horizons and their thicknesses, soil structure, consistence of soil, soil texture, soil colour, description of coarse fragments, effervescence with hydrochloric acid, transition between horizons, etc. The soil colours were described using a Munsell Soil Colour Chart (1992). This information and the resulting classification for each profile is given in Appendix-I. Reference to existing photographs of the pits, the type of vegetation surrounding the pits, and the distances to public roads and cultivated lands is also provided. Additionally, note was taken if agro-chemicals had been applied to the soil.

### **2.4. WHOLE-SOIL ANALYSIS**

The whole-soil analyses were performed using X-Ray Fluorescence Spectrometry (XRFS) and Inductively Coupled Plasma Mass Spectrometry (ICP-MS). The major and minor elements Na, Mg, Al, Si, P, K, Ca, Ti, Fe and the trace elements F, S, Cl, V, Cr, Mn, Co, Ni, Cu, Zn, Ga, Ge, As, Se, Br, Rb, Sr, Y, Zr, Nb, Mo, Sn, I, W, Pb, Bi, Th, and U were determined using XRFS. The aim of the ICP-MS analysis was to achieve lower detection limits for the elements Co, As, Se, Mo, Sn and I, and to determine the

concentrations of elements which could not be determined using XRFS (Li, Be, Cd, Sb). As a result of financial restrictions, only 44 soil samples were selected for the ICP-MS analysis. For the elements of which the concentrations were available from both instruments (Co, As, Se, Mo, Sn and I), a decision had to be made whether ICP-MS or XRFS results should be used to compile the final data set. The criteria for decision making and the results are given in Table 2.1.

**Table 2.1:** Analyses of trace elements. Tabulation of the criteria used when deciding if XRFS or ICP-MS results should be used for the data set. The deviations of the duplicates reflect not only the reproducibility of the instrumental measurements, but also the reproducibility of the dissolution procedure for the ICP-MS analysis. LLDs are given in ppm in air-dried soil.

Criterion	Co	As	Se	Mo	Sn	I
Agreement between XRFS and ICP-MS	generally reasonable but poor for concentrations lower than 4 ppm	poor	ICP-MS <LLD	good	good	poor
LLD ICP-MS (ppm in soil)	0.24	215	150	0.8	0.19	0.14
LLD XRFS (ppm in soil)	1.7	0.8	0.8	0.5	1.2	2.5
Comparison of duplicates (ICP-MS)	good	modest	< LLD	good	good	modest
Reference material, error (ICP-MS)	< 25 %	results not related to given concentrations	unknown	unknown	unknown	unknown
Check solutions, error (ICP-MS)	5-10 %	5-10 %	> 50 %	5-10 %	< 5 %	5-10 %
Wavelength scans (XRF)	-	confirmed XRFS	confirmed XRFS	-	confirmed XRFS	confirmed XRFS
Data used	ICP-MS	XRFS	XRFS	Both	XRFS	XRFS

### 2.4.1. X-Ray Fluorescence Spectrometry

The spectrometers of the Department of Geological Sciences (University of Cape Town), namely a Siemens-303AS and a Philips PW1400 XRF spectrometer, were used to determine the whole-soil geochemistry. The soil samples were analysed for nine major and minor elements and 28 trace elements. A Hewlett-Packard 9000 computer and the in-house programs NAVAL, MAJOR, AVERG, and the program TRACE (Duncan, 1975) were used to convert the intensity data into elemental concentrations.

The basic principle of this conversion is summarised by Equation 1 (Willis, 1991):

$$C_S = C_{STD} \times \frac{I_S}{I_{STD}} \times \frac{F(MCT)_S}{F(MCT)_{STD}} \quad (\text{Equ. 1})$$

Where:	C	=	element concentration
	I	=	net peak intensity
	MCT	=	matrix correction term: mass absorption coefficient for a specific wavelength for trace element analysis and influence coefficients for major element analysis
	F(MCT)	=	some function of a matrix correction term.
	STD	=	standard
	S	=	sample

#### 2.4.1.1. Sample preparation for the analysis of major and minor elements

A carbon-steel swingmill was used to grind the air-dried soil samples to a particle size of approximately -300 mesh (approx. -40  $\mu\text{m}$ ). Subsequently the samples were dried for four hours at 110°C. The loss of water ( $\text{H}_2\text{O}^-$ ) was determined as the mass difference between air-dried soil powder and oven dried (110°C) soil powder. To determine the combined water,  $\text{CO}_2$  and organic material present in the samples, the temperature was increased to 950°C for a further four hours. The loss of ignition (LOI) was determined from the corresponding loss in mass. The ashed samples were then quantitatively mixed with a Lithium Tetraborate flux with La as a heavy absorber (Johnson Matthey Spectroflux 105), fused according to the method of Norrish and Hutton (1969) and cast into 30 mm diameter glass discs, suitable for the sample holders of the two XRF spectrometers. The fusion discs were used to determine the concentrations of the major and minor elements  $\text{SiO}_2$ ,  $\text{Al}_2\text{O}_3$ ,  $\text{TiO}_2$ ,  $\text{Fe}_2\text{O}_3$ ,  $\text{MgO}$ ,  $\text{CaO}$ ,  $\text{K}_2\text{O}$ , and  $\text{P}_2\text{O}_5$ .  $\text{Na}_2\text{O}$  was determined separately on undiluted powder briquettes.

#### 2.4.1.2. *Sample preparation for the analysis of trace elements*

The trace elements F, S, Cl, V, Cr, Mn, Co, Ni, Cu, Zn, Ga, Ge, As, Se, Br, Rb, Sr, Y, Zr, Nb, Mo, Sn, I, W, Pb, Bi, Th, and U were determined on undiluted powder briquettes. Six grams of air-dried and  $-40\ \mu\text{m}$  ground soil powder were pressed into briquettes of 30 mm diameter with boric acid backing, using 5-8 tons of pressure on the ram. Samples with little clay and a high proportion of quartz were mixed with six drops of Mowiol solution (2 % Hoechst Mowiol N 70-88 in distilled water) because their natural cohesion was not sufficient to make stable briquettes.

#### 2.4.1.3. *Mass absorption coefficients*

The analyte spectral lines used for the elements F, S, Cl, V, Cr, Mn and Co have a longer wavelength than the absorption edge of iron, the major element with the shortest wavelength absorption edge. The absorption of these spectral lines is strongly related to both their position relative to major element absorption edges and the concentrations of the corresponding major elements. The specific wavelength of the analyte element and the concentrations of individual major elements are, therefore, critical for the determination of the mass absorption coefficients for these elements. Consequently, the mass absorption coefficients (MACs) for S, Cl, V, Cr, Mn and Co were calculated individually for each wavelength from major element concentrations, using the in-house program XRMAC.

The analyte lines of the remaining trace elements are on the short wavelength side of the shortest wavelength major element absorption edge ( $\text{Fe K}_{\text{abs}}$ ). For these elements the MAC was determined at the  $\text{Mo K}_{\alpha}$  wavelength using  $\text{Rh K}_{\alpha}$  Compton peak intensities. This single determination of the MAC at the  $\text{Mo K}_{\alpha}$  wavelength could be used for all the elements whose wavelengths are shorter than the  $\text{Fe K}_{\text{abs}}$  edge, because there are no major or minor element absorption edges between the  $\text{Rh K}_{\alpha}$  Compton peak and the  $\text{Fe K}_{\text{abs}}$  wavelengths (Willis, 1991). The program TRACE (Duncan, 1975) was used to perform the necessary calculations. For sodium and fluorine differences in MACs between samples and standards were small. It was assumed that errors caused by ignoring differences in mass absorption between samples and standards were insignificant compared with errors caused by particle size, mineralogical and surface effects (Prof. J.P. Willis, Department of Geological Sciences, University of Cape Town; pers. comm., 1993). Accordingly no corrections were made for differences in MACs.

#### 2.4.1.4. *Lower limit of detection and errors*

True and determined concentration of trace elements for some of the standards used to set up the calibration curves are given in Table 2.2. The results are generally of high quality. The concentrations determined for F and Sn, however, deviate to some degree from the true concentrations.

**Table 2.2:** Quality control for XRF analyses. Certified and determined concentrations of trace elements for some of the standards used to set up the calibration curves.

Element	Name of Standard	Concentration in ppm		Name of Standard	Concentration in ppm	
		Certified	Determined		Certified	Determined
F	W-1	220	274	BCR-1	490	536
S	only one standard used					
Cl	only one standard used					
V	G-2	36	28	BCR-1	365	368
Cr	G-2	8.0	8.2	GSP-1	12	11.4
Mn	G-2	263	256	GSP-1	310	313
Co	JG-1	4.0	3.8	W-1	50	49
Ni	JG-1	6.0	5.0	NIM-N	120	117
Cu	GSP-1	33	37	MRG-1	129	128
Zn	PG-11	32	32	GSP-1	105	103
Ga	NBS1365	.9	.9	SARM19	11	11
Ge	NBS1632A	2.1	1.6	SARM19	10.4	9.8
As	SARM20	3.8	3.7	NBS1632A	7.4	6.6
Se	SE8PPM	8.0	8.8	SE40PPM	40	40
Br	BR2/7/A	7.0	4.5	BR2/3/A	19	18
Rb	MRG-1	8.0	7.8	M-38	208	211
Sr	SARM18	35	32	SARM20	264	266
Y	SARM18	9.6	8.8	SARM19	16	16
Zr	W-1	95	94	G-2	320	319
Nb	W-1	6.8	7.2	M-38	18	20
Mo	W-1	.6	1.0	AGV-1	3.2	2.1
Sn	SN-11	900	838	SN-10	1350	1391
I	BR2/7/A	10	10.5	BR2/3/B	47	46
W	W30PPM	30	27	W62PPM	62	64
Pb	M-38	27	27	PG-11	57	57
Bi	BI11PPM	11	10	BI47PPM	47	48
Th	M-38	17	18	PG-11	63	62
U	JG-1	3.3	4.6	PG-11	13	13

The lower limit of detection (LLD) was calculated by the program TRACE (Duncan, 1975) for each trace element in each individual sample. The equation used to calculate the LLD is given below (Equation 2). The random counting error is caused by the counting chain and by the nature of X-ray emissions from a sample. By definition, the counting error is the standard deviation of the net peak intensity (Bertin, 1975). For trace elements, the counting error normally forms the major part of the total error. The program TRACE (Duncan, 1975), therefore, calculates counting errors for each trace element concentration in each sample. The determined elemental concentrations should be within  $\pm$  two standard deviations of the true concentrations if other errors are insignificant (95 % confidence level). Table 2.3 shows estimated averages for both the LLDs and counting errors for all elements determined with XRFS. The equations for the calculation of the LLD and the counting error are given below.

$$LLD = \frac{6}{\text{cps/ppm}} \sqrt{\frac{R_b}{T}} \quad (\text{Equ. 2})$$

Where:

- LLD = lower limit of detection  
 cps = net counts per second for analyte peak  
 ppm = concentration in parts per million (in % for major elements)  
 T = total counting time (peak + background)  
 $R_b$  = background count rate in cps

$$S.D. = \sqrt{\frac{R_p}{T_p} + \frac{R_b}{T_b}} \quad (\text{Equ. 3})$$

Where:

- S.D. = counting error, defined as the standard deviation of the net peak intensity and expressed in ppm  
 $T_p$  = counting time on peak  
 $T_b$  = counting time on background  
 $R_b$  = background count rate (including spectral overlap and tube peaks)  
 $R_p$  = gross peak count rate

For the major elements the counting error causes only a minor fraction of the total error. The average error was calculated for each major element as the average relative

difference between true and determined concentrations of standards. The results are expressed in percent and given in the left column of Table 2.3.

**Table 2.3:** Lower limits of detection (LLD) and estimate of errors for XRFS analyses. AE = average error for major elements (oxides) in percent of the true standard concentration; S.D. = estimated average counting error for trace elements in ppm. The unit for the LLD is percent for major elements and ppm for trace elements.

Oxide	AE	LLD	Element	S.D.	LLD	Element	S.D.	LLD	Element	S.D.	LLD	Element	S.D.	LLD
Na <sub>2</sub> O	.07	.02	F	50	140	Ni	.8	2.3	Br	.3	.9	Sn	.4	1.2
MgO	.09	.02	S	3	6*	Cu	.6	1.8	Rb	.3	.7	I**	.8	2.5
Al <sub>2</sub> O <sub>3</sub>	.09	.01	Cl	2	4	Zn	.5	1.2	Sr	.2	.6	W	1.0	2.6
SiO <sub>2</sub>	.4	.02	V	.4	1.2	Ga	.3	.8	Y	.3	.7	Pb	.7	2.1
P <sub>2</sub> O <sub>5</sub>	.03	.005	Cr	.6	1.3	Ge	.3	.9	Zr	.3	.6	Bi	.9	2.8
K <sub>2</sub> O	.03	.004	Mn	.7	1.5	As	.3	.8	Nb	.2	.6	Th	.6	1.7
CaO	.1	.005	Co	.6	1.7	Se	.3	.8	Mo	.2	.5	U	.5	1.3
TiO <sub>2</sub>	.02	.007												
Fe <sub>2</sub> O <sub>3</sub>	.09	.009												

\* The LLD for sulfur is likely to be higher due to mineralogical effects.

\*\* Natural sediment standards were used for the determination of iodine because the iodine salts in artificial standards are unstable under X-ray radiation and vacuum conditions.

#### 2.4.1.5. Analytical difficulties experienced

**High total in a sample with abundant halite:** The major element analysis of the sample 39Sap repeatedly gave a total of 108 percent. The XRF analysis of the powder briquette of the same sample indicated high concentrations of chlorine (5.7 %) and sodium (9.3 %). The XRD analysis of sample 39Sap showed that the sample contains halite (section 3.2.). Assuming that most of the Na and the Cl is present in the form of halite, it was concluded that the halite content of the sample is approximately 15 percent.

When examining possible reasons for the high total it appeared likely that most of the chlorine and the sodium present in the sample was lost when preparing the glass discs for the analysis of major elements. The loss took place when the sample was ignited at 950°C. The melting point of halite is 801°C, and the boiling point 1413°C (Weast, 1975-1976). Vaporisation of NaCl at 950°C should thus be limited. However, it was experimentally shown that approximately two thirds of 1 g (pure) NaCl can be lost

from a platinum crucible when heating to 950°C for eight hours. This loss is probably due to vaporisation of NaCl. The loss of NaCl from the sample took place before the weighing of an aliquot of the roasted sample for the preparation of the fusion discs and thus increased the magnitude of the LOI. The concentration of sodium was determined separately on a briquette of unheated powder. Adding the true concentration of Na<sub>2</sub>O, as determined from the powder briquette, the too high LOI and the concentrations of the other oxides resulted in the high total.

**Fluorine in fertilisers:** The fluorine concentration of one of the sampled fertilisers was analysed several times over a period of one month. The concentrations showed a variation that was higher than the calculated counting error (section 2.4.1.4.). A general trend towards lower concentrations with progressing time indicated a possible loss of fluorine from the sample. However, the fact that the reference counts obtained from a CaF<sub>2</sub> briquette also decreased over the same period of time indicated a possible equipment error or a loss of F from both the CaF<sub>2</sub> briquette and the fertiliser. The data reduction was performed using standard intensities that were measured immediately before and after the samples were run in order to minimise the errors corresponding to a possible equipment error. Nevertheless the quality of the fluorine data for the fertilisers remains uncertain.

#### 2.4.2. Inductively Coupled Plasma Mass Spectrometry

The whole-soil analysis for the elements Li, Be, Co, As, Se, Mo, Cd, Sn, Sb and I was performed using Inductively Coupled Plasma Mass Spectrometry (ICP-MS). Cobalt, As, Se, Mo, Sn and I were also determined using XRFS. Table 2.1 shows which results were chosen to compile the final data set.

**Instrument:** The analysis was performed utilizing a VG ISOTOPES Plasma Quad PQ2+ Inductively Coupled Plasma Mass Spectrometer at MINTEK, Johannesburg. A detailed description of the chosen instrumental settings and the analytical procedure is given in section 2.5.2.1.

**Sample preparation:** An aliquot (approximately 0.5 g) of the powder used to make the briquettes for the XRFS analyses (section 2.4.1.2.) was weighed into a teflon beaker, and 10 ml HNO<sub>3</sub> and 5 ml HClO<sub>4</sub> were added. The covered beaker was placed on a hot plate and the sample was allowed to reflux for two hours. The lid was removed and the sample was evaporated to incipient dryness. Five ml HF and 5 ml HClO<sub>4</sub> were added and the sample was evaporated to dryness. Ten ml distilled water and 10 ml nitric acid were added to dissolve the residue and the sample was made up to volume with distilled water in a 100 ml volumetric flask. The sample was diluted a further 2.5 times because samples can only be analysed with MINTEK's ICP-MS if the dissolved solids do not exceed 0.2 percent. The oxidising, acidic conditions during the sample preparation could result in vaporisation of I because I<sup>-</sup> may be oxidised to I<sub>2</sub>.

The quality of the results for I (ICP-MS) is thus doubtful and preference was given to the results from the XRFS analyses (Table 2.1).

**Calculation of LLD:** The LLD was calculated in accordance with Equation 4. The results of the calculations are tabulated in Table 2.4. More information on these calculations and procedures to achieve relatively low LLDs are given in section 2.5.2.1.

$$LLD = 3 \times S.D. \times 500 \quad (\text{Equ. 4})$$

Where:

LLD = Lower Limit of Detection at the 99 % confidence level.

S.D. = Relative standard deviation of blanks (outliers were excluded;  $n \approx 12$ ).

500 = Approximate dilution factor.

**Table 2.4:** Lower limits of detection (LLD) and the estimate of errors for the analyses of trace elements using ICP-MS. The LLD is given in ppb in air-dried soil. Relative deviation of the duplicates (Dupl.): + = small;  $\approx$  = small for higher concentrations, but large close to the LLD. Check solution error: estimated average difference between determined and true check solution concentration. Reference material error: relative difference between recommended and determined concentration in reference material (marine sediment, MESS 1, NRC-Canada).

	LLD	Dupl.	Check solution error	Reference material error
Li	220	+	10-15 %	no rec. value
Be	270	+	5-10 %	<5 %
Co	240	+	5-10 %	<25 %
Mo	800	+	5-10 %	no rec. value
Cd	690	<LLD	<5 %	<10 %
Sn	190	+	<5 %	no rec. value
Sb	310	$\approx$	<5 %	20-40 %
I	140	$\approx$	5-10 %	no rec. value

**Quality of analyses:** The comparison of the duplicates, the analysis of solutions with known concentrations (check solutions) and the concentrations determined for the reference material (marine sediment: MESS 1, NRC-Canada) showed that the results were reliable for most elements (Table 2.4). The LLDs for As and Se were too high for the purpose of the present study (Table 2.1). The As concentration determined for the reference material showed that results for As were generally not reliable. The large differences between the true and the determined Se concentrations of the check solutions suggest that the Se results were also not reliable.

**Analyses of Se and As using the hydride generation method:** The analytical problems encountered with Se and As are presumably due to peak overlapping with ArCl. The analysis of Se is particularly difficult because the individual isotopes only account for relatively small fractions of the element (Mr R. Robert, MINTEK, Johannesburg; pers. comm., 1993). Some selected samples were analysed for Se and As using the hydride generation method. This resulted in lower background counts and, therefore, data of better quality and lower limits of detection. The achieved LLDs in air-dried soil were 0.3 ppm for Se and 1.5 ppm for As. More information on the hydride generation method is given in section 2.5.2.1.

## **2.5. ANALYSIS OF EXTRACTABLE ELEMENT PORTIONS**

The determination and interpretation of the concentrations of the extractable element fractions form an important part of this study. Experiments to assess the suitability for this study of leaching techniques used by other authors are discussed in the following sections. Problems which were encountered when analysing the soil leachates using an Inductively Coupled Plasma Mass Spectrometer and an Inductively Coupled Plasma Atomic Emission Spectrometer are also discussed.

### **2.5.1. Selection of an appropriate leaching method**

Extractable element concentrations in soils are normally determined to establish the availability of elements to ground water, plants, animals and humans. For the present study, it was of particular interest to determine the extractable concentrations in a way which enables comparison of the results with the whole-soil analysis data and the data given in the literature. Since an international standard leaching procedure for soils for environmental purposes is not established yet (Hortensius and Nortcliff, 1991), one of the numerous leaching methods described in the literature had to be selected for the present study.

2.5.1.1. *Finding a suitable way of preparation of samples for the extraction*

**Errors introduced by air-drying of soil samples:** Methods for extraction of elements given in the literature without exception include drying of the soil because the results are to be based on soil dry weight. It is important to note that drying of soil causes immediate changes by altering chemical properties of the soil (Bartlett and James, 1980). Changes include increased surface acidity and increased solubilities of organic matter and Mn. The proportion of exchangeable K may be increased or decreased. Bartlett and Jones (1980) also showed that drying of the soil greatly lowers the ability of a soil sample to oxidise Cr. They suggested that the Cr oxidation test is a useful tool to exemplify the redox changes that occur in soils as a result of drying and storing. A remoistened sample may require a fairly long period of time (more than 16 days) before it regains properties similar to those of continuously moist soil. It can be summarised that drying of the soil may irreversibly change extractable proportions and speciations of elements. The speciation of elements was not determined in this thesis. The possible effect of drying on the size of the extractable portions of certain elements can not be quantified and has to be accepted.

**Description of potential methods:** The standard approach of soil scientists to prepare a sample for extraction is to sieve the air-dried soil sample through a 2 mm nylon mesh sieve after gentle crushing. The fraction coarser than 2 mm is discarded and the fraction smaller than 2 mm is used for the leaching procedure. This method will be referred to as Method-I. No corrections are made for the discarded coarse fraction, because the total surface area of the coarse fraction is very small compared to the total surface area of the fine fraction. The Non-Affiliated Soil Analysis Working Committee (1990) recommends crushing the material coarser than 2 mm until all the soil passes the 2 mm sieve. This is referred to as Method-II. The elimination of particles coarser than 2 mm, as in Methods I and II, makes it feasible to obtain representative subsamples in quantities small enough for the leaching procedure. Leaching the entire soil is referred to as Method-III. Using the subsamples that were powdered when preparing the samples for the whole-soil analyses is referred to as Method-IV. The powder is representative of the whole sample and was ground to a particle size finer than 50 microns.

**Experiment:** Experiments were carried out to compare Method-I with Method-IV. Two soil samples from the same pit, one sample with a major gravel fraction and one with a minor gravel fraction, were selected from most soil groups. Only one sample was selected from the coastal sand-derived soils because all soils derived from this material have only a minor gravel fraction. Two subsamples were taken from each selected sample, one from the ground powder (Method-IV) which represents the whole soil and one from the -2 mm sieved soil (Method-I). Each subsample was leached with 1 M  $\text{NH}_4\text{NO}_3$  and the leachate was analysed for Ca, Mg, Na, Zn, Mn, Fe, B and K. A complete description of the leaching procedure is given

in Appendix-II. For each sample, a ratio of [elemental concentration in leachate obtained from powdered sample] over [elemental concentration in leachate obtained from sieved sample] was calculated (Table 2.5).

**Conclusions:** Observations and conclusions from the results presented in Table 2.5:

(a) samples with a major gravel component generally have lower ratios than samples with a minor gravel component. This is particularly apparent for Ca, Mg, Na, K and B. Sample treatment according to Method-I includes the removal of the gravel fraction (> 2 mm) and results in an increased percentage of the finer fraction. It is, therefore, assumed that the leachable fractions of Ca, Mg, Na, K and B are mainly associated with particles smaller than 2 mm.

(b) manganese, and in one case iron, show the opposite trend, indicating that leachable Mn(Fe) is enriched in the coarse soil fraction. The coarse fraction of the selected samples consists mainly of sesquioxide concretions. It appears that sesquioxide concretions account for a higher concentration of extractable Mn and Fe.

(c) overall it can be concluded that the results from the differently pretreated samples show profound differences. It is thus inappropriate to compare data sets obtained using differently pretreated samples. Consequently, the choice of the most appropriate method is very important. Table 2.6 shows a comparison of the different methods for soil pretreatment. From the table it becomes clear that Method-I is the most suitable compromise for the present study. It is important to note that all methods have disadvantages. The disadvantage of the chosen method is that the exclusion of the coarse fraction makes it difficult to compare the results with the whole-soil analyses.

**Table 2.5:** Experiments to find a suitable method for sample preparation prior to leaching. Powdered (Method-IV) and < 2 mm sieved (Method-I) soil samples were leached with 1 M  $\text{NH}_4\text{NO}_3$ . The ratios of [concentration in extract of powdered soil] over [concentration in extract of sieved soil] are tabulated.

	Ca	Mg	Na	Zn	Mn	Fe	B	K
DERIVED FROM COASTAL SANDS								
Sample 17A, gravel: 0 %	1.1	1.2	1.3	1.6	6.5	17	1.5	2.1
ASSOCIATED WITH UNCONSOLIDATED SANDS OF GRANITIC ORIGIN								
Sample 25A, gravel: 6 %	1.2	2.3	1.6	0.8	1.6	8.8	0.9	6.5
Sample 25G, gravel: 24 %	0.3	0.1	0.3	0.7	10	0.8	0.3	1.3
DERIVED FROM GRANITE								
Sample 31AE, gravel: 5 %	3.3	8.8	5.8	1.4	0.7	2.2	3.7	7.0
Sample 31B, gravel: 52 %	0.8	0.8	1.0	0.4	2.5	0.8	0.5	3.4
ASSOCIATED WITH THE SEDIMENTS OF THE MALMESBURY GROUP								
Sample 43Top, gravel: 46 %	0.9	1.3	1.0	0.8	1.1	1.3	1.1	5.1
Sample 43E, gravel: 81 %	0.6	0.7	0.7	0.5	1.3	1.5	0.9	3.5
ASSOCIATED WITH THE FERRUGINIZED MATERIALS								
Sample 46A, gravel: 8 %	1.0	1.7	1.3	0.6	2.0	4.2	1.0	1.6
Sample 46B2, gravel: 57 %	0.5	0.6	1.1	0.7	0.9	3.7	1.0	1.5

**Table 2.6:** Comparison of possible soil treatments prior to leaching. The row "worst case strategy" indicates whether the corresponding method is suitable to quantify the maximum leachability. The row "simulation of present *in situ* conditions" indicates whether the corresponding method is suitable to quantify the present availability of the elements.

	<b>METHOD-I</b> Sieved soil, coarse fraction discarded	<b>METHOD-II</b> Sieved soil, coarse fraction crushed to pass 2 mm sieve	<b>METHOD-III</b> Untreated soil	<b>METHOD-IV</b> Powdered soil
Comparison with literature	good	reasonable	impossible	impossible
Comparison with whole-soil analysis	limited	good	good	good
Time needed for pretreatments	little	long	none	none for the present study
Possibility of contamination	small	large	no	yes
Representative subsampling	possible	difficult to possible	difficult to impossible	easy
Worst case strategy	no, exclusion of coarse fraction	yes, possible disaggregation or solution of concretions	no	yes, disaggregation of concretions
Simulation of present <i>in situ</i> conditions	limited, elements associated with fine fraction over-represented (see Table 2.5)	reasonable to limited, due to increase of surface of coarse fraction	reasonable	limited, elements associated with coarse fraction considerably over-represented due to increased surface area

### 2.5.1.2. Selection of a suitable extraction method

Several leaching techniques were evaluated and tested on soil samples to establish their suitability for the present study. The methods which seemed most relevant are listed below:

- (a) Toxicity characteristic leaching procedure (EPA US, 1990).  $\text{CH}_3\text{CH}_2\text{OOH}$  and  $\text{NaOH}$  (pH = 4.9) or  $\text{CH}_3\text{CH}_2\text{OOH}$  only (pH = 2.9), 1 part solids to 20 parts extractant, 18 hours.
- (b) A standard leaching test for combustion residues (maximum leachability; Van der Sloot *et al.*, 1984). First step:  $\text{HNO}_3$  (pH = 4), 1 part solids to 20 parts

extractant, 24 hours. Second step:  $\text{HNO}_3$  (pH = 4), 1 part of the previously leached solids to 80 parts extractant, 24 hours.

- (c)  $\text{HNO}_3$  leaching test (suggested by the author; unpublished).  $\text{HNO}_3$  (pH = 4), 1 part soil to 10 parts extractant, 4 hours.
- (d) Citric acid leaching test for agricultural purposes (Mr G.R. Thompson, Department of Agriculture and Water Supply, Elsenburg; pers. comm., 1993). Citric acid (pH = 2.7), 1 part soil to 10 parts extractant, 4 hours.
- (e) Extraction of heavy metals from soils to establish their availability to plants, and the risk of ground water pollution as first used by Symeonides and McRae (1977) and modified by Zeien and Brümmer (1992) and Prüß *et al.* (1991). 1 M  $\text{NH}_4\text{NO}_3$  (pH = 4.7), 4 parts soil to 10 parts extractant, 2 hours. A full description of this method is given in Appendix-II.
- (f)  $\text{H}_2\text{O}$  extraction to establish the contamination potential of contaminated materials with respect to ground water (Dr. A. Ruck, Umweltbundesamt Berlin, Germany; pers. comm., 1993).  $\text{H}_2\text{O}$ , 1 part solids to 100 parts extractant, 4 hours.

A comparison of most of the leaching methods listed above led to the following conclusions:

- (a) In agreement with Hortensius and Nortcliff (1991) it was found that concentrations determined using different leaching methods were very different. Comparison of data obtained using different leaching techniques is thus not possible.
- (b) The concentrations of the elements in the leachates were generally in the order: citric acid (Method d) >  $\text{NH}_4\text{NO}_3$  (Method e) >  $\text{HNO}_3$  (Method c) >  $\text{HNO}_3$  (Method b) >  $\text{H}_2\text{O}$  (Method f).
- (c) For  $\text{HNO}_3$  (Method b) and  $\text{H}_2\text{O}$  (Method f) more than half of the elements had concentrations close to or below the LLD of ICP-AES (Department of Agriculture and Water Supply, Elsenburg). The LLDs were 10 ppm for Mg, 25 ppm for Ca, 0.08 ppm for Zn, 0.5 ppm for Mn, 0.05 ppm for Cu, 0.5 ppm for Fe, 2 ppm for Al, 0.5 ppm for K, 0.5 ppm for Na, 0.5 ppm for P and 0.025 for B (Mr G.R. Thompson, Department of Agriculture and Water Supply, Elsenburg; pers. comm., 1993).
- (d) The contamination from filter papers and from chemicals used for the extraction can be significant and has to be monitored by means of analysing blanks.
- (e) The method given in Prüß *et al.* (1991; Method e) was found to be the most suitable for the present study for the following reasons:
  1. The method was an established one and soon to be a legislative leaching method in Germany. It was proposed as an internationally recognised soil leaching method for environmental purposes.

2. The concentrations of most elements were generally higher than the LLD\*.
3. Most other leaching techniques were devised primarily for municipal land-fill wastes, combustion residues and agricultural purposes.
4. Opposingly to some of the other methods the pH of the leachate usually stabilised within the acid range which ensured that leached elements stayed in solution.
5. The procedure was relatively simple and rapid.
6. Prüß *et al.* (1991) determined and published acceptable maximum concentrations in the  $\text{NH}_4\text{NO}_3$  leachates for the assessment of polluted soils (Table 9.2). Using this method it was thus possible to quantify the risk associated with contaminated soils. The highest acceptable concentrations were based on correlations between elemental concentrations in soil-leachates and elemental concentrations in plants that were grown on the corresponding soils. The publication demonstrated that the correlation between total plant and soil leachate concentration may be poor if the concentration of the extractable fraction is lower than 20 ppb in air-dried soil. The method is, therefore, less suitable for the assessment of minimal concentrations needed for the growth of plants. However, for concentrations higher than approximately 20 ppb, a good correlation between total plant concentrations and soil leachate concentrations was found. Hence, this leaching method was found to be suitable for assessment of contaminated soils.

Prüß *et al.* (1991) also indicated which soil function is most jeopardised if a particular element exceeds the recommended maximum concentration (Table 9.2). The following soil functions were considered:

- a) Substrate for the growth of plants used in human and
  - b) animal consumption.
  - c) Substrate for the growth plants not to be used for consumption.
  - d) Habitat for the soil-fauna.
  - e) Pollution buffer for ground water.
7. Aiming to justify the extraction with 1 M  $\text{NH}_4\text{NO}_3$  as described above, Prüß (1992) summarised the results of the experiments which were conducted to determine the optimal method for extraction. This included arguments for the chosen extractant, molarity, extractant/solid ratio and extraction time. It is beyond the scope of this study to discuss these arguments.

---

\* During the later use of this method it was found that the 1 M  $\text{NH}_4\text{NO}_3$  matrix causes relatively high LLDs if the leachates are analysed using ICP-MS. The concentrations of many elements were, therefore, below the LLD.

8. The results obtained with the method were shown to be reproducible. Laboratory-internal, repetitive extractions of one soil sample showed variability coefficients between 1 % for Zn and 50 % for V (Prüeb, 1992). A test that was performed using 10 different laboratories and three soil samples showed variability coefficients between 6 % for Zn and 46 % for Tl (Prüeb, 1992).

#### **2.5.2. Analysis of leachates**

Eighty eight soil leachates were analysed using Inductively Coupled Plasma Atomic Emission Spectrometry (ICP-AES) and Inductively Coupled Plasma Mass Spectrometry (ICP-MS). The elements Na, Mg, Al, P, S, K, Ca, Fe, Co, Ni, Cr, Cu, Zn and V were analysed using ICP-AES, and the elements Be, B, Al, V, Cr, Co, Ni, Cu, Zn, As, Se, Mo, Cd, Sb, Ba, Tl, Pb, Bi and U were analysed using ICP-MS; i.e. results for V, Co, Cu, Zn, Al, Cr and Ni were available from both techniques. The comparative data showed a high degree of dissimilarity between the MS and AES results for these elements. As a result of generally higher concentrations of the elements under investigation and using the same extraction technique, Faure (1993) observed reasonable agreement for the elements V, Co, Cu and Zn, but poor agreement for the elements Al, Cr and Ni. The recommendations of MINTEK's analytical staff, the LLDs and the results of the duplicates were considered when deciding which results should be used to compile the final data set. For some of the elements the number of samples with concentrations above the LLD was used as a supplementary criterion (Table 2.7). With the exception of Se and As, all analyses were performed within 20 days of the leaching of the samples.

**Table 2.7:** Determination of 1 M  $\text{NH}_4\text{NO}_3$  extractable element concentrations. Tabulation of the criteria used when deciding if ICP-AES or ICP-MS results should be used for the data set. The table is based on both the results of the present study and the results of Faure (1993). It is important to note that the results for the duplicates reflect not only the reproducibility of the instrumental measurements, but also the reproducibility of the leaching procedure. LLDs are given in ppb in air-dried soil.

	Agreement AES/MS	LLD ICP-MS in ppb	LLD ICP-AES in ppb	Duplicates ICP-MS	Duplicates ICP-AES	MINTEK's advice*	Number of values above LLD	Data used
V	modest for higher concentrations, but very poor for concentrations lower than 500 ppb	9	25	good for higher concentrations, but poor for concentrations lower than 30 ppb	good	-	not a criterion for V**	ICP-MS
Co	modest for concentrations higher than 500 ppb	13	125	modest to good	good	-	MS: 40 AES: 3	ICP-MS
Cu	generally good in Faure (1993) (concentrations ranging from 100 to 4000 ppb), but very poor for the samples of the present study where all concentrations were lower than 500 ppb	103	50	modest for higher concentrations, but poor for concentrations lower than 200 ppb	good	-	MS: 17 AES: 7	ICP-AES
Zn	modest for concentrations higher than 4000 ppb, but very poor for lower concentrations	665	125	poor	good	use ICP-AES	not a criterion for Zn**	ICP-AES
Al	very poor	110	500	poor	good	use ICP-AES	not a criterion for Al	ICP-AES
Cr	very poor	65	50	poor	very good	-	MS: 4 AES: 25	ICP-AES
Ni	very poor	70	250	poor	very good	use ICP-AES	not a criterion for Ni	ICP-AES

### 2.5.2.1. Inductively Coupled Plasma Mass Spectrometry

**Instrumentation:** The analysis was performed utilizing a VG ISOTOPES Plasma Quad PQ2+ Inductively Coupled Plasma Mass Spectrometer, at MINTEK, Johannesburg. A general introduction to ICP-MS technology is given in Houk (1986) and Date and Gray (1989).

A polypropylene V-groove de Galan type nebuliser, manufactured at MINTEK, was used. The sample solution was pumped into the nebuliser using a Gilson Miniplus

\* Mr R. Robert, MINTEK, Johannesburg; pers. comm., 1993.

\*\* Numerous samples have concentrations above the LLD.

3 peristaltic pump. Data were acquired in pulse counting mode using the peak scanning option. Table 2.8 lists the instrumental settings that were chosen to analyse the soil leachates.

**Dilution of samples and use of internal standards:** The interface cones and the ICP torch injector tube have small orifices through which the sample solution must pass. These orifices become easily blocked. The amount of dissolved solids in the sample, therefore, needs to be kept lower than 0.2 percent. Accordingly, the ammonium nitrate leachates had to be diluted by a factor of 50. Two millilitres of the obtained leachates were made up to a volume of 100 ml. This included the addition of 10 ml nitric acid (10 %) containing 1 ppm In, 1 ppm Sc and 1 ppm Re as internal standards to correct for possible drift and matrix effects. Since a correction for possible matrix effects was ensured for samples and standards it was acceptable to use standard solutions that were not made up with 1 M  $\text{NH}_4\text{NO}_3$ , i.e. not matrix matched.

**Calculation of the LLDs:** The LLD is mainly dependant on the variability of the blank readings because the calculated elemental concentrations are blank-subtracted. The standard deviation of the blank readings is therefore the most important parameter for the calculation of the LLDs (Equation 5). The calculated LLDs indicate whether a specific sample count rate is significantly higher than the corresponding average blank count rate.

A high proportion of the concentrations were below or near to the achieved LLDs. In order to retain more data values above the LLD it was decided to calculate the LLD at the 95 % confidence level rather than the 99 % confidence level. The usage of LLDs calculated at the 95 % confidence levels is in agreement with the recommendations of the International Union of Pure and Applied Chemists.

**Table 2.8:** ICP-MS instrumental settings.

Forward Power	1.35 kW
Reflected Power	< 10 W
Auxiliary Gas Flow (Ar)	0.30 l/min.
Carrier Gas Flow (Ar)	0.80 l/min.
Nebuliser Pressure	2 bar
Solution Uptake Rate	0.8 ml/min.
Sampler Cone Aperture	1 mm
Skimmer Cone Aperture	0.7 mm
Peristaltic pump	setting 40.0
ICP Plasma	Argon
Coolant Flow (Ar)	16 l/min.

$$LLD = 2 \times S.D. \times 2.5 \quad (\text{Equ. 5})$$

Where:

- LLD = Lower Limit of Detection (95 % confidence level).  
 S.D. = Relative standard deviation of blanks (n ≈ 32; outliers were excluded).  
 2.5 = Dilution factor (soil in extractant).

**Lowering the LLDs:** The 1 M  $\text{NH}_4\text{NO}_3$  solution used for the leaching of the samples resulted in relatively high and variable blank readings, leading to relatively high LLDs. Another reason for relatively high LLDs is the large number and variety of samples that are normally analysed with MINTEK's ICP-MS. This results in significant contamination of the instrument and causes high background counts and LLDs for many of the elements below mass 80. In an attempt to lower the LLDs, the instrument was specially stripped and thoroughly cleaned.

**Comparison of achieved LLDs with recommended maximum LLDs for assessment of polluted soils:** Table 2.9 compares the achieved LLDs with the highest acceptable LLDs for the assessment of polluted soils, as recommended by the NAW (1993). The purpose of the recommended maximum LLDs is to ensure that elemental concentrations usually encountered in leachates from uncontaminated soil samples can be determined with confidence. It is interesting to note that a high proportion of the elements analysed for have concentrations mainly below the LLD, although the achieved LLDs are generally acceptable (Table 2.9). The LLDs for Be, Se, Cd and U are too high.

**Quality control:** For each element, check solutions of known concentration were analysed. The average difference between the true concentrations and the determined concentrations was generally lower than 20 percent (Table 2.9). An evaluation of the results for the duplicates showed that the quality of the analyses was generally satisfactory (Table 2.9).

The precision of the ICP-MS equipment is checked on a weekly basis. The average degree of instrumental variation over 10 measurements of the same sample was determined to be less than 2 percent. Calibration is performed on a daily basis (Mr R. Robert, MINTEK, Johannesburg; pers. comm., 1993).

**Analyses of As and Se:** The LLDs for As and Se were too high for the purpose of the present study. Selected samples (1E, 4A, 32G, 46B2) were, therefore, analysed for Se and As by ICP-MS using the hydride generation method as described by Price (1979). In this method, the Se and As present in the sample solution are converted to gaseous hydrides. Only the gaseous phase is used for the analysis, whereas the ammonium nitrate solution is not. This method resulted in lower background counts and, therefore, lower detection limits. The achieved LLDs were 12 ppb for Se and 7 ppb for As ( $\text{NH}_4\text{NO}_3$  extractable in air-dried soil).

**Table 2.9:** Determination of 1 M  $\text{NH}_4\text{NO}_3$  extractable element concentrations using ICP-MS. The achieved LLDs are compared with the highest acceptable LLDs for the assessment of polluted soils, as recommended by the NAW (1993). The relative deviation of the duplicates and the estimated average differences between the true and the determined check solution concentrations are listed in order to demonstrate the quality of the analyses [Abbreviations for the deviation of duplicates: + = small;  $\approx$  = small for higher concentrations, but high close to the LLD;  $\downarrow$  = large]. Both, the deviations of the duplicates of the present study and the results of Faure (1993) were considered when compiling this table. LLDs in brackets were obtained using the hydride generation method.

	LLD in ppb (air-dried soil)		Duplicates	Deviation of check solutions
	Achieved	Highest Acceptable (NAW, 1993)		
Be	67	2.5	+	< 10 %
B	362	-	$\downarrow$	10-20 %
V	9	25	$\approx$	< 15 %
Co	13	50	+	< 15 %
Cu	103	250	$\approx$	< 15 %
As	71(7)	50	$\approx$	10-20 %
Se	877(12)	-	<LLD	10-30 %
Mo	49	25	$\approx$	20-30 %
Cd	17	5	$\approx$	< 15 %
Sb	23	25	$\approx$	10-20 %
Ba	61	-	+	10-20 %
Tl	2.7	12.5	+	10-20 %
Pb	54	50	+	10-20 %
Bi	3.2	-	+	15-35 %
U	30	2.5	+	10-20 %

### 2.5.2.2. Inductively Coupled Plasma Atomic Emission Spectrometry

The analysis of the leachates was performed utilizing a Spectroflame Inductively Coupled Plasma Atomic Emission Spectrometer, at MINTEK, Johannesburg. The routine operating conditions used for the analysis are listed in Table 2.10.

Prior to the analysis, 15 ml of the soil leachates were transferred to 20 ml volumetric flasks. Three ml HCl and 1 ml of a 0.2 g l<sup>-1</sup> Sc standard solution were added. The solutions were subsequently made up to volume with distilled water (dilution factor 1.33). Assuming that no Sc was present in the leachates, this resulted in a concentration of 10 ppm Sc in all sample solutions\*. The added scandium was used as an internal standard in order to correct for possible matrix effects; i.e. the intensity of each element was divided by the intensity of Sc and the ratios were used to set up the calibration lines and to calculate the concentration of each element. A further dilution by a factor of 5-10 was performed if one or more of the elemental concentrations were not within the calibration range (Table 2.11). The calibration standards were prepared in the same manner as the samples. The equation to calculate the theoretical LLDs is given below (Equation 6):

**Table 2.10:** ICP-AES instrumental settings.

Torch Power Setting	1.2 kW
All Ar Coolant	14 l/min
Auxiliary Gas (Ar)	1 l/min
Carrier Gas Flow (Ar)	1 l/min
Observation Height	10 mm above the coil

$$LLD = \frac{3 [ S_{r(Ib)} ] \times C}{I_n / I_b} \quad (\text{Equ. 6})$$

Where:	LLD	=	lower limit of detection
	I <sub>b</sub>	=	background intensity at peak position
	S <sub>r(Ib)</sub>	=	standard deviation of background signal
	I <sub>n</sub>	=	net intensity of elemental signal
	C	=	elemental concentration

\* The scandium contents of the soil samples under investigation are not known. Vinogradov (1959) determined an average content of 7 ppm Sc for the soils of Europe and North America. Only a small fraction of Sc is likely to be extractable using NH<sub>4</sub>NO<sub>3</sub>.

**Table 2.11:** Tabulation of theoretical LLDs and calibration ranges for the determination of the 1 M NH<sub>4</sub>NO<sub>3</sub> extractable element concentrations using ICP-AES. It is important to note that the realistic LLD ( $\approx 10$  times the theoretical LLD) is close to the elemental concentration in the lower calibration standard, as given in the right column of the table (see text). Concentrations which were below the calibration range were, therefore, reported to be below the LLD.

Element	Theoretical lower limit of detection in 1 M NH <sub>4</sub> NO <sub>3</sub> [mg l <sup>-1</sup> or ppm]	Calibration range in 1 M NH <sub>4</sub> NO <sub>3</sub> [mg l <sup>-1</sup> or ppm]
Co	0.006	0.05 - 5
Zn	0.004	0.05 - 5
Mg	0.0004	0.01 - 20
V	0.001	0.01 - 5
Ca	0.002	0.02 - 50
Cr	0.002	0.02 - 5
Cu	0.0015	0.02 - 5
Fe	0.0015	0.02 - 5
Ni	0.0082	0.1 - 5
Al	0.016	0.2 - 50
K	0.039	0.5 - 20
Na	0.026	0.5 - 50
P	0.011	0.2 - 20
S	0.015	0.2 - 25

Meaningful, reproducible results can only be obtained at approximately ten times the theoretical LLD (Mrs G. Russell, MINTEK, Johannesburg; pers. comm., 1993). This value is referred to as the real LLD. The concentrations of the lowest calibration standards were chosen close to the real LLD (Table 2.11). Concentrations lower than the lowest calibration standards were, therefore, reported to be below the LLD. The spectral lines used were free of any spectral overlap. It was, therefore, not necessary to perform any interference corrections (Mrs G. Russell, MINTEK, Johannesburg; pers. comm., 1993).

## 2.6. MINERALOGICAL ANALYSIS

**Instrumentation:** Twenty-four samples were selected for a qualitative mineralogical analysis using a Philips PW 1130/90 X-Ray Diffractometer equipped with a graphite Harshaw/Filtrol Monochromator and a NaI Scintillation Detector (PLN 1964/60). The Cu X-ray tube was run at 40 kV and 30 mA. No filter was used. Each sample was scanned from three to sixty five degrees  $2\theta$  in steps of 0,05 degrees per second. From three to seventeen degrees, a  $0.5^\circ$  divergence slit, a  $0.5^\circ$  receiving slit and a  $1^\circ$  antiscatter slit were used. From seventeen to sixty five degrees, a  $1^\circ$  divergence slit, a  $1^\circ$  receiving slit and no antiscatter slit were used.

**Sample preparation:** The powder used to make the briquettes for the XRF analyses (section 2.4.1.2.) was loaded in an aluminium sample holder and levelled off with a glass slide.

**Collection and interpretation of XRD data:** The data collection and the conversion to  $2\theta$  versus intensity plots were performed using the computer programmes COLLECT, XCONV (in-house programs), XPLOT (Raven, 1990) and GRAFIT (Graphicus, Inc.). Peaks were identified using the software package JCPDS PDF-2 Data Base Retrieval/Display System (International Centre for Diffraction Data; Swarthmore, PA 19081, US).

## 2.7. PARTICLE SIZE DISTRIBUTION, pH(KCl), ORGANIC MATTER AND CONDUCTIVITY OF WATER-SUSPENDED SOIL

The parameters listed above were determined utilizing the equipment of the Marine Geoscience Unit (Department of Geological Sciences, University of Cape Town). The Handbook of Standard Soil Testing Methods for Advisory Purposes (Non-Affiliated Soil Analysis Working Committee, 1990) was used for guidance through the laboratory work. However, some of the methods suggested in this handbook were adapted to the facilities of the Marine Geoscience Unit. The steps which were involved in the determination of the parameters listed above are outlined in key-words:

### GENERAL PREPARATION

- (1) Air drying of soil.
- (2) Mixing of soil in sampling container using a "Turbula" mixer (5-15 minutes).
- (3) Representative subsampling of soil samples: The method of subsampling and the size of the subsample were adapted to the physical appearance of individual soils. Relatively well sorted and fine textured soils were **spooned** (40 to 100 g sample). Poorly sorted and coarser textured soils which contained considerable amounts of gravel were subsampled using a **rifle splitter** (up to 500 g sample). Soil

samples which were too coarse textured for the riffle splitter were subsampled by means of the **cone-and-quartering technique**.

- (4) Drying of subsample at 60°C overnight.

### DRY SIEVING

- (5) The soil was sieved through 63, 31.5, 16, 8, 4 and 2 mm sieves. Organic matter was, regardless of its size, added to the fraction < 2 mm. The dry-mass of the various soil fractions was recorded.

### CONDUCTIVITY AND pH

- (6) Twenty five ml of a 1 M KCl solution were mixed with 10 g of -2 mm sieved soil. The pH value of the supernatant was measured using a M90 pH/Conductivity Meter (Electronic Scientific Instrumentation, cc) and is referred to as the pH(KCl) of the soil\*. A pH(KCl) between 5.3 and 6 is regarded to be neutral (Mr G.R. Thompson, Department of Agriculture and Water Supply, Elsenburg; pers. comm., 1991).
- (7) Conductivity of water-suspended soil: Ten grams of the soil fraction < 2 mm were mixed with 25 ml distilled water. The conductivity of the supernatant was measured using a M90 pH/Conductivity Meter (Electronic Scientific Instrumentation, cc) and is referred to as the conductivity of the water-suspended soil.

### PREPARATION OF FRACTION < 2 mm FOR SEDIGRAPH AND SETTLING COLUMN

- (8) The -2 mm sieved soil was dried at 60°C and subsampled. The weight of the subsample was recorded. Steps 9 to 13 describe the preparation of the subsamples for the more detailed particle size analyses using the sedigraph and the settling column.
- (9) Removal of organic matter: The subsamples were treated with H<sub>2</sub>O<sub>2</sub> in order to remove organic matter\*.
- (10) Removal of carbonates: Only four samples showed effervescence with HCl (10 : 1), indicating the presence of carbonates (Appendix-I). The corresponding subsamples were treated with HCl in order to remove the carbonates\*.
- (11) Removal of soluble salts: The subsamples were washed with distilled water until the conductivity of the supernatant was lower than 3333  $\mu\text{S cm}^{-1}$ .
- (12) Loss on pretreatment: Subsequent to steps 9, 10 and 11 the subsamples were dried at 60°C. The weight difference, expressed in percent, between the

---

\* Details of the method are given in Non-Affiliated Soil Analysis Working Committee (1990).

untreated and treated subsamples is referred to as the **loss on pretreatment (LOP)**.

- (13) Separation of sand from silt and clay: The pretreated subsamples were wet-sieved through a 53  $\mu\text{m}$  sieve.

#### USE OF SETTLING COLUMN AND SEDIGRAPH

- (14) The particle size distribution of the sand fraction ( $< 2 \text{ mm}$  and  $> 53 \mu\text{m}$ ) was analysed using a settling column, designed and built by staff members of the Marine Geoscience Unit.
- (15) The particle size distribution of the mud fraction ( $< 53 \mu\text{m}$ ) was analysed using a Micrometrics Sedigraph (Model 5000 D).
- (16) The computer programs SIZE, PHI, NORMAL (in-house programs) and GRAFIT (Graphicus, Inc.) were used to help with the collection, presentation and interpretation of the particle size data.

**Suitability of the LOP as a measure for the proportion of organic matter:** The ratios of [LOP] over [ $|100 - \text{sum of all soil fractions in \%|}$ ] demonstrate that the LOP is generally much higher than the deviation of the sum of all determined soil fractions from 100 percent (Table 2.12), indicating that the accuracy of the pretreatment (steps 8 to 12) was sufficient to make quantitative use of the LOP.

It is explained above that the LOP of a sample is the difference in weight after and before treatment with  $\text{H}_2\text{O}$ ,  $\text{H}_2\text{O}_2$  and  $\text{HCl}$ . The weight difference could be due to the loss of carbonates, soluble salts or organic matter. Only 4 samples showed effervescence with  $\text{HCl}$ , indicating the presence of carbonates. The data in Table 2.12 show that the sum of total  $\text{Cl}$  and 1 M  $\text{NH}_4\text{NO}_3$  extractable  $\text{Ca}$ ,  $\text{K}$ ,  $\text{Mg}$  and  $\text{Na}$  is generally much less than the LOP. Presuming that the proportion of soluble salts is not significantly higher than the sum of total  $\text{Cl}$  and 1 M  $\text{NH}_4\text{NO}_3$  extractable  $\text{Ca}$ ,  $\text{K}$ ,  $\text{Mg}$  and  $\text{Na}$  it is deduced that the loss of soluble salts generally accounts only for a minor proportion of the LOP. It is concluded that the loss of organic matter accounts for most of LOP. The LOP was, therefore, used as a measure of the proportion of organic matter.

**Table 2.12:** Suitability of the loss on pretreatment (LOP) as a measure for the proportion of organic matter. The ratios of [LOP] over [ $|100 - \text{sum of all soil fractions in \%}|$ ] demonstrate that the LOP is generally much higher than the deviation of the sum of all determined soil fractions from 100 percent. The ratio of [LOP] over [sum of total Cl and 1 M  $\text{NH}_4\text{NO}_3$  extractable Ca, K, Mg and Na] (% extractable) demonstrates that the LOP is generally much larger than the proportion of extractable elements.

Sample	%Gravel	%Sand	%Mud	%LOP	Sum	100-sum	LOP/ 100-sum	Sample	%LOP	%Extractable	LOP/Extract.
4A	1.9	85.1	1.7	11.3	100.0	<0.1	>113	26B	8.1	0.16	49
20Top	0.1	90.7	2.4	6.8	100.0	<0.1	>68	4A	11.3	0.23	49
30Top	5.6	74.8	17.5	2.1	100.0	<0.1	>21	20Top	6.8	0.16	43
37A	14.4	34.6	49.2	1.8	100.0	<0.1	>18	19A	0.9	0.02	43
37B	24.5	26.6	47.8	1.1	100.0	<0.1	>11	30Top	2.1	0.05	40
33Top	4.5	89.7	4.8	1.0	100.0	<0.1	>10	25G	6.6	0.17	38
17A	0.2	98.2	0.9	0.7	100.0	<0.1	>7	10A	1.9	0.06	32
45BA	0.7	70.5	28.1	0.7	100.0	<0.1	>7	17A	0.7	0.02	30
21Top	0.1	98.3	1.0	0.6	100.0	<0.1	>6	24Top	0.7	0.02	30
40E	48.2	32.8	18.4	0.6	100.0	<0.1	>6	25A	0.6	0.02	28
25Top	5.3	51.1	43.0	0.6	100.0	<0.1	>6	34A	0.7	0.03	28
25A	6.1	86.6	6.7	0.6	100.0	<0.1	>6	18Top	0.5	0.02	23
6AE	21.5	67.8	10.1	0.5	100.0	<0.1	>5	32A	0.5	0.02	23
41Top	52.5	34.5	12.5	0.5	100.0	<0.1	>5	36Top	1.0	0.04	23
18Top	0.1	98.7	0.7	0.5	100.0	<0.1	>5	46C	1.3	0.06	23
29E	0.3	92.2	7.0	0.5	100.0	<0.1	>5	46A	1.0	0.05	22
33AE	3.7	90.8	5.0	0.5	100.0	<0.1	>5	32Top	0.9	0.04	22
26AE	3.8	88.1	7.7	0.5	100.0	<0.1	>5	16A	0.6	0.03	21
5A	8.6	80.8	10.2	0.4	100.0	<0.1	>4	36B	1.6	0.08	21
36E	64.1	17.4	18.1	0.4	100.0	<0.1	>4	33Top	1.0	0.05	21
29G	0.1	83.7	15.9	0.3	100.0	<0.1	>3	37A	1.8	0.09	20
9A	7.4	84.6	7.8	0.3	100.0	<0.1	>3	30A	0.7	0.03	20
43Top	45.8	41.1	12.8	0.3	100.0	<0.1	>3	24A	0.3	0.01	20
28E	76.4	19.0	4.4	0.2	100.0	<0.1	>2	32G	2.4	0.12	19
43AE	50.0	38.8	11.1	0.1	100.0	<0.1	>1	21Top	0.6	0.03	19
26B	6.0	59.1	26.8	8.1	99.9	0.1	81	45BA	0.7	0.04	19
32G	0.6	38.5	58.7	2.4	100.1	0.1	24	45A	0.9	0.05	19
10A	2.9	91.4	3.8	1.9	100.1	0.1	19	33AE	0.5	0.03	18
38A	11.9	32.2	54.1	1.9	100.1	0.1	19	5A	0.4	0.02	18
38BC	3.2	21.6	71.8	3.7	100.2	0.2	18	31AE	0.8	0.04	18
36B	0.1	13.2	85.2	1.6	100.1	0.1	16	31Top	1.2	0.07	17
45B	1.3	38.0	59.7	1.1	100.1	0.1	11	6AE	0.5	0.03	16
28B	66.4	17.4	13.9	2.1	99.8	0.2	11	38A	1.9	0.12	16
46A	7.9	69.6	21.4	1.0	99.9	0.1	10	46B1	0.6	0.04	15
47A2	3.0	62.4	33.7	1.0	100.1	0.1	10	25Top	0.6	0.04	15
33G	5.4	46.9	46.7	0.9	99.9	0.1	9	16E	0.2	0.01	14
19A	0.2	98.1	0.9	0.9	100.1	0.1	9	45B	1.1	0.08	13
45A	0.4	76.4	22.4	0.9	100.1	0.1	9	26AE	0.5	0.04	13
40Top	42.4	37.7	19.1	0.9	100.1	0.1	9	47A1	0.6	0.04	13
32Top	5.4	87.2	6.5	0.9	99.9	0.1	9	9A	0.3	0.02	12
46B2	56.9	16.1	26.3	0.8	100.1	0.1	8	47B1	0.6	0.05	12
31AE	5.1	78.4	15.6	0.8	99.9	0.1	8	46B2	0.8	0.07	12
34A	12.7	71.2	15.3	0.7	99.9	0.1	7	40Top	0.9	0.08	11
24Top	1.2	94.7	3.5	0.7	100.1	0.1	7	38BC	3.7	0.33	11
46C	2.8	35.6	60.6	1.3	100.2	0.2	6	36E	0.4	0.03	11
46B1	21.4	52.2	25.9	0.6	100.1	0.1	6	29E	0.5	0.05	11
38B	12.0	20.4	66.6	1.2	100.2	0.2	6	44Top	0.7	0.07	9.9
16A	0.1	98.1	1.3	0.6	100.1	0.1	6	37B	1.1	0.12	9.7
47A1	5.4	67.6	26.5	0.6	100.1	0.1	6	41Top	0.5	0.06	8.7
36Top	36.4	37.8	24.6	1.0	99.8	0.2	5	47B2	0.8	0.09	8.6
25G	22.3	20.2	49.5	6.6	98.6	1.4	5	40B	0.8	0.09	8.4
31Top	4.0	80.6	13.9	1.2	99.7	0.3	4	47C	1.1	0.15	7.3
40B	28.0	22.1	49.3	0.8	100.2	0.2	4	40E	0.6	0.09	6.4
47B2	40.4	33.6	25.4	0.8	100.2	0.2	4	32GB	0.1	0.02	5.9
44Top	27.8	45.9	25.7	0.7	100.2	0.2	4	38B	1.2	0.25	4.9
24G	13.0	55.8	30.7	0.3	99.9	0.1	3	31B	0.6	0.14	4.6
30A	4.5	76.2	18.5	0.7	99.8	0.2	3	33G	0.9	0.24	3.9
31B	51.3	33.0	14.9	0.6	99.8	0.2	3	44C	0.4	0.11	3.7
24A	2.8	91.0	6.0	0.3	100.1	0.1	3	43Top	0.3	0.08	3.6
32A	3.8	87.9	7.6	0.5	99.8	0.2	2	24G	0.3	0.11	3.3
47B1	8.6	57.6	33.5	0.6	100.3	0.3	2	44A2	0.2	0.06	2.6
16E	0.1	98.5	1.3	0.2	100.1	0.1	2	44B	0.4	0.15	2.6
47C	2.4	22.9	74.2	1.1	100.6	0.6	2	43AE	0.1	0.08	1.2
44A2	58.9	25.0	16.0	0.2	100.1	0.1	2	29G	0.3	0.32	0.9
44B	2.7	19.3	78.0	0.4	100.3	0.3	1	43E	0.04	0.07	0.6
44C	3.2	40.1	56.6	0.4	100.3	0.3	1	41E	0.04	0.11	0.4
32GB	4.5	83.7	11.6	0.1	99.9	0.1	1	41B1	-0.1	0.17	-0.3
28A	2.4	82.0	15.8	1.2	101.4	1.4	1	41B2	-0.2	0.21	-0.9
43E	81.1	13.0	6.2	0.04	100.4	0.4	0.1				
41E	79.5	9.9	11.6	0.04	101.0	1.0	<0.1				
41B1	41.0	8.0	51.3	-0.1	100.2	0.2	-0.3				
41B2	7.4	12.9	80.2	-0.2	100.3	0.3	-0.6				

## **2.8. APPLYING THE RESULTS OF A PRINCIPAL COMPONENT ANALYSIS TO DEFINE THE PARTICLE SIZE CLASSES USED IN THIS THESIS**

**Introduction:** A rotated Principal Component Analysis (PCA; SAS Institute Inc., 1988) was applied to the data on the particle size distributions to reduce the total number of variables. This made it possible to display the results of the particle size analyses more simply.

The data set used for the analysis contained information on 46 soil samples from four underlying materials and different soil horizons. Soils derived from coastal sands had to be excluded from the PCA, because of incomplete data. The particle size classes used for the PCA and their loadings on the different principal components are shown in Table 2.13. Fine clay did not correlate with any of the principal components of a preliminary PCA and was, therefore, excluded from the final PCA analysis presented here.

**Results and combination of particle size classes:** The first five components of the PCA explained 94 % of the total variance of the data set (Table 2.13). By definition particle size classes strongly loaded on the same principal component have good correlation. It was, therefore, possible, in a way that minimised the loss of variance, to combine the initial Wentworth size classes into wider ones, by grouping classes that were strongly loaded onto the same principal component. This reduced the number of particle size classes from 13 to 6. The initial particle size classes and those resulting from the PCA are shown in Table 2.14.

The results of the PCA suggested that very coarse sand and coarse sand could be combined into a single particle size class which is referred to as 'coarse sand'. Furthermore fine sand and very fine sand were combined and are referred to as 'fine sand'. Very coarse silt and coarse silt were combined and are referred to as 'coarse silt'. All particle size fractions finer than coarse silt and coarser than fine clay were also combined. The resulting particle size fraction is referred to as 'fines' (particles  $> 0.5 \mu\text{m}$  and  $< 16 \mu\text{m}$ ). Fine clay was kept as an individual particle size class because it did not correlate with any of the other size classes (see above).

**Implication for future particle size analyses:** The reduction in the overall number of particle size classes could also be useful for future particle size analyses of soils. Firstly, the number of phi-sieves could be reduced with a minimal loss of information (variance). Secondly, the time taken for an analytical run using the sedigraph could be reduced by finishing the run at 16  $\mu\text{m}$  instead of 0.5  $\mu\text{m}$ . All particles smaller than 16  $\mu\text{m}$  could be reported as one particle size class, because the resulting loss of information is likely to be relatively small. In the case of the Department of Geological Sciences sedigraph (University of Cape Town), this would save more than 30 minutes of the 35 minutes per sample needed to analyse down to a particle size of 0.5  $\mu\text{m}$ .

**Table 2.13:** Variables (size classes) used for the Principal Component Analysis of the particle size distributions and their loadings on the different principal components. The highest loading of each size class is illustrated in bold. The variance accounted for by a principal component is given below its name. The total variance accounted for by the first five principal components equals 93.9 percent.

SIZE CLASS	PC 1	PC 2	PC 3	PC 4	PC 5
Variance (%)	37.3	17.8	17.4	14.9	6.5
very fine silt	<b>.937</b>	-.233	.171	-.081	-.122
coarse clay	<b>.921</b>	-.250	.124	-.084	-.115
fine silt	<b>.879</b>	-.244	.270	-.092	-.176
medium silt	<b>.801</b>	-.248	.408	-.088	-.175
medium clay	<b>.784</b>	-.321	.001	-.159	-.110
very coarse sand	-.312	<b>.927</b>	-.023	-.130	-.029
coarse sand	-.369	<b>.877</b>	.023	-.082	.261
very coarse silt	.075	.076	<b>.974</b>	.119	.035
coarse silt	.409	-.096	<b>.878</b>	.010	-.118
very fine sand	-.011	-.010	.247	<b>.946</b>	-.019
fine sand	-.265	-.250	-.159	<b>.815</b>	.306
medium sand	-.496	.311	-.060	.372	<b>.708</b>
fine clay	Excluded from final PCA (see text).				

**Table 2.14:** Combination of particle size classes according to the results of a Principal Component Analysis (PCA). The principal components on which individual size classes have their highest loading are tabulated. The combined size fractions are given in the right column. Fine clay was excluded from the final PCA because it did not show significant loadings on any of the initially calculated principal components.

Wentworth size class	Range of sizes within the class in mm, $\mu\text{m}$ and in values of phi	PC with highest loading	Name of the combined fraction
very coarse sand	2mm (-1.0 phi) - 1mm (0.0 phi)	PC 2: 0.93	coarse sand
coarse sand	1mm (0.0 phi) - 0.5mm (1.0 phi)	PC 2: 0.88	
medium sand	0.5mm (1.0 phi) - 0.25mm (2.0 phi)	PC 5: 0.70	medium sand
fine sand	0.25mm (2.0 phi) - 0.125mm (3.0 phi)	PC 4: 0.81	fine sand
very fine sand	0.125mm (3.0 phi) - 0.053mm (4.3 phi)	PC 4: 0.95	
very coarse silt	53 $\mu\text{m}$ (4.3 phi) - 31 $\mu\text{m}$ (5.0 phi)	PC 3: 0.97	coarse silt
coarse silt	31 $\mu\text{m}$ (5.0 phi) - 16 $\mu\text{m}$ (6.0 phi)	PC 3: 0.88	
medium silt	16 $\mu\text{m}$ (6.0 phi) - 8 $\mu\text{m}$ (7.0 phi)	PC 1: 0.80	fines
fine silt	8 $\mu\text{m}$ (7.0 phi) - 4 $\mu\text{m}$ (8.0 phi)	PC 1: 0.88	
very fine silt	4 $\mu\text{m}$ (8.0 phi) - 2 $\mu\text{m}$ (9.0 phi)	PC 1: 0.94	
coarse clay	2 $\mu\text{m}$ (9.0 phi) - 1 $\mu\text{m}$ (10.0 phi)	PC 1: 0.92	
medium clay	1 $\mu\text{m}$ (10.0 phi) - 0.5 $\mu\text{m}$ (11.0 phi)	PC 1: 0.78	
fine clay	<0.5 $\mu\text{m}$ (>11.0 phi)	excluded from final PCA analyses	fine clay

# CHAPTER 3.

## MINERALOGY

---

### 3.1. INTRODUCTION

Time and financial constraints did not allow for a comprehensive mineralogical analysis. The analysis was purely qualitative with no attempt at detailed study of clay minerals. The clay fraction was not separated prior to analysis and no other pretreatments were implemented. The main object was to aid the interpretation of the geochemical results in the following chapters.

X-ray diffractometry (XRD) was used to determine the mineralogy of 24 samples. This included the analysis of top- and subsoils associated with the different underlying materials as well as the parent rocks. Soil samples with particularly high proportions of clay, sesquioxides, feldspars or quartz were selected to ensure that most of the encountered mineralogical variance was represented by them. The analytical techniques were described in section 2.6. Figure 2.2 depicts the sampling localities. Sections of the sampled soil sequences are given in Figures 4.1, 5.2, 6.1, 7.1 and 8.1.

### 3.2. RESULTS

The XRD patterns and their interpretations are given in Figures 3.1 to 3.5. The results can be summarised as follows:

(a) **Coastal sand-derived soils:** Only quartz is present in detectable concentrations (Figure 3.1; samples 20Top and 21Top).

(b) **Soils associated with unconsolidated sands of granitic origin (USGO):** Only two samples were analysed. Sample 28E was taken from the E-horizon of Pit 28. The only minerals identified from the diffractogram of this sample are quartz and goethite (Figure 3.1). Sample 25G was taken from the G-horizon of Pit 25. The presence of a 7 Å peak ( $12.3^\circ 2\theta$ ) without a corresponding 14 Å peak (chlorite) indicates that this sample contains additionally a mineral of the kaolinite-group. For reasons explained above, no distinction was made between dickite, nacrite and metahalloysite. The mineral(s) associated with a 7 Å peak will be referred to as kaolinite.

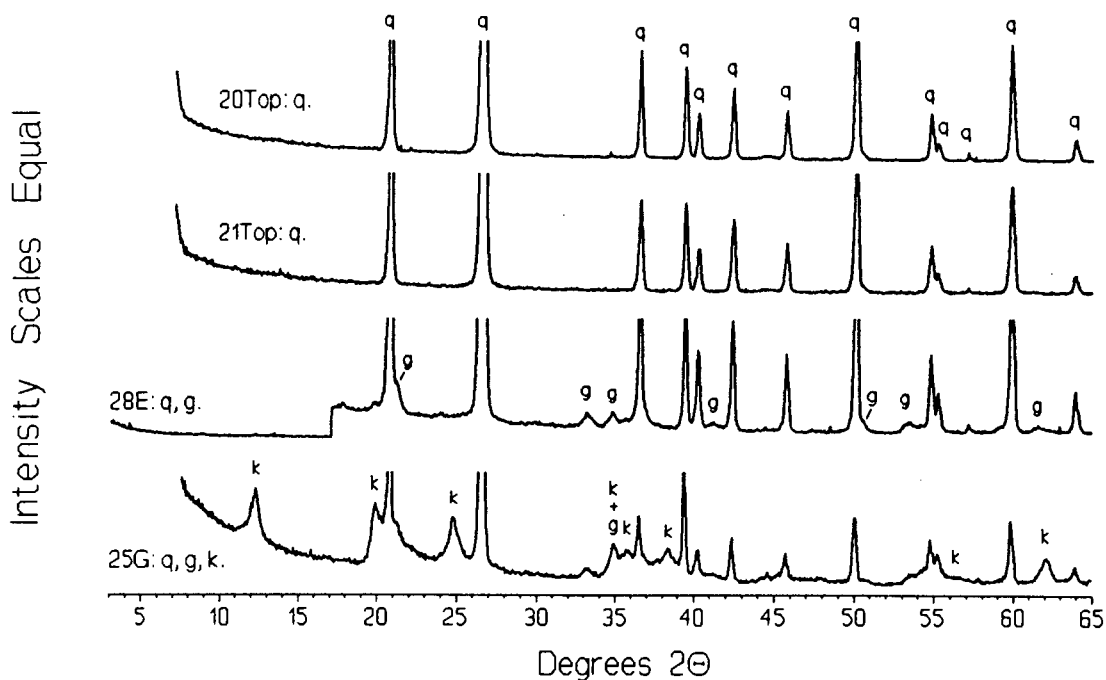


**Figure 3.1:** Stacked XRD patterns of a subset of samples taken from the soils associated with the coastal sands (20Top and 21Top) and the unconsolidated sands of granitic origin (28E and 25G). Symbol classification: q = quartz, g = goethite, k = kaolinite. The change of the intensity of sample 28E at 17° 2 $\theta$  is due to the changing of divergence slits from 0.5° to 1.0°.

(c) **Granite-derived Soils:** Four soil samples and the granite that formed their parent material were analysed. Orthoclase, plagioclase and quartz are the only minerals that could be identified from the diffractogram of the granite (Figure 3.2).

The granite-derived soil samples contain generally less feldspar than their parent material. The proportion of feldspars decreases with increasing distance from the granite (sample 30Top to 32G). Sample 32G, a sample from a heavy-textured subsoil at the bottom of the toposequence, contains only traces of feldspar. This sample is the only one that contains kaolinite. The diffractograms of sample 32G and sample 31B exhibit minor amounts of goethite. The results for the granite-derived soils are in agreement with Bühmann and Kirsten (1991) who showed kaolinite, metahalloysite, gibbsite, goethite and hematite to occur as weathering products in South African granite-derived soils.

(d) **Soils associated with schist of the Malmesbury Group:** Four soil samples and the strongly weathered underlying material (saprolite: sample 35Sap) were analysed (Figure 3.3). All samples contain quartz, goethite and plagioclase. Only the saprolite and the subsoil (samples 38BC and 37B) contain orthoclase. The proportions of feldspar and kaolinite decrease from the saprolite to the subsoil and further to the

topsoil (samples 36E and 37A). The sample that was taken from the E-horizon of Pit 36 (36E) is the only one that contains hematite.

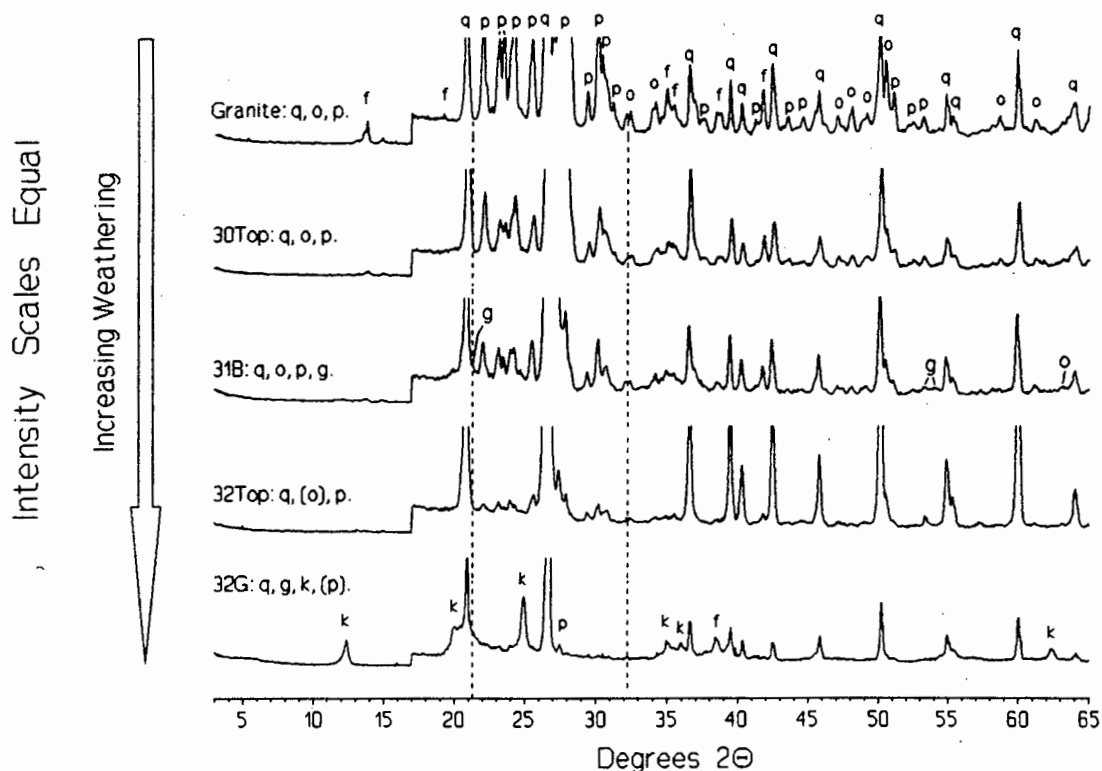


**Figure 3.2:** Stacked XRD patterns of a subset of granite-derived soils. Symbol classification: q = quartz, o = orthoclase, p = plagioclase, f (feldspar) = o + p, g = goethite, k = kaolinite. Dotted guidelines are drawn to facilitate the interpretation. The change of the intensity at  $17^\circ 2\theta$  is due to the changing of divergence slits from  $0.5^\circ$  to  $1.0^\circ$ .

The diffractograms of the saprolite and the subsoil of Pit 37 (sample 37B) exhibit  $10 \text{ \AA}$  peaks ( $9^\circ 2\theta$ ). It is suggested that the  $10 \text{ \AA}$  peak is either due to illite, halloysite, muscovite, biotite, or a combination of them. The relatively broad shape of the  $10 \text{ \AA}$  peak indicates the presence of a  $10 \text{ \AA}$  clay mineral such as illite. The presence of biotite is less likely because of its instability in the weathering environment (Rösler, 1981). The minerals associated with a  $10 \text{ \AA}$  peak will be referred to as  $10\text{\AA}$ -phyllosilicates. The saprolite contains a high proportion of  $10\text{\AA}$ -phyllosilicates while the soil samples contain either little or none.

**(e) Soil associated with feldspathic sandstone of the Malmesbury Group:** All samples analysed were taken from Pit 44 (Figure 3.4). This included one sample of the B-horizon (44B), one of the C-horizon (44C) and one of the feldspathic sandstone that underlies the soils (44Rock). All samples contain quartz, plagioclase, orthoclase, goethite and  $10\text{\AA}$ -phyllosilicates. The feldspathic sandstone also contains hematite.

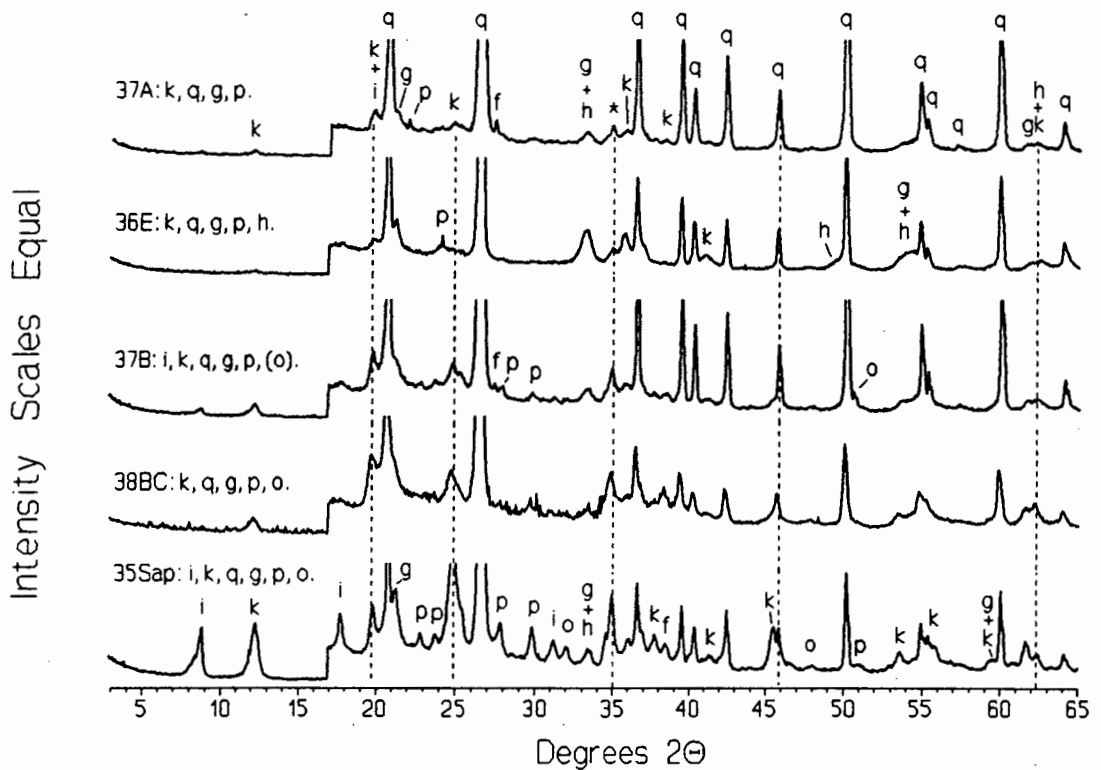


**Figure 3.3:** Stacked XRD patterns of a subset of samples taken from the soils associated with the schists of the Malmesbury Group. Symbol classification: q = quartz, o = orthoclase, p = plagioclase, f(feldspar) = o + p, g = goethite, k = kaolinite, i = 10Å-phyllsilicates, h = hematite, \* = p+o+k+g. Dotted guidelines are drawn to facilitate the interpretation. The change of the intensity at 17° 2θ is due to the changing of divergence slits from 0.5° to 1.0°.

The proportion of 10Å-phyllsilicates and feldspars decreases from the underlying material to the C-horizon and the B-horizon. Kaolinite occurs only in the soil samples and its proportion increases from the C- to the B-horizon.

The diffractogram of the feldspathic sandstone is the only one that exhibits a 14 Å peak (6.25° 2θ). The presence of a 14 Å peak without a corresponding 7 Å peak (chlorite) indicates the presence of either montmorillonite or vermiculite.

**(f) Soil associated with phyllite of the Malmesbury Group:** Two soil samples and one saprolite were analysed (Figure 3.4). All samples contain 10Å-phyllsilicates, kaolinite, quartz, goethite and plagioclase. Only sample 41B2 does not contain orthoclase. The proportions of 10Å-phyllsilicates, kaolinite and feldspar decrease from the saprolite to the soils. The identification of halite in sample 39Sap was confirmed by both the XRF-analyses of sodium and chlorine and the determination of the conductivity of the water-suspended soil (Chapter 6).

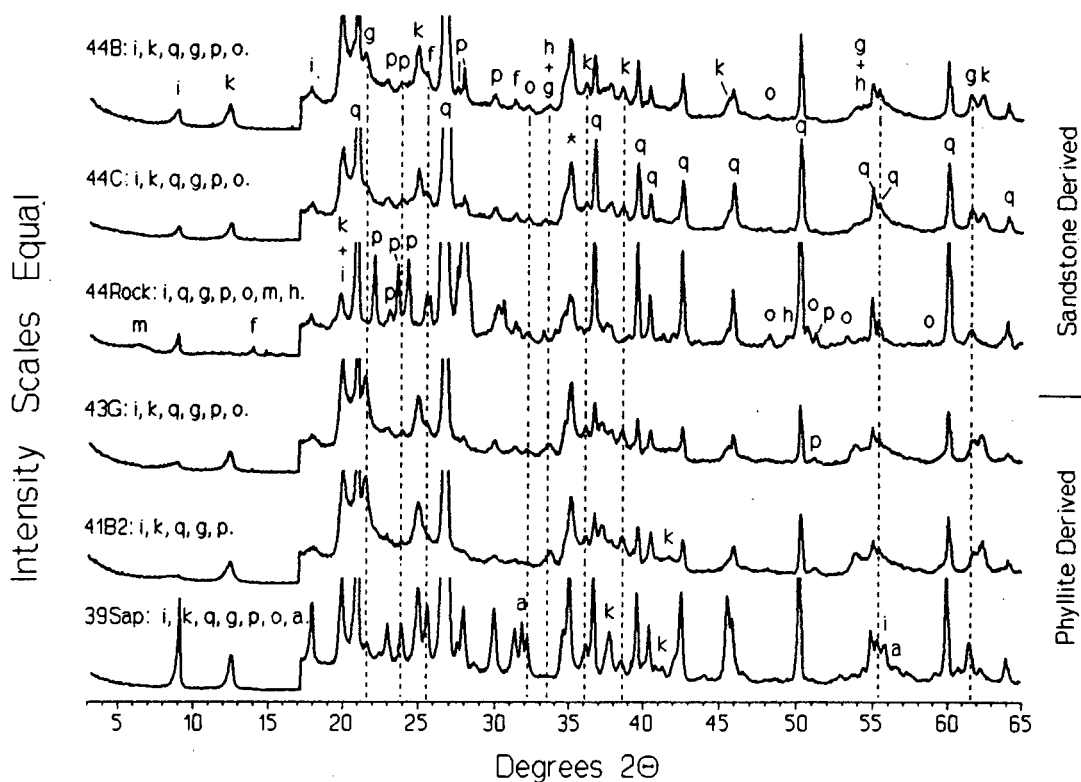


**Figure 3.4:** Stacked XRD patterns of a subset of samples taken from the soils associated with the feldspathic sandstone and phyllite of the Malmesbury Group. Symbol classification: q = quartz, o = orthoclase, p = plagioclase, f(feldspar) = o + p, g = goethite, k = kaolinite, i = 10Å-phyllsilicates, m = 14Å-montmorillonite and(or) vermiculite, h = hematite, a = halite, \* = p+o+k+g. Dotted guidelines are drawn to facilitate the interpretation. The change of the intensity at 17° 2θ is due to the changing of divergence slits from 0.5° to 1.0°.

**(g) Soil associated with ferruginized materials:** The samples of the B- and C-horizons (samples 46B2, 46C and 47C; Figure 3.5) contain detectable amounts of quartz, goethite, kaolinite, feldspar and hematite.

Sample 47A2 was taken from a burrow between the B1- and the C-horizon of Pit 47 at the top of the toposequence (Figure 7.1). The burrow was filled with material from the A-horizon (section 7.3.). The mineralogy of sample 47A2 differs in three aspects from the mineralogy of the samples taken from the B- and C- horizons; it contains more feldspars, less kaolinite and little or no hematite.

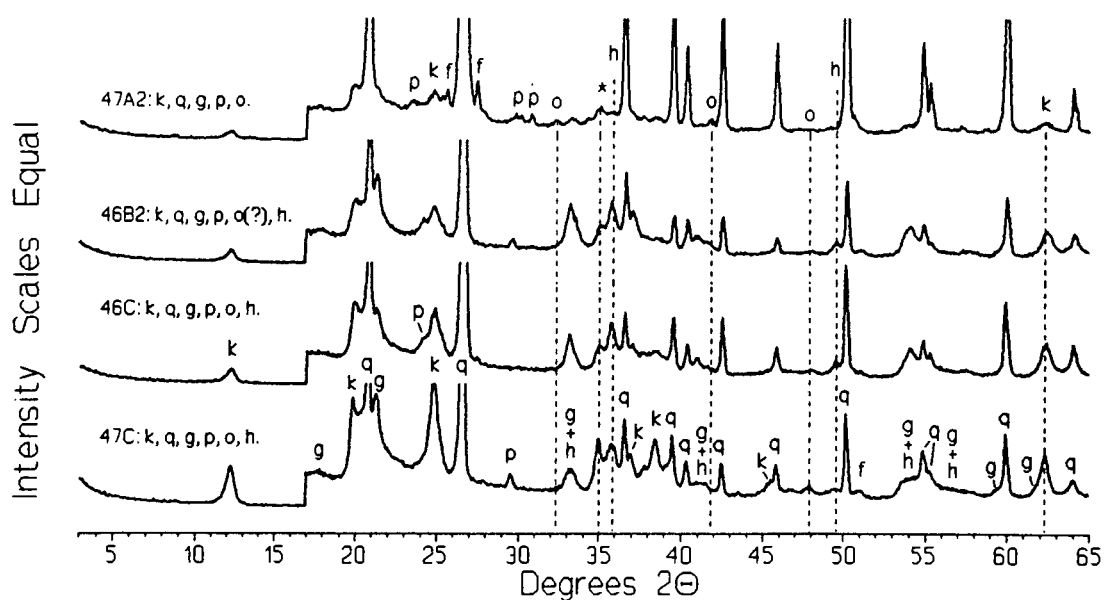


**Figure 3.5:** Stacked XRD patterns of a subset of samples taken from the soils associated with the ferruginized materials. Symbol classification: q = quartz, o = orthoclase, p = plagioclase, f(feldspar) = o + p, g = goethite, k = kaolinite, h = hematite, \* = p+o+k+g. Vertical guidelines are drawn to facilitate the interpretation. The change of the intensity at 17° 2θ is due to the changing of divergence slits from 0.5° to 1.0°.

### 3.3. DISCUSSION

#### Mineralogical differences between soils associated with different underlying materials:

The soils derived from coastal sand contain only quartz while the soils associated with the USGO may contain also goethite and kaolinite. The granite-derived soils contain additionally feldspars. Phyllosilicates with a d-spacing of 10 Å, probably illite, halloysite or muscovite, occur exclusively in the sediments of the Malmesbury Group and the associated soils. Small proportions of feldspars and relatively large proportions of hematite and goethite are characteristic for the soils associated with the ferruginized materials.

**Alteration of feldspars during weathering:** The proportion of feldspars generally decreased from the underlying material to the soil. This trend reflects the alteration of feldspars during weathering. In the soils associated with granites (Figure 3.2) and feldspathic sandstones of the Malmesbury Group (Figure 3.4) the proportion of kaolinite increases with progressive weathering of feldspars. It is apparent that in these soils the product of feldspar alteration is kaolinite.

It is important to note that the soils associated with the sands of granitic origin do not contain feldspars. A sample of a G-horizon derived from USGO (25G;

Figure 3.1), however, showed that the subsoil may contain a large proportion of kaolinite. It is thus likely that the underlying material originally contained feldspars which were altered to kaolinite. Subsequent eluviation of the kaolinite from the topsoil resulted in its accumulation in the subsoil.

**Pedogenic formation of kaolinite:** Neither the sample of the feldspathic sandstone (Malmesbury Group) nor the one of the granite contained kaolinite (Figures 3.2 and 3.4). The associated soils do contain kaolinite and its proportion increases with progressing weathering from the C- to the B-horizon (Figure 3.4). It is concluded that the kaolinite in these soils is pedogenic.

**Kaolinite inherited from the underlying material:** The proportions of kaolinite in the soils associated with schist, phyllite and ferruginized material increase from the A- and B-horizons to the underlying material (saprolites and C-horizons). It is, therefore, probable that the fresh rock also contains kaolinite. The kaolinite in these soils can thus be both pedogenic and inherited from the underlying rock.

**Alteration of 10Å-phyllsilicates during weathering:** The proportion of 10Å-phyllsilicates decreases from the underlying material (sample 35Sap in Figure 3.3; samples 39Sap and 44Rock in Figure 3.4) to the soil. This trend is probably a result of weathering of 10Å-phyllsilicates. It can be assumed that the alteration of 10Å-phyllsilicates results in kaolinite because no other clay minerals are present in the soils. This hypothesis is in agreement with Smith (1972) who observed the alteration of illite, muscovite and feldspar to kaolinite in three weathering profiles in rocks of the Malmesbury Group.

The decreasing proportion of 10Å-phyllsilicates from the underlying material to the soil may also reflect the dehydration of halloysite to metahalloysite or could be the result of processes other than weathering. Possible processes are (a) the dilution of *in situ* material with colluvial quartz gravel and (b) the loss of 10Å-phyllsilicates from a soil horizon by means of eluviation. The latter may only be applicable to the samples from the A- and E-horizons (37A and 36E). Pedogenic formation of 10Å-phyllsilicates was not evident from the samples studied in this work.

# CHAPTER 4.

## GRANITE-DERIVED SOILS

---

### 4.1. INTRODUCTION

**Occurrence and topography of the granites:** Three major occurrences of granite are in the field area (Figure 1.2). The two larger ones are of elongated shape, approximately 40 km long and follow a north-north-west south-south-east strike. One occurrence is centred on Darling while the other one is centred on Malmesbury. The third major occurrence of granite is just west of Paarl.

The Cape granites intruded into the older Malmesbury Group and are more resistant to the processes of degradation than the Malmesbury material. As a result the granites became more prominent with time and formed a number of smooth, rounded granite batholith exposures. These exposures are up to 729 m high (Paarlberg) and form the highest hills in the coastal plain.

**Sampling locations:** The samples discussed in this chapter were taken from the granite-derived soils in the Darling area. Two locations were sampled:

(a) Most of the samples were taken from a toposequence down the southern slope of the granite hill Klipberg, approximately 5 km north-west of Darling (location 4 in Figure 2.2). The hill has an altitude of 271 m amsl and lies within the north-eastern periphery of the Darling granite exposures, directly at the geological border to the unconsolidated, quaternary sands of the Groenrivier depression (Figure 1.2).

(b) Samples were also taken from different slope positions of two granite-derived toposequences, approximately 12 km south-east of Darling (location 5 in Figure 2.2).

The coordinates of all pits sampled are given in Appendix-I. A simplified section through the Klipberg toposequence (location 4) and the pits at location 5 is depicted in Figure 4.1.

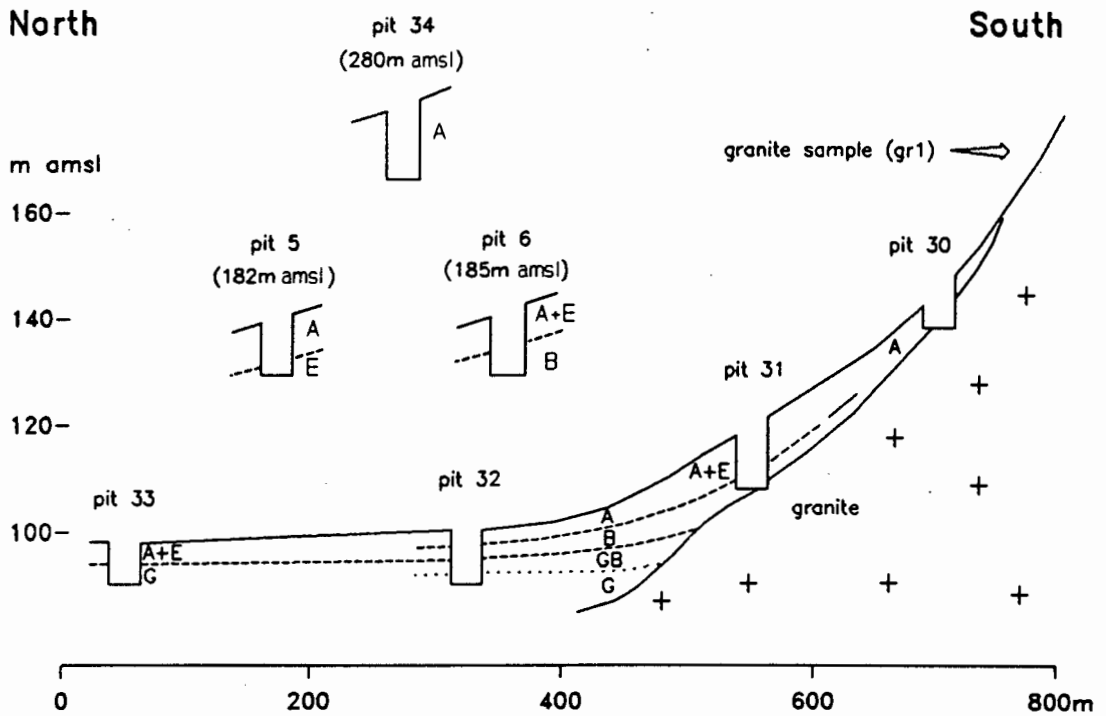


**Figure 4.1:** Simplified section through the granite-derived toposequence. Figure 2.4 can be used as a key to the abbreviations for the different soil horizons. Features other than the topography are not to scale. The vertical scale is exaggerated. The toposequence is situated on the northern slope of Klipberg and has an average gradient of 75 ‰ (location 4 in Figure 2.2). A slightly weathered sample of the granite was taken from an exposure at the top of the toposequence. Pits 5, 6 and 34 are approximately 20 km SE of the Klipberg toposequence (location 5 in Figure 2.2).

#### 4.2. ANALYTICAL RESULTS - AN OVERVIEW

**Tabulated summary of results:** A summary of the analytical results is given in Tables 4.1 to 4.4. The lower limit of detection (LLD), the total number of analysed samples and the number of samples that had values above the LLD are presented for each element. The range of concentrations is given if at least one sample had a concentration above the LLD. The mean, standard deviation and coefficient of variation were only calculated if the majority of the samples had concentrations above the LLD. The means calculated for the elements which occasionally have concentrations below the LLD are biased towards higher concentrations because only values above the LLD were included to derive the statistics. Table 4.5 summarises the affinity of elements for Fe-oxides, organic matter and kaolinite in the Klipberg toposequence. The major and trace element composition of the slightly weathered granite which forms the parent material of the Klipberg toposequence is given in Table 4.6. A full listing of the results is given in Appendix-III.

**Table 4.1:** Basic statistics of the major elements in the granite-derived soils. Only values above the lower limit of detection ( $n > \text{LLD}$ ) were included to derive the statistics. The analyses were performed using XRFS and all concentrations are given in percent in dried soil (LLD = lower limit of detection; S.D. = standard deviation; C.V. = coefficient of variation).

Oxide	n	n > LLD	Approx. LLD (%)	Mean (%)	S.D. (%)	C.V. (%)	Min. in % (sample)	Max. in % (sample)
Na <sub>2</sub> O	15	15	0.02	1.3	1.2	94	0.09 (32G)	3.6 (30Top)
MgO	15	13	0.02	0.13	0.13	107	< LLD	0.46 (33G)
Al <sub>2</sub> O <sub>3</sub>	15	15	0.01	8.0	4.7	59	1.5 (33Top)	17.7 (32G)
SiO <sub>2</sub>	15	15	0.02	82.9	8.8	11	67.2 (32G)	94.9 (33Top)
P <sub>2</sub> O <sub>5</sub>	15	15	0.005	0.04	0.02	53	0.01 (33AE)	0.08 (31B)
K <sub>2</sub> O	15	15	0.004	2.5	1.4	57	0.66 (33AE)	4.6 (30A)
CaO	15	15	0.005	0.1	0.1	109	0.01 (32GB)	0.35 (5A)
TiO <sub>2</sub>	15	15	0.007	0.14	0.06	43	0.07 (33Top)	0.27 (33G)
Fe <sub>2</sub> O <sub>3</sub>	15	15	0.009	2.1	1.4	69	0.77 (33AE)	5.5 (31B)

**Table 4.2:** Basic statistics summarising the pH(KCl) values, the conductivities of the water-suspended soil samples and the percentages of various particle size fractions and organic matter for the granite-derived soils (S.D. = standard deviation; C.V. = coefficient of variation).

Parameter	n	Mean	S.D.	C.V. (%)	Min. (sample)	Max. (sample)
pH (KCl)	15	4.8	0.4	8	4.3 (30A)	5.8 (31Top)
Conductivity ( $\mu\text{S cm}^{-1}$ )	15	145	182	126	30 (6AE)	610 (31B)
% Organic Matter	15	0.9	0.6	70	0.1 (32GB)	2.4 (32G)
% Gravel	15	9	13	133	0.6 (32G)	51 (31B)
% Sand	15	72	18	25	33 (31B)	91 (33AE)
% Mud	15	17	15	89	5 (33Top)	59 (32G)
% Fine Clay	14	7	12	166	0.01 (32Top)	40 (33G)

**Table 4.3:** Basic statistics of the trace elements in the granite-derived soils. Only values above the lower limit of detection ( $n > \text{LLD}$ ) were included to derive the statistics. Li, Be, Co, Cd and Sb were analysed using ICP-MS, all other elements were analysed using XRFs. The concentrations are given in ppm in dried soil (LLD = lower limit of detection; S.D. = standard dev.; C.V. = coefficient of variation; \* = pollution suspected [2 samples]; \*\* = one outlier excluded [426 ppm]).

Elem.	n	n > LLD	Approx. LLD in ppm	Mean in ppm	S.D. in ppm	C.V. (%)	Min. in ppm (sample)	Max. in ppm (sample)
Li	8	8	0.2	20	27	131	5.3 (34A)	84 (32G)
Be	8	7	0.3	1.9	1.7	87	< LLD	5.1 (30Top)
F	16	15	140	517	587	113	< LLD	1927 (33G)
S	15	15	6	160	78	48	59 (31AE)	340 (31B)
Cl	15	15	4	148	120	81	52 (6AE)	540 (31B)
V	15	15	1.2	19	11	61	7.6 (32A)	36 (31B)
Cr	15	15	1.3	25	7.9	31	16 (31AE)	49 (33G)
Mn	15	15	1.5	90	28	31	57 (31B)	135 (31Top)
Co	8	6	0.2	0.5	0.2	44	< LLD	0.9 (34A)
Ni	16	16	2.3	7.8	5.1	66	4.6 (32G)	26 (6B)
Cu	16	15	1.8	4.3	2.2	50	< LLD	8.3 (6B)
Zn	16	16	1.2	12	14	124	1.5 (32GB)	63 (6B)
Ga	3	3	0.8	12	8.2	68	6.1 (5A)	21 (6B)
Ge	16	12	0.9				< LLD	1.4 (32G)
As	16	16	0.8	83	188	226	1.9 (5A)	743 (32G)
Se	16	6	0.8				< LLD	5.3 (31B)
Br	16	15	0.9	5.4	5.0	92	< LLD	15 (31B)
Rb	16	16	0.7	194	114	59	51 (33Top)	373 (31B)
Sr	16	16	0.6	26	25	97	5.7 (32A)	77 (6AE)
Y	16	16	0.7	20	7.9	40	9.4 (33Top)	35 (30Top)
Zr	16	16	0.6	383	131	34	174 (33G)	584 (30Top)
Nb	16	16	0.6	127	87	68	4.6 (5A)	234 (30Top)
Mo	16	16	0.5	3.0	2.2	75	1.1 (6AE)	10 (31B)
Cd	8	0	0.7					
Sn*	16	16	1.2	14	17	127	2.2 (34A)	65 (33AE)
Sb	8	5	0.3				< LLD	8.0 (32G)
I	16	9	2.5				< LLD	12 (32G)
W**	15	16	2.6	19	102	231	9.8 (32GB)	35 (31B)
Pb	16	15	2.1	16	10	66	< LLD	43 (32G)
Bi	16	5	2.8				< LLD	6.4 (31B)
Th	16	16	1.7	27	38	140	5.2 (33AE)	165 (32G)
U	16	16	1.3	4.5	2.7	60	2.2 (33AE)	13 (32G)

**Table 4.4:** Basic statistics of the extractable element concentrations for the granite-derived soils. Only values above the lower limit of detection ( $n > \text{LLD}$ ) were included to derive the statistics. The results in the first part of the table are given in ppm in dried soil (fraction  $< 2$  mm) and were obtained using ICP-AES. The results in the second part of the table are given in ppb in dried soil (fraction  $< 2$  mm) and were obtained using ICP-MS (LLD = lower limit of detection; S.D. = standard deviation; C.V. = coefficient of variation).

## Part 1

Elem.	n	n > LLD	Approx. LLD in ppm	Mean in ppm	S.D. in ppm	C.V. (%)	Min. in ppm (sample)	Max. in ppm (sample)
Na	15	15	1.2	111	202	182	13 (32A)	725 (33G)
Mg	15	15	0.03	133	227	170	16 (5A)	810 (33G)
Al	15	11	0.5				< LLD	9 (30A)
P	15	6	0.5				< LLD	2.1 (31Top)
S	15	7	0.5				< LLD	70 (31B)
K	15	15	1.2	30	19	61	4.2 (32GB)	80 (30Top)
Ca	15	15	0.05	196	153	78	25 (32GB)	575 (33G)
Cr	15	2	0.05				< LLD	0.2 (33G)
Fe	15	4	0.05				< LLD	0.7 (33G)
Ni	15	2	0.2				< LLD	0.7 (33G)
Cu	15	1	0.05				< LLD	0.08 (33G)
Zn	15	7	0.1				< LLD	0.7 (33G)

## Part 2

Elem.	n	n > LLD	Approx. LLD in ppb	Mean in ppb	S.D. in ppb	C.V. (%)	Min. in ppb (sample)	Max. in ppb (sample)
Be	15	0	67					
B	14	2	362				< LLD	510 (32A)
V	15	3	9				< LLD	24 (31B)
Co	15	3	13				< LLD	65 (5A)
As	15	0	71					
Se	15	0	877					
Mo	15	0	49					
Cd	15	1	17				< LLD	22 (6AE)
Sb	15	0	23					
Ba	15	15	61	2079	1856	89.3	473 (32GB)	7334 (33G)
Tl	15	4	3				< LLD	21 (33G)
Pb	15	2	54				< LLD	314 (31B)
Bi	15	0	3					
U	15	0	30					

**Table 4.5:** Enrichment factors from (a) the granite to the subsoil with abundant Fe-oxide concretions [calculated as: concentration in Fe-oxide-rich soil over concentration in granite; based on one pit], (b) the composite samples of the topsoil to the samples of the organic-rich top 15 cm of the topsoil [calculated as: concentration in organic-rich soil over concentration in composite sample; based on four pits] and (c) the topsoil to the fine textured subsoil at the bottom of the toposequence [calculated as: concentration in fine textured subsoil over concentration in topsoil; based on two pits]. Blank cells indicate that the corresponding concentrations were not determined, below the LLD or ambiguous. Abbreviations: OM = organic matter, KAOL = kaolinite, FEOX = iron oxides. It is important to note that the enrichment factors reflect not only the affinity of the elements to clay, Fe-oxides and organic matter but also the quantity of elements released from their primary hosts and available for accumulation.

Element	Enrichment Factors			Interpretation
	(a) FE-OXIDES	(b) TOP 15	(c) CLAY	
<b>GROUP-I</b>				
Li			9.7*	Associated with KAOL.
P <sub>2</sub> O <sub>5</sub>	3	1 - 2.1	1 - 2	Associated with FEOX, OM and KAOL.
TiO <sub>2</sub>	1.9	±1	1.3 - 3	Confirms eluviation from topsoil.
V	14	1 - 2	4.3	Associated with OM, FEOX and KAOL.
Fe <sub>2</sub> O <sub>3</sub>	7.5	1 - 1.8	2.7 - 4.7	Associated with OM, FEOX and KAOL.
Zn	±1	±1	5	Associated with KAOL.
Zr	±1	±1	0.6 - 1	Not illuviated into the G-horizon.
Sn	±1	±1	2.4*	Associated with KAOL.
<b>GROUP-II</b>				
Cr	1.7	1 - 1.5	1.2 - 2.5	Associated with FEOX, OM and KAOL.
Mn	±1	1 - 1.7	±1	Associated with OM.
Co			2*	Associated with KAOL.
Ni	±1	0.9 - 1.4	0.5 - 1.4	
Cu	2.7	0.9 - 1.9	2 - 5	Associated with FEOX, OM and KAOL.
Sr	±1	±1	1.9 - 3.8	Association with KAOL.
Mo	5	1 - 1.4	1.3 - 2.5	Associated with FEOX, OM and KAOL.
W	2.5**	1 - 1.4	1.3 - 1.5	Association with FEOX, OM and KAOL.
<b>GROUP-III</b>				
F	1.7		8.8 - 10	Associated with FEOX and KAOL.
Na <sub>2</sub> O	0.3	±1		
Al <sub>2</sub> O <sub>3</sub>	0.8	±1	5 - 7.5	Associated with KAOL.
K <sub>2</sub> O	0.8	±1	0.5 - 1	

continued ...

\* Based on only one pit because the concentrations in the samples from the other pits were (a) below the LLD, (b) not determined or (c) affected by pollution (Sn).

\*\* The enrichment factor from the topsoil to subsoil rather than from granite to the subsoil is given because the interpretation of the latter would be misleading. See section 4.5.3. for explanation.

... Table 4.5 continued

Element	Enrichment Factors			Interpretation
	FE-OXIDES	TOP 15	CLAY	
<b>GROUP-III</b>				
CaO	0.6	1.4 - 2.5	3 - 5.6	Associated with OM and KAOL.
Rb	±1	±1	1.6 - 2.7	Associated with KAOL.
Y	0.5	±1	2.2	Associated with KAOL.
Pb	1.4	1 - 5	6 - 12	Associated with FEOX, OM and KAOL.
Th	1.5	±1	4.6 - 16	Associated with FEOX and KAOL.
U	±1	1 - 1.3	2.3 - 4.3	Associated with OM and KAOL.
<b>GROUP-IV</b>				
S	9	1.5 - 2.6	1.7 - 2.5	Association with FEOX, OM and KAOL.
As	188	1 - 4.3	5 - 42	Association with FEOX, OM and KAOL.
Se	> 7		2.5*	Association with FEOX and KAOL.
Br	15	±1	4 - 6	Association with FEOX and KAOL.
<b>GROUP-V (LEACHABLE ELEMENT FRACTIONS)</b>				
Na	11**	0.5 - 2.4	17 - 27	Associated with FEOX, OM and KAOL.
Mg	15	1 - 2.2	23 - 31	Associated with FEOX, OM and KAOL.
Al	> 2.7			Associated with FEOX.
P		2 - > 4	1 - > 2	Associated with OM and KAOL.
S	17		5 - > 28	Associated with FEOX and KAOL.
K	1.3**	1.5 - 2.6	1.8 - 4	Associated with OM and KAOL.
Ca		1.7 - 2.3	4 - 8	Associated with OM and KAOL.
V			1 - > 4	Associated with KAOL.
Cr			2 - > 4	Associated with KAOL.
Ni			1 - > 2.7	Associated with KAOL.
Cu			> 1.6*	Associated with KAOL.
Zn		> 3.2*	> 6*	Associated with OM and KAOL.
Ba	1.3	1 - 1.5	4.4 - 9.6	Associated with FEOX, OM and KAOL.
Tl			2.9 - > 7.8	Associated with KAOL.
Pb	> 6			Associated with FEOX.
<b>ELEMENTS WHICH WERE NOT ASSIGNED TO GROUPS</b>				
MgO	3.7	0.3 - > 3.8	13.5 - 23	Associated with FEOX and KAOL.
Cl	5.3	1.4 - 1.8	1.7 - 2.3	Associated with FEOX, OM and KAOL.
I	2		2.6 - 4.1	Associated with FEOX and KAOL.

\* Based on only one pit because the concentrations in the samples from the other pits were (a) below the LLD, (b) not determined or (c) affected by pollution (Sn).

\*\* The enrichment factor from the topsoil to subsoil rather than from granite to the subsoil is given because the interpretation of the latter would be misleading. See section 4.5.3. for explanation.

**Table 4.6:** Whole-rock analyses of the slightly weathered granite which forms the parent material of the Klipberg toposequence. Concentrations in percent for major elements and ppm for trace elements.

SiO <sub>2</sub>	74.0	Li	16	Zn	5.0	Mo	2.0
TiO <sub>2</sub>	0.06	Be	7.4	Ge	0.9	Cd	<0.7
Al <sub>2</sub> O <sub>3</sub>	14.3	F	404	As	1.3	Sn	7.3
Fe <sub>2</sub> O <sub>3</sub>	0.74	S	38	Se	<0.7	Sb	<0.3
MgO	0.02	Cl	101	Br	1.0	I	2.5
CaO	0.08	V	2.5	Rb	357	W	52
Na <sub>2</sub> O	5.6	Cr	15	Sr	7.7	Pb	11
K <sub>2</sub> O	5.2	Mn	62	Y	34	Bi	18
P <sub>2</sub> O <sub>5</sub>	0.03	Co	0.24	Zr	343	Th	31
H <sub>2</sub> O <sup>-</sup>	0.20	Ni	5.2	Nb	208	U	4.9
LOI	0.18	Cu	2.5				
TOTAL	100.4						

#### 4.3. PARTICLE SIZE DISTRIBUTIONS AND FIELD OBSERVATIONS

A photograph from the pit in the uppermost slope position (Pit 30) shows the sampling line down the Klipberg toposequence (Figure 4.2). Abundant granite exposures occur just above the pit from which the photograph was taken. The exposed granite showed signs of chemical and physical weathering. Granite detritus on the rock surfaces was probably subjected to surface wash towards the upper limit of the soil cover.

**Soil horizons and classification (summarised from Appendix-I):** Orthic A-horizons, E-horizons, soft plinthic and lithocutanic B-horizons and G-horizons were encountered in the field. The soil profiles along the toposequence down Klipberg were classified as belonging to the following soil forms: Pit 30, Mispah; Pit 31, Longlands; Pit 32, Westleigh; Pit 33, Kroonstad. The brown colour of the soil at the top of the toposequence indicates the presence of goethite and well drained conditions. The soil in middle and lower slope position has dominantly grey colours, indicating imperfectly and poorly drained conditions (Figure 2.1). The soil in the upper slope position is

coarse textured and directly underlain by granite (Figure 4.3). In the lower slope positions (Pits 32 and 33) coarse textured topsoil is underlain by fine textured and gleyed subsoil. The proportion of coarse sand in the topsoil increases continuously with increasing distance from the granite while all other particle size classes have decreasing proportions (Figure 4.3). This trend is discussed together with the geochemical results (section 4.5.4.).



**Figure 4.2:** The view from the uppermost pit down the granite-derived toposequence.

**Throughflow as important pathway of water:** Throughflow in a gravelly E-horizon in footslope position was observed during winter when performing the sampling of the toposequence at location 5 (Pit 5). The topography and the parent material of this toposequence are very similar to those of the Klipberg toposequence, suggesting that throughflow may also occur in the Klipberg toposequence. The coarse texture of the topsoil of the Klipberg toposequence (Figure 4.3) suggests a high infiltration rate. The granite probably acts as an aquiclude, causing lateral subsurface flow of infiltrated water through the soil down the toposequence (throughflow). Overland flow can only occur if the soil is water saturated or during catastrophic rain storms, if the precipitation exceeds the maximum infiltration rate.

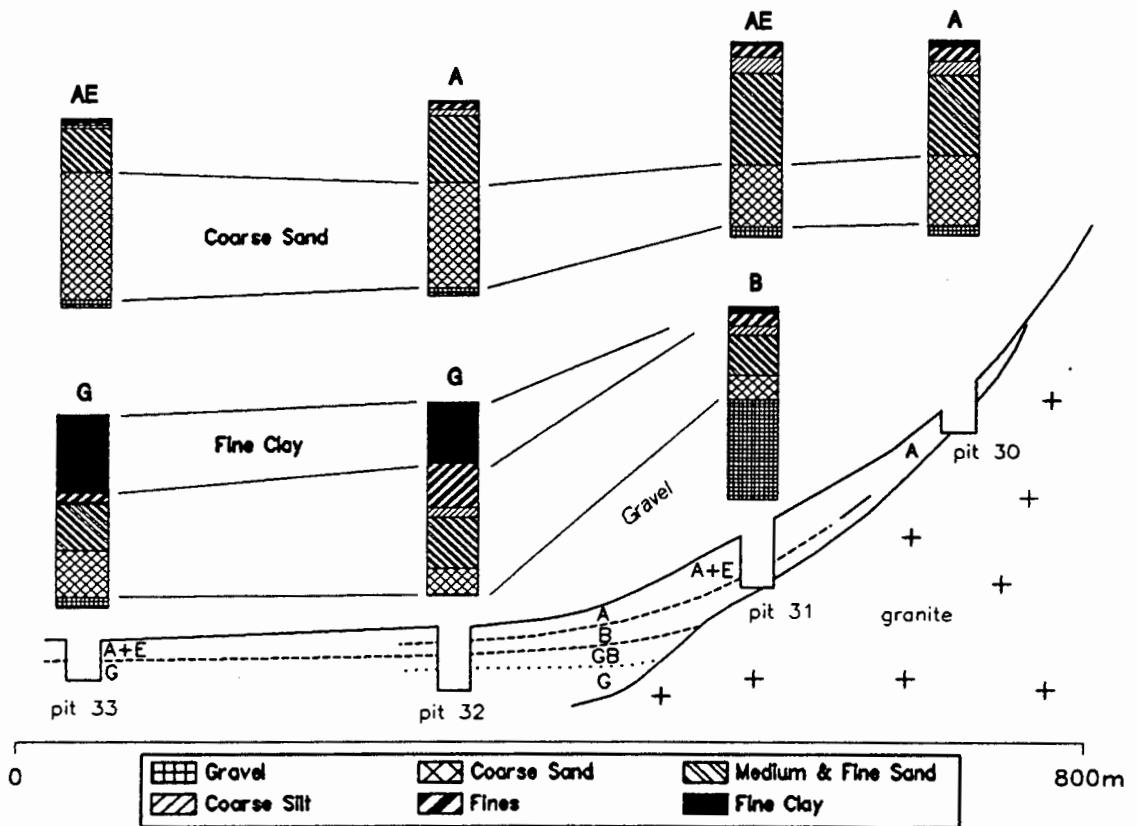


**Figure 4.3:** Particle size distributions of the samples taken from the granitic toposequence at Klipberg. The full size of each bar represents 100 weight % of the inorganic soil fraction. AE refers to a composite sample of the A- and the E-horizons. The particle size distribution of the top 15 cm of the soil profiles are not shown because they are similar to those of the corresponding A-horizons. The data for the top 15 cm are given in Appendix-III.

**Lateral eluviation by means of throughflow:** The particle size distribution of the soil at the upper limit of the soil cover (Pit 30) probably reflects the particle size distribution of the material available from the weathering granite above the soil cover. In contrast to this particle size distribution the subsoil in the steepest slope position consists mainly of sesquioxide gravel (sample 31B in Figure 4.3). The high gravel content, the steep gradient of the slope at Pit 31 and the underlying impermeable granite are strong indications for lateral eluviation being a major soil forming factor for this horizon. Eluviation probably depleted all particles smaller than gravel and, therefore, relatively enriched the horizon in gravel. In spite of the strong eluviation of this horizon, and due to the presence of coarse Fe-oxide concretions, it was decided to classify this horizon as a soft plinthic B-horizon (Figure 4.8: text box 3).

**Illuvial character of the subsoil at Pit 32:** The gravel fraction of the G-horizon at Pit 32 at the footslope of the toposequence (sample 32G) is very small and consists of rounded, and thus most likely transported, quartz grains. An *in situ* formation of this

horizon is, therefore, unlikely. It is thus proposed that the subsoil of Pit 32 is primarily the result of the deposition of material that was eluviated further up the toposequence (Figure 4.8: text box 4). The illuvial subsoil at Pit 32 has higher proportions of fines, coarse silt, medium sand and fine sand than the subsoil which is more distant from the steeper slope (Pit 33), probably indicating that the illuviation at Pit 32 resulted mainly in the accumulation of these particle size classes.

***In situ* character of the subsoil at Pit 33:** The differences between the particle size distributions of the subsoils at Pit 33 and Pit 32 suggest that the physical processes that were involved in their formation differ substantially (Figure 4.3). Sample 33G contains more gravel, coarse sand and fine clay than sample 32G. The smaller proportions of fines, coarse silt, medium sand and fine sand probably indicate that the proposed transport of particles eluviated from the upper part of the toposequence and deposited in the subsoil of Pit 32, does not reach as far as Pit 33. Gravel, coarse sand and fine clay are, therefore, relatively enriched.

**Comparison with other authors:** Munnik *et al.* (1992) investigated soils on hillslopes in a South African granite landscape and found sequences of soils which are similar to the Klipberg toposequence. Well drained soils were found in the higher slope positions and plinthic subsoils occurred in the midslope. The downslope profiles showed signs of wetness. The gradient of the investigated hillslopes was similar to the gradient of the Klipberg toposequence (average 75 ‰) and lateral flow of water was postulated. Nyamapfene (1986) investigated toposequences in Zimbabwe associated with gneiss and granite and postulated that throughflow causes the eluviation, transport and deposition of clay. Purves (1976) concluded from his field work and laboratory experiments that dispersed clay is transported by means of throughflow. He found that clay can be dispersed at exchangeable sodium percentages (ESP) lower than four and that dispersed clay is especially mobile in a coarse sand matrix.

**Conclusion:** It was demonstrated that lateral transport of particles in toposequences by means of throughflow, as proposed for the Klipberg toposequence, is a process also described elsewhere. It is, however, not described in the literature that particles as coarse as medium sand were subjected to lateral eluviation, transportation and illuviation. The lateral dislocation of medium sand in the Klipberg toposequence would suggest a very rapid flow of water through the very permeable, soft plinthic B-horizon in the steepest part of the toposequence (Pit 31). The geochemical results substantiated the important role of throughflow in the Klipberg toposequence (section 4.5.5.).

#### 4.4. MAJOR SOIL COMPONENTS

**Mineralogy:** XRD analyses showed that quartz is the most abundant mineral component. Plagioclase and orthoclase are abundant mineral components at the top of the toposequence. The soil further down the toposequence contains only small proportions of feldspars. The very fine-textured G-horizon at the bottom of the toposequence additionally contains detectable amounts of kaolinite (Chapter 3).

**Elemental composition and organic matter:**  $\text{SiO}_2$  is the most abundant component. Its concentration varies between 67 and 95 percent.  $\text{Al}_2\text{O}_3$  is generally the second most abundant constituent, ranging between 1.5 and 18 percent. Other abundant constituents are  $\text{K}_2\text{O}$ ,  $\text{Fe}_2\text{O}_3$  and  $\text{Na}_2\text{O}$ . The mean concentrations of the remaining elements are lower than 0.2 percent. The proportion of organic matter ranges between 0.1 and 2.4 percent (Table 4.1).

**A- and E-horizon:** The proportion of  $\text{SiO}_2$  within the topsoil increases from the top to the bottom of the toposequence while the concentrations of the other major elements decrease. The topsoil contains 74 %  $\text{SiO}_2$  at the top of the toposequence (Pit 30) and 95 %  $\text{SiO}_2$  at the bottom of the toposequence (Pit 33). The concentrations of  $\text{K}_2\text{O}$  and  $\text{Na}_2\text{O}$  decrease from approximately 4 to less than 1 percent. The concentration of  $\text{Al}_2\text{O}_3$  decreases from 13 to 1.5 % and the concentration of  $\text{Fe}_2\text{O}_3$  decreases from 1.8 to 0.8 % (Figure 4.4).

**High concentrations of  $\text{Fe}_2\text{O}_3$  and  $\text{Al}_2\text{O}_3$  in the subsoil:** The subsoil of Pit 31 was observed in the field to contain many sesquioxide concretions. This accumulation of sesquioxides in the subsoil resulted in the highest  $\text{Fe}_2\text{O}_3$  concentration found (5.5 %). The highest concentration of  $\text{Al}_2\text{O}_3$  coincides with high proportions of mud and kaolinite in the subsoil at the bottom of the toposequence (samples 32G and 33G).

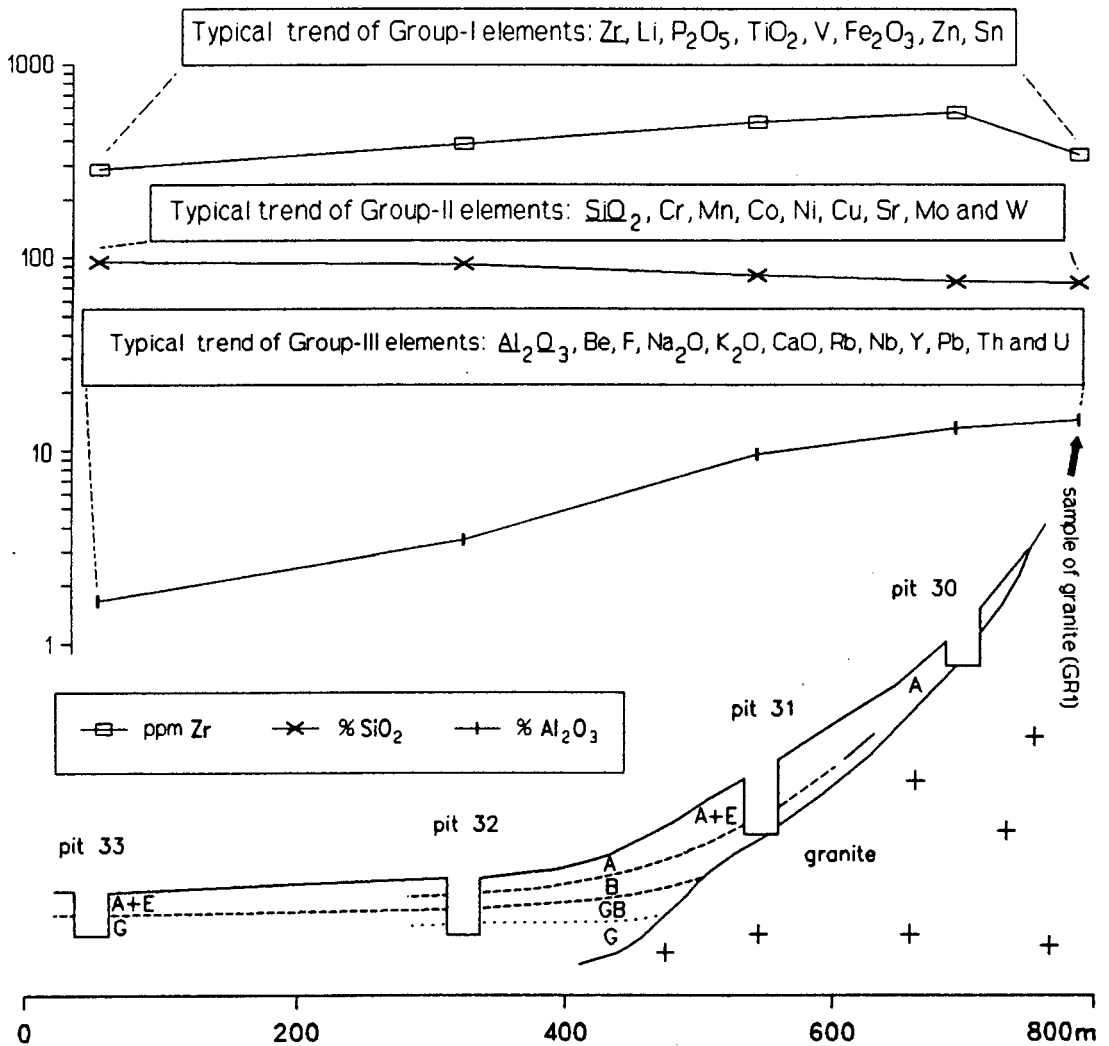


**Figure 4.4:** Change of the  $\text{Al}_2\text{O}_3$ ,  $\text{SiO}_2$  and Zr concentrations from the exposed granite down the topsoil (samples GR1, 30A, 31AE, 32A and 33AE). The increase of the Zr concentration from the granite to the topsoil and its decreasing concentration down the toposequence is typical for all elements in Group-I. The rather small variation of  $\text{SiO}_2$  is typical for all elements in Group-II. The continuously decreasing concentration of  $\text{Al}_2\text{O}_3$  is typical for all elements in Group-III.

#### 4.5. FACTORS WHICH DETERMINE THE LATERAL AND VERTICAL CHANGES OF THE CONCENTRATIONS

**Discussion of elements in groups:** The elements were allocated to groups in order to facilitate their discussion. The manner in which the elements were grouped is explained in section 1.2. The elements were allocated to four groups:

(Group-I) Elements with increasing concentrations from the granite to the uppermost part of the toposequence and decreasing concentrations towards the footslope (Figure 4.4; section 4.5.2.).

(Group-II) Elements with relatively constant concentrations. Some of the elements in this group have slightly increasing or decreasing concentrations from the granite to the footslope. The enrichment factors, however, are  $< 1.4$  and  $> 0.8$  (Figure 4.4; section 4.5.3.).

(Group-III) Elements with continuously decreasing concentrations from the granite to the footslope (Figure 4.4; section 4.5.4.).

(Group-IV) Elements which have strongly increasing concentrations from the granite to the soil (Figure 4.5; section 4.5.5.).

The leachable portions of the elements and the elements which could not be assigned to groups are discussed in sections 4.5.6. and 4.5.7., respectively. It is important to note that not all elements are in perfect agreement with the patterns described for their groups.

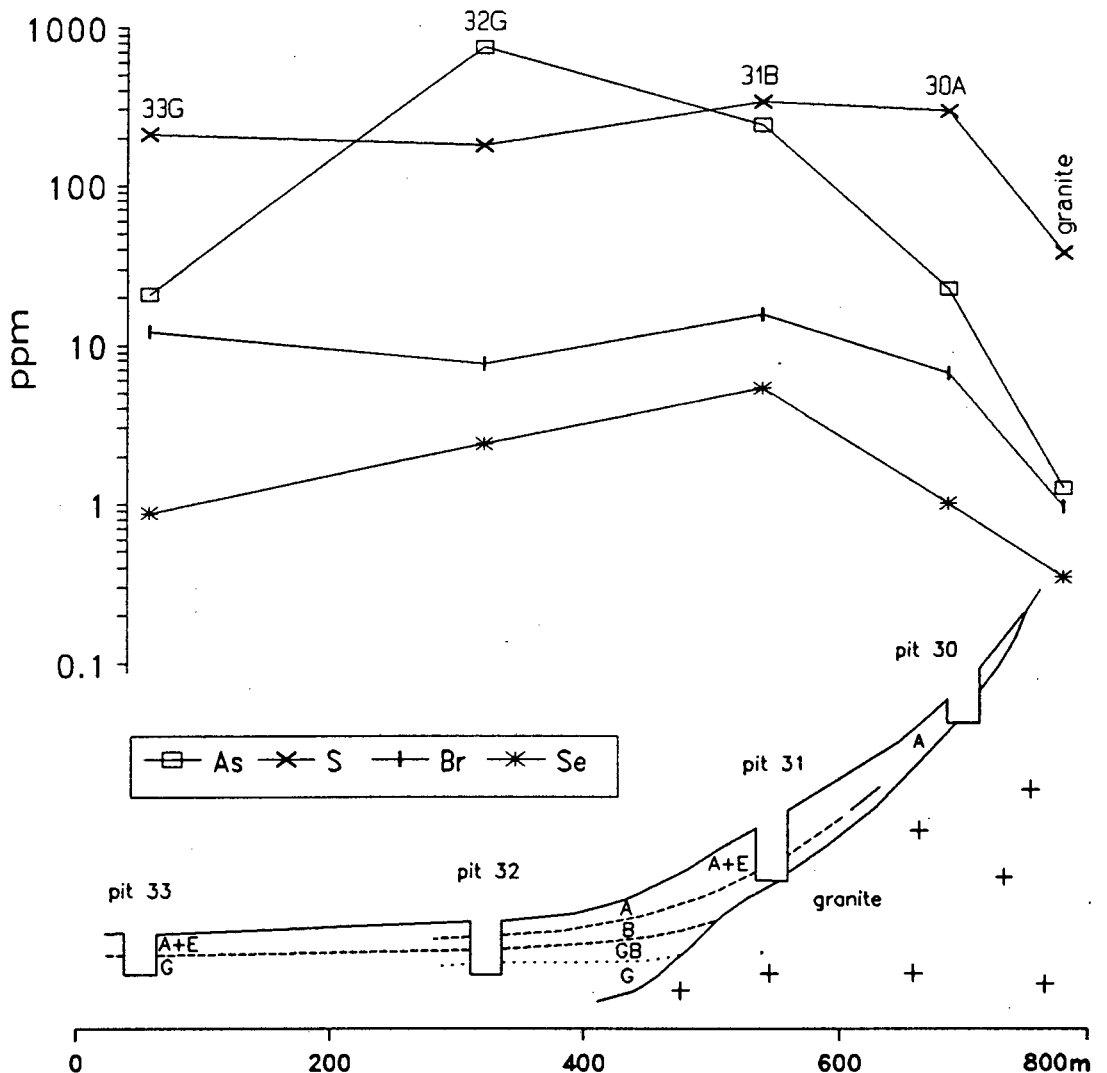


**Figure 4.5:** The concentrations of As, S, Br and Se (Group-IV) from the granite to the topsoil of Pit 30 and further to the subsoils of Pits 31, 32 and 33 in ppm (samples GR1, 30A, 31B, 32G and 33G). The graphs show the strong accumulation of Group-IV elements in the soil.

#### 4.5.1. Loss and gain of elements during soil formation

**Real loss(gain) of an element:** Changes in the concentration of a particular element from a less to a more weathered sample may be due to loss(gain) of other elements, especially major elements. An attempt was made to calculate the real loss(gain) of an element from concentrations which were corrected for this effect.

**Suitability of TiO<sub>2</sub> concentrations for calculating the real loss(gain) of elements during weathering:** Titanium occurs in soils chiefly in the form of insoluble, rock-derived minerals (Vinogradov, 1959; Scheffer and Schachtschabel, 1989). Common Ti minerals in soils are ilmenite, anatase and rutile. The portion of Ti which is released by minerals which are less resistant to weathering (e.g. biotite and amphibole) precipitates as TiO<sub>2</sub> (Scheffer and Schachtschabel, 1989). Loss and gain of Ti during weathering is, therefore, minimal. Titanium concentrations are thus suitable to correct the difference between concentrations in more and less weathered samples for loss and gain of other elements, provided no other mechanism for removing(adding) Ti is operating. The corrected difference is referred to as the real loss(gain) of a particular element during soil formation. An equation was formulated to calculate the real loss(gain) of an element (Equation 7). The suggested calculations are similar to the procedure given in Krauskopf (1979).

$$\text{Loss (Gain)} = \left[ \left[ \frac{\text{El } c_m}{\text{El } c_l} \cdot \frac{\text{Ti } c_l}{\text{Ti } c_m} \right] - 1 \right] \cdot 100 \quad (\text{Equ. 7})$$

Where:

Real Loss (Gain)	=	real loss (gain) of a particular element from a less to a more weathered sample in %
El c <sub>m</sub>	=	elemental concentration in the more weathered sample
El c <sub>l</sub>	=	elemental concentration in the less weathered sample
Ti c <sub>m</sub>	=	titanium concentration in the more weathered sample
Ti c <sub>l</sub>	=	titanium concentration in the less weathered sample

**Limitations and possible sources of error:** The distribution of TiO<sub>2</sub> in the granite-derived toposequence at Klipberg indicates depletion and accumulation of TiO<sub>2</sub> as a result of eluviation from the topsoil and illuviation into the subsoil (section 4.5.2.). It may be assumed that the effect of this process is minimal in the uppermost part of the

toposequence (Pit 30) because the soil in this part of the toposequence consists of one (uniform) soil horizon (Figure 4.1). Conclusions with respect to real loss and gain of elements using  $\text{TiO}_2$  concentrations as a reference concentration are thus restricted to the changes from the granite to the uppermost part of the toposequence.

Possible sources of error are (a) dissolution and loss of minor quantities of Ti from weathering resistant Ti minerals (Ajmone Marsan *et al.*, 1988), (b) the slightly weathered state of the sampled granite and (c) the possible lateral eluviation of relatively fine particles from the soil at the top of the toposequence due to throughflow, as described by Purves (1976). Error (a) would result in underestimation of the loss of all elements. Error (b) would result in underestimation of the loss of soluble elements. Error (c) would result in overestimation of the loss of those elements which are enriched in the finer soil fraction.

**Calculation of the real loss(gain) of elements from the exposed granite to the uppermost part of the soil cover:** The uppermost part of the toposequence has a steep gradient and consists of a coarse-textured A-horizon (Figure 4.1; section 4.3). It is assumed that the material contained in the A-horizon at the upper limit of the soil cover (Pit 30) originates from the granite exposed above the toposequence. The real loss(gain) of elements from the granite to the uppermost part of the soil cover was calculated according to Equation 7 and is presented in Figure 4.6.

The gained portion of an element probably originates from percolating rock leachates (e.g. As and S). Elements supplied by rock leachates may be become adsorbed or incorporated into organic matter and secondary soil minerals. High losses are best explained by soil leaching (e.g. Ca and Na). Both processes, precipitation and leaching, indicate a certain solubility of the corresponding elements. Elements of which only minor portions were lost(gained) are probably hosted by less soluble compounds (e.g. P and Zr). Alternatively, such elements may be released from their primary hosts but fully retained by other soil components such as clay, Fe-oxides and organic matter. This will be discussed for individual elements in sections 4.5.2. to 4.5.5. and in Chapter 9.

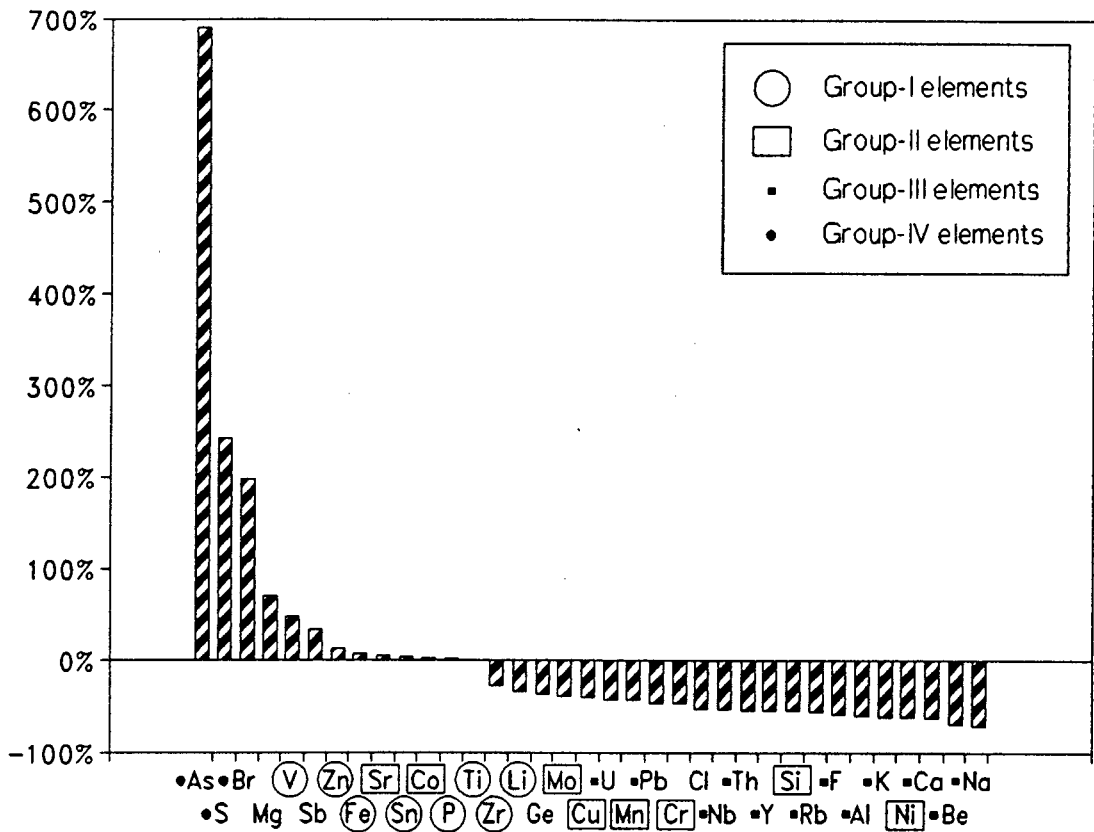


**Figure 4.6:** Real loss and gain of elements from the granite (sample Gr1) to the uppermost part of the toposequence (sample 30A) in percent. Titanium concentrations were used to correct for the relative changes in concentration due to loss(gain) of other elements, especially major elements, in order to calculate the real loss(gain) of elements (Equation 7).

#### 4.5.2. Group-I: Li, $P_2O_5$ , $TiO_2$ , V, $Fe_2O_3$ , Zn, Zr and Sn

**Observations:** Figure 4.6 shows that the real loss(gain) of the elements in Group-I from the granite to the uppermost part of the toposequence is relatively small. The concentrations of the elements in Group-I increase from the granite (sample Gr1) to the uppermost part of the topsoil (sample 30A; Figure 4.4). The concentrations in the topsoil generally decrease from the top to the bottom of the toposequence (samples 30A to 33AE). The concentrations of the Group-I elements generally increase from the topsoil to the fine-textured and(or) Fe-oxide-enriched subsoils (Table 4.5).

**Relative accumulation of Group-I elements from the granite to the uppermost part of the toposequence:** Titanium and Zr are chiefly hosted by insoluble minerals (Vinogradov, 1959). The increasing concentrations of these elements from the granite to the uppermost part of the toposequence are, therefore, best explained by loss of major elements. Figure 4.6 shows a small loss of Zr from the granite to the uppermost part of the toposequence. This loss could be the result of (a) preferential eluviation of Zr-hosts from the soil at the top of the toposequence due to throughflow (section 4.5.1.;

possible sources of error) or (b) partial dissolution of zircon. Partly weathered zircons in granitic soil were observed by Purves (1976).

Iron, Zn, Sn and Li can be hosted by minerals that may or may not be resistant to weathering. The similar behaviour of these elements and the other Group-I elements indicates that Fe, Zn, Sn and Li ions were not leached from the soil, even if they were released during the weathering of the detritus in the uppermost part of the toposequence. The Fe needed to form the abundant Fe-oxide concretions in the subsoil further down the toposequence (Pit 31) may originate from (a) deeper leaching of the granite above the toposequence and (b) leaching of the topsoil above Pit 31 (Figure 4.8: text boxes 2 and 7).

The most common inorganic host of P in rocks and soils is apatite (Scheffer and Schachtschabel, 1989). It may thus be presumed that the Klipberg granite supplies P to the toposequence mainly in the form of apatite. Apatite is unstable if the pH of the soil is lower than 7 (Scheffer and Schachtschabel, 1989). The pH of the uppermost part of the toposequence is in the acidic range ( $\text{pH}(\text{KCl}) = 4.3$ ), suggesting that P ions may be released from weathering apatite. However, the correlation of  $\text{P}_2\text{O}_5$  with the insoluble Group-I elements suggests that any P ions which were released during the weathering of apatite were fixed by other soil compounds such as organic matter and Fe-oxides. Association of P with Fe-oxides is also demonstrated in Table 4.5 and was reported by various authors which are reviewed by Torrent (1994).

**Vanadium:** Vanadium in granites may be hosted by minerals susceptible to weathering (e.g. mica and sulfides) or resistant to weathering (e.g. titanite; Landergren, 1974). A comparison with the literature showed that the weathered sample of the granite which formed the parent material of the granite-derived toposequence has a very low V concentration (2.5 ppm; Table 9.1). The subsoils with high proportions of secondary soil minerals (Fe-oxides and kaolinite) have relatively high V concentrations (32 to 36 ppm). It is open to speculation whether (a) the fresh granite has a normal V concentration (44 to 88 ppm; Table 9.1) and the low concentration in the weathered sample of the granite reflects the loss of V during the early stages of weathering or (b) the fresh granite has a low V concentration.

The conspicuous accumulation of V with secondary soil minerals indicates that the primary host of V did release V and, therefore, favours hypothesis (a). The hypothesis that the primary host of V released V during early weathering could also explain the (real) gain of V from the granite to the uppermost part of the derived toposequence, because V leached from the granite above the toposequence could be retained by secondary soil minerals and soil organic matter at the top of the toposequence (Figure 4.6). This process would be in agreement with the solubility of vanadium in the oxidised state and its affinity with Fe-oxides and organic matter, as proposed by other authors (section 9.13.).

The results obtained for the Group-IV elements (S, As and Se; section 4.5.5.) are best explained by postulating the early oxidation of sulfides during the weathering of the granite and leaching of the associated trace elements. Pyrites and other sulfides were shown to host considerable portions of V in sediments, particularly shales (Landergrén, 1974). It may, therefore, be speculated that sulfides are an important host of V in Klipberg granite, and that their oxidation resulted in release of soluble V.

It is concluded that (a) minerals susceptible to weathering are an important host of V in the granite and (b) the oxidation of these minerals results in water-soluble forms of V. Mobilised V was fixed by secondary soil minerals and organic matter or leached into the ground water.

**Loss of Group-I elements from the topsoil as a result of eluviation of detritus with a particle size smaller than 0.5 mm:** The results discussed in section 4.5.4. indicated that (a) the whole topsoil is subjected to gravitational transport and (b) any particles smaller than 0.5 mm are continuously eluviated from the topsoil during its gravitational transport to the bottom of the toposequence. The increasing loss of finer particles coincides with the decrease of the concentrations of the elements in Group-I described above. This correlation is best explained by proposing that the hosting minerals of the Group-I elements occur mainly in particles smaller than 0.5 mm and are thus continuously eluviated from the topsoil. This hypothesis is in agreement with (a) Vinogradov (1959) who observed that Ti may be present to a larger extent in the colloid fractions than in the coarser fraction and (b) the fact that the concentrations of the Group-I elements normally increase from the top- to the subsoil. Leaching of the Group-I elements from the topsoil is less likely because they are mainly hosted by insoluble substances.

**Tin pollution by means of agro-chemicals:** The concentration of Sn in the topsoil increases from Pit 32 (5 ppm) to Pit 33 (65 ppm) while the concentrations of the other Group-I elements decrease. The high Sn concentration in the topsoil of Pit 33 is possibly a result of soil treatment with agro-chemicals (Chapter 9).

**Particle size of zirconium minerals:** The eluviation of Zr from the topsoil did not result in higher Zr concentrations in the fine-textured subsoil (Table 4.5). The sample of the relatively coarse-textured GB-horizon of Pit 32 (sample 32GB) is the only one which contains more Zr than the topsoil and the granite. The high Zr concentration in sample 32GB coincides with the highest proportion of medium and fine sand observed in the Klipberg toposequence (60 % particles < 0.5 mm and > 0.053 mm). It was suggested above that medium and fine sand was eluviated from the upper part of the toposequence and accumulated in the vicinity of Pit 32 (section 4.3). The similar behaviour of medium sand, fine sand and Zr suggests that most of the zircons and (or) other zirconium minerals in the Klipberg toposequence have a particle size ranging between 0.053 mm and 0.5 mm. The almost exclusive occurrence

of Zr in the form of sand-sized zircons was also observed by Moura and Kroonenberg (1988).

#### 4.5.3. Group-II: SiO<sub>2</sub>, Cr, Mn, Co, Ni, Cu, Sr, Mo and W

**Observations:** Figure 4.6 shows significant losses of all Group-II elements, except for Sr, Co and W, from the granite to the uppermost part of the toposequence. The loss ranges between 40 % for Mo and 61 % for Ni. A loss of 55 % was calculated for SiO<sub>2</sub>.

The variation of the concentrations of the Group-II elements down the topsoil is generally small. The concentration of SiO<sub>2</sub> increases from the top to the bottom of the toposequence while the concentration of Mn decreases slightly (Figure 4.4). Many of the elements in Group-II have relatively high concentrations in the organic-rich top 15 cm of the soil profiles and in the fine-textured and(or) Fe-oxide-enriched subsoil (Table 4.5).

**Loss of Group-II elements and solubility of hosting minerals:** The losses from the granite to the uppermost part of the toposequence are best explained by leaching. The leaching of elements may have occurred (a) during the weathering of the granite, (b) during the gravitational transport of the detritus from the granite above the toposequence to the soil or (c) in the soil. The losses of most elements in Group-II are smaller than the loss of SiO<sub>2</sub>, indicating that the hosting minerals were less soluble than SiO<sub>2</sub> but more soluble than TiO<sub>2</sub>.

**Even distribution of Group-II trace elements in the topsoil:** The increasing concentration of SiO<sub>2</sub> in the topsoil from top to the bottom of the toposequence is due to the loss of most of the other major elements (section 4.4.). The concentrations of the trace elements of Group-II in the topsoil vary only within a relatively small range, indicating that the hosting minerals are neither enriched nor depleted relatively to SiO<sub>2</sub>. This confirms that the hosts of most Group-II elements have solubilities similar to SiO<sub>2</sub>.

**Strontium:** Strontium should be susceptible to weathering because it commonly substitutes Ca in the relatively soluble plagioclase. The association of Sr with the other Group-II elements may indicate that Sr is hosted mainly by minerals more resistant to weathering. Alternatively it could be speculated that Sr ions released from their primary hosts (e.g. plagioclase) are retained to become a constituent of secondary soil minerals or organic matter.

**Separation of Fe and Mn:** The formation of Fe-oxide concretions in the subsoil of Pit 31 did not result in higher Mn concentrations, suggesting that the Mn which was leached with the Fe at higher elevation did not precipitate with Fe but was removed in the ground water. This is in agreement with Scheffer and Schachtschabel (1989) who state that Mn is commonly more easily leached than Fe.

**Tungsten:** The concentrations of W in the granite and the derived soil are much higher than W levels recorded in the literature (Table 9.1). The concentration increases from 52 ppm in the granite to 426 ppm in the top 15 cm of the soil profile at Pit 30.

The composite sample of the topsoil at Pit 30 has a much lower W concentration (18 ppm), indicating a sharp decrease of the W concentration from the top 15 cm of the soil profile to the lower topsoil. The W concentrations further down the toposequence range between 10 and 35 ppm. High W concentrations and wolframite mineralisations associated with Western Cape granites are also reported in Robson (1980) and Scott (1969). In these studies it was observed that high W concentrations normally coincide with high Sn concentrations. The Sn concentration in the sample of the Klipberg granite, however, is only slightly higher than the background concentration, as reported by other authors (Table 9.1). A possible mechanism for the observed concentration of W in the top 15 cm of the soil profile is discussed in the following paragraph.

The results presented in section 4.5.5. (S, As, Se and Br) are best explained by assuming that the granite above the toposequence contains sulfides which are oxidised during the early stages of weathering. It was suggested that this oxidation would lower the pH of the rock leachates. Krauskopf (1970) reports that W minerals are slowly attacked by acid surface waters, especially by the strongly acid waters of weathering sulfide deposits. Tungsten released by acid attack is probably partly dissolved as  $\text{HWO}_4^-$ . Movement of W in near-surface solutions is shown by the existence of "haloes" in soils around ore deposits. It is thus reasonable to postulate that acidic leachates from the granite above the toposequence supply the soil with W. The surface run-off from the exposed granite infiltrates the toposequence through the topsoil at Pit 30 (Figure 4.8). The chemical interaction between the run-off and the soil could result in instant changes of the Eh(pH)-conditions and may thus cause precipitation of W. Adsorption of W by Fe-oxides, clay minerals and organic matter may also cause the observed accumulation (Swaine, 1990; Krauskopf, 1970). Further research is needed to substantiate this hypothesis. This should include a confirmation of the analytical results and the identification of the tungsten-hosting components in rock and soil.

#### **4.5.4. Group-III: Depletion of Be, F, $\text{Na}_2\text{O}$ , $\text{Al}_2\text{O}_3$ , $\text{K}_2\text{O}$ , CaO, Rb, Y, Nb, Pb, Th and U during soil formation**

**Observations:** Figure 4.6 shows major losses of the elements in Group-III from the granite to Pit 30. The losses range between 43 % for U and 72 % for  $\text{Na}_2\text{O}$ .

The concentrations of the Group-III elements decrease from the granite to the soil in the uppermost part of the toposequence and further to the topsoil in the lower slope positions (Figure 4.4). Except for  $\text{Na}_2\text{O}$ ,  $\text{K}_2\text{O}$  and Be, all elements have higher concentrations in the fine-textured subsoil than in the granite and the topsoil (Table 4.5). The decrease of the concentrations from the top to the bottom of the toposequence coincides with (a) decreasing proportions of feldspars (section 4.4.), (b) increasing proportions of coarse sand and decreasing proportions of all other particle size classes (Figure 4.3), (c) decreasing concentrations of Group-I elements and (d) increasing  $\text{SiO}_2$  concentrations (section 4.5.3.).

**Hypothesising gravitational transport and continuous weathering and leaching of the topsoil down the slope:** The loss of feldspars,  $\text{Na}_2\text{O}$ ,  $\text{Al}_2\text{O}_3$ ,  $\text{K}_2\text{O}$  and  $\text{CaO}$  down the toposequence implies that the degree of weathering increases down-slope. It was suggested that the exposed granite continuously supplies relatively fresh mineral detritus to the soil at the top of the toposequence (section 4.3.). As discussed below, the soil is probably subjected to gravitational transport. Weathering, leaching and eluviation results in depletion of (a) feldspars, (b) Group-I elements, (c) Group-III elements and (d) particles finer than coarse sand. This depletion causes relative accumulation of coarse sand and  $\text{SiO}_2$  as the soil moves down the slope.

**Sheet wash as an alternative hypothesis to explain observed lateral trends:** It may be argued that transport of particles by overland and(or) shallow flow of water during rain storms, referred to as sheet wash (Selby, 1982), caused the lateral trends described above. Gerrard (1992) quotes Webster (1965) who describes a complex situation in Zambia where erosion by sheet wash is greatest on the lower steeper parts of the slope leading to preferential removal of fine particles and leaving a coarse grained soil at the base of the slope. A similar process could explain the continuous coarsening of the topsoil down the Klipberg toposequence if the energy of the sheet wash would be sufficient to transport particles as coarse as medium sand beyond the lowermost pit (Pit 33). It is, however, suggested that sheet wash was not a process of major importance for the Klipberg toposequence because (a) the coarse texture of the topsoil facilitates fast infiltration and limits overland flow and (b) the almost level terrain in the lowermost slope position would probably not allow for overland flow, if it existed to be, turbulent enough to transport particles as coarse as medium sand. The possibility of predominantly vertical leaching and eluviation of the topsoil during gravitational transport was thus investigated in greater detail.

**Rates and importance of gravitational transport as reported by other authors:** Various other authors report gravitational transport as an important process in toposequences. The average slope of the Klipberg toposequence is 75 permille. The steepest part of the toposequence between Pits 30 and 32 is 124 ‰ or 7°. Scheffer and Schachtschabel (1989) reported that toposequences which have gradients steeper than 20 ‰ are commonly subjected to gravitational transport. Schumm (1967) showed that surficial rock creep on a slope approximately equivalent to the steepest part of the Klipberg toposequence may range between 10 and 20 mm per year. Williams (1974) found that the mean rate of surficial rock creep ranges between 1 cm per year on a 3° (50 ‰) slope and 3 cm per year on a 18° (320 ‰) slope. A comparative study suggested that these mean rates were not affected by contrasting climates. It is, however, important to note that the rate of surficial rock creep would overestimate the rate of soil movement. Buol *et al.* (1980) quotes Troeh (1975) who reported 11.5 mm soil movement at 15 cm depth and 1.2 mm movement at 105 cm depth in two years on a 40 ‰ slope.

Purves (1976) found evidence for colluvial action in granite-derived toposequences in Zimbabwe. In contrast to the Klipberg toposequence, the investigated toposequences showed a decreasing degree of weathering down the slope. Purves concluded that any soil added was at a similar stage of weathering to the recipient soil. Munnik *et al.* (1992) investigated granite-derived toposequences in South Africa and found signs of substantial mass movements. The gradients of the investigated toposequences are similar to the gradient of the Klipberg toposequence. They reported an average increase of the coarse sand fraction and a decrease of the clay fraction down the topsoil of the toposequence, similar to this study. Swanson (1985) investigated toposequences on moraines and found that soils are transported by creep. From his observations he concluded that the soil material undergoes weathering throughout its movement down the slope. The soils on the shoulder are thus less developed than the soils in footslope position.

**Conclusion:** The reviewed literature demonstrated that the slope of the Klipberg toposequence (average 75 ‰) is steep enough to experience gravitational transport. The coarse texture (gravel) and the loose consistency (lack of a cohesive clay matrix) of the soil in the upper parts of the toposequence would facilitate such transport.

It was further shown that gravitational transport of soil down toposequences was reported by other authors and resulted in lateral changes of the soil properties similar to those observed in this study. It is thus suggested that continuous weathering and eluviation during gravitational transport is an acceptable explanation for the results stated above. The hypothesis must be regarded as provisional until gravitational transport can be confirmed by direct field evidence (e.g. disturbed horizonation).

**Type and extent of gravitational transport:** Accepting the hypothesis of gravitational transport it may be asked which form of gravitational transport takes place, which soil horizons are affected by the transport and at what slope position the transport terminates. No definitive answers can be offered because of the lack of data from more observation points. Some aspects of the problem, however, are discussed below. The transport of the soil may be due to creep or runoff creep, the latter being defined as relatively slow movement of coarse material induced by runoff (Ploey and Moeyersons, 1975). Ploey and Moeyersons showed runoff creep to be particularly effective in moving sandy materials and granite gruss. In the upper slope positions coarse textured (gravelly) and loose soil that lacks a cohesive clay matrix directly overlies granite. It could, therefore, be speculated that in the upper slope positions all soil horizons are subjected to transport.

**Eluviation of Pb, Nb, Th, Y and U in form of detritus:** Figure 4.6 suggests that the hosts of Pb, Nb, Th, Y and U have solubilities slightly lower than SiO<sub>2</sub>, while the hosts of the remaining elements in Group-III have higher solubilities than SiO<sub>2</sub>. The decreasing concentrations of the Group-III elements down the topsoil, however, suggest that all Group-III elements are depleted relative to the most abundant soil component SiO<sub>2</sub>. It may thus be speculated that the loss of Pb, Nb, Th, Y and U from the topsoil

is partly due to eluviation of these elements in form of detritus rather than in a dissolved form.

#### 4.5.5. Group-IV: Accumulation of S, As, Se and Br in the soil

**Observations:** Figure 4.6 shows that the elements As, S and Br were added to the soil at the top of the toposequence. The concentrations of all Group-IV elements increase markedly from the granite to the uppermost part of the toposequence (Pit 30) and further to the subsoil of Pit 31 (Figure 4.5). Arsenic reaches its maximum concentration in the fine-textured subsoil at Pit 32 (743 ppm) while all other Group-IV elements reach their maximum concentration in the Fe-oxide-rich subsoil at Pit 31. The concentrations of As and Se decrease with increasing distance from the footslope (Pit 32 to 33).

**Possible sources of Group-IV elements:** The large increase in the concentrations from the granite to the soil suggests the accumulation of Group-IV elements from soil water. The Br, Se, As and S in the soil water may originate from the atmosphere and(or) deeper leaching of the granite above the toposequence (Vinogradov, 1959; Sposito, 1989; Scheffer and Schachtschabel, 1989). Bromine is more likely to originate from the atmosphere while Se and As are more likely to originate from the granite. This is discussed in more detail in Chapter 9. In the granite the elements As, Se, and S may occur together in primary sulfides (Vinogradov, 1959; Chapter 9).

#### **Possible concept for the accumulation of Group-IV elements in the soil:**

(a) Sulfides are common constituents of granites and are easily oxidised in the weathering environment (Rösler, 1981). It may thus be assumed that the primary sulfides present in the granite are oxidised during the early stages of weathering. This process may take place well below the present rock-surface. The oxidation lowers the pH of the weathering solution and results in formation of soluble selenites, arsenates and sulfates (Vinogradov, 1959). The lowering of the pH could permit the dissolution of Fe, even in the proposed oxidising conditions. The soluble compounds of the Group-IV elements are leached from the granite (Figure 4.8: text box 7). This is in agreement with the very low S concentration in the sample of the slightly weathered granite (Table 9.1). In order to test the proposed leaching of S, As, Se and Fe from the granite it would be interesting to test whether the concentrations of these elements in the granite increase with increasing depth (see also section 9.20.).

(b) The rock leachates infiltrate into the soil and cause the observed eluviation of the subsoil in the steeper section of the toposequence (Pit 31). The reaction of the leachates with weathering soil minerals causes higher pH values (Scheffer and Schachtschabel, 1989). Increasing pH values may form a geochemical barrier which could initiate the precipitation of the Fe-oxide concretions observed in the B-horizon at Pit 31 (Kasimov and Perel'man, 1994). Arsenic, Se and S were reported by Vinogradov (1959) to coprecipitate readily with secondary  $\text{Fe}(\text{OH})_3$ . It is proposed that this process caused the high concentrations of Group-IV elements in subsoil at Pit 31 (Figure 4.8: text box 3).

(c) The throughflow water reaches the footslope and percolates through the fine textured G-horizon at Pit 32 when the relief flattens out. The element load which remained in the throughflow water becomes partially adsorbed onto the clay minerals present in the G-horizon. It is interesting to speculate about the Fe-oxide concretions as an additional source of trace elements. The gravitational transport proposed in section 4.5.4. may also include the Fe-oxide concretions and their trace metal load, contributing to the gravel fraction in the B-horizon at the footslope (Pit 32). The high supply of throughflow water during winter probably causes longer periods of water saturation and a lack of oxygen at the footslope. This is reflected by the presence of a G-horizon, which by definition forms if reducing conditions prevail. Schwertmann and Taylor (1989) state that iron oxides can easily be remobilised through a reductive reaction. This takes place wherever and whenever  $O_2$  becomes deficient. It could thus be speculated that the Fe-oxide concretions breakdown when they reach the footslope. The decomposition could be a source of trace elements for the underlying G-horizon. The brown and grey mottles in the G-horizon could be possible remnants of the Fe-oxide concretions. The soft Fe-oxide concretions in the transitional GB-horizon could represent decomposing Fe-oxide concretions. This hypothesis, however, is speculative and more work needs to be carried out in order to determine whether (a) the Fe-oxide concretions are included in the gravitational transport and (b) the vertical succession from hard Fe-oxide concretions to soft concretions and further to mottles at the footslope (Pit 32) reflects the formation or the breakdown of the Fe-oxide concretions.

(d) The distinct decrease of the As and Se concentrations in the subsoil from Pit 32 to Pit 33 may indicate that the throughflow does not reach Pit 33. This is manifested in the disappearance of the eluviated, Fe-oxide-rich B-horizon between Pit 32 and Pit 33.

#### 4.5.6. Group-V: 1 M $NH_4NO_3$ extractable element fractions

The 1 M  $NH_4NO_3$  extractable concentrations of the elements were often below the LLD (Table 4.4). The values which were above the LLD indicated whether the extractable fraction of an element was associated mainly with Fe-oxides, kaolinite and(or) organic matter (Table 4.5). Magnesium, Ca, Al, K, Na and Ba are the only elements with extractable concentrations mostly above the LLD. The trends of their concentrations from the granite to the bottom of the toposequence (topsoil) are shown in Figure 4.7.

**Sodium and potassium:** The concentration of extractable Na and K is very high in the (pulverised) granite and declines rapidly towards the topsoil. This is in agreement with Matthes (1983) who states that the  $Na^+$  and  $K^+$  of feldspars is relatively easily soluble and Scheffer and Schachtschabel (1989) who state that the affinity of these cations for exchange sites in soils is relatively small.

**Calcium and magnesium:** The concentrations of extractable Ca and Mg increase from the (pulverised) granite to the topsoil. Krauskopf (1979) states that Ca and Mg

in rocks dissolve in larger amounts than other cations (e.g. Na and K). Pye (1986) found calcic plagioclase to be less stable in the weathering environment than K-feldspar. The affinity of  $\text{Ca}^{2+}$  and  $\text{Mg}^{2+}$  for exchange sites in soils is relatively large (Scheffer and Schachtschabel, 1989). In conclusion it is suggested that the increase of the concentrations from granite to soil reflects the leached state of the slightly weathered sample of the granite and the retention of extractable Ca and Mg in the soil. The relatively high concentrations of extractable Ca and Mg in the topsoil of Pit 31 coincide with the highest pH values of the Klipberg toposequence (pH(KCl) of top 15 cm = 5.8; pH(KCl) of sample 31AE = 5.2). The relatively high pH value may have caused a higher cation exchange capacity of the soil and could thus be the reason for the relatively high concentration of extractable Mg and Ca in the soil at this pit.

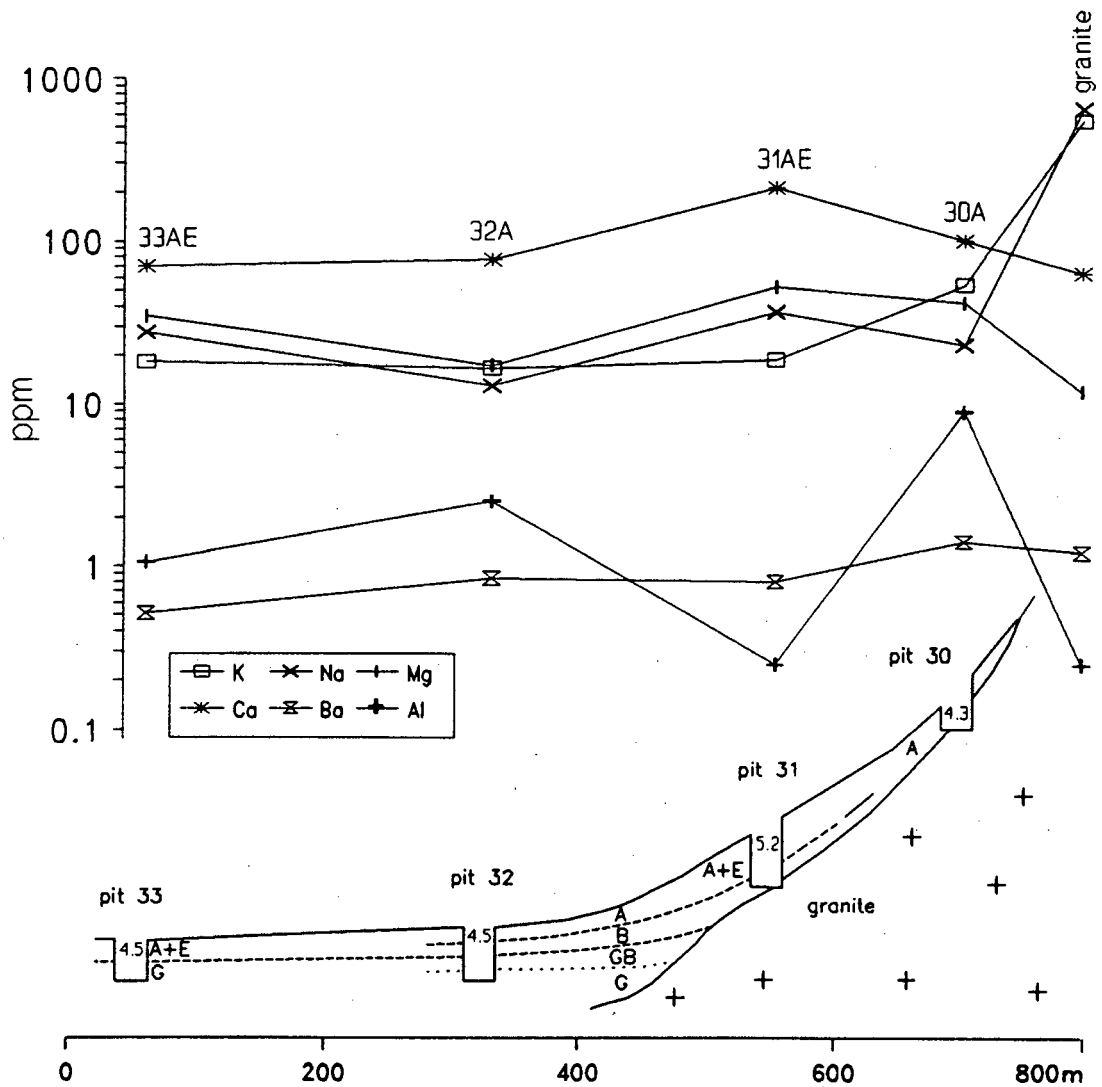


**Figure 4.7:** The concentrations of the 1 M  $\text{NH}_4\text{NO}_3$  extractable portions of K, Na, Mg, Ca, Ba and Al from the granite down the topsoil of the toposequence in ppm. The numbers in the pits refer to the pH(KCl) values of the topsoil.

**Barium:** The concentration of 1 M  $\text{NH}_4\text{NO}_3$  extractable Ba decreases continuously with increasing distance from the granite. A more detailed discussion of

extractable Ba is given in section 9.27. In this section it is suggested that K-feldspars are an important source of extractable Ba.

**Aluminium:** The concentration of extractable Al in the (pulverised) granite is small, indicating that Al is not easily released from its hosting minerals. The distribution of extractable Al in the topsoil seems to be determined by the soil pH. Samples with higher pH values have lower extractable concentrations than samples with low pH values (Figure 4.7). This observation is in agreement with Scheffer and Schachtschabel (1989) who state that a lowering of the pH results in release of  $Al^{3+}$  from oxides and silicates.

**Increase of 1 M  $NH_4NO_3$  extractable element concentrations in the G-horizon with increasing distance from the steeper slope of the toposequence:** The concentrations of the extractable element concentrations generally increase from the top- to the subsoil. All elements which had extractable concentrations above the LLD in the G-horizon showed increasing concentrations from Pit 32 to Pit 33 (Zn, Mg, V, Ca, Cr, Cu, Fe, Ni, Al, K, Na, P, S, Ba and Tl). This increase coincides with an increasing proportion of particles smaller than  $0.5 \mu m$  (Figure 4.3) and may, therefore, be linked to an increasing retention ability of the soil. The increase could also be the result of the strong leaching of the G-horizon near to the footslope (Pit 32; text boxes 5 and 6 in Figure 4.8).

#### 4.5.7. Elements which were not assigned to groups: Mg, Cl, Ge, I and Bi

**Chlorine and iodine:** The concentrations of Cl and I show little variation within the topsoil. Association with kaolinite and Fe-oxides in the subsoil was demonstrated (Table 4.5).

**Magnesium:** The concentration of MgO is generally close to the LLD and increases from the granite to the uppermost part of the toposequence. Its concentration in the topsoil ranges from  $< 0.013$  to  $0.071$  percent. Association of Mg with Fe-oxides and kaolinite in the subsoil is demonstrated in Table 4.5.

**Germanium:** Twenty five percent of the Ge concentrations are below the LLD ( $0.9$  ppm). Even the highest Ge concentration ( $1.4$  ppm) is close to the LLD.

**Bismuth:** The Bi concentration in the granite which forms the parent material of the toposequence is unusually high. Ahrens and Erlank (1969) report Bi concentrations ranging between  $0.02$  and  $2$  ppm for granitic rocks. The concentration in the investigated granite (sample GR1) is  $18$  ppm. Most of the samples taken from the derived soils have Bi concentrations below the LLD ( $\approx 2.8$  ppm). Samples which have concentrations above the LLD originate from (a) the soil just below the granite exposures at the top of the toposequence, (b) the subsoil with high proportions of Fe-oxide-concretions and (c) the fine textured subsoil at the bottom of the toposequence. It is concluded that Bi was leached and depleted during soil formation. This is consistent with the fact that Bi is commonly hosted by sulfide minerals (Ahrens and Erlank, 1969) because these are easily attacked during rock weathering and soil

formation (Rösler, 1981). Some of the dissolved Bi was retained by Fe-oxides and kaolinite.

#### 4.6. SUMMARY

The sampled soils derived from the granites of the Darling area. Soil samples from seven pits and different soil horizons were analysed for major and trace elements, 1 M  $\text{NH}_4\text{NO}_3$  extractable element concentrations, particle size distribution and various other properties. Pits 30, 31, 32 and 33 were positioned down a toposequence (Figures 2.1 and 4.1). A graphical summary of the physical and chemical soil forming processes is given in Figure 4.8. The numbers in brackets [ ] below refer to the text boxes in Figure 4.8.

**Transport of matter between pits:** The following transport mechanisms were postulated as being important in determining the observed geochemical trends: (a) gravitational transport, (b) lateral and vertical eluviation and illuviation of particles and (c) dissolved transport in throughflow water.

**Accumulation of elements hosted by minerals resistant to weathering [1]:** Physical weathering of the granite exposed above the toposequence continuously supplies detritus to the toposequence. The leaching of some of the major elements during the transportation of the detritus results in relative accumulation of Group-I elements\* in the uppermost part of the toposequence (Pit 30).

**Gravitational transport, eluviation and leaching of upper soil horizons [2]:** The data were best explained by proposing that gravity caused the soil to move down the toposequence. Continuous eluviation and leaching of the topsoil during gravitational transport resulted in depletion of (a) particles smaller than 0.5 mm, (b) feldspars, (c) Group-I\* elements and (d) Group-III elements\*\*.

**Eluviation and illuviation by means of throughflow [3, 4]:** Particles smaller than gravel were laterally eluviated from the subsoil in the steeper part of the toposequence (Pit 31) and deposited at the footslope of the toposequence by means of throughflow (Pit 32). The illuviation resulted in accumulation of fines, coarse silt, medium sand and fine sand in the subsoil of the footslope near to the steeper part of the toposequence. The G-horizon in the vicinity of Pit 33 has the highest proportion of particles smaller than  $0.5 \mu\text{m}$  because the illuviation of coarser particles was restricted to the footslope in closest proximity to the steeper part of the toposequence.

---

\* Li,  $\text{P}_2\text{O}_5$ ,  $\text{TiO}_2$ , V,  $\text{Fe}_2\text{O}_3$ , Zn, Zr and Sn.

\*\* Be, F,  $\text{Na}_2\text{O}$ ,  $\text{Al}_2\text{O}_3$ ,  $\text{K}_2\text{O}$ , CaO, Rb, Y, Nb, Pb, Th and U

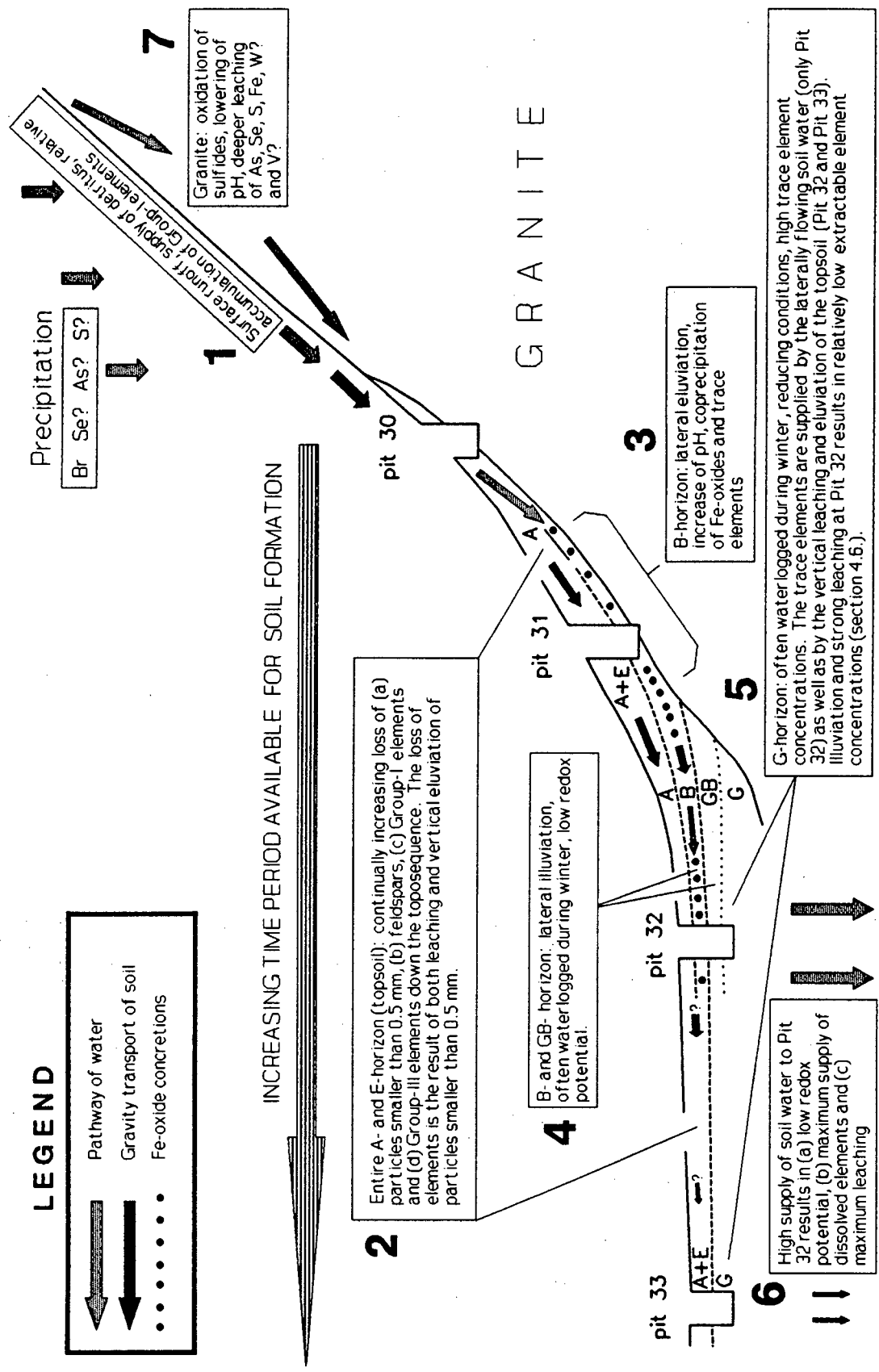


**Figure 4.8:** Interpretative diagram of the granite-derived toposequence (Klipberg). The numbers next to the text boxes correspond to the numbers in section 4.6.

**Changes of the particle size distribution and leaching as cause for lower concentrations of extractable element fractions [5, 6]:** The dilution of kaolinite with illuviated, coarse particles at Pit 32 presumably resulted in a lower retention ability of the soil. The relatively low retention ability and the strong leaching of the G-horizon near to Pit 32 resulted in relatively small amounts of 1 M  $\text{NH}_4\text{NO}_3$  extractable elements. The G-horizon at Pit 33 was less affected by leaching and illuviation and thus has higher extractable element concentrations.

**Accumulation of elements in the subsoil:** The depletion of elements in the topsoil coincided with an accumulation of most trace elements in the Fe-oxide and(or) kaolinite-rich subsoil (B- and G-horizon). It was suggested that higher pH values initiated the coprecipitation and accumulation of Fe-oxide concretions and trace elements from throughflow water in the subsoil at Pit 31. The Fe-oxide-rich subsoil, therefore, has generally high trace element concentrations [3]. The trace elements accumulated in the fine-textured G-horizon at the footslope (Pit 32) originate partly from the throughflow water [5]. The importance of throughflow as supplier of trace elements decreases towards Pit 33, suggesting that eluviation and leaching of the topsoil was the most important source of the elements accumulated in the subsoil at Pit 33 [5, 6].

**Particularly strong accumulation of As, Se, S and Br:** Mass balance calculations and the particularly strong increase of the As, Se, S and Br concentrations from the granite to the uppermost part of the toposequence (Pit 30) suggested that these elements were added to the soil (Figures 4.5 and 4.6). Aerial deposition is the most likely source of Br (sea-derived aerosols) while the oxidation of sulfides in the granite exposed above the toposequence is a possible source of As and Se [7]. Sulfur may originate from both the granite and the sea. The oxidised ions had higher solubilities and their transportation by throughflow water and subsequent precipitation in the soil resulted in very high concentrations of As and Se (Chapter 9). It is important to keep in mind that the high concentrations of As and Se in the soil may also result from aerial deposition of these elements (Chapter 9).

## CHAPTER 5.

# SOILS ASSOCIATED WITH UNCONSOLIDATED SANDS OF GRANITIC ORIGIN

---

### 5.1. INTRODUCTION

**Occurrence (Figure 5.1):** Both Van Niekerk (1967) and the results of this thesis suggest that the unconsolidated sands north-east of the Darling granite complex are partly of granitic origin. The unconsolidated sands between the granites and the course of the Groenrivier are thus referred to as unconsolidated sands of granitic origin (USGO). The unconsolidated sands which occur close to the outcrops of the Malmesbury Group were not sampled. These sands may originate partly from the Malmesbury sediments and are, therefore, not included when the abbreviation USGO is used.

**Underlying material and topography:** The geological map suggests that most of the area covered by USGO is underlain by sediments of the Malmesbury Group, mainly consisting of greywackes and phyllites. Only close to the granite exposures are the USGO underlain by granites (Theron, 1991; Van Niekerk, 1967). The area is drained by usually dry, slightly meandering streams. The relief is low and slightly undulating.

**Formation of the USGO:** The depression in which the sands were deposited formed during the Quaternary when a lowering of the erosion base, probably linked to the abstraction of water to the Pleistocene ice caps, resulted in active incision to a level lower than the present sea level. The rising sea level during the late Pleistocene resulted in the deposition of the unconsolidated sands east and west of the present Groenrivier (Van Niekerk, 1967).

**Sampling locations:** Figure 5.1 shows the position of the sampled pits. A simplified section through the sampling sites is given in Figure 5.2. Pits 26, 24 and 25 were, according to the map of Van Niekerk (1967), positioned along a common sequence of soils from the lower-lying areas towards the slightly higher-lying areas nearer the granite. The soil at Pit 26 is adjacent to the floodplain while the soils at Pits 24 and 25 occupy the slightly higher-lying areas closer to the granite. Downslope transport of matter from Pit 25 towards Pit 26 and further towards the floodplain is probably negligible because the average slope of soil sequence is only 3 permille. Pit 29 was positioned in the floodplain of the sporadically flowing Groenrivier, relatively distant from Pits 25, 24 and 26. Van Niekerk's (1967) soil map, however, shows that the

soil in the floodplain close to Pit 26 is very similar to the soil in the floodplain at Pit 29. Chemical and physical changes from Pit 29 to Pit 26 and further to Pits 24 and 25 are thus reported as changes with increasing distance from the floodplain and towards the granite.

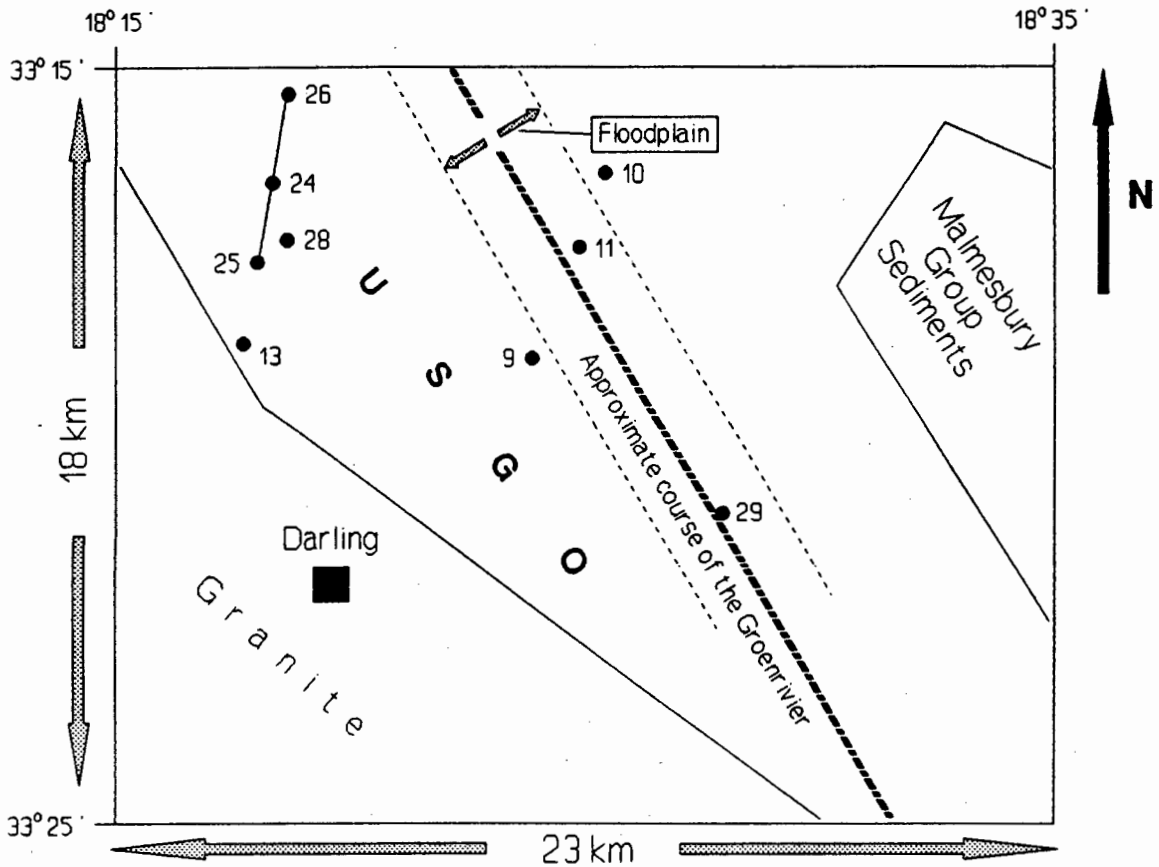


**Figure 5.1:** Simplified map of the sampling sites in the soils associated with the unconsolidated sands of granitic origin (USGO). The numbered points refer to the sampled pits. Pits 25, 24 and 26 are joined with a line because they are positioned down a common sequence of soils, as mapped by Van Niekerk (1967).

Pit 28 is in the same area, but the encountered soil type is not characteristic for the soils associated with the USGO because the soil developed on a small occurrence of Malmesbury quartzites within the USGO. The data for the pits not mentioned above but shown in Figure 5.1 are not discussed in greater detail because of incomplete chemical analyses. The coordinates and a full pedological description of all pits sampled are given in Appendix-I.

**Soil horizons and classification (summarised from Appendix-I):** Orthic A-horizons, E-horizons, prisma-cutanic B-horizons and G-horizons were encountered in the field. Pits 9, 13 and 26 are members of the Escourt soil form, Pits 10 and 29 are members of the Kroonstad soil form and Pits 24 and 25 are members of the Katspruit soil form.

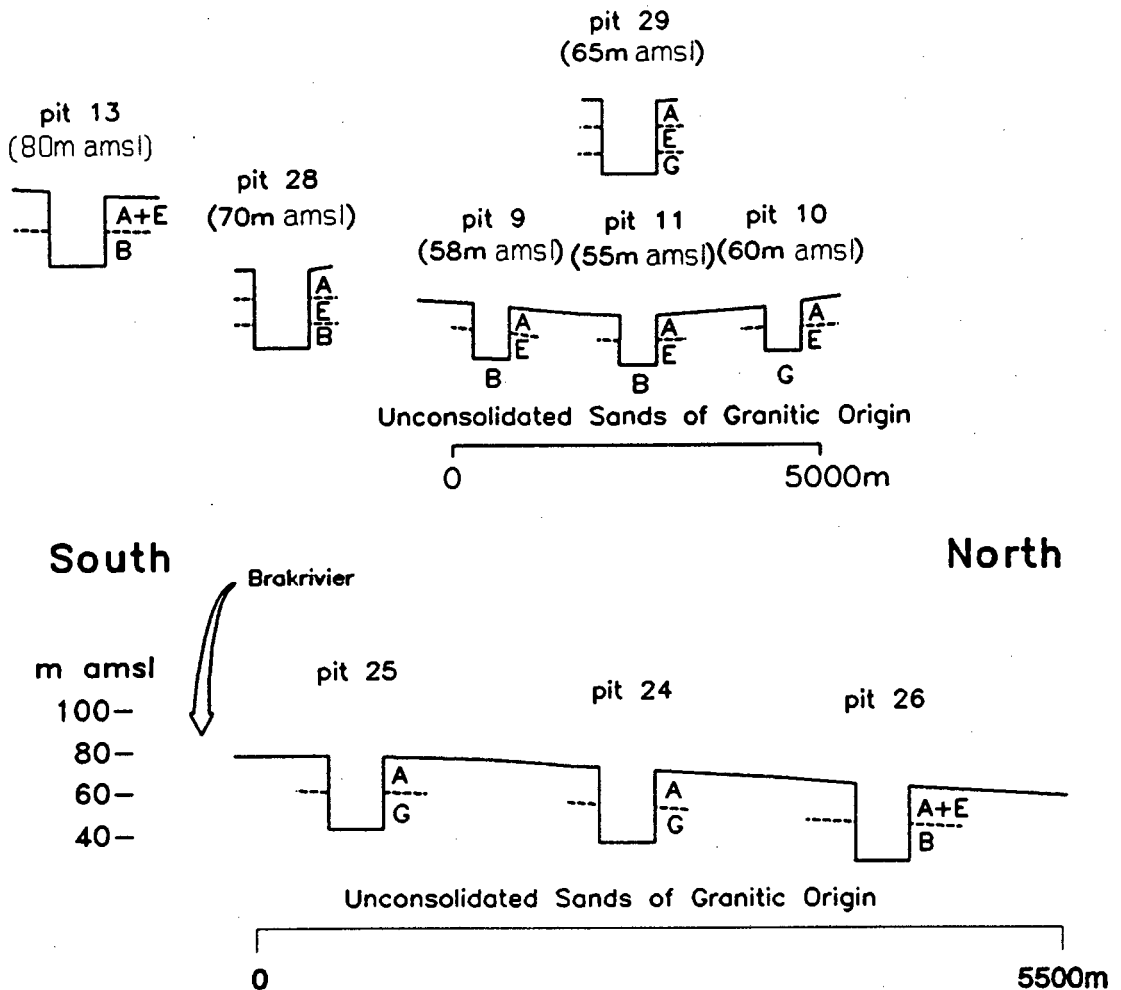


**Figure 5.2:** Simplified section through the sampling sites in the soils associated with the unconsolidated sands of granitic origin (locations 2 and 3 in Figure 2.2). Figure 2.4 can be used as a key to the abbreviations for the different soil horizons. Features other than the topography are not to scale. The vertical scale is exaggerated. Pits 13, 24, 25 and 28 are situated in the slightly higher-lying areas. The average gradient of the slope between Pit 25 and Pit 26 is 3 permille. Pits 9, 10, 11, 26 and 29 are situated in or close to the floodplain.

## 5.2. ANALYTICAL RESULTS - AN OVERVIEW

A summary of the analytical results is given in tabulated form (Tables 5.1 to 5.4). The manner in which the statistics were calculated is discussed in section 4.2. A graphical display of the geochemical trends from the floodplain (Pit 29) towards the granite (Pit 25) is presented in Figures 5.5 and 5.6. A complete listing of the results is given in Appendix-III.

**Table 5.1:** Basic statistics of the major elements in the soils associated with the unconsolidated sands of granitic origin. All values were above the lower limit of detection. The analyses were performed using XRFS and all concentrations are given in percent in dried soil (LLD = lower limit of detection; S.D. = standard deviation; C.V. = coefficient of variation).

Oxide	n	Approx. LLD (%)	Mean (%)	S.D. (%)	C.V. (%)	Min. in % (sample)	Max. in % (sample)
Na <sub>2</sub> O	14	0.02	0.15	0.14	88	0.03 (9A)	0.56 (29G)
MgO	14	0.02	0.13	0.11	82	0.03 (26AE)	0.33 (25G)
Al <sub>2</sub> O <sub>3</sub>	14	0.01	3.8	4.4	118	0.78 (10A)	16.6 (25G)
SiO <sub>2</sub>	14	0.02	89	10	11	59.5 (25G)	96.1 (9A)
P <sub>2</sub> O <sub>5</sub>	14	0.005	0.05	0.02	47	0.01 (29G)	0.09 (25G)
K <sub>2</sub> O	14	0.004	0.4	0.15	38	0.14 (10A)	0.68 (26B)
CaO	14	0.005	0.06	0.02	37	0.03 (9A)	0.1 (29Top)
TiO <sub>2</sub>	14	0.007	0.23	0.12	50	0.11 (24Top)	0.55 (25G)
Fe <sub>2</sub> O <sub>3</sub>	14	0.009	2.6	2.1	83	1.1 (10A)	8.9 (25G)

**Table 5.2:** Basic statistics summarising the pH(KCl) values, the conductivities of the water-suspended soil samples, and the percentages of various particle size fractions and organic matter for the soils associated with the unconsolidated sands of granitic origin (S.D. = standard deviation; C.V. = coefficient of variation).

Parameter	n	Mean	S.D.	C.V. (%)	Min. (sample)	Max. (sample)
pH (KCl)	13	5.3	0.5	9	4.6 (24A)	6.5 (29G)
Conductivity ( $\mu\text{S cm}^{-1}$ )	13	283	528	186	32 (25A)	2000 (29G)
% Organic Matter	13	1.7	2.6	151	0.3 (9A)	8.1 (26B)
% Gravel	13	5.5	6.2	113	0.0 (29Top)	22 (25G)
% Sand	13	76	22	30	20 (25G)	95 (24Top)
% Mud	13	17	16	93	3.5 (24Top)	49 (25G)
% Fine Clay	13	9.4	12	132	0.8 (10A)	40 (25G)

**Table 5.3:** Basic statistics of the trace elements in the soils associated with the unconsolidated sands of granitic origin. Only values above the lower limit of detection ( $n > \text{LLD}$ ) were included to derive the statistics. Li, Be, Co, Cd and Sb were analysed using ICP-MS, all other elements were analysed using XRFs. The concentrations are given in ppm in dried soil (LLD = lower limit of detection; S.D. = standard deviation; C.V. = coefficient of variation).

Elem.	n	n > LLD	Approx. LLD in ppm	Mean in ppm	S.D. in ppm	C.V. (%)	Min. in ppm (sample)	Max. in ppm (sample)
Li	7	7	0.2	9.4	8.0	85	4.5 (26AE)	26 (24G)
Be	7	3	0.3				< LLD	0.9 (24G)
F	17	5	140				< LLD	362 (26B)
S	14	14	6.0	228	105	46	82 (24A)	464 (10A)
Cl	13	13	4.0	239	385	161	45 (24A)	1459 (29G)
V	14	14	1.2	55	45	82	20 (29E)	182 (25G)
Cr	14	14	1.3	41	20	49	27 (24Top)	100 (25G)
Mn	14	14	1.5	86	28	32	55 (24G)	137 (29Top)
Co	7	7	0.2	1.0	0.5	55	0.4 (24Top)	1.8 (29G)
Ni	17	17	2.3	8.8	3.6	41	5.6 (13AE)	22 (25G)
Cu	17	17	1.8	4.0	0.8	20	2.6 (13AE)	6.0 (25G)
Zn	17	17	1.2	5.7	3.5	62	1.7 (11E)	16 (25G)
Ga	5	4	0.8	1.9	1.4	71	< LLD	3.9 (13AE)
Ge	17	2	0.9				< LLD	0.8 (10A)
As	17	17	0.8	9.5	9.6	101	1.6 (29Top)	38 (25G)
Se	17	3	0.8				< LLD	1.8 (25G)
Br	17	17	0.9	3.6	2.5	70	0.8 (11E)	10 (26B)
Rb	17	17	0.7	21	17	80	4.7 (11E)	65 (25G)
Sr	17	17	0.6	15	7.4	51	5.2 (9A)	30 (26B)
Y	17	17	0.7	13	5.6	42	5.4 (10A)	25 (25G)
Zr	17	17	0.6	281	75	27	162 (25G)	443 (25A)
Nb	17	17	0.6	8.9	7.0	80	2.7 (11E)	28 (25Top)
Mo	17	17	0.5	2.2	0.5	24	1.0 (11A)	2.9 (25G)
Cd	7	0	0.7					
Sn	16	14	1.2	5.2	5.8	111	< LLD	24 (25Top)
Sb	7	4	0.3				< LLD	4.2 (24A)
I	16	10	2.5				< LLD	16 (26B)
W	17	16	2.6	17	3.5	20	< LLD	22 (29G)
Pb	17	17	2.1	8.7	8.1	94	2.2 (11E)	35 (25G)
Bi	17	2	2.8				< LLD	3.1 (25Top)
Th	17	16	1.7	6.2	5.0	81	< LLD	21 (25G)
U	17	13	1.3				< LLD	3.4 (24G)

**Table 5.4:** Basic statistics of the extractable element concentrations for the soils associated with the unconsolidated sands of granitic origin. Only values above the lower limit of detection ( $n > \text{LLD}$ ) were included to derive the statistics. The results in the first part of the table are given in ppm in dried soil (fraction  $< 2$  mm) and were obtained using ICP-AES. The results in the second part of the table are given in ppb in dried soil (fraction  $< 2$  mm) and were obtained using ICP-MS (LLD = lower limit of detection; S.D. = standard deviation; C.V. = coefficient of variation).

## Part 1

Elem.	n	n > LLD	Approx. LLD in ppm	Mean in ppm	S.D. in ppm	C.V. (%)	Min. in ppm (sample)	Max. in ppm (sample)
Na	14	14	1.2	231	336	146	8.5 (24A)	1210 (29G)
Mg	14	14	0.03	151	174	115	12 (25A)	492 (25G)
Al	14	5	0.5				< LLD	3.2 (24A)
P	14	5	0.5				< LLD	2.2 (24Top)
S	14	9	0.5				< LLD	45 (29G)
K	14	14	1.2	39	40	104	12 (25A)	155 (26B)
Ca	14	14	0.05	206	137	67	52 (9A)	527 (25G)
Cr	14	4	0.05				< LLD	0.15 (26B)
Fe	14	2	0.05				< LLD	1.8 (10A)
Ni	14	3	0.2				< LLD	0.38 (26B)
Cu	14	0	0.05					
Zn	14	9	0.1				< LLD	0.75 (10A)

## Part 2

Elem.	n	n > LLD	Approx. LLD in ppb	Mean in ppb	S.D. in ppb	C.V. (%)	Min. in ppb (sample)	Max. in ppb (sample)
Be	14	0	67					
B	14	5	362				< LLD	1509 (25G)
V	14	3	9				< LLD	102 (29G)
Co	14	8	13				< LLD	47 (29Top)
As	14	0	71					
Se	14	0	877					
Mo	14	0	49					
Cd	14	0	17					
Sb	14	1	23				< LLD	35 (29Top)
Ba	14	14	61	1503	1327	88	196 (9A)	4783 (25G)
Tl	14	4	3				< LLD	10 (25G)
Pb	14	7	54				< LLD	169 (26B)
Bi	14	0	3					
U	14	1	30				< LLD	57 (26B)

### 5.3. PARTICLE SIZE DISTRIBUTIONS AND FIELD OBSERVATIONS

**Results for the subsoil:** The subsoils (here G- and B-horizons) have a decreasing proportion of medium and fine sand with increasing distance from the floodplain (Figure 5.3). The proportions of gravel and fine clay increase from the floodplain (Pit 29) towards the granite (Pit 25).

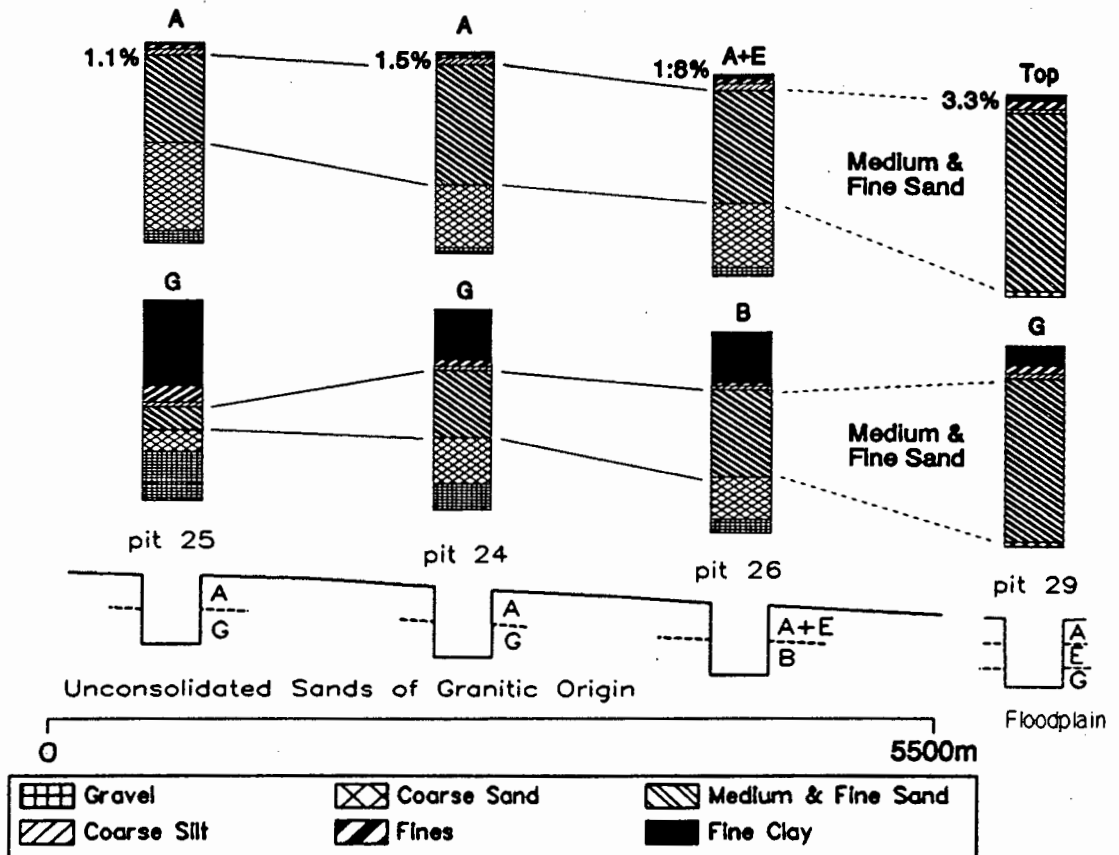


**Figure 5.3:** Particle size distributions of the top- and subsoils from the slightly higher lying areas near the Darling granite exposure (Pit 25) towards the floodplain (Pit 29). The full size of the bars represents 100 weight % of the inorganic soil fraction. "Top" refers to a sample which was taken from the top 15 cm of the A-horizon. The percentages of fine clay in the A-horizons are given to the left of the bars.

**Results for the topsoil:** The topsoil has higher proportions of coarse, medium and fine sand than the subsoil. The lateral trends are very similar to those of the subsoil: the proportions of medium and fine sand decrease with increasing distance from the floodplain towards the granite and the proportions of coarse sand and gravel increase towards the granite. The proportion of fine clay, however, decreases slightly with increasing distance from the floodplain (Figure 5.3).

**Constituents of individual particle size classes:** The particles contained in the gravel fraction are mainly concretions which consist of quartz grains cemented by

sesquioxides. The coarse sand fraction consists mainly of sesquioxide coated and irregular quartz grains. Well rounded and bleached quartz grains are the major component of the medium and fine sand fractions. The fine clay fraction probably consists mainly of pedogenic kaolinite (Chapter 3).

**Interpretation:** It is proposed that the observed trends are the function of three factors:

(a) The particle size distribution of the underlying material. Van Niekerk (1967) implied that the USGO consist of aeolian and fluvially transported sands and colluvium. The results of the present study suggest that the colluvial component consists mainly of irregular, coarse quartz sand because the proportion of this material increases towards a potential source of colluvium, the Darling granite complex, south-east of the USGO (Figure 5.7). With increasing distance from the granites and towards the floodplain, well rounded, moderately well sorted (standard deviation =  $0.65 \phi$  to  $0.72 \phi$ ), medium and fine grained quartz sand becomes more dominant. The highest proportion of medium and fine quartz sand occurs in the present floodplain, indicating that this size fraction is the major component of the local river deposits. The well rounded medium and fine sand may, however, also be of aeolian origin and is thus referred to as fluvial(aeolian) sand.

The lateral changes within the underlying material were inherited by the soils and resulted in increasing proportions of coarse sand (topsoil) and decreasing proportions of medium and fine sand (topsoil and subsoil) with increasing distance from the floodplain and towards the granite (Pit 29 to Pit 25 in Figure 5.3).

The importance of colluvial input of coarse sand from the granite and aeolian(fluvial) input of medium and fine sand is also reflected by the bimodal particle size distribution of the sand fraction (Figure 5.4). The figure shows that the proportion of colluvial, coarse sand ( $-1 \phi$  to  $1 \phi$ ) is maximal nearest to the granites (Pit 25) and decreases towards the floodplain (Pit 29).

(b) The mineralogy of the underlying material. The geochemistry of the soils suggests that the granite-derived, colluvial detritus initially contained minerals such as feldspars and mica (section 5.5.5.). It is proposed that these minerals were altered to pedogenic clay minerals and oxides, causing the observed higher proportions of fine clay and Fe-oxide gravel in the subsoils closer to the granite (Pit 25).

(c) The time available for soil forming processes. The study of weathering profiles and chronosequences associated with river terraces showed that time is an important factor for the formation of clay minerals and Fe-oxides. Older soils often have higher proportions of clay minerals, ferruginized zones and sesquioxides than younger equivalents (Gerrard, 1992; Swanson, 1985; Buol *et al.*, 1980).

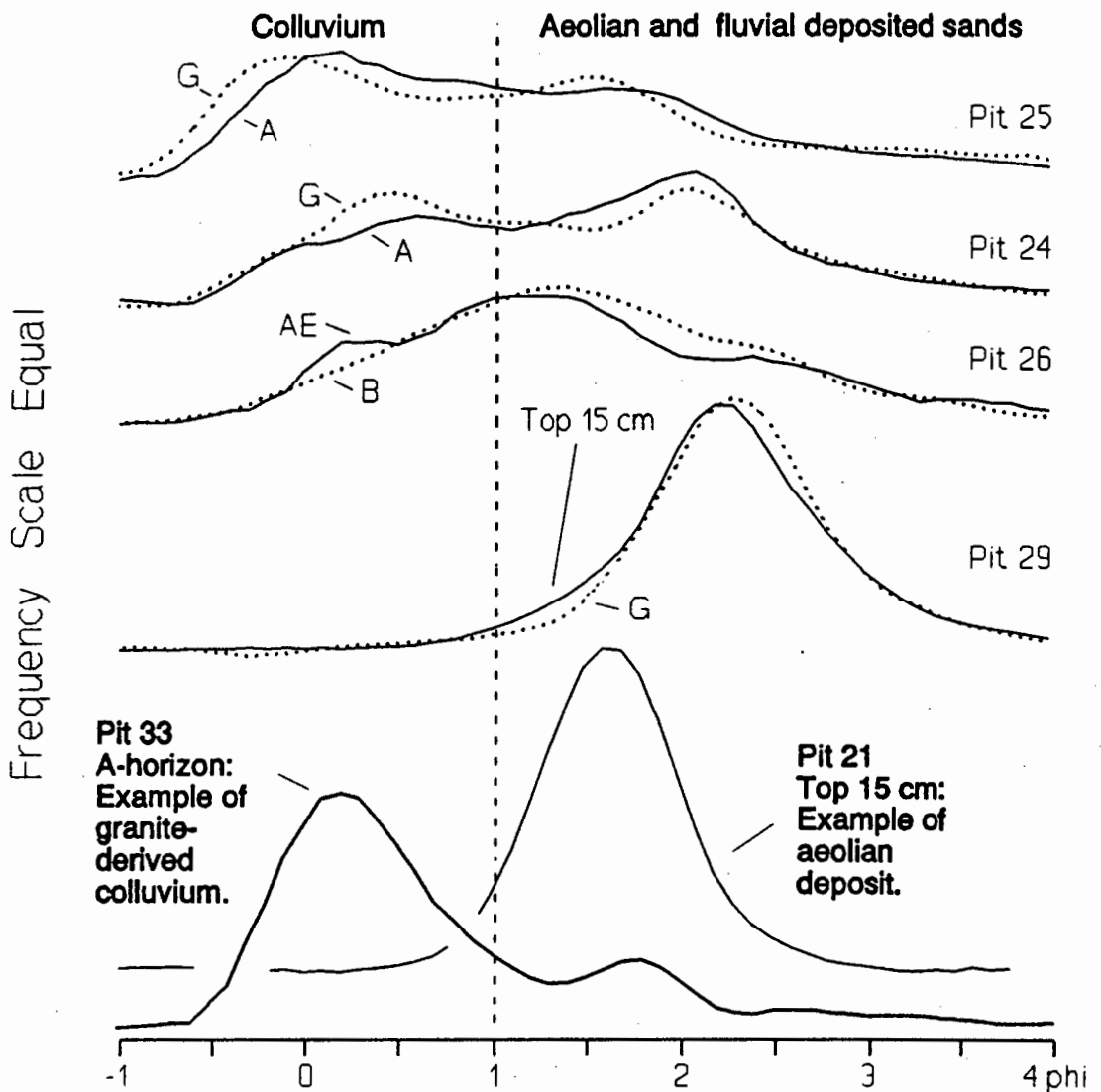


**Figure 5.4:** Particle size frequency curves of the sand fraction (class intervals = 0.1 phi units; lines = topsoil; dotted lines = subsoil). The soil sample from Pit 21 derived from coastal sands and exhibits a frequency curve that is typical for soils which derived from a wind-deposited underlying material. The soil sample from Pit 33 derived from granite and shows a frequency curve that is characteristic for soils which derived from granitic colluvium. The soils associated with the unconsolidated sands of granitic origin (Pits 25, 24, 26 and 29) show a shift from a bimodal to a unimodal particle size distribution. This shift demonstrates the change from a partly colluvial and partly fluvial(aeolian) underlying material near to the granite (Pit 25) to an exclusively fluvial(aeolian) underlying material in the floodplain (Pit 29).

Emergence of the land during the Holocene caused the Groenrivier and its tributaries to gradually expose the slopes of the Groenrivier depression; i.e. the sampled soil sequence (Van Niekerk, 1967). It is, therefore, possible that the time period, that was available for the formation and accumulation of sesquioxides and clay minerals, increases with increasing distance from the floodplain and towards the slightly higher-lying areas closer to the granite (Pit 29 to Pit 25). The decreasing proportion of fluvial

medium and fine sand in the subsoil towards the granite may thus also be the result of increasing dilution with pedogenic clay minerals (fine clay) and sesquioxide concretions (gravel) with progressing time (Figure 5.3). This hypothesis is in agreement with the increase of the concentrations of Ti and Zr (section 5.5.) towards the granite because these elements are commonly hosted by minerals resistant to weathering and would thus be concentrated in the older soils. Absolute age determinations and(or) more detailed field mapping are required to ascertain the increasing age of the soils from the floodplain towards the granite.

**Fine clay in the topsoil:** It was stated above that the lateral trends of fine clay in top- and subsoil are inverse. The proportion of fine clay in the topsoil decreases from 3.3 % in the floodplain to 1.1 % at Pit 25 nearer to the granite (Figure 5.3). If the input of feldspars and micas and the time period available for their alteration to clay minerals was maximal for the soil near to the granite the opposite trend could be expected. It could be speculated that the relatively low concentration of fine clay in the soil near to the granite reflects that the eluviation of clay from the topsoil nullified the positive effect of primary minerals and time available for the formation of clay minerals.

#### 5.4. MAJOR SOIL COMPONENTS

**Mineralogy:** The mineralogical composition of samples 25G and 28E was determined using XRD analyses (Chapter 3). The analyses showed that quartz is the major mineral component of the soils associated with the USGO. Other detected minerals are kaolinite and goethite. Feldspar is not present in detectable proportions. The occurrence of kaolinite in the subsoil, however, suggests that feldspar and(or) mica were initially constituents of the underlying material.

**Elemental composition (Table 5.1):** The most abundant compound is  $\text{SiO}_2$ . The topsoils have the highest concentrations of  $\text{SiO}_2$  (92 to 96 %). The concentration of  $\text{SiO}_2$  in the subsoil increases from the soils nearer to the granite (Pit 25G; 59 %) to the floodplain (Pit 29G; 90 %). This is in agreement with the decreasing proportion of  $\text{Al}_2\text{O}_3$  and fine clay towards Pit 29.

Other abundant components are  $\text{Al}_2\text{O}_3$  (0.8 to 17 %) and  $\text{Fe}_2\text{O}_3$  (1.1 to 9 %). The means for  $\text{K}_2\text{O}$  and  $\text{TiO}_2$  are 0.4 % and 0.2 %, respectively. All other elements and oxides have means lower than 0.2 percent.

**Organic matter:** The proportion of organic matter varies between 0.3 % and 8.1 % (Table 5.2). The highest proportions of organic matter occur in the subsoils (sample 25G: 6.6 %; sample 26B: 8.1 %).

## 5.5. FACTORS WHICH DETERMINE THE LATERAL CHANGES OF THE CONCENTRATIONS

**Discussion of elements in groups:** The elements were grouped in order to facilitate their discussion. The manner in which the elements were grouped is explained in section 1.2. A discussion of the individual groups follows in sections 5.5.1. to 5.5.7.

**Elements which were excluded from the discussion:** The total concentrations of Be, Ge, Cd and the concentrations of the 1 M  $\text{NH}_4\text{NO}_3$  extractable fractions of Be, B, Al, P, Fe, Cu, V, As, Se, Mo, Cd, Sb and Bi were mainly below the LLD and are not discussed. The elements Sb and Ga were excluded from the discussion because the number of samples analysed was too low to recognise horizontal and vertical trends.

### 5.5.1. Group-I (topsoil): Detrital input of $\text{Na}_2\text{O}$ , $\text{MgO}$ , $\text{Al}_2\text{O}_3$ , $\text{K}_2\text{O}$ , $\text{CaO}$ , $\text{TiO}_2$ , $\text{Mn}^*$ , $\text{Co}^*$ , $\text{Zn}^*$ , Rb, Sr, $\text{Th}^*$ , $\text{U}^*$ and 1 M $\text{NH}_4\text{NO}_3$ extractable $\text{Co}^*$ and Ba

**Observations:** The concentrations of the elements in Group-I in the topsoil increase towards both the floodplain (Pit 29) and the granite (Pit 25 in Figure 5.5). The concentrations at Pits 24 and 26 are relatively low.

**Input of granite-derived colluvium as controlling factor:** The elements in Group-I may be hosted by traces of feldspar, mica, biotite and heavy minerals. Pit 25 is relatively close to the outcropping granites and is possibly underlain by granite (Figure 5.7). It is, therefore, proposed that the increase of the concentrations towards Pit 25 is caused by input of detritus from the nearby granite. This is in good agreement with the results of the particle size distribution which suggested that the soil near to the granite contains considerable proportions of granite-derived colluvium (coarse sand; section 5.3.). The concentration of extractable Co may be determined by its total concentration. The concentration of extractable Ba could be controlled by the input of K-feldspar from the granite (section 9.27.).

**Input of fluvial detritus:** The increase of the concentrations towards the floodplain (Pit 29) suggest that the recent river deposits contain more feldspars, mica and heavy minerals than the soil in the slightly higher-lying areas.

### 5.5.2. Group-II (topsoil): Detrital input of Y, Zr, Nb and Sn

The concentrations of the Group-II elements in the topsoil are at a maximum near to the granite (Pit 25; Figure 5.5). The increase towards the granite suggests that the granitic colluvium also contains minerals which host Group-II elements (e.g. zircon and cassiterite). The concentrations of the Group-II elements in the floodplain are not increased, as in Group-I.

---

\* The allocation of this element to the group is debatable because the agreement between the variation of its concentration and the group pattern is poor.

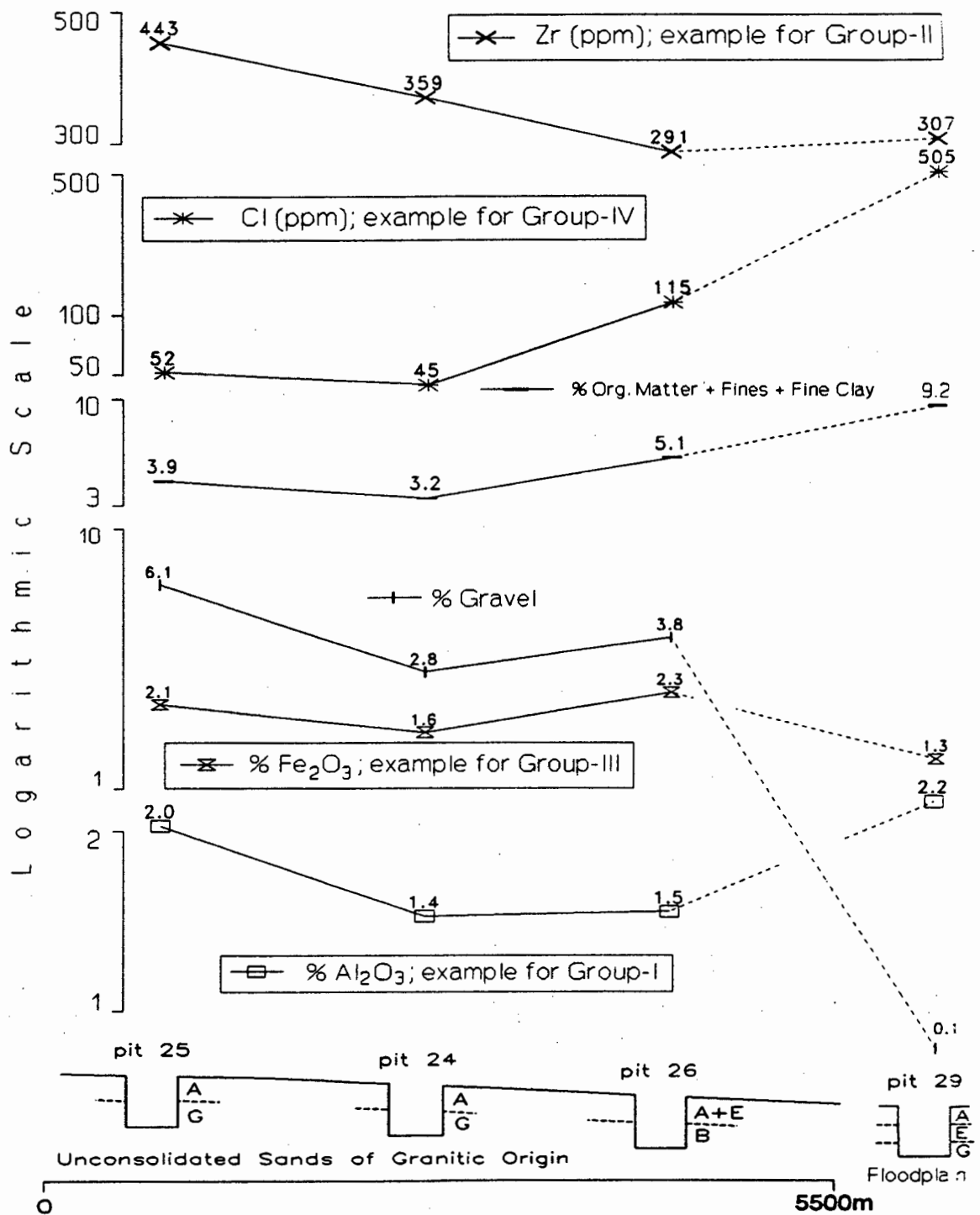


**Figure 5.5:** Horizontal changes of the concentrations of selected elements in the topsoils associated with the USGO. The increase of the  $\text{Al}_2\text{O}_3$  concentration towards Pit 25 and the floodplain is characteristic for all elements in Group-I ( $\text{Na}_2\text{O}$ ,  $\text{MgO}$ ,  $\text{Al}_2\text{O}_3$ ,  $\text{K}_2\text{O}$ ,  $\text{CaO}$ ,  $\text{TiO}_2$ ,  $\text{Mn}$ ,  $\text{Co}$ ,  $\text{Zn}$ ,  $\text{Rb}$ ,  $\text{Sr}$ ,  $\text{Th}$ ,  $\text{U}$  and extractable  $\text{Co}$  and  $\text{Ba}$ ). The high concentration of  $\text{Zr}$  at Pit 25 is typical for all elements in Group-II ( $\text{Y}$ ,  $\text{Zr}$ ,  $\text{Nb}$  and  $\text{Sn}$ ). The similar behaviour of  $\text{Fe}_2\text{O}_3$  and gravel demonstrates the lateral variation of the Group-III elements ( $\text{P}_2\text{O}_5$ ,  $\text{V}$ ,  $\text{Fe}_2\text{O}_3$ ,  $\text{As}$ , and  $\text{Pb}$ ). The concentrations of the elements in Group-IV ( $\text{S}$ ,  $\text{Cl}$ ,  $\text{Br}$ ,  $\text{I}$  and extractable  $\text{Na}$ ,  $\text{Mg}$ ,  $\text{S}$ ,  $\text{K}$ ,  $\text{Ca}$  and  $\text{Zn}$ ) increase with the proportions of organic matter, fines and fine clay towards the floodplain. This trend was demonstrated using  $\text{Cl}$  as an example.

### 5.5.3. Group-III (topsoil): Association of $P_2O_5$ , V, $Fe_2O_3$ , As, and Pb\* with Fe-oxides

**Observations:** The concentrations of the Group-III elements in the topsoil are at a maximum in samples which also have the highest proportions of gravel (samples 25A and 26AE; Figure 5.5). It was observed in the field that the gravel fraction consists partly of Fe-oxides.

**Association of Group-III elements and Fe-oxide gravel:** The results discussed earlier for the granite-derived soils (Table 4.5) showed that the elements in Group-III, except for Pb, may be strongly associated with Fe-oxides. It is, therefore, suggested that the elements in Group-III are accumulated in Fe-oxides. The Fe-oxides preferentially form gravel-sized concretions.

### 5.5.4. Group-IV (topsoil): Retention of S, Cl, Br, I and 1 M $NH_4NO_3$ extractable Na, Mg, S, K, Ca and Zn

The concentrations of the Group-IV elements in the topsoil increase from the granite (Pit 25) towards the floodplain. The proportions of fines, fine clay and organic matter and the conductivity of the water-suspended soil also increase towards the floodplain (Pit 29; Figure 5.5). It is, therefore, suggested that the retention ability of the topsoil for water and dissolved salts is the most important factor in determining the concentrations of the Group-IV elements. The increasing concentration of S could reflect both the fact that this element is a common constituent of organic matter and the retention of  $SO_4^{2-}$ .

It could also be speculated that the ground water table in the lower slope positions is relatively shallow (Figure 2.1). Capillary elevation and evaporation of ground water can result in the accumulation of salts in the soil (Buol *et al.*; 1980). This process could supply the soil with Group-IV elements and cause the increased concentrations at the footslope.

### 5.5.5. Group-V (subsoil): Detrital input of $Al_2O_3$ , $P_2O_5$ , $TiO_2$ , V, Cr, $Fe_2O_3$ , Ni\*, Zn, As, Rb, Y, Nb, Sn, Pb, Th, U\* and 1 M $NH_4NO_3$ extractable Ba and Tl

**Observations:** The concentrations of the Group-V elements in the subsoil increase from the floodplain towards the granite (Pit 29 to Pit 25 in Figure 5.6). This trend follows the increasing proportions of gravel and fine clay.

---

\* The allocation of this element to the group is debatable because the agreement between the variation of its concentration and the group pattern is poor.

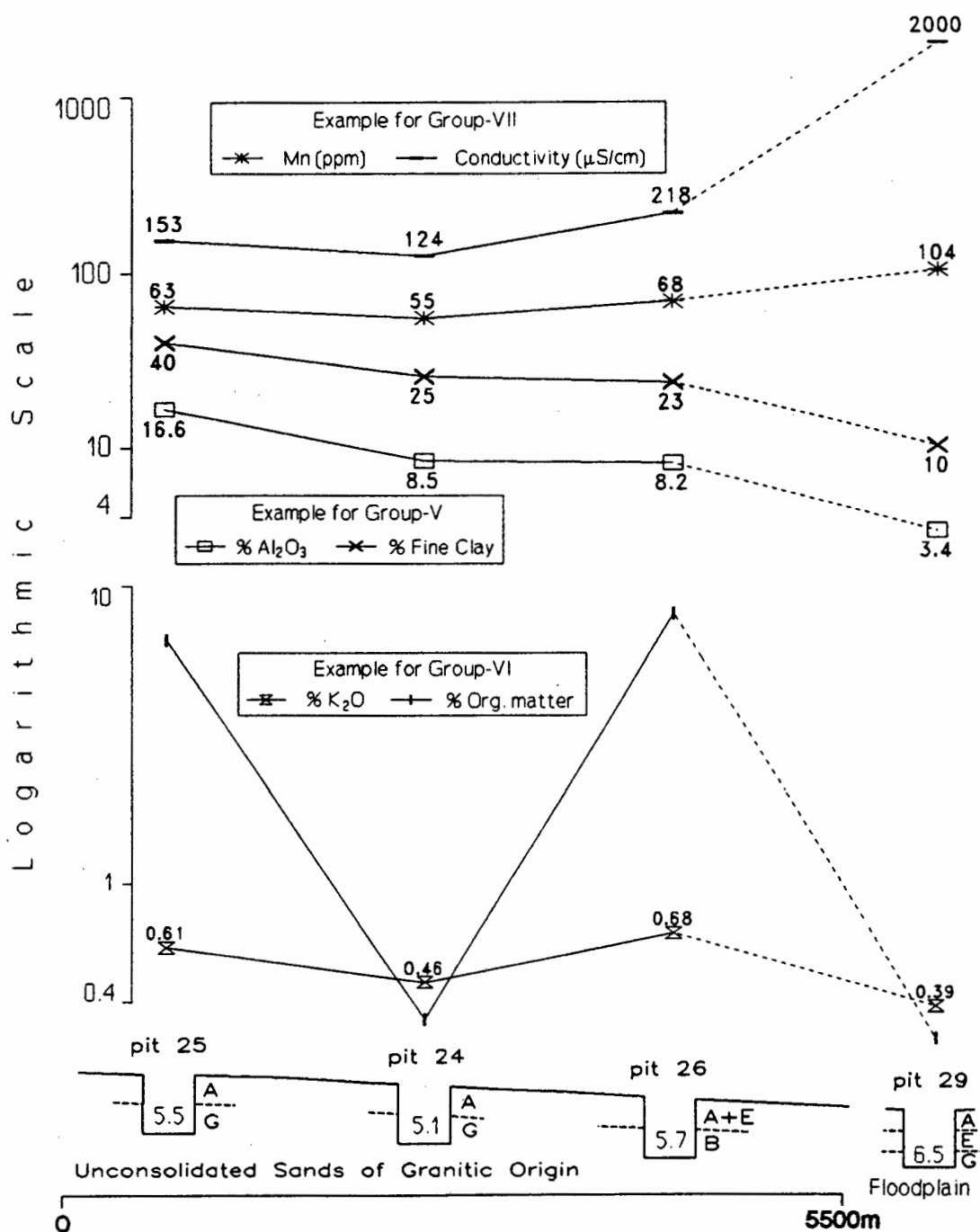


**Figure 5.6:** Horizontal changes of the concentrations of selected parameters in the subsoils associated with the USGO. The increasing proportion of fine clay and  $\text{Al}_2\text{O}_3$  towards Pit 25 is characteristic for all elements in Group-V ( $\text{Al}_2\text{O}_3$ ,  $\text{P}_2\text{O}_5$ ,  $\text{TiO}_2$ , V, Cr,  $\text{Fe}_2\text{O}_3$ , Ni, Zn, As, Rb, Y, Nb, Sn, Pb, Th, U and extractable Ba and Tl). The relatively high concentrations of  $\text{K}_2\text{O}$  and organic matter in samples 25G and 26B is typical for all elements in Group-VI (F, MgO, S,  $\text{K}_2\text{O}$ , CaO, Br, Sr and extractable B, Mg, K, Ca, Cr, Ni and Pb). The concentrations of the elements in Group-VII ( $\text{Na}_2\text{O}$ , Cl, Mn, W and extractable Na, S and Zn) increase with the conductivity of the water-suspended soil towards the floodplain. The concentration Mn was used as an example for the lateral variation of the Group-VII elements. The numbers in the pits refer to the pH(KCl) values of the subsoil.

**Input of colluvium and age of soil as controlling factors:** It was suggested that the Darling granite complex supplied the USGO with colluvium in the upper slope positions (section 5.3.). The relatively high concentrations of the Group-V elements near to the granite suggests that this detritus was an important source of Group-V elements. Some of the Group-V elements were probably hosted by minerals such as feldspar and mica, even if such minerals could not be detected in the corresponding samples (XRD-analyses; Chapter 3). It is possible that the age of the soil increases from the floodplain towards the slightly higher-lying areas near the granite (Pit 25; section 5.3). The older age of the soil near to the granite may have facilitated the complete alteration of feldspars and(or) micas into secondary clay minerals and oxides. More soluble constituents which could not be retained by the soil (e.g. Ca, K and Na) became leached while the elements in Group-V became relatively enriched as the alteration of primary minerals to pedogenic clay minerals and Fe-oxide gravel progressed. This would be in agreement with various other authors who studied the geochemical changes in soils with time. Kesel and Spicer (1985) investigated soils on alluvial fans in Costa Rica and found that the older soils in the upper slope positions have higher  $\text{Al}_2\text{O}_3$  and  $\text{Fe}_2\text{O}_3$  concentrations and lower  $\text{SiO}_2$  concentrations. They also found that in the older soils primary minerals were completely altered to secondary soil minerals. Young *et al.* (1987) investigated 40000 year old soils in Australia and found that Fe accumulated to high concentrations. Nesbitt and Young (1989) showed that the concentrations of Fe and Al commonly increase with the degree of weathering.

The increasing concentrations of extractable Ba and Tl towards the granite are probably linked to the increasing proportion of fine clay because finer textured soils can retain more extractable Ba and Tl (sections 9.27. and 9.29.).

#### **5.5.6. Group-VI (subsoil): Similar behaviour of F, MgO, S, $\text{K}_2\text{O}$ , CaO, Br\*, Sr and 1 M $\text{NH}_4\text{NO}_3$ extractable B, Mg, K, Ca, Cr\*, Ni, Pb and organic matter**

**Observations:** Samples 25G (Pit 25) and 26B (Pit 26) contain between 6 % and 8 % organic matter whereas the subsoils of Pits 24 and 29 contain less than 0.5 % (Figure 5.6). The concentrations of the Group-VI elements in the subsoil are slightly higher in samples with high proportions of organic matter.

**Control of organic matter on Group-VI elements:** The similar behaviour of the elements in Group-VI and organic matter could indicate that (a) Group-VI elements were introduced to the soil as a constituent of organic matter or (b) Group-VI elements have an affinity for organic matter and are thus retained in the organic-rich subsoils. The correlation of organic matter and Group-VI elements can be weak (e.g.  $\text{K}_2\text{O}$  in Figure 5.6) and it is important to note that the association or introduction with organic

---

\* The allocation of this element to the group is debatable because the agreement between the variation of its concentration and the group pattern is poor.

matter is probably restricted to only a certain portion of an element. The mode of occurrence may be different for individual Group-VI elements. Elements may be associated with clay minerals, adsorbed by organic matter or incorporated into organic matter. Accumulation of Group-VI elements in the form of soluble salts is less likely because the conductivity of the water-suspended soil does not follow the same enrichment pattern (Figure 5.6).

#### 5.5.7. Group-VII (subsoil): Na<sub>2</sub>O, Cl, Mn, W and 1 M NH<sub>4</sub>NO<sub>3</sub> extractable Na, S\* and Zn

**Observations:** The concentrations of the elements in Group-VII in the subsoil increase from the soils near the granite (Pit 25) towards the floodplain (Pit 29). This increase coincides with higher conductivities of the water-suspended soil and higher pH(KCl) values (Figure 5.6).

**Exclusion of soil retention ability as controlling factor:** The trend of the elements in Group-VII is inverse to the trend of fine clay (Figure 5.3). Also the high proportion of organic matter in the subsoils at Pits 25 and 26 does not affect the concentrations of the Group-VII elements. It is concluded that the retention ability of the soil does not control the concentrations of the elements in Group-VII.

**Depth of ground water table as controlling factor:** The distance between soil and ground water table would normally decrease towards the floodplain (Figure 2.1). The conductivity of the water-suspended soil reaches 2000  $\mu\text{S cm}^{-1}$  in the floodplain (Figure 5.6), indicating high proportions of soluble salts. Capillary elevation and evaporation of ground water can result in the accumulation of salts in the soil (Buol *et al.*, 1980). This process could supply the soil with all Group-VII elements, except for W, and cause the increased concentrations. The high pH of the subsoil in the floodplain (Pit 29) is probably linked to the alkaline reaction of exchangeable Na<sup>+</sup>.

**Tungsten:** The increase of the concentrations of the elements in Group-VII does coincide with higher proportions of fine and medium sand (Figure 5.3). The similar behaviour of W and fine and medium sand is also evident in soils associated with other underlying materials. It is thus suggested that considerable portions of W are hosted by (medium and fine) sand-sized, weathering resistant mineral particles, likely to be scheelite or wolframite (section 10.27). The results discussed in section 5.3. indicated that the medium and fine sand is of fluvial and(or) aeolian origin.

---

\* The allocation of this element to the group is debatable because the agreement between the variation of its concentration and the group pattern is poor.

## 5.6. VERTICAL CHANGES OF THE CONCENTRATIONS

Pits 24, 25, 26, 28 and 29 were sampled at different soil depths. Where possible, the top 15 cm, the A-horizon, the E-horizon and the subsoil (here B- and G-horizons) were sampled. The results can be summarised as follows:

**Results (a):** The concentrations of  $\text{Al}_2\text{O}_3$ ,  $\text{Fe}_2\text{O}_3$ ,  $\text{MgO}$ ,  $\text{Na}_2\text{O}$ ,  $\text{Se}^*$ , Cr, Sn, Li, Be,  $\text{Co}^*$  and 1 M  $\text{NH}_4\text{NO}_3$  extractable Mg, Ca, Cr,  $\text{Ni}^*$ , Na, S and B increase downwards in all pits sampled.

**Interpretation:** The mineralogical and the particle size analyses, as well as the field observations, suggest that the proportion of clay minerals and sesquioxides increases from the topsoil to the subsoil (Chapter 3, section 5.3 and Appendix-I). This is in agreement with the downwards increasing concentrations of  $\text{Al}_2\text{O}_3$  and  $\text{Fe}_2\text{O}_3$ . It is proposed that elements which have downwards increasing concentrations in all pits are typically associated with clay minerals and oxides. Organic matter may also be considered to be a possible host of the elements listed above because some of the subsoils are organic-rich (section 5.5.6.). Some of the elements (e.g. Sn) may be hosted by weathering resistant minerals such as sphene and cassiterite.

**Results (b):** The concentrations of  $\text{TiO}_2$ ,  $\text{K}_2\text{O}$ , Th, Pb, Br, As, Zn, Ni, Cu, Y, Sr, U, Rb, V, S, F, I and extractable Zn, K, Ba and Tl increase downwards only in the soil near to the granite (Pit 25).

**Interpretation:** The results of this chapter gave reason to speculate that the age of the soil increases from the floodplain towards the granite (sections 5.3. and 5.5.5.). The accumulation of elements which are exclusively enriched in the subsoil near to the granite could thus be a function of (a) their association with clay minerals and oxides and (b) the time period available for the processes that facilitate this association. Such processes are eluviation, illuviation, leaching and alteration of minerals. Some of the elements listed above (e.g.  $\text{TiO}_2$  and U) are probably hosted by weathering resistant (heavy) minerals.

**Results (c):** The concentrations of  $\text{SiO}_2$ , Zr, Mn and the extractable P and Co decrease downwards.

**Interpretation:** The concentration of  $\text{SiO}_2$  decreases downwards because the secondary minerals which characterise the subsoil (clay minerals and oxides) contain less  $\text{SiO}_2$  than the major soil component quartz.

The results presented in section 4.5.2. implied that zirconium minerals which derived from the Darling granite complex have mostly a particle size between 0.053 mm and 0.5 mm (fine and medium sand). The proportion of fine and medium sand in the USGO-derived soils decreases, like the Zr concentration, with soil depth. It is,

---

\* The allocation of this element to the group is debatable because the agreement between the variation of its concentration and the group pattern is poor.

therefore, possible that the relative accumulation of fine and medium sand in the topsoil resulted also in accumulation of similar sized Zr minerals. The vertical distribution of Mn and extractable P and Co is discussed in Chapter 9.

**Results (d):**  $\text{TiO}_2$ ,  $\text{Al}_2\text{O}_3$ ,  $\text{Fe}_2\text{O}_3$ , MgO, CaO,  $\text{Na}_2\text{O}$ ,  $\text{K}_2\text{O}$ , Br, Zn, Rb, V, S, Cl, I and extractable Mg, Ca, K, Na and S are depleted in the E-horizon of Pit 29, while  $\text{SiO}_2$  is relatively enriched in this horizon.

**Interpretation:** The low concentrations in the E-horizon are due to leaching and eluviation and confirmed the classification of this horizon as an E(luviated)-horizon. The relatively high concentration of  $\text{SiO}_2$  is due to removal of other soil components.

**Results (e):**  $\text{MgO}^*$ , CaO,  $\text{P}_2\text{O}_5$ ,  $\text{Zn}^*$ ,  $\text{Cl}^*$  and extractable  $\text{Zn}^*$ , Mg, Ca and P are enriched in the top 15 cm of the soil. This trend coincides in two out of three pits with higher proportions of organic matter in the top 15 cm.

**Interpretation:** The elements may be associated with organic matter.

## 5.7. SUMMARY

**Introduction:** The sampled soils are associated with unconsolidated, granitic, Pleistocene sands (USGO) north-east of the Darling granite complex. Soil samples from nine pits and different soil horizons were analysed for major and trace elements, 1 M  $\text{NH}_4\text{NO}_3$  extractable element concentrations, particle size distribution and various other parameters. The soils at Pits 29, 26, 24 and 25 exemplify a common sequence of soils from the floodplain of the Groenrivier to the granite. The trends of the physical and chemical properties of the soil from the floodplain towards the granite were discussed in detail.

**Major soil components:** The soil consists mainly of  $\text{SiO}_2$  (59 to 96 %). Other important components are  $\text{Al}_2\text{O}_3$  (0.78 to 16 %),  $\text{Fe}_2\text{O}_3$  (1.1 to 9 %) and organic matter (0.3 to 8.1 %).

**Input of colluvial and fluvial(aeolian) detritus:** The proportion of coarse sand generally increases towards the granite complex while the proportions of medium and fine sand increase towards the floodplain. It was suggested that the higher proportion of coarse sand near to the granite is due to input of granite-derived colluvium. The high proportion of medium and fine sand in the floodplain is the result of deposition of these particles during flood events (text boxes 1, 2 and 3 in Figure 5.7).

**Alteration of feldspars and(or) mica to kaolinite and oxides:** It was proposed that the granite-derived colluvium contained initially feldspars and(or) mica. The alteration of these minerals to kaolinite and oxides resulted in relatively high proportions of fine clay and gravel in the subsoil near to the granite (text boxes 1 and 3 in Figure 5.7).

---

\* The allocation of this element to the group is debatable because the agreement between the variation of its concentration and the group pattern is poor.

**Factors that determine the lateral geochemical variations in the USGO-derived soils:** The lateral variation of the elemental concentrations from the floodplain towards the granite indicated which factors are most important in determining the elemental concentrations. These factors are explained below and illustrated in Figure 5.7.

(a) Colluvial input of feldspars, mica and heavy minerals from the granite to the soils which are relatively close to the granite caused relatively high concentrations of Na<sub>2</sub>O, MgO, Al<sub>2</sub>O<sub>3</sub>, P<sub>2</sub>O<sub>5</sub>, K<sub>2</sub>O, CaO, TiO<sub>2</sub>, V, Cr, Fe<sub>2</sub>O<sub>3</sub>, Zn, As, Rb, Sr, Y, Zr, Nb, Sn, Pb, Th and 1 M NH<sub>4</sub>NO<sub>3</sub> extractable Ba and Tl [*topsoil and(or) subsoil*; text box 1 in Figure 5.7].

(b) Time period available for soil forming processes. The topography, particle size distributions, geochemical results and a comparison with the results of other authors together may have indicated that the age of the soil increases from the floodplain towards the slightly higher-lying areas near the granite complex. The older age of the soil near to the granite may have facilitated the complete alteration of feldspars and(or) micas into secondary clay minerals and oxides. More soluble constituents which could not be retained by the soil (e.g. Ca, K and Na) became leached while Al<sub>2</sub>O<sub>3</sub>, P<sub>2</sub>O<sub>5</sub>, TiO<sub>2</sub>, V, Cr, Fe<sub>2</sub>O<sub>3</sub>, Zn, As, Rb, Y, Nb, Sn, Pb, Th and extractable Ba and Tl became relatively enriched as soil formation progressed (*subsoil*; text box 4 in Figure 5.7). Absolute age determinations are required to confirm this hypothesis.

(c) Fluvial deposition of feldspars, mica and heavy minerals during flood events probably caused relatively high concentrations of Na<sub>2</sub>O, MgO, Al<sub>2</sub>O<sub>3</sub>, K<sub>2</sub>O, CaO, TiO<sub>2</sub>, Rb, Sr and extractable Ba in the *topsoil* of the floodplain (text box 2 in Figure 5.7).

(d) Accumulation of P<sub>2</sub>O<sub>5</sub>, V, Fe<sub>2</sub>O<sub>3</sub> and As in Fe-oxides probably resulted in higher concentrations of these elements in the *topsoil* at Pits 25 and 26. It was observed in the field that the Fe-oxides occur partly in the form of gravel-sized concretions.

(e) High proportions of organic matter in the *subsoil* coincided with high concentrations of F, MgO, S, K<sub>2</sub>O, CaO, Sr and extractable B, Mg, K, Ca, Ni and Pb.

(f) It was suggested that an increased retention ability, as determined by higher proportions of fine clay, fines and organic matter, caused the relatively high concentrations of S, Cl, Br, I and extractable Na, Mg, S, K, Ca and Zn in the *topsoil* of the floodplain (text box 3 in Figure 5.7).

(g) Distance of soil to ground water table. The relatively high concentrations of Na<sub>2</sub>O, Cl, Mn and extractable Na and Zn in the *subsoil* of the floodplain may be the result of capillary elevation and evaporation of ground water (text box 5 in Figure 5.7).

**Vertical distribution of elements:** Most elements have increasing concentrations from the topsoil to the kaolinite-, goethite- and sometimes organic matter-enriched subsoil. The magnitude of this increase reaches its maximum in possibly the oldest soil profile, nearest to the granite. Only the elements SiO<sub>2</sub>, Zr, Mn and 1 M NH<sub>4</sub>NO<sub>3</sub> extractable P and Co have higher concentrations in the topsoil. The elements CaO, P<sub>2</sub>O<sub>5</sub> and extractable Mg, Ca and P have higher concentrations in the organic-rich top 15 cm of the soil profiles.

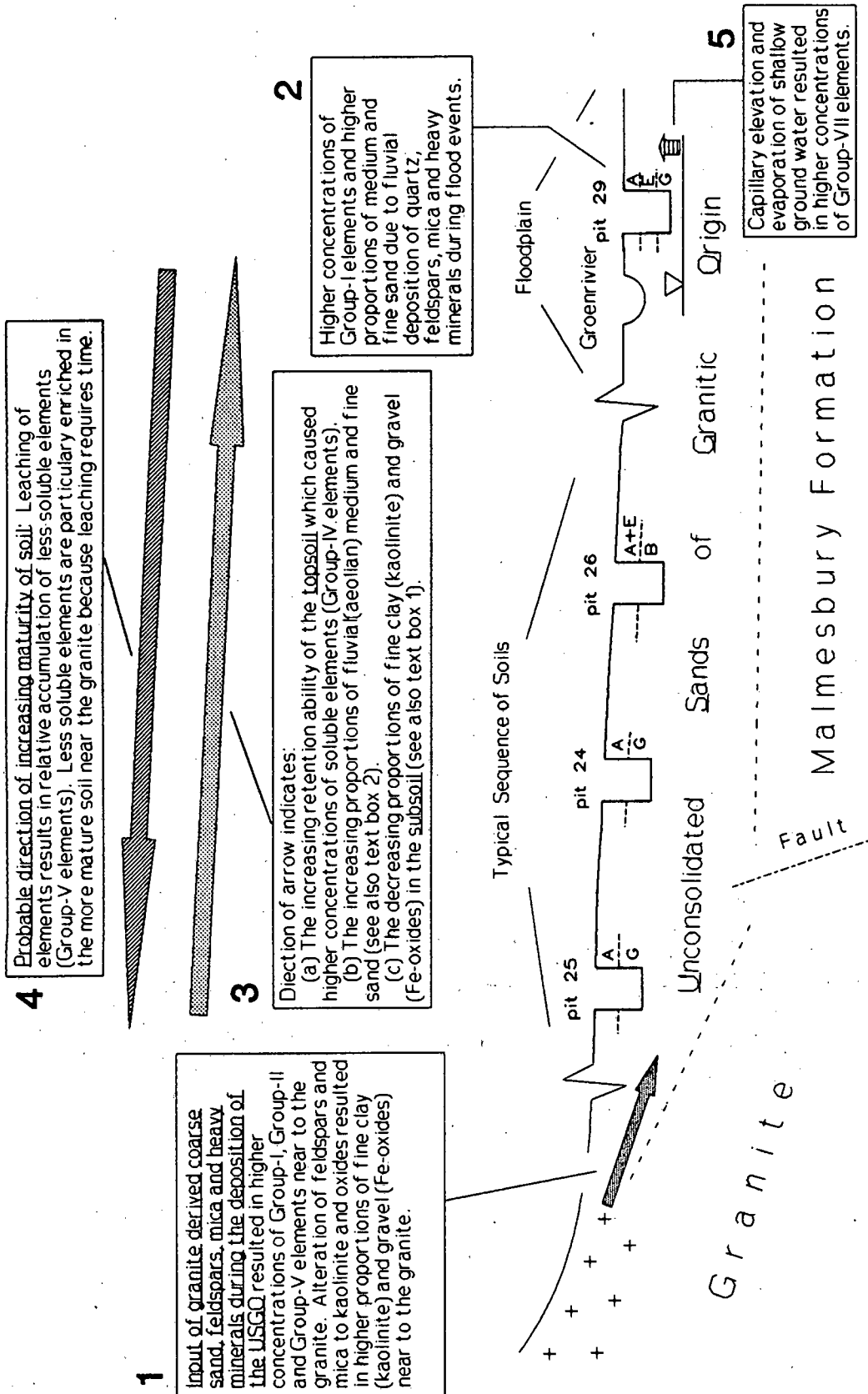


**Figure 5.7:** Interpretative diagram of the soils associated with the unconsolidated sands of granitic origin (USGO). The numbers next to the text boxes correspond to the numbers in the summary of this chapter.

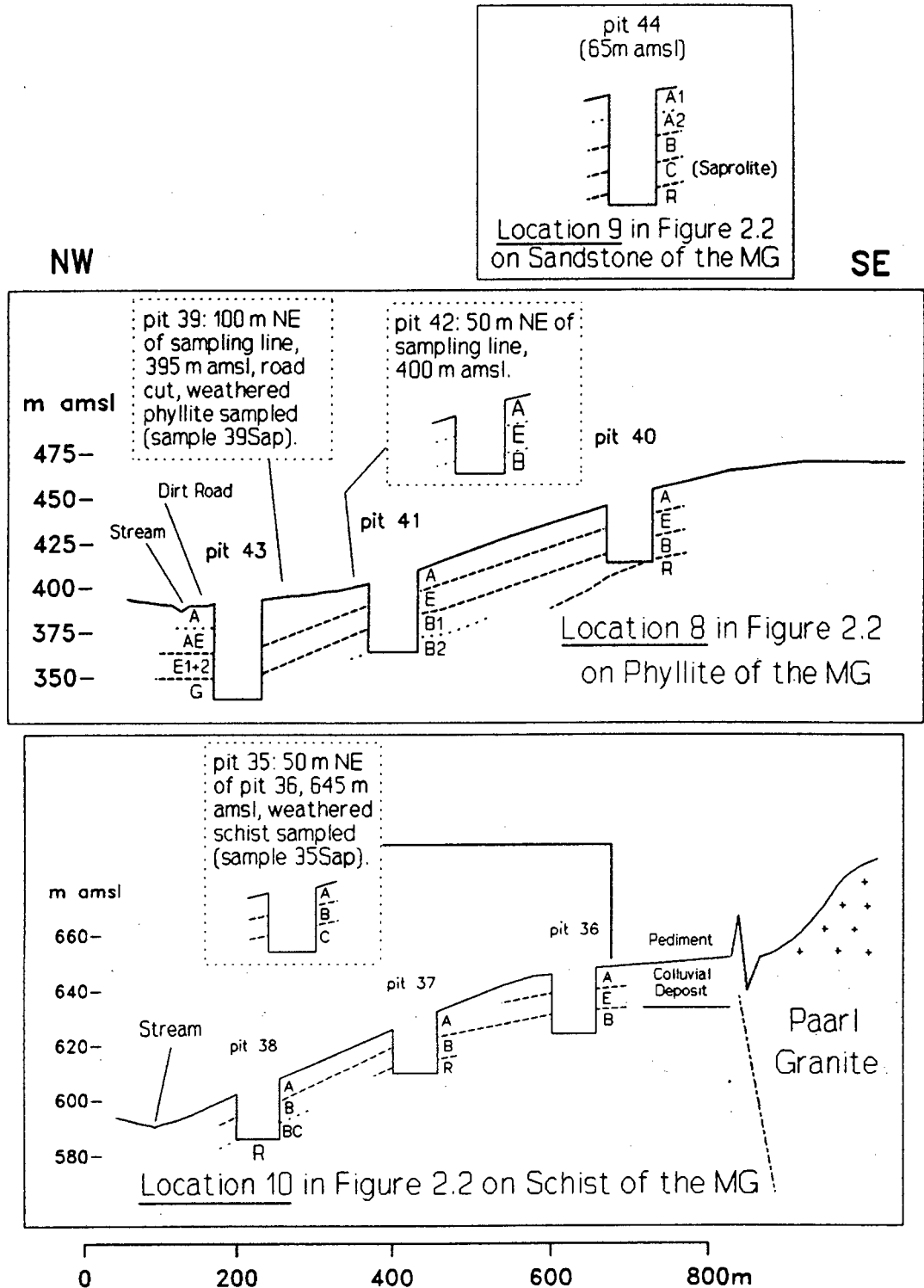


**Figure 6.1:** Simplified sections through the sampling sites in the soils associated with the sediments of the Malmesbury Group (MG). Figure 2.4 can be used as a key to the abbreviations for the different soil horizons. Features other than the topography are not to scale. The vertical scale is exaggerated. The average gradients of the slopes are approximately 100 ‰ for both toposequences.

**Pits 39 to 43:** The toposequence associated with phyllite is approximately 5 km north-west of Wellington and just west of the road between Paarl and Malmesbury (location 8 in Figure 2.2). Figure 6.1. shows a simplified section through the toposequence and the pits sampled. Figure 6.3 shows the view from the pit at top of the toposequence (Pit 40) towards the footslope.

**Pit 44:** Only a single pit was dug into the soil associated with sandstone (location 9 in Figure 2.2; Figure 6.1). The coordinates and a full pedological description of all pits sampled are given in Appendix-I.

**Soil horizons and classification (summarised from Appendix-I):** Orthic A-horizons, E-horizons, lithocutanic B-horizons, pedocutanic

B-horizons, prismaeutanic B-horizons and G-horizons were encountered in the field. The profiles were classified to belong to the following soil forms: Glenrosa (Pit 35), Klapmuts (Pit 36), Sterkspruit (Pits 37, 38 and 44), Cartref (Pit 40), Escourt (Pits 41 and 42) and Kroonstad (Pit 43).



**Figure 6.2:** View from the midslope (Pit 37) down the toposequence on schist of the Malmesbury Group.



**Figure 6.3:** View from the top (Pit 40) towards the footslope of the toposequence on phyllite of the Malmesbury Group.

## **6.2. ANALYTICAL RESULTS - AN OVERVIEW**

A summary of the analytical results is given in tabulated form (Tables 6.1 to 6.4). The manner in which the statistics were calculated is discussed in section 4.2. A graphical display of the geochemical trends from the top to the bottom of the toposequences is presented in Figures 6.5 and 6.6. A complete listing of the results is given in Appendix-III.

**Quality of analyses of 1 M  $\text{NH}_4\text{NO}_3$  extractable Se:** Samples 41B1 and 41B2 were determined to have very high concentrations of extractable Se (23 ppm and 24 ppm). These results are probably incorrect because (a) the extractable Se concentration is in both cases higher than the total Se concentration, which was checked by re-analysing qualitatively and quantitatively using XRFS, and (b) the analysis of Se by ICP-MS is known to be problematic (section 2.4.2.). It is, however, remarkable that the two samples which were determined to be high in extractable Se originate from the same location and soil horizon, and, further, that both samples are relatively high in total Se. Therefore, it is concluded that the results are quantitatively wrong but qualitatively correct.

**Table 6.1:** Basic statistics of the major elements in the soils associated with the sediments of the Malmesbury Group. All values were above the lower limit of detection. The analyses were performed using XRFS and all concentrations are given in percent in dried soil (LLD = lower limit of detection; S.D. = standard deviation; C.V. = coefficient of variation).

Oxide	n	Approx. LLD (%)	Mean (%)	S.D. (%)	C.V. (%)	Min. in % (sample)	Max. in % (sample)
Na <sub>2</sub> O	23	0.02	0.11	0.08	72	0.03 (36E)	0.32 (43G)
MgO	23	0.02	0.46	0.34	74	0.09 (43Top)	1.1 (38BC)
Al <sub>2</sub> O <sub>3</sub>	23	0.01	11	6.8	62	2.3 (43AE)	23 (41B2)
SiO <sub>2</sub>	23	0.02	71	12.9	18	50 (41B2)	92 (43AE)
P <sub>2</sub> O <sub>5</sub>	23	0.005	0.08	0.05	58	0.03 (43G)	0.19 (40Top)
K <sub>2</sub> O	23	0.004	1.3	0.82	63	0.28 (43Top)	2.9 (44B)
CaO	23	0.005	0.12	0.16	135	0.02 (43E)	0.84 (38BC)
TiO <sub>2</sub>	23	0.007	0.52	0.2	38	0.17 (43E)	0.98 (36B)
Fe <sub>2</sub> O <sub>3</sub>	23	0.009	8.7	4.1	47	3.8 (43AE)	21 (36E)

**Table 6.2:** Basic statistics summarising the pH(KCl) values, the conductivities of the water-suspended soil samples and the percentages of various particle size fractions and organic matter for the soils associated with the sediments of the Malmesbury Group (S.D. = standard deviation; C.V. = coefficient of variation).

Parameter	n	Mean	S.D.	C.V. (%)	Min. (sample)	Max. (sample)
pH(KCl)	23	5.5	0.9	17	4.0 (36B)	7.2 (38BC)
Conductivity ( $\mu\text{S cm}^{-1}$ )	23	347	355	102	47 (44A2)	1470 (43G)
% Organic Matter	23	0.8	0.9	116	0.0 (41B2)	3.7 (38BC)
% Gravel	23	32	25	77	0.1 (36B)	81 (43E)
% Sand	23	26	12	46	8 (41B1)	46 (44Top)
% Mud	23	41	27	66	6 (43E)	85 (36B)
% Fine Clay	13	34	21	61	6 (36E)	63 (41B2)

**Table 6.3:** Basic statistics of the trace elements in the soils associated with the sediments of the Malmesbury Group. Only values above the lower limit of detection ( $n > \text{LLD}$ ) were included to derive the statistics. Li, Be, Co, Cd and Sb were analysed using ICP-MS, all other elements were analysed using XRFs. The concentrations are given in ppm in dried soil (LLD = lower limit of detection; S.D. = standard deviation; C.V. = coefficient of variation).

Elem.	n	n > LLD	Approx. LLD in ppm	Mean in ppm	S.D. in ppm	C.V. (%)	Min. in ppm (sample)	Max. in ppm (sample)
Li	11	11	0.2	14	13	94	3.1 (43Top)	40 (44B)
Be	11	11	0.3	1.9	1.4	75	0.6 (43Top)	4.3 (44B)
F	25	14	140				< LLD	720 (43G)
S	23	23	6.0	321	121	38	165 (43AE)	669 (41B2)
Cl	23	23	4.0	225	208	92	42 (44B)	806 (43G)
V	23	23	1.2	120	55	46	48 (43AE)	258 (36E)
Cr	23	23	1.3	97	29	30	54 (41Top)	165 (44A2)
Mn	23	23	1.5	157	97	62	58 (41E)	391 (38A)
Co	11	11	0.2	4.8	4.3	91	1.1 (41Top)	15 (44B)
Ni	25	25	2.3	17	12	70	4.5 (36Top)	57 (44B)
Cu	25	25	1.8	19	14	72	6.7 (42Top)	63 (44C)
Zn	25	25	1.2	26	12	47	9.2 (43E)	55 (44B)
Ge	25	2	0.9				< LLD	0.9 (42B)
As	25	25	0.8	16	8.6	55	5.4 (38BC)	40 (44A2)
Se	25	18	0.8	1.9	0.8	45	< LLD	3.2 (36E)
Br	25	25	0.9	13	9.9	75	1.7 (43E)	29 (41B2)
Rb	25	25	0.7	79	54	68	17 (43Top)	170 (43G)
Sr	25	25	0.6	23	14	60	7.7 (43AE)	64 (38BC)
Y	25	25	0.7	20	15	74	7.5 (43E)	73 (44C)
Zr	25	25	0.6	217	90	41	74 (41E)	373 (44Top)
Nb	25	25	0.6	10	3.9	39	3.1 (43E)	20 (36B)
Mo	25	25	0.5	1.7	0.5	26	0.7 (38BC)	2.6 (44A2)
Cd	11	0	0.7					
Sn	25	23	1.2	4.9	2.4	48	< LLD	10 (43G)
Sb	11	11	0.3	4.3	3.6	83	1.6 (43Top)	13 (44Top)
I	25	20	2.5	48	56	117	< LLD	209 (41B2)
W	25	25	2.6	11	3.3	31	6.4 (36E)	18 (43AE)
Pb	25	25	2.1	22	7.7	35	8.9 (42Top)	40 (44A2)
Bi	25	0	2.8					
Th	25	25	1.7	13	5.3	42	3.3 (43AE)	20 (36E)
U	25	25	1.3	3.8	1.5	39	2.1 (43AE)	7.1 (40B)

**Table 6.4:** Basic statistics of the extractable element concentrations for the soils associated with the sediments of the Malmesbury Group. Only values above the lower limit of detection ( $n > \text{LLD}$ ) were included to derive the statistics. The results in the first part of the table are given in ppm in dried soil (fraction  $< 2$  mm) and were obtained using ICP-AES. The results in the second part of the table are given in ppb in dried soil (fraction  $< 2$  mm) and were obtained using ICP-MS (LLD = lower limit of detection; S.D. = standard deviation; C.V. = coefficient of variation; \* see section 6.2.).

## Part 1

Elem.	n	n > LLD	Approx. LLD in ppm	Mean in ppm	S.D. in ppm	C.V. (%)	Min. in ppm (sample)	Max. in ppm (sample)
Na	25	25	1.2	279	412	148	21 (40E)	1825 (43G)
Mg	25	25	0.03	266	271	102	24 (40E)	982 (42B)
Al	25	16	0.5				< LLD	21 (36B)
P	25	18	0.5				< LLD	5.8 (44Top)
S	25	25	0.5	30	36	117	4.5 (44A2)	132 (41B2)
K	25	25	1.2	38	18	46	8.5 (43AE)	87 (42B)
Ca	25	25	0.05	466	267	57	110 (43E)	1102 (38BC)
Cr	25	11	0.05				< LLD	0.2 (38BC)
Fe	25	17	0.05				< LLD	7.8 (41B1)
Ni	25	16	0.2				< LLD	0.9 (38BC)
Cu	25	3	0.05				< LLD	0.1 (38BC)
Zn	25	23	0.1	0.46	0.2	44	< LLD	1.0 (38BC)

## Part 2

Elem.	n	n > LLD	Approx. LLD in ppb	Mean in ppb	S.D. in ppb	C.V. (%)	Min. in ppb (sample)	Max. in ppb (sample)
Be	25	0	67				< LLD	< LLD
B	25	8	362				< LLD	1894 (41B2)
V	25	14	9				< LLD	112 (41B1)
Co	25	15	13				< LLD	82 (42Top)
As	25	3	71				< LLD	90 (44A2)
Se	25	4	877				< LLD	24000* (41B2)
Mo	25	3	49				< LLD	61 (40E)
Cd	25	8	17				< LLD	43 (41B2)
Sb	25	5	23				< LLD	72 (42Top)
Ba	25	25	61	10274	7326	71	2273 (36E)	32646 (44C)
Tl	25	15	3				< LLD	16 (41B1)
Pb	25	5	54				< LLD	297 (42B)
Bi	25	4	3				< LLD	6 (44A2)
U	25	.1	30				< LLD	66 (38B)

### 6.3. PARTICLE SIZE DISTRIBUTIONS AND FIELD OBSERVATIONS

The particle size distributions of 22 soil samples were determined. The initial Wentworth size classes were grouped into wider ones in order to reduce the number of variables (section 2.8.). The results are summarised in Figure 6.4.

#### 6.3.1. Soil associated with schist

**Pit 36:** The soil profile at Pit 36 formed at the border of the pediment and the slope of the incision. The A- and the E-horizons derived from the colluvial coverage and consist mainly of sesquioxide, quartz and granite gravel. The B-horizon derived probably directly from schist of the Malmesbury Group. The soil horizons have distinctly different particle size distributions (Figure 6.4). The B-horizon contains very high proportions of fines and fine clay while the A- (not illustrated) and the E-horizon contain very high proportions of gravel. The transition between the E- and the B-horizon is abrupt.

**Source of gravel:** Neither the B-horizon at Pit 36 nor the saprolite of the schist at Pit 35 contain gravel, probably indicating that the schist which underlies the toposequence contains no or very little gravel. The colluvial deposit at the top of the toposequence is the only possible source of granite and quartz gravel.

**Colluviation of the soils at Pits 37 and 38:** The literature discussed in section 4.5.4. demonstrated that the gradient between Pits 37 and 38 (approximately 100 ‰) is steep enough to expect gravitational transport of the soil. This was confirmed by the occurrence of quartz and granite gravel in the top- and subsoil of the lower slope positions.

**Mixing during colluviation:** The change of the particle size distribution from the top- and subsoil at Pits 37 and 38 is, in contrast to the soil profile at Pit 36, indistinct. Neither the finer particle size classes nor gravel occur in very large proportions. This is best explained by hypothesising that colluviation resulted in mixing of the coarse material from the top of the toposequence and the finer weathering products of the underlying schist. This would be in agreement with Munnik *et al.* (1992) who studied the hillslope properties of a granitic landscape in South Africa and considered that gravitational transport could be important in determining observed particle size distributions and resulted in admixture of colluvium and materials weathered from a nearby saprolite. Removal of relatively fine particles from the top of the toposequence and their deposition in the lower slope positions by means of sheet floods and throughflow water, as observed by Purves (1976), may have contributed to the mixing of coarse and fine materials.

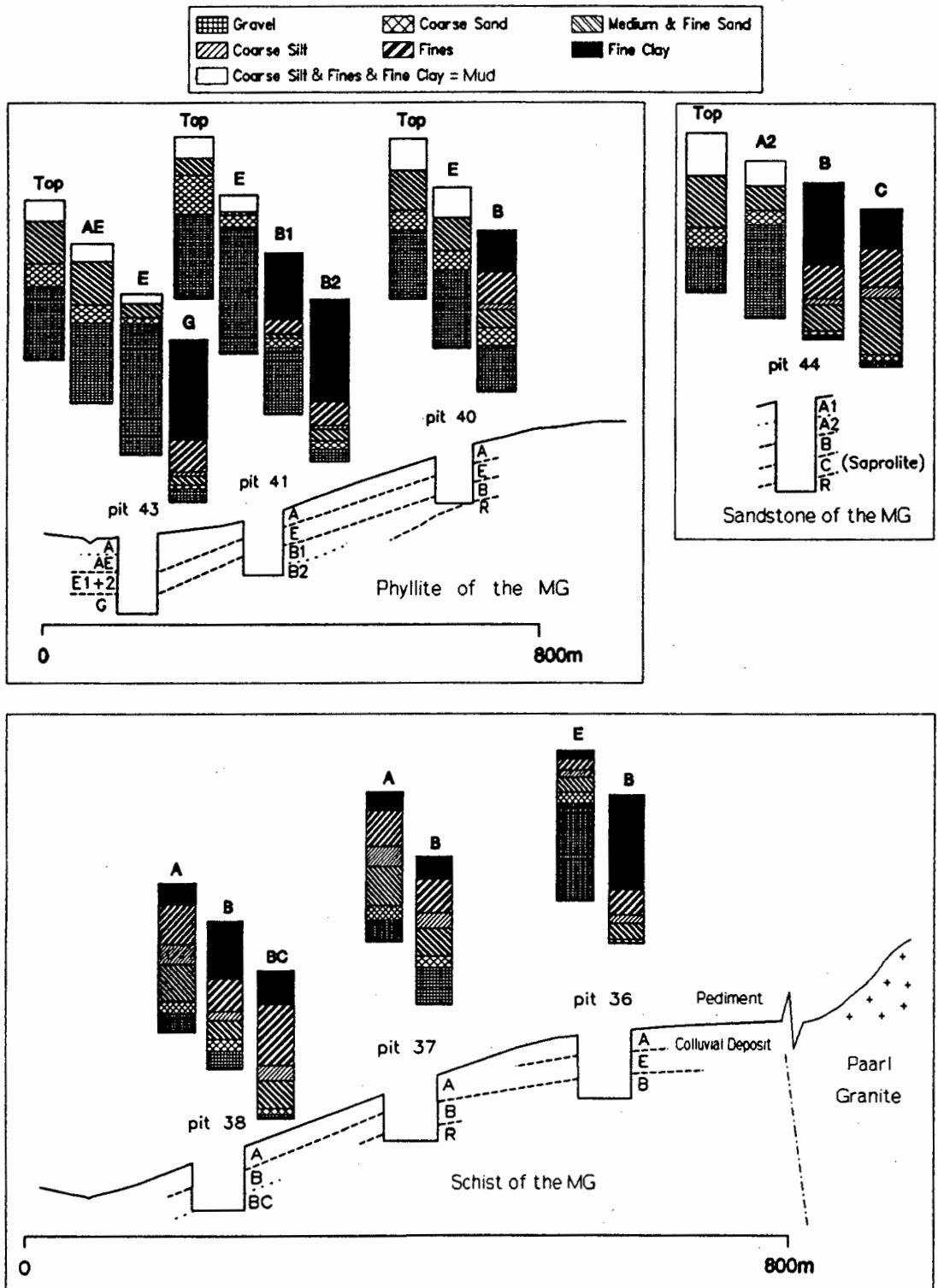


**Figure 6.4:** Particle size distributions of the soils associated with the sediments of the Malmesbury Group (MG). The full size of the bars represents 100 weight % of the inorganic soil fraction. The particle size distribution of sample 36Top was not determined in detail and is, therefore, not displayed. For some samples the proportions of coarse silt, fines and fine clay were not determined and are reported together as "mud" (white areas).

### 6.3.2. Soil associated with phyllite

The proportion of gravel is generally high (Figure 6.4). Quartz gravel is not restricted to the soil and occurs also in the underlying phyllite (sample 39Sap; Appendix-I). The proportion of relatively fine particles increases from the top- to the subsoil and within the subsoil from the top to the bottom of the toposequence, possibly indicating that finer particles are eluviated from the topsoil and partly illuviated into the subsoil near to the bottom of the toposequence. Suspension in throughflow water may be an important mechanism for the transportation of the clay particles (Purves, 1976). A very gravelly E-horizon probably acting as permeable pathway for the throughflow was recognised in all pits.

### 6.3.3. Soil associated with sandstone

Figure 6.4 shows the particle size distribution of Pit 44. The distinct increase in the proportion of fine clay from the C- to the B-horizon probably reflects both the alteration of relatively coarse grained minerals (e.g. feldspars) to clay minerals and the illuviation of fine clay from the topsoil into the subsoil. The upper horizons are relatively enriched in coarse sand and gravel. The particles in the coarse sand and gravel fractions consist chiefly of sesquioxide concretions and quartz.

## 6.4. MAJOR SOIL COMPONENTS

**Mineralogy (summarised from Chapter 3):** The mineralogical composition was determined from 8 soil samples and the three (weathered) underlying materials. The XRD scans showed that quartz is the most abundant mineral component in all samples analysed. Feldspars and goethite also occur in all samples but in smaller proportions. The proportion of feldspars was shown to decrease generally from the underlying material to the subsoil and further to the topsoil. The samples of the schist and the phyllite contain kaolinite while the sample of the sandstone does not. It was thus concluded that the kaolinite present in the soil on sandstone is pedogenic while the kaolinite present in the soil on schist and phyllite may be both inherited from the underlying material and pedogenic. The proportions of 10Å-phyllsilicates (illite, halloysite and(or) muscovite) decrease from the underlying material to the soil. Alteration of these minerals to kaolinite during soil formation was, therefore, suggested. The sandstone and the E-horizon of Pit 36 contain hematite in detectable amounts.

The phyllite which underlies the toposequence at Location 8 (sample 39Sap) was taken from a road embankment. The high proportion of halite in sample 39Sap (approximately 15 %; section 2.4.1.5.) is probably the result of surface evaporation of ground water.

**Elemental composition (Table 6.1):**  $\text{SiO}_2$  is the most abundant compound. Its concentration ranges between 50 and 92 percent. The proportions of  $\text{Al}_2\text{O}_3$  vary between 2.3 and 22.6 percent. The mean of the  $\text{Fe}_2\text{O}_3$  concentration is 8.7 percent.  $\text{K}_2\text{O}$ ,  $\text{TiO}_2$  and  $\text{MgO}$  have means between 1.3 and 0.5 percent. All other compounds have means lower than 0.5 percent.

## 6.5. FACTORS WHICH DETERMINE THE SOIL CHEMISTRY

**Effect of different underlying rock, fertilisation and sampling technique on the analytical results:** Average concentrations were calculated separately for soils associated with schist, phyllite and sandstone of the Malmesbury Group. The chemical differences between these soil groups are discussed in section 6.5.1. A discussion of the possible effects of fertilisation and sampling technique is given in section 6.5.2.

**Lateral change of concentrations:** The lateral change of the concentrations down the toposequences is discussed in sections 6.5.3. to 6.5.5. Elements which are not discussed in these sections were excluded because (a) their concentrations are mainly below the LLD, (b) the number of samples analysed for these elements was too low to recognise lateral trends (Tables 6.1 to 6.4), or (c) the lateral change in the concentrations was insignificant.

### 6.5.1. Effect of underlying rock-type on soil chemistry

**Introduction:** Average concentrations were calculated for all elements. This was accomplished separately for the soils on schist, phyllite and feldspathic sandstone and included the calculation of separate average concentrations for top- and subsoil. The data were examined using a (non-parametric) Kruskal-Wallis Test (95 % confidence level; Statgraphics, 1993) to determine the significance of the differences between the average concentrations.

**The average concentrations are based on the following numbers of samples and pits:**

(a) Soil associated with *schist* of the Malmesbury Group.

Topsoil group: 4 samples from 3 pits.

Subsoil group: 4 samples from 3 pits.

(b) Soil associated with *phyllite* of the Malmesbury Group.

Topsoil group: 7 samples from 3 pits.

Subsoil group: 4 samples from 3 pits.

(c) Soils associated with *feldspathic sandstone* of the Malmesbury Group.

Topsoil group: 2 samples from 1 pit.

Subsoil group: 2 samples from 1 pit.

**Meaning of the #-symbol in the presentation of the results:** The differences between the soil groups were compared with the differences between the underlying rocks. A # was used if the differences between the underlying materials could be controlling the differences between the soil groups; i.e. if a higher concentration in a particular soil group corresponded with a higher concentration in its underlying material.

#### Results for the topsoil

##### **Comparison of soil on schist with soil on phyllite:**

The concentrations of Th, Br, Nb#, Zr#, Mn#, Cr#, V# and S are higher in the soil on schist. The concentrations of SiO<sub>2</sub># and W# are higher in the soil on phyllite.

##### **Comparison of soil on schist with soil on feldspathic sandstone:**

The concentration of P<sub>2</sub>O<sub>5</sub># is higher in the soil on feldspathic sandstone.

##### **Comparison of soil on feldspathic sandstone with soil on phyllite:**

The concentrations of SiO<sub>2</sub> and extractable S# are higher in the soil on phyllite. The concentrations of TiO<sub>2</sub>#, Fe<sub>2</sub>O<sub>3</sub>#, MgO#, Na<sub>2</sub>O, K<sub>2</sub>O, Th, Pb#, As, Zn#, Ni#, Cu, Nb, Zr#, Y#, Sr#, Rb, Mn#, Cr and V are higher in the soil on feldspathic sandstone.

#### Results for the subsoil

##### **Comparison of soil on schist with soil on phyllite:**

The concentrations of TiO<sub>2</sub>#, Nb#, Zr#, Sr and Mn# are higher in the soil on schist. The concentrations of Fe<sub>2</sub>O<sub>3</sub>, K<sub>2</sub>O#, As#, Ni, Rb#, Cr and Sn are higher in the soil on phyllite.

##### **Comparison of soil on schist with soil on feldspathic sandstone:**

None of the calculated average concentrations are significantly different at the 95 % confidence level.

##### **Comparison of soil on feldspathic sandstone with soil on phyllite:**

None of the calculated average concentrations are significantly different at the 95 % confidence level.

**Conclusions:** The differences between the soils associated with different rock-types are generally small, although significant for some of the investigated elements. The similarity of the soil groups could be the result of (a) the small chemical differences between the underlying rocks and (b) the similar chemical differentiation of the underlying rock during soil formation. Trying to explain the described differences for individual elements would be too speculative and was thus not attempted. It is, however, interesting to note that some of the differences between the soil groups cannot be linked to the differences between the underlying materials and must be due to soil forming processes (elements without #).

### 6.5.2. Effect of agro-chemicals and sampling procedure on the analytical results

**Introduction:** The results of soil samples from two pits (41 and 42) were compared to determine the possible effects of agro-chemicals and sampling technique on the analytical results. Top- and subsoil were compared separately. Pits 41 and 42 are in a similar slope position and only 50 m apart from each other. The phenotype of the two soil profiles is almost identical (Appendix-I). It is thus proposed that the chemical composition of the soil exposed in the two pits was initially very similar. The recent history of the soil at the two pits differs in three points:

(a) the soil at Pit 41 is under recent cultivation and was treated with agro-chemicals while the soil at Pit 42 is not cultivated. The cultivation of the soil at Pit 41 may have caused chemical differences between the soil samples from the two pits.

(b) Pit 41 was dug shortly before the sampling was performed while Pit 42 was an old erosion gully. The longer exposure of the soil profile in the erosion gully (Pit 42) may have resulted in chemical alterations.

(c) Pit 42 was sampled using plastic tools while Pit 41 was sampled using metal tools. The sampling with metal tools may have resulted in contamination of the soil samples taken from Pit 41.

**Method of comparison:** The elemental concentrations determined from the samples of the two pits are considered different if the ratio [concentration in sample from Pit 41] over [concentration in sample from Pit 42] is  $> 1.3$  or  $< 0.7$ . The LLD was used to substitute for the concentration if the concentration was below the LLD.

#### Results for the topsoil

The concentrations of Br and 1 M  $\text{NH}_4\text{NO}_3$  extractable Ca and B are higher in the sample from Pit 41. The concentrations of extractable Zn, Sb, Fe, Co, Al, Ba and Mg are higher in the sample from Pit 42.

#### Results for the subsoil

The concentrations of I and 1 M  $\text{NH}_4\text{NO}_3$  extractable Se, Fe, Cd, Bi, B and S are higher in the sample from Pit 41. The concentrations of extractable Ba, P, K, Ca and Co are higher in the sample from Pit 42.

**Conclusions:** The chemical differences between the two pits are limited to relatively soluble elements and the concentrations of the extractable element fractions. It is not possible to resolve whether the differences are natural or due to the dissimilar recent history of the two pits (see above; points a to c). It is, however, possible to conclude that the concentrations of the elements which are not listed above are hardly affected by (a) the cultivation (e.g. agro-chemicals and ploughing), (b) the time period between first exposure of soil profile and sampling and (c) the usage of metal tools for the sampling procedure.

### 6.5.3. Lateral change of the concentrations down the topsoil

**Allocation of elements to groups:** The elements were allocated to groups in order to facilitate their discussion. The manner in which the elements were grouped was explained in section 1.2. Elements which are allocated to Group-I and Group-III are illustrated in **bold**.

- Group-I: (based on toposequence associated with schist) **Li, Be, Na<sub>2</sub>O, MgO, Al<sub>2</sub>O<sub>3</sub>, S, K<sub>2</sub>O, CaO, TiO<sub>2</sub>, Mn, Co, Ni, Cu, Zn, Br, Rb, Sr, Y, Nb, Sn\*, I, U\*** and 1 M NH<sub>4</sub>NO<sub>3</sub> extractable **Na, Mg, P\*, K\*, Ca, Ni, Zn, Ba** and Tl.
- Group-II: (based on toposequence associated with schist) V, Fe<sub>2</sub>O<sub>3</sub>, As, Se, Mo, Sb and 1 M NH<sub>4</sub>NO<sub>3</sub> extractable Co.
- Group-III: (based on toposequence associated with phyllite) **Li\*, Be\*, MgO, Al<sub>2</sub>O<sub>3</sub>, P<sub>2</sub>O<sub>5</sub>, S\*, K<sub>2</sub>O, CaO, TiO<sub>2</sub>, V, Cr, Mn, Fe<sub>2</sub>O<sub>3</sub>, Ni, Cu, Zn, Rb, Sr, Y, Nb, Sn, Sb\*, Pb, Th, U** and 1 M NH<sub>4</sub>NO<sub>3</sub> extractable **K, Ca** and **Ba**.
- Group-IV: (based on toposequence associated with phyllite) Na<sub>2</sub>O, SiO<sub>2</sub>, Cl, Co\* and 1 M NH<sub>4</sub>NO<sub>3</sub> extractable Na and Co.

**Results for toposequence associated with schist (Figure 6.5):** The concentrations of the elements in Group-I increase down the toposequence. The concentrations of the elements in Group-II are at a maximum at the top of the toposequence (Pit 36).

**Results for toposequence associated with phyllite (Figure 6.5):** The concentrations of the elements in Group-III decrease down the toposequence. The concentrations of the elements in Group-IV are at a maximum at the bottom of the toposequence (Pit 43).

**Input of Group-I elements from the underlying material and the top of the toposequence (toposequence associated with schist):** It was suggested in section 6.3.1. that the colluviation down the toposequence associated with schist resulted in mixing of the coarse material from the top of the toposequence and the finer grained weathering products of the underlying schist. An examination of the vertical elemental distribution showed that most of the elements in Group-I have higher concentrations in the subsoil and in the underlying saprolite than in the topsoil (section 6.5.6.). It is thus proposed that the increasing concentrations of the Group-I elements down the toposequence reflect the mixing of the topsoil with the underlying material.

Lateral transport of relatively fine particles and dissolved solids from the top of the toposequence towards the lower slope positions (Pits 37 and 38) by means of throughflow or sheet wash (section 6.3.1.) may be an additional source of Group-I elements. This would be in agreement with Selby (1982) who described a case where this mechanism resulted in an increase of the soil fertility at the footslope.

---

\* Allocation of the element to the group is debatable because (a) some of the samples have concentrations below the LLD, (b) some of the samples were not analysed for this particular element and (c) the agreement between the lateral variation of the elemental concentration and the group pattern is poor.

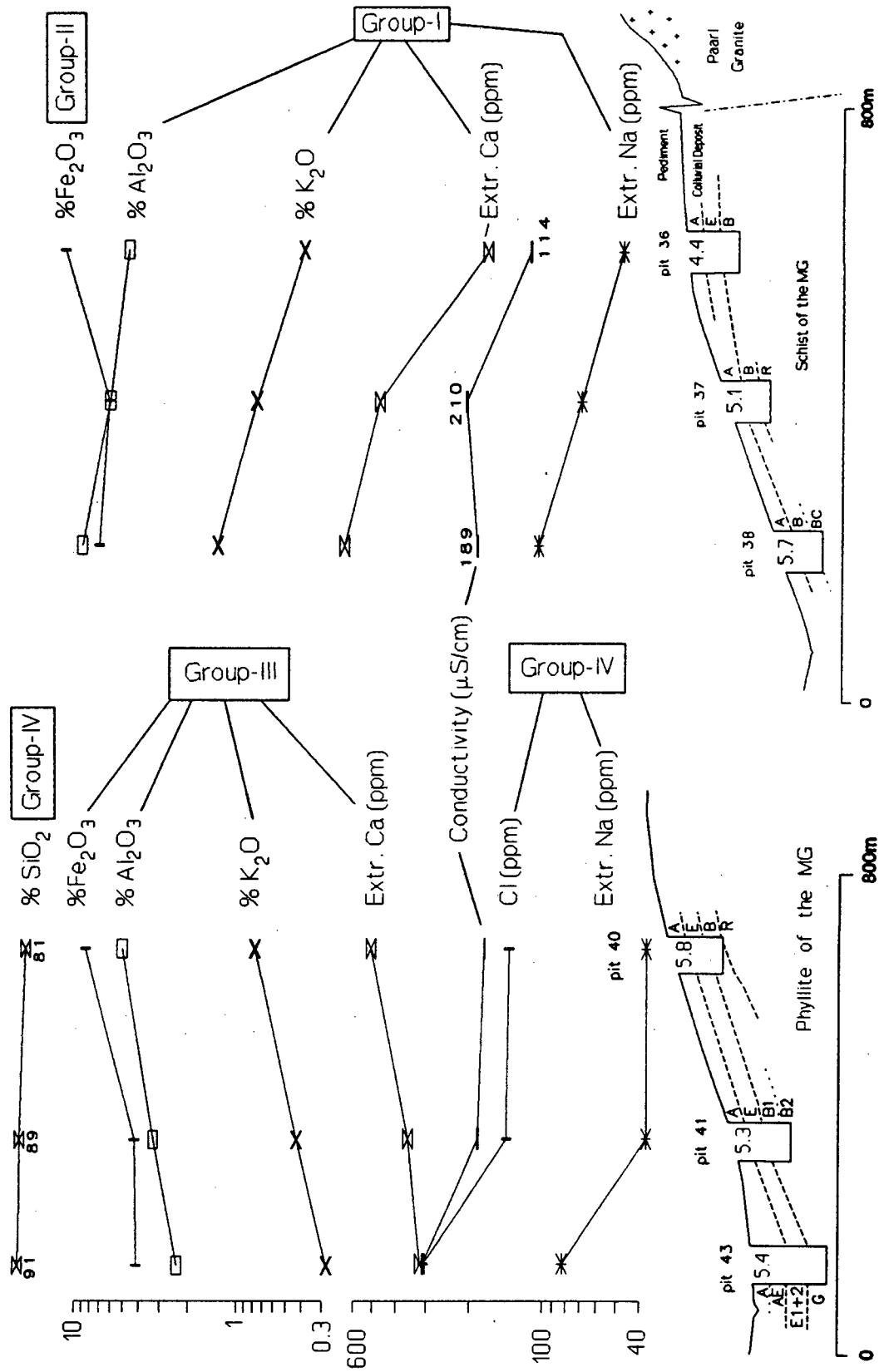


**Figure 6.5:** Lateral change of the concentrations down the topsoil of the toposequences associated with sediments of the Malmesbury Group. A subset of elements was selected to demonstrate the trends which are typical for the different element-groups. A full list of the elements allocated to the groups is given in the text. The numbers in the pits refer to the pH(KCl) values of the topsoil.

**Increasing retention ability down the toposequence associated with schist as secondary control for some of the Group-I elements:** The underlying schist is fine grained and contains clay minerals such as illite and kaolinite (section 6.4). The admixture of clay minerals from the underlying material and the top of the toposequence to the topsoil at Pits 37 and 38 explains the increasing proportions of mud down the toposequence (Figure 6.4). A resulting increase of the retention ability for water and dissolved solids may be a secondary cause for the increasing concentrations of Br, I and the extractable element fractions (Na, Mg, P, K, Ca, Ni, Zn, Ba and Tl). The alkaline reaction of exchangeable  $\text{Na}^+$  could explain the relatively high pH value at the bottom of the toposequence. Retained salts increased the conductivity of the (water-suspended) topsoil at the bottom of the toposequence.

**Accumulation Group-II elements in Fe-oxides at the top of the toposequence associated with schist:** The similar behaviour of  $\text{Fe}_2\text{O}_3$  and Group-II elements indicates association of Group-II elements with Fe-oxides. Higher concentrations of the Group-II elements occur in the top part of the toposequence (Pit 36). The decrease of the concentrations towards the lower slope positions may be due to the dilution with Group-I elements.

**Eluviation of Group-III elements from the topsoil down the toposequence associated with phyllite:** The literature discussed in section 4.5.4. demonstrated that the gradient of the toposequence associated with phyllite (approximately 100 ‰) is steep enough to expect gravitational transport of the soil. The very high proportion of gravel in the A- and E-horizons of the toposequence associated with phyllite (section 6.3.2.) presumably results in a high permeability for water and descending clay particles (Blume, 1992). The mean percentage of exchangeable sodium (ESP) is relatively high (29 %) and would thus favour the dispersion and eluviation of clay particles (Purves, 1976). It could thus be speculated that the topsoil is continuously leached and eluviated during its transport towards the footslope. The continuous loss of finer particles and dissolved solids from the topsoil could explain the decrease of the Group-III element concentrations and the decrease of the proportion of organic matter towards the lower slope positions. The loss of Group-III elements results in relative accumulation of  $\text{SiO}_2$ . The eluviated particles may be both illuviated into the subsoil or removed from the toposequence into the drainage line by means of throughflow in the very gravelly and permeable E-horizon (section 6.3.2.). The hypothesis presented in this paragraph would be in agreement with the results for the granite-derived toposequence which suggested eluviation and depletion of elements during the gravitational transport of the soil and with increasing distance from the top of the toposequence (section 4.5.4).

**Possible precipitation of NaCl in the lowest slope position of the toposequence associated with phyllite:** The relatively high concentrations of Cl and extractable Na in the lowest slope position (Figure 6.5; sample 43Top) are probably due to evaporation of throughflow water and capillary uplifted ground water, as described in Buol *et al.*

(1980) and Conacher (1975). The precipitation of NaCl could account for the observed increase of the total Na concentration ( $\text{Na}_2\text{O}$ ). The increased concentrations of Na and Cl correspond with higher conductivities of the water-suspended soil.

**Comparison of the toposequences associated with schist and phyllite:** The two toposequences are similar with respect to aspect, gradient and shape of the slope and climate. Both toposequences are underlain by a clay-rich metamorphosed sediment. In spite of these similarities the elements demonstrated in bold (see above) have increasing concentration down the toposequence associated schist and decreasing concentration down the toposequence associated phyllite. It was suggested that the colluviation down the toposequence associated with schist results in admixture of weathering products from the underlying rock into the topsoil and causes increasing elemental concentrations down the slope. The decrease of the elemental concentrations down the toposequence associated with phyllite may be the result of continuous eluviation during gravitational transport. The higher percentage of gravel and the accompanied increase of the permeability as well as higher ESP values (see above) probably favour the eluviation of clay in the toposequence associated with phyllite. The higher percentage of gravel could also increase the proportion of the precipitation which infiltrates into the soil (Poesen and Lavee, 1994; Brakensiek and Rawls, 1994; Valentin, 1994) and in this way increase the quantity of water available for eluviation. Statham (1977) concluded from laboratory experiments that the quantity of water available for eluviation is by far the most important factor in determining vertical clay displacement.

Many of the elements illustrated in bold are important nutrients. More research should be directed in order to investigate in more detail why eluviation of finer particles and removal of nutrients from the topsoil predominates in the toposequence associated with phyllite while admixture of finer particles and nutrients from the underlying material into the topsoil predominates in the toposequence associated with schist. The clay mineralogy and the structure of the soil are important determinants of the permeability and should be investigated in greater detail. The toposequence associated with phyllite is used for crop production while the toposequence associated with schist is vegetated with shrubveld. The possible effects of cultivation and vegetation type with regard to eluviation and colluviation should be considered when examining the possible reasons for the differences between the toposequences.

#### 6.5.4. Lateral change of the concentrations down the subsoil of the toposequence on schist

Results for F, Na<sub>2</sub>O, MgO, P<sub>2</sub>O<sub>5</sub>, Cl, K<sub>2</sub>O, Cr\*, Ni\*, Cu, Rb and 1 M NH<sub>4</sub>NO<sub>3</sub> extractable Na and V (Group-V elements; Figure 6.6): The concentrations of the elements in Group-V, the conductivity of the water-suspended soil and the pH values increase down the toposequence. The highest concentrations occur in the underlying material (saprolite; sample 35Sap).

**Assimilation of Group-V elements from the underlying material:** The results discussed above suggested that colluviation resulted in mixing of the soil and weathering products of the schist. It is suggested that the mixing also resulted in the assimilation of Group-V elements from the underlying material and caused the observed increase of the concentrations down the toposequence.

Uptake of salts (e.g. NaCl) from the underlying material could best explain the increasing conductivity of the (water-suspended) soil down the toposequence. The increase of the pH towards the lower slope positions may be due to the alkaline reaction of exchangeable Na<sup>+</sup>.

**Results for Al<sub>2</sub>O<sub>3</sub> and 1 M NH<sub>4</sub>NO<sub>3</sub> extractable B, Mg, Al, S, K, Cr, Fe and Zn (Group-VI elements; Figure 6.6):** High concentrations of the elements in Group-VI at the top and the bottom of the toposequence coincide with higher proportions of finer particles (fine clay and fines; samples 36B and 38B in Figure 6.4). The similar behaviour of Al<sub>2</sub>O<sub>3</sub>, mud, fine clay and the Group-VI elements suggests that the retention ability of clay minerals for water and dissolved solids is an important control for the concentrations of the elements in Group-VI.

**Results for S, CaO, Mn, Sr, I and 1 M NH<sub>4</sub>NO<sub>3</sub> extractable P, Ca, Ni and Ba (Group-VII elements; Figure 6.6):** The concentrations of the elements in Group-VII are relatively low in the underlying material and increase from the top to the bottom of the toposequence.

**Evaporation of soil water and pH as controlling factors:** Continuous evaporation of water from the soil could result in accumulation of most Group-VII elements. The distance between soil and ground water table would normally decrease towards the footslope (Figure 2.1). Possible sources of soil water available for evaporation are, therefore, capillary elevation of ground water as well as overland flow and throughflow from the upper part of the toposequence. The importance of throughflow in the salinisation of soils in the footslope position was demonstrated by Conacher (1975).

---

\* Allocation of this element to the group is debatable because the agreement between the lateral trend of its concentration and the group pattern is poor.

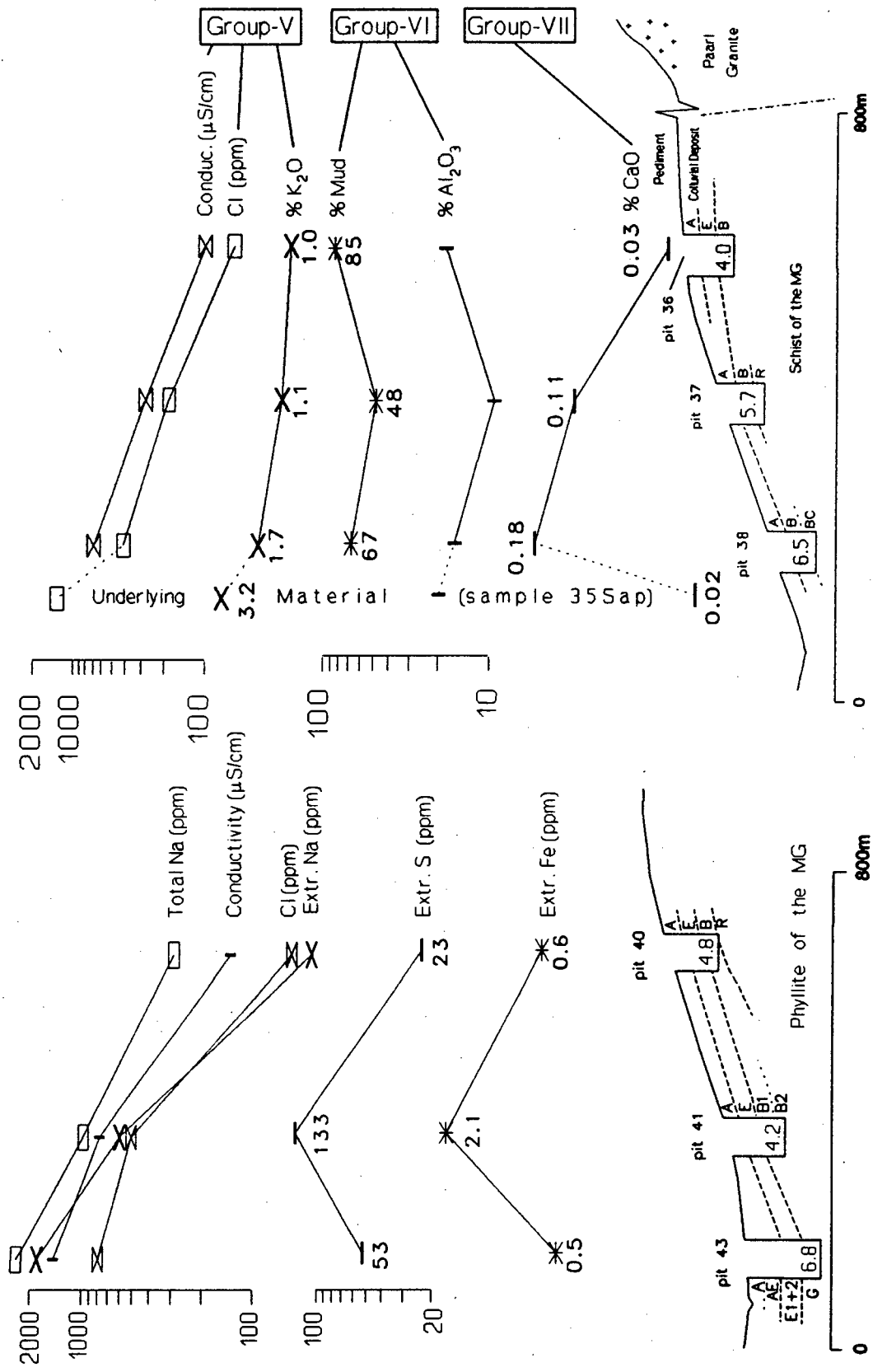


**Figure 6.6:** Lateral change of the elemental concentrations down the subsoil of the toposequence associated with schist (right side). A subset of elements was selected to demonstrate the trends which are typical for the different element-groups. A full list of the elements allocated to the groups is given in the text. The high concentrations of extractable S and Fe in the subsoil at Pit 41 (toposequence on phyllite) are also characteristic for total S and I and extractable B, Al, V, Cr, Co, Se, Pb and Bi. The numbers in the pits refer to the pH(KCl) values of the subsoil.

The lower part of the B-horizon in footslope position (sample 38BC) contains carbonate in detectable proportions (Appendix-I). Association of Group-VII elements with carbonates is, therefore, possible.

The increase of the concentrations towards the bottom of the toposequence coincides with higher pH values (Figure 6.6). The ability of soils to adsorb cations increases with increasing pH values. It is, therefore, suggested that the soil pH may be a secondary factor in controlling the increase of the concentrations (e.g. extractable Ni).

**Gravel, SiO<sub>2</sub> and Zr (Figure 6.7; text box 5):** The concentrations of SiO<sub>2</sub>, Zr and the proportion of gravel are at a maximum in midslope position (subsoil). The subsoil in the footslope and the uppermost slope position as well as the underlying material have lower concentrations. The highest proportions of gravel and Zr overall occur in the partly granite-derived topsoil at the top of the toposequence. Admixture of material from the colluvial deposit at the top of the toposequence by means of colluviation may thus be the reason for the increased concentrations in the subsoil at midslope position (see above).

**Bromine and Pb:** The concentrations of Br and Pb are at a maximum in the fine textured subsoil at the top of the toposequence, indicating the association of Br and Pb with clay minerals.

#### 6.5.5. Lateral change of the concentrations down the subsoil of the toposequence on phyllite

The variation of most elemental concentrations is small. Only elements which showed meaningful changes in concentration are discussed in this section.

**Accumulation of Na and Cl at the bottom of the toposequence:** The concentrations of Cl, extractable Na and total Na as well as the conductivity of the water-suspended soil and the pH value increase towards the lowest slope position (sample 43G; Figure 6.6; Table 6.5). This increase coincides with higher proportions of finer particles (mud and fine clay; Figure 6.4). It is suggested that the increasing salinisation of the soil down the toposequence is controlled by the evaporation of water from the soil. The salinisation reaches its maximum in the lowest slope position because (a) the finer textured soil can retain more water and solubles and (b) the distance between soil and ground water table presumably decreases down the toposequence (Figure 2.1). Evaporation of throughflow water at the bottom of the toposequence may also result in higher concentrations of Na and Cl (Conacher, 1975). The alkaline reaction of exchangeable Na<sup>+</sup> probably caused the increased pH values [pH(KCl) in subsoil at footslope = 6.8].

**Table 6.5:** High concentrations of S, I and some  $\text{NH}_4\text{NO}_3$  extractable element fractions in the subsoil at the midslope position of the toposequence associated with the phyllite of the Malmesbury Group. The concentrations of extractable Na, the pH(KCl) values, the conductivity of the water-suspended soil and the total concentrations of the anomalous elements are listed in the lower part of the table.

Parameter	Units	SLOPE POSITION AND SAMPLE				
		Top 40B	Middle 41B1	Middle 41B2	Middle 42B	Bottom 43G
Extr. B	ppb	<362	1799	1893	1025	<362
Extr. Al	ppm	1.5	17	6	8	0.8
Extr. S	ppm	23	62	132	92	52
Total S	ppm	279	445	669		213
Extr. V	ppb	10	111	64	83	37
Extr. Cr	ppm	0.05	0.13	0.13	0.18	0.10
Extr. Fe	ppm	0.55	7.7	2.0	0.78	0.45
Extr. Co	ppb	<13	29	19	31	<13
Extr. Se#	ppb	<875	23000	24000	<875	<875
Total I	ppm	85	98	208	55	49
Extr. Pb	ppb	<52	219	210	297	<52
Extr. Bi	ppb	<3	6	6	<3	<3
Extr. Na	ppm	45	425	597	880	1825
$\text{Na}_2\text{O}$	%	0.04	0.11	0.13		0.32
$\text{Al}_2\text{O}_3$	%	14.3	20.0	22.6		22.2
Total Cl	ppm	59	377	506		806
Total V	ppm	123	156	158		175
Total Cr	ppm	101	123	126		138
$\text{Fe}_2\text{O}_3$	%	8.2	9.7	9.9		9.8
Total Se	ppm	2.8	3.2	2.8	2.4	1.4
Total Pb	ppm	29	25	19	22	22
Total Bi	ppm	<2.8	<2.9	<2.9	<2.9	<2.9
pH(KCl)		4.8	4.2	4.2		6.8
Conductivity	$\mu\text{S cm}^{-1}$	134	600	783		1470

# The quality of the analyses of extractable Se is discussed in section 6.2.

**High concentrations of 1 M  $\text{NH}_4\text{NO}_3$  extractable B, Al, S, V, Cr, Fe, Co, Se\*, Pb, Bi and total S and I in midslope position:** The concentrations of extractable B, Al, S, V, Cr, Fe, Co, Se, Pb, Bi and total S and I are particularly high in the subsoil in

\* See section 6.2.

midslope position (samples 41B1, 41B2 and 42B; Figure 6.6; Table 6.5). The total concentrations of the corresponding elements are not anomalous (Table 6.5). There is no obvious explanation for the concentration of the listed elements in midslope position.

#### 6.5.6. Vertical changes of the concentrations

**Results (a):** The concentrations of SiO<sub>2</sub>, P<sub>2</sub>O<sub>5</sub>, Mn, Zr and 1 M NH<sub>4</sub>NO<sub>3</sub> extractable P\* and Co decrease from the top- to the subsoil. This is in agreement with the results from soil profiles which are underlain by different rock-types (e.g. section 5.6.). A discussion of the accumulation of P, Mn and Co in the topsoil is given in Chapter 9.

**Results (b):** The concentrations of Li\*, Be\*, F, Na<sub>2</sub>O, MgO, Al<sub>2</sub>O<sub>3</sub>, K<sub>2</sub>O, TiO<sub>2</sub>, Co\*, Ni, Zn, Se\*, Br, Rb, Sr, Y, Nb, Mo\*, Sn, I, W, Th, U and extractable B\*, Na, Mg, Al, S, Cr, Ni and Ba\* increase from the top- to the subsoil.

**Interpretation:** The increasing concentrations towards the subsoil coincide with higher proportions of clay minerals, feldspar and goethite (Chapter 3; sections 6.3 and 6.4). Association of the above listed elements with these minerals is, therefore, likely. Some of the elements (e.g. TiO<sub>2</sub>, W, Nb and U) may be hosted by heavy minerals and could thus indicate accumulation of heavy minerals in the subsoil.

**Results (c):** The elements Na<sub>2</sub>O, TiO<sub>2</sub>, Mn, Y, Zr and extractable Na, S, K, Ca and Zn are partly depleted in the E-horizons while the elements V, Cr, Fe<sub>2</sub>O<sub>3</sub>, Cu, As, Se and extractable Fe as well as gravel are enriched in some of the E-horizons.

**Interpretation:** The low elemental concentrations in the E-horizon are due to leaching and eluviation. The elements which have relatively high concentrations in the E-horizon are likely to be accumulated in the partly gravel-sized Fe-oxide concretions.

**Other elements:** Elements which are not mentioned in this section were not discussed because (a) they have mainly concentrations below the LLD, (b) the number of samples analysed for these elements was too low to recognise vertical trends, (c) they have relatively constant concentrations with increasing soil depth or (d) they showed dissimilar vertical trends. The vertical distribution of individual elements is discussed in Chapter 9.

## 6.6. SUMMARY

**Introduction:** The sampled soils are associated with the sediments of the Malmesbury Group. Soil samples from 10 pits and different soil horizons were analysed for major and trace elements, 1 M NH<sub>4</sub>NO<sub>3</sub> extractable element concentrations, particle size distribution and various other parameters. The toposequence at location 8 is underlain

---

\* Allocation of element to group is not definite. This could be because (a) some of the samples have concentrations below the LLD, (b) some of the samples were not analysed for this particular element and (c) the vertical increase or decrease of the concentration was not observed in all pits.

by phyllite while the toposequence at location 10 is underlain by schist (Figure 2.2). The soil at Pit 44 is underlain by sandstone (location 9 in Figure 2.2).

**Major soil components:** All samples contain quartz, feldspars and goethite in detectable proportions. The proportions of feldspar and 10Å-phyllsilicates (illite, halloysite and/or muscovite) decrease from the underlying material to the subsoil and in some pits further to the topsoil. Kaolinite was shown to be partly of pedogenic origin. The concentration of SiO<sub>2</sub> ranges between 50 and 92 percent. Other major components are Al<sub>2</sub>O<sub>3</sub>, Fe<sub>2</sub>O<sub>3</sub>, K<sub>2</sub>O, TiO<sub>2</sub> and MgO (Table 6.1).

**Differences between the soils associated with different rock-types of the Malmesbury Group:** The averages of the elemental concentrations in the soils associated with sandstone, schist and phyllite were compared. The differences are generally small and thus difficult to interpret.

**Effect of agro-chemicals and sampling technique on analytical results:** The data for soil samples from two pits were compared to establish the possible effects of (a) agro-chemicals, (b) sampling with metal in contrast to plastic tools and (c) the time period between exposure of soil profile and sampling. Chemical differences between the samples were limited to soluble elements and extractable element concentrations. It was concluded that the total elemental concentrations were not significantly affected by a), b) and c).

**Toposequence associated with schist:** Colluviation probably resulted in admixture of minerals and their associated elements from the underlying material into the topsoil. The concentrations of most elements\* increase consequently from the top to the bottom of the toposequence. The uptake of finer particles from the underlying material into the topsoil could result in an increase of the retention ability and may thus be a secondary cause for the increasing concentrations of Br and I and the extractable element fractions down the toposequence (text box 1 in Figure 6.7).

**Toposequence associated with phyllite:** Continuous eluviation during gravitational transport may have caused the depletion of most elements\*\*, mud and organic matter and relative accumulation of SiO<sub>2</sub> down the toposequence (text box 2 in Figure 6.7).

**Critical differences between the two toposequences:** The set of elements in Group-I and Group-III is similar, meaning that many elements which have increasing concentrations down the toposequence associated with schist have decreasing concentrations down the toposequence associated with phyllite. Possible reasons for the strong eluviation and the depletion of Group-III elements down the toposequence associated with phyllite are higher exchangeable sodium percentages (ESP) and very

---

\* Group-I elements: Li, Be, Na<sub>2</sub>O, MgO, Al<sub>2</sub>O<sub>3</sub>, S, K<sub>2</sub>O, CaO, TiO<sub>2</sub>, Mn, Co, Ni, Cu, Zn, Br, Rb, Sr, Y, Nb, Sn, I, U and 1 M NH<sub>4</sub>NO<sub>3</sub> extractable Na, Mg, P, K, Ca, Ni, Zn, Ba and Tl.

\*\* Group-III elements: Li, Be, MgO, Al<sub>2</sub>O<sub>3</sub>, P<sub>2</sub>O<sub>5</sub>, S, K<sub>2</sub>O, CaO, TiO<sub>2</sub>, V, Cr, Mn, Fe<sub>2</sub>O<sub>3</sub>, Ni, Cu, Zn, Rb, Sr, Y, Nb, Sn, Sb, Pb, Th, U and 1 M NH<sub>4</sub>NO<sub>3</sub> extractable K, Ca and Ba.

## Toposequence on Phyllite

**2** Strong vertical eluviation results in continuous depletion of Group-III elements, mud and organic matter and relative accumulation of SiO<sub>2</sub> as the soil moves down the toposequence.

**3**

The set of elements in Group-I and Group-III is similar, indicating that the same elements may have increasing or decreasing concentrations down a toposequence. The very high proportion of gravel and the relatively high exchangeable sodium percentage may facilitate the eluviation of the toposequence on phyllite (section 6.5.3). More research should be directed to explain the very different development of the soil down the two toposequences because many of the affected elements are important nutrients.

## Toposequence on Schist

**1** Colluvium and accompanied mixing results in admixture of Group-I and Group-V elements from the underlying material into the soil. Increasing concentrations from the top to the bottom of the toposequence are the consequence. The admixture of relatively fine particles may increase the retention ability of the soil and could favour the increasing concentrations of the extractable element fractions down the toposequence (Group-I).

**4**

*In situ* part of toposequence: Accumulation of V, As, Se, Mo and Sb in partly gravel sized Fe-oxides.

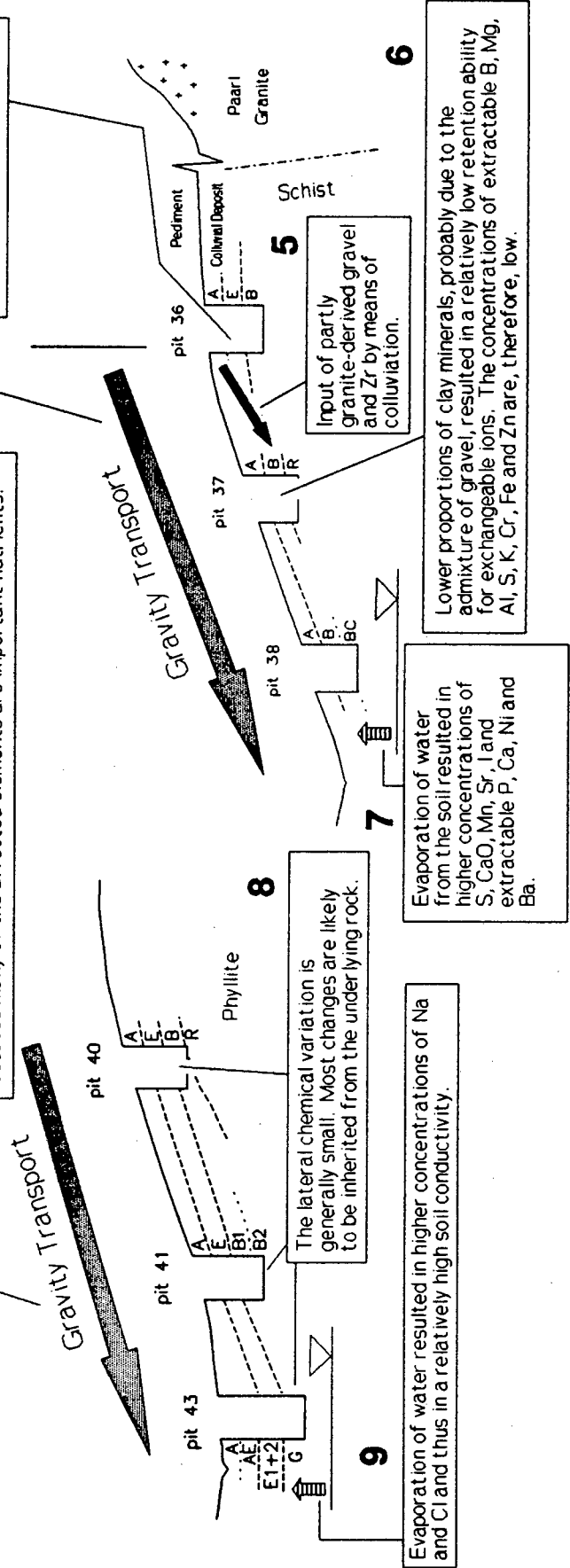


**Figure 6.7:** Interpretative diagram of the toposequences associated with schist and phyllite of the Malmesbury Group.

much higher proportions of gravel (text box 3 in Figure 6.7). Higher ESP values facilitate the dispersion and eluviation of clay and higher proportions of gravel increase the permeability of the soil. Higher proportions of gravel could also increase the infiltration rate and thus increase the quantity of water available for eluviation. It was suggested that the reasons for the very different geochemical development of the soil down the two toposequences be investigated in more detail because, many of the elements which showed reversed behaviour are important nutrients.

**Association of elements with Fe-oxides:** Higher concentrations of Group-II\* elements coincided with higher concentrations of  $\text{Fe}_2\text{O}_3$ . Association with Fe-oxides was thus suggested. Highest concentrations of  $\text{Fe}_2\text{O}_3$  and Group-II elements occur in the top part of the toposequence associated with schist (Pit 36). The decrease of the concentrations towards the lower slope positions of this toposequence may result from dilution with admixed (Group-I) major elements (text box 4 in Figure 6.7).

**Factors which determine the lateral change of the concentrations down the subsoil of the toposequence on schist:**

(a) Increasing concentrations of Group-V elements\*\* down the toposequence suggested that admixture of these elements from the underlying material during colluviation of the slope was an important factor in determining their concentrations (text box 1 in Figure 6.7).

(b) The retention ability, as determined by the proportion of finer particles, seems to be most important in determining the concentrations of 1 M  $\text{NH}_4\text{NO}_3$  extractable B, Mg, Al, S, K, Cr, Fe and Zn (text box 6 in Figure 6.7).

(c) Relatively high concentrations of S, CaO, Mn, Sr, Y, I and 1 M  $\text{NH}_4\text{NO}_3$  extractable P, Ca, Ni and Ba at the footslope suggested that these elements originate partly from evaporated water. Association of some of the above listed elements with carbonates is possible (text box 7 in Figure 6.7). Increased concentrations of carbonates and(or) exchangeable  $\text{Na}^+$  in the lowest slope position could explain relatively high soil pH values. High conductivities of the water-suspended soil coincided with higher concentrations of Na and Cl.

**Vertical distribution:** Many elements have increasing concentrations with increasing soil depth while  $\text{SiO}_2$ ,  $\text{P}_2\text{O}_5$ , Mn, Zr and 1 M  $\text{NH}_4\text{NO}_3$  extractable P and Co have decreasing concentrations. Depletion as well as accumulation of certain elements in the E-horizons was evident.

---

\* Group-II elements: V,  $\text{Fe}_2\text{O}_3$ , As, Se, Mo, Sb and 1 M  $\text{NH}_4\text{NO}_3$  extractable Co.

\*\* Group-V elements: F,  $\text{Na}_2\text{O}$ , MgO,  $\text{P}_2\text{O}_5$ , Cl,  $\text{K}_2\text{O}$ , Cr, Ni, Cu, Rb and 1 M  $\text{NH}_4\text{NO}_3$  extractable Na and V.

# CHAPTER 7.

## SOILS ASSOCIATED WITH FERRUGINIZED MATERIALS

---

### 7.1. INTRODUCTION

**Ferruginization of the underlying material:** The tropical climate during the earlier Cenozoic resulted in deep and intense weathering of soil and underlying rock in the field area (Lambrechts, 1983). Those minerals which are susceptible to weathering (e.g. feldspars) were mainly altered to form Fe-oxides, Al-oxides and kaolinite. This process is referred to as ferruginization (Scheffer and Schachtschabel, 1989). The soils associated with the ferruginized materials are typically red in colour, suggesting that hematite is one of the products of the ferruginization (Torrent, 1994).

Ferruginization can nullify the chemical differences between different rock-types. A Principal Component Analysis of the analytical results presented in this study showed that the soils associated with (a) ferruginized granites and (b) ferruginized sediments of the Malmesbury Group have very similar chemical properties (Schloemann, 1992).

**Occurrence of ferruginized materials (summarised from Lambrechts, 1983):** Similar ferruginized materials may derive from different rock-types. Due to the age of the ferralitic weathering profiles, the original landscapes in which they developed were subsequently modified by incision and stripping. In addition, younger transported material such as marine clays, aeolian sands and colluvium may overlie the older ferruginized materials. The result is that the distribution of the ferruginized materials in the landscape is irregular and that a considerable variety of soils may be found on erosional surfaces in areas characterised by ferralitic preweathering. Ferruginized materials are widespread on high-lying pediments and footslopes adjacent to the Cape Fold Belt east of the field area because these areas were less affected by subsequent erosion and sedimentation. In the field area the ferruginized materials are less abundant and derived from granite and sediments of the Malmesbury Group. Colluviation of high-lying ferruginized materials in the Darling granite hills has resulted in the occurrence of red soils adjacent to fresh granite in the lower-lying areas. Occurrences of ferruginized materials in the west of the field area are irregular and mainly underlain by sediments of the Malmesbury Group.

**Sampling locations:** Samples were taken from six pits (Figure 7.1). Pits 7, 8 and 12 are at different locations in the Darling area (Location 6 in Figure 2.2). The underlying material of these pits consists of ferruginized granite (Theron, 1991).

Pits 47, 46 and 45 were dug down a toposequence, approximately 3500 m north-west of Malmesbury (Location 7 in Figure 2.2). The toposequence strikes south-west north-east, is approximately 1500 m long and has an average gradient of 44 permille. Figure 7.2 shows the view from the pit in the lowermost slope position (Pit 45) towards the top of the toposequence. The geological map shows that the contact between the granite and the sediments of the Malmesbury Group runs through the sampled toposequence (Figure 7.1; Theron, 1991). The relatively large scale of the map (1 : 250000) and a lack of outcrop made it difficult to locate the exact position of the contact. The coordinates and a full pedological description of all pits sampled are given in Appendix-I.

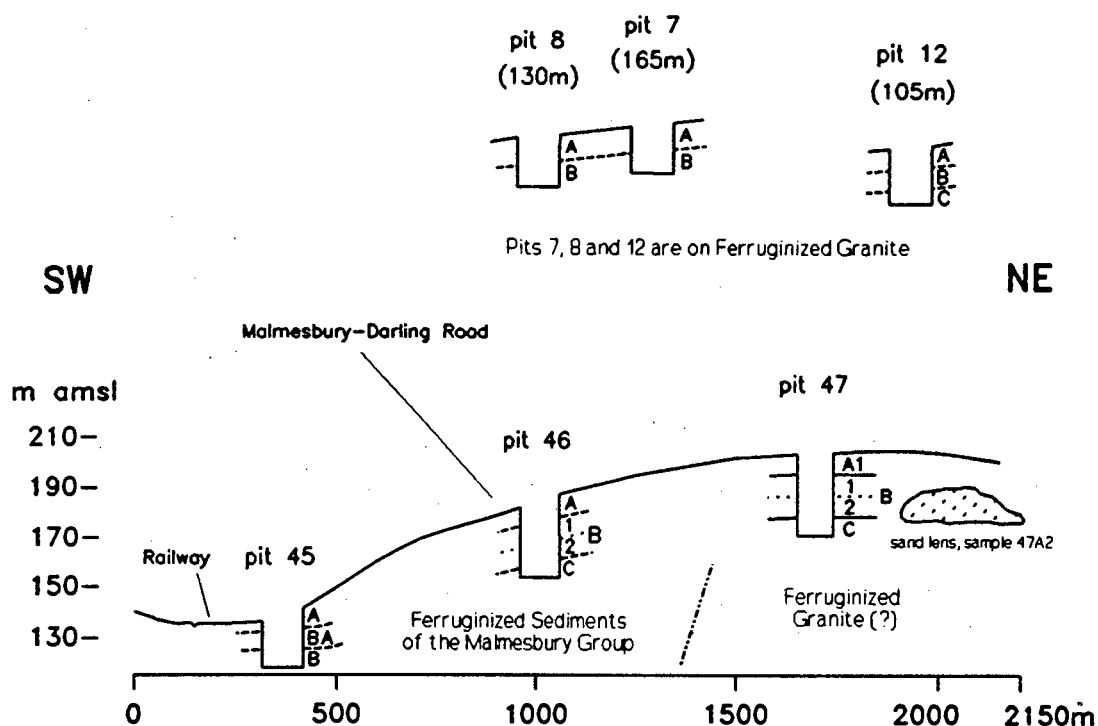


**Figure 7.1:** Simplified sections through the sampling sites in the soils associated with the ferruginized materials. Pits 7, 8, and 12 are at location 6 and Pits 45, 46 and 47 are at location 7 in Figure 2.2. Figure 2.4 can be used as a key to the abbreviations for the different soil horizons. Features other than the topography are not to scale. The vertical scale is exaggerated. The average gradient of the slope from Pit 47 to Pit 45 is 44 permille.



**Figure 7.2:** A photograph showing the view from the footslope (Pit 45) towards the higher slope positions of the toposequence associated with the ferruginized materials.

**Soil horizons and classification (summarised from Appendix-I):** Orthic A-horizons, red apedal B-horizons, yellow-brown apedal B-horizons and neocutanic B-horizons were encountered in the field. The profiles were classified to belong to the following soil forms: Hutton (Pits 8, 12 and 46), Clovelly (Pit 45) and Oakleaf (Pit 47). The soil profile at Pit 7 could not be classified because the B-horizon was partly below the ground water table.

## **7.2. ANALYTICAL RESULTS - AN OVERVIEW**

A summary of the analytical results is given in tabulated form (Tables 7.1 to 7.4). The manner in which the statistics were calculated is discussed in section 4.2. A graphical display of the geochemical trends from the top to the bottom of the toposequence is presented in Figure 7.4. A complete listing of the results is given in Appendix-III.

**Table 7.1:** Basic statistics of the major elements in the soils associated with the ferruginized materials. Only values above the lower limit of detection ( $n > \text{LLD}$ ) were included to derive the statistics. The analyses were performed using XRFs and all concentrations are given in percent in dried soil (LLD = lower limit of detection; S.D. = standard deviation; C.V. = coefficient of variation).

Oxide	n	n > LLD	Approx. LLD (%)	Mean (%)	S.D. (%)	C.V. (%)	Min. in % (sample)	Max. in % (sample)
Na <sub>2</sub> O	18	17	0.02	0.10	0.06	64	< LLD	0.28 (7A)
MgO	18	18	0.02	0.18	0.09	52	0.08 (12A)	0.47 (8A)
Al <sub>2</sub> O <sub>3</sub>	18	18	0.01	11	6.2	58	4.1 (45A)	22.8 (47C)
SiO <sub>2</sub>	18	18	0.02	74	15	20	47.6 (46B2)	90.0 (45A)
P <sub>2</sub> O <sub>5</sub>	18	18	0.005	0.07	0.03	42	0.04 (47A2)	0.15 (47B2)
K <sub>2</sub> O	18	18	0.004	0.71	0.36	51	0.22 (46B2)	1.6 (7A)
CaO	18	18	0.005	0.14	0.22	151	0.03 (12B)	0.77 (8A)
TiO <sub>2</sub>	18	18	0.007	0.59	0.20	34	0.28 (7A)	1.1 (47C)
Fe <sub>2</sub> O <sub>3</sub>	18	18	0.009	7.8	5.9	75	1.8 (7A)	22.7 (46B2)

**Table 7.2:** Basic statistics summarising the pH(KCl) values, the conductivities of the water-suspended soil samples and the percentages of various particle size fractions and organic matter for the soils associated with the ferruginized materials (S.D. = standard deviation; C.V. = coefficient of variation).

Parameter	n	Mean	S.D.	C.V. (%)	Min. (sample)	Max. (sample)
pH(KCl)	12	5.5	0.8	15	4.7 (45BA)	7.8 (47C)
Conductivity ( $\mu\text{S cm}^{-1}$ )	12	138	77	56	49 (47B1)	291 (45A)
% Organic Matter	12	0.9	0.2	25	0.6 (47A1)	1.3 (46C)
% Gravel	12	13	18	144	0.4 (45A)	57 (46B2)
% Sand	12	50	20	40	16 (46B2)	76 (45A)
% Mud	12	36	18	49	21 (46A)	74 (47C)
% Fine Clay	7	25	13	53	11 (45BA)	40 (47C)

**Table 7.3:** Basic statistics of the trace elements in the soils associated with the ferruginized materials. Only values above the lower limit of detection ( $n > \text{LLD}$ ) were included to derive the statistics. Li, Be, Co, Cd and Sb were analysed using ICP-MS, all other elements were analysed using XRFS. The concentrations are given in ppm in dried soil (LLD = lower limit of detection; S.D. = standard deviation; C.V. = coefficient of variation).

Elem.	n	n > LLD	Approx. LLD in ppm	Mean in ppm	S.D. in ppm	C.V. (%)	Min. in ppm (sample)	Max. in ppm (sample)
Li	8	8	0.2	10	5.9	56	5.6 (47Top)	23 (45B)
Be	8	7	0.3	0.9	0.5	55	< LLD	1.8 (45B)
F	18	1	140				< LLD	124 (45BA)
S	18	18	6.0	222	102	46	110 (45BA)	477 (8B)
Cl	18	18	4.0	64	14	22	40 (47B1)	88 (45B)
V	18	18	1.2	127	98	77	31 (7A)	371 (46B2)
Cr	18	18	1.3	81	55	68	30 (47Top)	205 (46B2)
Mn	18	18	1.5	127	70	55	44 (8B)	315 (47A2)
Co	8	8	0.2	2.9	1.2	43	1.6 (45A)	4.9 (45B)
Ni	18	18	2.3	11	5.3	48	6.6 (47Top)	25 (45B)
Cu	18	18	1.8	7.8	3.9	50	3.6 (12A)	18 (45B)
Zn	18	18	1.2	16	7.0	43	6.2 (12B)	31 (12A)
Ga	5	5	0.8	12	8.8	71	4.8 (7A)	26 (8B)
Ge	18	5	0.9				< LLD	1.6 (12B)
As	18	18	0.8	11	10	92	2.1 (7A)	41 (46B2)
Se	18	13	0.8	2.7	2.4	91	< LLD	8.9 (46B2)
Br	18	18	0.9	5.8	3.7	63	1.6 (47B1)	14 (46C)
Rb	18	18	0.7	41	13	32	24 (46A)	69 (7A)
Sr	18	18	0.6	17	10	61	7.1 (8B)	44 (47C)
Y	18	18	0.7	15	4.1	28	10 (8B)	24 (7A)
Zr	18	18	0.6	408	111	27	239 (47C)	568 (46A)
Nb	18	18	0.6	16	11	71	6.2 (7A)	50 (12A)
Mo	18	18	0.5	1.7	0.7	39	0.9 (47A2)	3.2 (12B)
Cd	8	0	0.7					
Sn	18	16	1.2	4.9	2.4	49	< LLD	9.6 (8B)
Sb	8	8	0.3	1.3	0.8	58	0.5 (46A)	3.0 (47B2)
I	18	15	2.5	19	18	96	< LLD	64 (47C)
W	18	18	2.6	9.2	2.6	29	4.9 (47B1)	14 (12B)
Pb	18	18	2.1	17	10	60	8.7 (12A)	42 (47B2)
Bi	18	3	2.8				< LLD	3.9 (47B2)
Th	18	18	1.7	19	14	73	3.8 (45A)	52 (46B2)
U	18	18	1.3	3.1	1.2	39	1.7 (7A)	5.5 (45B)

**Table 7.4:** Basic statistics of the extractable element concentrations for the soils associated with the ferruginized materials. Only values above the lower limit of detection ( $n > \text{LLD}$ ) were included to derive the statistics. The results in the first part of the table are given in ppm in dried soil (fraction  $< 2$  mm) and were obtained using ICP-AES. The results in the second part of the table are given in ppb in dried soil (fraction  $< 2$  mm) and were obtained using ICP-MS (LLD = lower limit of detection; S.D. = standard deviation; C.V. = coefficient of variation).

## Part 1

Elem.	n	n > LLD	Approx. LLD in ppm	Mean in ppm	S.D. in ppm	C.V. (%)	Min. in ppm (sample)	Max. in ppm (sample)
Na	16	16	1.2	28	12	43	14 (46A)	50 (47B2)
Mg	16	16	0.03	98	73	75	20 (12A)	257 (47C)
Al	16	9	0.5				< LLD	11 (12B)
P	16	8	0.5				< LLD	2.1 (45A)
S	16	16	0.5	20	17	85	4 (47Top)	62 (45B)
K	16	16	1.2	49	42	84	17 (47A1)	190 (45B)
Ca	16	16	0.05	346	220	63	125 (12B)	1055 (47C)
Cr	16	2	0.05				< LLD	0.1 (47C)
Fe	16	14	0.05	0.29	0.21	73	< LLD	0.7 (12B)
Ni	16	6	0.2				< LLD	0.7 (47C)
Cu	16	2	0.05				< LLD	0.1 (8A)
Zn	16	14	0.1	0.93	2.4	257	< LLD	9.3 (12A)

## Part 2

Elem.	n	n > LLD	Approx. LLD in ppb	Mean in ppb	S.D. in ppb	C.V. (%)	Min. in ppb (sample)	Max. in ppb (sample)
Be	16	3	67				< LLD	134 (45BA)
B	16	2	362				< LLD	656 (47C)
V	16	3	9				< LLD	18 (45A)
Co	16	10	13				< LLD	37 (12A)
As	16	3	71				< LLD	109 (45BA)
Se	16	2	877				< LLD	1353 (45B)
Mo	16	0	49					
Cd	16	2	17				< LLD	27 (45A)
Sb	16	1	23				< LLD	25 (45A)
Ba	16	16	61	5410	4966	92	1159 (8A)	18529 (47B2)
Tl	16	6	3				< LLD	10 (45B)
Pb	16	3	54				< LLD	59 (47A1)
Bi	16	0	3					
U	16	1	30				< LLD	68 (47C)

### 7.3. PARTICLE SIZE DISTRIBUTIONS AND FIELD OBSERVATIONS

The particle size distributions of the samples taken from the toposequence associated with the ferruginized materials are presented in Figure 7.3. Processes which could have caused these particle size distributions are discussed in this section. Field observations are discussed together with the particle size distributions.

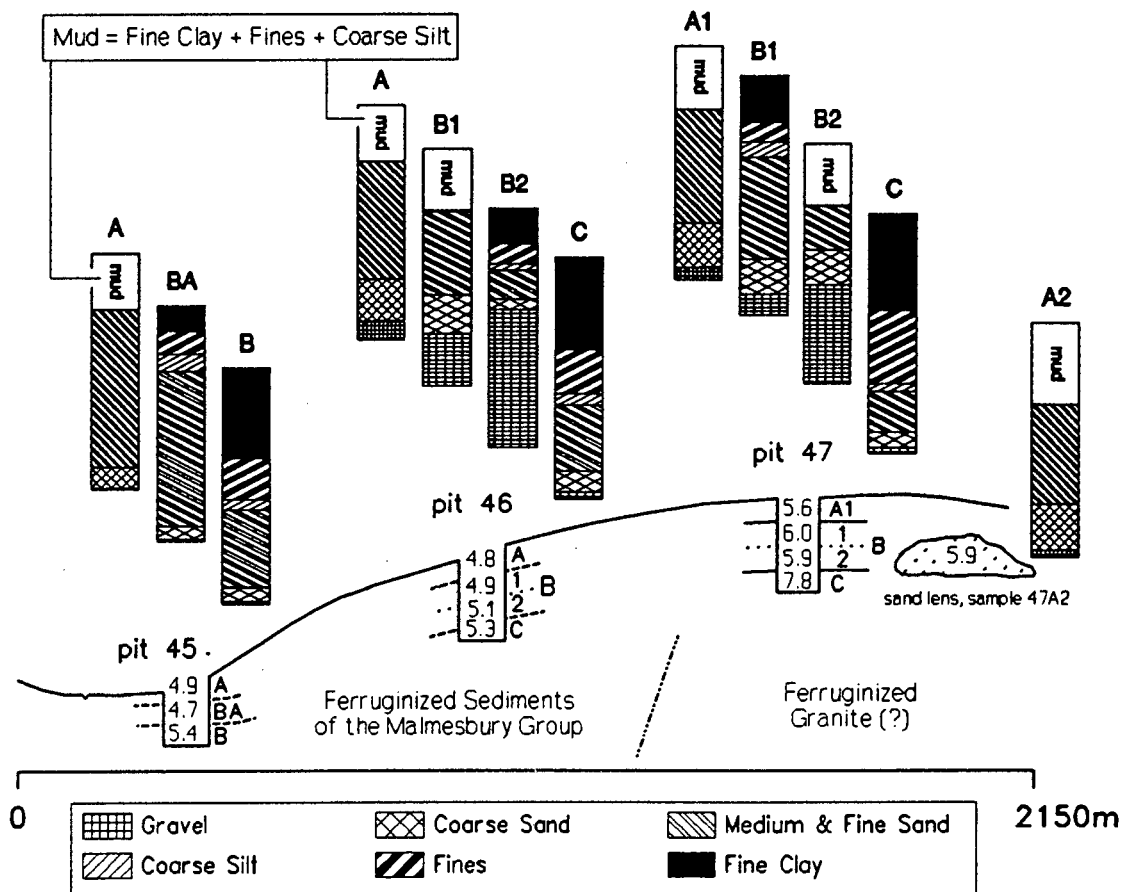


**Figure 7.3:** Particle size distributions of the toposequence associated with the ferruginized materials. The full size of the bars represents 100 weight % of the inorganic soil fraction. For some samples the proportions of coarse silt, fines and fine clay were not determined and are reported together as "mud" (white areas). The numbers in the pits refer to the pH(KCl) values. The sand lens (sample 47A2) was located between the B1- and the C-horizon of Pit 47, and is probably a burrow filled with material from the A1-horizon.

**Eluviation of A- and B-horizon at Pits 46 and 47 and formation of Fe-oxide concretions:** The C-horizon contains high proportions of fine clay and fines and is, therefore, relatively impermeable. The impermeable C-horizon could function as an aquiclude and cause a lateral flow of soil water down the slope (throughflow). The

overlying B-horizon contains much more gravel and less finer particles and is, therefore, more permeable. The gravel fraction consists mainly of Fe-oxides. The higher proportion of Fe-oxide gravel and the smaller proportion of finer particles are best explained by (a) vertical eluviation, (b) lateral eluviation of the finer particles by means of throughflow and (c) formation of coarse Fe-oxide concretions in the upper slope positions. This would be in agreement with the results and the literature review presented in Chapter 4. In this chapter it was suggested that processes (b) and (c) can be important soil forming factors (sections 4.3. and 4.5.5.).

The A-horizon is relatively enriched in medium and fine sand because (a) the formation of coarse Fe-oxide gravel was restricted to the B-horizons and (b) particles finer than fine sand were eluviated from the topsoil.

**Gravitational transport of Fe-oxide concretions:** The literature review presented in section 4.5.4. demonstrated that the average gradient between Pits 47 and 45 (44 ‰) is steep enough to expect gravitational transport of the soil. The absence of a cohesive clay matrix in the B-horizon at Pits 46 and 47 implies that the relatively loose Fe-oxide gravel in this horizon would be included in this transport. Fe-oxide concretions, however, were not found in the soil at the footslope (Pit 45). Red mottles in the B-horizon at Pit 45 are possible remnants of the Fe-oxide concretions. It could be speculated that the Fe-oxide concretions breakdown when they reach the footslope because longer periods of water saturation may cause a lack of oxygen in soils at the footslope position (Scheffer and Schachtschabel, 1989) and could, therefore, initiate the remobilisation of Fe-oxides (Schwertmann and Taylor, 1989). The possibility of remobilisation of Fe-oxides in the footslope position was also investigated for the Klipberg toposequence and is discussed in more detail in section 4.5.5. More research needs to be carried out to determine whether (a) the Fe-oxide concretions are included in the gravitational transport and (b) the lack of Fe-oxide concretions at the footslope reflects their breakdown.

**The burrow in the soil profile at Pit 47:** The soil profile at Pit 47 exhibited a sand lens between the B1 and the C-horizon (Figure 7.1.). The particle size distribution and the chemical composition of the sand lens are very similar to those of the A1-horizon (Figure 7.3; Appendix-III). The sand lens is thus probably a burrow which was filled up with material from the A-horizon. The sample taken from the sand lens is referred to as 47A2.

#### 7.4. MAJOR SOIL COMPONENTS

**Mineralogy (summarised from Chapter 3):** The mineralogical composition was determined from 4 soil samples (Figure 3.5). All samples analysed contain quartz, goethite, kaolinite and traces of feldspar. The proportion of feldspar increases from the

sub- to the topsoil. Hematite was detected by XRD only in the subsoil. The reddish colour of the topsoil indicates traces of hematite which, however, were undetectable by XRD. The samples of the top 15 cm and the C-horizon at Pit 47 were the only samples which contain  $\text{CaCO}_3$  (Appendix-I).

**Elemental composition (Table 7.1):**  $\text{SiO}_2$  is the most abundant compound. Its concentration ranges from 48 to 90 percent. The means of  $\text{Al}_2\text{O}_3$  and  $\text{Fe}_2\text{O}_3$  are 11 % and 8 %, respectively. Organic matter,  $\text{K}_2\text{O}$  and  $\text{TiO}_2$  have means between 1 and 0.5 percent. The proportion of organic matter varies, compared to the soils associated with other underlying materials, only within small limits (0.6 % to 1.3 %). All other compounds have means lower than 0.5 percent.

## 7.5. FACTORS WHICH DETERMINE THE LATERAL CHANGES OF THE CONCENTRATIONS

**Discussion of elements in groups:** The elements were allocated to groups in order to facilitate their discussion. The manner in which the elements were grouped is explained in section 1.2.

**Elements excluded from the discussion:** Elements which are not discussed in this section were excluded because (a) their concentrations are mainly below the LLD, (b) the number of samples analysed for these elements was too low to recognise horizontal trends (Tables 7.1 to 7.4) or (c) the lateral change of the concentrations was insignificant.

### 7.5.1. Group-I (top- and subsoil): Association of $\text{P}_2\text{O}_5$ , V, Cr, $\text{Fe}_2\text{O}_3$ , As, Se, Pb, Th and 1 M $\text{NH}_4\text{NO}_3$ extractable Mg and $\text{Co}^*$ with Fe-oxide concretions

**Results (Figure 7.4):** The elements in Group-I have moderate to relatively high concentrations in the middle and upper part of the toposequence. The soil at the footslope (Pit 45) has the lowest concentrations. Underlined elements showed this trend in top- and subsoil, the other elements only in the subsoil. Higher concentrations of the Group-I elements coincide with high proportions of gravelly Fe-oxide concretions. The similar behaviour of gravel,  $\text{Fe}_2\text{O}_3$  and the other Group-I elements implies the accumulation of Group-I elements in Fe-oxide gravel.

---

\* Allocation of the element to this group is debatable because the agreement between the lateral variation of the elemental concentration and the group pattern is poor.

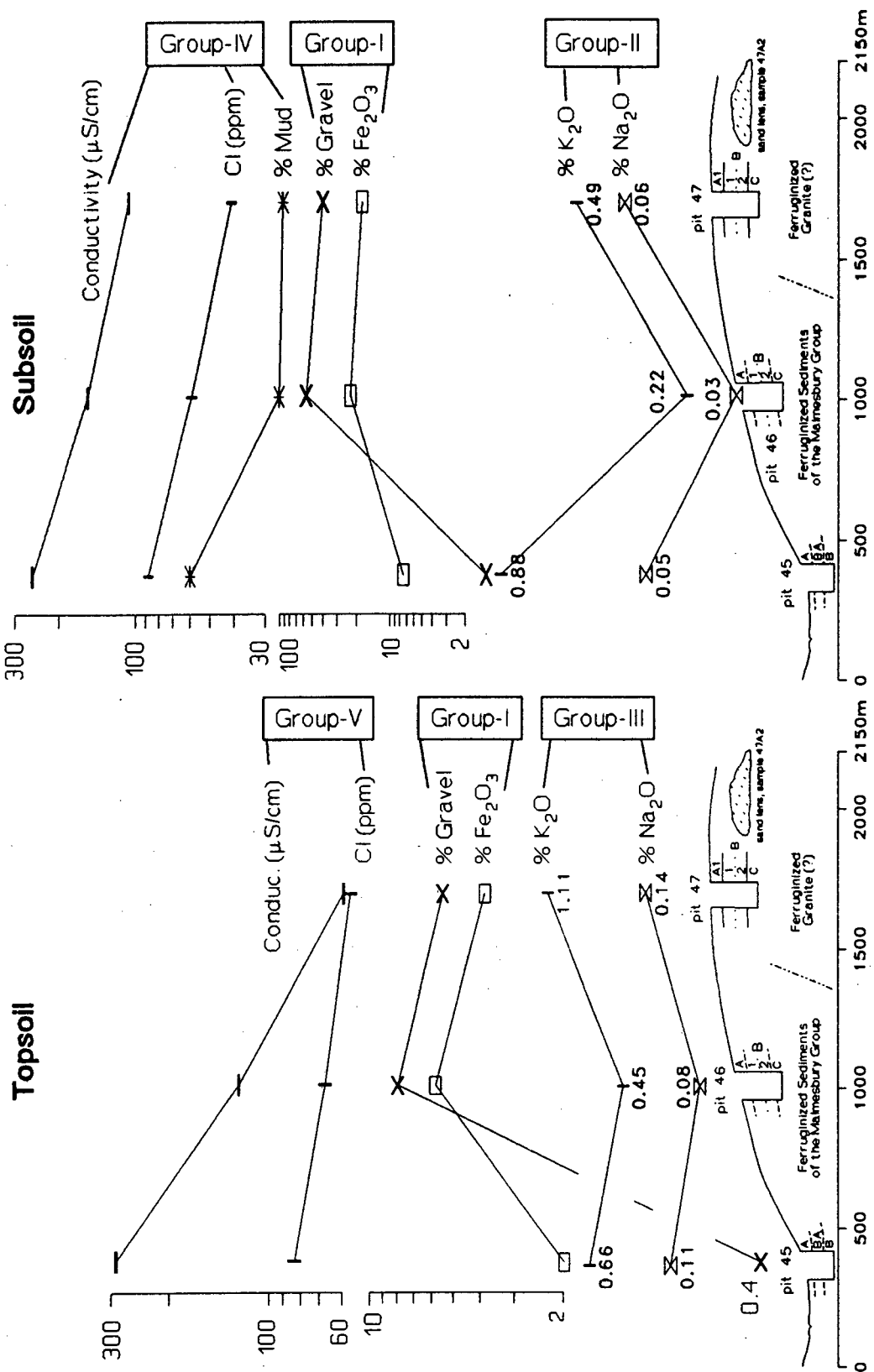


**Figure 7.4:** Lateral change of the concentrations down the top- and the subsoil of the toposequence associated with the ferruginized materials. A subset of elements was selected to demonstrate the trends which are typical for the different element-groups. A full list of the elements allocated to the groups is given in the text.

**7.5.2. Group-II (subsoil):** Lateral eluviation of  $\text{Na}_2\text{O}$ ,  $\text{MgO}$ ,  $\text{K}_2\text{O}$ ,  $\text{CaO}$ ,  $\text{Mn}$ ,  $\text{Ni}$ ,  $\text{Cu}$ ,  $\text{Zn}$ ,  $\text{Rb}$ ,  $\text{Sr}$ ,  $\text{Y}$ ,  $\text{W}^*$  and 1 M  $\text{NH}_4\text{NO}_3$  extractable  $\text{Na}$ ,  $\text{K}$  and  $\text{Ca}$

**Results (Figure 7.4):** The elements in Group-II have higher concentrations in the subsoil at the top and the bottom of the toposequence. The subsoil in midslope position (Pit 46) has the lowest concentrations.

**Lateral eluviation as most important control:** The relatively high gradient of the toposequence at midslope position probably resulted in lateral eluviation of finer particles from the B-horizon and thus in relative accumulation of gravel (section 7.3.). It is proposed that the elements in Group-II are mainly hosted by minerals which have a particle size smaller than gravel (e.g. remains of feldspars; section 7.6.: results d). The lateral eluviation of these mineral-particles towards the footslope and the leaching of  $\text{Na}$ ,  $\text{K}$  and  $\text{Ca}$  could explain the low concentrations in midslope position. The relatively high concentrations of extractable  $\text{Na}$ ,  $\text{K}$  and  $\text{Ca}$  in the soil at the footslope may also be controlled by evaporation of water from the soil (section 7.5.4.).

**7.5.3. Group-III (topsoil):**  $\text{Be}$ ,  $\text{Na}_2\text{O}$ ,  $\text{K}_2\text{O}$ ,  $\text{Mn}$ ,  $\text{Cu}$ ,  $\text{Zn}$ ,  $\text{Rb}$ ,  $\text{Sr}$ ,  $\text{Sb}$  and 1 M  $\text{NH}_4\text{NO}_3$  extractable  $\text{Mg}$

**Results (Figure 7.4):** The distribution of the Group-III elements in the topsoil is very similar to the distribution of the Group-II elements in the subsoil. The topsoil in midslope position (Pit 46) has slightly lower concentrations than the topsoil in the uppermost and lowest slope position. Elements which show the same trend in the subsoil are underlined (section 7.5.2.).

**Mixing of A- and B-horizon as possible control of the lateral trend:** There is no obvious explanation for the lower concentrations of the Group-III elements in midslope position and the explanation given here is very speculative. The gradient between Pits 47 and 45 is steep enough to expect gravitational transport (section 7.3.). The importance of soil mixing during gravitational transport in controlling lateral chemical trends was demonstrated in section 6.5.3. It could be speculated that the steeper gradient at midslope position results in faster gravitational transport and, therefore, in mixing of the A- and the B-horizon. This would explain the low concentrations of the Group-III elements in the A-horizon at Pit 46 because the underlying B-horizon has particularly low  $\text{Na}_2\text{O}$ ,  $\text{K}_2\text{O}$ ,  $\text{Mn}$ ,  $\text{Cu}$ ,  $\text{Zn}$ ,  $\text{Rb}$  and  $\text{Sr}$  concentrations (section 7.5.2.). This hypothesis would also explain the increase from 5 % gravel in the A-horizon at Pit 47 to 8 % gravel in the A-horizon at Pit 46 because the mixing of horizons could result in assimilation of gravel from the B-horizon.

The concentrations of  $\text{Be}$  and  $\text{Sb}$  in the subsoil at midslope position were not determined. It is thus not possible to resolve whether soil mixing can explain the lateral trend of these elements in the topsoil. The lateral trend of extractable  $\text{Mg}$  is difficult to explain.

---

\* Allocation of the element to this group is debatable because the agreement between the lateral variation of the elemental concentration and the group pattern is poor.

**7.5.4. Group-IV (subsoil): S\*, Cl, Br, I and 1 M NH<sub>4</sub>NO<sub>3</sub> extractable Al, S, Fe and Tl concentrations controlled by retention and evaporation of soil water**

**Results (Figure 7.4):** The concentrations of the elements in Group-IV increase down the subsoil of the toposequence. The increase of the concentrations coincides with higher proportions of mud and higher conductivities of the water-suspended soil.

**Retention ability and evaporation of soil water as possible controls:** The higher proportion of mud in the subsoil at the footslope probably results in a higher retention ability for water and dissolved solids. Increased retention of Group-IV elements is, therefore, a possible reason for their relatively high concentrations at the footslope.

It could also be speculated that the ground water table in the lower slope positions is relatively shallow (Figure 2.1). Evaporation of ground water, overland flow and(or) throughflow water from the soil can result in the accumulation of salts (Buol *et al.*, 1980; Conacher, 1975). This process could supply the soil with Group-IV elements and cause the increased concentrations at the footslope.

**7.5.5. Group-V (topsoil): S, Cl, W and 1 M NH<sub>4</sub>NO<sub>3</sub> extractable Na, P, S, K, Co, Zn and Tl\***

The elements in Group-V have increasing concentrations from the top to the bottom of the toposequence (topsoil). The increase of the concentrations coincides with a higher conductivity of the water-suspended soil. This trend is best explained by the evaporation of water from the soil in the footslope position (see section above for more information; tungsten excluded).

**Tungsten:** The increase of the concentrations of the elements in Group-V also coincides with higher proportions of fine and medium sand (Figure 7.3). The similar behaviour of W and fine and medium sand is also evident in soils associated with other underlying materials. It is thus suggested that considerable portions of W are hosted by (medium and fine) sand-sized, weathering resistant mineral particles, probably scheelite or wolframite (section 9.28.).

**7.5.6. Other elements (SiO<sub>2</sub>, Zr and 1 M NH<sub>4</sub>NO<sub>3</sub> extractable Fe, Ni, Zn and Ba)**

**SiO<sub>2</sub>:** The concentration of SiO<sub>2</sub> in the subsoil increases from 51 % at the top of the toposequence to 64 % at the bottom of the toposequence and is inversely proportional to the concentrations of the elements in Group-I (section 7.5.1.). It is, therefore, suggested that the formation of Fe-oxides in the upper slope positions resulted in dilution of SiO<sub>2</sub> while the hypothesised illuviation of clay minerals and decomposition of Fe-oxides at the footslope could have resulted in higher SiO<sub>2</sub> concentrations.

**Effect of soil pH:** Extractable Ni, Zn and Ba have decreasing concentrations down the subsoil and extractable Ba and Fe have decreasing concentrations down the topsoil of the toposequence. Different amounts of atmospheric deposition and plant

---

\* Allocation of the element to this group is debatable because the agreement between the lateral variation of the elemental concentration and the group pattern is poor.

uptake are unlikely to be the cause for these trends because the sampled soils are only 1500 m apart and are very similarly utilised (crop production). The decrease of the concentrations coincides with lower pH values (Figure 7.3). The ability of soils to adsorb cations decreases with decreasing pH values. It is, therefore, suggested that the soil pH controls the decrease of the concentrations. The observed trend may also reflect the redistribution of extractable Fe, Ni, Zn and Ba by throughflow and(or) overland flow.

## 7.6. VERTICAL CHANGES OF THE CONCENTRATIONS

**Results (a):** The concentrations of MgO, Al<sub>2</sub>O<sub>3</sub>, TiO<sub>2</sub>, Zn, Br, Nb, Sn, I, U and 1 M NH<sub>4</sub>NO<sub>3</sub> extractable Na, Mg, Al, Fe, Ni and Tl generally increase with increasing soil depth.

**Interpretation:** The increase of the concentrations from the A- to the Fe-oxide-rich B-horizons at Pits 46 and 47 could indicate association with Fe-oxides. The highest concentrations, however, occur in the fine-textured and kaolinite-rich C-horizons. Association of certain elements with clay minerals has been discussed at length earlier. For the above listed elements an association with clay minerals is an important characteristic. Some of the elements (e.g. TiO<sub>2</sub>, Nb and U) may be hosted by heavy minerals and could thus indicate accumulation of heavy minerals in the C- and the B-horizons.

**Results (b):** The concentrations of Li, Be, S\*, V, Cr, Fe<sub>2</sub>O<sub>3</sub>, Co, Ni, Cu, As, Se, Mo, Pb, Th and extractable S\* and Ba increase from the A- to the B-horizons and decrease from the B- to the C-horizons.

**Interpretation:** The highest concentrations occur in the B-horizons of Pits 46 and 47 and coincide with very high proportions of Fe-oxide gravel. Association with Fe-oxides seems thus an important characteristic of the above listed elements. The lateral change of the concentrations substantiated the association with Fe-oxides for the underlined elements (section 7.5.1.).

**Results (c):** The concentration of SiO<sub>2</sub> decreases from the A- to the B-horizons and increases from the B- to the C-horizons.

**Interpretation:** The vertical changes of the SiO<sub>2</sub> concentrations are inversely proportional to the concentrations(proportions) of Fe<sub>2</sub>O<sub>3</sub> and gravel (see above). Lower SiO<sub>2</sub> concentrations are the consequence of dilution with Fe-oxide gravel.

---

\* Allocation of the element to this group is debatable because the described vertical change of the concentration was not observed in all pits.

**Results (d):** The concentrations of  $\text{Na}_2\text{O}$ ,  $\text{K}_2\text{O}$ , Mn, Zr and extractable Co\* generally decrease with increasing soil depth. A discussion of the vertical distribution of Mn and extractable Co is given in Chapter 9.

**Interpretation ( $\text{Na}_2\text{O}$ ,  $\text{K}_2\text{O}$ ):**  $\text{Na}_2\text{O}$  and  $\text{K}_2\text{O}$  are possibly hosted by remains of feldspars. This would be in agreement with the results of the mineralogical analyses which indicated that the proportion of feldspars decreases slightly from the top- to the subsoil (Chapter 3 and section 7.4.). The vertical decrease of the concentrations coincides also with decreasing proportions of sand (Figure 7.5). It is, therefore, suggested that the particle size of the  $\text{Na}_2\text{O}$ - and  $\text{K}_2\text{O}$ -hosting feldspars is chiefly in the sand range (0.053 mm - 2 mm). The accumulation of sand in the topsoil (section 7.3.) resulted in relatively high  $\text{Na}_2\text{O}$  and  $\text{K}_2\text{O}$  concentrations while the low proportion of sand in the B- and the C-horizons resulted in lower concentrations.

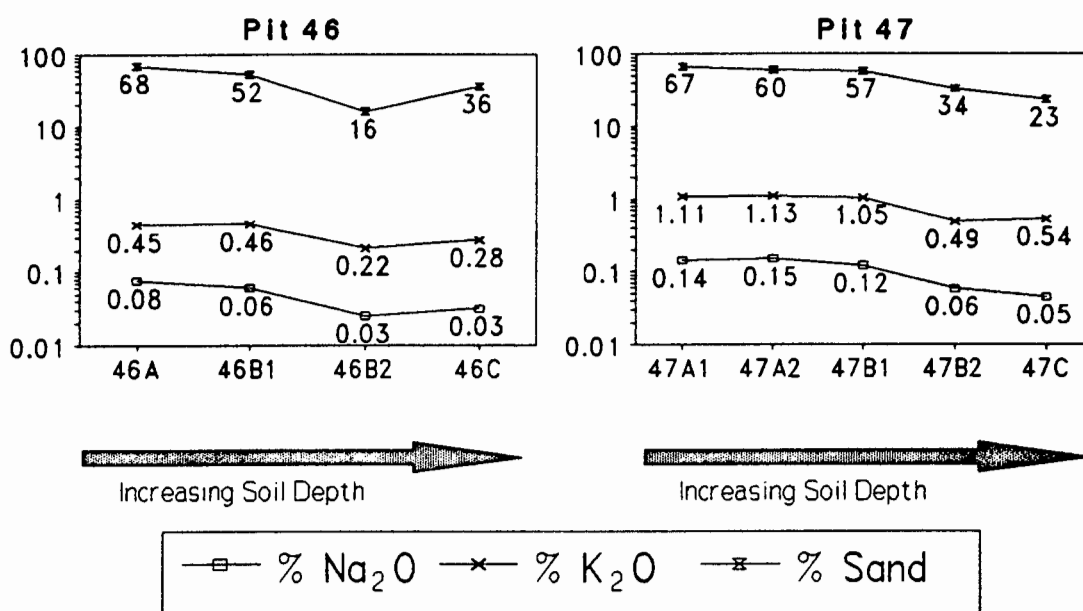


**Figure 7.5:** The similar vertical change of the  $\text{Na}_2\text{O}$ ,  $\text{K}_2\text{O}$  and sand percentages in Pits 46 and 47.

**Other elements:** Elements which are not mentioned in this section were not discussed because (a) they have mainly concentrations below the LLD, (b) the number of samples analysed for these elements was too low to recognise vertical trends [see Tables 7.1 to 7.4], (c) they have relatively constant concentrations with increasing soil depth [Cl, Sr and Rb] or (d) they showed dissimilar vertical trends [ $\text{P}_2\text{O}_5$ , CaO, Y, W and extractable P, K, Ca and Zn]. The vertical distribution of individual elements is discussed in Chapter 9.

\* Allocation of the element to this group is debatable because the described vertical change of the concentration was not observed in all pits.

## 7.7. SUMMARY

**Introduction (Figure 7.1):** The sampled soils are associated with ferruginized sediments of the Malmesbury Group or ferruginized granite (locations 6 and 7 in Figure 2.2). Soil samples from 6 pits and different soil horizons were analysed for major and trace elements, 1 M  $\text{NH}_4\text{NO}_3$  extractable element concentrations, particle size distribution and various other parameters.

**Major soil components:** All samples analysed contain quartz, goethite, kaolinite and traces of feldspar. Some of the samples contain detectable amounts of hematite and  $\text{CaCO}_3$ . The concentration of  $\text{SiO}_2$  ranges between 48 and 90 percent. Other major components are, in decreasing order of the means of their concentrations,  $\text{Al}_2\text{O}_3$ ,  $\text{Fe}_2\text{O}_3$ , organic matter,  $\text{K}_2\text{O}$  and  $\text{TiO}_2$  (Table 7.1).

The interpretation of the particle size distributions and the horizontal and vertical changes of the concentrations in the toposequence at location 7 (Pits 47 to 45) are summarised below. The numbers in brackets, for example [1], refer to more explanations in the text boxes of Figure 7.6:

- [1]: The formation of Fe-oxide concretions resulted in higher concentrations of elements with an affinity for Fe-oxides (Group-I<sup>1</sup>).
- [2]: The preferential lateral eluviation of the hosts of Group-II<sup>2</sup> elements from the B-horizon in midslope position is the best explanation for relatively low concentrations.
- [3]: The transportation by gravity should supply the observed Fe-oxide concretions to the footslope. The lack of concretions at the footslope gave reason to speculate about their decomposition.
- [4]: Increased evaporation of water from the soil at the footslope caused higher concentrations of Group-IV<sup>3</sup> elements (subsoil) and Group-V<sup>4</sup> elements (topsoil).
- [5]: The accumulation of sand-sized remains of feldspars in the topsoil probably caused higher  $\text{Na}_2\text{O}$  and  $\text{K}_2\text{O}$  concentrations.
- [6]: Increasing concentrations of  $\text{MgO}$ ,  $\text{Al}_2\text{O}_3$ ,  $\text{TiO}_2$ , Zn, Br, Nb, Sn, I, U and 1 M  $\text{NH}_4\text{NO}_3$  extractable Na, Mg, Al, Fe, Ni and Tl from the topsoil to the fine-textured subsoil indicated (a) association of trace elements with kaolinite [e.g. extractable element fractions] and (b) accumulation of heavy minerals in the subsoil [e.g. possible hosts of  $\text{TiO}_2$  and Nb].

---

<sup>1</sup>  $\text{P}_2\text{O}_5$ , V, Cr,  $\text{Fe}_2\text{O}_3$ , As, Se, Pb and Th.

<sup>2</sup>  $\text{Na}_2\text{O}$ ,  $\text{MgO}$ ,  $\text{K}_2\text{O}$ , CaO, Mn, Ni, Cu, Zn, Rb, Sr, Y, W and 1 M  $\text{NH}_4\text{NO}_3$  extractable Na, K and Ca.

<sup>3</sup> S, Cl, Br, I and 1 M  $\text{NH}_4\text{NO}_3$  extractable Al, S, Fe and Tl

<sup>4</sup> S, Cl and 1 M  $\text{NH}_4\text{NO}_3$  extractable Na, P, S, K, Co, Zn and Tl.

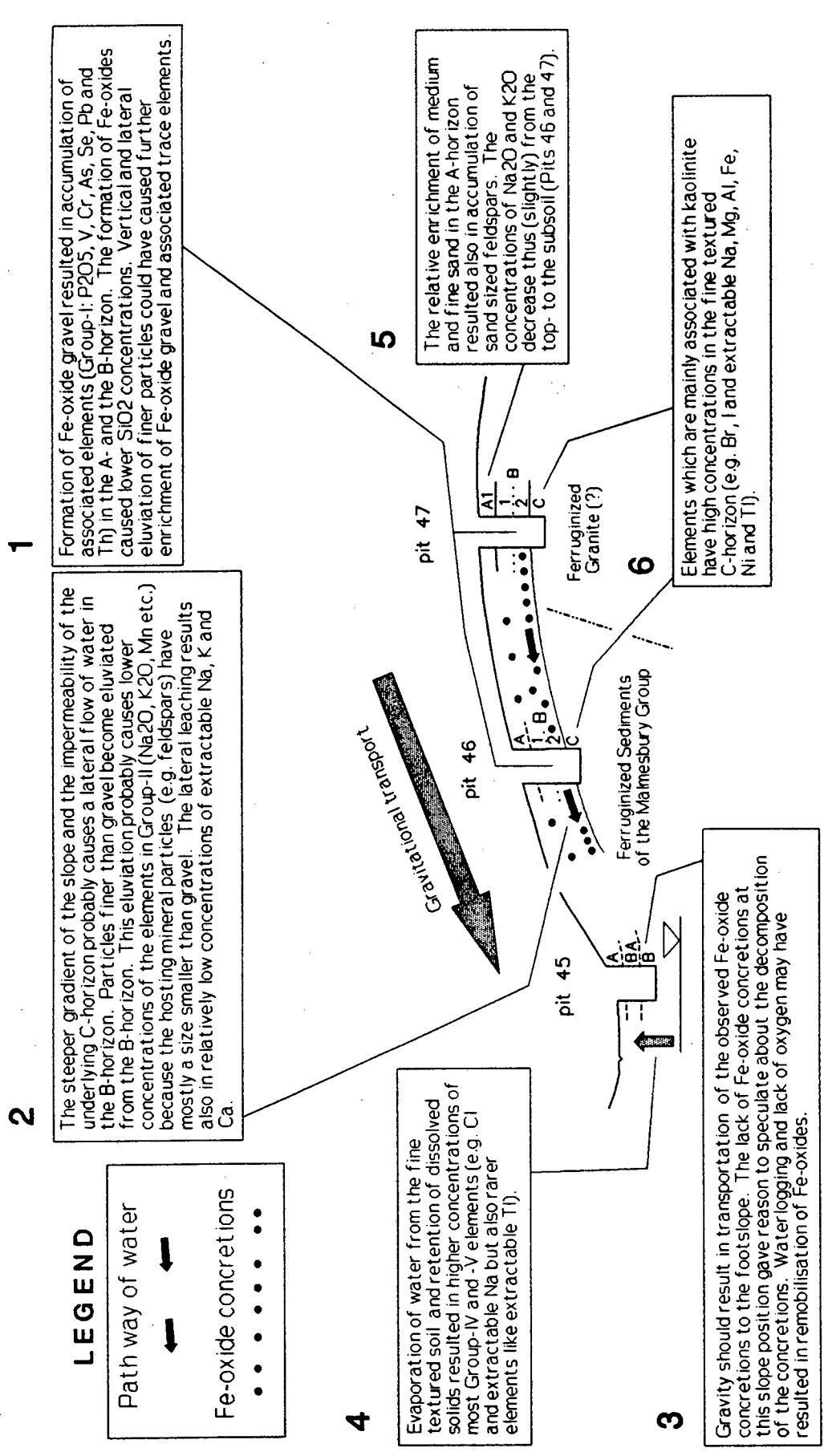


**Figure 7.6:** Interpretative diagram of the toposequence associated with the ferruginized materials. The numbers next to the text boxes correspond to the [numbers] in the summary of this chapter.

# CHAPTER 8.

## COASTAL SAND-DERIVED SOILS

### 8.1. INTRODUCTION

**Sampling location:** The location of the sampled soil sequence is approximately 10 km south-west of Darling in close proximity to the west coast (Location 1 in Figure 2.2). Most of the pits were dug along an approximately 6000 m long, south-west north-east striking sampling line. A simplified section through the sampled soil sequence is given in Figure 8.1. Figure 8.2 shows the view from the coastal dunes at Pit 4 inland towards Rondeberg. The coordinates of individual pits are given in Appendix-I.

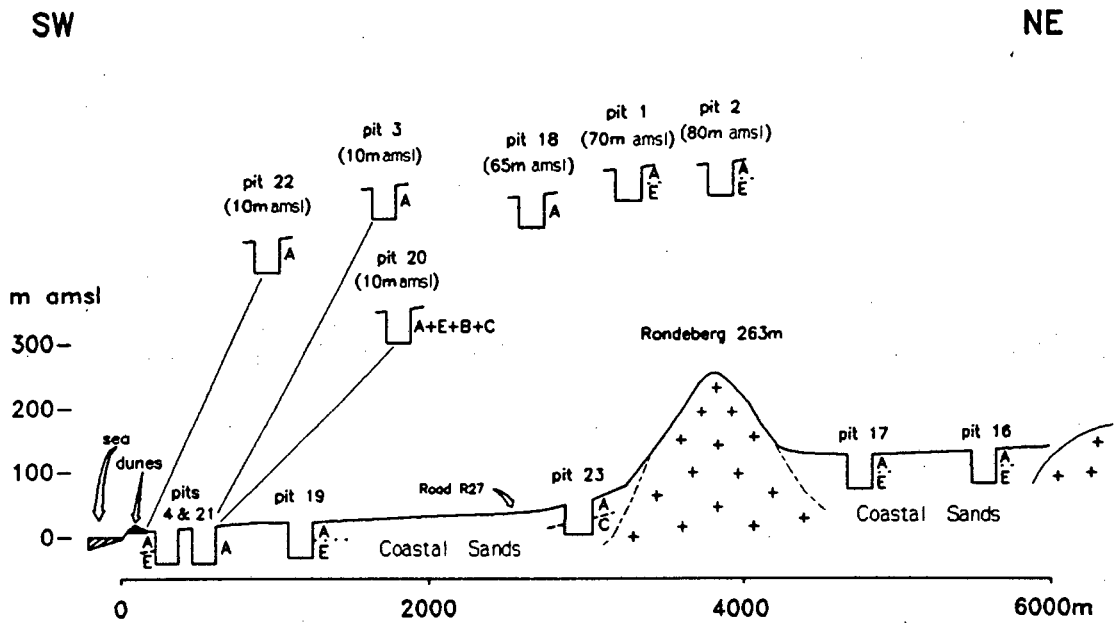


**Figure 8.1:** Simplified section through the sampling sites in the soils derived from the coastal sands (location 1 in Figure 2.2). Figure 2.4 can be used as a key to the abbreviations for the different soil horizons. Features other than the topography are not to scale. The vertical scale is exaggerated. Pits 1, 2 and 18 are approximately 3 km north of the cross-section. Pits 3, 20 and 22 are in line with the cross-section. It was, however, impossible to accommodate them in the drawing of the cross-section. The average gradient along the sampling line is 22 permille.



**Figure 8.2:** A photograph showing the view from the coastal dunes at Pit 4 towards Rondeberg.

**Occurrence and topography of coastal sands:** The occurrence of wind deposited, unconsolidated coastal sands in the study area is restricted to an approximately 10 km wide strip along the west coast (Sandveld in Figure 1.1). Inland the coastal sands overlap outcropping granites and sediments or change gradually into the partially fluviially deposited and colluvially influenced sands of the Groenrivier depression (Figure 1.2). The topography of the sands can be classified into three terrain units (Figure 8.1): (a) the recent dune fields, usually near to the sea (e.g. at Pits 4 and 21); (b) the relicts of terraces (e.g. at Pits 17 and 19); and (c) the sand covered slopes of the granite outcrops further inland (e.g. at Pit 23).

**Soil horizons and classification (summarised from Appendix-I):** Three diagnostic soil horizons were encountered in the field, orthic A-horizons, E-horizons and podsolic horizons. Criteria used to discriminate between these horizons were the colour of a horizon, mainly indicating different amounts of organic matter, and the vertical position of a horizon in relation to the other soil horizons. Most of the soil profiles showed orthic A-horizons over E-horizons and were thus classified as members of the Fernwood soil form. Other soils encountered were either members of the Lamotte

(Orthic A-horizon over E-horizon over Podzol B-horizon) or the Namib soil forms (Orthic A-horizon over Regic Sand).

**Particle size distribution:** All soil samples taken from profiles that derived from coastal sands showed similar particle size distributions. The samples consist mainly of medium and fine sand (particle size between 1 and 3 phi). Slightly different proportions of fine sand, medium sand and organic matter are the only variations. Figure 8.3 shows three examples of typical particle size distributions.

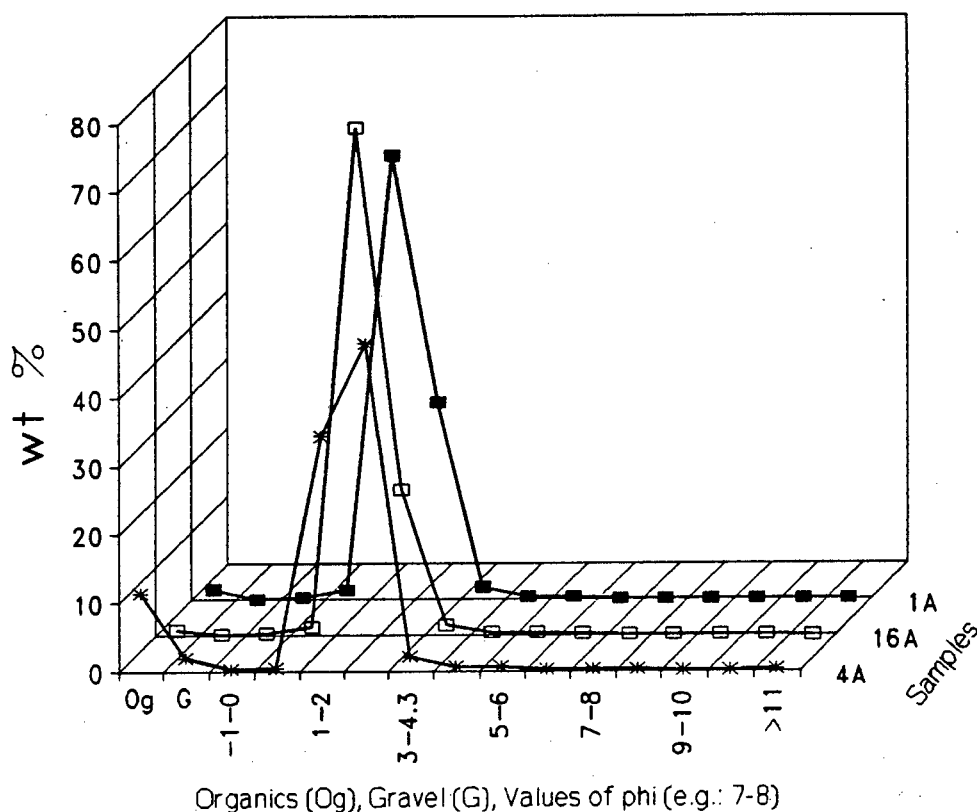


**Figure 8.3:** Particle size distributions of three A-horizons (samples 1A, 4A and 16A) which derived from the wind-deposited coastal sands. The weight percentages were calculated on a whole soil basis; i.e. organic matter was not excluded from the calculations.

## 8.2. ANALYTICAL RESULTS - AN OVERVIEW

A summary of the analytical results is given in tabulated form (Tables 8.1 to 8.4). The manner in which the statistics were calculated is discussed in section 4.2. A graphical display of typical geochemical trends from the sea towards the north-eastern end of the soil sequence (topsoil) is presented in Figures 8.4, 8.5 and 8.8. A complete listing of the results is given in Appendix-III.

**Table 8.1:** Basic statistics of the major elements in the coastal sand-derived soils. Only values above the lower limit of detection ( $n > \text{LLD}$ ) were included to derive the statistics. The analyses were performed using XRFs and all concentrations are given in percent in dried soil (LLD = lower limit of detection; S.D. = standard deviation; C.V. = coefficient of variation).

Oxide	n	n > LLD	Approx. LLD (%)	Mean (%)	S.D. (%)	C.V. (%)	Min. in % (sample)	Max. in % (sample)
Na <sub>2</sub> O	14	11	0.02	0.05	0.04	76	< LLD	0.14 (23Top)
MgO	14	14	0.02	0.06	0.04	69	0.01 (18Top)	0.19 (4A)
Al <sub>2</sub> O <sub>3</sub>	14	14	0.01	0.6	0.4	66	0.2 (18Top)	1.8 (23Top)
SiO <sub>2</sub>	14	14	0.02	96	3.2	3.4	86.4 (4A)	98.2 (1E)
P <sub>2</sub> O <sub>5</sub>	14	14	0.005	0.04	0.05	135	0.01 (18Top)	0.19 (4A)
K <sub>2</sub> O	14	14	0.004	0.12	0.15	130	0.04 (17A)	0.64 (23Top)
CaO	14	14	0.005	0.2	0.56	278	0.03 (17E)	2.1 (4A)
TiO <sub>2</sub>	14	14	0.007	0.1	0.04	38	0.04 (18Top)	0.18 (23Top)
Fe <sub>2</sub> O <sub>3</sub>	14	14	0.009	0.7	0.1	14	0.5 (1E)	0.87 (21Top)

**Table 8.2:** Basic statistics summarising the percentages of mud and organic matter, pH(KCl) values and the conductivities of the water-suspended soil samples for the coastal sand-derived soils (S.D. = standard deviation; C.V. = coefficient of variation).

Parameter	n	Mean	S.D.	C.V. (%)	Min. (sample)	Max. (sample)
% Mud	10	1.3	0.5	38	0.7 (18Top)	2.4 (20Top)
pH(KCl)	10	5.1	0.9	17	4.1 (19A)	7.3 (4A)
Conductivity ( $\mu\text{S cm}^{-1}$ )	10	92	122	132	22 (18Top)	402 (20Top)
% Organic Matter	10	2.3	3.7	159	0.2 (16E)	11.3 (4A)

**Significance of the calculated standard deviations given in Tables 8.1 to 8.4:** A test for normality was performed for the distributions of all elements(oxides) presented in Tables 8.1 to 8.4. The results showed for most parameters that it is unlikely that the samples were taken from a normal distribution. The calculated standard deviations are, therefore, only rough estimates of the variation of a parameter.

**Chemical differences between A- and E-horizons:** An Analysis of Variance was performed for all elements using the program SAS/STAT (SAS Institute Inc., 1988). This was to determine the significance of the chemical differences between A- and E-horizons. For the purpose of this investigation the samples of the top 15 cm of the soil profile and the composite samples of the A-horizon were grouped together to represent the chemical composition of the A-horizon. None of the parameters showed significant differences between A- and E-horizons (95 % confidence level). A visual assessment of the vertical change of the elemental concentrations, however, showed that the differences between the A- and E-horizons are consistent and meaningful for some of the investigated parameters (section 8.5.).

**Table 8.3:** Basic statistics of the trace elements in the coastal sand-derived soils. Only values above the lower limit of detection ( $n > \text{LLD}$ ) were included to derive the statistics. Li, Be, Co, Cd and Sb were analysed using ICP-MS, all other elements were analysed using XRFs. The concentrations are given in ppm in dried soil (LLD = lower limit of detection; S.D. = standard deviation; C.V. = coefficient of variation).

Elem.	n	n > LLD	Approx. LLD in ppm	Mean in ppm	S.D. in ppm	C.V. (%)	Min. in ppm (sample)	Max. in ppm (sample)
Li	7	7	0.2	2.9	0.9	31	1.7 (19A)	4.2 (21Top)
Be	7	0	0.3					
F	17	2	140				< LLD	281 (4A)
S	14	14	6	210	294	140	52 (1E)	1036 (4A)
Cl	14	14	4	100	102	101	42 (1E)	422 (20Top)
V	14	14	1.2	7.7	1.1	14	6 (1E)	9.4 (23Top)
Cr	14	14	1.3	28	4.0	15	22 (1E)	37 (19A)
Mn	14	14	1.5	70	14	20	47 (1E)	103 (4A)
Co	7	5	0.2	0.4	0.22	51	< LLD	0.81 (4A)
Ni	17	17	2.3	8.6	1.5	18	4.9 (4A)	11 (17A)
Cu	17	17	1.8	3.9	0.59	15	2.8 (16E)	5.1 (16A)
Zn	17	17	1.2	2.5	1.6	65	1.1 (18Top)	8.1 (4A)
Ga	6	1	0.8				< LLD	0.76 (4A)
Ge	17	5	0.9				< LLD	1.0 (3A)
As	17	16	0.8	1.1	0.46	42	< LLD	2.5 (23Top)
Se	17	0	0.8					
Br	17	17	0.9	8.9	13.5	152	0.79 (2E)	46 (20Top)
Rb	17	16	0.7	4.5	6.1	136	< LLD	26 (23Top)
Sr	17	17	0.6	25	26	105	5.5 (18Top)	113 (4A)
Y	17	17	0.7	3.8	1.6	42	2.0 (18Top)	7.3 (4A)
Zr	17	17	0.6	258	164	64	95 (18Top)	643 (23Top)
Nb	17	17	0.6	2.4	1.1	48	1.1 (1A)	5.5 (23Top)
Mo	17	17	0.5	2.2	0.5	24	1.0 (4A)	2.9 (17E)
Cd	7	0	0.7					
Sn	17	14	1.2	2.2	0.4	18	< LLD	3.1 (1A)
Sb	7	7	0.3	2.6	2.5	96	0.9 (20Top)	8.1 (16Top)
I	17	3	2.5				< LLD	8.8 (4A)
W	17	17	2.6	22	4.6	21	11 (4A)	28 (19A)
Pb	17	8	2.1				< LLD	3.9 (23Top)
Bi	17	0	2.8					
Th	17	7	1.7				< LLD	2.0 (1E)
U	17	9	1.3				< LLD	2.0 (16A)

**Table 8.4:** Basic statistics of the extractable element concentrations for the coastal sand-derived soils. Only values above the lower limit of detection ( $n > \text{LLD}$ ) were included to derive the statistics. The results in the first part of the table are given in ppm in dried soil (fraction  $< 2$  mm) and were obtained using ICP-AES. The results in the second part of the table are given in ppb in dried soil (fraction  $< 2$  mm) and were obtained using ICP-MS (LLD = lower limit of detection; S.D. = standard deviation; C.V. = coefficient of variation).

## Part 1

Elem.	n	n > LLD	Approx. LLD in ppm	Mean in ppm	S.D. in ppm	C.V. (%)	Min. in ppm (sample)	Max. in ppm (sample)
Na	14	14	1.2	32	44	138	9.7 (1E)	172 (20Top)
Mg	14	14	0.03	64	91	143	16 (16E)	305 (20Top)
Al	14	10	0.5				< LLD	8.5 (4A)
P	14	8	0.5				< LLD	18 (4A)
S	14	14	0.5	6.8	8.0	118	2.5 (16E)	30 (20Top)
K	14	14	1.2	6.3	4.8	76	1.4 (17E)	20 (4A)
Ca	14	14	0.05	286	445	156	47 (16E)	1740 (4A)
Cr	14	2	0.05				< LLD	0.05 (4A)
Fe	14	14	0.05	0.9	2.1	225	0.13 (17E)	8.0 (4A)
Ni	14	2	0.2				< LLD	0.83 (4A)
Cu	14	0	0.05					
Zn	14	4	0.1				< LLD	0.88 (4A)

## Part 2

Elem.	n	n > LLD	Approx. LLD in ppb	Mean in ppb	S.D. in ppb	C.V. (%)	Min. in ppb (sample)	Max. in ppb (sample)
Be	14	0	67					
B	14	1	362				< LLD	1318 (4A)
V	14	1	9				< LLD	16 (4A)
Co	14	1	13				< LLD	20 (4A)
As	14	0	71					
Se	14	0	877					
Mo	14	0	49					
Cd	14	1	17				< LLD	24 (4A)
Sb	14	1	23				< LLD	82 (20Top)
Ba	14	14	61	634	213	34	229 (19A)	997 (20Top)
Tl	14	0	3					
Pb	14	7	54				< LLD	400 (17Top)
Bi	14	0	3					
U	14	0	30					

### 8.3. MAJOR SOIL COMPONENTS

**Quartz:** The soils consist mainly of medium and fine-grained sand, i.e. particles smaller than 0.5 mm and greater than 0.125 mm (1-3 phi; Figure 8.3). The XRD analyses of two soils derived from coastal sands showed quartz to be the only major mineral component (Chapter 3). The SiO<sub>2</sub> concentrations, as determined by XRFS, indicate that the proportion of quartz ranges approximately from 86 to 98 percent (Table 8.1).

**Other components:** Organic matter commonly is the second most abundant soil component after quartz. The samples analysed for this study had proportions of organic matter ranging from 0.2 to 11 percent (Table 8.2). The mean values of the Fe<sub>2</sub>O<sub>3</sub>, Al<sub>2</sub>O<sub>3</sub>, CaO and K<sub>2</sub>O concentrations vary between 0.1 and 0.7 percent (Table 8.1). All other elements have means < 0.1 percent.

**Calcium carbonate:** Only the two samples taken from the topsoils at the pits nearest to the coast (samples 4A and 22A; Figure 8.1.) contain carbonate (Appendix-I). The concentration of calcium carbonate in sample 4A, calculated from the XRFS results for CaO, is approximately 3.8 percent.

The occurrence of calcium carbonate as observed in this study is in agreement with the geological map (Theron, 1991). The map shows that the occurrence of calcium carbonate is generally restricted to the recent, 500-3000 m wide sand deposits of the active dune fields in close proximity to the shoreline. The absence of calcium carbonate in the soils further inland is presumably the result of carbonate leaching by percolating rain water. At two localities, however, the windblown coastal sands formed substantial calcareous deposits further inland, south-west of Atlantis and south-west of Hopefield. The calcium carbonate in the coastal sands may be of biogenic origin (Theron, 1991).

### 8.4. FACTORS WHICH DETERMINE THE LATERAL CHANGES OF THE CONCENTRATIONS

**Lateral transport of matter between pits:** A general understanding of possible transport mechanisms for material between the sampled pits is important for the discussion of the observed geochemical trends. As stated above, the soil consists almost exclusively of medium and fine sand. Typical permeabilities of sandy soils range from 3 m per day to 300 m per day (Scheffer and Schachtschabel, 1989). The existence of laterally flowing, perched ground water as a possible pathway for transport of material between the relatively widely spaced pits is, therefore, unlikely.

The field sampling was performed during winter. The high rainfall during winter resulted in high water tables in Pit 19 and Pit 20. Both pits are in close proximity to the

sea (Figure 8.1) and showed a ground water table at approximately 1 m depth. Matter could thus be transported between these pits via ground water flow. This transport mechanism, however, is limited to localities and seasons with higher water tables. The sparse vegetation cover of the loose sands and the presence of dunes suggest that aeolian transport is the most important mechanism in transporting matter between pits.

**Discussion of elements in groups:** The elements were allocated to groups in order to facilitate their discussion. The manner in which the elements were grouped is explained in section 1.2. The elements were allocated to three groups:

(Group-I) Elements with increasing concentrations towards the granite batholiths and the coast (section 8.4.1.).

(Group-II) Elements with generally constant concentrations but low concentrations in samples with high proportions of organic matter (section 8.4.3.).

(Group-III) Elements and extractable fractions thereof which have high concentrations in samples that have high proportions of organic matter and mud (section 8.4.4.).

Elements which could not be assigned to groups are discussed in section 8.4.5. The vertical distribution of the elements is discussed in section 8.5.

#### **8.4.1. Group-I: Na<sub>2</sub>O, MgO, Al<sub>2</sub>O<sub>3</sub>, P<sub>2</sub>O<sub>5</sub>, K<sub>2</sub>O, CaO, Zn\*, Rb, Sr, Y\*, Nb\* and Pb\* concentrations controlled by aeolian and colluvial input of detritus**

**Observed trends (Figure 8.4):** The concentrations decrease from the coast towards Pit 19 and increase from Pit 19 towards the sand covered slope of a granite outcrop (Rondeberg; sample 23Top). The concentrations at Pit 17 are low while the concentrations at the lower-most footslope of the granite complex at the north-east end of the sampling line are relatively high (sample 16A).

Pits 1 and 18 are 3 km north of the main sampling line and a relatively long distance from granite outcrops and coast. The elemental concentrations in Pits 1 and 18 are relatively low.

**Input of detritus from different geological sources:** The observed trends are best explained by aeolian and(or) colluvial input of detritus from the coast and the granite batholiths. Hosting minerals could be traces of feldspar, mica, apatite and heavy minerals. It is assumed that granite-derived mineral detritus is the major source of Group-I elements for the soils near to the two granite batholiths (Pits 16, 17, and 23) while beach-derived mineral detritus is the major source of Group-I elements for the soils near to the coast (Pits 4, 20, and 21).

---

\* The lateral trend of the elemental concentrations is very similar to the trend of the other Group-I elements. The assignment to Group-I, however, is debatable because the concentrations are usually close to the LLD and do not exceed 10 ppm.

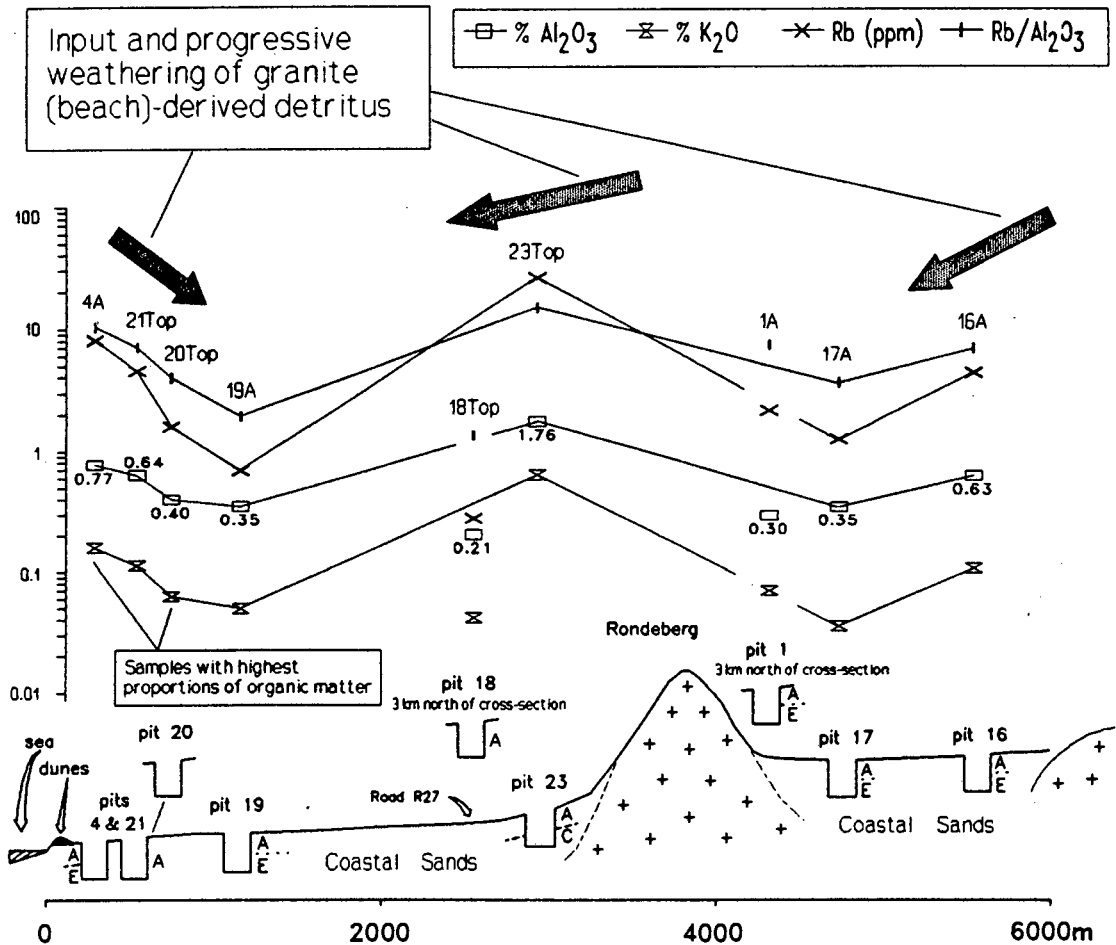


**Figure 8.4:** Variation of the  $\text{Al}_2\text{O}_3$ ,  $\text{K}_2\text{O}$  and Rb concentrations and the  $\text{Rb}/\text{Al}_2\text{O}_3$  ratios in the topsoil along the sampling line. The  $\text{Rb}/\text{Al}_2\text{O}_3$  ratio was plotted as a measure for the weathering state of the soils. The trends of the  $\text{Al}_2\text{O}_3$ ,  $\text{K}_2\text{O}$  and Rb concentrations are typical for all elements in Group-I ( $\text{Na}_2\text{O}$ ,  $\text{CaO}$ ,  $\text{MgO}$ ,  $\text{P}_2\text{O}_5$ , Sr and less distinct Nb, Pb, Y and Zn).

**Possible sources of the beach-derived detritus:** Presuming that the northerly directed longshore drift is more important in transporting the beach sediments than the wind, it is suggested that the beach detritus originates from outcrops which are south of the sampling sites. These could be submarine, littoral or terrestrial. The closest possible source of feldspars at the beach south of the sampling sites are outcrops of Malmesbury sediments. These outcrops are approximately 8 km distant from the sampling sites (Theron, 1991). Genthe (1987; Appendix-I) described samples of Malmesbury Group wackes dredged from the seafloor between Cape Town and the Rondeberg area. In the majority of cases he reported presence of various feldspars.

**Chemical index of alteration ( $\text{CIA} = \text{Al}_2\text{O}_3 / (\text{Al}_2\text{O}_3 + \text{CaO} + \text{Na}_2\text{O} + \text{K}_2\text{O}) * 100$ ):** The CIA, as first used by Nesbitt and Young (1982), is an established method to quantify the degree of weathering of geological materials. A plot of the CIA values of the coastal sand-derived soils (not illustrated) was difficult to interpret and

partly misleading because the variation of the CIA values was generally small (67-81) and only samples with high proportions of organic matter appeared to be relatively fresh (CIA values lower than 60). The results discussed in this thesis give reason to suggest that Ca, Na and K which are released from their weathering host-minerals may be retained by secondary soil minerals and organic matter (sections 8.4.2., 8.4.4. and 9.11.). This would cause the CIA values in organic-rich samples to be too low, especially since the total concentrations of the elements involved are very low in the coastal sand-derived soils (Table 8.1). For these reasons the CIA was not used for this study.

**Suitability of the Rb/Al<sub>2</sub>O<sub>3</sub> ratio to quantify the degree of weathering:** Rubidium is, similarly to Ca, Na and K, typically contained in minerals which, if present in significant proportions, indicate relative freshness of geological materials (e.g. feldspars). Rubidium, according to Billings (1970), is more rapidly depleted during weathering than K, although the cation exchange capacity of Rb is relatively high (Scheffer and Schachtschabel, 1989). Rb/Al<sub>2</sub>O<sub>3</sub> ratios could thus be a suitable measure for the different degrees of weathering of the coastal sand-derived soils. Organic-rich samples (4A and 20Top in Figure 8.4) have Rb/Al<sub>2</sub>O<sub>3</sub> ratios which are within the range of samples with lower proportions of organic matter and are not outliers as they are with regard to their CIA values (see above). This may reflect that Rb is incorporated into organic substances to a lesser degree than K, Ca and Na because it is not essential to plants. The Rb/Al<sub>2</sub>O<sub>3</sub> ratio was, therefore, used in this study to quantify the degree of weathering of the coastal sand-derived soils.

**Lateral change of the Rb/Al<sub>2</sub>O<sub>3</sub> ratio and conclusion:** Figure 8.4 shows that the lateral trends of the Rb/Al<sub>2</sub>O<sub>3</sub> ratio and the Rb and Al<sub>2</sub>O<sub>3</sub> concentrations are similar. It is suggested that progressive weathering, leaching and eluviation of the mineral detritus supplied from the coast and the granite causes (a) depletion of Group-I elements, (b) preferred loss of Rb over Al<sub>2</sub>O<sub>3</sub> and (c) decreasing Rb/Al<sub>2</sub>O<sub>3</sub> ratios with increasing distance from its source.

#### **8.4.2. Relative loss of Na, Mg, Al, P, K, Ca, Rb and Sr during soil weathering**

An attempt was made to rank the elements in Group-I that are most commonly associated with feldspars and(or) micas by their tendency to become depleted during soil weathering. The tendency to become depleted was quantified for individual elements using the ratio of [elemental concentration in a strongly weathered sample (sample 17A)] over [elemental concentration in the freshest sample (sample 23Top)] (Table 8.5). The two samples were selected to fulfil the following criteria:

(a) As indicated by the Rb/Al<sub>2</sub>O<sub>3</sub> ratios shown in Figure 8.4, they have a high contrast in their degree of weathering. This made it easier to interpret the results.

(b) They were taken from pits that are near to one another to ensure that the colluvial detritus supplied to the pits derived from the same granite outcrop. This

helped to minimise the errors resulting from possible input of detritus from other sources.

(c) Both samples were selected from pits that are distant from the sea in order to minimise errors that could be introduced by aeolian input of beach-derived mineral detritus and sea spray.

The following ranking was established for the elements: the tendency of elements to be leached from the soil by percolating water is  $Rb > K > Na > P > Al > Mg > Sr = Ca$  (Table 8.5).

**Table 8.5:** The  $Rb/Al_2O_3$  ratios and the concentrations of CaO, Sr, MgO,  $Al_2O_3$ ,  $P_2O_5$ ,  $Na_2O$ ,  $K_2O$  and Rb in the freshest (sample 23Top) and in a strongly weathered sample (sample 17A) of the coastal sand-derived soils. The ratios of [concentration in weathered sample] over [concentration in fresh sample] were calculated to quantify the tendency of a particular element to become depleted during soil weathering. Lower ratios indicate higher rates of depletion.

Samples	$Rb/Al_2O_3$	CaO %	Sr ppm	MgO %	$Al_2O_3$ %	$P_2O_5$ %	$Na_2O$ %	$K_2O$ %	Rb ppm
17a (weathered)	4.3	0.03	12.9	0.03	0.35	0.01	0.01	0.04	1.2
23Top (fresh)	15	0.07	30.2	0.11	1.76	0.08	0.14	0.64	26.2
Ratio: 17A/23Top		0.4	0.4	0.3	0.2	0.1	0.07	0.06	0.05

**Retention of Ca, Mg and P released from weathering minerals:** Scheffer and Schachtschabel (1989) state that Ca, Mg and phosphates are readily available from weathering minerals while K containing minerals are more resistant to chemical weathering. The results of this study, however, showed that Ca, Mg and P have a smaller tendency to become leached from the coastal sand-derived soils than K. It is, therefore, proposed that considerable proportions of the Ca, Mg and P which are released during the weathering of minerals are retained by vegetation and soil organic matter. This implies that most of the Ca, Mg and P present in the strongly weathered samples is adsorbed onto and(or) incorporated into organic matter. The association of Ca and organic matter is also demonstrated in Figure 9.7.

#### 8.4.3. Group-II: Association of $Fe_2O_3$ , Ni, Mo and W in Fe-oxides and heavy minerals

**Observations:** The lateral variation of the Group-II element concentrations is low. Figure 8.5 shows that the Group-II elements are slightly depleted in the organic-rich samples of the A-horizon at Pits 4 and 20 (Figure 8.5). The concentrations of the elements in Group-II show covariance with the proportions of medium sand (particles  $< 0.5$  mm and  $> 0.25$  mm; Figure 8.6).

**Hosts of Group-II elements:** Samples, which have relatively low  $\text{Fe}_2\text{O}_3$  concentrations ( $\approx 0.5\%$ ), were noted in the field to have bleached sand grains, whereas the samples with the highest  $\text{Fe}_2\text{O}_3$  concentrations ( $\approx 0.85\%$ ) have brown coloured grains. It is thus assumed that a substantial proportion of Fe is present in the form of iron oxides which form sand grain coatings. Heavy minerals associated with the medium sand fraction of the soil probably account for most of the remaining Fe (Figure 8.6). Wilding *et al.* (1977) quote Frondel (1962) and Dennen (1966) who report that trace amounts of Fe occur as occlusions in quartz, either interstitially or as isomorphous replacements. It may thus be speculated that some of the Fe is hosted by quartz grains. The similar behaviour of the elements in Group-II indicates the association of Ni, W and Mo with the above suggested, iron-(hosting) minerals.

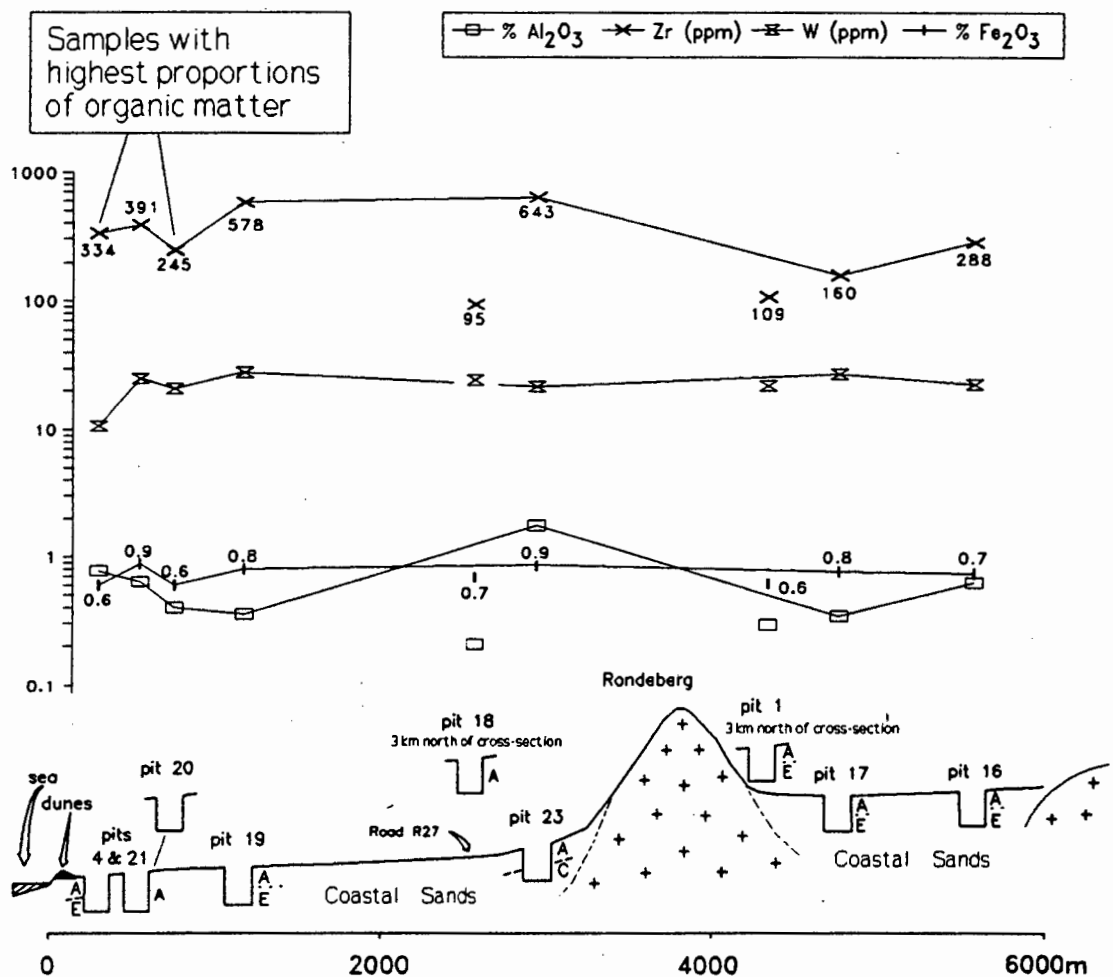


**Figure 8.5:** Trends of the  $\text{Fe}_2\text{O}_3$ , W, Zr and  $\text{Al}_2\text{O}_3$  concentrations in the topsoil along the sampling line. The variability of the  $\text{Fe}_2\text{O}_3$  and W concentrations is generally low. Both elements have low concentrations in the organic-rich samples 4A and 20Top. This distribution is typical for all elements in Group-II ( $\text{Fe}_2\text{O}_3$ , Ni, W and Mo). The Zr concentration is at a maximum in samples which originate from pits close to the granite batholites and can change over short distances. The  $\text{Al}_2\text{O}_3$  concentration was plotted to facilitate the comparison of the trends of Group-I elements, Group-II elements and Zr.

**Depletion of Group-II elements:** Samples with higher concentrations of 1 M  $\text{NH}_4\text{NO}_3$  extractable Fe generally have lower total Fe concentrations and higher proportions of organic matter (Figure 8.7). The highest concentrations of extractable Fe and the lowest concentrations of total Fe and the other Group-II elements occur together in samples with high proportions of organic matter (samples 4A and 20Top). The presence of organic matter may result in complexation and reduction of Fe. Both processes increase the solubility of Fe and can cause the decomposition of Fe-oxides (Scheffer and Schachtschabel, 1989). It is, therefore, proposed that the proportion of organic matter controls the concentration of extractable Fe. High proportions of organic matter result in higher concentrations of extractable Fe. Long-term leaching of extractable Fe and the other Group-II elements may result in depletion of these elements.

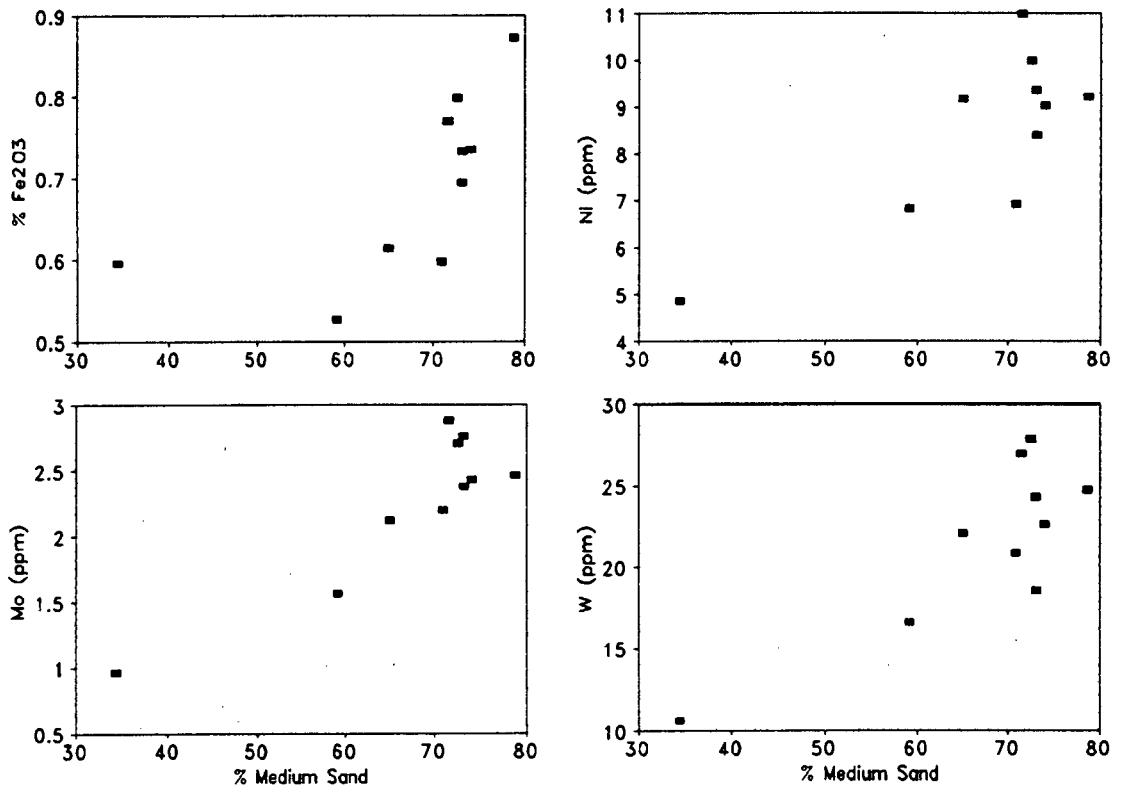


**Figure 8.6:** The covariance of  $\text{Fe}_2\text{O}_3$ , Ni, Mo, W and medium sand in the coastal sand-derived soils.

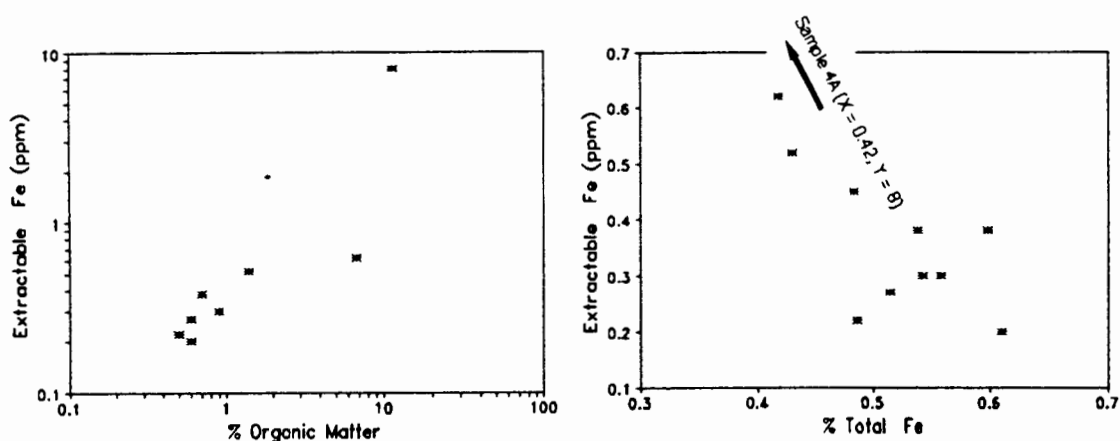


**Figure 8.7:** The 1 M  $\text{NH}_4\text{NO}_3$  extractable concentrations of Fe in the coastal sand-derived topsoils versus the total Fe concentration and the proportion of organic matter. Samples with higher concentrations of extractable Fe generally have lower total Fe concentrations and higher proportions of organic matter. The number of data points displayed in the two plots is not equal because the proportion of organic matter was not determined in all samples.

#### 8.4.4. Group-III: Total S, Cl, Br and 1 M $\text{NH}_4\text{NO}_3$ extractable Na, Mg, Al, P, S, K, Ca, Fe and Ba concentrations controlled by the retention ability

**Observations (Figure 8.8):** The lateral trends of total Br, Cl, S and the extractable element portions, except for K, are similar to the trends of organic matter and mud in the topsoil. The vertical distribution of many Group-III elements confirmed that the proportion of organic matter is an important determinant of their concentrations, because they often have decreasing concentrations with increasing soil depth and decreasing proportions of organic matter (section 8.5.).

**Proportion of organic matter as main determinant for the concentrations of the elements in Group-III:** The quantity of organic matter and mud can affect the elemental concentrations in different ways:

(i) It is proposed that the Br and Cl concentrations and the elemental concentrations in the  $\text{NH}_4\text{NO}_3$  extracts are at least partially a function of the retention ability of soil organic matter and mud. Possible sources of the Group-III elements are *in situ* weathering of minerals and precipitation of sea spray and rain. The retained elements (ions) can be (a) adsorbed onto or (b) incorporated into organic matter and (c) present as salts. The important contribution of organic matter to the cation exchange capacity of coastal soils was also demonstrated by Stevenson (1982).

(ii) The similar behaviour of total S and organic matter probably reflects that S is a common constituent of organic matter (Orr, 1974).

(iii) The solubilities of Al and Fe under normal surface conditions are low. The complexation of Al and Fe by organic acids as well as the lowering of the redox-potential, caused by the oxygen demand of decaying of organic matter, can, however,

increase their solubilities (Scheffer and Schachtschabel, 1989) and result in higher concentrations of Fe and Al in the  $\text{NH}_4\text{NO}_3$  extracts of the samples which contain more organic matter.

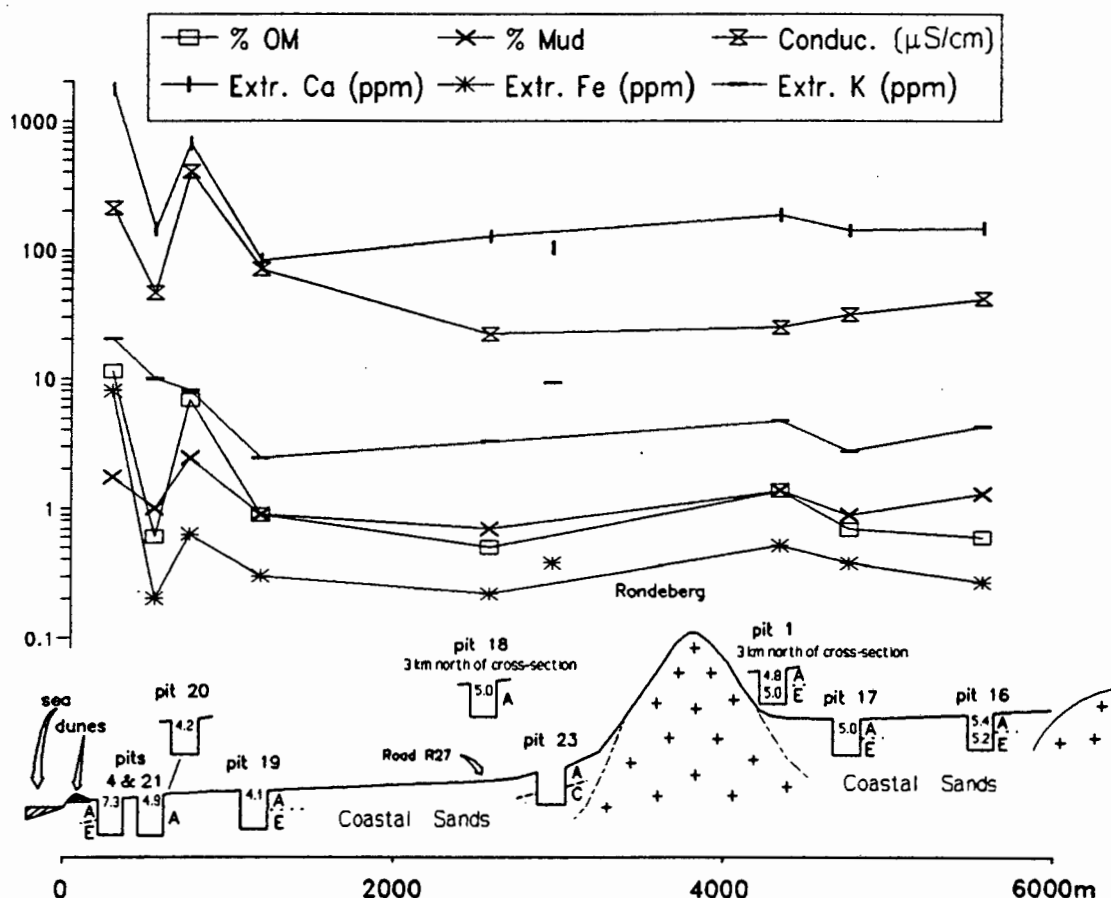


**Figure 8.8:** Similar lateral trends of organic matter (OM), mud, conductivity of water-suspended soil and extractable Ca and Fe in the topsoil. The proportions of organic matter and mud and the conductivity of the soil at Pit 23 were not determined. The lateral trend demonstrated by extractable Ca and Fe is typical for the Group-III elements (total Br, Cl, S and extractable Mg, Ba, S, Na, P, Fe, Al, Ca; extractable K excluded). The numbers in the pits refer to the pH(KCl) values.

**Seasonal changes:** The sampling of the coastal sand-derived soils was performed during winter. It may be speculated that the absence of rainfall during summer allows the accumulation of large amounts of precipitated sea spray in all soils, regardless of the proportions of organic matter and mud. The distribution of Group-III elements during summer could, therefore, differ from the distribution presented in this study. Only those elements of Group-III which belong to the major, dissolved constituents of sea-water would be affected by seasonal changes. These elements are Br, Cl, S, P, Mg, Na, K and Ca (Henderson, 1986).

**Extractable portion of K:** A comparison of Figures 8.4 and 8.8 shows that the concentrations of K in the  $\text{NH}_4\text{NO}_3$  extracts correlates not only with the proportion of organic matter but also with its total concentrations. It is, therefore, suggested that the total concentration of K is an important control of its concentrations in the  $\text{NH}_4\text{NO}_3$  extracts.

#### **8.4.5. Elements which were not assigned to groups (Li, Ti, V, Cr, Mn, As, Zr, Sb and U)**

**Antimony and Li:** Only seven samples were analysed for Sb and Li. The concentration of Sb ranges between 0.9 ppm and 8 ppm and the concentration of Li ranges between 1.7 ppm and 4.2 ppm. All concentrations were above the LLD but the number of samples analysed was too low to draw conclusions about the lateral distribution of Sb and Li. The increase of the Sb concentration from 1 ppm in the E-horizon to 8 ppm in the top 15 cm of the soil profile at Pit 16 may be due to association of Sb and organic matter, or to poor analysis (see also section 9.26.).

**TiO<sub>2</sub>, Mn, V, Cr and U:** The lateral variation of TiO<sub>2</sub>, Mn, V, Cr and U is very small. It is suggested that the concentrations are mainly predetermined by the underlying material.

**Zirconium (Figure 8.5):** The concentration of Zr increases slightly towards the granite batholiths, as do the concentrations of the Group-I elements. In contrast to the concentrations of the Group-I elements the concentration Zr does not increase towards the coast.

It is suggested that the lateral distribution of Zr on the landward side of the sampling line is determined mainly by input of granite-derived detritus. The Zr concentration of the detritus supplied from the beach must be lower than or equal to the concentrations in the sands underlying Pits 4, 20 and 21 because the Zr concentrations do not increase from Pit 19 towards the beach (Figure 8.5).

Despite the short distance between Pits 20 and 21 (100 m), these pits have considerably different Zr concentrations in their A-horizons (Pit 21 = 391 ppm, Pit 20 = 245 ppm; Figure 8.5). This is discussed together with the vertical change of the concentrations in section 8.4.6.

**Arsenic:** The concentration of As is generally very close to its LLD (0.8 ppm). The only sample which has a slightly higher As concentration originates from the sand-covered slope of a granite outcrop (sample 23Top).

#### **8.4.6. Particularly rapid lateral change of some soil properties**

The content of this section is illustrated in Figure 8.9 (text boxes marked with A).

**Comparison of two differently coloured soils:** It was noted in the field that soil colours can change over very short distances. A good example is the change from a dark grey A-horizon in the vicinity of Pit 20 to brownish yellow A-horizon in the vicinity

of Pit 21. The two pits are only 100 m apart and occupy identical slope positions. The dark grey colour of the A-horizon at Pit 20 is the result of abundant organic matter in a matrix of bleached sand grains. The brownish yellow colour of the A-horizon at pit 21 is due to iron oxide coated quartz grains and a lack of large amounts of organic matter.

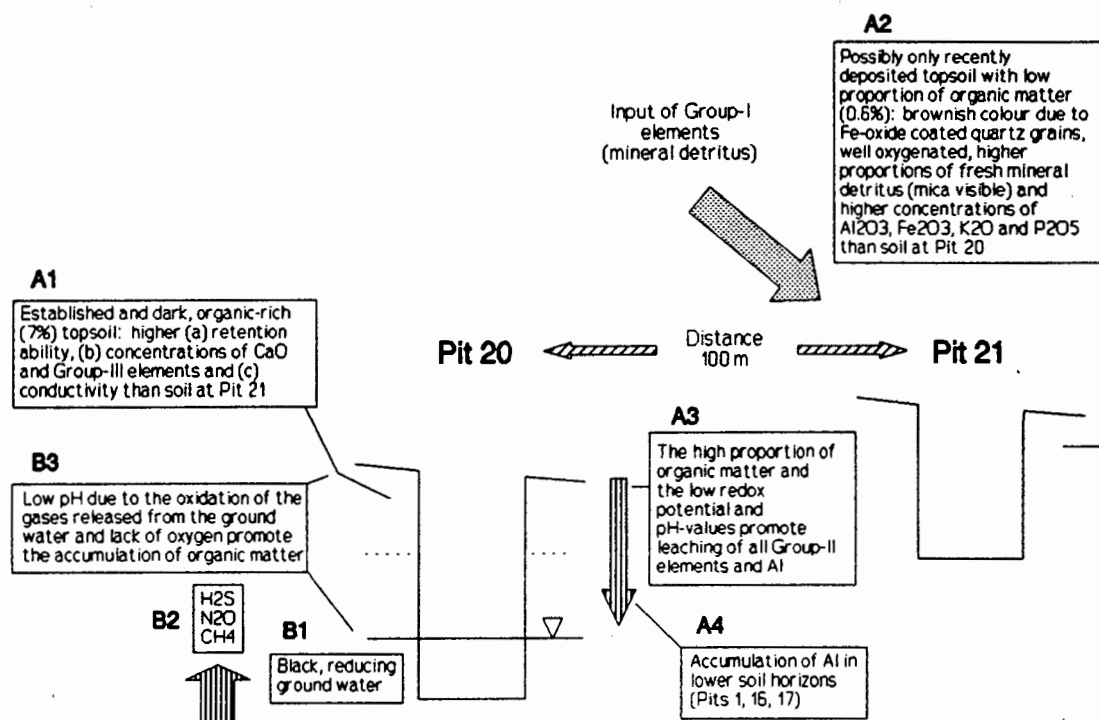


**Figure 8.9:** Conceptual diagram summarising the processes which caused the rapid lateral change of some soil properties from Pit 20 to Pit 21 (text boxes marked with A) and the low pH values in Pits 20 and 19 (text boxes marked with B).

Pit 20 was flooded with black-coloured ground water from a depth of 1 m. The smell of H<sub>2</sub>S indicated that the ground water and possibly the soil air were reducing (Scheffer and Schachtschabel, 1989). Pit 21, which was 0.5 m deep, did not reach the ground water table.

The sample taken from the brownish yellow soil at Pit 21 has higher Al<sub>2</sub>O<sub>3</sub>, Fe<sub>2</sub>O<sub>3</sub>, K<sub>2</sub>O, P<sub>2</sub>O<sub>5</sub> and Zr concentrations than the A-horizon at Pit 20 and is one of the few which contains mica in visible amounts. The dark grey A-horizon at Pit 20 has higher CaO, S, Br, Cl and I concentrations, a higher conductivity (water-suspended) and higher concentrations of 1 M NH<sub>4</sub>NO<sub>3</sub> extractable Mg, Ca, Fe, Ni, Al, Na, P and S than the A-horizon at Pit 21.

**Organic matter as control of lateral chemical and colour changes:** The differences between the two differently coloured soils appear to be controlled by the different quantities of organic matter. The high proportion of organic matter in the

A-horizon at Pit 20 probably enables the soil to retain higher quantities of precipitated sea spray and elements such as I, Br, Cl as well as the extractable fractions of the elements listed above. The relatively high concentration of CaO in the organic-rich soil reflects the retention of Ca by organic matter (section 9.12). The concentration of S is higher in the organic-rich soils because S is a common constituent of organic substances.

The decay of organic matter can cause lower redox-potentials, higher acidities and complexation of Fe and Al. Such conditions would explain the relatively low concentrations of  $\text{Fe}_2\text{O}_3$  and  $\text{Al}_2\text{O}_3$  in sample 20Top because they could cause higher solubilities and consequently increased leaching of Fe and Al. In conclusion it is suggested that the different proportions of organic matter can account for the observed chemical differences.

**Possible reasons for abrupt lateral change of the proportion of organic matter:** Three factors may determine the conspicuous decrease in the proportion of organic matter from Pit 20 to Pit 21.

(a) The ground water table in the organic-rich soil at Pit 20 was shallow when the field sampling was performed. Increased soil moisture could facilitate plant growth and, therefore, cause an increased supply of plant material to the soil.

(b) The field observations indicated that the soil air at Pit 20 was reducing (see above and section 8.4.7.). It may be speculated that the reducing conditions facilitated the accumulation of organic matter because a lack of oxygen results in slower decomposition of organics (Scheffer and Schachtschabel, 1989)

(c) It could also be speculated that the soil at Pit 21 consists mainly of recently deposited and less weathered mineral detritus. The time period available for soil forming processes was not long enough for (i) organic matter to accumulate in the soil, (ii) K and P to be leached, (iii) Zr to be eluviated from the topsoil (section 8.5.) and (d) mica to be altered.

**Conclusion:** Laterally changing proportions of organic matter cause abrupt geochemical changes in the coastal sand-derived soils. This could have important implications for the indigenous fynbos vegetation. More detailed research is required to conclude the reasons for the laterally changing proportions of organic matter.

#### 8.4.7. Control of ground water and calcium carbonate on soil pH

**Observations:** The pH(KCl) of the soil samples is shown in Figure 8.8. Samples taken closer to the coast (Pits 4, 19, 20 and 21) were both acidic and alkaline [pH(KCl) between 4.1 and 7.3]. The pH(KCl) values of the samples taken from the soils further inland were less variable and slightly acidic to neutral\*.

---

\* A pH(KCl) between 5.3 and 6 is considered to be neutral (Mr G.R. Thompson, Department of Agriculture and Water Supply, Elsenburg; pers. comm., 1993).

**Possible determinants of soil pH:** The pH of a soil is dependant on various factors. According to Scheffer and Schachtschabel (1989) these may be:

(a) Turnover of organic matter - the decay of organic matter results in organic acids and  $\text{CO}_2$ , causing the generation of carbonic acid.

(b) The type of vegetation - the decay of organic substances from different vegetation types may contribute different quantities of  $\text{H}^+$  ions.

(c) Input and weathering of minerals - the weathering of minerals can buffer the acidity. For the coastal sand-derived soils it is particularly calcium carbonate that plays an important role in determining the soil pH.

(d) Aerial deposition and retention of sea-derived Na - exchangeable  $\text{Na}^+$  reacts alkaline and is a common cause of high pH values in soil.

(e) Different redox-potentials of the soil water and air - the effect of different redox-potentials is due to the use and release of  $\text{H}^+$  ions in redox reactions. A more detailed discussion of the effect of the redox-potential is given below.

The slightly acid to neutral pH values of the soils further inland are presumably a result of an inter-play between factors a, b, c and d. The more extreme pH values closer to the coast depend strongly on one of the factors and are thus easier explained:

**Alkaline effect of carbonate:** The only sample that contains free carbonate (4A) was the only one to have a pH(KCl) in the alkaline range (7.3). It is important to note that the alkalinity of calcium carbonate buffered the  $\text{H}^+$  ions that are likely to be generated during the turnover of the abundant organic matter in this sample.

**Acidification induced by reducing ground water (Figure 8.9; text boxes marked with B):** Black-coloured ground water, releasing gases smelling of  $\text{H}_2\text{S}$  and low with pH values (4.1 and 4.2), occur exclusively in Pit 20 and Pit 19 (Figure 8.8; Appendix-I). Scheffer and Schachtschabel (1989) state that the presence of  $\text{H}_2\text{S}$  indicates the activity of anaerobic microorganisms and is thus a reflection of the strongly reducing character of the ground water. The decomposition of organic substances in the ground water by anaerobe microorganisms can also result in the formation of  $\text{N}_2\text{O}$  and  $\text{CH}_4$ . The oxidation of these gases in the more oxygenated upper part of the soil profile can donate  $\text{H}^+$  ions (Scheffer and Schachtschabel, 1989). It is, therefore, proposed that the low pH values of Pits 20 and 19 are induced by reducing ground water.

**Seasonal changing of pH values:** The soils in the vicinity of Pit 20 and Pit 19 are probably most acidic during the winter season because the winter rainfall raises the ground water table. The pH during the dry summer months may rise because a lower ground water table would also result in a lowering of the zone of oxidation from the soil into the underlying sands.

**Anion exchange capacity and soil pH:** Lower pH values could result in a higher anion exchange capacity of the soil (Scheffer and Schachtschabel, 1989). The anion exchange capacity of the coastal sand-derived soils is particularly important since, as discussed by Cowling (1992), the availability of phosphates and nitrates is a limiting

factor for the primary production of the fynbos ecosystem. However, it has to be considered that a lowering of the pH also delays the decomposition of organic material and the associated release of nutrients (Scheffer and Schachtschabel, 1989).

### 8.5. VERTICAL CHANGES OF THE CONCENTRATIONS

**Observations (Table 8.6):** The vertical chemical variation was only determined in pits 1, 16 and 17. The differences between the concentrations in the top 15 cm of a soil profile, the A-horizons and E-horizons are generally small and the vertical trends are non-uniform for some of the elements. Only elements which have meaningful vertical changes in concentration are discussed in this section.

The concentrations of  $\text{Al}_2\text{O}_3$ ,  $\text{TiO}_2$  and Zr increase with soil depth (Table 8.6). The increase of  $\text{TiO}_2$  in Pits 1 and 16, however, is smaller than the analytical error. The vertical increase of the concentrations in the most weathered soil at Pit 17\* is generally greater. The concentration of CaO, the proportion of organic matter and the concentrations of the 1 M  $\text{NH}_4\text{NO}_3$  extractable portions of K, Ca, S, Na, P and Ba decrease with increasing soil depth. The concentration of Br increases with soil depth; i.e. against the general vertical trend of the other elements in Group-III.

**Association of CaO and extractable K, Ca, S, Na, P, Ba with organic matter:** The relatively high concentrations of extractable K, Ca, S, Na, P and Ba in the organic-rich A-horizons confirm their association with organic matter (section 8.4.4.). The decrease of the (total) CaO concentration with increasing soil depth and decreasing proportions of organic matter suggests that the Ca hosted by organic matter may form a major proportion of the total Ca content (section 9.12.).

**Leaching of Al from the A-horizon:** The higher proportion of organic matter in the A-horizon may result in higher mobility of Al (Scheffer and Schachtschabel, 1989). It is, therefore, proposed that the downwards increasing concentration of  $\text{Al}_2\text{O}_3$  is the result of Al leaching from the A-horizon. Clay minerals are neither visible nor detectable in the coastal sand-derived soils and accumulation of Al in the lower soil horizons in the form clay minerals is thus improbable.

**Eluviation of  $\text{TiO}_2$  and Zr from the topsoil:** The particle size of Ti- and Zr-hosting minerals may be smaller than sand (Vinogradov, 1959; Erlank *et al.*, 1978). It is, therefore, possible that the downwards increasing concentrations of  $\text{TiO}_2$  and Zr are due to eluviation of fine-grained Ti- and Zr-hosting mineral particles from the A-horizon. Eluviation of Ti- and Zr-hosting minerals from the A-horizon was also deduced from the results for the granite-derived toposequence (Chapter 4).

---

\* The strong weathering of the soil at Pit 17 was demonstrated using Rb/ $\text{Al}_2\text{O}_3$  ratios (section 8.4.1.).

**Table 8.6:** Vertical changes of the concentrations in the coastal sand-derived soils. The concentrations of  $\text{Al}_2\text{O}_3$ , Zr,  $\text{TiO}_2$  and Br increase with soil depth. The increase of  $\text{TiO}_2$  in Pits 1 and 16 and Br in Pit 1, however, is smaller than the analytical error. The concentrations of CaO, organic matter (OM) and the extractable element concentrations decrease with soil depth. The proportion of organic matter was not determined for samples 16Top, 17Top and 17E.

	Pit 1		Pit 16			Pit 17		
	A	E	Top 15	A	E	Top 15	A	E
% $\text{Al}_2\text{O}_3$	0.30	0.38	0.56	0.63	0.95	0.38	0.35	1.02
% $\text{TiO}_2$	0.07	0.08	0.09	0.10	0.11	0.06	0.07	0.12
Br (ppm)	2.4	2.7	1.4	2.7	3.5	2.8	3.6	11.0
Zr (ppm)	109	135	208	288	267	137	160	376
% CaO	0.05	0.03	0.06	0.05	0.03	0.05	0.03	0.03
% OM	1.4	0.3		0.6	0.2		0.7	
<b>EXTRACTABLE CONCENTRATIONS</b>								
K (ppm)	4.8	3.5	8.3	4.3	4.8	5.5	2.8	1.4
Ca (ppm)	185	83	200	148	48	250	140	83
S (ppm)	4.3	2.7	4	3.2	2.5	4.5	3.8	3.2
Na (ppm)	14	10	17	13	10	16	14	17
P (ppm)	0.5	0.3	1	0.3	0.3	0.7	0.3	0.3
Ba (ppm)	0.77	0.41	0.72	0.68	0.50	0.73	0.39	0.58

## 8.6. SUMMARY

The sampled soils derived from unconsolidated, aeolian sands near the coast. Soil samples from nine pits were analysed for trace and major elements, 1 M  $\text{NH}_4\text{NO}_3$  extractable element concentrations, particle size distribution and various other parameters. Most of the sampled pits were positioned along a 6 km long sampling line which runs inland from the coast (Figure 8.1; location 1 in Figure 2.2).

**Major soil components:** The soil consists almost exclusively of fine and medium sand (0.125 mm to 0.5 mm) and organic matter. The proportion of quartz ranges approximately between 86 and 98 percent. Considerable proportions  $\text{CaCO}_3$  occur only near to the coast.

**Input of beach- and granite-derived detritus (Figure 8.4):** The concentrations of  $\text{Al}_2\text{O}_3$ ,  $\text{K}_2\text{O}$ ,  $\text{Na}_2\text{O}$ , CaO, MgO,  $\text{P}_2\text{O}_5$ , Rb, Sr and possibly Nb, Pb, Y and Zn (Group-I) increase towards the coast and the granite batholiths. It was suggested that aeolian and colluvial input of beach- and granite-derived mineral detritus controls the concentrations of the Group-I elements along the sampling line. The association of the elements in this group implied that the supplied detritus may contain small amounts of feldspars, mica,

apatite, carbonates and possibly hornblende, tourmaline and other heavy minerals. Rb/Al<sub>2</sub>O<sub>3</sub> ratios were used as a measure of the degree of weathering.

**Retention of mineral-released elements by organic matter:** The tendency of elements to become leached from the coastal sand-derived soil is Rb > K > Na > P > Al > Mg > Sr = Ca. The results suggested that large proportions of the Ca, Mg and P released from their primary host minerals were retained by organic matter.

**Fe<sub>2</sub>O<sub>3</sub>, Ni, W and Mo (Group-II; Figure 8.5):** The variation of the concentrations of the elements in Group-II is generally low. It was proposed that Ni, W and Mo occur together with Fe-oxides which were observed in the field to form quartz grain coatings. Higher proportions of organic matter increased the solubility of Fe and probably resulted in leaching and depletion of Group-II elements. Heavy minerals associated with the medium sand fraction probably account for the proportion of Group-II elements which is not hosted by Fe-oxides.

**Retention of elements by soil organic matter (Figure 8.8):** The concentrations of total Br, Cl and S and 1 M NH<sub>4</sub>NO<sub>3</sub> extractable Mg, Ba, S, Na, P, Fe, Al and Ca (Group-III) were shown to correlate with the proportions of organic matter and mud. It was thus suggested that the retention ability of organic matter and mud for water and dissolved solids controls the distribution of the elements in Group-III. Possible sources of the elements(ions) in Group-III are *in situ* weathering of minerals and precipitation of sea spray and rain.

**Vertical distribution (Table 8.6):** The vertical variation of the concentrations is generally small. The most important determinant of the observed vertical changes was the downwards decreasing proportion of organic matter. The relatively high proportion of organic matter in the A-horizons probably resulted in:

- (a) Increased retention of extractable K, Ca, S, Na, P and Ba.
- (b) Higher Al solubilities and leaching of Al from the A-horizon, explaining the increase of the Al<sub>2</sub>O<sub>3</sub> concentrations with soil depth.

The increase of the TiO<sub>2</sub> and Zr concentrations from the topsoils to the E-horizons may be due to eluviation of their possibly fine-grained hosts from the A-horizon.

**Rapid, lateral geochemical changes near to the coast (Figure 8.9; text boxes marked with A):** The concentrations of Al<sub>2</sub>O<sub>3</sub>, Fe<sub>2</sub>O<sub>3</sub>, K<sub>2</sub>O, P<sub>2</sub>O<sub>5</sub>, CaO, S, Br, Cl, Zr and 1 M NH<sub>4</sub>NO<sub>3</sub> extractable Mg, Ca, Fe, Ni, Al, Na, P and S may change substantially over short distances (e.g. within 100 m from Pit 20 to Pit 21). It was suggested that laterally changing proportions of organic matter are most important in controlling the observed changes. Several hypotheses were presented in order to explain the abrupt lateral changes in the proportion of organic matter.

**Ground water induced acidification of soils (Figure 8.9; text boxes marked with B):** The results indicated that the occurrence of shallow and reducing ground water can lower the pH of the overlying soil. This acidity, however, is dependant on high ground water tables. Lower ground water tables during summer could cause higher soil pH values.

## CHAPTER 9.

# SUMMARY AND EXTENDED DISCUSSION OF INDIVIDUAL ELEMENTS AND SOIL FORMING FACTORS

---

### 9.1. INTRODUCTION

In this chapter individual elements are discussed in detail. This includes general information on their relevance to the environment and behaviour during soil formation. Elements will be discussed in order of ascending atomic number. Elements which behaved similarly in the soil environment are discussed together. The results from the preceding chapters are briefly summarised and compared with those of other authors in order to identify anomalies such as high and low concentrations and unusual distribution patterns. This comparison is partly provided in a tabulated form (Table 9.1). The data used to compile Table 9.1 are summarised from this thesis, Blume (1992), Scheffer and Schachtschabel (1989), Shacklette and Boerngen (1984) and Bowen (1979) in Sposito (1989), Fiedler and Rösler (1987), Merian (1984), Wedepohl (1969-1978), Aubert and Pinta (1977), Shacklette *et al.* (1971), Turekian and Wedepohl (1961), Vinogradov (1959) and Green (1959). The importance of the soil forming factors time, parent material, topography, climate, biota and man is summarised in sections 9.32. to 9.35.

### 9.2. LITHIUM

**Essentiality and toxicity:** Lithium is essential for certain biological processes and is also known to be toxic if the concentration in the soil is too high (Heier and Billings, 1970a; Vinogradov, 1959).

**Primary host minerals:** The relatively small size of the  $\text{Li}^+$  ion (0.78 Å) allows  $\text{Li}^+$  to substitute for  $\text{Mg}^{2+}$  and  $\text{Fe}^{2+}$ . Pyroxene, amphibole and mica are often relatively enriched in Li. The amount of Li in feldspars is restricted. Concentrations higher than 5 ppm are exceptional for feldspars (Heier and Billings, 1970a; Vinogradov, 1959). The similar behaviour of Li, Ti and Zr in the granite-derived soil suggested a Li host which is resistant to weathering .

**Table 9.1:** Comparison of concentrations in underlying materials and soil groups with concentrations reported in the literature. Symbols and abbreviations: † = extractable concentration; ∇ = mean; ↔ = range of means from more than one author; ‡ = normal range of concentrations from one author; MG = Malmesbury Group; \* = generally increasing concentrations during soil formation (from the granite and the sediments of the MG to the associated soils); +(-) = investigated soils have relatively high(low) concentrations. USGO = unconsolidated sands of granitic origin. The standard deviation is given in brackets [ ]. The means and the ranges in the column "Soils - Other Authors" may be from different authors. References used for this table are given in section 9.1.

Element (Oxide)	UNDERLYING MATERIALS			SOILS ASSOCIATED WITH ~ increasing degree of weathering and transport of the underlying material ~						SOILS OTHER AUTHORS	
	Granite This Study <sup>1</sup>	Other Authors	Pelites This Study <sup>2</sup>	Other Authors	Granite	Sedim. of the MG	USGO	Ferrugin. Materials	Coastal Sands	Means	Range
Li (ppm) -	17	24↔40	25	60↔159	20∇[27]	14∇[13]	9.4∇[8]	10∇[6]	2.9∇[0.9]	24∇	10∇169
Be (ppm)	7.4	2↔5.5	3	2↔3	1.9∇[1.7]	1.9∇[1.4]	<0.3∇0.9	0.9∇[0.5]	<0.3	0.9↔6	5∇140
lBe (ppb)	<65		<65		<67	<67	<67	<67∇134	<67		
F (ppm)	404	520↔2950	793	500↔800	517∇[587]	<140∇1720	<140∇362	<140	<140∇1281	90↔980	20∇1400
% Na <sub>2</sub> O -	5.6	3.3↔3.8	0.23	1.2↔1.6	1.3∇[1.2]	0.11∇[0.08]	0.15∇[0.14]	0.1∇[0.06]	<0.02∇0.14	1.62∇	
lNa (ppm)	662		1677		111∇[202]	279∇[412]	231∇[336]	28∇[12]	32∇[44]		
% MgO -	0.02	0.26↔1.56	1.0	2.5↔2.6	0.13∇[0.13]	0.46∇[0.34]	0.13∇[0.11]	0.18∇[0.09]	0.06∇[0.04]	1.5∇	0.08∇0.83
lMg (ppm)	12		370		133∇[227]	266∇[271]	151∇[174]	98∇[73]	64∇[91]		
% Al <sub>2</sub> O <sub>3</sub>	14.3	13.8∇	19.0	16.7∇	8.0∇[4.7]	11∇[6.8]	3.8∇[4.4]	11∇[6.2]	0.6∇[0.4]	13.6∇	
lAl (ppm)	<0.5		0.6		<0.5∇19	<0.5∇121	<0.5∇13.2	<0.5∇11	<0.5∇18.5		
% SiO <sub>2</sub> *	74		61		83∇[8.8]	71∇[13]	89∇[10]	74∇[15]	96∇[3.2]		

... continued

<sup>1</sup> The sampled granite was slightly weathered (sample Gr1) and formed the parent material to most of the granite-derived soils investigated in this study (Figure 5.1).  
<sup>2</sup> Based on one or two strongly weathered samples from schist and(or) phyllite of the Malmesbury Group (saproplites; samples 35Sap and 39Sap; Figure 6.1). Most of the soil samples summarised in the column "soils associated with the sediments of the Malmesbury Group (MG)" are associated with these rocks.

... Table 9.1 continued

Element (Oxide)	UNDERLYING MATERIALS			SOILS ASSOCIATED WITH - increasing degree of weathering and transport of the underlying material -					SOILS OTHER AUTHORS		
	Granite This Study <sup>1</sup>	Granite Other Authors	Pelites This Study <sup>2</sup>	Other Authors	Granite	Sedim. of the MG	USGO	Ferrugin. Materials	Coastal Sands	Means	Range
% P <sub>2</sub> O <sub>5</sub> *	0.03	0.14*	0.06	0.16*	0.04*[0.02]	0.08*[0.05]	0.05*[0.02]	0.07*[0.03]	0.04*[0.05]	0.1*	0.04:0.18
IP (ppm)	<0.5		<0.5		<0.5:2.1	<0.5:5.8	<0.5:2.2	<0.5:2.1	<0.5:1.8		
S (ppm) *	38	300*	151	2400*	160*[78]	321*[121]	228*[105]	222*[102]	210*[294]	1600*	200:2000
IS (ppm)	4.3		42		<0.5:170	30*[36]	<0.5:45	20*[17]	6.8*[8]		
Cl (ppm)	101	130-200	1300	180*	148*[120]	225*[208]	239*[385]	64*[14]	100*[102]	100*	
% K <sub>2</sub> O	5.2	5.1*	3.8	3.6*	2.5*[1.4]	1.3*[0.8]	0.4*[0.15]	0.71*[0.4]	0.12*[0.15]	1.8*	0.2:1.4
IK (ppm)	557		9.6		30*[19]	38*[18]	39*[40]	49*[42]	6.3*[4.8]		
% CaO *	0.08	0.7-3.5	0.02	2.2*	0.1*[0.1]	0.12*[0.16]	0.06*[0.02]	0.14*[0.22]	0.2*[0.56]		0.1:1.7
ICa (ppm)	65		55		196*[153]	466*[267]	206*[137]	346*[220]	286*[445]		
% TiO <sub>2</sub>	0.06	0.2-0.6	0.8	0.76*	0.14*[0.06]	0.52*[0.2]	0.23*[0.12]	0.59*[0.2]	0.1*[0.04]	0.48*	
V (ppm)	2.5	44-88	122	130*	19*[11]	120*[55]	55*[45]	127*[98]	7.7*[1.1]	56-100	
IV (ppb)	<9		141		<9:24	<9:112	<9:147	<9:118	<9:116		
Cr (ppm)	15	4-22	118	90*	25*[7.9]	97*[29]	41*[20]	81*[55]	28*[4]	37-54	5:1100
ICr (ppm)	<0.05		<0.05:0.1		<0.05:0.2	<0.05:0.2	<0.05:0.15	<0.05:0.1	<0.05:0.05		
Mn (ppm) *-	62	325-540	109	100:14000	90*[28]	157*[97]	86*[28]	127*[70]	70*[14]	550*	20:1800

continued ...

<sup>1</sup> The sampled granite was slightly weathered (sample Gr1) and formed the parent material to most of the granite-derived soils investigated in this study (Figure 5.1).

<sup>2</sup> Based on one or two strongly weathered samples from schist and(or) phyllite of the Malmesbury Group (sapolites; samples 35Sap and 39Sap; Figure 6.1). Most of the soil samples summarised in the column "soils associated with the sediments of the Malmesbury Group (MG)" are associated with these rocks.

... Table 9.1 continued

Element (Oxide)	UNDERLYING MATERIALS			SOILS ASSOCIATED WITH → increasing degree of weathering and transport of the underlying material →						SOILS OTHER AUTHORS	
	Granite This Study <sup>1</sup>	Other Authors	Pelites This Study <sup>2</sup>	Other Authors	Granite	Sedim. of the MG	USGO	Ferrugin. Materials	Coastal Sands	Means	Range
Co (ppm) * -	0.24	1-4	2.1	20*	0.5*[0.2]	4.8*[4.3]	1.0*[0.5]	2.9*[1.2]	0.4*[0.22]	3-9.1	1-140
Co (ppb)	<13		<13		<13165	<13182	<13147	<13137	<13120		
Ni (ppm) * -	5.2	7*	12	70*	7.8*[5.1]	17*[12]	8.8*[3.6]	11*[5.3]	8.6*[1.5]	19*	5150
Ni (ppb)	<0.2		<0.2		<0.210.7	<0.210.9	<0.210.38	<0.210.7	<0.210.83		
Cu (ppm) -	2.5	13*	24	45*	4.3*[2.2]	19*[14]	4.0*[0.8]	7.8*[3.9]	3.9*[0.6]	25*	2140
Cu (ppb)	<0.05		<0.05		<0.0510.08	<0.0510.1	<0.05	<0.0510.1	<0.05		
Zn (ppm) -	5.0	50*	30	95*	12*[14]	26*[12]	5.7*[3.5]	16*[7.0]	2.5*[1.6]	60*	10180
Zn (ppb)	<0.1		0.17		<0.110.7	<0.111.0	<0.110.75	0.93*[2.4]	<0.110.88		
As (ppm) * +	1.3	1.5-1.9	9.6	13*	83*[188]	16*[8.6]	9.5*[9.6]	11*[10]	1.1*[0.5]	3.6-7.2	2120
Se (ppm)	<0.8	0.05*	<0.8	0.6*	<0.815.3	1.9*[0.8]	<0.811.8	2.7*[2.4]	<0.8	0.4*	0.0212
Br (ppm) +	<1.0	0.1315	36	1-60	5.4*[5]	13*[9.9]	3.6*[2.5]	5.8*[3.7]	8.9*[13.5]	0.85-1	
Mo (ppm) *	1.9	1-1.3	0.7	1-2.6	3*[2.2]	1.7*[0.5]	2.2*[0.5]	1.7*[0.7]	2.2*[0.5]	0.9-2	0.215
Sn (ppm)	7.3	2.414.2	6.8	6*	14*[17]	4.9*[2.4]	5.2*[5.8]	4.9*[2.4]	2.2*[0.4]		1120
Sb (ppm) *	<0.3	0.0910.6	1.9	0.114	<0.318	4.3*[3.6]	<0.314.2	1.3*[0.8]	2.6*[2.5]	0.66-6	0.213

continued ...

<sup>1</sup> The sampled granite was slightly weathered (sample Gr1) and formed the parent material to most of the granite-derived soils investigated in this study (Figure 5.1).

<sup>2</sup> Based on one or two strongly weathered samples from schist and(or) phyllite of the Malmesbury Group (saprolites; samples 35Sap and 39Sap; Figure 6.1). Most of the soil samples summarised in the column "soils associated with the sediments of the Malmesbury Group (MG)" are associated with these rocks.

... Table 9.1 continued

Element (Oxide)	UNDERLYING MATERIALS			SOILS ASSOCIATED WITH - increasing degree of weathering and transport of the underlying material -						SOILS OTHER AUTHORS	
	This Study <sup>1</sup>	Granite Other Authors	Pelites This Study <sup>2</sup>	Other Authors	Granite	Sedim. of the MG	USGO	Ferrugin. Materials	Coastal Sands	Means	Range
I (ppm) *	2.5	0.14-0.2	15	0.2-1.7	<2.5-12	48*[56]	<2.5-116	19*[18]	<2.5-18.8	1.2-5	0.1-150
Ba (ppm) *	1.2		1.2		2.1*[1.9]	10*[7.3]	1.5*[1.3]	5.4*[5.0]	0.6*[0.2]		
W (ppm) +	52	1.5*	7	1.5-3.8	44*[102]	11*[3.3]	17*[3.5]	9.2*[2.6]	22*[4.6]		4-110
Tl (ppb)	24		5		<3-21	<3-116	<3-110	<3-110	<3		
Pb (ppm) *	11	15-19	18	20*	16*[10]	22*[7.7]	8.7*[8.1]	17*[10]	<2.1-13.9	15-19	2-160
Pb (ppb)	<54		<54-1288		<54-1314	<54-1297	<54-1169	<54-159	<54-1400		
Th (ppm)	31	8-156	17	12*	27*[38]	13*[5.3]	6.2*[5.0]	19*[14]	<1.7-12.0	5-9.4	1-135
U (ppm)	4.8	3*	6	3.7*	4.5*[2.7]	3.8*[1.5]	<1.3-13.4	3.1*[1.2]	<1.3-12.0	2.7*	0.7-19

<sup>1</sup> The sampled granite was slightly weathered (sample Gr1) and formed the parent material to most of the granite-derived soils investigated in this study (Figure 5.1).

<sup>2</sup> Based on one or two strongly weathered samples from schist and(or) phyllite of the Malmesbury Group (saprolites; samples 35Sap and 39Sap; Figure 6.1). Most of the soil samples summarised in the column "soils associated with the sediments of the Malmesbury Group (MG)" are associated with these rocks.

**Highest concentrations in fine textured subsoil:** The eluviation of Li from the topsoil and its concentration in the kaolinite-rich subsoil was shown in Chapters 4 to 7. The enrichment factor from the top- to the subsoil may be as high as 9.7 (Table 4.5) and the highest determined Li concentration was 84 ppm (subsoil at Pit 32). The concentration in the subsoil is quite often higher than the concentration in the underlying rock. Association of Li with clay was also observed by other authors (Heier and Billings, 1970a; Vinogradov, 1959). Accumulation of illuviated mica may also be considered to be a possible reason for high Li concentrations in the subsoil. Highest acceptable concentrations for the assessment of Li polluted soils were not found in the literature.

**Other factors which determine the concentrations:** Heier and Billings (1970a) observed low Li concentrations in lateritic soils. This is in agreement with the general decrease of the Li concentrations from the granite-derived soils to the soils associated with the sediments of the Malmesbury Group and further to the soils associated with the ferruginized materials (Table 9.1). It could be deduced that long periods of weathering may result in depletion of Li. The accumulation of Li in strongly eluviated soil horizons which contain abundant Fe-oxide concretions (Chapter 7) contradicts the above suggested depletion of Li during weathering and suggests association of Li and Fe-oxides. It is recommended that the Fe-oxide concretions be analysed for Li.

**Comparison of underlying materials and soil groups (Table 9.1):** The differences between the Li concentrations in the underlying materials and the concentrations in the corresponding soils are relatively small. It is, therefore, suggested that most of the Li that was released during soil weathering was adsorbed onto or incorporated into secondary soil minerals rather than removed from the soil.

**Comparison with literature (Table 9.1):** The samples of the rocks underlying the investigated soils have relatively low Li concentrations. This could reflect the relatively high degree of weathering of the sampled material. The Li concentrations in the investigated soils are generally lower than the values reported by other authors.

### 9.3. BERYLLIUM

**General:** An important characteristic of Be is the small size of its cation (0.31 Å). The size of the Be<sup>2+</sup> ion allows it to substitute for Si (0.41 Å) and results in a high ionic potential (Merian, 1984; Hörmann, 1969). The mobility of the ion should thus be relatively high (Scheffer and Schachtschabel, 1989).

The toxicity of Be is agreed on by various authors (e.g. Blume, 1992; Merian, 1984). Water-soluble forms of Be are particularly toxic to plants. The highest risk for humans occurs if unusually high concentrations of Be are inhaled. Blume (1992) states that Be is not essential to plants and animals.

### 9.3.1. Total Be concentrations

**Primary host minerals:** Most of the world's Be is hosted by plagioclase, hornblende, pyroxene, mica and clay-minerals (Merian, 1984; Hörmann, 1969). Be-minerals (e.g. Beryl) are less important. A comparison of data published by Hörmann (1969) demonstrates that muscovite is the rock-forming mineral with the highest Be concentrations (10 to 50 ppm). The results from the granite-derived soil indicated that the host of Be is relatively susceptible to weathering.

**Maximum concentrations close to the granite:** The granite has the highest Be concentration overall (sample Gr1; 7 ppm). The soil sample with the highest Be concentration (sample 30Top; 5 ppm) originates from the soil nearest to the granite outcrops. The highest acceptable Be concentration for the assessment of polluted soils is 10 ppm (Kloke, 1980) and was not exceeded.

**Continuous depletion of Be during soil formation:** The Be concentration in the granite-derived soil decreases with increasing distance from the granite, indicating that Be becomes continuously depleted during soil formation.

**Accumulation of Be:** The sample taken from a sandstone of the Malmesbury Group has lower Be concentrations than the associated soil, indicating that formation of soils may also result in accumulation of Be.

**Other controls on concentration:** Merian (1984) as well as Hörmann (1969) report that Be is commonly associated with clay. This is in agreement with the results from the soils associated with the USGO and sediments of the Malmesbury Group, because the Be concentrations in these soils increase from the topsoil to the clay-enriched subsoil. The granite-derived soils, however, did not show an increase in the Be concentrations from the top- to the subsoil.

Correlations of  $\text{Fe}_2\text{O}_3$ , Fe-oxide gravel and Be in the toposequence associated with the ferruginized materials indicated association of Be with Fe-oxides (Chapter 7).

**Comparison with literature (Table 9.1):** The Be concentrations of the underlying rocks are within the normal range, as determined by other authors. The means of the Be concentrations for the investigated soil groups compare well with the data published by other authors. Only the soils associated with the USGO and the coastal sands have relatively low Be concentrations.

### 9.3.2. 1 M $\text{NH}_4\text{NO}_3$ extractable concentrations of Be

Only 8 % the 89 soil samples analysed for extractable Be have concentrations above the LLD (67 ppb). The highest concentrations of extractable Be occur at the footslope of the toposequence associated with the ferruginized material (Pit 45). The concentrations of extractable Be in Pit 45 range from 70 ppb to 135 ppb and greatly exceed the highest acceptable concentrations for the assessment of polluted soil (20 ppb; Table 9.2). It was speculated that the footslope of the toposequence associated with the ferruginized materials is characterised by decomposition of Fe-oxide concretions (Chapter 7).

Extractable Be may thus originate from decomposing Fe-oxide concretions. In conclusion it is suggested that Fe-oxide concretions be analysed for Be.

**Table 9.2:** Concentrations of ammonium nitrate extractable element fractions that should not be exceeded in the soil (Prüß *et al.*, 1991). A concentration that is higher than the recommended maximum concentration can limit the functioning of the soil. It is indicated which of the soil functions is most threatened by a pollutant in order to help in deciding which countermeasures are most important. Abbreviations for the ranking of concerns if the maximum concentrations are not excessively exceeded: PC = primary concern, C = concern, INV = further investigations needed to assess risk. Limited soil functioning only if the maximum concentrations are excessively exceeded: ⊗.

	Recommended maximum extractable concentrations (ppb in soil fraction < 2 mm)	SOIL FUNCTIONS AND RANKING OF CONCERNS				
		Pollutant buffer with regard to plants for human consumption	Pollutant buffer with regard to plants for animal consumption	Habitat for plants	Habitat for soil organisms	Pollutant filter with regard to ground water
As	100	PC	⊗	C	⊗	C
Be	20	⊗	⊗	⊗	⊗	INV
Bi	100	⊗	INV	⊗	⊗	⊗
Cd	20	PC	C	⊗	C	C
Co	500	⊗	C	C	⊗	⊗
Cr	100	⊗	⊗	⊗	PC	C
Cu	2000	⊗	C	C	PC	C
Mo	1000	⊗	PC	C	⊗	⊗
Ni	1000	⊗	⊗	C	⊗	⊗
Pb	2000	PC	C	⊗	C	C
Sb	1000	⊗	⊗	⊗	⊗	C
Tl	30	PC	C	C	C	INV
U	40	⊗	⊗	⊗	⊗	INV
V	100	⊗	⊗	INV	⊗	⊗
Zn	10000	⊗	⊗	C	⊗	⊗

## 9.4. FLUORINE

**Relevance of F to health:** Fluorine increases the resistance of teeth to caries if it is included into the lattice of tooth-apatite. High intake of F can result in fluorosis and other diseases (Fiedler and Rösler, 1987; Scheffer and Schachtschabel, 1989). Fluorosis may arise if the concentration of F in soil is higher than 500 ppm or higher than 2 ppm in drinking water (Brouwer *et al.*, 1988; Vinogradov, 1959). Mertz (1981) states that essentiality of F for animals was reported but not confirmed.

**Primary host minerals and mobility:** Topaz, fluorite and fluor-apatite are the only rock-forming minerals that have F as an essential constituent. Fluorine is a common replacement of the OH-groups in mica and hornblende. The F concentration of feldspars is relatively low (Vinogradov, 1959; Koritnig, 1972). Major losses of F from the granite-derived topsoil suggested that the primary host of F is relatively soluble. Koritnig (1972) reported that the F hosted by micas was leached out soon after onset of weathering. Mica could thus be an important host of F in the granite-derived toposequence. It is important to note that the complexation of F by Al can increase the solubility of both elements (Scheffer and Schachtschabel, 1989).

### Maximum concentrations:

The highest F concentrations occur in the G-horizon of the granite-derived toposequence ( $\approx 1900$  ppm). Highest acceptable F concentrations for the redevelopment of contaminated land vary, depending on the author, from 200 ppm to 1000 ppm (Eidgenössisches Department des Inneren, 1986; Smith, 1980; Kloke, 1980). It is, however, important to note that the use of the acceptable maximum concentrations is problematic because the natural distribution of F in rocks and soils is very variable and natural concentrations may well be higher than 1000 ppm (Scheffer and Schachtschabel, 1989).

**Important controls of the concentration:** Subsoils and underlying rocks have generally higher F concentrations than the topsoils, reflecting that the eluviation and leaching of the topsoil results in depletion of F. The enrichment factor from the topsoil to the clay-rich subsoil may be as high as 10 (Table 4.5). The accumulation of F in the

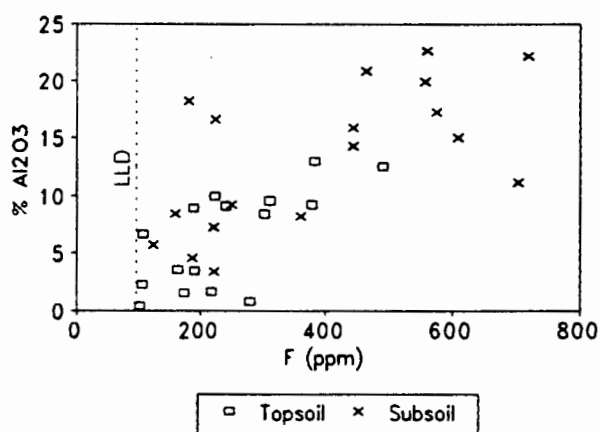


**Figure 9.1:** Fluorine versus  $\text{Al}_2\text{O}_3$  in soil samples, showing that high F concentrations occur mainly in subsoils with high  $\text{Al}_2\text{O}_3$  concentrations.

subsoil reflects its strong affinity for clay minerals (Scheffer and Schachtschabel, 1989). A plot of F versus  $\text{Al}_2\text{O}_3$  (Figure 9.1) shows that high F concentrations occur mainly in subsoils with high  $\text{Al}_2\text{O}_3$  concentrations. On the assumption that subsoils with high  $\text{Al}_2\text{O}_3$  concentrations contain high proportions of clay minerals, the plot substantiates the affinity for F to clay minerals.

In the soils associated with the USGO high F concentrations coincided with high proportions of organic matter (6.6 to 8.1 %), suggesting an association of organic matter and F. This association is difficult to explain because (a) F is generally not enriched in organic substances and (b) the affinity of  $\text{F}^-$  ions for organic matter is small (Swaine, 1990; Scheffer and Schachtschabel, 1989; Koritnig, 1972).

**Comparison with literature:** Table 9.1 indicates that the F concentration in the granite is relatively low. The slightly weathered state of the sample taken from the granite is the best explanation for this anomaly. The means of the F concentrations in the investigated soils compare well with values reported by other authors.

## 9.5. SODIUM

### 9.5.1. Total $\text{Na}_2\text{O}$ concentrations

**Lateral change of the concentrations along the sampling lines:** The lateral change of the  $\text{Na}_2\text{O}$  concentrations is controlled by the colluvial, fluvial or aeolian input of  $\text{Na}_2\text{O}$ -hosting minerals (e.g. feldspars) from near-by granites (sections 4.5.4., 5.5.1 and 8.4.1.), and the evaporation of water and accumulation of soluble salts at the footslope of a toposequence (sections 5.5.7. and 6.5.5.). The eluviation and depletion of Na-hosting minerals particles is the best explanation for the lateral trend of the  $\text{Na}_2\text{O}$  concentrations observed in the toposequence associated with the ferruginized materials (section 7.5.2.).

**Early release during weathering:** Mass balance calculations and leaching experiments showed that Na is readily released during the early stages of granite weathering. The real  $\text{Na}_2\text{O}$  loss from the granite to the uppermost part of the granite-derived toposequence is 72 % (sections 4.5.1. and 4.5.6.).

**Comparison with literature (Table 9.1):** Sposito (1989) reported a world average of 1.61 % for  $\text{Na}_2\text{O}$  in soils. The means of the investigated soils range from 0.1 to 1.3 %  $\text{Na}_2\text{O}$ .

### 9.5.2. 1 M $\text{NH}_4\text{NO}_3$ extractable concentrations of Na

**Variation of the concentrations in the coastal sand-derived soils:** The concentrations of extractable Na in the coastal sand-derived soils correlate mainly with the organic matter contents. It was suggested that organic matter enables the soil to

retain higher quantities of Na. The proportion of organic matter, and, therefore, also the concentration of extractable Na, decreases with increasing soil depth (Chapter 8).

**Aerial deposition of Na:** Aerial deposition is an important source of Na for soils, particularly in close proximity to the sea (Scheffer and Schachtschabel, 1989). It is interesting to note that the concentration of extractable Na in the coastal sand-derived soils does not increase towards the sea, probably indicating that Na deposited on the soil is easily leached into the ground water. Only coastal sand-derived soils with higher proportions of organic matter can retain and accumulate extractable Na to higher concentrations. The distance to the sea is of secondary importance. This is substantiated by the fact that the coastal sand-derived soils, being closest to the sea, have extractable Na concentrations lower than or similar to the soils which occur further inland (Table 9.1).

**Comparison of underlying rock and soil groups (Table 9.1):** The concentration of extractable Na in the (pulverised) granite was lower than the concentration in the (pulverised) pelites of the Malmesbury Group. This trend was inherited by the associated soils.

The soils have generally much lower concentrations of extractable Na than the underlying rocks. This substantiates the conclusion that Na is readily released by its host minerals and easily leached into the ground water (see above).

## 9.6. MAGNESIUM

**Highest concentrations:** The highest MgO concentrations occur in the subsoils associated with the sediments of the Malmesbury Group. These subsoils also have high concentrations of 1 M  $\text{NH}_4\text{NO}_3$  extractable Mg. This is in agreement with the relatively high concentrations of total and extractable Mg in the underlying rock (Table 9.1). The decrease of the Mg concentrations from the sediments of the Malmesbury Group and the subsoils to the overlying topsoils reflects the loss of Mg due to leaching and eluviation of the topsoils (Figure 9.2).

**Possible atmospheric deposition of Mg:** The concentrations of total and extractable Mg increase from the granite to the derived soils. The increase coincides with lower [non-extractable Mg] over [1 M  $\text{NH}_4\text{NO}_3$  extractable Mg] ratios (Figure 9.2), reflecting the relatively large proportion of extractable Mg in the soil. It is stated in Scheffer and Schachtschabel (1989) that the deposition of aerosols may contribute considerable quantities of Mg to soils if the locality is relatively close to the sea. The increase of the Mg concentration from the rock to the soil may, therefore, reflect atmospheric input of Mg. This explanation, however, is conflicting with the results obtained from the soils associated with the coastal sands and USGO which indicated that aeolian and colluvial input of granitic detritus is an important source of Mg. It

could be argued that the increase of the Mg concentrations from the granite to the soil is the result of the accumulation of Mg from throughflow water. This explanation, however, is conflicting with the fact that the highest Mg concentrations occur in the soil which is most distant from the steeper part of the slope (Pit 33) and probably least affected by throughflow.

**Vertical distribution:** The concentration of total and extractable Mg increases often from the top- to the subsoil. This was attributed to the association of Mg with clay minerals and Fe-oxides (e.g. Table 4.5.). High Mg concentrations in the relatively organic-rich top 15 cm of the soil profiles and in the organic-rich subsoils suggested the association of Mg with organic matter (Chapter 5 and section 8.4.2.). E-horizons are sometimes depleted in both total and extractable Mg.

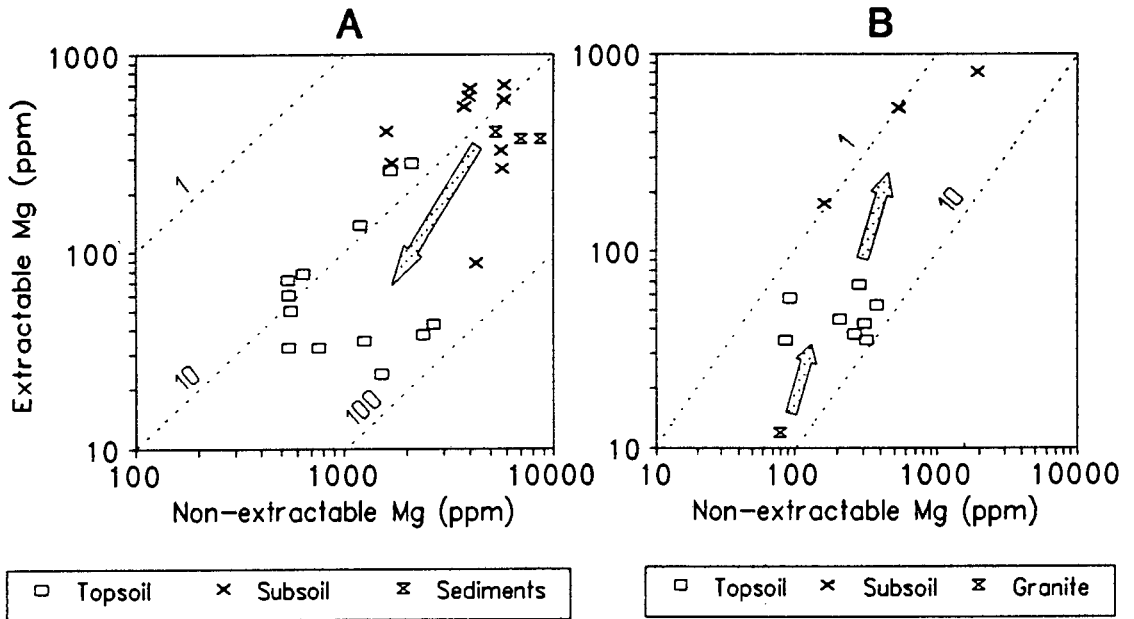


**Figure 9.2:**  $\text{NH}_4\text{NO}_3$  extractable versus non-extractable Mg for the soils associated with the sediments of the Malmesbury Group (A) and the granite (B). Diagonal lines were drawn to indicate different ratios. The arrows demonstrate the chemical changes with progressing soil formation.

**Comparison with literature (Table 9.1):** The MgO concentrations reported in the literature indicate that the concentrations in the investigated soils and rocks are low. The low concentrations in the sediments of the Malmesbury Group and the soils possibly reflect the absence of Mg-enriched source rocks (parent materials) in the field area (e.g. basic rock-types).

## 9.7. ALUMINIUM

**Highest concentrations:** The  $\text{Al}_2\text{O}_3$  concentrations generally increase from the top- to the subsoil. This is attributed to the accumulation of clay minerals in the subsoil (Chapter 3). The highest  $\text{Al}_2\text{O}_3$  concentrations occur in the subsoils associated with the sediments of the Malmesbury Group, reflecting the relatively high proportion of clay minerals in this rock-type (Chapter 3).

**Controlling factors:** It was stated above, that the accumulation of clay minerals in the subsoil causes a conspicuous increase of the  $\text{Al}_2\text{O}_3$  concentrations from the top- to the subsoils. The horizontal variations of the concentration are smaller and were attributed to the effects of colluvial, fluvial and(or) aeolian input of feldspathic detritus (Chapters 4, 5 and 8). It was also shown that colluviation may cause uptake of clay minerals from the underlying material into the soil and thereby affect the  $\text{Al}_2\text{O}_3$  concentrations (Chapter 6). Some of the E(luviated)-horizons are particularly depleted in  $\text{Al}_2\text{O}_3$ .

The results from the coastal sand-derived soils showed that samples with high proportions of organic matter have low  $\text{Al}_2\text{O}_3$  concentrations but high concentrations of 1 M  $\text{NH}_4\text{NO}_3$  extractable Al. It was proposed that the decay of organic matter results in lower redox-potentials and higher acidities, causing complexation, solution, leaching and finally depletion of Al. The  $\text{Al}_2\text{O}_3$  concentrations increase from the top- to the subsoil because the proportion of organic matter normally decreases from the top- to the subsoil (Chapter 8).

**1 M  $\text{NH}_4\text{NO}_3$  extractable Al:** 42 % of the 89 soil samples had extractable Al concentrations below the LLD (0.5 ppm). Relatively high concentrations of extractable Al occur in samples with high proportions of organic matter (see above), low pH values (Chapter 4) and high proportions of clay (Chapters 6 and 7). A lowering of the soil-pH may cause release of  $\text{Al}^{3+}$  ions from oxides and silicates (Scheffer and Schachtschabel, 1989). Higher proportions of clay provide more exchange sites for extractable  $\text{Al}^{3+}$  ions.

## 9.8. PHOSPHORUS

**Highest concentrations:** The soils with the highest total P concentrations are associated with the sediments of the Malmesbury Group. This is in agreement with the relatively high P concentration in the underlying sediments (Table 9.1). It is, however, important to note that the accumulation of organic matter in the soils derived from coastal sands also resulted in high total P concentrations.

**Factors which control the concentrations of total P ( $\text{P}_2\text{O}_5$ ):** The distribution of  $\text{P}_2\text{O}_5$  in the soil associated with USGO and coastal sand indicated that the fluvial,

aeolian and colluvial input of detritus is an important determinant of the lateral change of the  $P_2O_5$  concentration.

It was generally noted in the preceding chapters that P is not depleted during soil formation. This was attributed to insoluble host-minerals (e.g. apatite) and fixing of released P-compounds by soil constituents such as organic matter and Fe-oxides (e.g. Table 4.5, section 8.4.2.). The differences between the  $P_2O_5$  concentrations in the underlying rocks and the more and less weathered soil groups is relatively small compared to other elements (Table 9.1; depletion factor 1-2). The tendency of P to have similar concentrations in underlying rocks and different soil groups substantiates the hypothesis that the investigated soils commonly retain P during soil formation.

**1 M  $NH_4NO_3$  extractable concentration:** 48 % of the 89 soil samples have extractable P concentrations below the LLD (0.5 ppm). The concentration of extractable P is higher in soils that have higher retention abilities for P-compounds; i.e. higher proportions of clay minerals and organic matter (e.g. sections 6.5.3. and 8.4.4.). Particularly, the accumulation of organic matter in the soils derived from the coastal sands results in high concentrations of extractable P (section 8.4.4.; Table 9.1).

It was also observed that the concentration of extractable P increases down a toposequence towards the footslope (sections 6.5.4. and 7.5.5.). It was suggested that the evaporation of water from the soils at the footslopes caused the accumulation of extractable or soluble P-compounds.

The (powdered) rocks have extractable P concentrations below the LLD (Table 9.1), indicating that their P is hosted by insoluble minerals such as apatite.

**Vertical distribution:** The total and the extractable concentrations of P often increase from the sub- to the topsoil. The highest concentrations commonly occur in the organic-rich top 15 cm of the soil profiles.

**Other authors:** Accumulation of P in the topsoil and its association with organic matter and Fe-oxides is also reported elsewhere (e.g. Torrent, 1994; Scheffer and Schachtschabel, 1989; Division of Soils CSIRO, 1983). The concentrations in the soils are within the normal range (Table 9.1).

**Agro-chemical inputs:** The distribution of total and extractable P in the sampled soils gave no reason to suggest that agro-chemical inputs of P were important in determining the observed concentrations (e.g. section 6.5.2.). All concentrations are within the normal range as suggested by other authors (Table 9.1). This could indicate that (a) no P was applied to the soils, (b) the quantity of P applied to the soils was relatively small compared to the background concentration of P and (c) the P added to the soil was not retained by the soil. It is important to note that the sampling strategy was designed to avoid, as far as possible, the effects of the application of agro-chemicals (section 2.2.).

## 9.9. SULFUR

**Factors which control the lateral and vertical change of the concentrations along the sampling lines:** It was shown in Chapters 4 to 8 that high concentrations of total and 1 M  $\text{NH}_4\text{NO}_3$  extractable S coincide with high proportions of organic matter, clay minerals or Fe-oxides. The results suggested that the affinity of S, probably in the form of sulfates, for Fe-oxides is particularly strong (e.g. Table 4.5; section 7.6.). The retention of S by these substances resulted in its accumulation in top- and subsoils and presumably caused the general increase of the S concentrations from the underlying rocks to the soils (Table 9.1). E-horizons are partly depleted in total and extractable S. The results also suggested the accumulation of S due to the evaporation of water from the soil (Chapters 5, 6, 7).

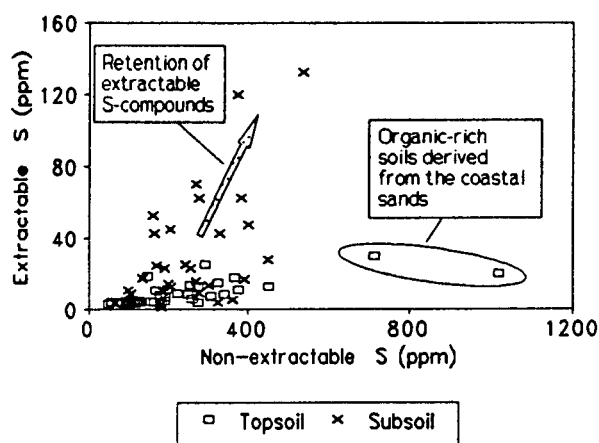


**Figure 9.3:**  $\text{NH}_4\text{NO}_3$  extractable S versus non-extractable S for all soils.

**Insolubility of S in the topsoil:** Figure 9.3 shows that the subsoils may have both high concentrations of non-extractable and extractable S. The topsoils are characterised by a wide range of non-extractable S concentrations and generally low concentrations of extractable S. Scheffer and Schachtschabel (1989) state that 60 to 98 % of the S present in the topsoil is hosted by organic matter. In this study high S concentrations in the topsoil coincided with high proportions of organic matter and(or) Fe-oxides (see above). Association of S with these substances in the topsoil was thus suggested. In the organic-rich topsoils S may also be present in the form of sulfides. Figure 9.3 shows that these substances host S mainly in a non-extractable (insoluble) form.

## 9.10. CHLORINE

**General:** Chlorine is essential to plants, animals and humans. High concentrations of Cl can be toxic. The chlorine concentration in magmatic rocks ranges commonly from 50 ppm to 500 ppm. Marine sediments and sedimentary rocks with high proportions of clay may contain as much as 3 % Cl (Scheffer and Schachtschabel, 1989). The Cl concentrations of the investigated rocks and soils are within the normal range, as outlined above (Table 9.1).

Apatite is a common host of Cl in igneous, metamorphic and sedimentary rocks. The Cl ion can substitute for the hydroxyl ion in hydroxysilicate minerals, despite the fairly large difference in the respective ionic radii ( $\text{OH}^-$  1.40 Å;  $\text{Cl}^-$  1.81 Å; Fuge, 1974).

Chloride ions released during weathering form easily soluble salts with alkaline and alkaline-earth cations. These salts are easily leached from the soils. They can accumulate in the soil if considerable amounts of soil water evaporate. It is important to note that *in situ* weathering of minerals accounts only for a small proportion of the Cl present in soils. The largest proportion of Cl in soils is accounted for by atmospheric deposition (Scheffer and Schachtschabel, 1989).

Figure 9.4 shows the correlation of the conductivity of the water-suspended soil and the Cl concentration, indicating that Cl forms a major proportion of the total dissolved solids. The subsoils show a higher degree of correlation than the topsoils, probably reflecting that a considerable proportion of the Cl present in the topsoils is hosted by insoluble minerals.

**Factors which control the vertical and lateral change of the concentrations along the sampling lines:** High Cl concentrations occur in soils which have high proportions of organic matter and(or) fine particles. This was attributed to the retention ability of clays and organic matter for water and dissolved solids. Evaporation of retained water could contribute to the observed accumulation of Cl. The highest Cl concentrations (650 ppm to 1459 ppm) occur in the fine textured subsoils at the bottom of the toposequences, suggesting that the evaporation of uplifted shallow ground water, throughflow water and overland flow resulted in high Cl concentrations (Chapters 5, 6 and 7). It is interesting to note that the Cl concentration in the coastal sand-derived soils does not increase towards the sea, probably showing that aerial deposition of Cl results in higher concentrations only if the soil has the ability to retain soluble salts.

The high Cl concentration in a leached, coarse-textured and Fe-oxide-enriched E-horizon in midslope position of the granite-derived toposequence is unusual (sample 31B: 540 ppm Cl). The accumulation of Cl in this soil horizon could suggest an affinity of  $\text{Cl}^-$  ions for Fe-oxides (Table 4.5). Adsorption of Cl by Fe-oxides is possible at pH values lower than 5 (Scheffer and Schachtschabel, 1989). The pH(KCl) of sample 31B is 4.9 and Cl could thus be adsorbed to Fe-oxides in sample 31B. The conductivity of the water-suspended soil, however, is also relatively high and could

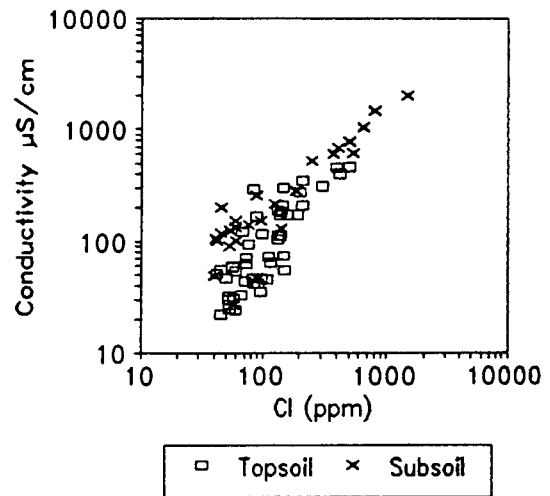


**Figure 9.4:** Correlation of the conductivity of the water-suspended soil and the chlorine concentration.

indicate that Cl is (a) present in the form of salts or (b) easily desorbed when the soil is suspended in water.

### 9.11. POTASSIUM

**Factors which determine the lateral and vertical change of the  $K_2O$  concentrations:** The samples of the granite and the sediments of the Malmesbury Group have higher  $K_2O$  concentrations than most of the investigated soils (Table 9.1), indicating a general loss of K during soil formation. Relatively high concentrations of  $K_2O$  were found in soil horizons which contain high proportions of feldspars or fine particles (Chapters 4, 5, 6 and 8). The relatively high concentration of K in feldspars is well known and will not be discussed further. The possible presence of clay minerals which can host and accumulate relatively high proportions of K could explain why fine textured soil horizons may have high  $K_2O$  concentrations (e.g. fixation of K in illite; Scheffer and Schachtschabel, 1989).

The results obtained from the soils associated with the USGO showed that subsoils which have high proportions of organic matter also have slightly higher  $K_2O$  concentrations (section 5.5.6.). Heier and Billings (1970b) reported K concentrations in dried tissue of plants which were often higher than 1 percent. Maximum concentrations were as high as 11.5 percent. The average K concentration in the soils associated with the USGO is lower than 1 percent. It is thus suggested that the increased concentration of K in the organic-rich subsoils reflects that K was introduced to the subsoil as a constituent of organic matter. A concentration of approximately 2.7 % K in the organic matter is required in order to account for the observed increase of the K concentration in the soil. Potassium is easily released by organic substances and may thus be associated with the clay minerals in the organic-rich soil horizons. Less than ten percent of the gained K is exchangeable with  $NH_4^+$ .

The lateral change of the  $K_2O$  concentrations in the topsoils associated with granite, USGO and coastal sand was explained by aeolian, fluvial and(or) colluvial input of  $K_2O$ -hosting minerals (Chapters 4, 5 and 8).

**Source of 1 M  $NH_4NO_3$  extractable K:** The quantity of K extractable from the (powdered) granite is much larger than the quantity extractable from the associated soils, indicating that a fraction of the K hosted by feldspars and other rock-forming minerals is easily soluble (Figure 9.5). Long-term leaching of the granite-derived topsoils resulted in continuous depletion of both total and extractable K (section 4.5.4.). During this process the relatively organic-rich top 15 cm of the soil retained more extractable K than the underlying topsoil, indicating the association of extractable K and organic matter (Figure 9.5).

Illite, muscovite and feldspars are known to host considerable quantities of K. The XRD-analyses indicated decreasing proportions of these minerals from the sediments of the Malmesbury Group to the overlying soils (Chapter 3). The alteration and leaching of feldspars, illite and muscovite to kaolinite is, therefore, a possible source of extractable K.

**Accumulation of 1 M  $\text{NH}_4\text{NO}_3$  extractable K:** Higher concentrations of extractable K coincided often with higher proportions of organic matter and(or) finer particles (Chapters 5 to 8), indicating that the adsorption of K to organic matter and clay is an important factor in determining the quantity of K extractable. The covariance of extractable and total K, as demonstrated in Chapters 4 and 8, indicated that the quantity of mineral-hosted K is the most important factor in determining the concentration of extractable K if less or no potential K-adsorbents are present in the soil.

**Agro-chemical inputs:** The distribution of total and extractable K in the sampled soils gave no reason to suggest that agro-chemical inputs of K were important in determining the observed concentrations (e.g. section 6.5.2.). All concentrations are within the normal range as suggested by other authors (Table 9.1). This could indicate that (a) no K was applied to the soils, (b) the quantity of K applied to the soils was relatively small compared to the background concentration of K and (c) the K added to the soil was not retained by the soil. It is important to note that the sampling strategy was not designed to determine the effect of the application of agro-chemicals (section 2.2.). On the contrary the sampling of cultivated soils was deliberately avoided.

## 9.12. CALCIUM

**Changes from the underlying rock to the soils (Table 9.1):** The CaO concentrations in the samples taken from the granite and the sediments of the Malmesbury Group are much lower than the means for similar rocks reported by other authors. This probably reflects the weathering (leaching) of the sampled rocks, because it was shown by Krauskopf (1979) that  $\text{Ca}^{2+}$ , hosted by common rock-forming minerals, dissolves faster in water than most other cations. The increasing concentration of 1 M  $\text{NH}_4\text{NO}_3$  extractable Ca from the underlying rock to the associated soils (Table 9.1) may indicate both the leaching and depletion of Ca during the weathering of the rocks and the

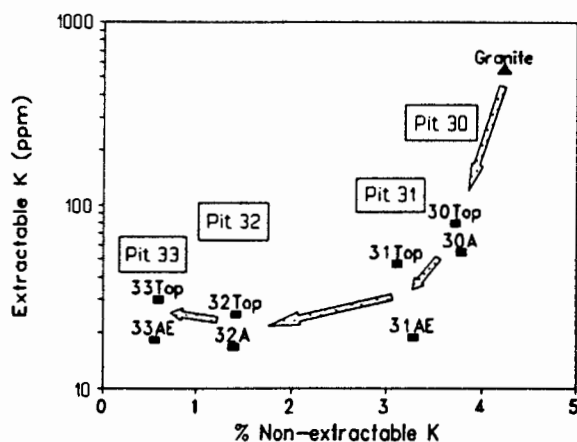


**Figure 9.5:**  $\text{NH}_4\text{NO}_3$  extractable K versus non-extractable K for the topsoils of the granite-derived toposequence. The arrows indicate increasing distance from the granite and progressive leaching.

general ability of soils to retain larger quantities of exchangeable Ca.

**Non-extractable and 1 M  $\text{NH}_4\text{NO}_3$  extractable Ca in the soils associated with the sediments of the Malmesbury Group:** The extractable concentration of Ca in the soils associated with the sediments of the Malmesbury Group is larger than the non-extractable concentration. A plot of extractable versus non-extractable Ca shows a weak correlation of the two Ca fractions (Figure 9.6). This could indicate that (a) Ca hosted by rock-derived minerals is an important source for extractable Ca and (b) soluble or exchangeable Ca becomes incorporated into organic matter or secondary soil minerals and causes higher non-extractable concentrations. The very low (total) CaO concentration in the underlying sediments (see above), the (weak) covariance of CaO and organic matter in the topsoils (Figure 9.7) and the relatively high affinity of Ca to adsorbents favour the latter hypothesis.

**Factors which determine the lateral and vertical change of the Ca concentrations along the sampling lines:** High total and extractable Ca concentrations coincided often with high proportions of organic matter (e.g. Figure 9.7) and fine particles, or were found in soils which were subjected to input of relatively fresh mineral detritus (Chapters 4 to 8). It was, therefore, suggested that the colluvial, fluvial and aeolian input of mineral detritus and the accumulation of Ca in soils with higher retention abilities is important in determining the lateral and vertical change of the Ca concentrations.

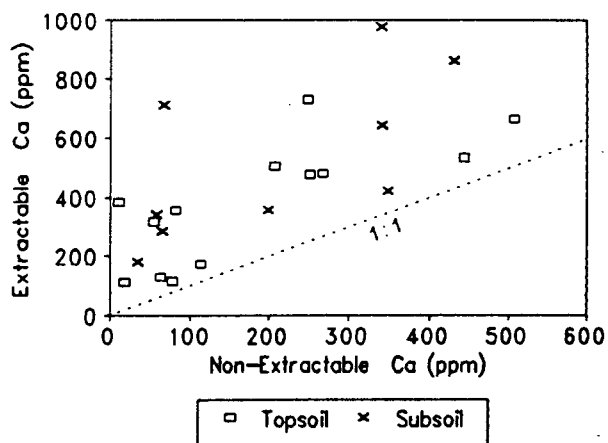


**Figure 9.6:** The (weak) covariance of  $\text{NH}_4\text{NO}_3$  extractable Ca and non-extractable Ca in the soils associated with the sediments of the Malmesbury Group.

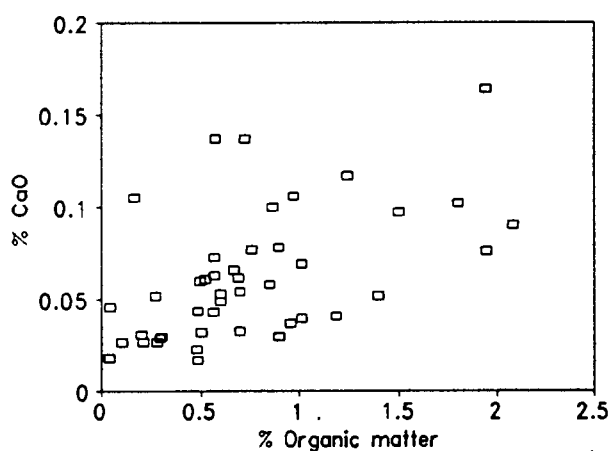


**Figure 9.7:** The (weak) covariance of organic matter and CaO in the topsoils.

### 9.13. VANADIUM

**General:** The  $V^{3+}$  ion has an ionic radius (0.61 Å) which is very similar to that of the  $Fe^{3+}$  ion (0.73 Å). Vanadium, therefore, tends to follow iron in mineral formation during magmatic processes. Mica is known to be an important host of V in granites. Pyrite and other sulfides were shown to host considerable portions of V in sediments, particularly shales (Landergren, 1974).

**Essentiality and toxicity:** Vanadium is known to be essential to animals and its essentiality for humans was suggested (Merian, 1984; Mertz, 1981). High concentrations of V are toxic to plants, animals and humans (Blume, 1992; Merian, 1984; Mertz, 1981).

**Behaviour during weathering:** The behaviour of V during weathering is primarily determined by the initial host of V. Vanadium is enriched in residual soils if hosted by minerals resistant to weathering (e.g. in a study by Minarik *et al.*, 1983). Vanadium which is hosted by mica, sulfides and other minerals more susceptible to weathering may become mobile during weathering. The mobility of V during weathering is dependant on numerous factors. Important are the concentrations of other ions, the Eh- and pH-conditions and the speciation of V. Common oxidation states of V in natural systems are +III, +IV and +V. The chemistry which determines the solubility of these species in natural waters is very complex and the subject of present research. A review of the literature on this subject is given in Dodds (1994). Vinogradov (1959) reports that the more oxidised species of V (+IV and +V) are very mobile in soils. The mobility of the more oxidised V species is also mentioned in Landergren (1974). Wanty and Goldhaber (1992) reported that ligands such as  $F^-$ ,  $Cl^-$  and perhaps  $SO_4^{2-}$  may form complexes with Vanadium(+IV)-compounds. Mobile V may be fixed and accumulated by organic matter, clay minerals and Fe-oxides (Swaine, 1990; Division of Soils CSIRO, 1983; Aubert and Pinta, 1977).

#### 9.13.1. Total V concentrations

**Factors which determine the lateral and vertical change of the V concentrations along the sampling lines:** High concentrations of V coincided with high proportions of organic matter, clay minerals or Fe-oxides, confirming the affinity of V for these substances (see above and Chapters 4 to 7). The enrichment of V in soil horizons which contain large proportions of Fe-oxides concretions is most conspicuous (Figure 9.8). The enrichment factor of V from the topsoil to the Fe-oxide-enriched subsoil may be as high as 14 (Table 4.5).

**Highest concentrations:** The highest V concentrations observed occur in the subsoil of the toposequence associated with the ferruginized materials (Chapter 7). The corresponding soil horizons contain abundant Fe-oxide-gravel and the V concentrations

range from 266 ppm to 371 ppm. The soils are used for crop production and are subject to the application of agro-chemicals. The V concentration of fertilisers, as reported by Nriagu and Pacyna (1988), generally ranges from 0.2 ppm to 0.8 ppm. It is a subject of speculation whether the relatively high concentration of V in the soils mentioned above is the result of anthropogenic activities or caused by natural processes.

The plot of V versus  $\text{Fe}_2\text{O}_3$  shows that high proportions of Fe can sufficiently account for very high levels of V (Figure 9.8).

Kelly (1980) classified soils which have V concentrations between 100 ppm and 200 ppm to be "slightly contaminated" and soils which have V concentrations between 200 ppm and 500 ppm to be "contaminated". These guidelines for the assessment of V pollution are similar to the guidelines suggested by Kloke (1980). In terms of these guidelines some of the soils associated with the ferruginized materials are to be classified "contaminated".

**Vanadium in the granite-derived toposequence:** A comparison with the literature shows that the sample of the granite which formed the parent material of the granite-derived toposequence has a very low V concentration (2.5 ppm; Table 9.1). A discussion of the possible reasons for the low concentration in the granite and the distribution of V in the granite-derived toposequence is given in section 4.5.2. In this section it was suggested that (a) minerals susceptible to weathering are probably an important host of V in the granite (e.g. mica or sulfides) and (b) the oxidation of these minerals results in water-soluble forms of V.

**Comparison with literature (Table 9.1):** The means of the V concentration for the soils associated with the sediments of the Malmesbury Group and the ferruginized materials are relatively high, probably reflecting both the relatively high concentration of V in the underlying materials and the affinity of V for Fe-oxides.

### 9.13.2. 1 M $\text{NH}_4\text{NO}_3$ extractable concentrations of V

Only 30 % of the 89 soil samples analysed have extractable V concentrations above LLD (9 ppb). The highest concentrations generally occur in the sediments of the Malmesbury Group and in the associated subsoils (26 ppb to 213 ppb). Two subsoils (samples 29G and 41B1) and the weathered phyllite of the Malmesbury Group, underlying the toposequence at Location 8 (sample 39Sap), have extractable V concentrations which exceed the highest acceptable concentrations for the assessment

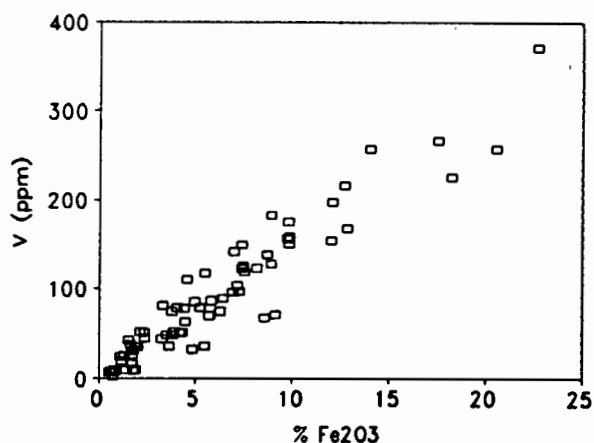


Figure 9.8: The correlation of V and  $\text{Fe}_2\text{O}_3$  in the soil.

of polluted soils (Table 9.2). A harmful effect on any of the soil functions listed in Table 9.2 is unlikely because the recommended maximum concentration of 100 ppb is only slightly exceeded. The weathered schist of the Malmesbury Group which underlies the toposequence at Location 10 also has a relatively high extractable V concentration (69 ppb), while the associated soils have generally lower concentrations (Table 9.1).

#### 9.14. CHROMIUM

**In rocks and during weathering:** Igneous processes may result in accumulation of Cr in minerals resistant (e.g. chromite) and relatively susceptible (e.g. biotite) to weathering. Accumulation and depletion of Cr in residual soils is, therefore, possible. Ruppert (1987) reports relatively high Cr concentrations for biotite, amphibole and pyroxene. Chromium in soils occurs in the Cr(III) and Cr(VI) valence states. Both ions may form compounds in soils which may be, dependant on the Eh-/pH-conditions, soluble in the soil water (Scheffer and Schachtschabel, 1989). Compared to Cr(III), chromate(VI) has a higher mobility in most soils at moderate or high pH because the anion binding ability is high only at relatively low pH (Fischer and Cram, 1994). Chromium is, despite its solubility, immobile in the soil environment because it has strong affinities to Fe-oxides and clay minerals (Scheffer and Schachtschabel, 1989; Shiraki, 1978). Shiraki (1978) refers to Cr as the element which is most effectively fixed during soil formation. The affinity of Cr for humic acid, especially at higher pH values, was demonstrated by Kerndorff and Schnitzer (1980). Nair and Narayanaswamy (1983) investigated polluted soils associated with laterites and showed that major proportions of the total Cr content may be hosted by the organic fraction of the soil.

**Essentiality and toxicity:** Chromium is probably essential to animals and humans but is possibly dispensable for plants (Scheffer and Schachtschabel, 1989; Mertz, 1981). Cr(VI)-compounds are toxic to plants, animals and humans. The toxicity of Cr(VI)-compounds is 100 to 1000 times higher than the toxicity of Cr(III)-compounds (Merian, 1984).

##### 9.14.1. Total Cr concentrations

**Factors which determine the lateral and vertical change of the Cr concentrations along the sampling lines:** Higher Cr concentrations coincided with higher proportions of clay minerals and Fe-oxide-concretions (Chapters 4 to 7), confirming the above stated affinity of Cr for these substances. Overall, the affinity of Cr for Fe-oxides is the most important factor in controlling the concentration of Cr in the investigated soils (Figure 9.9). The results obtained from the soil sequence associated with the USGO suggested that the lateral variation of the Cr concentration in this soil sequence is a function of both the input of Cr in the form of colluvial detritus and the period of time available for the accumulation of Cr during soil formation. Table 4.5 demonstrates the

accumulation Cr in the organic-rich top 15 cm of the granite-derived soil profiles.

**Highest concentrations:** The highest Cr concentrations occur in the subsoils associated with the sediments of the Malmesbury Group and the ferruginized materials, probably mainly reflecting the relatively high Cr concentration in the corresponding underlying materials (Table 9.1). A large proportion of these subsoils

have Cr concentrations which exceed 100 ppm. One hundred ppm is the highest acceptable concentration for the assessment of Cr polluted soils (Löfl, 1987, 1988; Ministerie Vrom, 1983; Kelly, 1980; Kloke, 1980). Hoffmann *et al.* (1981), however, suggested that a value of 120 ppm should be used for the assessment of soils which naturally have higher Cr concentrations. The subsoils with the three highest Cr concentrations (165 ppm to 205 ppm Cr) have higher concentrations than the underlying sediments of the Malmesbury Group (103 ppm and 134 ppm Cr) and are presently used for crop production. The long-time application of fertilisers and other agro-chemicals to these soils was confirmed by the farmers. There is reason to speculate about the application of agro-chemicals being the reason for the high Cr concentrations in these soils because:

(a) the accumulation of Cr in soils due to the application of fertilisers was also suggested by Scheffer and Schachtschabel (1989) and Nriagu and Pacyna (1988).

(b) Cr is immobile in soils and may thus accumulate with time if continuously added to the soil (see above). Scheffer and Schachtschabel (1989), however, observed that the long-term application of high Cr sewage to soils did not result in higher Cr concentrations in the subsoil because the immobility of Cr limits its accumulation to the uppermost part of the soil profile.

The plot of Cr versus  $\text{Fe}_2\text{O}_3$  shows that high proportions of Fe could sufficiently account for the observed high levels of Cr (Figure 9.9). More detailed research in the areas with high Cr concentrations is required to establish the reason for the highest Cr concentrations.

#### 9.14.2. 1 M $\text{NH}_4\text{NO}_3$ extractable concentrations of Cr

The LLD for extractable Cr in this study is 0.05 ppm. 73 % of the 86 analysed soil samples have concentrations below the LLD. Concentrations above the LLD are normally restricted to fine textured subsoils. The results obtained from the soil sequence associated with the USGO showed that high extractable Cr concentrations

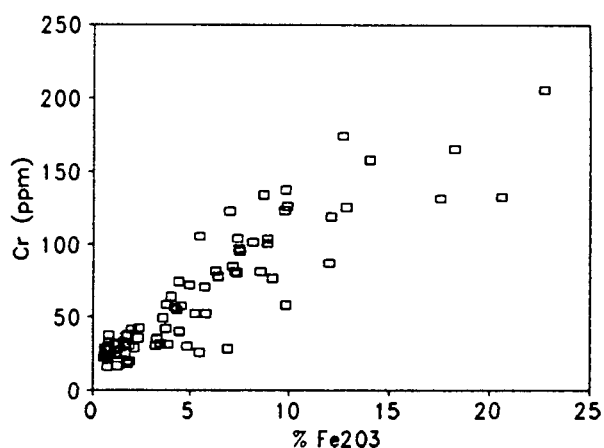


**Figure 9.9:** The correlation of Cr and  $\text{Fe}_2\text{O}_3$  in the soil.

coincide with high proportions of organic matter. The highest acceptable extractable Cr concentration for the assessment of polluted soil is 0.1 ppm (100 ppb; Table 9.2). This concentration is exceeded in 8 soil samples. The highest extractable Cr concentrations overall (0.2 ppm) occur in two subsoils which, according to the farmers, had not been treated with agro-chemicals for more than 20 years (samples 38BC and 33G).

### 9.15. MANGANESE

**In rocks and during weathering:** Biotite, hornblende and plagioclase are common primary hosts of Mn in soils. Ruppert (1987) determined the concentration of Mn in granite-derived biotites to be 1200 ppm to 8300 ppm. Low pH values and redox-potentials increase the solubility of Mn in the soil water and, therefore, facilitate the leaching of Mn from its hosts. Manganese which is released into the soil solution may become (a) adsorbed, (b) fixed by plants or (c) incorporated into secondary soil minerals such as Mn-oxides, carbonates and clay minerals (Scheffer and Schachtschabel, 1989; Aubert and Pinta, 1977; Wedepohl, 1978). The average concentration of Mn in terrestrial vegetation is 400 ppm (Wedepohl, 1978). Trees extract Mn from the soil and concentrate it in leaves and needles, in which it plays a biochemical role. When leaves and needles fall, Mn accumulates in the humic topsoil. The concentration of Mn, therefore, commonly decreases from the top- to the subsoil (Vinogradov, 1959). Gorbanov (1994) investigated the distribution of Fe, Mn, Ti, Cu, Zn, Co, Ni and Cr in soils and found that Mn is the element which is most accumulated in organic-rich horizons.

**Factors which determine the lateral and vertical change of the Mn concentrations along the sampling lines:** Many soil profiles have slightly decreasing Mn concentrations from top- to the subsoil (Chapters 4 to 7), probably confirming the concentration of Mn in fallen plant material (see above).

High Mn concentrations in the subsoils of the soil sequences associated with USGO and schist of the Malmesbury Group are restricted to the lower-most slope position (bottom land) and coincided with detectable proportions of carbonate and higher conductivities of the water-suspended soil (sections 5.5. and 6.5.4). It was suggested that Mn coprecipitated with the carbonates when soil water evaporated from the soil. The lateral change of the Mn concentration in the topsoil of the soil sequence associated with the USGO was best explained by colluvial and alluvial input of Mn-containing mineral detritus (section 5.5).

It is interesting to note that the data gave no indication of the association of Mn with Fe-oxides.

**Changes from the underlying rocks to the soils (Table 9.1):** The Mn concentration increases from the underlying rocks to the soils. The differences between the Mn concentrations in the more and less weathered soil groups are relatively small. It is thus suggested that the loss of Mn during soil formation is similar to or smaller than the loss of major elements.

**Comparison with literature (Table 9.1):** The Mn concentration in the granite which forms the parent material of the Klipberg toposequence is much lower than Mn concentrations in granitic rocks reported by other authors.

The means of the Mn concentrations in the investigated soils are lower than the average concentrations in soils, as suggested by other authors. This could reflect the absence of parent materials with typically high Mn concentrations in the field area (e.g. basic and ultrabasic rocks).

## 9.16. COBALT

**In rocks and during weathering:** Mafic minerals are typical host minerals of Co in igneous rocks. The concentration of Co in biotites from granites investigated by Ruppert (1987) varied between 3 ppm and 77 ppm. Cobalt may be easily mobilised during weathering because many of its common salts are extremely soluble (e.g. cobalt chloride, sulfate and nitrate). Cobalt phosphates and carbonates are less soluble (Turekian, 1978). Sposito (1989) reports that the average concentration of Co in soils is lower than its average concentration in the crust (depletion factor 0.46), suggesting that Co is generally leached and depleted during soil formation. However, it is well known that Co may be accumulated in

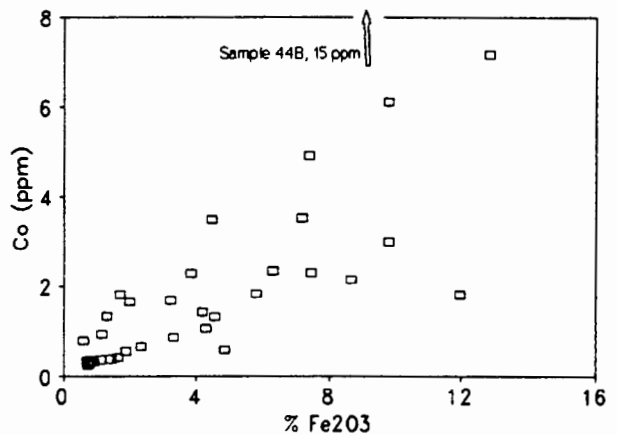


**Figure 9.10:** The correlation of Co and Fe<sub>2</sub>O<sub>3</sub> in the soil.

pedogenic Fe-oxides (Figure 9.10; Scheffer and Schachtschabel, 1989; Division of Soils, CSIRO 1983). The results of this study suggested that the accumulation of Co in pedogenic Fe-oxides resulted in increasing Co concentrations from the underlying rock to the soils (see below). Aubert and Pinta (1977) recorded high Co concentrations in soils with high proportions of organic matter and(or) clay minerals. The accumulation of Co in organic-rich soils was also observed by Vinogradov (1959). Alkaline soils can adsorb more Co than acid soils and often have higher Co concentrations (Scheffer and Schachtschabel, 1989).

**Essentiality and toxicity:** Cobalt is essential for animals and humans. It is, for example, a constituent of vitamin B<sub>12</sub>. Its function in higher plants is not yet established (Scheffer and Schachtschabel, 1989). Cobalt is carcinogenic and can cause damage to skin, heart and lungs (Merian, 1984).

#### 9.16.1. Total Co concentrations

**Highest concentrations:** The samples with the three highest Co concentrations originate from Pit 44 (7.2 ppm to 15 ppm). Highest acceptable concentrations for the assessment of Co polluted soils were not exceeded (25 ppm to 50 ppm; Eidgenössisches Department des Inneren, 1986; Ministerie Vrom, 1983).

**Factors which determine the lateral and vertical change of the Co concentrations along the sampling lines:** The reason for the relatively high Co concentrations in the samples from Pit 44 is probably the relatively high Co level in the underlying sandstone (Malmesbury Group). The Co concentration in the sandstone is 7.4 ppm while the other underlying rocks have much lower concentrations (Table 9.1). Soils associated with the sediments of the Malmesbury Group and the ferruginized materials have generally higher Co concentrations than the soils underlain by other rock-types (Table 9.1).

The Co concentration increases from the underlying rock to the soils (Table 9.1), probably indicating that most of the Co mobilised during weathering was fixed by Fe-oxides (Figure 9.10). The increase of the Co concentrations from the topsoils to the fine textured subsoils demonstrated the association of Co and clay minerals (e.g. Table 4.5). The lateral variation of the Co concentrations along the soil sequence associated with the USGO indicated that colluvial and alluvial input of detritus can also be an important factor in determining the concentration of Co in soils (Chapter 5).

**Comparison with literature (Table 9.1):** The rocks and soils investigated in this study have relatively low Co concentrations (Table 9.1). The low concentration in the pelites and the soils may reflect the absence of source (parent) rocks which have potentially high Co concentrations (e.g. basic and ultrabasic rocks).

#### 9.16.2. 1 M NH<sub>4</sub>NO<sub>3</sub> extractable concentrations of Co

The LLD for extractable Co in this study is 13 ppb. 57 % of the 89 soil samples analysed have concentrations below the LLD. The highest extractable Co concentration occurs in the top 15 cm of the toposequence associated with the phyllites of the Malmesbury Group (Pit 42; 82 ppb). Highest acceptable concentrations for the assessment of Co polluted soils were not exceeded (500 ppb; Table 9.2). The concentrations of extractable Co often decrease from the top- to the subsoil. This decrease normally coincides with decreasing proportions of organic matter. Different hypotheses to explain this observation are discussed below:

(a) The decomposition of organic material in the upper part of the soil profiles could be an important source of extractable Co. High concentrations of (total) Co in organic-rich soils were observed by other authors (see above). This is in contradiction to Scheffer and Schachtschabel (1989) who report that the range of Co concentrations normally encountered in plants is 0.02 ppm to 0.5 ppm and lower than the concentration encountered in most soils (Table 9.1).

(b) The affinity of dissolved Co ions for organic matter could be stronger than their affinity for other adsorbents (e.g. Fe-oxides and clay minerals). Kerndorff and Schnitzer (1980), however, demonstrated that the affinity of dissolved Co ions for humic acid is lower than the affinities of most other metals which were investigated. Hg, Fe, Pb, Al, Cr, Cu, Cd and Zn have higher affinities to humic acid than Mn and Co.

(c) Extractable Co may have been added to the topsoil in the form of fertilisers. This, however, is unlikely because Co is normally only applied to pastures (Scheffer and Schachtschabel, 1989) and such areas were not sampled.

(d) Ruppert (1987) observed the accumulation of Pb and Cd in organic-rich topsoils and argued that their accumulation was the result of aerial deposition. He stated further that the fraction of heavy metals which were introduced to the soil by means of aerial deposition should be "easily available". It could, therefore, be speculated that the accumulation of extractable Co in the topsoil reflects the aerial deposition of Co. The relatively low affinity of Co for humic acid (see above) and the absence of larger industries in the field area, however, contradict this hypothesis.

(e) Scheffer and Schachtschabel (1989) state that the complexation of Co by organic substances is an important factor in determining the solubility of Co in soils. At soil pH(CaCl<sub>2</sub>) values higher than six, 90 % of the Co dissolved in the soil solution is complexed by organic substances. The decreasing concentration of extractable Co with increasing soil depth could thus also reflect the complexation of Co by organic substances in the topsoil.

## 9.17. NICKEL, COPPER AND ZINC

**Essentiality and toxicity:** Particularly Zn and Cu, but also Ni, are essential to various life processes. Uptake of high quantities of Zn, Cu or Ni can be damaging to plants, animals and humans (Merian, 1984). Jackson *et al.* (1986) related higher frequencies of cancers of the stomach and the oesophagus to low concentrations of Zn and Mo in soils.

**Literature:** The distribution of the elements Ni, Cu and Zn in soil has been widely studied because they are important micro-nutrients for plants (Zn and Cu) and common pollutants (Zn, Cu and Ni). A summary of their role and distribution in soils is given, among others, in Blume (1992), Scheffer and Schachtschabel (1989) and

Division of Soils, CSIRO (1983). Current, normal levels and distribution patterns of Ni, Cu and Zn in Swiss, Dutch and German soils were, among others, determined by Hessischer Minister für Landwirtschaft und Forsten (1986), Driel and Smilde (1981) and Häni *et al.* (1981). Excessive concentrations due to pollution are normally restricted to the floodplain of polluted rivers and areas close to industrial developments. Soils associated with ultrabasic rocks (e.g. basalt) naturally have high Ni concentrations which often exceed acceptable maximum concentrations for the assessment of polluted soils (50 ppm to 100 ppm).

**Behaviour during soil formation:** A large proportion of the Ni, Cu and Zn present in igneous rocks is hosted by biotite and other mafic minerals (Ruppert, 1987; Wedepohl, 1969-1978). The weathering of these minerals during soil formation results in the release of Ni, Cu and Zn ions to the soil solution. Released ions are commonly adsorbed by or incorporated into organic matter and secondary soil minerals such as Fe-oxides and clay minerals. The adsorption of Ni, Cu and Zn is favoured by higher soil pH values (Scheffer and Schachtschabel, 1989). The presence of organic matter can facilitate and inhibit the transport of Cu(II) because complexes with organic matter may, depending on the type of organic matter, the concentration of Cu and the pH, be more soluble or more adsorbable than Cu(II) alone (Oden *et al.*, 1993).

#### 9.17.1. Total Ni, Cu and Zn concentrations

**Highest concentrations in the area of study:** The concentrations of Ni, Cu and Zn normally increase from the top- to the subsoil. This increase coincides with increasing proportions of clay minerals and Fe-oxides. The highest concentrations of Ni, Cu and Zn occur in the subsoils associated with the sediments of the Malmesbury Group (Table 9.1). Highest acceptable concentrations for the assessment of polluted soils were not exceeded.

**Comparison with literature:** A comparison with the values reported by other authors indicates that the investigated rocks and soils have relatively low Ni, Cu and Zn concentrations (Table 9.1). The relatively low concentrations in the pelites probably indicate the absence of source rocks which potentially have high Ni, Cu and Zn concentrations (ultrabasic and basaltic rocks). Low concentrations in the rocks were inherited by the associated soils.

**Covariance with other soil components:** The correlations of Ni, Cu and Zn with  $\text{Al}_2\text{O}_3$ ,  $\text{Fe}_2\text{O}_3$ , mud and organic matter are generally weak, reflecting that the concentrations of Ni, Cu and Zn are controlled by numerous factors. An exception is the conspicuous covariance of Ni and  $\text{Al}_2\text{O}_3$  in Pit 44 (Figure 9.11). The concentrations of Ni,  $\text{Al}_2\text{O}_3$  and  $\text{Fe}_2\text{O}_3$  increase from the underlying sandstone to the C-horizon and further to the B-horizon (samples 44R to 44B). The topsoil has low Ni and  $\text{Al}_2\text{O}_3$  concentrations but high  $\text{Fe}_2\text{O}_3$  concentrations (samples 44Top and 44A2). The increase of the concentrations from the sandstone to the B-horizon is accompanied by increasing

proportions of fine clay (particles  $< 0.5 \mu\text{m}$ ; Figure 6.4) and alteration of montmorillonite and feldspars to kaolinite (Chapter 3). The topsoil at Pit 44 has relatively low proportions of finer particles while the gravel fraction, mainly consisting of Fe-oxide concretions, is relatively enriched (Figure 6.4). The high proportion of gravel in the topsoil probably reflects eluviation of particles finer

than gravel and the formation of Fe-oxide concretions. It is concluded that the Ni in the soil at Pit 44 is mainly hosted by, and accumulated in, relatively fine mineral particles. These could be pedogenic clay minerals and Fe-oxides. The formation and accumulation of gravel-sized Fe-oxide concretions in the topsoil did not result in higher Ni concentrations.

**Coastal sand-derived soils:** The results from the coastal sand-derived soils showed that the concentration of Ni is particularly low in samples with high proportions of organic matter. The association of Fe and Ni in Fe-oxides was suggested. Higher proportions of organic matter increase the solubility of Fe and result in leaching and depletion of elements associated with Fe-oxides. Heavy minerals associated with the medium sized sand fraction probably account for the portion of Ni which is not associated with Fe-oxides (section 8.4.3.).

#### 9.17.2. 1 M $\text{NH}_4\text{NO}_3$ extractable concentrations of Ni, Cu and Zn

The concentrations of extractable Ni, Cu and Zn normally increase with increasing soil depth. Relatively high concentrations in the subsoils coincide with higher proportions of clay minerals and Fe-oxides. High concentrations sometimes coincide with high pH values (Ni and Zn) and high proportions of organic matter (Ni; Chapters 5, 6 and 7). Highest acceptable concentrations for the assessment of polluted soils were not exceeded (Table 9.2).

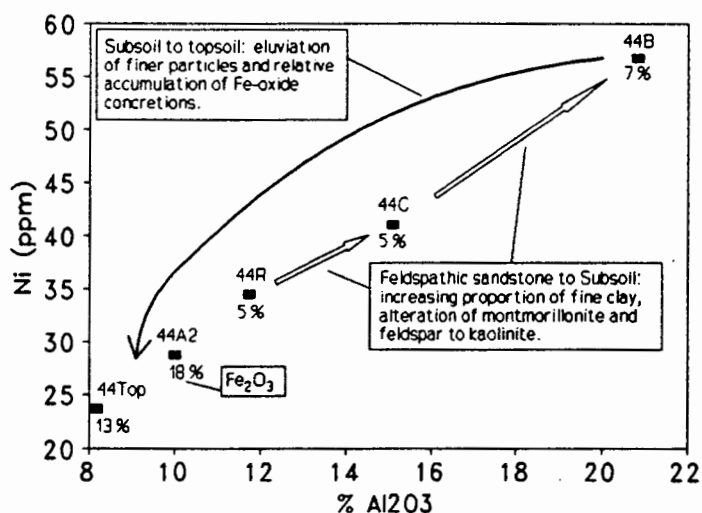


**Figure 9.11:** Covariance of Ni and  $\text{Al}_2\text{O}_3$  in Pit 44. The sample names and the concentrations of  $\text{Fe}_2\text{O}_3$  are given with the corresponding data points.

### 9.18. GALLIUM

A biological function of Ga is not known (Mertz, 1981). Only 19 soil samples were analysed for Ga. These included soils associated with granites, USGO, ferruginized materials and coastal sands. Six samples have concentrations below the LLD (0.8 ppm). The highest concentration determined is 26 ppm. The corresponding sample originates from a B-horizon associated with ferruginized materials (sample 8B). The determined range of concentrations (< 0.8 ppm to 26 ppm) is in agreement with the mean Ga content of soils (17 ppm), as reported by Sposito (1989).

Gallium concentrations at different soil depth were obtained from two soil profiles (Pits 8 and 12). The concentrations of Ga increase from the A- to the B-horizon (enrichment factors 2.3 and 2.6). This increase coincides with higher concentrations of  $Al_2O_3$  and  $Fe_2O_3$  as well as higher proportions of clay and Fe-oxides (field observations; Appendix-I). Association of Ga with clay minerals and Fe-oxides is, therefore, probable.

### 9.19. GERMANIUM

No biological function of Ge is known (Mertz, 1981). Seventy two of 100 analysed samples had concentrations below the LLD (0.9 ppm). The remaining samples have concentrations close to the LLD (maximum concentration = 1.6 ppm). This is in agreement with the mean Ge content of soils (1.2 ppm), as reported by Sposito (1989). Many of the soils which have concentrations above the LLD are associated with granites and ferruginized materials.

### 9.20. ARSENIC

**In Rocks:** The variability of As concentrations in common igneous rock-types is relatively low. Concentrations range often from < 1 ppm to 3 ppm. Most rock-forming minerals have low As concentrations. Higher concentrations of As may occur in magnetite and sulfides. Soils and sediments have higher As concentrations than igneous rocks (Table 9.1; Onishi, 1969a).

**Behaviour during weathering:** The weathering of minerals during soil formation is the source of oxidised and, therefore, soluble forms of As. Vinogradov (1959) reports that the oxidation of arsenic sulfides is an important source of water-soluble As. Coprecipitation of As with Fe-oxides as well as adsorption of As by Fe-oxides is reported by Onishi (1969a) and Vinogradov (1959). The specific adsorption of arsenate

by clay minerals and Fe-oxides is explained in Scheffer and Schachtschabel (1989). The affinity of As for Fe-oxides and clay minerals is the best explanation for the enrichment of As in soils and sediments compared to igneous rocks.

The connection between arsenic content and organic material has attracted the attention of many authors but could not be confirmed in an investigation of peat gleys and humus-alluvial soils from northern Russia (Vinogradov, 1959).

**Input of As from the atmosphere:** Introduction of As from the atmosphere is an important source for soil As. This process is the result of both the natural As content of the atmosphere (e.g. volcanic exhalations) and emission of As from industries (Lux, 1981; Vinogradov, 1959; Onishi and Sandell, 1955a). Blume (1992) reports the ratio of [total anthropogenic emission] over [total natural emission] to be 2786. Onishi (1969a) reports As concentrations in rain water ranging from 0.01 ppb to 13.9 ppb. The annual precipitation of As ranges between  $0.03 \mu\text{g m}^2$  (unpolluted atmosphere) and  $2000 \mu\text{g m}^2$  in major cities (Blume, 1992). Another possible source of As in soils is the application of insectofungicides (Merian, 1984; Vinogradov, 1959).

**Essentiality and toxicity:** It is reported by Mertz (1981) that As is essential to certain life processes. The occurrence of natural As deficiencies is not described. Higher concentrations of As are toxic to plants, animals and humans (Blume, 1992; Merian, 1984).

#### 9.20.1. Total As concentrations

**Granite-derived toposequence:** Mass balance calculations and the particularly strong increase of the As, Se, S and Br concentrations from the granite to the uppermost part of the toposequence (Pit 30) suggested that these elements were added to the soil (section 4.5.5.). The extra As may originate from (a) the atmosphere or (b) the leachates of the granite outcropping above the toposequence. The latter would confirm that the oxidation of sulfides in igneous rocks is an important source of water-soluble As (see above). It is important to note that there is no obvious source of atmospheric As in the region. Soil horizons which contain high proportions of Fe-oxides concretions or kaolinite are most enriched in As. The enrichment factors from the granite and the topsoil to the clay and Fe-oxide enriched subsoils are 42 and 188, respectively (Table 4.5).

**Toxic levels of As:** Soils with As concentrations higher than 50 ppm are considered to have toxic implications (Kelly, 1980). This concentration is greatly exceeded in samples from the subsoil of the granite-derived toposequence [Pit 31: 244 ppm As; Pit 32: 743 ppm As]. The critical concentration of 100 ppb  $\text{NH}_4\text{NO}_3$  extractable As in dried soil, as recommended by Prüeb *et al.* (1991), was not exceeded (Table 9.1). The best explanation for the immobility of As is the specific adsorption of arsenates by Fe-oxides and clay minerals, as explained in Scheffer and Schachtschabel (1989). The fixation of arsenates on the surface of growing Fe-oxides and clay minerals

may also have resulted in the incorporation of As into these substances. Alternatively, it could be argued that the extractable concentration is only low because the Fe-oxide gravel was excluded from the leaching experiments (section 2.5.1.1.).

**Other soil groups:** The results discussed in Chapters 5 to 7 confirmed the concentration of As in soil horizons with relatively high proportions of clay and Fe-oxides (see above).

#### **9.20.2. 1 M NH<sub>4</sub>NO<sub>3</sub> extractable concentrations of As**

Only 10 % of the 88 samples analysed have extractable As concentrations above the LLD (70 ppb). Soils with concentrations above the LLD belong exclusively to the soil groups associated with the sediments of the Malmesbury Group and the ferruginized materials. The determined concentrations range from the LLD to 109 ppb. The highest acceptable concentration of extractable As for the assessment of polluted soils is 100 ppb (Table 9.1). This concentration was only (slightly) exceeded in one soil sample (sample 45BA = 109 ppm As). The underlying sediments of the Malmesbury Group have also concentrations above the LLD (72 ppb to 133 ppb). The high concentration of extractable As in these sediments is the most plausible explanation for the relatively high concentration in some of the associated soils.

### **9.21. SELENIUM**

The concentration of Se in common rock and soil types is normally lower than 2 ppm (Table 9.1). The narrow range between toxic and sub-optimal Se concentrations in humans, however, resulted in a wide interest in Se. Davies (1980) provides a comprehensive review of the different aspects of Se in soils.

**Behaviour during weathering:** Selenium probably accompanies the accessory sulfide minerals in igneous rocks, reflecting its close relationship to S. Several analyses reported in Leutwein (1972) showed that the concentration of Se in common sulfides ranges normally between 5 ppm and 60 ppm. A very characteristic feature of selenium is that under oxidising conditions selenium-bearing sulfides and selenides are rapidly oxidised. The resulting selenite ions are very stable and can migrate until they are adsorbed on Fe-oxides (Leutwein, 1972; Vinogradov, 1959). The ability of soils to adsorb selenites increases with decreasing pH values (Scheffer and Schachtschabel, 1989). Aubert and Pinta (1977) report relatively high concentrations of Se in organic-rich and fine textured soils. Lakin (1972) describes the cycling and chemistry of Se in more detail.

**Input from the atmosphere:** Selenium precipitation from the atmosphere contributes significantly to the Se content of soils (Scheffer and Schachtschabel, 1989). Emission into the atmosphere results from volcanic exhalations, sea water and anthropogenic sources (Blume, 1992; Scheffer and Schachtschabel, 1989; Leutwein,

1972). Blume (1992) reports that the ratio of [total anthropogenic emission of Se] over [total natural emission of Se] is 3390.

**Essentiality and toxicity:** Selenium can increase the growth rate of plants and is essential to animals and humans. High concentrations of Se are toxic to plants, animals and humans. It was mentioned above, that the range between toxic and sub-optimal Se concentrations in humans is narrow. The Se intake of humans in Central Europe is regarded to be sub-optimal (Scheffer and Schachtschabel, 1989). Significant inverse correlations of dietary Se intakes, Se blood levels and Se concentrations in crops with human mortalities from cancers were, among others, shown by Jackson (1986), Salonen *et al.* (1984), Schrauzer *et al.* (1977) and Shamberger and Willis (1971).

**Analytical problems:** The LLD for the analyses of total Se was 0.7 ppm (XRFS). Only 42 of 100 analysed samples have concentrations above the LLD. The interpretation of the data is, therefore, restricted.

It is discussed in section 2.5.2.1. that the analysis of Se in the NH<sub>4</sub>NO<sub>3</sub> extracts is problematic. The LLDs obtained with ICP-MS were relatively high (877 ppb in air-dried soil). As a consequence most samples have concentrations below the LLD. The quality of the results for the few samples which have concentrations above the LLD is presumably poor (section 6.2.). It was, therefore, unfortunately not possible to quantify

the levels of available Se in Western Cape soils. Lower detection limits and better quality data could be obtained using the hydride generation method (section 2.5.2.1.).

**Granite-derived toposequence:** Sharply increasing concentrations of Se from the granite to the derived soil indicated that Se was added to the soil. Extra Se may originate from (a) the atmosphere or (b) the leachates of the granite outcropping above the toposequence. The latter would confirm that the oxidation of sulfides in igneous rocks is an important source of water-soluble Se (see above and section 4.5.5.).

**Highest concentrations:** The samples which have the highest Se concentrations (3 ppm to 9 ppm) contain high proportions of Fe-oxide gravel. Most of these samples originate from subsoils associated with the ferruginized materials and the sediments of the Malmesbury Group. In his guidelines for contaminated soils Kelly (1980) states that soils with Se concentrations higher than 3 ppm may be considered polluted. Most of the Se, however, is probably incorporated into the Fe-oxide concretions, and, therefore, immobile. Toxic implications are thus not likely.

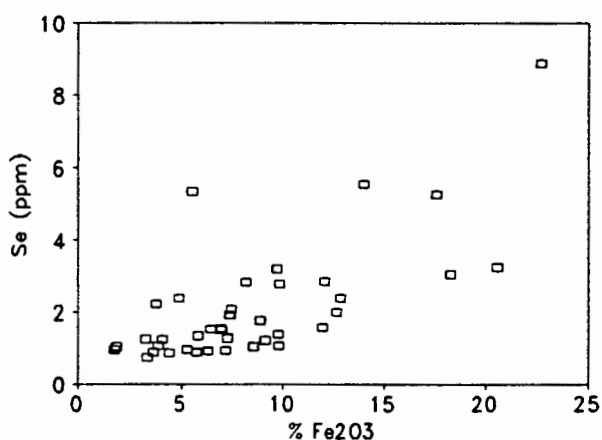


**Figure 9.12:** The (weak) correlation of Fe<sub>2</sub>O<sub>3</sub> and Se in the soils.

The above discussed association of Se with Fe-oxides was confirmed by the moderate covariance of Se and  $\text{Fe}_2\text{O}_3$  (Figure 9.12). The concentrations of Se often increase from the topsoils to the fine textured and Fe-oxide-rich subsoils.

## 9.22. BROMINE AND IODINE

**General:** The concentrations of Br and I in igneous rocks are generally below 2 ppm. Sediments and soils often have higher concentrations (Table 9.1). The principal source of Br and I in soils is the atmosphere. Both elements may be introduced to the soil directly by means of meteoric precipitation (Vinogradov, 1959). Absorption of aerial Br and I by plants is also known (Vinogradov, 1959). Wedepohl (1969-1978) reported terrestrial plants to contain between 1 ppm and 10 ppm I and vegetables to contain between 10 ppm and 25 ppm Br. Decaying plant material, therefore, also contributes to the Br and I content of soils. Once in the soil, Br and I can be adsorbed by the soil organic matter and clay minerals. Association of Br and I with organic matter in coal was shown by various authors reviewed by Swaine (1990).

The concentrations of Br and I in sea-water are 67 ppm and 0.06 ppm, respectively. Sea spray is a major source of atmospheric Br and I. The distance between the sea and a particular soil is thus an important control of its Br and I concentrations (Vinogradov, 1959). Other important controls are the proportion of organic matter and the texture of the soil, because soils with higher proportions of clay and organic matter can retain higher quantities of Br and I. Afyuni *et al.* (1994) surface applied KBr at different slope positions of three toposequences. They found that solute transport of  $\text{Br}^-$  is highly variable and dependant on profile characteristics, slope gradient, and hydrologic processes at different landscape positions.

**Detection limits:** Only two samples have Br concentrations below the LLD (0.9 ppm). The LLD for I (approximately 2.5 ppm) is more problematic because 37 of 100 samples have concentrations below the LLD.

**Highest concentrations:** The highest Br concentrations (20 ppm to 45 ppm) occur in the subsoils associated with the sediments of the Malmesbury Group and in organic-rich coastal sand-derived soils. High concentrations in the coastal sand-derived soils reflect the close proximity of the sampling sites to the sea and the retention ability of organic matter (section 8.4.4.). High proportions of mud (retention ability) and high Br concentrations in the underlying material (Table 9.1) are the best explanations for the concentration of Br in the subsoils associated with the sediments of the Malmesbury Group (Chapter 6).

The highest I concentrations (10 ppm to 210 ppm) occur in the subsoils associated with the sediments of the Malmesbury Group and the ferruginized materials. The two samples of the underlying sediments contain 7 and 23 ppm I. This is relatively

high, but cannot account for I concentrations as high as 210 ppm. Iodine contributions from the atmosphere and pedogenic redistributions are, therefore, likely to play an important role in the concentration of I in some soil horizons.

Figure 9.13 demonstrates that high proportions of mud (> 40 %) are a condition for higher levels of Br and I in the investigated soils. The only exceptions are high Br concentrations in samples which contain high proportions of Fe-oxides or organic matter, reflecting that these substances can also accumulate Br. The strong affinity of Br for Fe-oxides is also shown in Table 4.5 (enrichment factor 15).

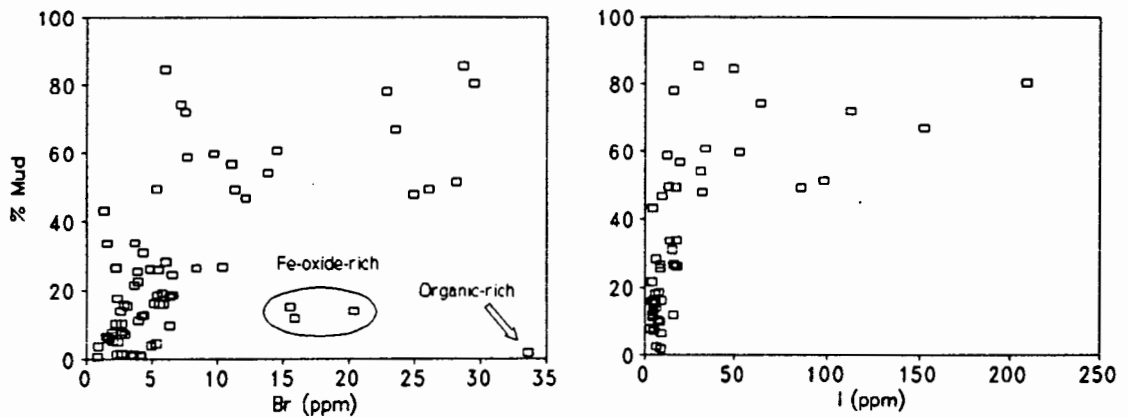


**Figure 9.13:** The plots of bromine and iodine versus mud show that higher proportions of mud (> 40 %) are a condition for higher levels of Br and I in the investigated soils.

**Factors which determine the lateral and vertical change of the concentrations along the sampling lines:** It can be generalised that soil horizons with higher retention abilities have higher Br and I concentrations. Changes in the proportions of organic matter and mud are thus most important in determining lateral and vertical changes of the concentrations within individual soil sequences. The concentrations generally increase, along with the proportion of mud, from the top- to the subsoil. It was further suggested that time is an important factor for the accumulation of Br and I because their concentrations probably increase with the length of the time period available for soil formation (Chapters 5 and 6).

**Comparison with literature (Table 9.1):** The investigated soils have relatively high Br concentrations, probably reflecting the close proximity of the sampling lines to the sea. It is not conclusive from the data that the I concentrations of the investigated soils are higher than the levels reported by other authors, because many of the concentrations in the investigated soils and the I levels reported elsewhere are close to or below the LLD achieved in this study. Samples which have I concentrations above the LLD, however, indicate that some soils and rocks have relatively high I levels.

### 9.23. MOLYBDENUM

Ninety four of 96 soil samples have Mo concentrations between 0.7 ppm and 3.2 ppm. The two samples which have higher concentrations originate from the subsoil of the granite-derived toposequence (samples 31B and 32G). Sample 31B contains abundant Fe-oxide-concretions and has a Mo concentration of 10 ppm. Sample 32G contains a high proportion of kaolinite and 6.3 ppm Mo. The accumulation of Mo in these samples demonstrates the affinity of Mo for clay minerals and Fe-oxides (Table 4.5). The leachate from the granite above the toposequence is probably the most important source for the accumulation of Mo in the subsoil (Figure 5.7). The only soluble form of Mo under aerobic conditions is  $\text{MoO}_4^{2-}$ . The sorption of  $\text{MoO}_4^{2-}$ , mainly by Fe-oxides and less by clay, is also reported in Scheffer and Schachtschabel (1989).

Association of Mo and Fe-oxides was also suggested in Chapters 6 to 8 because slightly higher concentrations of Mo coincide with higher concentrations of  $\text{Fe}_2\text{O}_3$  or higher proportions of Fe-oxide concretions. The results obtained from the coastal sand-derived soils indicated that high proportions of organic matter and the accompanying increase in the solubility of Fe caused leaching and depletion of Fe-oxides. The loss of Fe-oxides resulted also in lower concentrations of associated trace elements (Ni, Mo and W). The results for the coastal sand-derived soils suggested further that Mo may be hosted by heavy minerals associated with the medium-sized sand fraction.

The Mo concentrations increase slightly from the underlying rocks to the soils (Table 9.1). It is thus suggested that the loss of Mo during soil formation is relatively small compared to the loss of major elements.

The encountered range of the Mo levels as well as the low degree of the variability of the concentrations is in agreement with the findings of other authors (Table 9.1; Scheffer and Schachtschabel, 1989; Vinogradov, 1959).

### 9.24. CADMIUM

Only the concentration of 1 M  $\text{NH}_4\text{NO}_3$  extractable Cd was determined. Eighty five percent of the 88 samples analysed have extractable Cd concentrations below the LLD (17 ppb). The concentrations above the LLD vary between the LLD and 43 ppb. Most of the concentrations above the LLD exceed the highest acceptable concentration for the assessment of Cd polluted soils (20 ppb; Table 9.2). The samples with high extractable Cd concentrations are used for crop production and originate almost exclusively from the soils associated with the phyllite and sandstone of the Malmesbury Group (Pits 40, 41, 42 and 44) and the ferruginized materials (Pit 45). The extractable concentrations in the underlying phyllite and sandstone are lower than the concentrations in the soil. All samples from comparable uncultivated soils (associated

with the schists of the Malmesbury Group) have extractable Cd concentrations below the LLD.

**Fertilisers as a possible source of Cd:** The increase of the extractable Cd concentrations from the uncultivated to the cultivated soils and the relatively low concentration in the underlying rock give reason to speculate about the accumulation of extractable Cd due to the application of fertilisers. Phosphates applied to the soil often contain between 7 and 170 ppm Cd (Kabata-Pendias and Pendias, 1985). Naidu *et al.* (1994) observed that the presence of  $\text{PO}_4^{3-}$  enhances the sorption of Cd by the soil. A calculation based on fertilisers used in Germany showed that the application of phosphates may increase the Cd content of the soil by 0.4 ppb per year (Jung *et al.*, 1979). Possible accumulation of Cd in Western Cape soils due to the application of phosphates should be the subject of further research. It is important to bear in mind that all Cd concentrations determined in this study need confirmation because they are close to the obtained LLD.

## 9.25. TIN

**Essentiality and toxicity:** The toxicity of elemental Sn is, quite different to many other heavy metals (e.g. Pb and Hg), very low. Tin compounds have different degrees of toxicity. Organo-tin compounds are more toxic than inorganic salts of Sn. The most toxic organo-tin compounds are constituents of pesticides (Merian, 1984). Mertz (1981) reports that too low intake of Sn can result in deficiency and cause growth depression in animals.

**Primary hosts:** Analyses reported in Hamaguchi and Kuroda (1969) showed that 60 to 70 % and more of the Sn in granitic rocks may be hosted by hornblende, biotite and sphene. Cassiterite ( $\text{SnO}_2$ ), the most abundant Sn mineral, typically forms part of post-magmatic and hydrothermal mineral associations and is known to be very resistant to weathering (Rösler, 1981). Accumulation of cassiterite in sediments and residual soils is thus possible.

**Behaviour of Sn in the granite-derived toposequence during soil formation:** The ratio of [average tin content of natural waters] over [average tin content in standard rocks] indicates that the migration capacity of tin is low and comparable to those of Ba, Ti and Zr (Hamaguchi and Kuroda, 1969). This is in agreement with the results from the granite-derived toposequence which showed that Sn was neither lost from nor added to the soil during the early stages of soil formation (section 4.5.1.). It was, therefore, suggested that the primary host of Sn in the granite-derived toposequence is resistant to weathering and does not allow for leaching of Sn. Granite-derived soil horizons which contain relatively high proportions of substances which typically adsorb and accumulate free metal ions are not enriched in Sn, substantiating that most of the Sn

is locked up in its primary host (Table 4.5). The slight enrichment of Sn in the fine textured subsoil of the granite-derived toposequence is probably the result of eluviation of relatively fine grained, Sn-hosting mineral particles from the topsoil into the subsoil (section 4.5.2.).

**Other soil groups:** The above discussed increase of the Sn concentrations from the topsoil to the subsoil was also noted in soil profiles associated with the USGO, ferruginized materials and sediments of the Malmesbury Group. The magnitude of the increase is more pronounced in soil profiles which were suggested to be more mature (section 5.6.). It was, therefore, proposed that time is an important factor for the accumulation of Sn in the subsoil. The Sn concentrations in the soil associated with the USGO increase towards the Darling granite outcrops. It was, therefore, suggested that the colluvial input of granitic detritus is an important source of Sn for these soils (sections 5.5.2. and 5.5.5.). Association of Sn with organic matter, as proposed by Aubert and Pinta (1977) and Vinogradov (1959), was not observed in this study.

**Moderate covariance of Sn and  $Al_2O_3$ :** Moderate covariance of Sn and  $Al_2O_3$  is demonstrated in Figure 9.14. The cause for the covariance is probably different for top- and subsoil.

**Topsoil:** Along the sampling lines higher  $Al_2O_3$  concentrations in the topsoil reflected relatively high proportions of primary, rock-derived aluminosilicates (e.g. feldspars). It was shown in the previous chapters that their concentration in the topsoil is often due to colluvial(aeolian) input of granitic detritus. Particle size effects may also play a role in their accumulation (sections 7.5.2. and 8.5.3.). The best explanation for the correlation of  $Al_2O_3$  and Sn in the topsoil is that granitic detritus is also important in introducing Sn to the soil.

**Subsoil:** High concentrations  $Al_2O_3$  in the subsoil normally indicate high proportions of clay minerals. High proportions of clay minerals are the result of advanced soil formation; i.e. amongst other processes pedogenic formation, illuviation and accumulation of clay minerals. The increased concentration of Sn in such soil horizons could be due to both the direct association of Sn and clay minerals or the illuviation of weathering-resistant and Sn-hosting minerals into the subsoil.

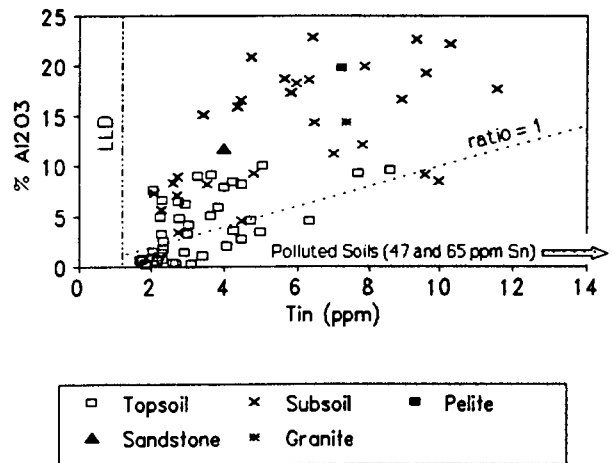


**Figure 9.14:** Tin versus  $Al_2O_3$  for rock and soil samples. Lines were drawn to indicate the LLD and the ratio 1.

**Highest concentrations:** The two soil samples with the highest Sn levels originate from the footslope of the granite-derived toposequence (Pit 33; Figure 4.1). The Sn concentration of the two samples, 33AE and 33Top, are 65 ppm and 47 ppm, respectively. The application of pesticides is a possible reason for high Sn concentrations in soils (see above). The owner of the land stated that the area had not been treated with agro-chemicals for at least 50 years. The results of this study, however, indicate that the cause for the high Sn levels are connected to the cultivation of the soil:

(a) The surrounding of Pit 33 was being used as a pasture when the field sampling was performed.

(b) The low gradient at the footslope (Pit 33) makes this part of the toposequence more accessible for cultivation.

(c) The Sn concentrations at Pit 33 are much higher than the concentrations in the rest of the toposequence and the granite (4 to 24 ppm).

(d) Elements which were shown to behave similarly to Sn in the upper part of the toposequence have relatively low concentrations in the soil at Pit 33 (Group-I elements in section 4.5.2.).

(e) The  $\text{Al}_2\text{O}_3/\text{Sn}$  ratios of the potentially polluted soil horizons are approximately 0.03 while unpolluted soils have ratios close to or greater than 1 (Figure 9.14).

The highest acceptable Sn concentration for the assessment of polluted soils is 50 ppm (Kloke, 1980). Further research is required to investigate the cause and consequences of the high Sn concentrations at Pit 33.

**Comparison with literature:** A comparison of the determined concentrations with the levels reported by other authors indicated that the concentrations in the underlying rocks and the different soil groups are within the normal range (Table 9.1).

## 9.26. ANTIMONY

**Comparison with literature:** An early review of the abundance of Sb in chondrites, igneous rocks and sediments is given by Onishi and Sandell (1955b). In this publication an average Sb concentration of 0.24 ppm for granites and 1.2 ppm for shales is suggested. The ranges of the Sb concentrations in granites and shales listed in Table 9.1 are taken from Onishi (1969b). From the table it can be seen that the Sb concentrations of the rocks which underlie some of the investigated soils have concentrations in the normal range.

Information on the concentration of Sb in soils is scarce. Estimated means for soil range from 0.66 ppm (Sposito, 1989) to 6 ppm (Davies, 1980). Assessing the results reported in Driel and Smilde (1981) and Onishi (1969b) it seems that Sb concentrations

between 0.2 ppm and 3 ppm are common in soils. This estimate is substantiated by the results of this study. Of the 44 samples analysed for Sb, 16 % have levels below the LLD (0.3 ppm), 66 % have concentrations between the 0.3 ppm and 3 ppm and 18 % have concentrations between 3 ppm and 13 ppm.

**Highest concentrations:** The highest acceptable Sb concentration for the assessment of polluted soils, as recommended by Kloke (1980), is 5 ppm. This concentration is slightly exceeded in 7 soil samples (5 ppm to 13 ppm). The corresponding samples originate from both top- and subsoils as well as from various locations and underlying rocks, giving no indication of soil pollution being the reason for the high concentrations.

**Concentration during soil formation:** There seems to be a general increase of the Sb concentrations from the underlying rock to the soil (Table 9.1). This trend is particularly conspicuous in the soil associated with the sandstone of the Malmesbury Group (Pit 44; not shown in Table 9.1). The concentrations at this pit increase from 3.4 ppm in the rock to 7 ppm in the B-horizon and further to 13 ppm in the top 15 cm of the soil profile. The increasing concentration towards the top of this cultivated soil profile could indicate Sb pollution by means of agro-chemicals. The reviewed literature gave no indication of Sb being a constituent of agro-chemicals. In conclusion it is suggested that the loss of Sb during soil formation is relatively small compared to the loss of major elements. Antimony is thus relatively enriched during soil formation.

**Affinity of Sb for Fe-oxides and organic matter:** The highest concentration of Sb in the topsoils associated with the schist of the Malmesbury Group coincides with high  $\text{Fe}_2\text{O}_3$  concentrations (section 6.5.3.). The association of Sb and Fe-oxides, which is also mentioned in Onishi (1969b), was thus suggested. Driel and Smilde (1981) observed that Dutch fen-peat soils generally have higher Sb concentrations than loess, mossy-peaty-sand, sandy and clay soils ( $n = 381$ ). The mean calculated for the fen-peat soils was 1.6 ppm while the other soil groups had means ranging between 0.4 and 0.8 ppm. The relatively high concentration in the organic-rich fen-peat soils probably indicates that Sb has a certain affinity for organic matter.

## 9.27. BARIUM

**In rocks and soils:** Potassium feldspars are the most important Ba hosts in igneous rocks. The concentration of Ba in granites is very variable. An overall mean of 732 ppm is reported in Puchelt (1972). The means of the Ba concentrations for shales range from 250 to 800 ppm. The overall mean of the Ba concentrations in soils is estimated to be 580 ppm (Sposito, 1989).

**During weathering:** Leaching experiments with water showed that Ba is easily released from K feldspar and granite powder. The residence of Ba in the weathering

solution is mainly restricted by the low solubility of  $\text{BaSO}_4$  and the adsorption of Ba by clays, Fe-oxides and organic substances. Both increases and decreases of the Ba concentrations with increasing degrees of weathering have been observed (Puchelt, 1972).

In this study only the concentration 1 M  $\text{NH}_4\text{NO}_3$  extractable Ba was determined. The determined concentrations of extractable Ba range between 0.2 and 33 ppm ( $n = 86$ ). The vertical and horizontal changes of the extractable Ba concentrations in the soil are controlled by the factors discussed below.

**Role of feldspars:** It was shown in Chapter 3 and section 4.4. that the proportion of feldspars decreases down the topsoil of the granite-derived toposequence. This was attributed to the increasing degree of weathering and leaching down this toposequence (Chapter 3; Figure 4.8: text box 2).

The decreasing concentration of  $\text{K}_2\text{O}$  down the granite-derived topsoil (section 4.5.4.) is presumably a good relative measure for the loss of feldspars with progressing weathering. Figure 9.15 shows the corresponding samples in a plot of extractable Ba versus  $\text{K}_2\text{O}$ . It can be seen from the figure that the concentrations of  $\text{K}_2\text{O}$  and extractable Ba generally decrease from the granite to the footslope.

The correlation of extractable Ba and  $\text{K}_2\text{O}$  improves if the soil samples from the top 15 cm of the profiles and the composite samples of the topsoil are assessed separately. The samples from the top 15 cm of the soil profiles have lower  $[\text{K}_2\text{O}]$  over  $[\text{Extractable Ba}]$  values than the composite samples, probably reflecting that the relatively high proportion of organic matter in the samples from the top 15 cm retains extractable Ba. In conclusion it is suggested that the proportion of feldspars, if present, and organic matter are important in determining the concentration of extractable Ba. This is in support of the laboratory experiments reported in Puchelt (1972; see above).

**Retention ability of the soil:** The retention ability of the soil for Ba is determined by the proportions of clay, Fe-oxides and organic matter (see above). Higher proportions of these substances may thus result in higher concentrations of extractable Ba (Table 4.5). In addition it is the pH of the soil which affects the retention ability. Alkaline soils can retain more Ba than acidic soils (Scheffer and Schachtschabel, 1989; section 7.5.6.). The affinity of  $\text{Ba}^{2+}$  ions for clay minerals and

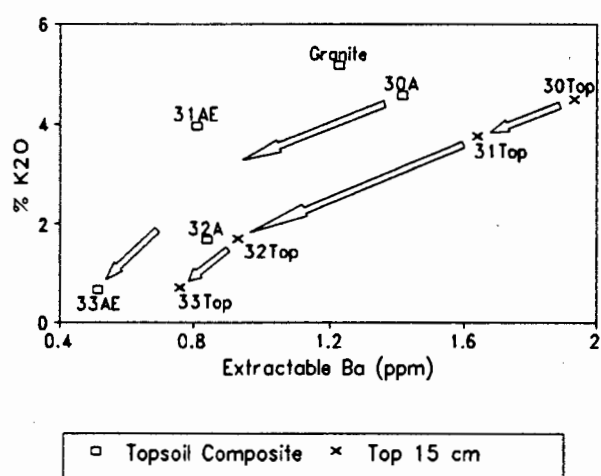


**Figure 9.15:** The loss of  $\text{K}_2\text{O}$  and  $\text{NH}_4\text{NO}_3$  extractable Ba down the granite-derived toposequence. The arrows indicate increasing degree of weathering and distance from the granite.

Fe-oxides often causes an increase of the concentrations from the top- to the subsoils (e.g. sections 5.6 and 7.6.). In other examples the retention ability also determines the lateral change of the extractable Ba concentrations (sections 5.5.5. and 8.4.4.). It is interesting to note that the retention ability of the soils associated with the granite and the sediments of the Malmesbury Group is strong enough to cause a general increase of the extractable Ba concentrations from the underlying rocks to the soils (Table 9.1).

Figure 9.16 shows that samples with high extractable Ba concentrations always have a minimum concentration of  $\text{Al}_2\text{O}_3$  and(or)  $\text{Fe}_2\text{O}_3$  ( $\pm > 5\%$ ). On the assumption that high  $[\text{Al}_2\text{O}_3 + \text{Fe}_2\text{O}_3]$  values reflect relatively high proportions of Fe-oxides, clay minerals or feldspars this diagram summarises the importance of these substances for the accumulation of extractable Ba in the soil (see above).

## 9.28. TUNGSTEN

**Association with medium and fine sand:** Fine textured sediments normally have higher trace metal concentrations than sandstones. The average concentrations of W in shale and sandstone are 1.8 and 1.6 ppm, respectively (Turekian and Wedepohl, 1961). This similarity is unusual and was explained with the assumption that W in sandstones is concentrated in heavy minerals or clay cement (Krauskopf, 1970). The tendency of W to have relatively high concentrations in sandy materials is substantiated by the results of this study:

(a) In the study area, W is one of the few elements which has relatively high concentrations in the sandy soils on transported underlying materials (Table 9.1; soils associated with the USGO and coastal sand).

(b) The lateral change of the W levels along the sampling lines often covaries with the proportion of medium and fine sand (sections 5.5.7., 7.5.2., 7.5.5. and 8.4.3.).

It is deduced that processes which resulted in the relative accumulation of medium and fine sand also resulted in enrichment of W-hosting minerals. Such processes are, among others, leaching of soluble constituents during weathering as well as separation of particles during eluviation and colluvial, aeolian and fluvial transport. In conclusion it is suggested that considerable proportions of W are hosted by (medium

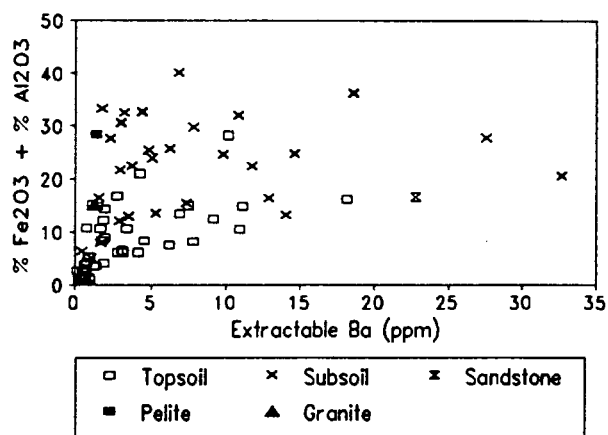


**Figure 9.16:**  $[\text{Al}_2\text{O}_3 + \text{Fe}_2\text{O}_3]$  versus  $\text{NH}_4\text{NO}_3$  extractable Ba for rock and soil samples.

and fine) sand-sized and weathering resistant mineral particles, likely to be scheelite or wolframite.

**Concentration from rock-leachates:** The lateral change of the W concentration down the granite-derived toposequence indicated that the concentration of W from rock-leachates may be the reason for unusually high levels of W at the top of the toposequence (426 ppm; section 4.5.3.). More detailed research should be undertaken in order to confirm the dissolved transport of W in the granite-derived toposequence.

**Depletion in organic-rich samples:** In the coastal sand-derived soils particularly low levels of Fe<sub>2</sub>O<sub>3</sub> and W coincided with high proportions of organic matter. The association of Fe and W in Fe-oxides was suggested. Higher proportions of organic matter increase the solubility of Fe and resulted probably in leaching and depletion of elements associated with Fe-oxides (section 8.4.3.).

**Adsorption:** The results presented in Table 4.5 indicate that the association of W with clay, Fe-oxides and organic matter may result in relative enrichment of W (enrichment factors 1 to 2.5).

**Comparison with literature:** An overall mean for the concentrations of W in soils is not given in the references listed in section 9.1. The normal range of concentrations given in Table 9.1 (4 to 10 ppm) is based on several soil analyses reported by Krauskopf (1970). The means of the W concentrations for the soil groups investigated in this study range from 9.2 ppm to 44 ppm, possibly indicating that the level of W in Western Cape soils is relatively high. This is in agreement with the high W concentrations in the underlying rocks (Table 9.1) and Robson (1980) and Scott (1969) who reported high W concentrations and wolframite mineralisation in Western Cape granites.

## 9.29. THALLIUM

**General:** In this study only the concentration of 1 M NH<sub>4</sub>NO<sub>3</sub> extractable Tl was analysed for. Only 36 % of the 88 analysed samples have concentrations above the LLD (2.7 ppb). The determined concentrations range between 2.8 and 24 ppb. The highest acceptable Tl concentration for the assessment of polluted soils (30 ppb) is not exceeded (Table 9.2). The soil samples with the highest extractable Tl concentrations (> 7 ppb) originate exclusively from fine textured subsoils, probably reflecting the affinity of dissolved Tl for clay minerals observed elsewhere (De Albuquerque and Shaw, 1972). The enrichment factor of extractable Tl from the topsoil to the fine textured subsoil horizons may be as high as 7.8 (Table 4.5).

**Loss during soil formation:** Biotite and K-feldspars are important hosts of Tl in granitic rocks (De Albuquerque and Shaw, 1972). The (powdered) granite which formed the parent material of the toposequence down Klipberg has the highest

extractable Tl concentration overall (24 ppb). All derived soils, except for the fine texture subsoils, have Tl levels below the LLD. This may reflect that Tl is readily released from biotite and feldspar and rapidly leached during soil formation. This hypothesis is in contradiction to the enrichment of Tl from fresh rocks to their weathering products, as reported in (De Albuquerque and Shaw, 1972). The analyses of the total Tl concentrations would be essential in order to draw a definite conclusion.

### 9.30. LEAD

**Enrichment during soil formation:** In igneous rocks lead occurs mainly in the structure of K-feldspars and mica (Wedepohl, 1974). The loss of Pb during weathering may be as high as 40 % (Figure 4.6; Wedepohl, 1974). The fact that the mean of the Pb concentrations in the investigated soils is slightly higher than the Pb concentrations in the underlying rocks reflects that the loss of Pb was relatively small compared to the loss of major elements (Table 9.1). The relatively small loss is presumably due to the particularly strong specific adsorption of Pb by clay and Fe-oxides (Scheffer and Schachtschabel, 1989).

**Lateral and vertical changes of the concentrations along the sampling lines:** The results presented in Table 4.5 and sections 5.5.3., 5.6., 7.5.1., 7.6. indicated that the retention ability of the soil for Pb, as determined mainly by the proportions of Fe-oxides and clay, is of major importance in controlling lateral and vertical changes of the Pb concentration. The concentration of Pb often increases from the top- to the subsoil because the subsoils frequently have higher proportions of Fe-oxides and clay minerals than the topsoils. The soils associated with the coastal sands, granites and USGO have increasing Pb concentrations towards the granite batholiths (sections 4.5.4., 5.5.5. and 7.5.1.). It was, therefore, suggested that the input of granite-derived minerals (e.g. feldspars) is an important source of Pb and can control the lateral change of its concentration.

Figure 9.17 shows the covariance of  $[Al_2O_3 + Fe_2O_3]$  and Pb in the investigated soil samples. On the assumption that high  $[Al_2O_3 + Fe_2O_3]$  values reflect relatively high proportions of Fe-oxides, clay minerals and(or) feldspars this diagram supports the importance of these substances for the concentration of Pb in the soil.

**Acceptable maximum concentrations:** The acceptable maximum concentrations for the assessment of Pb polluted soils range, dependant on the author, between 100 and 500 ppm (Bundesverband Deutscher Geologen, 1990). The highest lead level determined in this study is 43 ppm.

**1 M  $NH_4NO_3$  extractable concentration of Pb:** Only 28 % of the 88 analysed samples have extractable Pb concentrations above the LLD (54 ppb). The determined concentrations range between the LLD and 400 ppb. The acceptable maximum

concentration for the assessment of soils polluted with Pb (2000 ppb; Table 9.2) was not exceeded. Relatively high concentrations of extractable Pb are not restricted to soils associated with certain underlying rocks and may occur in the top- and subsoil. Covariation of extractable Pb with the pH values or the proportions of organic matter and clay minerals was generally not evident. Only the results obtained from the subsoil associated with the USGO (section 5.5.6.) indicated the association of extractable Pb with organic matter.

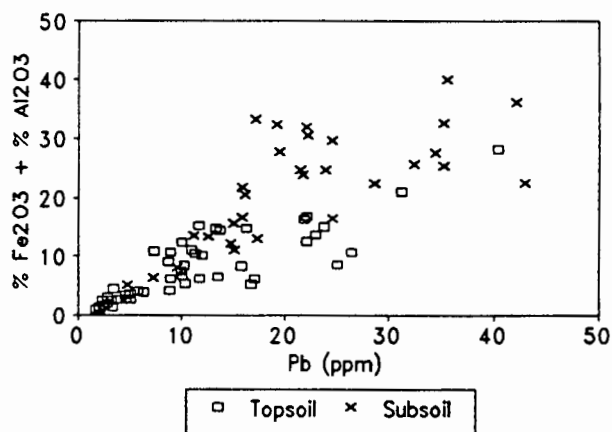


Figure 9.17: Correlation of  $[\text{Fe}_2\text{O}_3 + \text{Al}_2\text{O}_3]$  and Pb in the investigated soils.

### 9.31. THORIUM AND URANIUM

**In rocks and during weathering:** Thorium and U are both concentrated in biotite, hornblende and zircon of igneous rocks. During weathering they commonly become fractionated owing to oxidation of U to the soluble uranyl ion ( $\text{UO}_2^{2+}$ ). Carbonate ions strongly complex uranyl ions and may, therefore, increase the solubility of U (Rogers and Adams, 1969). The low solubility of most U-phosphates can limit the mobility of U (Vinogradov, 1959). Uranium becomes concentrated in organic-rich sediments. The concentration of U in coals is well known. Swaine (1990) suggested that U is predominantly organically bound in coals. In contrast to U the relatively immobile Th becomes concentrated in residual materials. Braun and Pagel (1994) suggested the immobilisation of Th in soils as thorianite ( $\text{ThO}_2$ ).

**Enrichment of Th and U in the granite-derived subsoil:** It was shown that 43 % of the U and 54 % of the Th was leached during the early stages of weathering; i.e. from the outcropping granite to the uppermost part of the toposequence (section 4.5.1.; Figure 4.6). The loss of U and Th is similar to the loss of  $\text{SiO}_2$  (55 %). It was thus suggested that the hosts of U and Th in the granite are relatively insoluble. A portion of the Th and U leached from the soil and rock at the top of the soil sequence was retained by the fine textured subsoil in the lower slope positions. This resulted in the highest Th and U concentrations overall (Th = 165 ppm and U = 13 ppm; sample 32G in Figure 9.18). The Th/U ratio increases from 6 in the granite to 13 in the U and Th enriched subsoil. The stronger enrichment of Th probably indicates that the affinity of dissolved Th for clay minerals is particularly strong while U passes more easily through the kaolinite-rich subsoil. The strong affinity of Th for kaolinite is also reflected by the

sharp increase of the Th concentration from the coarse textured topsoils to the kaolinitic subsoils (enrichment factor 4.6 to 16; Table 4.5).

It is important to note that the illuviation of fine grained and weathering resistant mineral detritus into the subsoil may contribute to the enrichment of U and Th at the bottom of the toposequence (section 4.5.4.). Even though the significance of this process cannot be quantified, it is suggested that its

contribution does not account completely for the enrichment in the subsoil because it was shown that major proportions of Th and U were leached during the weathering of the granite and were, therefore, available in a dissolved form.

It is further important to bear in mind that accumulation of Th and U to high concentrations is restricted to the footslope of the toposequence. The concentrations at Pit 33, which is more distant from the granite, are not above background. It is concluded that the supply of Th and U from the weathering granite above the toposequence is essential for the accumulation of Th and U to unusually high concentrations.

**Lateral and vertical changes of the concentrations along the sampling lines:** Similar to many of the previously discussed elements (e.g. Pb; section 9.29.), the observed variation of the Th and U concentrations is best explained by (a) the accumulation of these elements in clay- and(or) Fe-oxide-rich soil horizons and (b) the input of Th and U in the form of granite-derived detritus (Table 4.5; sections 4.5.4., 5.5.1., 5.5.5., 5.6., 6.5.6., 7.5.1. and 7.6.). Uranium and  $Al_2O_3$  are correlated in the topsoil while the covariance in the subsoil is ambiguous (Figure 9.19). It was shown that the concentration of  $Al_2O_3$  in the topsoils normally increases towards the granite outcrops (sections 4.5.4., 5.5.1. and 8.4.1.). This was attributed to the input of aluminosilicates from the granites. The correlation of U and  $Al_2O_3$  in the topsoil, therefore, substantiates the observations that the input of granitic detritus is an important source of U. Higher concentrations of  $Al_2O_3$  in the subsoil reflect higher proportions of clay minerals. The lesser degree of covariance of U and  $Al_2O_3$  in the subsoil substantiates the suggestion that the proportion of clay minerals is not the only factor that controls the U concentration. The covariance of Th and  $Al_2O_3$  (not shown) is similar to the covariance of U and  $Al_2O_3$  and, therefore, substantiates the importance of the above mentioned processes in controlling the concentration of Th.

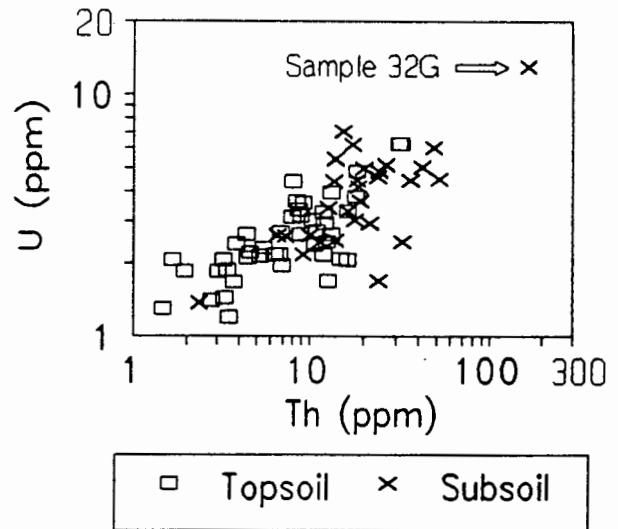


**Figure 9.18:** Thorium versus U for all soil samples. Note the logarithmic scales.

**Covariance of Th and U:** It is known that the different solubilities of Th and U normally result in the fractionation of these elements during weathering (see above). Figure 9.18 shows that the concentrations of U and Th covary in the investigated soils. The covariance is particularly strong for the topsoils. It is concluded that the different solubilities of Th and U do not result in complete fractionation of these elements during soil formation. The

covariation may be attributed to the observation that both elements are accumulated in fine textured subsoils and depend on the input of granitic detritus (see above).

**Different behaviour during ferruginization:** The mean of the Th concentrations increases from the soils associated with the sediments of the Malmesbury Group to those associated with the ferruginized materials while the mean of the U concentrations decreases slightly (Table 9.1). The relatively high concentration of Th in the soils associated with the ferruginized materials may be the result of higher Th concentrations in the underlying, fresh rock (not determined). Alternatively it could be speculated that the strong weathering of the ferruginized materials resulted in accumulation of the rather immobile Th and in depletion of the more mobile U.

**Comparison with literature:** Information on the levels of U and Th in soils is relatively scarce. The normal range of the Th and U concentrations in soils, as given in Table 9.1, was taken from Swaine (1990) and was first published in Swaine (1955). The Th and U concentrations in the investigated soils and rocks are comparable with the levels reported by Swaine (Table 9.1). It is, however, important to bear in mind that natural accumulation during soil formation resulted in unusually high concentrations of U and Th in the field area. This is especially interesting for U because this element is typically depleted during weathering (see above).

**1 M  $\text{NH}_4\text{NO}_3$  extractable fractions:** The concentrations of extractable Th were not determined. Only 3 of the 88 samples analysed for extractable U have concentrations above the LLD (30 ppb). The corresponding samples originate from subsoils associated with different rock-types and have extractable U concentrations ranging from 57 to 68 ppb. The acceptable U concentration for the assessment of polluted soils is 40 ppb. A harmful affect on any of the soil functions listed in Table 9.2 is unlikely because the recommended maximum concentration is not greatly exceeded.

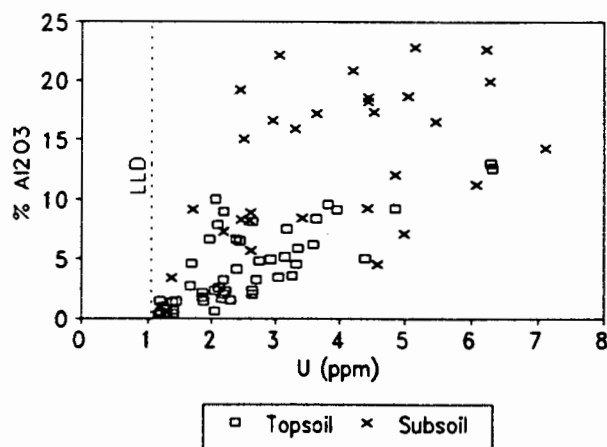


**Figure 9.19:** The correlation of U and  $\text{Al}_2\text{O}_3$  in the investigated topsoils.

### 9.32. TIME

**General:** The importance of the role of time in the formation of soils was recognised by Jenny (1941) who wrote: "The estimation of relative age or degree of maturity of soils is universally based on horizon differentiation. In practice, it is generally maintained that the larger the number of horizons and the greater their thickness and intensity the more mature is the soil. ... it is evident that the issues centre around the factor time in soil formation".

One method of studying the effects of time as a soil-forming factor is to recognise and investigate a chronosequence, wherein all soil-forming factors except for time are constant or vary ineffectively. Thus, observed differences between soils can be related to the lapse of different periods of time since the initiation of soil formation. Results can only be meaningful and comparable if it is possible to assign ages to various ground surfaces with a reasonable degree of accuracy (Stevens and Walker, 1970). In the present study no attempt was made to determine the age of the sampled soils. Therefore, any attempt to discuss the importance of time in the formation of the sampled soils would be speculative. Nevertheless, the effect of time has been discussed qualitatively in relation to the soils associated with the granite, USGO and Malmesbury sediments.

**Lapse of time during gravitational transport (summarised from sections 4.5.2., 4.5.4. and 6.5.3.):** The slope of the toposequences on granite, phyllite and schist was steep enough (between 75 and 100 ‰) to suggest gravitational soil transport. For the toposequence on schist this was confirmed by the presence of granitic fragments in the lower slope positions (Pit 38; Figure 6.1).

The concentrations of Li, Be, F, Na<sub>2</sub>O, MgO, Al<sub>2</sub>O<sub>3</sub>, P<sub>2</sub>O<sub>5</sub>, S, K<sub>2</sub>O, CaO, TiO<sub>2</sub>, V, Cr, Mn, Fe<sub>2</sub>O<sub>3</sub>, Ni, Cu, Zn, Rb, Sr, Y, Zr, Nb, Sn, Sb, Pb, Th and U (Group-I elements) decrease down the topsoils of the toposequences on granite and phyllite. This decrease coincided with depletion of finer particles, feldspars and organic matter. It is hypothesised that continuous soil weathering, leaching and eluviation during gravitational transport of the topsoil caused the gradual depletion of the soil components listed above. The transport of the soil requires time; i.e. the soil components at the bottom of the sequence were exposed for longer to the processes of weathering and soil formation than the components at the top of the sequence. Accepting the hypothesis as explained above, it can be concluded that the time period available for weathering, leaching and eluviation may partly account for the depletion of the elements and soil components listed above. It is important to keep in mind that time is not the only soil forming factor that varies down the toposequence. The contribution of time to the formation of these soils can thus not be quantified.

Colluviation down the toposequence on schist and admixture of minerals and their associated elements from the underlying material into the topsoil probably caused

the concentrations Li, Be, Na<sub>2</sub>O, MgO, Al<sub>2</sub>O<sub>3</sub>, S, K<sub>2</sub>O, CaO, TiO<sub>2</sub>, Mn, Co, Ni, Cu, Zn, Br, Rb, Sr, Y, Nb, Sn, I, U and NH<sub>4</sub>NO<sub>3</sub>, extractable Na, Mg, P, K, Ca, Ni, Zn, Ba and Tl (Group-II elements) to increase down the toposequence. A comparison of the elements in Group-I and Group-II shows that many elements which have decreasing concentration down the toposequences on granite and phyllite have increasing concentration down the toposequence on schist. This may simply reflect the fact that the effect of time as a factor for soil chemical composition is variable.

**Chemistry of soils on USGO as affected by time (summarised from sections 5.3. and 5.5.5.):** The topography, particle size distributions and geochemical results agree with the hypothesis that the age of the soil increases from the floodplain towards the slightly higher-lying areas near the granite complex. The geochemical results showed that the supposedly older subsoil has lower CaO, K<sub>2</sub>O and Na<sub>2</sub>O concentrations and higher Al<sub>2</sub>O<sub>3</sub>, P<sub>2</sub>O<sub>5</sub>, TiO<sub>2</sub>, V, Cr, Fe<sub>2</sub>O<sub>3</sub>, Zn, As, Rb, Y, Nb, Sn, Pb and Th concentrations than the younger subsoil. This was partly attributed to the complete alteration of feldspars and(or) micas into secondary clay minerals and oxides in the older soils. More soluble constituents which could not be retained by the soil (e.g. Ca, K and Na) became leached while the less soluble elements (e.g. Al, P, Ti, Cr, Fe, Sn and Pb) became relatively enriched as the alteration of primary minerals to pedogenic clay minerals and Fe-oxide gravel progressed. It is thus suggested that the age of the soil is one important control for the concentrations of the elements listed above. The higher concentration of Al, Fe and Ti in the older soils would be in agreement with various other authors who have studied the geochemical changes in soils with time (Nesbitt and Young, 1989; Young *et al.*, 1987; Kesel and Spicer, 1985).

### 9.33. PARENT MATERIAL

**General:** Soil parent materials vary with respect to many characteristics (Fanning and Fanning, 1989). Some of the most important characteristics for the formation of soils are texture, mineralogy and degree of consolidation of the parent material. The effects of parent material are more obvious if a soil is young. As the soil becomes older, inherited properties typically become less obvious as the environment molds the soil. Inherited resistant minerals, however, may endure even after the soil is old. The properties of the parent materials are also important in controlling the direction and rate of soil genesis.

**Other authors:** Litaor *et al.* (1989) investigated a lithosequence in the northeastern Samaria steppe (Israel). Seventeen soil samples were analysed for pH, electrical conductivity, alkalinity, soluble ions (Na, K, Ca, Mg, Cl), cation exchange capacity, exchangeable cations (Na, K, Ca, Mg), organic matter, water retention, calcium carbonate and several particle size classes. The exchangeable sodium percentages were

calculated. A Factor Analysis was used to show that different quantities of clay, salt and calcium carbonate were the main controls of the physical and chemical differences between the soils. The quantities of clay, salt and calcium carbonate were related to different underlying materials.

The importance of the underlying material for the soils in the study area was emphasised by Talbot (1947), Lambrechts (1979) and Schloms *et al.* (1983). Mr J.J.N. Lambrechts (Department of Soil Science, University of Stellenbosch; pers. comm., 1990) suggested grouping the soils of the study area according to the underlying material as listed below:

- Group-I: Deep sandy soils derived from recent coastal sands.
- Group-II: Duplex soils of the flat terrain, associated with unconsolidated sands of (partly) granitic origin.
- Group-III: Soils associated with ferruginized materials of Miocene to Pliocene age.
- Group-IV: Soils of the undulating, hilly terrain associated with granitic rocks.
- Group-V: Soils of the rolling terrain associated with the sediments of the Malmesbury Group.

**In this study:** The importance of the parent material in determining the abundance of elements in the sampled soils was initially ascertained when a preliminary set of samples was analysed for Ni, Cu, Zn, As, Se, Br, Rb, Sr, Zr, Nb, Mo, W, Pb, Th and U (section 2.2.). Various multivariate statistical methods showed that many elements have significantly different concentrations in soils associated with different underlying materials.

This was confirmed when individual elements were discussed earlier in this chapter (Table 9.1). The soils associated with sandy underlying materials (USGO and coastal sands) inherited high proportions of quartz sand and thus have lower retention capacities than the other soils. The concentration of SiO<sub>2</sub> is typically high in these soils while most other elements have relatively low concentrations. The soils associated with granite inherited feldspars which were partly altered to clay minerals. The clay minerals present in the soils on the sediments of the Malmesbury Group are both pedogenic and inherited (Chapter 3). The relatively high proportions of clay minerals and Fe-oxides in the soils on granite and sediments of the Malmesbury Group resulted in lower concentrations of SiO<sub>2</sub> and presumably in higher retention capacities, explaining the relatively high concentrations of most other elements (Table 9.1).

A Principal Component Analysis was used to demonstrate the geochemical variance of 77 soil and associated rock samples (Figure 9.20). Principal Component 1 (PC 1) explains 36 % of the total variance and correlates negatively with Si and positively with Mg, Al, Ti, V, Cr, Fe, Ni, Cu, Zn, Y and Pb ("*Quartz Negative; Clay and Oxide Positive Component*"). Subsoils which have high proportions of clay and(or) sesquioxides have

high PC 1 values while sandy topsoils have low values. It was inferred that the variation explained by PC 1 is partly due to the accumulation and loss of clay minerals, sesquioxides and quartz during soil genesis. However, it can also be seen in Figure 9.20 that the highest PC 1 values are exclusively due to soils associated with the sediments of the Malmesbury Group and the ferruginized materials while the lowest values correspond to the soils associated with the sandy underlying materials (coastal sands and USGO). It is inferred that both the underlying material and pedogenic processes are important in controlling the concentrations of the elements represented by PC 1.

Principal Component 2 (PC 2) accounts for 18 % of the total variance, correlates with F, Na, K, Rb, Nb, Mo, Th and U and has been named "*Granitic Component*". Granite-derived soil samples have high PC 2 values while all other soil groups have low values. Variations in the values of PC 2 mainly represent different stages of weathering of a granitic parent material.

It is concluded that the different parent materials accounted for a substantial portion of the chemical variance explained by PC 1 and PC 2. The parent material is thus a soil forming factor of major importance for the investigated soils.

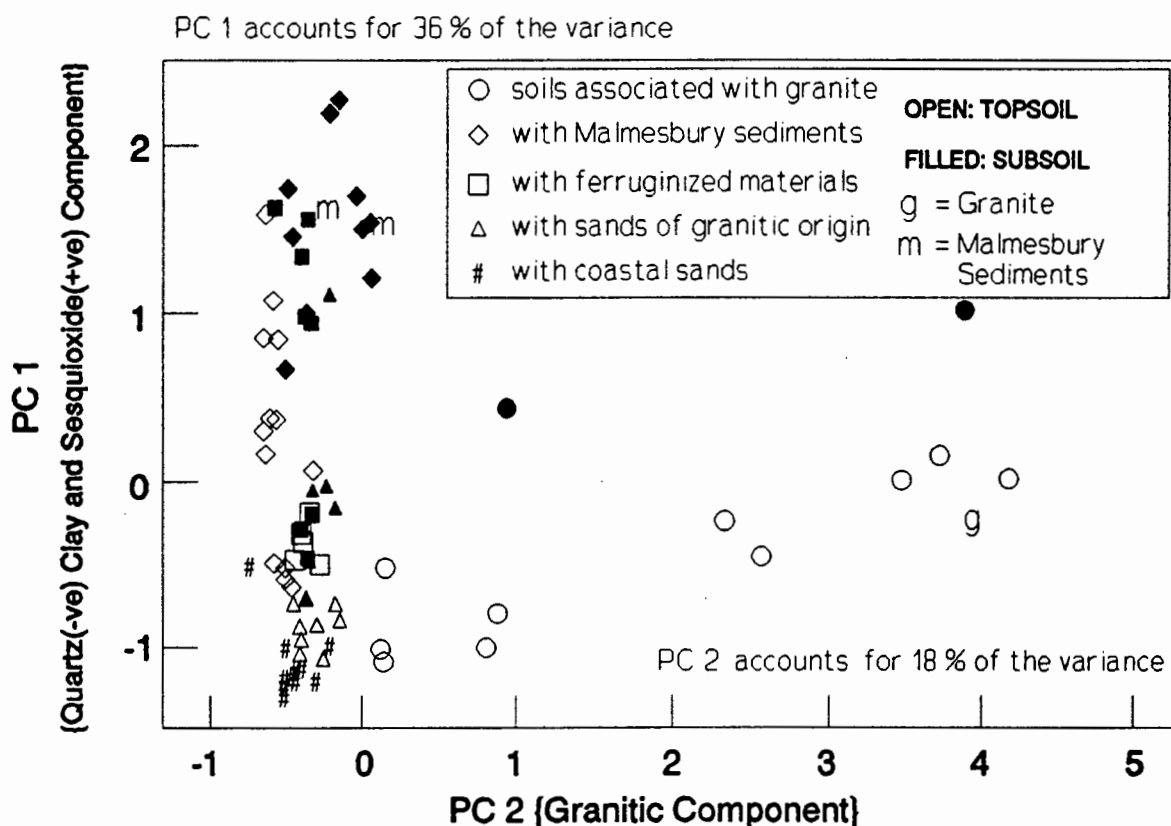


**Figure 9.20:** Principal Component Analysis of the chemical composition of soils and parent rocks. Principal Component 1 (PC1) explains 36 % of the total variance and correlates negatively with Si and positively with Mg, Al, Ti, V, Cr, Fe, Ni, Cu, Zn, Y and Pb ("*Quartz Negative; Clay and Oxide Positive Component*"). Principal Component 2 (PC 2) accounts for 18 % of the total variance, correlates with F, Na, K, Rb, Nb, Mo, Th and U and has been named "*Granitic Component*".

### 9.34. TOPOGRAPHY

**General:** Topography, or local relief, controls much of the distribution of soils in the landscape. This can result in markedly contrasting soils merging laterally with one another and yet be in equilibrium under existing local conditions (Birkeland, 1974). It has become clearer in the past decades that soils are interdependent and the processes that occur in the soils of the higher lying portions of the landscape have an influence on soils that occur in the lower parts of the landscape (Hugget, 1975; Ruhe and Walker, 1968). Most of the soil properties that vary with topography are controlled by aspect, shape and gradient of slope, elevation, soil age and drainage conditions. Processes such as erosion and deposition (colluviation), lateral leaching and precipitation, lateral eluviation and illuviation, and alluviation cause typical differences between soils which occupy different topographic positions (Buol *et al.*, 1989; Fanning and Fanning, 1989; Hall, 1983).

**The geochemistry of the sampled soils as affected by hillslope processes:** In this study many soils were sampled along relatively steep toposequences (40 to 100 permille). It was demonstrated that the chemical and physical properties of soils in different topographic positions are substantially different. Possible reasons for the changes down the toposequences have been discussed at length earlier. The following processes were identified as being of probable importance:

(a) The evaporation of soil water in the lower slope positions often resulted in higher concentrations of soluble elements (e.g. Na, S, Cl, Br and I).

(b) The erosion, transport and deposition of solids, as well as the solution and precipitation of solubles, by throughflow water resulted in translocation of particles and chemical elements. In the granite-derived toposequence relatively fine particles and elements such as S, V, As, Se, Br, Th and U were depleted in the upper part of the toposequence and accumulated in the subsoil at the footslope.

(c) Transportation of soil by gravity was suggested. Continuous weathering, leaching and eluviation caused the concentrations of most major and trace elements to decrease from the top to the bottom of the toposequence (topsoil). The depletion of elements coincided with weathering of feldspars and eluviation of organic matter and clay. The data for the toposequence on schist, however, indicated that colluviation down a toposequence may result in admixture of weathering products from the underlying rock into the topsoil, and may cause increasing elemental concentrations down a toposequence.

(d) It was previously mentioned (e.g. section 9.32.) that the data for the soils associated with the USGO agree with the hypothesis that the age of the soil increases from the floodplain towards the slightly higher-lying areas near the granite exposures. The supposedly older soils in the slightly higher-lying areas were exposed to the

processes of weathering for longer time periods. Insoluble elements were relatively enriched whereas more soluble elements were depleted in the older soils. A list of the affected elements is given in section 9.32.

### 9.35. CLIMATE, BIOTA AND MAN

**Climate:** The climatic factor is often considered to be the most important in determining the properties of many soils (Birkeland, 1974). On a global scale climatic and soil gradients seem to be congruent, judging by similarity of patterns on world soil maps and climatic maps (Buol *et al.*, 1989). On a smaller scale and within one climatic zone other soil forming factors become much more important. Nevertheless, different microclimatic conditions, such as wind, aspect and shade, may greatly affect soil formation.

All sampling locations lie within the Coastal Foreland, a smoothly undulating coastal plain with a maximum elevation of less than 200 m. The surface is, however, broken by a number of granite batholiths. The macro-climatic conditions in the field area (temperature and precipitation) are considered fairly homogeneous and are described in section 1.7. Possible effects of slightly different temperatures and precipitation rates on the sampled soils would be negligible compared to the effects of slope position and parent material. It was thus not possible to evaluate the importance of small climatic differences between the sampling sites.

The ferruginized materials are considered to have been preweathered during a tropical climate in the earlier Cenozoic. Minerals susceptible to weathering were altered to form Fe-oxides, Al-oxides and kaolinite. The chemical properties of the ferruginized materials, as induced by the palaeoclimate, were partly inherited by the overlying soils (Chapter 7).

**Biota:** The interactions between soil and biota are complex. Animals and plants live in and on soils and depend upon them as a source of food. The habitation of soils by plants and animals controls nitrogen and carbon cycling and causes different forms of bioturbation. Biota are thus considered an important soil forming factor. The most conspicuous evidence of biota affecting soils in the Coastal Foreland is the abundant occurrence of earth mounds, colloquially called "heuweltjies". An examination of earth mounds close to the field area indicated that they are well-established active termitaria of the harvester termite *Microhodotermes viator*. The most obvious effects on the soils were bioturbation and calcretisation (Moore and Picker, 1991).

In this study sampling sites were selected to eliminate, as far as possible, the effects of termites, molerats and other burrowing animals. In two cases, however, soils showed signs of bioturbation. These were the burrow in the soil profile at Pit 47

(Chapter 7) and the molehills close to Pit 33 (Chapter 4). In both cases the bioturbation had no apparent effect on the observed geochemical trends.

**Man:** The impact of humans on soils is manifold. In the study area impacts are mainly caused by agricultural activities. Cultivation may result in compaction and erosion of soils. Gully erosion is an obvious phenomenon in the field area and was surveyed by Talbot (1947).

The application of agro-chemicals often introduces toxic substances into soils. In this study sampling sites were selected to minimise the effects of cultivation (section 2.2.). In some cases, however, samples had to be taken from cultivated soils. Only the results for V, Cr, Sn and Cd gave reason to speculate about soil contamination.

Rates of aerial deposition of toxic substances are probably close to background because of the lack of industry in the field area.

## CHAPTER 10.

# CONCLUSIONS AND RECOMMENDATIONS FOR FUTURE RESEARCH

---

The aim of this study was to investigate the geochemistry of some common Western Cape soils. Very little was previously known about the geochemistry of Western Cape soils and this thesis was primarily a reconnaissance study. It was, therefore, not attempted to focus on any particular elements or to prove or disprove existing pedogenic hypotheses. The broad nature of this study resulted in an array of observations, conclusions and hypotheses in different fields of geochemistry and soil science, many of which still require confirmation. Observations and conclusions are summarised in section 10.1, and some hypotheses with recommendations for future research are given in section 10.2.

### 10.1. CONCLUSIONS

**Importance of the underlying material for sampling strategy:** Various statistical tests on a preliminary data set indicated that the underlying material is the most important factor in determining the composition of the overlying soils. Soils from all abundant underlying materials were sampled in order to cover the largest possible proportion of the total chemical variance with a limited number of soil samples.

**Extensive cultivation of the soils in study area:** The degree to which the field area is cultivated is remarkable. Extensive field excursions were undertaken to locate suitable uncultivated sampling sites. It was realised that it is generally difficult, and for the soils associated with the USGO and the ferruginized materials impossible, to find sampling sites which are characterised by uncultivated, common soil types. However, in all instances sampling sites were selected to eliminate, as far as possible, the effects of cultivation.

**Leaching experiments:** Several leaching methods were compared in order to find the technique which was most suitable for the present study. It was found that results obtained using differently pretreated samples or using different leaching methods were substantially different. Extraction with 1 M  $\text{NH}_4\text{NO}_3$  (Appendix-II) was found to be most suitable to quantify (a) the proportion of an element which is "readily mobilised" and (b) the environmental risk associated with contaminated soils. It is, however,

important to note that the  $\text{NH}_4\text{NO}_3$  matrix resulted in relatively high detection limits and that many of the investigated elements had concentrations mainly below the LLD.

**Combination of particle size classes:** A rotated Principal Component Analysis proved to be a useful statistical technique for reducing the overall number of particle size classes in a way that minimised the loss of variance. Although the number of particle size classes was reduced from 13 to 6, the accompanied loss of variance was less than 10 percent.

**Data base of best possible background concentrations:** Two important aims of this study were to produce a geochemical data base for the use of other scientists and to provide the best possible background concentrations of a range of elements. The mean, minimum and maximum concentrations, and the corresponding standard deviations, of all investigated elements have been reported separately for soils associated with different underlying materials. Analytical results for soils underlain by the same geological materials but from different locations are still needed in order to examine how representative the reported concentrations are. Although the presented mean concentrations may be influenced by various forms of soil pollution only the results for V, Cr, Sn and Cd gave reason to speculate about such contamination (section 10.2.).

**Lateral and vertical changes of the soil characteristics were best explained by:**

(a) *Affinity of trace elements for organic matter, clay minerals and Fe-oxides.* Most trace metals have higher concentrations in soil horizons with higher proportions of clay minerals. Phosphorus, S, V, Fe, As, Se and Cr are typically enriched in soils with high proportions of Fe-oxides. The elements Mg, P, S, K, Ca and Mn and the 1 M  $\text{NH}_4\text{NO}_3$  extractable fractions of P and Ca often have increasing concentrations from the subsoil to the relatively organic-rich topsoil. An affinity with organic matter was thus suggested.

(b) *Retention of dissolved elements from evaporating water.* Lateral changes in the concentrations of Na, S, Cl, Br, I and  $\text{NH}_4\text{NO}_3$  extractable Na, Mg, P, S, K, Ca, Zn and Tl are commonly controlled by the retention capacity and the slope position of the soil. Higher concentrations occur in soils which have higher proportions of relatively fine particles and organic matter and(or) occupy the lowest slope position. Manganese and extractable Ni, Ba, Al and Fe sometimes show the same behaviour. It was concluded that the retention capacity of the soil for water and dissolved solids, and the evaporation of throughflow water or uplifted ground water from the soil, are important in determining the observed lateral changes in elemental concentration.

(c) *Aeolian, fluvial and colluvial input of detritus.* The soils associated with the granites, USGO and the coastal sands have increasing concentrations of numerous major and trace elements towards the potential sources of relatively fresh detritus. It was concluded that the aeolian, fluvial and colluvial input of mineral detritus from the beach and nearby granites is an important factor in determining the observed lateral changes in elemental concentration.

(d) *Transportation of soil by gravity.* Downslope geochemical changes in toposequences with steeper average gradients ( $> 40 \text{ ‰}$ ) were closely related to hillslope processes. It was proposed that the soil of the granite-derived toposequence was subjected to gravitational transport. The continuous weathering, leaching and eluviation of the soil during transport caused the concentrations of most major and trace elements to decrease with increasing distance from the granite. The continuous loss of Na, Al, K and Ca and relatively fine particles resulted in high concentrations of Si and high proportions of coarse sand in the most leached soil at the lowermost slope position.

(e) *Various effects of throughflow water.* The results suggested that leachates from granites outcropping above the Klipberg toposequence infiltrated into the soil at the top of the sequence. The flow of water continued down-slope in the form of throughflow. This throughflow water was a source of trace elements. Their adsorption and(or) precipitation resulted in high concentrations of S, V, As, Se, Br, Th, U in the soil. Leaching of elements by throughflow provided the best explanation for the low concentrations of the  $1 \text{ M NH}_4\text{NO}_3$  extractable element fractions at the footslope. Preferential eluviation and illuviation of relatively fine particles caused lateral changes in the particle size distributions within the granite-derived toposequence, and probably partly determined the lateral change of elemental concentrations in the toposequence associated with the ferruginized materials.

**Extensive loss of elements during the very early stage of weathering:** Chemical changes from the outcropping granite to the upper limit of the soil cover of the Klipberg toposequence indicated a major loss of the more soluble elements during the early stages of weathering (losses in percent: Na: 72, Ca: 63, K: 61, Si: 55 and Mn: 44).

**Retention of mineral-released elements by organic matter:** The tendency of elements to become leached from the coastal sand-derived soil was  $\text{Rb} > \text{K} > \text{Na} > \text{P} > \text{Al} > \text{Mg} > \text{Sr} = \text{Ca}$ . The results suggested that large proportions of the Ca, Mg and P released from their primary host minerals were retained by organic matter.

**Pedogenic accumulation of elements to high concentrations:** Pedogenic processes alone accounted sufficiently for high concentrations of As and Se. High concentrations F, Sb and  $1 \text{ M NH}_4\text{NO}_3$  extractable V were not indicative of soil pollution. The maximum concentrations of the elements mentioned above exceeded recommended maximum levels for the assessment of polluted soils. It was concluded that recommended maximum concentrations can only be considered as guidelines, and not as absolute limits.

## 10.2. RECOMMENDATIONS FOR FUTURE RESEARCH

**Granite-derived toposequence:** In the granite-derived toposequence trace elements accumulated together with Fe-oxide concretions. Leachates from the granite outcropping

above the toposequence were proposed as important sources of accumulated S, V, As, Se, Th and U. It was speculated that the transportation of the Fe-oxide concretions by gravity and their subsequent breakdown due to reducing conditions at the footslope could be a potential source of trace elements for the underlying subsoil and the ground water. More information is needed to provide better evidence for this hypothesis:

(a) *More comprehensive field observations.* More observation points (pits or trenches) could provide information that is needed in order to determine (a) whether the Fe-oxide concretions are included in the gravity transport; (b) whether the vertical succession from hard Fe-oxide concretions to soft concretions and further to mottles at the footslope reflects the formation or the breakdown of the Fe-oxide concretions; and (c) what form of gravitational transport takes place.

(b) *Geochemical changes of granite with increasing depth.* A drill core of the granite above the toposequence could be analysed for S, V, As, Se, Th and U at different depths. Increasing concentrations with increasing depth would confirm that surficial leaching of the granite is an important source of the corresponding elements. Constant concentrations would indicate that atmospheric deposition of elements, or some other process, is significant and important in order to explain the high concentrations of the corresponding elements in the soil.

**Proton microprobe analyses of Fe-oxide concretions:** The change of the concentrations of the anomalous trace elements along sections through individual Fe-oxide concretions could be determined. The results could reflect fluctuations of the element supply to the soil and, therefore, provide a possible indication of either fluctuations in atmospheric deposition or different rates of leaching of the granite.

**Soils associated with the sediments of the Malmesbury Group:** The results showed that the elements Li, Be, Mg, Al, S, K, Ca, Ti, Mn, Ni, Cu, Zn, Rb, Sr, Y, Nb, Sn, U and 1 M  $\text{NH}_4\text{NO}_3$  extractable K, Ca and Ba may have increasing and decreasing concentrations down a toposequence. It was suggested that colluviation down the toposequence associated with schist resulted in admixture of weathering products from the underlying rock into the topsoil and caused increasing concentrations down the slope. The decrease of the concentrations of the same elements down the toposequence associated with phyllite may be the result of continuous eluviation during gravitational transport. The strong eluviation of the toposequence on phyllite may be favoured by very high percentages of gravel and higher exchangeable sodium percentages.

Many of the elements listed above are important nutrients. More research should be directed in order to investigate in more detail why eluviation of finer particles and removal of nutrients from the topsoil predominates in the toposequence associated with phyllite while admixture of finer particles and nutrients from the underlying material into the topsoil predominates in the toposequence associated with schist. The two toposequences are similar with respect to aspect, gradient and shape of the slope and climate. Both toposequences are underlain by a clay-rich metamorphosed sediment.

The clay mineralogy and the structure of the soil are important determinants of the permeability and should be investigated in greater detail. The toposequence associated with phyllite is used for crop production while the toposequence associated with schist is vegetated with shrubveld. The possible effects of cultivation and vegetation type with regard to eluviation and colluviation should be considered when examining the possible reasons for the observed differences between the toposequences.

**Dissolved transport of tungsten:** This study suggested that W is commonly hosted by sand-sized, weather-resistant mineral particles, likely to be scheelite or wolframite. However, high concentrations of W (426 ppm) in the granite-derived toposequence gave reason to speculate about the occurrence of acidic leaching, dissolved transport and precipitation or adsorption of W. The possible transport of W in acidic solutions and its concentration in certain soil horizons requires further research. This should include a confirmation of the analytical results reported in this study and the identification of the tungsten-hosting components in rock and soil. Tungsten analyses of surface run-off and throughflow water could provide important evidence for the transport of W in solution.

**Ages of the soils associated with the USGO:** Field observations, particle size distributions and the geochemical results could have indicated that the age of the soils associated with the USGO increases from the floodplain towards the Darling granite complex. Absolute age determinations and(or) more detailed mapping are required to substantiate this hypothesis.

**Possible Cd contamination by fertilisers:** The results obtained for the soils associated with the sediments of the Malmesbury Group gave reason to speculate about a link between fertilisation and higher concentrations of 1 M  $\text{NH}_4\text{NO}_3$  extractable Cd. Research should be directed to investigate in greater detail this possible link.

**Geochemistry and pH values of the coastal sand-derived soil:** Results for the coastal sand-derived soils indicated abrupt lateral geochemical changes and that the occurrence of shallow and reducing ground waters can cause acidification of the overlying soil. This could have important implications for the indigenous fynbos vegetation and should be examined in more detail.

**Extractable Co:** The concentrations of the extractable element fractions normally increase from the topsoils to the fine-textured subsoils. Several hypotheses were presented to explain the conspicuous decrease in the concentration of 1 M  $\text{NH}_4\text{NO}_3$  extractable Co with increasing soil depth. The anomalous behaviour should be investigated in more detail because Co is an environmentally significant element.

**Elements which have relatively low or high concentrations in the investigated soils:** A comparison of the mean elemental concentrations with levels reported in the literature indicated that the investigated soils generally have high As, Br and W concentrations. The concentrations of Li, Na, Mg, Mn, Co, Ni, Cu and Zn are relatively

low. Further research is necessary to confirm these results and to investigate whether the anomalous concentrations affect plant, animal or human health.

**Possible link between low Zn, Cu and Se concentrations and kwashiorkor:** There has been a debate in the literature about the connection between low daily Se intakes and low Se blood levels with higher susceptibilities to kwashiorkor (Hadjimarkos, 1965; Waterlow, 1965; Schwarz, 1965; Burk *et al.*, 1967). Kwashiorkor occurs frequently in the Western Cape and it was observed that kwashiorkor patients in this region have low Zn, Cu and Se blood levels (Prof. Heeser, Red Cross Children's Hospital, Cape Town; pers. comm., 1990). Possible relationships between areas with high frequencies of kwashiorkor and soils with lower concentrations of Zn, Cu and(or) Se should be investigated. Elemental concentrations in crops and drinking water should also be determined.

The relatively high LLD for the analysis of total Se (0.8 ppm) made it impossible to determine whether the concentrations of Se in the soils of the field area are generally lower than the mean concentration of Se in soils (0.4 ppm; Sposito, 1989). The high LLDs for the analysis of 1 M  $\text{NH}_4\text{NO}_3$  extractable Se experienced in this study could be lowered by using the hydride generation method.

## REFERENCES CITED

- ADRIANO, D.C. (1986): Trace elements in the terrestrial environment. Springer Verlag, New York.
- AFYUNI, M.M., CASSEL, D.K. and ROBARGE, W.P. (1994): Lateral and vertical bromide ion transport in a Piedmont landscape. *Soil Sci. Soc. Am. J.*, 58: 967-74.
- AHRENS, L.H. and ERLANK, A.J. (1969): Bismuth. In: *Handbook of geochemistry* (section 83; editor: Wedepohl, K.H.). Springer Verlag, Berlin.
- AJMONE MARSAN, F., BAIN, D.C. and DUTHIE, D.M.L. (1988): Parent material uniformity and degree of weathering in a soil chronosequence, northwestern Italy. *Catena*, 15: 507-17.
- ALLOWAY, B.J. (1993): *Heavy metals in soils*. Blackie, London.
- AUBERT, H. and PINTA, M. (1977): *Trace elements in soils*. Elsevier Scientific, Amsterdam.
- AXELSON, E. (1973): *Congo to Cape: early portuguese explorers*. Faber and Faber, London.
- BARROW, J. (1806): *Travels into the interior of Southern Africa*. Cadell and Davies, London.
- BARTLETT, R. and JAMES, B. (1980): Studying dried, stored soil samples - some pitfalls. *Soil Sci. Soc. Am. J.*, 44: 721-4.
- BERTIN, E.P. (1975): *Principles and practise of X-ray spectrometric analysis*. Plenum Press, second edition.
- BILLINGS, G.K. (1970): Rubidium. In: *Handbook of geochemistry* (section 37; editor: Wedepohl, K.H.). Springer Verlag, Berlin.
- BIRKELAND, P.W. (1974): *Pedology, weathering and geomorphological research*. Oxford University Press, New York.
- BLUME, H.P. (1992): *Handbuch des Bodenschutzes*. Ecomed, second edition, Landsberg/Lech.
- BOUCHER, C. (1987): *A phytosociological study of transects through the Western Cape Coastal Foreland*. Ph.D. thesis, University of Stellenbosch.
- BOWEN, H.J.M. (1979): *Environmental chemistry of the elements*. Academic Press, London.

- BRAKENSIEK, D.L. and RAWLS, W.J. (1994): Soil containing rock fragments: effects on infiltration. *Catena*, 23: 99-110.
- BRAUN, J.J. and PAGEL, M. (1994): Geochemical and mineralogical behaviour of REE, Th and U in the Akongo lateritic profile (SW Cameroon). *Catena*, 21: 173-77.
- BRIDGEMAN, D., PALMER, I. and THOMAS, W. (editors; 1992): South Africa on a leading edge? A guide to the Western Province economy, Wesgro, Cape Town.
- BROUWER, I.D., BACKER DIRKS, O., DE BRUIN, A. and HAUTVAST, J.G.A.J. (1988): Unsuitability of World Health Organisation Guidelines for fluoride concentrations in drinking water in Senegal. *The Lancet*, 8579: 223-25.
- BRUCE, R.W. and BEUKES, D.J. (1992): Effects of parent rock and cultivation on element status and other properties of soils in two landtypes in the Western Transvaal. Proceedings of the 17th Congress of the Soil Science Society of SA, Stellenbosch, January, 1992.
- BRÜNE, H. and ELLINGHAUS, R. (1982): Schwermetallgehalte in landwirtschaftlich genutzten Ackerböden Hessens. *Landwirtschaftliche Forschung (Sonderheft)*, 38: 338-49.
- BRUNKE, E.G. (1973): Some geochemical aspects of weathering profiles of Cape granite and associated minerals. Unpublished honours project. Department of Geological Sciences, University of Cape Town.
- BÜHMANN, C. and KIRSTEN, W.F.A. (1991): The mineralogy of five weathering profiles developed from Archaean granite in the eastern Transvaal, Republic of South Africa. *S. Afr. J. Plant Soil*, 8(3): 146-52.
- BUNDESVERBAND DEUTSCHER GEOLOGEN (1990): Höchstmengenwerte für Schadstoffe in Boden, Grundwasser und Luft. Schriftenreihe des BDG Nr. 5, Bonn.
- BUOL, S.W., HOLE, F.D., McCracken, R.J. (1980): Soil genesis and classification. Second edition, Iowa State University Press, Ames.
- BUOL, S.W., HOLE, F.D., McCracken, R.J. (1989): Soil genesis and classification. Third edition, Iowa State University Press, Ames.
- BURK, R.F., PEARSON, W.N., WOOD, R.P. and VITERI, F. (1967): Blood-selenium levels and *in vitro* red blood cell uptake of <sup>75</sup>Se in Kwashiorkor. *Am. J. Clinical Nutrition*, 20(7): 723-33.
- CAMPBELL, B.M. (1985): Montane vegetation structure in the fynbos biome. Ph.D. thesis, Rijksuniversiteit te Utrecht.

- CONACHER, A.J. (1975): Throughflow as a mechanism responsible for excessive soil salinisation in non-irrigated, previously arable lands in the Western Australian Wheatbelt: a field study. *Catena*, 2: 31-68.
- COWLING, R.M. (1992): *The ecology of fynbos*. Oxford University Press, Cape Town.
- DATE, A.R. and GRAY, A.L. (editors; 1989): *Applications of Inductively Coupled Plasma Mass Spectrometry*. Chapman and Hall, New York.
- DAVIES, B.E. (1980): *Applied soil trace elements*. Wiley-Interscience, Chichester.
- DEACON, H.J. (1983): The peopling of the Fynbos Region. South African National Scientific Programmes Report, 75: 183-204.
- DE ALBUQUERQUE, C.A.R. and SHAW, D.M. (1972): Thallium. In: *Handbook of geochemistry* (section 81; editor: Wedepohl, K.H.). Springer Verlag, Berlin.
- DENNEN, W.A. (1966): Stoichiometric substitution in natural quartz. *Geochim. Cosmochim. Acta*, 30: 1235-41.
- DENT, R.H. (1973): A geochemical investigation of weathering profiles of the Cape granite. Unpublished honours project. Department of Geological Sciences, University of Cape Town.
- DIVISION OF SOILS, CSIRO (1983): *Soils: an Australian viewpoint*. CSIRO, Melbourne Academic Press, London.
- DODDS, H.A. (1994): The fate and geochemistry of vanadium in effluent-treated soils. M.Sc. thesis (unpublished), Department of Geological Sciences, University of Cape Town.
- DUNCAN, A.R. (1975): TRACE. Department of Geological Sciences, University of Cape Town.
- EIDGENÖSSISCHES DEPARTMENT DES INNEREN (1986): *Verordnung über Schadstoffgehalte des Bodens*, Bern.
- ELLIS, F., SCHLOMS, B.H.A., RUDMAN, R.B. and OOSTHUIZEN, A.B. (1979): Soil association map - Western Cape (1:250000; unpublished preliminary version). Department of Agriculture and Water Supply, Elsenburg.
- EPA US (ENVIRONMENTAL PROTECTION AGENCY OF THE UNITED STATES; 1990): Toxicity characteristic leaching procedure (TCLB). US Govt. Documents, 40 CFR Ch. 1 (7-1-90 Edition), Part 261, Appendix-II.

ERLANK, A.J., SMITH, H.S., MARCHANT, J.W., CARDOSO, M.P. and AHRENS, L.H. (1978): Zirconium. In: Handbook of geochemistry (section 40; editor: Wedepohl, K.H.). Springer Verlag, Berlin.

FANNING, D.S. and FANNING, M.C.B. (1989): Soil: Morphology, genesis and classification. John Wiley, New York.

FAURE, K. (1993): Mineralogy and geochemistry of the carbonaceous mudstones, and coal petrogenesis of the Grootegeluk Formation in the Waterberg coal field, South Africa. Ph.D. thesis, Department of Geological Sciences, University of Cape Town.

FIEDLER, H.J. and RÖSLER, H.J. (editors; 1987): Spurenelemente in der Umwelt. Gustav Fischer Verlag, Jena.

FISCHER, W.R. and CRAM, S. (1994): Behaviour and analysis of chromium in soils. Transactions of the 15th International Congress of Soil Science, Acapulco, Mexico, Volume 3A, Commission II, p 181.

FRONDEL, C. (1962): Dana's system of mineralogy. Volume III: Silica Minerals, John Wiley, New York.

FUGE, R. (1974): Chlorine. In: Handbook of geochemistry (section 17; editor: Wedepohl, K.H.). Springer Verlag, Berlin.

GENTHE, R.I. (1987): The geology of the inner continental shelf and Agulhas Arch: Cape Town to Port Elizabeth. Bulletin: Joint Geological Survey and University of Cape Town (Marine Geoscience Unit), 20: 1-129.

GERRARD, J. (1992): Soil Geomorphology: An integration of pedology and geomorphology. Chapman and Hall, London.

GLAZOVSKAYA, M.A. (1968): Geochemical landscapes and types of geochemical soil sequences. Trans. 9th Int. Congress Soil Sci. Adelaide, 4: 303-12.

GORBANOV, S.P. (1994): Distribution of metal microelements by genetic soil horizons as depending on profile differentiation. Transactions of the 15th International Congress of Soil Science, Acapulco, Mexico, Volume 6b, Commission V, 109-110.

GREEN, J. (1959): Geochemical table of elements for 1959. Bull. Geol. Soc. Am., 70: 1127-84.

GREEN L.G. (1949): In the land of the afternoon. H.B. Jimmins, Standard Press Ltd., Cape Town.

HADJIMARKOS, D.M. (1965): Selenium content of fish flour in relation to kwashiorkor and dental caries. Lancet, i: 605.

HALL, G.F. (1983): Pedology and geomorphology. In: Pedogenesis and soil taxonomy, I. Concepts and interactions (editors Wilding, L.P., Smeck, N.E. and Hall, G.F.). Elsevier, Amsterdam.

HAMAGUCHI, H. and KURODA, R. (1969): Tin. In: Handbook of geochemistry (section 50; editor: Wedepohl, K.H.). Springer Verlag, Berlin.

HÄNI, H., GUPTA, S. and SIEGENTHALER, A. (1981): Schwermetallgehalte einiger wenig belasteter typischer Böden in der Schweiz. Landwirtschaftliche Forschung (Sonderheft), 38: 314-23.

HARTMANN, M.O. (1969): The soil heterogeneity of some soils in the south-western Cape Province and its relationship to soil classification. M.Sc. thesis (unpublished), University of Stellenbosch.

HEIER, K.S. and BILLINGS, G.K. (1970a): Lithium. In: Handbook of geochemistry (section 3; editor: Wedepohl, K.H.). Springer Verlag, Berlin.

HEIER, K.S. and BILLINGS, G.K. (1970b): Potassium. In: Handbook of geochemistry (section 19; editor: Wedepohl, K.H.). Springer Verlag, Berlin.

HENDERSON, P. (1986): Inorganic Geochemistry. Third edition, M.C. Robert Maxwell, Pergamon Press, Oxford.

HESSISCHER MINISTER FÜR LANDWIRTSCHAFT UND FORSTEN (1986): Bericht zur Schwermetall-Situation landwirtschaftlich genutzter Böden in Hessen. Die kleine Hessen-Bibl. Erkenntnisse, Einblicke.

HOFFMANN, G.G., SCHWEIGER, P., SCHOLL, W. and SCHMID, R. (1981): Grundbelastung der Böden von Baden-Württemberg mit Schwermetallen. Landwirtschaftliche Forschung (Sonderheft), 38: 324-37.

HÖRMANN, P.K. (1969): Beryllium. In: Handbook of geochemistry (section 4; editor: Wedepohl, K.H.). Springer Verlag, Berlin.

HORTENSIUS, D. and NORTCLIFF, S. (1991): International standardization of soil quality measurement procedures for the purpose of soil protection. Soil Use and Management, 7(3): 163-66.

HOUK, R.S. (1986): Mass spectrometry of inductively coupled plasmas. Analytical Chemistry, Vol. 58, 1: 97-105.

JACKSON, M.L. (1986): Geochemical characteristics of land and its effect on human heart and cancer death rates in the United States and China. Applied Geochemistry, 1: 175-80.

JACKSON, M.L., ZHANG, J.Z., LI, C.S. and MARTIN, D.F. (1986): The geochemical availability of soil Zn and Mo in relation to stomach and oesophageal cancer in the People's Republic of China and U.S.A. *Appl. Geochem.*, 1: 487-92.

JENNY, H. (1941): *Factors of soil formation - A system of quantitative pedology.* McGraw-Hill, New York.

JUNG, J., ISERMANN, K. and HENJES, G. (1979): Einfluß von cadmiumhaltigen Düngerphosphaten auf die Cadmiumanreicherung von Kulturböden und Nutzpflanzen. *Landwirtschaftliche Forschung*, 32: 262-82.

KABATA-PENDIAS, A. and PENDIAS, H. (1985): *Trace elements in soils and plants.* CRC Press, Florida.

KASIMOV, N.S. and PEREL'MAN, A.I. (1994): Geochemical barriers in environmental aspects. *Transactions of the 15th International Congress of Soil Science, Acapulco, Mexico, Volume 3B, Commission II*, 38-39.

KELLY, R.T. (1980): Site investigation and materials problems. In: *Reclamation of contaminated land. Proceedings of the Society of Chemical Industry conference held at the Congress Theatre, Eastbourne, UK, October 1979, London (Society of Chemical Industry).*

KERNDORFF, H. and SCHNITZER, M. (1980): Sorption of metals on humic acid. *Geochim. Cosmochim. Acta*, 44: 1701-8.

KESEL, R.H. and SPICER, B.E. (1985): Geomorphologic relationships and ages of soils on alluvial fans in the Rio General Valley, Costa Rica. *Catena*, 12: 149-66.

KIRKBY, M.J. (1969): Infiltration, throughflow and overland flow. In: *Water, earth and man* (editor Chorley, R.J.), Methuen, London, 215-27.

KLOKE, A. (1980): Richtwerte 80': Orientierungsdaten für tolerierbare Gesamtgehalte einiger Elemente in Kulturböden. *Mitt. VDLUFA*, 1-3: 9-11.

KORITNIG, S. (1972): Fluorine. In: *Handbook of geochemistry* (section 9; editor: Wedepohl, K.H.). Springer Verlag, Berlin.

KRAUSKOPF, K.B. (1970): Tungsten. In: *Handbook of geochemistry* (section 74; editor: Wedepohl, K.H.). Springer Verlag, Berlin.

KRAUSKOPF, K.B. (1979): *Introduction to geochemistry. Second edition,* McGraw-Hill, Tosho Printing, Tokyo.

LAKIN, H.W. (1972): Selenium accumulation in soils and its absorption by plants and animals. *Geol. Soc. Am. Bull.*, 83: 181-90.

LAMBRECHTS, J.J.N. (1979): Geology, geomorphology and soils. In: Fynbos ecology: a preliminary synthesis (editors Day J., Siegfried W.R., Louw G.N. and Jarman M.L.), South African National Scientific Programmes Report No. 40.

LAMBRECHTS, J.J.N. (1983): Soils, soil processes and soil distribution in the fynbos region: an introduction. In: Fynbos ecology: a preliminary synthesis (editors Deacon H.J., Hendey Q.B. and Lambrechts J.J.N.), South African National Scientific Programmes Report No. 75.

LANDERGREN, S. (1974): Vanadium. In: Handbook of geochemistry (section 23; editor: Wedepohl, K.H.). Springer Verlag, Berlin.

LAWLESS, P.J. (1972): Some aspects of the geochemistry of weathering profiles of Malmesbury Formation rocks in the Diep River catchment area. Unpublished honours project. Department of Geological Sciences, University of Cape Town.

LEUTWEIN, F. (1972): Selenium. In: Handbook of geochemistry (section 34; editor: Wedepohl, K.H.). Springer Verlag, Berlin.

LITAOR, M.I., DAN, Y. and KOYUMDJISKY, H. (1989): Factor Analysis of a lithosequence in the northeastern Samaria steppe (Israel). *Geoderma*, 44: 1-15.

LÖLF (Landesanstalt für Ökologie, Landschaftsentwicklung und Forstplanung Nordrhein-Westfalen; 1987): Mindestuntersuchungsprogramm Kulturboden (Authors: König, W. and Hembrock, A.), Düsseldorf, Germany.

LÖLF (Landesanstalt für Ökologie, Landschaftsentwicklung und Forstplanung Nordrhein-Westfalen; 1988): Mindestuntersuchungsprogramm Kulturboden zur Gefährdungsabschätzung von Altablagerungen und Altstandorten im Hinblick auf eine landwirtschaftliche oder gärtnerische Nutzung. Recklinghausen, Germany.

LUX, W. (1981): Gesamtgehalte von Schwermetallen (As, Pb, Cu, Zn) in Böden und Pflanzen im Südosten Hamburgs. *Landwirtschaftliche Forschung*, 38: 363-73.

MARTIN, B.A. (1973): A geochemical study of weathering profiles in Cape granites of the Cape Peninsula. Unpublished honours project. Department of Geological Sciences, University of Cape Town.

MATTHES, S. (1983): Mineralogy: Eine Einführung in die spezielle Mineralogie, Petrologie und Lagerstättenkunde. Springer-Verlag, Berlin.

MERIAN, E. (editor; 1984): Metalle in der Umwelt: Verteilung, Analytik und biologische Relevanz. Verlag Chemie, Weinheim, Florida, Basel.

MERRYWEATHER, F.R. (1965): The soils of the Wellington-Malmesbury area. M.Sc. thesis (unpublished), University of Stellenbosch.

- MERTZ, W. (1981): The essential trace elements. *Science*, 213: 1332-8.
- MINARIK, L., ABSOLON, K., KÖLLNEROVA, Z. and KLECKA, M. (1983): Chemical changes of granite during its weathering. In: *Leaching and diffusion in rocks and their weathering products* (editor Augustithis, S.S.). Theophrastus Publications S.A., Athens.
- MINISTERIE VROM (Ministerie van Volkshuisvestning, Ruimtelijke Ordening en Milieubeheer; 1983): *Leidraad bodemsanering*. s'Gravehage, Netherlands.
- MOORE, J.M. and PICKER, M.D. (1991): Heuweltjies (earth mounds) in the Clanwilliam district, Cape Province, South Africa: 4000-years old termite nests. *Oecologia*, 86: 424-32.
- MOURA, M.L. AND KROONENBERG, S.B. (1988): Major and minor elements geochemistry and mineralogy of four soil profiles from Araracuara, Colombian Amazonas. *Catena*, 15: 81-97.
- MUNNIK, M.C., VERSTER, E. and VAN ROOYEN, T.H. (1992): Spatial pattern and variability of soil and hillslope properties in a granitic landscape, 2. Pretoria - Johannesburg area. *S. Afr. J. Plant Soil*, 9(2): 43-51.
- MUNSELL SOIL COLOR CHARTS (1992): Macbeth Division of Kollmorgen Instruments Corporation, New York.
- NAIDU, R., deLACY, N.J., KOOKANA, R.S., BOLAN, N.S. and TILLER, K.G. (1994): Effect of inorganic ligands on adsorption of cadmium by soils. *Transactions of the 15th International Congress of Soil Science, Acapulco, Mexico, Volume 3B, Commission II*, 190-191.
- NAIR, A.M. and NARAYANASWAMY (1983): Leaching - diffusion - adsorption processes in rocks, clays and laterites from Kerala, India. In: *Leaching and diffusion in rocks and their weathering products* (editor Augustithis, S.S.). Theophrastus Publications S.A., Athens.
- NAW (Normenausschuß Wasserwesen im deutschen Institut für Normung e.V.; 1993): *Ammoniumextraktion zur Bestimmung mobiler Spurenelemente in Mineralböden (DIN V 19730: preliminary German standard method)*. Printed by and to be purchased from: Beuth Verlag GmbH, Burghafenstr. 6, 1000 Berlin 30, Germany.
- NESBITT, H.W. and YOUNG, G.M. (1982): Early proterozoic climates and plate motions inferred from major element chemistry of lutites. *Nature*, 299: 715-17.
- NESBITT, H.W. and YOUNG, G.M. (1989): Formation and diagenesis of weathering profiles. *J. Geology*, 97(2): 129-47.

NON-AFFILIATED SOIL ANALYSIS WORKING COMMITTEE (1990): Handbook of standard soil testing methods for advisory purposes. Soil Science Society of SA, Pretoria.

NORRISH, K. and HUTTON, J.T. (1969): An accurate X-ray spectrometric method for the analyses of a wide range of geological samples. *Geochim. Cosmochim. Acta*, 33: 431-53.

NRIAGU, J.O. and PACYNA, J.M. (1988): Quantitative assessment of worldwide contamination of air, water and soils by trace elements. *Nature*, 333: 134-9.

NYAMAPFENE, K.W. (1986): Some relationships between topography and sodic soils in Zimbabwe. *Z. Geomorph. N. F.*, 30(1): 47-52.

ODEN, W.I., AMY, G.L. and CONKLIN, M. (1993): Subsurface interactions of humic substances with Cu(II) in saturated media. *Environ. Sci. Technol.*, 27(6): 1045-51.

ONISHI, H. and SANDELL, E.B. (1955a): Geochemistry of arsenic. *Geochim. Cosmochim. Acta*, 7: 1-33.

ONISHI, H. and SANDELL, E.B. (1955b): Notes on the geochemistry of antimony. *Geochim. Cosmochim. Acta*, 8: 213-21.

ONISHI, H. (1969a): Arsenic. In: Handbook of geochemistry (section 33; editor: Wedepohl, K.H.). Springer Verlag, Berlin.

ONISHI, H. (1969b): Antimony. In: Handbook of geochemistry (section 51; editor: Wedepohl, K.H.). Springer Verlag, Berlin.

ORR, W. (1974): Sulfur. In: Handbook of geochemistry (section 16; editor: Wedepohl, K.H.). Springer Verlag, Berlin.

PLOEY, J. AND MOEYERSONS, J. (1975): Runoff creep of coarse debris: experimental data and some field observations. *Catena*, 2: 275-88.

POESEN, J. and LAVEE, H. (1994): Rock fragments in top soils: significance and processes. *Catena*, 23: 1-28.

PRICE, W.J. (1979): Spectrochemical analysis by atomic absorption. London, Philadelphia, Rheine.

PRÜEB, A., TURIAN, G. and SCHWEIKLE, V. (1991): Ableitung kritischer Gehalte an  $\text{NH}_4\text{NO}_3$ -extrahierbaren ökotoxikologisch relevanten Spurenelementen in Böden SW-Deutschlands. *Mitt. Dtsch. Bodenkundl. Gesellsch.*, 66(I):385-88.

PRÜEB, A. (1992): Vorsorgewerte und Prüfwerte für mobile und mobilisierbare, potentiell ökotoxische Spurenelemente in Böden. Verlag U.E. Grauer, Wendlingen.

PUCHELT, H. (1972): Barium. In: Handbook of geochemistry (section 56; editor: Wedepohl, K.H.). Springer Verlag, Berlin.

PURVES, W.D. (1976): A detailed investigation into the genesis of granite-derived soils. Ph.D. thesis, University of Rhodesia.

PYE, K. (1986): Mineralogical and textural controls on the weathering of granitoid rocks. *Catena*, 13: 47-57.

RAVEN, M.D. (1990): XPLO program: Manipulation of X-ray powder diffraction data. CSIRO, Division of Soils, Adelaide (Australia).

ROBSON, S. (1980): A report on a project to investigate the occurrence of cassiterite and wolframite on the farm "Langverwacht" at the Kuils River in the Cape Province. Unpublished report. Department of Geological Sciences, University of Cape Town.

ROGERS, J.J.W. and ADAMS, J.A.S. (1969): Uranium. In: Handbook of geochemistry (section 92; editor: Wedepohl, K.H.). Springer Verlag, Berlin.

RÖSLER, H.J. (1981): Lehrbuch der Mineralogie. VEB Deutscher Verlag für Grundstoffindustrie, second edition, Leipzig.

RUHE, R.V. and WALKER, P.H. (1968): Hillslope models and soil formation, I. Open Systems. *Trans. 9th Int. Congress Soil Sci.*, Adelaide, pp. 551-560.

RUPPERT, H. (1987): Natürliche Grundgehalte und anthropogene Anreicherungen von Schwermetallen in Böden Bayerns. Bayerisches Geologisches Landesamt (GLA-Fachberichte), München.

SALONEN, J.T., ALFTHAN, G., HUTTUNEN, J.K. and PUSKA, P. (1984): Association between serum selenium and the risk of cancer. *Am. J. Epidemiology*, 120(3): 342-49.

SAS INSTITUTE INC. (1988): SAS/STAT program, Release 6.03 Edition. Cary, NC: SAS Institute Inc.

SCHEFFER, F. and SCHACHTSCHABEL, P. (1989): Lehrbuch der Bodenkunde. 12. edition revised by: SCHACHTSCHABEL, P., BLUME, H.P., BRÜMMER, G., HARTGE, K.H. and SCHWERTMANN, U., Enke Verlag, Stuttgart.

SCHLOEMANN, H. (1992): The distribution of health-related elements in the different soil types between Piketberg and Cape Town. A poster presented at the 17th Congress of the Soil Science Society of SA, Stellenbosch, January, 1992.

SCHLOMS, B.H.A., ELLIS, F. and LAMBRECHTS, J.J.N. (1983): Soils of the Cape Coastal Platform. In: Fynbos ecology: a preliminary synthesis (editors Deacon H.J., Hendey Q.B. and Lambrechts J.J.N.), South African National Scientific Programmes Report No. 75.

SCHRAUZER, G.N., WHITE, D.A. and SCHNEIDER, C.J. (1977): Cancer mortality correlation studies-III: Statistical associations with dietary selenium intakes. *Bioinorganic Chemistry*, 7: 23-34.

SCHUMM, S.A. (1967): Rates of surficial rock creep on hillslopes in western Colorado. *Science*, 155: 560-61.

SCHWARZ, K. (1965): Selenium and kwashiorkor. *Lancet*, i: 1335.

SCHWEITZER, F.R. (1974): Excavations at Die Kelders, Cape Province, South Africa, in the Holocene Deposits. *Annals of the South African Museum*, 78: 101-233.

SCHWERTMANN, U. and TAYLOR, R.M. (1989): Iron oxides. In: *Minerals in soil environments* (editors Dinauer, R.C., Dixon, J.B. and Weed, S.B.), Soil Science Society of America, second edition, Madison, Wisconsin.

SCOTT, M.J. (1969): Cassiterite deposits at Kuils River, South Western Cape Province. Unpublished honours project. Department of Geological Sciences, University of Cape Town.

SELBY, M.J. (1982): *Hillslope materials and processes*. Oxford University Press, Oxford.

SHACKLETTE, H.T. and BOERNGEN, J.G. (1984): Element concentrations in soils and other surficial materials of the conterminous United States. U.S. Geol. Surv. Prof. Paper 1270.

SHACKLETTE, H.T., HAMILTON, J.C., BOERNGEN, J.G. and BOWLES, J.M. (1971): Elemental composition of superficial materials in the conterminous United States. U.S. Geol. Surv. Prof. Paper 574-D, U.S. Government Printing Office, Washington, D.C.

SHAMBERGER, R.J. and WILLIS, C.E. (1971): Selenium distribution and human cancer mortality. *CRC Critical Reviews Clin. Lab. Sci.*, 2: 211-21.

SHIRAKI, K. (1978): Chromium. In: *Handbook of geochemistry* (section 24; editor: Wedepohl, K.H.). Springer Verlag, Berlin.

SMITH, H.S. (1972): Some aspects of the geochemistry of weathering profiles of the Malmesbury rocks in the Diep River Catchment Area. Unpublished honours project. Department of Geological Sciences, University of Cape Town.

SMITH, M.A. (1980): Standards for the redevelopment of contaminated land. In: Reclamation of contaminated land. Proceedings of the Society of Chemical Industry conference held at the Congress Theatre, Eastbourne, UK, October 1979, London (Society of Chemical Industry).

SOIL CLASSIFICATION WORKING GROUP (1991): Soil Classification: A taxonomic system for South Africa. Soil and Irrigation Research Institute in the Department of Agricultural Development, Pretoria.

SPOSITO, G. (1989): The chemistry of soils. Oxford University Press, New York, Oxford.

STATGRAPHICS (1993): Version 7 for DOS. Manugistics, Inc., 2115 East Jefferson Street, Rockville, Maryland 20852-4999, USA.

STATHAM, I. (1977): Earth surface sediment transport. Clarendon Press, London.

STEPHEN, I. (1952): A study of rock weathering with reference to the soils of the Malvern hills. *J. Soil Sci.*, 3(1): 20-33.

STEVENS, P.R. and WALKER, T.W. (1970): The chronosequence concept and soil formation. *Q. Rev. Biol.*, 45(4): 333-50.

STEVENSON, F.J. (1982): Humus chemistry: genesis, compositions, reactions. Wiley-Interscience Publication, John Wiley and Sons, New York.

SWAINE, D.J. (1990): Trace elements in coal. Butterworths, London.

SWAINE, D.J. (1955): The trace element content of soils. *Commonw. Bur. Soil Sci. Tech. Commun.*, 48: 157 pp.

SWANSON, D.K. (1985): Soil catenas on Pinedale and Bull Lake moraines, Willow Lake, Wind River Mountains, Wyoming. *Catena*, 12: 329-42.

SYMEONIDES, C. and MCRAE, S.G. (1977): The assessment of plant-available cadmium in soils. *J. Environ. Qual.*, 6: 120-23.

TALBOT, W.J. (1947): Swartland and Sandveld: A survey of land utilization and soil erosion in the Western Lowland of the Cape Province. Oxford University Press, Cape Town.

THERON, G.N. (1991): Geological Map - Cape Town (3318, 1:250000). Geological Survey of South Africa.

TOPPING, N.J. (1972): Some aspects of the geochemistry of weathering profiles of Malmesbury rocks in the Diep River catchment area. Unpublished honours project. Department of Geological Sciences, University of Cape Town.

- TORRENT, J. (1994): Iron oxides in Mediterranean soils: properties and influence on soil behaviour. Transactions of the 15th International Congress of Soil Science, Acapulco, Mexico, Volume 8A, Symposium VIIA, 2-14.
- TROEH, F.R. (1975): Measuring soil creep. Soil Sci. Soc. Am. Proc., 39: 707-9.
- TUREKIAN, K.K. and WEDEPOHL, K.H. (1961): Distribution of the elements in some major units of the earth's crust. Geol. Soc. Am. Bull., 72: 175-92.
- TUREKIAN, K.K. (1978): Cobalt. In: Handbook of geochemistry (section 27; editor: Wedepohl, K.H.). Springer Verlag, Berlin.
- VALENTIN, C. (1994): Surface sealing as affected by various rock fragment covers in West Africa. Catena, 23: 87-97.
- VAN DER SLOOT, H.A., PIEPERS, O. and KOK, A. (1984): A standard leaching test for combustion residues (BEOP-31). Studiegroep Ontwikkeling Standaard Uitloogtesten Verbrandingsresiduen (SOSUV), Translation of BEOP-25, Amsterdam.
- VAN DRIEL, W. and SMILDE, K.W. (1981): Heavy-metal contents of Dutch arable soils. Landwirtschaftliche Forschung (Sonderheft), 38: 305-313.
- VAN NIEKERK, B.J. (1967): The soils of the Darling area. M.Sc. thesis (unpublished), University of Stellenbosch.
- VINOGRADOV, A.P. (1959): The geochemistry of rare and dispersed chemical elements in soils. Consultants Bureau, Inc., New York.
- WALTON, C., DAVIES, G. and O'HAGAN, T. (editors; 1984): Reader's Digest Atlas of Southern Africa. Cape Town.
- WANTY, R.B. and GOLDHABER, M.B. (1992): Thermodynamics and kinetics of reactions involving vanadium in natural systems: accumulation of vanadium in sedimentary rocks. Geochim. Cosmochim. Acta, 56: 1471-83.
- WATERLOW, J.C. (1965): Selenium content of fish flour and kwashiorkor. Lancet, i: 869.
- WEAST, R.C. (editor; 1975-1976): Handbook of Chemistry and Physics (56th Edition). Cleveland, Ohio.
- WEATHER BUREAU (1980): Climate of South Africa (Part 8). General survey, WB 28, Government Printer, Pretoria.
- WEBSTER, R. (1965): A catena of soils on the Northern Rhodesia plateau. J. of Soil Science, 16: 31-43.

WEDEPOHL, K.H. (1969-1978): Handbook of Geochemistry. Springer-Verlag, Berlin.

WEDEPOHL, K.H. (1974): Lead. In: Handbook of geochemistry (section 82; editor: Wedepohl, K.H.). Springer Verlag, Berlin.

WEDEPOHL, K.H. (1978): Manganese. In: Handbook of geochemistry (section 25; editor: Wedepohl, K.H.). Springer Verlag, Berlin.

WELLINGTON, J.H. (1955): South Africa, a geographical study. Cambridge University Press, London.

WILDING, L.P., SMECK, N.E. and DREES, L.R. (1977): Silica in soils: quartz, cristobalite, tridymite and opal. In: Minerals in soil environments, pp. 471-552 (Soil Sci. Soc. Am.: Wisc.).

WILLIAMS, M.A.J. (1974): Surface rock creep on sandstone slopes in the northern territory of Australia. Australian Geographer, XII(5): 419-24.

WILLIS, J.P. (1991): Mass absorption coefficient determination using Compton scattered tube radiation: applications, limitations and pitfalls. Advances in X-ray analysis, 34: 243-61.

YOUNG, R.W., NANSON, G.C. and JONES, B.G. (1987): Weathering of late Pleistocene alluvium under a humid temperate climate: Cranebrook Terrace, southeastern Australia. Catena, 14: 469-84.

ZEIEN, H. and BRÜMMER, G.W. (1992): Analysenvorschrift zur Extraktion der mobilen und leicht nachlieferbaren Schwermetalle. Methodenvorschrift des Institut für Bodenkunde der Universität Bonn (unpublished), Bonn.

## APPENDIX-I: Description and classification of individual soil profiles

Pit No: 1  
 Map/photo: 3318AD; P1 (profile)  
 Latitude & Longitude: 33° 24'6"/18° 18'16"  
 Vegetation/Landuse: Fynbos  
 Distance to next public road<sup>1</sup>: 1  
 Distance to arable land<sup>2</sup>: Unknown  
 Date described: 1990-07

Soil form: Fernwood  
 Soil family: Penicuik  
 Terrain unit<sup>3</sup>: 4  
 Water table: None  
 Distance to next pasture<sup>1</sup>: Unknown  
 Described by: H Schloemann & A B Oosthuizen<sup>2</sup>

Underlying material: Coastal sand

Horizon	Depth (cm)	Description	Diagnostic horizons	Samples
A	0- 60	Grey with blackish mottles (due to accumulation of organic matter); pure medium sand; single-grained; loose; effervescence with HCl: none; fine roots common; gradual smooth transition.	Orthic	1A
E	60- 100 +	Pale brownish grey; pure medium sand; single-grained; loose; effervescence with HCl: none.	E-horizon	1E

Remarks: None

<sup>1</sup> Explanation of code in table on last page of this appendix (Table App-1, page 286).

<sup>2</sup> ISCW - Institute for Soil, Climate and Water; Private Bag, Eisenburg, 7607.

Pit No: 2  
 Map/photo: 3318AD; P2 (profile)  
 Latitude & Longitude: 33° 23'57"/18° 18'27"  
 Vegetation/Landuse: Fynbos  
 Distance to next public road<sup>1</sup>: 1  
 Distance to next pasture<sup>1</sup>: Unknown  
 Date described: 1990-07

Soil form: Fernwood  
 Soil family: Penicuik  
 Terrain unit<sup>1</sup>: 4  
 Water table: None  
 Distance to arable land<sup>1</sup>: Unknown  
 Described by: H Schloemann & A B Oosthuizen<sup>2</sup>

Underlying material: Coastal sand

Horizon	Depth (cm)	Description	Diagnostic horizons	Samples
A	0- 65	Grey with blackish mottles (due to accumulation of organic matter); pure medium sand; single-grained; loose; effervescence with HCl: none; fine roots common; gradual smooth transition.	Orthic	2A
E	65- 110 +	Pale brownish grey; pure medium sand; single-grained; loose; effervescence with HCl: none.	E-horizon	2E

Remarks: None

<sup>1</sup> Explanation of code in table on last page of this appendix (Table App-1, page 286).

<sup>2</sup> ISCW - Institute for Soil, Climate and Water; Private Bag, Eisenburg, 7607.

Pit No: 3  
 Map/photo: 3318AD; none  
 Latitude & Longitude: 33° 26'0"/18° 16'12"  
 Vegetation/Landuse: pasture  
 Distance to next public road<sup>1</sup>: 1  
 Distance to next pasture<sup>1</sup>: 7  
 Date described: 1990-07

Soil form: Fernwood or Lamotte  
 Soil family: Unknown  
 Terrain unit<sup>1</sup>: Unknown  
 Water table: None  
 Distance to arable land<sup>1</sup>: Unknown  
 Described by: H Schloemann & A B Oosthuizen<sup>2</sup>

Underlying material: Coastal sand

Horizon	Depth (cm)	Description	Diagnostic horizons	Samples
A	0- 110+	Dark grey; pure medium sand; single-grained; loose; effervescence with HCl: none; fine roots common.	Orthic	3A

Remarks: High proportion of organic matter.

---

<sup>1</sup> Explanation of code in table on last page of this appendix (Table App-1, page 286).

<sup>2</sup> ISCW - Institute for Soil, Climate and Water; Private Bag, Eisenburg, 7607.

Pit No: 4  
 Map/photo: 3318AD; none  
 Latitude & Longitude: 33° 26'10"/18° 16'8"  
 Vegetation/Landuse: Fynbos  
 Distance to next public road<sup>1</sup>: 1  
 Distance to next pasture<sup>1</sup>: Unknown  
 Date described: 1990-07

Soil form: Fernwood or Namib  
 Soil family: Unknown  
 Terrain unit: Lower footslope of dune  
 Water table: None  
 Distance to arable land<sup>1</sup>: Unknown  
 Described by: H Schloemann & A B Oosthuizen<sup>2</sup>

Underlying material: Calcareous coastal sand

Horizon	Depth (cm)	Description	Diagnostic horizons	Samples
A	0- 30	Dark grey; pure medium sand; single-grained; loose; effervescence with HCl: strong; fine roots common; gradual smooth transition.	Orthic	4A
E	30- 50+	Light grey; pure medium sand; single-grained; loose.	E-horizon	None

Remarks: None

<sup>1</sup> Explanation of code in table on last page of this appendix (Table App-1, page 286).  
<sup>2</sup> ISCW - Institute for Soil, Climate and Water; Private Bag, Eisenburg, 7607.

Pit No: 5  
 Map/photo: 3318AD; P3 (profile)  
 Latitude & Longitude: 33° 28'24" / 18° 26'50"  
 Vegetation/Landuse: Cultivated pastures  
 Distance to next public road<sup>1</sup>: 3  
 Distance to next pasture<sup>2</sup>: 7  
 Date described: 1990-07

Soil form: Kroonstad  
 Soil family: Unknown  
 Terrain unit<sup>1</sup>: 4  
 Water table: 650 mm  
 Distance to arable land<sup>1</sup>: Unknown  
 Described by: H Schloermann & A B Oosthuizen<sup>2</sup>

Underlying material: Granite

Horizon	Depth (cm)	Description	Diagnostic horizons	Samples
A	0- 65	Wet; brown; loamy coarse sand; weak fine crumb; friable; effervescence with HCl: none; gradual smooth transition;	Orthic	5A
E	65- 75		E-horizon	None

Remarks: The occurrence of perched ground water did not allow to describe the E-horizon in more detail and suggested the existence of a relatively fine-textured subsoil (less permeable). It is presumed that the subsoil qualifies for a G-horizon because gleyed horizons were observed in near-by pits.

<sup>1</sup> Explanation of code in table on last page of this appendix (Table App-1, page 286).

<sup>2</sup> ISCW - Institute for Soil, Climate and Water; Private Bag, Eisenburg, 7607.

Pit No: 6  
 Map/photo: 3318AD; P4 (profile)  
 Latitude & Longitude: 33° 28'11" / 18° 26'41"  
 Vegetation/Landuse: Cultivated pastures  
 Distance to next public road<sup>1</sup>: 3  
 Distance to next pasture<sup>1</sup>: 7  
 Date described: 1990-07

Soil form: Cartref  
 Soil family: Frosterley  
 Terrain unit<sup>1</sup>: 3  
 Water table: None  
 Distance to arable land<sup>1</sup>: Unknown  
 Described by: H Schloemann & A B Oosthuizen<sup>2</sup>

Underlying material: Granite

Horizon	Depth (cm)	Description	Diagnostic horizons	Samples
A	0- 40	Wet; brown; loamy coarse sand; weak fine crumb; friable; effervescence with HCl: none; gradual smooth transition.	Orthic	6AE <sup>3</sup>
E	40- 50	Wet; light brown; loamy coarse sand; weak fine crumb; friable; effervescence with HCl: none; common fine quartz gravel; common fine sesquioxide concretions; clear smooth transition.	E-horizon	6AE <sup>3</sup>
B	50- 70+	Wet; red brown; clay; massive; firm; effervescence with HCl: none.	Lithocutanic	6B

Remarks: None

<sup>1</sup> Explanation of code in table on last page of this appendix (Table App-1, page 286).

<sup>2</sup> ISCW - Institute for Soil, Climate and Water; Private Bag, Eisenburg, 7607.

<sup>3</sup> The A-horizon and the E-horizon were sampled as a composite.

**Pit No: 7**

Map/photo: 3318AD; P5 (profile)  
Latitude & Longitude: 33° 24'40" / 18° 26'21"  
Vegetation/Landuse: Vineyards  
Distance to next public road<sup>1</sup>: 1  
Distance to next pasture<sup>1</sup>: Unknown  
Date described: 1990-07

Soil form: Unknown  
Soil family: Unknown  
Terrain unit<sup>1</sup>: Unknown  
Water table: 750 mm  
Distance to arable land<sup>1</sup>: 6  
Described by: H Schloemann & A B Oosthuizen<sup>2</sup>

**Underlying material: Ferruginized granite**

Horizon	Depth (cm)	Description	Diagnostic horizons	Samples
A	0- 70	Wet; brown; sandy loam; effervescence with HCl: none.	Orthic	7A
B	70- 75+	Wet; grey with brown red concretions; silty clay; loose; effervescence with HCl: none; few sesquioxide concretions; few quartz gravel.	Unknown	None

**Remarks:**

The B-horizon was not sampled due to the occurrence of perched ground water.

---

<sup>1</sup> Explanation of code in table on last page of this appendix (Table App-1, page 286).

<sup>2</sup> ISCW - Institute for Soil, Climate and Water; Private Bag, Eisenburg, 7607.

Pit No: 8  
 Map/photo: 3318AD; none  
 Latitude & Longitude: 33° 24'17" /18° 26'52"  
 Vegetation/Landuse: Vineyards  
 Distance to next public road<sup>1</sup>: 4  
 Distance to next pasture<sup>1</sup>: Unknown  
 Date described: 1990-07

Soil form: Hutton  
 Soil family: Suurbekom  
 Terrain unit<sup>1</sup>: 3  
 Water table: None  
 Distance to arable land<sup>1</sup>: 6  
 Described by: H Schloemann & A B Oosthuizen<sup>2</sup>

Underlying material: Ferruginized granite

Horizon	Depth (cm)	Description	Diagnostic horizons	Samples
A	0- 40	Reddish brown; loamy sand; massive; soft; effervescence with HCl: none; few quartz and feldspar gravel.	Orthic	8A
B	40- 65	Red laterite stones in light brown matrix; loam; weak fine crumb; hard; effervescence with HCl: none.	Red apedal	8B

Remarks: None

<sup>1</sup> Explanation of code in table on last page of this appendix (Table App-1, page 286).

<sup>2</sup> ISCW - Institute for Soil, Climate and Water; Private Bag, Eisenburg, 7607.

**Pit No: 9**

Map/photo: 3318AD; P6 (profile)  
Latitude & Longitude: 33° 18'24" /18° 26'21"  
Vegetation/Landuse: In between cultivated land and track  
Distance to next public road<sup>1</sup>: 3  
Distance to next pasture<sup>1</sup>: Unknown  
Date described: 1990-07

Soil form: Escourt  
Soil family: Zastron  
Terrain unit<sup>1</sup>: 5  
Water table: 500 mm  
Distance to arable land<sup>1</sup>: Unknown  
Described by: H Schloemann & A B Oosthuizen<sup>2</sup>

Underlying material: Unconsolidated sands of granitic origin

Horizon	Depth (cm)	Description	Diagnostic horizons	Samples
A	0- 30	Wet; dark brown; loamy medium to coarse sand; weak fine crumb; friable; effervescence with HCl: none; clear smooth transition.	Orthic	9A
E	30- 50	Wet; pale brown; loamy coarse sand; weak fine crumb; friable; effervescence with HCl: none.	E-horizon	None

**Remarks:**

The occurrence of perched ground water implies the existence of a fine-textured (less permeable) subsoil. It is presumed that this subsoil is prismaticcutanic because prismaticcutanic B-horizons were observed in near-by pits.

---

<sup>1</sup> Explanation of code in table on last page of this appendix (Table App-1, page 286).

<sup>2</sup> ISCW - Institute for Soil, Climate and Water; Private Bag, Eisenburg, 7607.

Pit No: 10

Map/photo: 3318AD; none

Latitude & Longitude: 33° 16'15"/18° 27'2"

Vegetation/Landuse: In between cultivated land and track

Distance to next public road<sup>1</sup>: 2

Distance to next pasture<sup>1</sup>: Unknown

Date described: 1990-07

Soil form: Kroonstad

Soil family: Unknown

Terrain unit<sup>1</sup>: 5

Water table: 350 mm

Distance to arable land<sup>1</sup>: Unknown

Described by: H Schloemann & A B Oosthuizen<sup>2</sup>

Underlying material: Unconsolidated sands of granitic origin

Horizon	Depth (cm)	Description	Diagnostic horizons	Samples
A	0- 30	Wet; brown; loamy fine sand; weak fine crumb; friable; effervescence with HCl: none; few sesquioxide concretions; gradual smooth transition;	Orthic	10A
E	30- 40+	Wet; pale brown; loamy fine sand; single-grained; loose; effervescence with HCl: none; many sesquioxide concretions.	E-horizon	None

Remarks:

The occurrence of perched ground water did not allow to describe the E-horizon in more detail and suggested the existence of a relatively fine-textured subsoil (less permeable). It is presumed that the subsoil qualifies for a G-horizon because gleyed horizons were observed in near-by pits.

<sup>1</sup> Explanation of code in table on last page of this appendix (Table App-1, page 286).

<sup>2</sup> ISCW - Institute for Soil, Climate and Water; Private Bag, Eisenburg, 7607.

Pit No: 11  
 Map/photo: 3318AD; P7 (profile)  
 Latitude & Longitude: 33° 17'0"/18° 26'52"  
 Vegetation/Landuse: In between cultivated land and public road  
 Distance to next public road<sup>1</sup>: 6  
 Distance to next pasture<sup>1</sup>: Unknown  
 Date described: 1990-07

Soil form: Unknown  
 Soil family: Unknown  
 Terrain unit<sup>1</sup>: 5  
 Water table: 500 mm  
 Distance to arable land<sup>1</sup>: Unknown  
 Described by: H Schloemann & A B Oosthuizen<sup>2</sup>

Underlying material: Unconsolidated sands of granitic origin

Horizon	Depth (cm)	Description	Diagnostic horizons	Samples
A	0- 20	Wet; grey, sandy loam; weak fine crumb; friable; effervescence with HCl: none; few roots; clear tonguing transition.	Orthic	11A
E	20- 45+	Wet; pale grey; sandy loam; weak fine crumb; friable; effervescence with HCl: none; with two burrows filled with material from the A-horizon.	E-horizon	11E

Remarks: The occurrence of perched ground water suggested the existence of a fine-textured (less permeable) subsoil. The soil profile is not classified because a description and classification of the subsoil was not possible.

<sup>1</sup> Explanation of code in table on last page of this appendix (Table App-1, page 286).

<sup>2</sup> ISCW - Institute for Soil, Climate and Water; Private Bag, Eisenburg, 7607.

Pit No: 12

Map/photo: 3318AD; P8 (profile)

Latitude & Longitude: 33° 20'10"/18° 22'48"

Vegetation/Landuse: In between public road and cultivated land

Distance to next public road<sup>1</sup>: 6

Distance to next pasture<sup>1</sup>: Unknown

Date described: 1990-07

Soil form: Hutton

Soil family: Suurbekom

Terrain unit<sup>1</sup>: 4

Water table: None

Distance to arable land<sup>1</sup>: 5

Described by: H Schloemann & A B Oosthuizen<sup>2</sup>

Underlying material: Ferruginized granite

Horizon	Depth (cm)	Description	Diagnostic horizons	Samples
A	0- 25	Wet; dark brown; sandy loam; weak medium crumb; friable; effervescence with HCl: none; clear smooth transition.	Orthic	12A
B	25- 45	Wet; reddish brown; loam; weak medium subangular blocky; slightly hard; effervescence with HCl: none; few sesquioxide concretions; few laterite gravel; clear smooth transition.	Red apedal	12B
C	45- 85+	Wet; yellowish red; clay loam; moderate crumb; hard; effervescence with HCl: none; many (coarse) laterite gravel.		None

Remarks: The C-horizon consists mainly of weathered laterite.

<sup>1</sup> Explanation of code in table on last page of this appendix (Table App-1, page 286).

<sup>2</sup> ISCW - Institute for Soil, Climate and Water; Private Bag, Eisenburg, 7607.

Pit No: 13

Map/photo: 3318AD; P10 (profile)

Latitude & Longitude: 33° 18'50"/18° 21'39"

Vegetation/Landuse: In between public road and cultivated land

Distance to next public road<sup>1</sup>: 6

Distance to next pasture<sup>1</sup>: Unknown

Date described: 1990-07

Soil form: Escourt

Soil family: Zastron

Terrain unit<sup>1</sup>: 5

Water table: 400 mm

Distance to arable land<sup>1</sup>: 5

Described by: H Schloermann & A B Oosthuizen<sup>2</sup>

Underlying material: Unconsolidated sands of granitic origin

Horizon	Depth (cm)	Description	Diagnostic horizons	Samples
A	0- 20	Wet; dark brown; coarse sandy loam; weak fine crumb; soft; effervescence with HCl: none; clear smooth transition.	Orthic	13AE <sup>3</sup>
E	20- 50	Wet; brown; coarse sandy loam; weak fine crumb; soft; effervescence with HCl: none.	E-horizon	13AE <sup>3</sup>

Remarks:

The occurrence of perched ground water implies the existence of a fine-textured (less permeable) subsoil. It is presumed that this subsoil is prismatic-tanic because prismatic-tanic B-horizons were observed in near-by pits.

---

<sup>1</sup> Explanation of code in table on last page of this appendix (Table App-1, page 286).

<sup>2</sup> ISCW - Institute for Soil, Climate and Water; Private Bag, Eisenburg, 7607.

<sup>3</sup> The A-horizon and the E-horizon were sampled as a composite.

Pit No: 16  
 Map/photo: 3318AD; S8, S9 (vegetation) & S10 (profile)  
 Latitude & Longitude: 33° 25'21"/18° 19'31"  
 Vegetation/Landuse: Fynbos  
 Distance to next public road<sup>1</sup>: 1  
 Distance to next pasture<sup>1</sup>: 1  
 Date described: 1990-11

Soil form: Fernwood  
 Soil family: Hopefield  
 Terrain unit<sup>1</sup>: 3  
 Water table: None  
 Distance to arable land<sup>1</sup>: 1  
 Described by: H Schloemann & A B Oosthuizen<sup>2</sup>

Underlying material: Coastal sand

Horizon	Depth (cm)	Description	Diagnostic horizons	Samples
A	0- 60	Dry; grey; pure medium sand; single-grained; loose; effervescence with HCl: none; gradual smooth transition.	Orthic	16Top & 16A
E	60- 110+	Wet; yellow; pure medium sand; single-grained; loose; effervescence with HCl: none.	E-horizon	16E

Remarks: None

<sup>1</sup> Explanation of code in table on last page of this appendix (Table App-1, page 286).

<sup>2</sup> ISCW - Institute for Soil, Climate and Water; Private Bag, Elsenburg, 7607.

Pit No: 17  
 Map/photo: 3318AD; S11 (vegetation)  
 Latitude & Longitude: 33° 25'28"/18° 19'2"  
 Vegetation/Landuse: Fynbos  
 Distance to next public road<sup>1</sup>: 1  
 Distance to next pasture<sup>1</sup>: 1  
 Date described: 1990-11

Soil form: Fernwood  
 Soil family: Hopefield  
 Terrain unit<sup>1</sup>: 5  
 Water table: None  
 Distance to arable land<sup>1</sup>: 1  
 Described by: H Schloemann & A B Oosthuizen<sup>2</sup>

Underlying material: Coastal sand

Horizon	Depth (cm)	Description	Diagnostic horizons	Samples
A	0- 100	Dry; grey; pure medium sand; single-grained; loose; effervescence with HCl: none; gradual smooth transition.	Orthic	17Top & 17A
E	100- 110+	Wet; yellow; pure medium sand; single-grained; loose; effervescence with HCl: none.	E-horizon	17E

Remarks: None

<sup>1</sup> Explanation of code in table on last page of this appendix (Table App-1, page 286).

<sup>2</sup> ISCW - Institute for Soil, Climate and Water; Private Bag, Eisenburg, 7607.

Pit No: 18  
 Map/photo: 3318AD; S12 (vegetation)  
 Latitude & Longitude: 33° 24'10"/18° 17'4"  
 Vegetation/Landuse: Fynbos & alien vegetation  
 Distance to next public road<sup>1</sup>: 3  
 Distance to next pasture<sup>1</sup>: 1  
 Date described: 1990-11

Soil form: Unknown  
 Soil family: Unknown  
 Terrain unit<sup>1</sup>: 5  
 Water table: None  
 Distance to arable land<sup>1</sup>: 1  
 Described by: H Schloemann & A B Oosthuizen<sup>2</sup>

Underlying material: Coastal sand

Horizon	Depth (cm)	Description	Diagnostic horizons	Samples
A	0- 20+	Dry; grey; pure medium sand; single-grained; loose; effervescence with HCl: none.	Orthic	18Top

Remarks: This pit is located in a distinct terrace of marine origin.

<sup>1</sup> Explanation of code in table on last page of this appendix (Table App-1, page 286).

<sup>2</sup> ISCW - Institute for Soil, Climate and Water; Private Bag, Eisenburg, 7607.

Pit No: 19

Map/photo: 3318AD; S14, S15 (vegetation)

Latitude & Longitude: 33° 26'16"/18° 16'54"

Vegetation/Landuse: Fynbos

Distance to next public road<sup>1</sup>: 1

Distance to next pasture<sup>1</sup>: 1

Date described: 1990-11

Soil form: Fernwood

Soil family: Unknown

Terrain unit<sup>1</sup>: 5

Water table: 1100 mm

Distance to arable land<sup>1</sup>: 1

Described by: H Schloemann & A B Oosthuizen<sup>2</sup>

Underlying material: Coastal sand

Horizon	Depth (cm)	Description	Diagnostic horizons	Samples
A	0- 110	Dry; grey; pure medium sand; single-grained; loose; effervescence with HCl: none; gradual smooth transition.	Orthic	19Top & 19A
E	110+	Wet; pale yellowish grey; pure medium sand; loose.	E-horizon	19E

Remarks:

The smell of H<sub>2</sub>S indicated reducing conditions in the water.

---

<sup>1</sup> Explanation of code in table on last page of this appendix (Table App-1, page 286).

<sup>2</sup> ISCW - Institute for Soil, Climate and Water; Private Bag, Eisenburg, 7607.

Pit No: 20

Map/photo: 3318AD; S16, S17, S18 (profile) & S19, S20 (vegetation)

Latitude & Longitude: 33° 26'24"/18° 16'35"

Vegetation/Landuse: Fynbos

Distance to next public road<sup>1</sup>: 1

Distance to next pasture<sup>1</sup>: 1

Date described: 1990-11

Soil form: Lamotte

Soil family: Kruisfontein

Terrain unit<sup>1</sup>: 4

Water table: 1000 mm

Distance to arable land<sup>1</sup>: 1

Described by: H Schloermann & A B Oosthuizen<sup>2</sup>

Underlying material: Coastal sand

Horizon	Depth (cm)	Description	Diagnostic horizons	Samples
A	0- 15	Wet; greyish black; pure medium sand; single-grained; loose; effervescence with HCl: none; few roots; gradual smooth transition.	Orthic	20Top & 20A <sup>3</sup>
E	15- 30	Wet; grey; pure medium sand; single-grained; loose; effervescence with HCl: none; clear wavy transition.	E-horizon	20A <sup>3</sup>
B	30- 60	Wet; black; pure medium sand; single-grained; loose; effervescence with HCl: none; clear smooth transition.	Podsolc	20A <sup>3</sup>
C	60+	Wet; blackish grey; pure medium sand; single-grained; loose; effervescence with HCl: none.	Unconsolidated material with signs of wetness	20A <sup>3</sup>

Remarks: The smell of H<sub>2</sub>S indicated reducing conditions in the water.

<sup>1</sup> Explanation of code in table on last page of this appendix (Table App-1, page 286).

<sup>2</sup> ISCW - Institute for Soil, Climate and Water; Private Bag, Eisenburg, 7607.

<sup>3</sup> The A-, E-, B- and C-horizons were sampled as a composite.

Pit No: 21

Map/photo: 3318AD; S21 (profile) & S22 (vegetation)

Latitude & Longitude: 33° 26'24"/18° 16'31"

Vegetation/Landuse: Fynbos

Distance to next public road<sup>1</sup>: 1

Distance to next pasture<sup>2</sup>: 1

Date described: 1990-11

Soil form: Fernwood

Soil family: Unknown

Terrain unit<sup>1</sup>: 4

Water table: None

Distance to arable land<sup>1</sup>: 1

Described by: H Schloemann & A B Oosthuizen<sup>2</sup>

Underlying material: Coastal sand

Horizon	Depth (cm)	Description	Diagnostic horizons	Samples
A	0- 50 +	Dry; yellow; pure medium sand; single-grained; loose; effervescence with HCl: none; few roots.	Orthic	21Top

Remarks:

None

---

<sup>1</sup> Explanation of code in table on last page of this appendix (Table App-1, page 286).

<sup>2</sup> ISCW - Institute for Soil, Climate and Water; Private Bag, Eisenburg, 7607.

Pit No: 22

Map/photo: 3318AD; S23 (profile) & S24 (vegetation) & S26 (dunes)

Latitude & Longitude: 33° 26'32"/18° 16'23"

Vegetation/Landuse: Fynbos

Distance to next public road<sup>1</sup>: 1

Distance to next pasture<sup>1</sup>: 1

Date described: 1990-11

Soil form: Probably Namib

Soil family: Unknown

Terrain unit<sup>1</sup>: 3, midslope of dune

Water table: None

Distance to arable land<sup>1</sup>: 1

Described by: H Schloemann & A B Oosthuizen<sup>2</sup>

Underlying material: Calcareous coastal sand

Horizon	Depth (cm)	Description	Diagnostic horizons	Samples
A	0- 50+	Dry; dark grey; pure medium sand; single-grained; loose; effervescence with HCl: strong.	Orthic	22Top

Remarks: The pit is positioned on the slope of a dune. With abundant mica.

---

<sup>1</sup> Explanation of code in table on last page of this appendix (Table App-1, page 286).

<sup>2</sup> ISCW - Institute for Soil, Climate and Water; Private Bag, Eisenburg, 7607.

Pit No: 23

Map/photo: 3318AD; S27, S29 (profile) & S28, S30 (vegetation)

Latitude & Longitude: 33° 25'25"/18° 17'45"

Vegetation/Landuse: Fynbos

Distance to next public road<sup>1</sup>: 2

Distance to next pasture<sup>1</sup>: 1

Date described: 1990-11

Soil form: Namib

Soil family: Nortler

Terrain unit<sup>1</sup>: 3 (steep)

Water table: None

Distance to arable land<sup>1</sup>: 1

Described by: H Schloemann & A B Oosthuizen<sup>2</sup>

Underlying material: Coastal sand

Horizon	Depth (cm)	Description	Diagnostic horizons	Samples
A	0- 15	Dry; dark yellow; pure medium sand; single-grained; loose; effervescence with HCl: none; few roots; gradual smooth transition.	Orthic	23Top
C	15- 50+	Dry; yellow; pure medium sand; single-grained; loose; effervescence with HCl: none.	Regic sand	None

Remarks: None

<sup>1</sup> Explanation of code in table on last page of this appendix (Table App-1, page 286).

<sup>2</sup> ISCW - Institute for Soil, Climate and Water; Private Bag, Eisenburg, 7607.

Pit No: 24

Map/photo: 3318AD; S35, S36 (profile) & S37 (vegetation)

Latitude & Longitude: 33° 17'5"/18° 22'4"

Vegetation/Landuse: Cultivated

Distance to next public road<sup>1</sup>: 2

Distance to next pasture<sup>1</sup>: 7

Date described: 1991-02

Soil form: Katspruit

Soil family: Lammermoor

Terrain unit<sup>1</sup>: 5

Water table: None

Distance to arable land<sup>1</sup>: 7

Described by: H Schloemann

Underlying material: Unconsolidated sands of granitic origin

Horizon	Depth (cm)	Description	Diagnostic horizons	Samples
A	0- 140	Dry; pale grey; Wet; yellowish grey; with dark horizontal layers of organic material; medium to coarse sand; weak crumb; soft; effervescence with HCl: none; gradual smooth transition.	Orthic	24Top & 24A
G	140- 170+	Wet; grey with yellow mottles; sandy clay loam; moderate massive; hard; effervescence with HCl: none.	G-horizon	24G

Remarks:

The soil was fertilised using 2:1:0 + 30 % N fertiliser (Nitrophosca, Darling) and KAN-fertiliser. A sample of the 2:1:0 + 30 % N fertiliser (sample 24fr) was analysed for trace elements.

---

<sup>1</sup> Explanation of code in table on last page of this appendix (Table App-1, page 286).

Pit No: 25

Map/photo: 3318AD: S42, S43 (profile) & S44 (vegetation)

Latitude & Longitude: 33° 18'3"/18° 21'50"

Vegetation/Landuse: Cultivated

Distance to next public road<sup>1</sup>: 1

Distance to next pasture<sup>1</sup>: 7

Date described: 1991-02

Soil form: Katspruit

Soil family: Lammermoor

Terrain unit<sup>1</sup>: 5

Water table: None

Distance to arable land<sup>1</sup>: 7

Described by: H Schloemann

Underlying material: Unconsolidated sands of granitic origin

Horizon	Depth (cm)	Description	Diagnostic horizons	Samples
A	0- 80	Dry; pale grey; coarse sand; massive; slightly hard; effervescence with HCl: none; very few quartz and Fe-oxide gravel; abrupt smooth transition.	Orthic	25Top & 25A
G	80- 110+	Dry; grey with yellow brown mottles; sandy clay; massive; hard; effervescence with HCl: none; few gravel.	G-horizon	25G

Remarks:

A possible E-horizon was ignored when this profile was classified. The soil was fertilised using 3:2:1 + 25 % N (Kynoch) fertiliser (sample ferA). A sample of the fertiliser was analysed for trace elements.

---

<sup>1</sup> Explanation of code in table on last page of this appendix (Table App-1, page 286).

Pit No: 26  
 Map/photo: 3318AD; S32 (profile) & S33 (vegetation)  
 Latitude & Longitude: 33° 16'11"/18° 22'23"  
 Vegetation/Landuse: Cultivated  
 Distance to next public road<sup>1</sup>: 2  
 Distance to next pasture<sup>1</sup>: 7  
 Date described: 1991-02

Soil form: Escourt  
 Soil family: Zastron (shallow phase)  
 Terrain unit<sup>1</sup>: 5  
 Water table: None  
 Distance to arable land<sup>1</sup>: 7  
 Described by: H Schloemann & A B Oosthuizen<sup>2</sup>

Underlying material: Unconsolidated sands of granitic origin

Horizon	Depth (cm)	Description	Diagnostic horizons	Samples
A	0- 20	Dry; pale grey; pure coarse to medium sand; massive; slightly hard; effervescence with HCl: none; abrupt smooth transition.	Orthic	26AE <sup>3</sup>
E	20- 30	Dry; paler grey; pure coarse to medium sand; massive; slightly hard; effervescence with HCl: none; abrupt smooth transition.	E-horizon	26AE <sup>3</sup>
B	30- 50 +	Dry; brownish dark grey; sandy clay loam; weak coarse prismatic; very hard; effervescence with HCl: none; few gravel.	Prismatic	26B

Remarks: The soil was not treated with agro-chemicals for two years.

<sup>1</sup> Explanation of code in table on last page of this appendix (Table App-1, page 286).

<sup>2</sup> ISCW - Institute for Soil, Climate and Water; Private Bag, Eisenburg, 7607.

<sup>3</sup> The A-horizon and the E-horizon were sampled as a composite.

Pit No: 28

Map/photo: 3318AD; S40 (profile) & S41 (vegetation)

Latitude & Longitude: 33° 17'52"/18° 22'33"

Vegetation/Landuse: Strip of shrubveld surrounded by cultivated land

Distance to next public road<sup>1</sup>: 3

Distance to next pasture<sup>1</sup>: 7

Date described: 1991-02

Soil form: Unknown

Soil family: Unknown

Terrain unit<sup>1</sup>: 3

Water table: None

Distance to arable land<sup>1</sup>: 4

Described by: H Schloemann

Underlying material: Unconsolidated sands of granitic origin and quartzite boulders.

Horizon	Depth (cm)	Description	Diagnostic horizons	Samples
A	0- 25	Dry; pale grey; loamy medium to fine sand; weak massive; slightly hard; effervescence with HCl: none; few quartz gravel; clear smooth transition.	Orthic	28A
E	25- 50	Dry; pale grey; sandy loam; single-grained; loose; effervescence with HCl: none; many (coarse) quartzite stones; clear smooth transition.	Possibly E-horizon	28E
B	50- 70+	Dry; reddish brown; sandy loam; massive; hard; effervescence with HCl: none; many sesquioxide gravel.	Unknown	28B

Remarks: The surrounding of the pit is not cultivated.

<sup>1</sup> Explanation of code in table on last page of this appendix (Table App-1, page 286).

Pit No: 29

Map/photo: 3318AD; S45, S46 (profile) & S47 (vegetation)

Latitude & Longitude: 33° 21' 21" / 18° 29' 43"

Vegetation/Landuse: Shrub- to treeveld

Distance to next public road<sup>1</sup>: 1

Distance to next pasture<sup>1</sup>: 7

Date described: 1991-02

Soil form: Kroonstad

Soil family: Morgendal

Terrain unit<sup>1</sup>: 5

Water table: None

Distance to arable land<sup>1</sup>: 2

Described by: H Schloermann & A B Oosthuizen<sup>2</sup>

Underlying material: Unconsolidated sands of granitic origin

Horizon	Depth (cm)	Description	Diagnostic horizons	Samples
A	0- 20	Dry; dark grey with red iron oxide mottles; fine sand; weak fine crumb; soft; effervescence with HCl: none; clear smooth transition.	Orthic	29Top & 29Top <sup>3</sup>
E	20- 75	Dry; pale grey with red iron oxide mottles; fine sand; weak fine crumb; soft; effervescence with HCl: none; clear smooth transition.	E-horizon	29E
G	75- 110+	Moist; dark grey; fine sandy loam; massive; slightly firm; effervescence with HCl: none.	G-horizon	29G

Remarks: The owner of the land stated that the soil was never treated with agro-chemicals.

<sup>1</sup> Explanation of code in table on last page of this appendix (Table App-1, page 286).

<sup>2</sup> ISCW - Institute for Soil, Climate and Water; Private Bag, Eisenburg, 7607.

<sup>3</sup> Sample 29Top<sub>1</sub> was taken with an auger while sample 29Top was taken with a plastic shovel.

**Pit No: 30**

Map/photo: 3318AD; S54 (profile) & S52, S53 (vegetation)  
Latitude & Longitude: 33° 19'49"/18° 21'56"  
Vegetation/Landuse: Shrubveld  
Distance to next public road<sup>1</sup>: 2  
Distance to next pasture<sup>2</sup>: 7  
Date described: 1991-02

Soil form: Mispah  
Soil family: Myhill  
Terrain unit<sup>3</sup>: 3  
Water table: None  
Distance to arable land<sup>1</sup>: 3  
Described by: H Schloemann & A B Oosthuizen<sup>2</sup>

**Underlying material: Granite**

Horizon	Depth (cm)	Description	Diagnostic horizons	Samples
A	0- 75	Dry; brown; medium to coarse loamy sand; moderate crumb; slightly hard; effervescence with HCl: none; very few gravel; wavy abrupt transition.	Orthic	30Top & 30A
R	75+	Fine-grained, chemically weathered granite.	Hard rock	see remarks

**Remarks:**

A sample of the granite (GR1) was taken in form of a boulder which was found 70 meters south-west of Pit 30. The owner of the land stated that agro-chemicals were not applied to the soil for at least 50 years.

<sup>1</sup> Explanation of code in table on last page of this appendix (Table App-1, page 286).

<sup>2</sup> ISCW - Institute for Soil, Climate and Water; Private Bag, Eisenburg, 7607.

Pit No: 31

Map/photo: 3318AD; S55, S56 (profile) & S57 (vegetation)

Latitude & Longitude: 33° 19'42"/18° 21'56"

Vegetation/Landuse: Shrubveld

Distance to next public road<sup>1</sup>: 2

Distance to next pasture<sup>1</sup>: 7

Date described: 1991-02

Soil form: Longlands  
Soil family: Sherbrook  
Terrain unit<sup>1</sup>: 3  
Water table: None  
Distance to arable land<sup>1</sup>: 3  
Described by: H Schloemann

Underlying material: Granite

Horizon	Depth (cm)	Description	Diagnostic horizons	Samples
A	0- 60	Dry; greyish brown; medium to coarse loamy sand; moderate crumb; slightly hard; effervescence with HCl: none; very few gravel; gradual smooth transition.	Orthic	31Top & 31AE <sup>2</sup>
E	60- 170	Dry; pale brown; medium to coarse loamy sand; moderate crumb; slightly hard; effervescence with HCl: none; very few gravel; gradual smooth transition.	E-horizon	31AE <sup>2</sup>
B	170- 250	Dry; reddish brown; medium to coarse sandy loam; single-grained; hard; effervescence with HCl: none; many sesquioxide concretions.	Soft plinthic	31B
R	250+	Granite.		

Remarks: The rock was only reached using an auger. The owner of the land stated that agro-chemicals were not applied to the soil for at least 50 years.

<sup>1</sup> Explanation of code in table on last page of this appendix (Table App-1, page 286).

<sup>2</sup> The A-horizon and the E-horizon were sampled as a composite.

Pit No: 32

Map/photo: 3318AD; S58 (profile) & P13 (vegetation)

Latitude & Longitude: 33° 19'36"/18° 22'6"

Vegetation/Landuse: Grassveld that was cultivated in the past

Distance to next public road<sup>1</sup>: 2

Distance to next pasture<sup>1</sup>: 7

Date described: 1991-02

Soil form: Westlelgh

Soil family: Helena

Terrain unit<sup>1</sup>: 4

Water table: None

Distance to arable land<sup>1</sup>: 2

Described by: H Schloemann

Underlying material: Granite

Horizon	Depth (cm)	Description	Diagnostic horizons	Samples
A	0- 55	Dry; pale grey; coarse sand; weak crumb; soft; effervescence with HCl: none; very few quartz gravel; clear smooth transition.	Orthic	32Top & 32A
B	55- 110	Dry; pale grey; coarse sand; single-grained; hard; effervescence with HCl: none; many sesquioxide concretions and quartz gravel; clear smooth transition.	Soft plinthic	32B
GB	110- 140	Wet; pale grey matrix with brown and pale grey clay accumulations (mottles); coarse to medium sandy loam; massive; slightly firm; effervescence with HCl: none; very few quartz gravel; softened sesquioxide concretions; diffuse smooth transition.	Non-diagnostic	32GB
G	140- 150+	Wet; pale grey matrix with brown and pale grey clay accumulations (mottles); clay; massive; firm; effervescence with HCl: none.	Non-diagnostic	32G

Remarks:

The owner of the land stated that agro-chemicals were not applied to the soil for at least 50 years.

---

<sup>1</sup> Explanation of code in table on last page of this appendix (Table App-1, page 286).

Pit No: 33

Map/photo: 3318AD; P14, P15, P17 (profile) & P16 (vegetation)

Latitude & Longitude: 33° 19'26"/18° 22'6"

Vegetation/Landuse: Grassveld that was cultivated in the past

Distance to next public road<sup>1</sup>: 3

Distance to next pasture<sup>2</sup>: 7

Date described: 1991-02

Soil form: Kroonstad

Soil family: Morgendal

Terrain unit<sup>1</sup>: 5

Water table: None

Distance to arable land<sup>1</sup>: 4

Described by: H Schloemann

Underlying material: Granite

Horizon	Depth (cm)	Description	Diagnostic horizons	Samples
A	0- 15	Dry; grey; coarse sand; single-grained; loose; effervescence with HCl: none; very few quartz gravel; gradual smooth.	Orthic	33Top & 33AE <sup>2</sup>
E	15- 60	Dry; pale grey; coarse sand; massive; slightly hard; effervescence with HCl: none; few quartz gravel; abrupt smooth.	E-horizon	33AE <sup>2</sup>
G	60- 140+	Wet; dark grey with brown mottles; coarse sandy clay; massive; hard; effervescence with HCl: none; very few gravel.	G-horizon	33G

Remarks:

The owner of the land stated that agro-chemicals were not applied to the soil for at least 50 years.

<sup>1</sup> Explanation of code in table on last page of this appendix (Table App-1, page 286).

<sup>2</sup> The A-horizon and the E-horizon were sampled as a composite.

Pit No: 34  
 Map/photo: 3318AD; none  
 Latitude & Longitude: approximately 33° 28'32" / 18° 28'40"  
 Vegetation/Landuse: Shrubveld  
 Distance to next public road<sup>1</sup>: 3  
 Distance to next pasture<sup>1</sup>: 7  
 Date described: 1991-02

Soil form: Unknown  
 Soil family: Unknown  
 Terrain unit<sup>1</sup>: 3  
 Water table: None  
 Distance to arable land<sup>1</sup>: 1  
 Described by: H Schloemann

Underlying material: Granite

Horizon	Depth (cm)	Description	Diagnostic horizons	Samples
A	0- 75+	Dry; brown; medium to coarse sandy loam; massive; slightly hard; effervescence with HCl: none; very few quartz gravel.	Orthic	34Top & 34A

Remarks: Pit not deep enough to classify soil profile.

---

<sup>1</sup> Explanation of code in table on last page of this appendix (Table App-1, page 286).

Pit No: 35  
 Map/photo: 3318AD; S60 (profile)  
 Latitude & Longitude: 33° 44'33"/18° 53'21"  
 Vegetation/Landuse: Cultivated grassland  
 Distance to next public road<sup>1</sup>: 3  
 Distance to next pasture<sup>1</sup>: 1  
 Date described: 1991-03

Soil form: Glenrosa  
 Soil family: Unknown  
 Terrain unit<sup>1</sup>: 3  
 Water table: None  
 Distance to arable land<sup>1</sup>: 2  
 Described by: H Schloemann

Underlying material: Schist of the Malmesbury Group

Horizon	Depth (cm)	Description	Diagnostic horizons	Samples
A	0- 20	Dry; grey; loamy sand; coarse moderate blocky; slightly firm; effervescence with HCl: none; very few granite, sesquioxide and quartz gravel.	Orthic	None
B	20- 40	Dry; dark grey; clay loam; blocky; hard; effervescence with HCl: none.	Lithocutanic	None
C	40+	Dry; yellow brown; effervescence with HCl: none; weathered schist.		35Sap

Remarks: The owner of the land stated that the area was not treated with agro-chemicals since 1976. Surface of soil with salt precipitations. Sample 35Sap was taken from a depth of 100 cm to 130 cm and represents the underlying material for the soils at Pits 36, 37 and 38.

---

<sup>1</sup> Explanation of code in table on last page of this appendix (Table App-1, page 286).

Pit No: 36

Map/photo: 3318DB; S68 (profile) & S69 (vegetation)

Latitude & Longitude: 33° 44'34" / 18° 53'18"

Surface stone: None

Occurrence of flooding: Nil

Vegetation/Land use: Open dwarf shrubveld

Water table: None

Distance to arable land<sup>1</sup>: 2

Aspect: NW

Microrelief: None

Soil form: Klapmuts

Soil family: Bossleveld

Surface rock: None

Terrain unit<sup>1</sup>: 1

Slope: 6 %

Slope shape: Convex

Distance to next public road<sup>1</sup>: 3

Distance to next pasture<sup>1</sup>: 1

Described by: A B Oosthuizen<sup>2</sup>

Date described: 1991-04

Underlying material: Schist of the Malmesbury Group  
Weathering of underlying material: Moderate physical, weak chemical

Horizon	Depth (cm)	Description	Diagnostic horizons	Sample
A	0- 10	Dry; dry very pale brown 10YR7/3; moist brown to dark brown 10YR4/3; fine sandy loam; massive; slightly hard; few pores; few rounded medium hard sesquioxide concretions; few irregular fine gravel (granite and quartz); water absorption: 10 seconds; few roots; clear smooth transition.	Orthic	36Top
E	10- 20	Dry; dry very pale brown 10YR7/3; moist yellowish brown 10YR5/4; loamy fine sand; single grain; slightly hard; few pores; many rounded medium hard sesquioxide concretions; common irregular fine gravel (granite and quartz); water absorption: 3 seconds; few roots; abrupt smooth transition.	E-horizon	36E
B	20- 40+	Dry; dry reddish yellow 7.5YR6/6; moist strong brown 7.5YR5/6; common medium distinct red sesquioxide mottles; clay loam; moderate coarse angular blocky; very hard; common clay cutans; few rounded fine hard sesquioxide concretions; few irregular fine gravel; water absorption: 6 seconds; few roots.	Pedocutanic	36B

Remarks: The land owner stated that the site was not treated with agro-chemicals since 1976. Surface of soil with salt precipitations.

<sup>1</sup> Explanation of code in table on last page of this appendix (Table App-1, page 286).

<sup>2</sup> ISCW - Institute for Soil, Climate and Water; Private Bag, Eisenburg, 7607.

Pit No: 37

Map/photo: 3318DB; S72 (profile) & S73 (vegetation)

Latitude & Longitude: 33° 44'31" / 18° 53'15"

Surface stone: None

Occurrence of flooding: Nil

Vegetation/Land use: Closed dwarf shrubveld

Water table: None

Distance to arable land<sup>1</sup>: 2

Aspect: NW

Microrelief: None

Soil form: Sterkspruit

Soil family: Hermon

Surface rock: None

Terrain unit<sup>1</sup>: 3

Slope: 8 %

Slope shape: Convex

Distance to next public road<sup>1</sup>: 3

Distance to next pasture<sup>1</sup>: 1

Described by: A B Oosthuizen<sup>2</sup>

Date described: 1991-04

Underlying material: Schist of the Malmesbury Group

Weathering of underlying material: Weak physical, weak chemical

Horizon	Depth (cm)	Description	Diagnostic horizons	Sample
A	0- 20	Dry; dry pale brown 10YR6/3; moist brown to dark brown 10YR4/3; fine sandy clay loam; massive; hard; few pores; few rounded fine hard sesquioxide concretions; few rounded fine gravel (granite and quartz); water absorption: 12 seconds; common roots; clear smooth transition.	Orthic	37A
B	20- 40	Dry; dry brown to dark brown 10YR4/3; moist dark brown 10YR3/3; few medium distinct yellowish brown saprolite mottles; clay loam; moderate coarse prismatic; very hard; few pores; few clay cutans; few rounded fine hard sesquioxide concretions; few rounded fine gravel (granite and quartz); water absorption: 13 seconds; few roots; clear tonguing transition.	Prismaeutanic	37B
R	40- 50+	Rock.		

Remarks: The land owner stated that the site was not treated with agro-chemicals since 1976. Surface of soil with salt precipitations.

<sup>1</sup> Explanation of code in table on last page of this appendix (Table App-1, page 286).

<sup>2</sup> ISCW - Institute for Soil, Climate and Water; Private Bag, Eisenburg, 7607.

Pit No: 38  
 Map/photo: 3318DB; S75 (profile) & S76 (vegetation)  
 Latitude & Longitude: 33° 44'28"/18° 53'13"  
 Surface stone: None  
 Occurrence of flooding: Nil  
 Vegetation/Land use: Closed dwarf shrubveld  
 Water table: None  
 Distance to arable land<sup>1</sup>: 2  
 Aspect: NW  
 Microrelief: None

Soil form: Sterkspruit  
 Soil family: Hermon  
 Surface rock: None  
 Terrain unit<sup>1</sup>: 4  
 Slope: 6 %  
 Slope shape: Concave  
 Distance to next public road<sup>1</sup>: 3  
 Distance to next pasture<sup>1</sup>: 1  
 Described by: A B Oosthuizen<sup>2</sup>  
 Date described: 1991-04

Underlying material: Schist of the Malmesbury Group  
 Weathering of underlying material: Moderate physical, weak chemical

Horizon	Depth (cm)	Description	Diagnostic horizons	Sample
A	0- 20	Dry; dry light yellowish brown 10YR6/4; moist brown to dark brown 7.5YR4/4; fine sandy clay loam; massive; hard; few pores; few rounded fine gravel (quartz and granite); few rounded fine hard sesquioxide concretions; water absorption: 8 seconds; common roots; abrupt smooth transition.	Orthic	38A
B	20- 30	Dry; dry dark greyish brown 10YR4/2; moist dark brown 10YR3/3; clay; moderate coarse prismatic; very hard; few pores; common clay cutans; few rounded fine quartz gravel; few rounded fine hard sesquioxide concretions; water absorption: 10 seconds; few roots; gradual smooth transition.	Prismacutanic	38B
BC	30- 55	Dry; dry yellowish brown 10YR5/4; moist dark yellowish brown 10YR4/6; clay; weak coarse prismatic; very hard; few pores; few slickensides; common clay cutans; very few shale fragments; very few sesquioxide concretions; few irregular medium gravel; water absorption: 8 seconds; effervescence with HCl: slight; clear wavy transition.	Prismacutanic	38BC
R	55+	Rock.		

Remarks: The land owner stated that the site was not treated with agro-chemicals since 1976. Surface of soil with salt precipitations.

<sup>1</sup> Explanation of code in table on last page of this appendix (Table App-1, page 286).

<sup>2</sup> ISCW - Institute for Soil, Climate and Water; Private Bag, Eisenburg, 7607.

Pit No: 39

Map/photo: 3318DB; S77 (location)  
Latitude & Longitude: 33° 37'18"/18° 56'25"  
Vegetation/Landuse: Road cut  
Distance to next public road<sup>1</sup>: 6  
Distance to next pasture<sup>1</sup>: 3  
Date described: 1991-03

Soil form: n.a.  
Soil family: n.a.  
Terrain unit<sup>1</sup>: n.a.  
Water table: None  
Distance to arable land<sup>1</sup>: 3  
Described by: H Schloemann

Underlying material: Phyllite of the Malmesbury Group

Remarks:

Road cut: the exposed material (sample 39Sap) represents the underlying material for the soil at Pits 40, 41, 42 and 43. Description of the exposed material: Soft, strongly chemically weathered phyllite. Abundant lenses of silt. Layered quartz precipitations common. The degree of weathering decreases towards the bottom of the road cut.

---

<sup>1</sup> Explanation of code in table on last page of this appendix (Table App-1, page 286).

Pit No: 40  
 Map/photo: 3318DB; S78 (profile) & S79 (vegetation)  
 Latitude & Longitude: 33° 37'28"/18° 56'33"  
 Surface stone: None  
 Occurrence of flooding: Nil  
 Vegetation/Land use: Cultivated, unknown  
 Water table: None  
 Distance to arable land<sup>1</sup>: 7  
 Aspect: NW  
 Microrelief: None

Soil form: Cartref  
 Soil family: Steenbras  
 Surface rock: None  
 Terrain unit<sup>1</sup>: 3  
 Slope: 6 %  
 Slope shape: Convex  
 Distance to next public road<sup>1</sup>: 4  
 Distance to next pasture<sup>1</sup>: 7  
 Described by: A B Oosthuizen<sup>2</sup>  
 Date described: 1991-04

Underlying material: Phyllite of the Malmesbury Group  
 Weathering of underlying material: Moderate physical, weak chemical

Horizon	Depth (cm)	Description	Diagnostic horizons	Sample
A	0- 20	Dry; dry light yellowish brown 10YR6/4; moist dark yellowish brown 10YR4/4; fine sandy clay loam; massive; slightly hard; few pores; common irregular medium quartz gravel; few rounded medium hard sesquioxide concretions; water absorption: 8 seconds; few roots; clear smooth transition.	Orthic	40Top
E	20- 40	Dry; dry light brown 7.5YR6/4; moist dark yellowish brown 10YR4/6; fine sandy loam; single grain; slightly hard; many pores; many irregular coarse quartz gravel; few rounded coarse hard sesquioxide concretions; water absorption: 6 seconds; clear wavy transition.	E-horizon	40E
B	40- 60	Dry; dry yellowish brown 10YR5/6; moist strong brown 7.5YR5/6; common fine faint yellowish brown saprolite mottles; clay; moderate fine subangular blocky; very hard; few pores; common clay cutans; common irregular medium quartz gravel; water absorption: 9 seconds; clear tonguing transition.	Lithocutanic	40B
R	60- 80+	Hard rock.		None

Remarks: No information about agro-chemicals.

<sup>1</sup> Explanation of code in table on last page of this appendix (Table App-1, page 286).

<sup>2</sup> ISCW - Institute for Soil, Climate and Water; Private Bag, Eisenburg, 7607.

Pit No: 41

Map/photo: 3318DB; S80, S81 (profile) & S82 (vegetation)

Latitude & Longitude: 33° 37'19"/18° 56'27"

Surface stone: None

Occurrence of flooding: Nil

Vegetation/Land use: Cultivated, unknown

Water table: None

Distance to arable land<sup>1</sup>: 7

Aspect: NW

Microrelief: None

Soil form: Estcourt  
Soil family: Haarlem  
Surface rock: None  
Terrain unit<sup>1</sup>: 3  
Slope: 10 %  
Slope shape: Convex  
Distance to next public road<sup>1</sup>: 4  
Distance to next pasture<sup>1</sup>: 7  
Described by: A B Oosthuizen<sup>2</sup>  
Date described: 1991-04

Underlying material: Phyllite of the Malmesbury Group

Weathering of underlying material: Unknown

Horizon	Depth (cm)	Description	Diagnostic horizons	Sample
A	0- 20	Dry; dry pinkish grey 7.5YR6/2; moist brown to dark brown 10YR4/3; fine sandy loam; massive; hard; few pores; few sesquioxide concretions; common irregular medium quartz gravel; water absorption: 6 seconds; few roots; clear smooth transition.	Orthic	41Top
E	20- 40	Dry; dry light grey 10YR7/2; moist yellowish brown 10YR5/4; fine sandy clay loam; massive; hard; few pores; few sesquioxide concretions; many irregular medium quartz gravel; water absorption: 7 seconds; abrupt smooth transition.	E-horizon	41E
B1	40- 50	Dry; dry yellowish brown 10YR5/8; moist yellowish brown 10YR5/8; few fine faint red sesquioxide mottles; clay; moderate coarse prismatic; very hard; few pores; many clay cutans; few irregular fine quartz gravel; water absorption: 5 seconds; clear smooth transition.	Prismacutanic	41B1
B2	50- 60+	Dry; dry yellowish brown 10YR5/8; moist yellowish brown 10YR5/8; few fine faint red sesquioxide mottles; clay; moderate coarse angular blocky; very hard; few pores; common clay cutans; few irregular fine gravel; water absorption: 3 seconds.		41B2

Remarks: No information about agro-chemicals.

<sup>1</sup> Explanation of code in table on last page of this appendix (Table App-1, page 286).

<sup>2</sup> ISCW - Institute for Soil, Climate and Water; Private Bag, Eisenburg, 7607.

Pit No: 42  
 Map/photo: 3318DB; S83 (profile)  
 Latitude & Longitude: 33° 37'16"/18° 56'24"  
 Vegetation/Landuse: Shrubveld between public road and cultivated land  
 Distance to next public road<sup>1</sup>: 4  
 Distance to next pasture<sup>1</sup>: 6  
 Date described: 1991-03

Soil form: Escourt  
 Soil family: Haarlem  
 Terrain unit<sup>1</sup>: 3  
 Water table: None  
 Distance to arable land<sup>1</sup>: 6  
 Described by: H Schloemann

Underlying material: Phyllite of the Malmesbury Group

Horizon	Depth (cm)	Description	Diagnostic horizons	Samples
A	0- 20	Very similar to the A-horizon of Pit 41	Orthic	42Top
E	20- 50	Very similar to the E-horizon of Pit 41	E-horizon	None
B	50- 60+	Very similar to the B horizon of Pit 41	Prismacutanic	42B

Remarks: The soil at this pit is not cultivated and was sampled in order to compare the results with those for Pit 41 (section 6.5.2.).

---

<sup>1</sup> Explanation of code in table on last page of this appendix (Table App-1, page 286).

Pit No: 43  
 Map/photo: 3318DB; S84 (profile) & S85 (vegetation)  
 Latitude & Longitude: 33° 37'15"/18° 56'23"  
 Surface stone: None  
 Occurrence of flooding: Nil  
 Vegetation/Land use: Cultivated, unknown  
 Water table: None  
 Distance to arable land<sup>1</sup>: 7  
 Aspect: NW  
 Microrelief: None  
 Underlying material: Phyllite of the Malmesbury Group  
 Weathering of underlying material: Unknown

Soil form: Kroonstad  
 Soil family: Morgendal  
 Surface rock: None  
 Terrain unit<sup>1</sup>: 4  
 Slope: 4 %  
 Slope shape: Straight  
 Distance to next public road<sup>1</sup>: 4  
 Distance to next pasture<sup>1</sup>: 7  
 Described by: A B Oosthuizen<sup>2</sup>  
 Date described: 1991-04

Horizon	Depth (cm)	Description	Diagnostic horizons	Sample
A	0- 35	Dry; dry very pale brown 10YR7/3; moist brown to dark brown 10YR4/3; loamy medium sand; massive; hard; few pores; few irregular medium gravel; few sesquioxide concretions; water absorption: 7 seconds; few roots; clear smooth transition.	Orthic	43Top
AE	35- 60	Dry; dry very pale brown 10YR7/4; moist yellowish brown 10YR5/4; loamy medium sand; massive; hard; few pores; few irregular medium gravel; few sesquioxide concretions; water absorption: 9 seconds; clear smooth transition.	Orthic	43AE
E1	60- 80	Dry; dry white 10YR8/1; moist light yellowish brown 10YR6/4; medium sand; single grain; slightly hard; few pores; common irregular medium gravel; few sesquioxide concretions; water absorption: 4 seconds; clear smooth transition.	E-horizon	43E <sup>3</sup>
E2	80- 100	Dry; dry pale yellow 2.5Y7/4; moist light yellowish brown 2.5Y6/4; loamy fine sand; single grain; hard; few pores; very many irregular medium gravel; sesquioxide concretions; water absorption: 4 seconds; abrupt smooth transition.	E-horizon	43E <sup>3</sup>
G	100-110+	Dry; dry yellowish brown 10YR5/6; moist dark yellowish brown 10YR4/6; common fine faint red sesquioxide mottles; clay; moderate coarse prismatic; very hard; common clay cutans; water absorption: 10 seconds.	G-horizon	43G
Remarks:	None			

<sup>1</sup> Explanation of code in table on last page of this appendix (Table App-1, page 286).

<sup>2</sup> ISCW - Institute for Soil, Climate and Water; Private Bag, Eisenburg, 7607.

<sup>3</sup> The E-horizon was sampled as a composite.

Pit No: 44

Map/photo: 3318DA; S95, S96, S98, S101 (profile) & S97 (vegetation) & S102, S103 (structure)

Latitude & Longitude: 33° 42'22"/18° 36'12"

Surface stone: Flat, 80 mm long, 0.6 m apart

Occurrence of flooding: Nil

Vegetation/Land use: Disturbed land/ploughed

Water table: None

Distance to arable land<sup>1</sup>: 7

Aspect: S

Microrelief: None

Soil form: Sterkspruit

Soil family: Hermon

Surface rock: None

Terrain unit<sup>1</sup>: 3

Slope: 12 %

Slope shape: Convex

Distance to next public road<sup>1</sup>: 1

Distance to next pasture<sup>1</sup>: 7

Described by: A B Oosthuizen<sup>2</sup>

Date described: 1991-05

Underlying material: Sandstone of the Malmesbury Group

Weathering of underlying material: Moderate physical, weak chemical

Horizon	Depth (cm)	Description	Diagnostic horizons	Sample
A1	0- 30	Moist; dry pale brown 10YR6/3; moist greyish brown 10YR5/2; fine sandy clay loam; massive; friable; few pores; common rounded medium hard sesquioxide concretions; few irregular medium gravel; water absorption: 8 seconds; common roots; clear smooth transition.	Orthic	44Top
A2	30- 40	Moist; dry light brownish grey 10YR6/2; moist dark greyish brown 10YR4/2; fine sandy clay loam; massive; friable; few pores; many rounded medium hard sesquioxide concretions; few irregular medium gravel; water absorption: 5 seconds; few roots; abrupt smooth transition.	Orthic	44A2
B	40- 60	Moist; moist brown to dark brown 10YR4/3; clay; moderate coarse prismatic; very firm; many clay cutans; very few small hard sesquioxide concretions; very few irregular medium quartz gravel; water absorption: 7 seconds; few roots; clear wavy transition.	Prismaeutanic	44B
C	60+	Saprolite		44C

Remarks: A well developed E-horizon occurs in some places. Mixing of the A- and the E-horizon due to ploughing in other places. The profile may, therefore, also qualify for the Estcourt soil form. The underlying material was sampled (sample 44R) in form of a sandstone boulder, found approximately 200 meters south-east of Pit 44. Agro-chemicals were recently applied to the soil.

<sup>1</sup> Explanation of code in table on last page of this appendix (Table App-1, page 286).

<sup>2</sup> ISCW - Institute for Soil, Climate and Water; Private Bag, Eisenburg, 7607.

Pit No: 45  
 Map/photo: 3318BC; S107, S108 (profile) & S110 (vegetation)  
 Latitude & Longitude: 33° 27'29"/18° 41'07"  
 Surface stone: None  
 Occurrence of flooding: Nil  
 Vegetation/Land use: Disturbed land/ploughed  
 Water table: None  
 Distance to arable land<sup>1</sup>: 2  
 Aspect: W  
 Microrelief: None

Soil form: Clovelly  
 Soil family: Leiden  
 Surface rock: None  
 Terrain unit<sup>1</sup>: 4  
 Slope: 6 %  
 Slope shape: Straight  
 Distance to next public road<sup>1</sup>: 2  
 Distance to next pasture<sup>1</sup>: 7  
 Described by: A B Oosthuizen<sup>2</sup>  
 Date described: 1991-06

Underlying material: Ferruginized material of the Malmesbury Group  
 Weathering of underlying material: Unknown

Horizon	Depth (cm)	Description	Diagnostic horizons	Sample
A	0- 30	Moist; dry light brown 7.5YR6/4; moist brown to dark brown 7.5YR4/4; loamy fine sand; single grain; friable; many pores; water absorption: 8 seconds; few roots; abrupt smooth transition.	Orthic	45A
BA	30- 60	Moist; dry light brown 7.5YR6/4; moist strong brown 7.5YR5/6; fine sandy loam; massive; friable; few rounded quartz gravel; many pores; water absorption: 4 seconds; clear smooth transition.	yellow-brown apedal	45BA
B	60- 90+	Moist; moist strong brown 7.5YR5/6; common medium distinct red iron oxide mottles; fine sandy clay loam; weak coarse subangular blocky; firm; few subangular quartz gravel; few pores with signs of wetness; common clay cutans; water absorption: 5 seconds.	yellow-brown apedal	45B

Remarks: The soil was recently fertilised with lime ammonium nitrate (LAN; Kynoch, Milnerton). A sample of the fertiliser was analysed for trace elements (samples ferB and ferC).

<sup>1</sup> Explanation of code in table on last page of this appendix (Table App-1, page 286).

<sup>2</sup> ISCW - Institute for Soil, Climate and Water; Private Bag, Eisenburg, 7607.

Pit No: 46

Map/photo: 3318BC; S114, S115 (profile)

Latitude & Longitude: 33° 27'19"/18° 41'29"

Surface stone: None

Occurrence of flooding: Nil

Vegetation/Land use: disturbed land/ploughed

Water table: None

Distance to arable land<sup>1</sup>: 7

Aspect: SW

Microrelief: None

Soil form: Hutton

Soil family: Suurbekom

Surface rock: None

Terrain unit<sup>1</sup>: 3

Slope: 12 %

Slope shape: Convex

Distance to next public road<sup>1</sup>: 5

Distance to next pasture<sup>1</sup>: 1

Described by: A B Oosthuizen<sup>2</sup>

Date described: 1991-06

Underlying material: Ferruginized material of the Malmesbury Group

Weathering of underlying material: Unknown

Horizon	Depth (cm)	Description	Diagnostic horizons	Sample
Ap	0- 15	Moist; dry yellowish red 5YR5/6; moist yellowish red 5YR4/6; loamy fine sand; massive; loose; few pores; few rounded coarse hard sesquioxide concretions; water absorption: 5 seconds; common roots; clear smooth transition.	Orthic	46A <sup>3</sup>
A	15- 40	Moist; dry yellowish red 5YR5/6; moist yellowish red 5YR4/6; loamy fine sand; massive; friable; few pores; few rounded coarse hard sesquioxide concretions; water absorption: 6 seconds; few roots; clear smooth transition.	Orthic	46A <sup>3</sup>
B1	40- 85	Moist; dry red 2.5YR4/8; moist red 2.5YR4/6; fine sandy loam; massive; slightly firm; few pores; common rounded coarse hard sesquioxide concretions; water absorption: 5 seconds; few roots; clear smooth transition.	Red apedal	46B1
B2	85- 155	Moist; dry red 2.5YR4/8; moist red 2.5YR4/6; fine sandy loam; weak medium subangular blocky; firm; few pores; few clay cutans; very many rounded very coarse hard sesquioxide concretions; water absorption: 4 seconds; clear smooth transition.	Red apedal	46B2

<sup>1</sup> Explanation of code in table on last page of this appendix (Table App-1, page 286).

<sup>2</sup> ISCW - Institute for Soil, Climate and Water; Private Bag, Eisenburg, 7607.

<sup>3</sup> The Ap-horizon and the A-horizon were sampled as a composite.

46C

155 + Moist; dry yellowish brown 10YR5/8; moist fine sandy clay loam; weak coarse subangular blocky; very firm; few angular quartz gravel; few rounded sesquioxide concretions; few pores; few clay cutans; water absorption: 8 seconds.

Remarks: The site was recently fertilised with lime ammonium nitrate (LAN; Kynoch, Milneron). A sample of the fertiliser was analysed for trace elements (sample ferB). Other agro-chemicals were also applied.

Pit No: 47  
 Map/photo: 3318BC; S116, S117, S118 (profile) & S120 (vegetation)  
 Latitude & Longitude: 33° 27'08"/18° 41'52"  
 Surface stone: None  
 Occurrence of flooding: Nil  
 Vegetation/Land use: Disturbed land/ploughed  
 Water table: None  
 Distance to arable land<sup>1</sup>: 7  
 Aspect: Level  
 Microrelief: None

Soil form: Oakleaf  
 Soil family: Patrysdal  
 Surface rock: None  
 Terrain unit<sup>1</sup>: 1  
 Slope: 4 %  
 Slope shape: Convex  
 Distance to next public road<sup>1</sup>: 3  
 Distance to next pasture<sup>1</sup>: 2  
 Described by: A B Oosthuizen<sup>2</sup>  
 Date described: 1991-06

Underlying material: Ferruginized material, probably granite  
 Weathering of underlying material: Unknown

Horizon	Depth (cm)	Description	Diagnostic horizons	Sample
Ap	0- 20	Moist; dry light brown 7.5YR6/4; moist brown 7.5YR5/4; loamy medium sand; massive; friable; few fine subangular quartz gravel; few fine rounded sesquioxide concretions; effervescence with HCl: slight; few pores; water absorption: 5 seconds; few roots; abrupt smooth transition.	Orthic	47Top
A1	20- 60	Moist; dry brown 7.5YR5/4; moist brown to dark brown 7.5YR4/4; medium sandy loam; massive; friable; few fine subangular quartz gravel; few fine rounded sesquioxide concretions; few pores; water absorption: 5 seconds; few roots; gradual smooth transition.	Orthic	47A1
B1	60- 100	Dry; dry strong brown 7.5YR5/6; moist yellowish red 5YR5/8; fine sandy clay loam; massive; hard; few fine subangular quartz gravel; few pores; common clay cutans; common rounded medium hard sesquioxide concretions; water absorption: 8 seconds; few roots; clear wavy transition.	Neocutanic	47B1
B2	100- 200	Dry; dry reddish yellow 7.5YR6/8; moist strong brown 7.5YR5/8; common medium distinct red iron oxide mottles; fine sandy clay loam; weak medium subangular blocky; very hard; few pores; common clay cutans; few fine subangular quartz gravel; many rounded coarse hard sesquioxide concretions; water absorption: 7 seconds; clear smooth transition.	Neocutanic	47B2

<sup>1</sup> Explanation of code in table on last page of this appendix (Table App-1, page 286).

<sup>2</sup> ISCW - Institute for Soil, Climate and Water; Private Bag, Eisenburg. 7607.

C 200-270+ Moist; reddish 10R4/6; clay; moderate fine blocky; very firm; few rounded medium sesquioxide concretions; angular quartz gravel; effervescence with HCL at 2,4 m depth: strong.

Remarks: Agro-chemicals were not applied to the soil for at least one year. An additional sample was taken from a sand lens (sample 47A2). The sand lens showed the properties of an A-horizon but was developed between the B1- and the C-horizon and cutting through the B2-horizon. The pit is situated between heuwelkies.

Table App-1: Code system used to report the distance of a pit from the next public road, arable land and pasture land. The right column explains the code system used to report the slope position of a pit.

DISTANCE TO NEXT PUBLIC ROAD		CODE SYSTEM USED TO REPORT:		TERRAIN UNIT	
		DISTANCE TO ARABLE AND PASTURE LAND			
1	> 1000 m	1	> 500 m	1	Crest
2	1000-500 m	2	500-100 m	2	Scarp
3	500-100 m	3	100-50 m	3	Midslope
4	100-50 m	4	50-20 m	4	Footslope
5	50-10 m	5	20-5 m	5	Valley Bottom
6	< 10 m	6	5-1 m		
		7	on cultivated land		

**APPENDIX-II: Method for extraction of elements with ammonium nitrate**

1. Sieving: Sieve the air-dried soil through a 2 mm nylon or stainless steel sieve and discard the coarse fraction.
2. Weighing: Weigh 20 g air-dried and < 2 mm sieved soil into a 100 ml acid-cleaned polypropylene centrifuge beaker.
3. Addition: Add 50 ml 1 M  $\text{NH}_4\text{NO}_3$  G.R. to the soil (80.04 g/l; No. 1188, Fa. Merck; extractant to soil ratio is 2.5).
4. Agitating: Agitate end-over-end for 2 hours at 20°C.
5. Centrifuging: Centrifuge for 15 minutes at 20°C and 2500 RPM.
6. Filtration: Filter the supernatant through a folded filter paper (Fa. Schleicher and Schuell, 595 1/2, 125 mm diameter) into an acid-cleaned 100 ml polyethylene bottle.
7. Stabilising: Stabilise the extract by adding 0.5 ml conc.  $\text{HNO}_3$  (65 %) G.R. (No. 452, Fa. Merck).

**APPENDIX-III: Elemental concentrations, pH values, conductivities of the water-suspended soils and particle size distributions**

**Table App-2: Concentrations of major elements in percent. Negative numbers refer to concentrations below the LLD. Analytical method: XRFS.**

Sample	Na <sub>2</sub> O	MgO	Al <sub>2</sub> O <sub>3</sub>	SiO <sub>2</sub>	P <sub>2</sub> O <sub>5</sub>	K <sub>2</sub> O	CaO	TiO <sub>2</sub>	Fe <sub>2</sub> O <sub>3</sub>	H <sub>2</sub> O-	LOI	Total
1A	0.02	0.05	0.3	97.3	0.013	0.07	0.05	0.07	0.62	0.14	1.00	99.64
1E	0.02	0.04	0.4	98.2	0.014	0.05	0.03	0.08	0.53	0.07	0.33	99.72
4A	0.13	0.19	0.8	86.4	0.192	0.16	2.14	0.14	0.60	1.40	7.44	99.62
5A	1.06	0.24	6.6	85.7	0.071	2.74	0.35	0.19	1.84	0.18	1.15	100.16
6AE	1.45	0.32	9.0	82.1	0.068	3.46	0.35	0.24	1.71	0.20	1.55	100.40
7A	0.28	0.23	4.6	87.5	0.062	1.58	0.21	0.28	1.83	0.26	1.75	98.60
8A	0.04	0.47	7.9	77.0	0.080	0.78	0.77	0.46	7.35	0.56	4.00	99.45
8B	-0.02	0.15	19.2	55.6	0.063	0.32	0.07	0.77	14.00	1.45	8.86	100.54
9A	0.03	0.05	1.1	96.1	0.037	0.16	0.03	0.23	1.54	0.13	0.57	99.98
10A	0.06	0.05	0.8	94.2	0.030	0.14	0.08	0.15	1.10	0.36	2.58	99.56
12A	0.11	0.08	4.5	85.9	0.051	0.54	0.04	0.29	4.41	0.45	2.74	99.14
12B	0.08	0.13	9.1	72.5	0.085	0.55	0.03	0.41	12.66	0.77	4.04	100.35
16Top	0.03	0.07	0.6	96.9	0.019	0.12	0.06	0.09	0.78	0.11	1.02	99.72
16A	0.04	0.08	0.6	97.4	0.019	0.11	0.05	0.10	0.74	0.11	0.68	99.93
16E	0.03	0.07	1.0	97.2	0.021	0.11	0.03	0.11	0.73	0.12	0.33	99.71
17Top	-0.02	0.05	0.4	97.4	0.017	0.05	0.05	0.06	0.69	0.11	1.10	99.92
17A	-0.02	0.03	0.3	98.1	0.010	0.04	0.03	0.07	0.77	0.09	0.64	100.17
17E	0.04	0.03	1.0	95.7	0.020	0.05	0.03	0.12	0.82	0.37	0.82	99.01
18Top	-0.02	0.01	0.2	98.2	0.009	0.04	0.03	0.04	0.70	0.06	0.59	99.86
19A	0.03	0.04	0.4	97.1	0.010	0.05	0.03	0.13	0.80	0.09	0.98	99.58
20Top	0.08	0.08	0.4	91.6	0.021	0.06	0.16	0.07	0.60	1.18	5.85	100.11
21Top	0.05	0.07	0.6	97.0	0.068	0.11	0.05	0.08	0.87	0.15	0.70	99.83
23Top	0.14	0.11	1.8	95.1	0.079	0.64	0.07	0.18	0.86	0.14	0.78	99.82
24Top	0.04	0.10	1.4	95.8	0.066	0.32	0.06	0.11	1.11	0.12	0.94	100.07
24A	0.05	0.04	1.4	94.9	0.037	0.28	0.03	0.13	1.65	0.11	0.74	99.39
24G	0.17	0.22	8.5	80.4	0.057	0.46	0.04	0.36	4.56	1.25	3.88	99.90
25Top	0.10	0.05	2.0	92.4	0.079	0.47	0.06	0.15	3.31	0.20	1.20	100.08
25A	0.11	0.07	2.0	93.6	0.058	0.50	0.04	0.16	2.11	0.17	1.00	99.85
25G	0.19	0.33	16.6	59.5	0.089	0.61	0.08	0.55	8.88	6.39	6.79	100.01
26AE	0.06	0.03	1.5	93.4	0.057	0.30	0.04	0.15	2.33	0.19	1.29	99.32
26B	0.19	0.30	8.2	80.6	0.046	0.68	0.08	0.32	4.02	1.81	3.76	99.95
28A	0.07	0.07	2.7	92.1	0.039	0.46	0.04	0.18	1.31	0.43	2.05	99.46
28E	0.03	0.08	3.3	86.1	0.127	0.44	0.03	0.19	6.92	0.66	2.24	100.07
28B	0.03	0.16	7.3	80.9	0.118	0.67	0.04	0.16	3.75	2.45	3.76	99.38
29Top	0.23	0.12	2.2	92.6	0.032	0.47	0.10	0.26	1.31	0.37	1.88	99.64
29Top <sub>t</sub>	0.19	0.12	2.1	93.2	0.031	0.43	0.10	0.25	1.30	0.43	2.10	100.32
29E	0.17	0.07	1.5	95.0	0.021	0.36	0.06	0.22	1.15	0.28	0.87	99.68
29G	0.56	0.29	3.4	90.4	0.013	0.39	0.07	0.23	1.71	1.27	1.35	99.73
Gr1	5.58	0.02	14.3	74.0	0.026	5.17	0.08	0.06	0.74	0.20	0.18	100.41
30Top	3.60	0.06	12.6	74.3	0.079	4.49	0.09	0.13	1.87	0.81	2.13	100.14
30A	3.54	0.06	13.0	75.1	0.060	4.56	0.07	0.14	1.80	0.59	1.63	100.54
31Top	2.68	0.03	9.3	80.1	0.042	3.75	0.12	0.10	1.43	0.76	2.17	100.45
31AE	2.85	0.07	9.6	81.0	0.043	3.96	0.08	0.11	1.25	0.35	0.95	100.24
31B	1.73	0.06	11.2	73.7	0.080	4.19	0.04	0.12	5.49	1.01	2.55	100.19
32Top	0.61	0.05	3.6	90.5	0.038	1.70	0.06	0.08	1.66	0.43	1.30	100.03
32A	0.64	-0.01	3.4	92.2	0.017	1.68	0.02	0.11	0.93	0.36	0.62	100.07
32GB	0.86	-0.01	4.6	90.4	0.016	2.16	0.01	0.12	1.75	0.31	0.00	100.21
32G	0.09	0.18	17.7	67.2	0.019	0.87	0.07	0.14	4.86	1.95	6.78	99.86
33Top	0.20	0.04	1.5	94.9	0.029	0.70	0.04	0.08	0.83	0.43	1.14	99.93
33AE	0.20	0.02	1.7	94.8	0.014	0.66	0.02	0.09	0.78	0.33	0.62	99.18
33G	0.26	0.46	12.0	74.2	0.028	0.76	0.10	0.27	3.62	3.17	5.11	100.03
34A	0.27	0.06	5.0	88.7	0.046	2.56	0.05	0.24	1.15	0.47	1.29	99.77
35Sap	0.23	0.95	19.8	56.1	0.094	3.20	0.02	0.86	8.66	1.53	6.66	98.11
36Top	0.06	0.10	4.8	77.4	0.091	0.41	0.04	0.47	11.98	0.62	3.40	99.42
36E	0.03	0.12	7.1	66.3	0.113	0.43	0.03	0.52	20.56	0.85	4.05	100.16
36B	0.06	0.33	18.2	61.9	0.051	0.98	0.03	0.98	7.46	1.57	7.98	99.56
37A	0.08	0.22	6.2	80.9	0.087	0.79	0.10	0.58	6.29	0.71	4.26	100.27

continued ...

Sample	Na <sub>2</sub> O	MgO	Al <sub>2</sub> O <sub>3</sub>	SiO <sub>2</sub>	P <sub>2</sub> O <sub>5</sub>	K <sub>2</sub> O	CaO	TiO <sub>2</sub>	Fe <sub>2</sub> O <sub>3</sub>	H <sub>2</sub> O-	LOI	Total
37B	0.12	0.33	9.3	75.8	0.078	1.12	0.11	0.68	7.25	0.95	4.70	100.40
38A	0.12	0.39	9.1	73.6	0.090	1.35	0.16	0.73	7.16	1.01	5.75	99.54
38B	0.20	0.75	15.9	63.0	0.068	1.68	0.18	0.71	8.89	2.26	6.77	100.51
38BC	0.22	1.08	17.3	61.0	0.067	1.56	0.84	0.78	7.49	2.64	7.65	100.57
39Sap	9.34	1.23	18.1	66.1	0.020	4.31	0.03	0.75	2.22	0.62	5.30	108.00
40Top	0.05	0.21	5.1	80.8	0.188	0.78	0.10	0.42	8.55	0.66	3.62	100.50
40E	0.05	0.26	5.9	79.9	0.173	0.91	0.14	0.42	9.14	0.58	3.52	100.99
40B	0.04	0.72	14.3	65.4	0.077	2.49	0.11	0.48	8.16	1.62	5.56	99.02
41Top	0.05	0.13	3.3	89.4	0.068	0.43	0.06	0.32	4.30	0.36	2.08	100.46
41E	0.06	0.32	8.4	79.1	0.046	0.94	0.05	0.24	6.41	0.98	3.75	100.34
41B1	0.11	0.71	20.0	53.2	0.047	1.94	0.06	0.36	9.72	4.70	8.52	99.36
41B2	0.13	0.77	22.6	49.9	0.045	2.01	0.05	0.43	9.86	5.17	9.00	100.01
43Top	0.07	0.10	2.3	91.3	0.056	0.28	0.05	0.28	4.19	0.33	1.49	100.51
43AE	0.12	0.10	2.3	91.6	0.038	0.30	0.03	0.30	3.78	0.32	1.21	100.11
43E	0.07	0.10	2.5	88.6	0.038	0.28	0.02	0.17	5.73	0.34	1.34	99.23
43G	0.32	1.06	22.2	52.8	0.025	2.52	0.08	0.56	9.79	2.66	8.14	100.13
44Top	0.31	0.40	8.2	70.8	0.147	1.41	0.14	0.60	12.83	0.89	3.63	99.38
44A2	0.17	0.45	10.0	63.2	0.146	1.56	0.11	0.61	18.23	1.42	4.14	100.04
44B	0.09	0.99	20.8	55.0	0.040	2.90	0.18	0.67	6.96	4.86	7.66	100.23
44C	0.09	0.99	15.1	61.8	0.035	2.59	0.14	0.72	5.49	7.59	5.26	99.79
44R	1.88	1.51	11.7	72.6	0.213	2.50	0.53	0.87	4.96	0.77	2.28	99.83
45A	0.11	0.14	4.1	90.0	0.080	0.66	0.08	0.44	1.99	0.53	2.51	100.71
45BA	0.10	0.15	5.7	87.1	0.044	0.71	0.04	0.54	2.38	0.51	2.42	99.65
45B	0.05	0.27	16.5	64.4	0.069	0.88	0.07	0.73	7.38	2.37	6.99	99.70
46A	0.08	0.10	6.5	82.8	0.083	0.45	0.07	0.56	5.81	0.66	3.33	100.45
46B1	0.06	0.12	8.3	79.9	0.050	0.46	0.05	0.59	5.26	0.86	3.63	99.26
46B2	0.03	0.15	17.3	47.6	0.139	0.22	0.04	0.65	22.69	2.34	8.66	99.88
46C	0.03	0.17	18.6	57.8	0.088	0.28	0.05	0.91	12.07	2.38	7.98	100.37
47Top	0.14	0.10	5.2	86.0	0.052	1.06	0.05	0.49	3.24	0.43	2.41	99.16
47A1	0.14	0.13	6.7	84.3	0.053	1.11	0.07	0.53	3.85	0.54	2.75	100.15
47B1	0.12	0.17	8.9	79.5	0.045	1.05	0.08	0.59	4.47	0.78	3.67	99.38
47B2	0.06	0.21	18.7	50.6	0.148	0.49	0.09	0.67	17.53	2.32	8.96	99.84
47C	0.05	0.28	22.8	52.9	0.076	0.54	0.69	1.09	9.80	2.70	9.75	100.74
47A2	0.15	0.17	7.6	83.2	0.036	1.13	0.11	0.60	3.47	0.89	3.31	100.65

**Table App-3 (part a):** Concentrations of trace elements in ppm. Negative numbers refer to concentrations below the LLD. ICP-MS: analysed using Inductively Coupled Plasma Mass Spectrometry. XRFS: analysed using X-Ray Fluorescence Spectrometry.

Sample	Li ICP-MS	Be ICP-MS	F XRFS	S XRFS	Cl XRFS	V XRFS	Cr XRFS	Mn XRFS	Co XRFS	Co ICP-MS	Ni XRFS	Cu XRFS	Zn XRFS
1A			-86	106	53	7.3	28.3	58.5	-1.7		9.2	4.4	3.0
1E			-84	52	42	6.0	21.7	46.9	-1.6		6.8	3.4	1.3
2A			-86								6.7	3.8	1.6
2E			-86								7.4	3.2	1.6
3A			-87								8.4	3.7	1.7
4A	3.3	-0.3	281	1036	212	7.4	23.8	102.9	-1.6	0.81	4.9	3.3	8.1
5A			107	168	66	34.8	30.3	131.3	2.5		7.3	5.0	13.2
6AE			189	132	52	30.1	29.4	122.8	3.4		9.2	6.7	16.8
6B			442								26.1	8.3	63.0
7A			-101	184	77	31.1	37.2	121.8	3.3		7.6	5.7	14.2
8A			-124	315	73	121.9	80.1	83.3	3.0		9.3	7.0	8.9
8B			-133	477	73	257.4	157.8	44.2	4.4		18.7	6.3	8.6
9A			-95	198	98	42.1	32.9	74.5	-1.9		7.8	4.5	3.4
10A			-89	464	159	23.5	30.5	70.8	-1.8		7.9	4.6	5.4
11A			-105								7.1	4.0	4.5
11E			-92								6.2	3.5	1.7
12A			-116	266	77	78.4	73.7	93.9	-2.3		8.8	3.6	31.3
12B			-138	286	66	216.3	174.2	70.4	3.3		11.9	7.8	6.2
13AE			-109								5.6	2.6	4.4
16Top	2.6	-0.3	-85	90	63	8.7	29.1	69.0	-1.7	0.30	9.8	3.6	2.2
16A	2.7	-0.3	-85	118	91	8.1	27.6	67.4	-1.7	0.31	9.0	5.1	2.3
16E	3.5	-0.3	-85	103	60	8.5	22.3	53.5	-1.6	0.35	8.4	2.8	2.3
17Top			-84	98	57	6.7	28.4	63.3	-1.6		9.3	4.1	2.1

continued ...

Sample	Li ICP-MS	Be ICP-MS	F XRFS	S XRFS	Cl XRFS	V XRFS	Cr XRFS	Mn XRFS	Co XRFS	Co ICP-MS	Ni XRFS	Cu XRFS	Zn XRFS
17A			-84	79	57	7.7	30.1	69.8	-1.6		11.0	3.7	1.5
17E			-86	117	84	9.2	32.9	74.8	-1.7		10.0	4.4	3.0
18Top			-86	61	45	6.2	27.7	63.8	-1.6		9.4	4.3	1.1
19A	1.7	-0.3	-86	131	72	7.9	36.9	76.8	-1.7	-0.24	10.0	4.6	2.5
20Top	2.0	-0.3	101	743	422	6.5	24.9	62.0	-1.6	-0.24	6.9	3.7	1.7
21Top	4.2	-0.3	-86	116	83	7.9	27.2	84.6	-1.7	0.34	9.2	4.5	2.4
23Top			-86	87	65	9.4	26.5	83.7	-1.7		9.3	3.9	4.1
24Top	5.4	-0.3	-91	91	60	23.7	27.3	69.8	-1.7	0.38	7.4	3.7	4.2
24A	5.2	-0.3	-94	82	45	37.3	31.5	68.1	-1.8	0.42	8.0	4.1	2.6
24G	26.1	0.9	159	183	55	109.6	57.0	55.0	-2.3	1.33	8.6	2.6	9.0
25Top	5.6	0.3	-109	178	150	81.5	34.6	90.7	-2.1	0.87	7.6	3.1	3.9
25A			-100	111	52	51.4	28.6	73.9	-1.9		7.4	4.1	3.4
25G			225	286	95	182.5	100.1	63.1	8.3		21.9	6.0	15.8
26AE	4.5	-0.3	-102	295	115	50.9	35.3	71.3	-2.0	0.66	7.0	3.7	4.0
26B			362	329	124	79.0	63.5	67.9	3.6		11.5	3.5	11.1
28A			-93	171	97	24.1	25.6	69.5	-1.8		7.2	4.1	3.9
28E			-130	196	53	96.3	28.3	58.5	-2.6		6.7	5.4	3.9
28B			222	186	57	74.5	41.6	71.9	2.2		24.3	7.3	5.8
29Top	5.3	-0.3	106	287	505	25.0	31.7	133.8	2.4	1.35	8.5	4.3	7.0
29Top <sub>1</sub>			-91	279		24.6	31.6	137.2	2.1		9.4	4.5	6.8
29E			-90	160	193	20.1	31.1	127.4	-1.7		9.5	4.5	3.7
29G	13.5	0.3	223	248	1459	25.6	36.4	103.6	3.1	1.81	8.8	4.0	5.2
Gr1	16.6	7.4	404	38	101	2.5	15.3	62.0	-1.7	0.24	5.2	2.5	5.0
30Top	25.1	5.1	490	164	148	9.4	19.4	120.1	-1.9	0.56	4.9	3.0	13.3
30A			383	296	107	8.6	18.5	79.1	-1.9		4.6	3.4	12.7
31Top	19.8	3.1	379	151	140	10.1	24.2	135.3	-1.8	0.39	6.5	3.2	7.6
31AE			312	59	95	9.3	16.4	78.2	-1.8		4.6	1.6	6.5
31B			705	340	540	35.9	25.4	56.7	-2.5		5.5	6.8	6.3
32Top	6.0	-0.3	163	136	131	15.4	25.2	75.6	-1.9	-0.24	7.0	1.9	3.1
32A	8.7	1.1	191	72	84	7.6	24.8	72.4	-1.7	0.31	8.2	1.6	2.3
32GB	9.2	1.8	187	76	89	17.9	17.2	56.8	-1.9	-0.24	5.3	-1.0	1.5
32G	84.0	1.5	1891	181	141	32.1	29.6	72.2	-2.3	0.59	4.6	7.5	11.6
33Top	5.5	0.5	174	185	203	9.3	27.1	77.9	-1.7	0.36	8.8	4.0	3.9
33AE			218	123	111	8.3	21.0	66.3	-1.7		6.8	2.7	2.9
33G			1927	213	251	35.7	49.0	83.5	2.4		9.4	5.1	13.6
34A	5.3	0.3	-90	114	71	17.4	23.4	120.1	-1.8	0.93	6.1	4.3	8.5
35Sap	25.0	2.7	551	151	1300	137.4	133.6	126.1	-2.9	2.15	15.0	31.6	31.9
36Top	4.1	0.6	-151	350	133	153.7	86.4	173.8	-3.2	1.81	4.5	13.8	18.9
36E	3.4	0.8	-172	366	72	257.6	132.5	145.7	-3.9	2.12	5.1	19.5	23.8
36B	5.7	0.7	181	269	60	125.4	96.7	155.1	-2.8	2.30	10.8	8.0	25.2
37A	6.9	1.1	-124	339	144	74.5	81.0	311.3	-2.6	2.35	8.1	15.9	20.0
37B			251	317	188	97.5	80.7	310.1	-2.7		8.9	17.1	22.4
38A	14.8	2.2	242	388	132	103.0	84.0	391.3	6.4	3.53	12.8	19.0	26.8
38B			444	448	407	127.1	103.6	332.6	6.8		19.2	22.1	28.8
38BC			575	493	650	118.5	94.7	268.5	3.8		19.2	22.7	28.0
39Sap			1035	1237	56921	106.2	102.9	92.7	-2.0		10.1	17.1	27.7
40Top			-134	269	137	67.5	80.6	139.4	-2.9		14.5	16.9	26.1
40E			-140	232	75	70.5	76.0	119.2	-3.0		14.0	16.9	28.5
40B			444	279	59	122.8	101.1	86.4	4.0		19.3	13.9	31.7
41Top	4.7	0.7	-116	178	141	50.7	54.4	91.1	-2.4	1.09	6.6	6.7	10.2
41E			303	319	146	89.1	77.2	58.4	-2.6		10.7	8.7	13.5
41B1			557	445	377	155.8	123.1	71.1	3.2		23.4	17.3	27.8
41B2			560	669	506	158.2	125.8	69.8	-3.0		22.7	15.4	28.4
42Top			-113								8.1	6.7	13.1
42B			508								24.6	17.1	30.3
43Top	3.1	0.6	-117	207	306	50.6	56.4	90.2	-2.4	1.43	7.9	6.8	10.7
43AE			-115	165	399	48.4	58.1	79.8	-2.3		9.5	6.8	10.9
43E			-126	384	212	69.6	70.0	70.3	-2.6		9.1	7.2	9.2
43G	34.6	3.4	720	213	806	175.0	137.6	77.5	7.5	6.11	26.9	15.2	41.8
44Top	12.7	2.5	-148	258	87	167.8	125.2	161.2	7.9	7.18	23.7	30.5	33.5
44A2			224	194	50	226.0	164.9	151.0	9.8		28.8	42.2	41.4
44B	40.4	4.3	464	196	42	141.2	122.9	118.8	29.0	14.79	56.8	45.5	54.9
44C	25.1	3.7	609	407	45	116.9	105.2	146.7	19.6	9.81	41.1	63.3	53.4
44R	16.0	2.7	579	24	46	85.4	71.2	209.0	13.8	7.45	34.5	16.0	60.5
45A	7.1	0.4	-104	217	83	35.0	41.2	172.9	2.1	1.65	8.7	7.1	13.3
45BA			124	110	75	44.2	42.2	108.1	2.7		8.6	7.2	12.1
45B	22.8	1.8	-131	339	88	149.4	103.9	97.4	6.2	4.91	24.6	18.5	24.2

continued ...

Sample	Li ICP-MS	Be ICP-MS	F XRFS	S XRFS	Cl XRFS	V XRFS	Cr XRFS	Mn XRFS	Co XRFS	Co ICP-MS	Ni XRFS	Cu XRFS	Zn XRFS
46A	6.4	-0.3	-124	187	67	85.9	51.5	133.1	-2.6	1.82	8.5	3.7	11.0
46B1			-121	152	54	78.9	51.6	111.2	-2.5		9.0	4.8	11.3
46B2			-158	372	59	371.4	205.2	53.6	-3.9		16.5	12.1	18.3
46C			-138	214	53	196.9	118.5	83.1	4.3		13.3	7.3	17.0
47Top	5.6	0.4	-112	124	61	43.6	30.1	185.2	-2.2	1.68	6.6	5.0	11.6
47A1	7.1	0.6	-116	116	56	51.9	31.0	248.2	3.8	2.29	7.0	7.0	15.9
47B1	11.3	0.7	-119	114	40	62.9	39.6	175.9	-2.4	3.48	7.9	6.2	18.5
47B2	15.1	1.4	-147	194	41	266.4	131.3	95.4	-3.6	4.30	20.4	15.9	28.1
47C	8.8	1.2	-130	206	45	150.3	57.6	92.8	-3.0	2.99	7.1	8.1	24.8
47A2			-113	133	56	48.3	31.5	314.7	4.7		6.8	7.0	18.1
24fr			237								5.1	72.2	2049.3
fer_a			3940								18.5	77.9	562.5
fer_c			415								-3.2	-0.6	4.2
fer_d			3605								9.6	46.9	289.4
fer_e			5677								-4.7	80.9	

**Table App-3 (part b):** Concentrations of trace elements in ppm. Negative numbers refer to concentrations below the LLD. ICP-MS: analysed using Inductively Coupled Plasma Mass Spectrometry. XRFS: analysed using X-Ray Fluorescence Spectrometry.

Sample	Ga XRFS	Ge XRFS	As XRFS	As ICP-MS	Se XRFS	Se ICP-MS	Br XRFS	Rb XRFS	Sr XRFS	Y XRFS	Zr XRFS	Nb XRFS	Mo XRFS
1A	-0.7	0.8	0.9		-0.6		2.4	2.2	12.6	2.6	109	1.1	2.1
1E	-0.7	0.8	0.9		-0.6		2.7	2.2	11.0	2.8	135	1.8	1.6
2A	-0.7	0.7	0.8		-0.6		1.2	3.1	14.1	2.6	95	1.7	1.8
2E	-0.7	0.7	1.3		-0.6		0.8	3.0	13.7	2.5	107	1.6	1.6
3A	-0.7	1.0	1.1		-0.6		28.9	3.4	32.8	3.4	216	1.8	1.8
4A	0.8	-0.6	0.6	-215	-0.6	-150	33.7	8.1	113.0	7.3	334	3.7	1.0
5A	6.1	0.8	1.9		-0.7		2.2	76.8	74.8	21.7	306	4.6	1.3
6AE	8.7	0.9	2.0		-0.7		2.7	107.9	77.0	23.8	265	5.5	1.1
6B	21.5	1.2	5.0		1.3		15.2	152.8	60.9	18.5	201	17.8	1.2
7A	4.8	-0.7	2.1		-0.7		2.9	68.8	36.6	23.6	394	6.2	1.2
8A	10.5	0.9	8.1		1.9		5.0	25.7	10.6	16.1	313	7.6	1.6
8B	26.5	1.6	15.3		5.5		13.8	40.6	7.1	9.9	267	16.4	2.3
9A	1.7	-0.7	5.7		-0.7		2.6	4.9	5.2	10.4	276	5.9	2.1
10A	0.8	0.8	3.2		-0.6		4.9	5.0	8.8	5.4	190	2.9	2.0
11A	1.3	-0.7	6.4		-0.7		1.9	8.1	9.1	8.0	242	3.5	1.0
11E	-0.7	0.8	2.5		-0.6		0.8	4.7	6.8	6.2	251	2.7	1.3
12A	5.7	1.2	7.2		0.9		3.7	37.7	9.7	16.6	566	50.0	1.2
12B	14.2	1.6	16.0		2.0		6.8	44.2	8.6	14.8	397	38.5	3.2
13AE	3.9	-0.7	13.6		-0.7		2.0	35.1	22.5	16.2	338	11.8	1.8
16Top		-0.7	0.8	-215	-0.7	-150	1.4	3.8	18.5	3.7	208	2.5	2.8
16A		-0.7	0.7	-215	-0.7	-150	2.7	4.3	18.2	5.5	288	2.5	2.4
16E		-0.7	1.3	-215	-0.7	-150	3.5	4.4	16.8	4.6	267	2.8	2.4
17Top		-0.7	0.8		-0.6		2.8	1.4	13.7	2.4	137	1.6	2.5
17A		-0.7	1.3		-0.7		3.6	1.3	12.9	2.2	160	1.8	2.9
17E		-0.7	1.5		-0.7		11.0	1.5	12.7	3.9	376	3.2	2.9
18Top		-0.7	-0.6		-0.7		0.8	-0.6	5.5	2.0	95	1.1	2.8
19A		-0.7	1.1	-215	-0.7	-150	4.1	0.7	8.2	4.4	578	3.5	2.7
20Top		-0.7	1.2	-215	-0.6	-150	45.7	1.6	31.4	2.9	245	1.6	2.2
21Top		-0.7	0.7	-215	-0.7	-150	4.0	4.6	63.6	4.4	391	2.2	2.5
23Top		-0.7	2.5		-0.7		2.1	26.2	30.3	6.9	643	5.5	2.2
24Top		-0.7	3.1	-215	-0.7	-150	0.9	12.2	6.8	9.2	236	6.1	2.2
24A		-0.7	6.6	-215	-0.7	-150	1.7	13.3	6.5	12.5	359	7.1	2.8
24G		-0.8	18.6	-215	-0.7	-150	4.3	39.3	19.0	15.7	267	14.0	2.4
25Top		-0.8	21.3	-215	0.7	-150	1.3	20.9	12.2	21.0	411	27.9	2.9
25A		-0.7	10.7		-0.7		2.0	21.9	10.7	22.5	443	11.2	2.1
25G		-0.9	38.2		1.8		5.3	65.2	26.5	25.2	163	22.4	2.9
26AE		-0.7	11.4	-215	-0.7	-150	2.7	13.4	14.4	12.5	291	7.4	2.7
26B		-0.8	13.7		1.2		10.4	50.9	30.4	16.0	211	10.3	2.7
28A		-0.7	3.9		-0.7		5.5	32.7	12.9	14.7	345	10.6	2.0
28E		-0.8	29.3		1.5		5.3	33.3	15.6	11.2	188	9.2	2.9
28B		-0.8	15.8		2.2		20.4	58.5	19.2	10.5	169	7.5	2.9

continued ...

Sample	Ga XRFS	Ge XRFS	As XRFS	As ICP-MS	Se XRFS	Se ICP-MS	Br XRFS	Rb XRFS	Sr XRFS	Y XRFS	Zr XRFS	Nb XRFS	Mo XRFS
29Top		-0.7	1.6	-215	-0.7	-150	6.3	17.8	19.5	13.6	307	4.6	2.1
29Top <sub>r</sub>		-0.7	2.0		-0.7		5.9	16.6	18.7	11.9	261	4.3	2.2
29E		-0.7	2.0		-0.7		2.9	12.6	14.6	10.8	306	3.9	2.3
29G		-0.7	1.9	-215	-0.7	-150	5.9	21.1	16.7	9.8	217	4.7	2.0
Gr1		0.9	1.3	403	-0.7	-150	1.0	356.9	7.7	34.2	343	207.6	2.0
30Top		1.2	27.4	246	-0.7	-150	2.4	346.2	18.9	34.9	584	234.3	2.9
30A		1.4	22.7		1.0		6.6	352.6	18.4	34.8	567	217.1	2.7
31Top		-0.7	9.4	-215	-0.7	-150	2.6	308.3	13.3	18.2	418	186.5	2.4
31AE		1.0	9.2		-0.7		2.8	320.2	9.9	20.2	506	205.2	2.2
31B		1.3	243.9		5.3		15.5	372.8	9.2	15.8	396	204.2	10.0
32Top		0.8	77.3	-215	-0.7	-150	1.5	153.4	6.7	9.9	354	136.9	3.1
32A		-0.7	17.6	-215	-0.7	-150	1.9	152.9	5.7	10.8	388	143.6	2.5
32GB		0.8	137.8	-215	0.9	-150	-0.9	190.3	6.4	15.8	570	198.6	2.9
32G		1.4	743.0	991	2.4	-150	7.6	245.9	10.7	23.5	365	221.8	6.3
33Top		-0.7	6.3	322	-0.7	-150	2.4	51.4	9.8	9.4	267	88.0	2.8
33AE		1.1	4.4		-0.7		2.0	53.7	9.7	10.7	286	89.8	2.1
33G		1.1	20.8		0.9		12.2	138.8	36.5	23.8	174	66.7	2.6
34A		-0.7	2.0	361	-0.7	-150	3.1	75.0	45.8	26.3	483	6.0	1.5
35Sap		-0.9	3.7	225	-0.8	-150	9.0	153.8	16.7	17.9	181	19.1	0.7
36Top		-1.0	15.9	-215	1.6	-150	6.5	23.0	11.1	9.8	345	9.4	2.2
36E		-1.1	27.2	-215	3.2	-150	6.4	24.9	11.0	9.5	280	9.8	2.3
36B		-0.8	6.4	-215	2.1	-150	28.7	61.7	20.6	14.6	287	19.9	1.5
37A		-0.8	5.5	-215	0.9	-150	11.3	42.6	27.0	10.7	329	11.8	1.5
37B		-0.8	6.5		1.3		25.0	61.1	36.3	12.6	323	13.8	1.3
38A		-0.8	6.8	-215	0.9	-150	13.9	70.9	35.8	19.2	347	14.7	1.5
38B		-0.9	7.2		-0.8		23.5	108.8	49.1	27.6	238	13.8	1.4
38BC		-0.8	5.4		-0.8		7.5	101.9	64.4	30.4	262	15.3	0.7
39Sap		1.1	15.6		-0.7		63.5	191.6	16.2	34.4	167	15.7	0.7
40Top		-0.9	13.8		1.0		5.8	41.2	19.0	18.2	189	7.4	1.9
40E		-0.9	12.9		1.2		5.4	47.4	20.2	18.7	163	7.3	1.6
40B		-0.9	13.1		2.8		26.0	140.0	22.5	27.6	148	9.9	1.1
41Top		-0.8	12.9	-215	-0.7	-150	4.2	26.3	10.3	14.5	157	6.2	1.7
41E		-0.8	17.9		1.5		15.9	65.4	10.4	9.7	74	5.6	1.7
41B1		-0.9	21.4		3.2		28.2	150.6	17.5	13.6	116	9.5	2.1
41B2		-0.9	20.9		2.8		29.5	154.5	17.6	10.9	135	9.8	1.5
42Top		-0.7	11.1		-0.7		2.4	20.4	8.1	13.0	167	5.3	1.9
42B		0.9	23.4		2.4		26.7	153.0	18.3	13.8	133	11.1	1.6
43Top		-0.8	15.6	-215	-0.7	-150	4.4	16.8	10.3	11.4	162	5.1	2.1
43AE		-0.8	15.5		-0.7		4.0	18.6	7.7	11.9	168	5.0	2.4
43E		-0.8	24.6		0.9		1.7	18.3	16.9	7.5	83	3.1	2.3
43G		-0.9	23.5	468	1.4	-150	5.9	170.4	20.1	16.0	133	11.8	1.7
44Top		-1.0	25.6	-215	2.4	-150	5.4	67.9	30.9	31.2	373	11.0	1.9
44A2		-1.1	39.8		3.0		5.1	77.3	25.9	33.2	307	11.2	2.6
44B		0.9	9.4	-215	1.5	-150	22.8	168.5	29.6	53.9	232	11.7	1.2
44C		-0.8	7.2	-215	-0.8	-150	11.0	143.5	44.8	72.6	279	13.4	1.4
44R		-0.8	4.5	-215	-0.8	-150	-1.0	103.3	116.0	47.0	340	15.0	1.2
45A		-0.7	3.1	-215	-0.7	-150	3.9	31.0	14.9	13.5	465	8.3	1.4
45BA		-0.7	2.9		-0.7		6.1	37.6	14.7	14.0	407	9.9	1.1
45B		1.1	9.6	-215	1.9	-150	9.7	67.5	16.0	21.4	269	14.2	1.9
46A		-0.8	8.4	-215	1.3	-150	3.6	23.7	9.5	10.6	568	11.0	1.5
46B1		-0.8	6.8		1.0		4.8	30.7	8.8	11.2	454	12.0	1.4
46B2		-1.1	41.2		8.9		8.4	24.6	7.5	10.8	321	12.8	2.7
46C		-0.9	18.2		2.8		14.5	30.1	9.0	14.3	421	17.6	2.1
47Top		-0.8	4.4	-215	1.2	-150	3.2	40.6	19.3	11.1	522	9.7	1.1
47A1		-0.8	5.5	-215	1.1	-150	2.2	45.4	22.3	12.3	482	10.6	1.2
47B1		-0.8	7.0	-215	-0.7	-150	1.6	51.3	22.9	12.3	467	11.7	1.1
47B2		-1.0	33.3	-215	5.3	-150	3.8	45.7	18.3	22.2	242	12.8	2.6
47C		-0.9	11.2	-215	1.1	-150	7.2	43.8	43.9	13.8	239	20.9	1.5
47A2		-0.7	4.9		-0.7		3.7	50.1	29.4	14.9	547	11.5	0.9
24fr		-0.6	5.4		-0.5		7.7	2.8	628.8	44.4	7	-0.4	1.0
fer_a	-0.9	-0.8	8.0		-0.7		47.4	5.6	902.0	50.9	14	1.0	1.1
fer_c	-0.5	-0.4	1.1		-0.4		1.6	0.7	27.3	-0.4	1	-0.3	-0.3
fer_d	-0.8	-0.8	5.3		-0.7		134.5	12.5	681.2	49.7	9	1.0	0.6
fer_e	-0.7	-0.6	8.9		-0.6		6.1	2.1	616.3	43.0	10	0.6	0.6

**Table App-3 (part c): Concentrations of trace elements in ppm. Negative numbers refer to concentrations below the LLD. ICP-MS: analysed using Inductively Coupled Plasma Mass Spectrometry. XRFS: analysed using X-Ray Fluorescence Spectrometry.**

Sample	Mo ICP-MS	Cd ICP-MS	Sn XRFS	Sn ICP-MS	Sb ICP-MS	I XRFS	I ICP-MS	W XRFS	Pb XRFS	Bi XRFS	Th XRFS	U XRFS
1A			3.1			-3.6		22.1	1.7	-2.1	-1.4	1.2
1E			-1.8			-3.6		16.6	2.0	-2.1	2.0	-1.1
2A			2.0			-3.3		18.1	2.8	-2.1	1.5	-1.1
2E			2.5			-3.3		15.8	2.5	-2.1	1.7	-1.1
3A			2.3			-3.3		19.0	-1.6	-2.1	2.0	-1.1
4A	1.3	-0.7	1.8	0.8	2.1	8.8	-0.1	10.6	3.3	-2.1	1.5	1.3
5A			2.3			7.4		11.4	25.2	-2.3	10.6	2.4
6AE			3.3			-3.9		11.3	26.4	-2.3	11.9	2.2
6B			6.3			8.6		23.7	21.4	-2.6	11.9	3.7
7A			4.7			-3.8		13.0	13.6	-2.3	12.6	1.7
8A			4.0			5.0		8.4	11.7	-2.6	14.8	2.1
8B			9.6			16.1		12.3	17.2	-2.9	32.3	2.5
9A			3.4			-3.7		18.5	5.0	-2.2	3.9	-1.2
10A			2.3			-3.7		19.4	2.8	-2.1	-1.4	-1.1
11A			3.1			5.4		13.4	7.0	2.5	4.4	-1.2
11E			1.6			-3.3		16.6	2.2	-2.2	2.3	-1.1
12A			6.3			-4.1		9.6	8.7	-2.4	16.3	3.3
12B			9.6			9.4		14.0	15.9	-3.0	24.0	1.7
13AE			3.0			4.1		11.2	12.7	-2.4	9.1	2.1
16Top	2.0	-0.7	2.2	0.9	8.1	-2.3	-0.1	26.3	-1.7	-2.3	-1.4	1.2
16A	2.1	-0.7	1.7	0.7	1.4	-2.3	-0.1	22.7	2.0	-2.3	1.7	2.1
16E	1.7	-0.7	2.0	0.6	1.0	-2.3	-0.1	18.6	-1.7	-2.3	-1.4	1.3
17Top			-1.8			-3.6		24.0	-1.7	-2.3	-1.4	1.3
17A			1.8			-3.7		27.0	-1.7	-2.3	-1.4	-1.1
17E			2.2			4.4		25.9	-1.7	-2.3	-1.4	-1.1
18Top			1.9			-3.7		24.3	-1.7	-2.3	-1.4	-1.1
19A	2.9	-0.7	2.7	0.6	2.8	-3.6	-0.1	27.9	-1.7	-2.3	-1.4	1.4
20Top	1.9	-0.7	2.6	0.7	0.9	6.6	0.3	20.8	-1.6	-2.2	-1.4	-1.1
21Top	2.3	-0.7	-1.8	0.5	2.0	-3.6	-0.1	24.8	2.5	-2.3	-1.4	1.4
23Top			2.3			-3.7		21.8	3.9	-2.4	2.0	1.9
24Top	2.5	-0.7	2.3	1.2	-0.3	-3.7	-0.1	20.3	3.2	-2.3	2.8	1.4
24A	2.5	-0.7	2.9	1.0	4.2	-3.8	-0.1	20.2	2.8	-2.4	3.4	1.9
24G	1.9	-0.7	10.0	3.5	2.3	15.0	0.4	12.6	17.4	-2.6	12.7	3.4
25Top	2.5	-0.7	23.6	1.3	2.4	4.5	-0.1	-2.6	10.3	3.1	6.4	2.2
25A			4.1			-2.4		18.4	8.8	-2.4	8.7	2.6
25G			8.9			12.9		14.4	35.2	-2.9	21.5	3.0
26AE	2.3	-0.7	2.0	0.8	-0.3	5.0	-0.1	17.9	6.3	-2.4	3.5	1.2
26B			3.5			15.8		13.9	14.8	-2.5	7.3	2.6
28A			4.5			4.6		15.5	5.8	-2.3	3.8	1.7
28E			3.0			-4.4		11.3	12.1	-2.8	6.8	2.7
28B			2.1			6.3		16.6	15.2	-2.5	9.2	2.2
29Top	1.8	-0.7	-1.8	1.1	1.3	8.5	0.2	18.9	5.0	-2.4	4.6	2.2
29Top <sub>t</sub>			0.0					20.9	4.6	-2.3	3.0	1.9
29E			-1.8			5.1		21.9	4.6	-2.4	3.3	1.4
29G	1.3	-0.7	2.8	3.6	-0.3	9.3	-0.1	22.5	4.7	-2.4	2.4	1.4
Gr1	1.7	-0.7	7.3	2.4	-0.3	2.5	-0.1	52.5	11.0	17.7	30.9	4.9
30Top	3.4	-0.7	22.1	3.1	0.9	-3.9	-0.1	426.1	13.8	5.6	30.8	6.3
30A			17.3			-3.9		18.1	13.4	2.6	32.0	6.3
31Top	3.0	-0.7	7.7	2.1	1.1	-3.8	-0.1	19.5	8.9	-2.5	18.3	4.8
31AE			8.6			4.0		14.3	7.3	-2.5	17.9	3.8
31B			7.0			5.1		35.4	15.9	6.4	48.3	6.1
32Top	3.4	-0.7	4.2	0.5	-0.3	-2.4	-0.1	19.9	16.8	-2.4	11.9	3.3
32A	2.5	-0.7	5.0	1.3	-0.3	3.0	-0.1	17.9	3.4	-2.4	10.3	3.0
32GB	2.7	-0.7	4.5	1.6	6.3	4.4	-0.1	9.8	7.2	3.1	23.8	4.6
32G	8.0	-0.7	11.6	8.1	8.0	12.5	0.9	22.5	43.0	5.0	165.0	13.0
33Top	2.7	-0.7	46.6	1.2	-0.3	-3.7	-0.1	19.5	-1.7	-2.3	5.4	2.3
33AE			64.7			-3.7		16.7	2.4	-2.3	5.2	2.2
33G			7.8			9.5		24.6	15.1	-2.5	24.0	4.8
34A	1.6	-0.7	2.2	1.7	0.6	5.9	-0.1	15.5	17.1	-2.4	12.0	2.9
35Sap	-0.8	-0.7	7.2	5.2	1.9	23.2	-0.1	5.6	22.5	-2.9	17.0	8.2
36Top	2.4	-0.7	2.8	1.7	2.1	-3.1	-0.1	8.1	22.1	-3.1	10.9	2.8
36E	2.6	-0.7	2.7	1.7	2.9	5.7	0.3	6.4	34.4	-3.8	20.0	5.0

continued ...

Sample	Mo ICP-MS	Cd ICP-MS	Sn XRFS	Sn ICP-MS	Sb ICP-MS	I XRFS	I ICP-MS	W XRFS	Pb XRFS	Bi XRFS	Th XRFS	U XRFS
36B	0.8	-0.7	6.0	5.4	1.7	29.6	1.7	7.1	32.4	-2.7	18.1	4.4
37A	1.7	-0.7	2.9	2.1	1.7	17.2	-0.1	10.3	22.2	-2.7	9.2	3.6
37B			4.8			31.9		8.7	24.6	-2.8	13.6	4.4
38A	1.2	-0.7	3.6	3.1	1.6	31.1	1.4	8.8	21.9	-2.8	13.2	4.0
38B			4.4			152.4		8.6	24.0	-2.9	16.3	3.3
38BC			5.8			112.6		7.8	21.5	-2.8	19.1	3.6
39Sap			6.5			7.2		8.1	12.5	-2.5	17.0	3.5
40Top			3.6			-4.6		11.8	23.0	-2.8	8.0	4.4
40E			3.8			7.9		11.4	23.8	-2.9	8.6	3.4
40B			6.4			86.0		7.1	28.6	-2.8	15.3	7.1
41Top	1.8	-0.7	2.3	1.6	2.8	4.8	0.2	14.2	9.9	-2.5	6.7	2.2
41E			4.2			15.9		11.3	16.3	-2.7	8.3	3.6
41B1			7.9			98.1		9.3	24.6	-2.9	17.1	6.3
41B2			9.3			209.0		9.5	19.2	-2.9	17.1	6.2
42Top			2.5			4.6		17.1	8.9	-2.5	5.0	2.7
42B			9.6			55.9		7.8	22.2	-2.9	18.4	6.7
43Top	2.1	-0.7	-2.0	1.0	1.6	-4.1	-0.1	13.4	10.1	-2.5	4.4	2.6
43AE			-2.0			4.4		18.5	11.8	-2.5	3.3	2.1
43E			2.3			9.2		14.9	15.8	-2.7	4.4	2.1
43G	1.2	-0.7	10.3	7.6	5.8	49.4	0.4	7.4	22.1	-2.9	17.8	3.0
44Top	1.9	-0.7	4.5	2.2	12.7	-5.0	-0.1	11.7	31.2	-3.2	13.3	2.6
44A2			5.0			-5.5		13.0	40.4	-3.6	16.2	2.1
44B	-0.8	-0.7	4.7	4.7	7.0	15.7	-0.1	10.8	19.5	-2.7	18.5	4.2
44C	1.3	-0.7	3.4	4.3	7.7	19.1	-0.1	15.9	16.2	-2.7	13.8	2.5
44R	1.0	-0.7	4.0	3.3	3.4	-2.7	-0.1	9.6	18.9	-2.7	13.0	3.0
45A	1.5	-0.7	3.0	1.6	0.6	-3.8	-0.1	12.8	8.9	-2.4	3.8	2.4
45BA			2.3			6.2		8.8	9.6	-2.4	6.5	2.6
45B	1.4	-0.7	4.5	4.3	1.2	52.7	3.3	11.0	21.7	3.1	13.7	5.5
46A	1.6	-0.7	2.7	1.6	0.5	4.1	-0.1	8.5	10.0	-2.7	12.4	2.5
46B1			2.6			17.9		6.5	11.2	2.7	11.4	2.5
46B2			5.8			16.4		5.7	35.4	-3.8	51.7	4.5
46C			6.3			33.7		8.6	22.2	-3.0	35.7	4.4
47Top	1.5	-0.7	-1.9	1.2	1.5	6.2	0.2	10.5	10.3	-2.5	7.9	3.1
47A1	1.1	-0.7	-2.0	1.6	1.6	8.6	-0.1	6.5	11.3	-2.5	6.9	2.0
47B1	1.5	-0.7	2.7	2.1	1.1	13.8	0.9	4.9	12.7	-2.6	10.0	2.6
47B2	2.4	-0.7	5.7	3.6	3.0	8.5	0.4	9.0	42.1	3.9	41.3	5.0
47C	1.1	-0.7	6.4	4.8	1.3	64.2	0.5	8.4	35.2	-2.9	26.3	5.1
47A2			2.0			17.5		6.7	11.0	-2.5	8.9	3.2
24fr								6.5	70.4	-1.9	22.6	4.3
fer_a			1.4			-2.2		2.7	21.4	-2.5	25.8	3.7
fer_c			2.4			-1.2		-1.4	-1.0	-1.4	-0.9	-0.7
fer_d			-1.7			-3.5		4.0	13.9	-2.5	26.1	2.5
fer_e			-1.4			-2.8		6.6	69.5	-1.9	19.3	3.4

**Table App-4:** Concentrations of 1 M  $\text{NH}_4\text{NO}_3$  extractable element fractions in ppm. The analyses were performed using ICP-AES. The method for extraction is given in Appendix-II and discussed in section 2.5. Negative numbers refer to concentrations below the LLD.

Sample	Na	Mg	Al	P	S	K	Ca	V	Cr	Fe	Ni	Cu	Zn
1A	14	30	1.8	0.5	4	5	185	-0.025	-0.05	0.52	-0.25	-0.05	0.43
1E	10	18	1.0	-0.5	3	4	83	-0.025	-0.05	0.35	-0.25	-0.05	-0.13
4A	80	248	8.5	18.3	20	20	1740	-0.025	0.05	8.00	0.82	-0.05	0.88
5A	13	17	5.5	-0.5	4	38	68	-0.025	-0.05	0.18	-0.25	-0.05	0.20
6AE	21	55	1.4	-0.5	4	28	190	-0.025	-0.05	0.10	-0.25	-0.05	0.23
8A	17	100	-0.5	1.0	7	40	355	-0.025	-0.05	0.08	-0.25	0.10	0.15
8B	24	133	2.5	1.0	28	45	423	-0.025	-0.05	0.57	0.25	-0.05	0.25
9A	28	17	1.3	-0.5	7	28	53	-0.025	-0.05	0.73	-0.25	-0.05	0.50
10A	68	65	1.2	1.3	13	63	258	-0.025	-0.05	1.85	-0.25	-0.05	0.75
12A	15	20	5.3	-0.5	6	24	138	-0.025	-0.05	0.20	-0.25	-0.05	9.25
12B	28	58	11.0	0.5	16	28	125	-0.025	-0.05	0.68	-0.25	-0.05	-0.13
16Top	17	35	-0.5	1.0	4	8	200	-0.025	-0.05	0.30	-0.25	-0.05	-0.13
16A	13	30	-0.5	-0.5	3	4	148	-0.025	-0.05	0.27	-0.25	-0.05	-0.13
16E	10	17	1.3	-0.5	3	5	48	-0.025	-0.05	0.60	-0.25	-0.05	-0.13
17Top	16	30	1.7	0.7	5	6	250	-0.025	-0.05	0.45	-0.25	-0.05	0.18
17A	14	20	1.1	-0.5	4	3	140	-0.025	-0.05	0.38	-0.25	-0.05	-0.13
17E	17	45	1.0	-0.5	3	1	83	-0.025	-0.05	0.13	-0.25	-0.05	-0.13
18Top	15	25	-0.5	0.7	4	3	128	-0.025	-0.05	0.22	-0.25	-0.05	-0.13
19A	24	28	0.5	1.0	5	2	83	-0.025	-0.05	0.30	-0.25	-0.05	-0.13
20Top	173	305	0.9	3.8	30	8	665	-0.025	0.05	0.62	0.40	-0.05	0.43
21Top	33	45	-0.5	0.7	5	10	145	-0.025	-0.05	0.20	-0.25	-0.05	-0.13
23Top	14	21	1.8	-0.5	3	9	103	-0.025	-0.05	0.38	-0.25	-0.05	-0.13
24Top	10	22	-0.5	2.2	-1	15	125	-0.025	-0.05	-0.05	-0.25	-0.05	0.15
24A	9	12	3.3	-0.5	-1	13	70	-0.025	-0.05	-0.05	-0.25	-0.05	-0.13
24G	410	373	-0.5	-0.5	1	38	180	-0.025	0.08	-0.05	0.25	-0.05	0.18
25Top	15	16	-0.5	1.6	-1	18	183	-0.025	-0.05	-0.05	-0.25	-0.05	-0.13
25A	18	12	0.9	-0.5	-1	13	105	-0.025	-0.05	-0.05	-0.25	-0.05	-0.13
25G	520	493	-0.5	-0.5	9	95	528	-0.025	0.10	-0.05	0.35	-0.05	0.33
26AE	25	43	-0.5	-0.5	-1	28	158	-0.025	-0.05	-0.05	-0.25	-0.05	0.25
26B	480	418	1.3	-0.5	4	155	458	0.050	0.15	-0.05	0.38	-0.05	0.53
29Top	223	133	-0.5	0.6	13	23	218	-0.025	-0.05	-0.05	-0.25	-0.05	0.20
29Top <sub>t</sub>	118	113	-0.5	0.6	4	25	230	-0.025	-0.05	-0.05	-0.25	-0.05	0.15
29E	98	68	-0.5	-0.5	4	13	100	-0.025	-0.05	-0.05	-0.25	-0.05	-0.13
29G	1210	340	-0.5	-0.5	45	23	218	-0.025	0.05	-0.05	-0.25	-0.05	-0.13
Gr1	663	12	-0.5	-0.5	4	558	65	-0.025	-0.05	-0.05	-0.25	-0.05	-0.13
30Top	28	68	-0.5	0.5	-1	80	203	-0.025	-0.05	-0.05	-0.25	-0.05	-0.13
30A	23	43	9.0	-0.5	-1	55	103	-0.025	-0.05	-0.05	-0.25	-0.05	-0.13
31Top	19	58	-0.5	2.1	-1	48	450	-0.025	-0.05	-0.05	-0.25	-0.05	0.13
31AE	38	53	-0.5	-0.5	-1	19	215	-0.025	-0.05	-0.05	-0.25	-0.05	-0.13
31B	420	175	1.4	-0.5	70	25	218	-0.025	-0.05	-0.05	-0.25	-0.05	-0.13
32Top	22	38	-0.5	0.9	-1	25	180	-0.025	-0.05	-0.05	-0.25	-0.05	-0.13
32A	13	17	2.5	-0.5	-1	17	78	0.050	-0.05	-0.05	-0.25	-0.05	-0.13
32GB	20	22	0.6	-0.5	-1	4	25	0.025	-0.05	-0.05	-0.25	-0.05	-0.13
32G	223	530	1.3	0.6	2	16	335	0.050	0.13	-0.05	0.32	-0.05	0.28
33Top	65	45	0.9	1.2	4	30	120	0.025	-0.05	0.20	-0.25	-0.05	0.40
33AE	28	35	1.1	-0.5	-1	18	70	-0.025	-0.05	-0.05	-0.25	-0.05	-0.13
33G	725	810	4.5	1.0	14	33	575	0.100	0.20	0.75	0.68	0.08	0.75
34A	18	35	2.3	-0.5	4	22	108	-0.025	-0.05	-0.05	-0.25	-0.05	0.23
35Sap	1678	370	-0.5	-0.5	43	8	88	-0.025	-0.05	-0.05	-0.25	-0.05	0.18
36Top	48	60	1.9	0.6	8	30	173	-0.025	-0.05	0.87	-0.25	-0.05	0.28
36E	28	78	4.5	-0.5	5	19	130	-0.025	-0.05	1.38	-0.25	-0.05	0.15
36B	88	408	20.8	-0.5	25	33	180	-0.025	0.08	1.20	-0.25	-0.05	0.43
37A	70	138	-0.5	1.6	15	55	478	-0.025	-0.05	-0.05	0.27	-0.05	0.38
37B	258	283	-0.5	-0.5	13	23	423	-0.025	-0.05	-0.05	-0.25	-0.05	0.35
38A	105	283	-0.5	1.0	11	43	665	-0.025	-0.05	-0.05	0.38	-0.05	0.45
38B	610	613	1.0	1.1	48	38	863	0.100	0.18	0.13	0.73	0.08	0.75
38BC	838	695	1.1	1.3	120	35	1103	0.100	0.20	0.10	0.90	0.10	1.00
39Sap	6900	370	0.6	-0.5	243	11	24	0.075	0.10	-0.05	-0.25	0.05	0.18
40Top	38	35	0.6	2.1	13	60	508	0.050	-0.05	0.15	0.38	-0.05	0.33
40E	22	24	0.7	1.4	9	38	730	0.075	-0.05	0.13	0.50	0.08	0.48
40B	45	88	1.5	0.7	23	40	713	0.075	0.05	0.55	0.50	-0.05	0.48
41Top	38	33	-0.5	1.0	11	33	355	-0.025	-0.05	-0.05	-0.25	-0.05	0.23

continued ...

Sample	Na	Mg	Al	P	S	K	Ca	V	Cr	Fe	Ni	Cu	Zn
41E	225	260	3.0	0.6	25	45	385	-0.025	0.05	1.95	0.32	-0.05	0.35
41B1	425	540	17.0	0.6	63	43	343	0.050	0.13	7.75	0.40	-0.05	0.45
41B2	598	673	6.0	0.7	133	35	285	0.050	0.13	2.05	0.40	-0.05	0.45
42Top	33	55	1.3	0.9	9	28	250	0.025	-0.05	0.15	-0.25	-0.05	0.83
42B	880	983	8.0	2.8	93	88	525	0.050	0.18	0.78	0.60	-0.05	0.68
43Top	83	33	-0.5	2.5	11	14	318	0.025	-0.05	0.40	-0.25	-0.05	0.33
43AE	238	50	-0.5	-0.5	19	9	115	-0.025	-0.05	-0.05	-0.25	-0.05	-0.13
43E	288	73	-0.5	-0.5	18	19	110	-0.025	-0.05	-0.05	-0.25	-0.05	-0.13
43G	1825	585	0.8	0.7	53	48	358	-0.025	0.10	0.45	0.35	-0.05	0.43
44Top	33	38	-0.5	5.8	8	40	535	0.025	-0.05	0.20	0.35	-0.05	0.35
44A2	25	43	-0.5	-0.5	5	35	483	-0.025	-0.05	-0.05	0.30	-0.05	0.28
44B	88	325	1.1	0.7	10	75	975	0.075	0.10	0.22	0.68	-0.05	0.65
44C	60	265	0.5	-0.5	17	35	645	0.050	0.08	-0.05	0.47	-0.05	0.43
44R	128	403	-0.5	0.6	7	100	780	0.050	0.10	-0.05	0.60	-0.05	0.60
45A	28	43	-0.5	2.1	13	63	268	-0.025	-0.05	0.05	-0.25	-0.05	0.48
45BA	25	33	-0.5	-0.5	11	68	173	-0.025	-0.05	-0.05	-0.25	-0.05	0.25
45B	50	88	1.4	-0.5	63	190	405	0.025	-0.05	0.62	0.27	-0.05	0.25
46A	14	24	0.6	1.2	8	35	328	0.050	-0.05	0.10	-0.25	-0.05	0.23
46B1	24	60	-0.5	-0.5	18	25	258	-0.025	-0.05	0.20	-0.25	-0.05	0.13
46B2	30	195	0.7	-0.5	43	35	340	0.025	-0.05	0.22	0.30	-0.05	0.28
46C	38	190	0.8	-0.5	23	24	250	-0.025	-0.05	0.40	-0.25	-0.05	0.20
47Top	19	43	-0.5	0.7	4	38	195	-0.025	-0.05	-0.05	-0.25	-0.05	-0.13
47A1	19	53	-0.5	-0.5	5	17	305	0.025	-0.05	0.35	-0.25	-0.05	0.25
47B1	25	80	-0.5	-0.5	9	21	373	-0.025	-0.05	0.05	0.27	-0.05	0.23
47B2	50	190	0.8	0.6	25	70	550	0.050	0.08	0.20	0.47	-0.05	0.43
47C	48	258	1.1	1.1	43	70	1055	0.075	0.10	0.32	0.73	0.05	0.70

**Table App-5: Concentrations of 1 M NH<sub>4</sub>NO<sub>3</sub> extractable element fractions in ppb. The analyses were performed using ICP-MS. The method for extraction is given in Appendix-II and discussed in section 2.5. Negative numbers refer to concentrations below the LLD.**

Sample	Be	B	V	Co	Cu	As	Sc	Mo	Cd	Sb	Ba	Tl	Pb	Bi	U
1A	-65	-363	-9	-13	-103	-70	-875	-50	-17	-23	767	-3	-53	-3	-30
1E	-65	-363	-9	-13	-103	-7	-12	-50	-17	-23	407	-3	-53	-3	-30
4A	-65	1318	16	20	160	-7	-12	-50	24	-23	935	-3	96	-3	-30
5A	-65	-363	-9	65	-103	-70	-875	-50	-17	-23	1802	-3	-53	-3	-30
6AE	-65	-363	-9	36	-103	-70	-875	-50	22	-23	3360	-3	-53	-3	-30
8A	-65	-363	-9	-13	-103	-70	-875	-50	-17	-23	1159	-3	-53	-3	-30
8B	-65	372	-9	-13	-103	-70	-875	-50	-17	-23	1738	-3	-53	-3	-30
9A	-65	-363	-9	16	-103	-70	-875	-50	-17	-23	196	-3	58	-3	-30
10A	-65	-363	-9	-13	-103	-70	-875	-50	-17	-23	532	-3	-53	-3	-30
12A	-65	-363	-9	37	-103	-70	-875	-50	-17	-23	1929	3	53	-3	-30
12B	-65	-363	-9	32	-103	-70	-875	-50	-17	-23	2918	7	-53	-3	-30
16Top	-65	-363	-9	-13	-103	-70	-875	-50	-17	-23	719	-3	-53	-3	-30
16A	-65	-363	-9	-13	-103	-70	-875	-50	-17	-23	675	-3	95	-3	-30
16E	-65	-363	-9	-13	-103	-70	-875	-50	-17	-23	502	-3	-53	-3	-30
17Top	-65	-363	-9	-13	-103	-70	-875	-50	-17	-23	730	-3	400	-3	-30
17A	-65	-363	-9	-13	-103	-70	-875	-50	-17	-23	390	-3	-53	-3	-30
17E	-65	-363	-9	-13	-103	-70	-875	-50	-17	-23	583	-3	150	-3	-30
18Top	-65	-363	-9	-13	-103	-70	-875	-50	-17	-23	532	-3	-53	-3	-30
19A	-65	-363	-9	-13	-103	-70	-875	-50	-17	-23	229	-3	82	-3	-30
20Top	-65	-363	-9	-13	250	-70	-875	-50	-17	82	997	-3	-53	-3	-30
21Top	-65	-363	-9	-13	242	-70	-875	-50	-17	-23	615	-3	72	-3	-30
23Top	-65	-363	-9	-13	-103	-70	-875	-50	-17	-23	795	-3	59	-3	-30
24Top	-65	-363	11	16	-103	-70	-875	-50	-17	-23	684	-3	-53	-3	-30
24A	-65	415	-9	-13	143	-70	-875	-50	-17	-23	742	-3	104	-3	-30
24G	-65	648	-9	-13	-103	-70	-875	-50	-17	-23	3486	5	-53	-3	-30
25Top	-65	-363	-9	16	-103	-70	-875	-50	-17	-23	961	-3	78	-3	-30
25A	-65	-363	-9	38	-103	-70	-875	-50	-17	-23	1888	-3	-53	-3	-30
25G	-65	1509	-9	-13	140	-70	-875	-50	-17	-23	4783	10	103	-3	-30
26AE	-65	-363	-9	21	333	-70	-875	-50	-17	-23	678	-3	-53	-3	-30
26B	-65	1219	-9	-13	-103	-70	-875	-50	-17	-23	2892	7	169	-3	57

continued ...

Sample	Be	B	V	Co	Cu	As	Se	Mo	Cd	Sb	Ba	Tl	Pb	Bi	U
29Top	-65	-363	12	24	345	-70	-875	-50	-17	35	1373	3	105	-3	-30
29Top <sub>Pt</sub>	-65	-363	-9	47	-103	-70	-875	-50	-17	-23	1240	-3	-53	-3	-30
29E	-65	-363	-9	21	198	-70	-875	-50	-17	-23	524	-3	58	-3	-30
29G	-65	966	102	-13	-103	-70	-875	-50	-17	-23	1061	-3	-53	-3	-30
Gr1	-65	-363	-9	-13	-103	-70	-875	-50	-17	-23	1227	24	-53	-3	-30
30Top	-65	-363	-9	-13	-103	-70	-875	-50	-17	-23	1933	-3	-53	-3	-30
30A	-65	-363	-9	-13	-103	-70	-875	-50	-17	-23	1414	-3	-53	-3	-30
31Top	-65	-363	-9	-13	-103	-70	-875	-50	-17	-23	1639	-3	-53	-3	-30
31AE	66	-363	10	-13	-103	-70	-875	-50	-17	-23	810	-3	-53	-3	-30
31B	-65		24	-13	-103	-70	-875	-50	-17	-23	1565	-3	314	-3	-30
32Top	-65	499	-9	-13	-103	-70	-875	-50	-17	-23	930	-3	-53	-3	-30
32A	-65	511	-9	-13	-103	-70	-875	-50	-17	-23	839	-3	73	-3	-30
32GB	-65	-363	-9	-13	-103	-70	-875	-50	-17	-23	473	-3	-53	-3	-30
32G	-65	-363	-9	-13	-103	52	-12	-50	-17	-23	3685	8	-53	-3	-30
33Top	-65	-363	18	-13	-103	-70	-875	-50	-17	-23	761	3	-53	-3	-30
33AE	-65	-363	-9	-13	-103	-70	-875	-50	-17	-23	514	-3	-53	-3	-30
33G	-65	-363	-9	-13	-103	-70	-875	-50	-17	-23	7334	21	-53	-3	-30
34A	-65	-363	-9	17	-103	-70	-875	-50	-17	-23	4119	5	-53	-3	-30
35Sap	-65	8885	69	-13	-103	86	-875	-50	-17	-23	1395	-3	288	-3	-30
36Top	-65	-363	-9	52	-103	-70	-875	-50	-17	-23	2732	4	-53	-3	-30
36E	-65	-363	-9	16	-103	-70	-875	-50	-17	-23	2273	-3	-53	-3	-30
36B	-65	546	-9	-13	-103	-70	-875	-50	-17	-23	6257	4	-53	-3	-30
37A	-65	459	10	19	-103	-70	-875	-50	-17	42	9161	4	-53	-3	-30
37B	65	-363	-9	-13	-103	-70	-875	-50	-17	-23	12860	3	-53	-3	-30
38A	-65	-363	-9	26	155	-70	-875	61	-17	-23	18129	7	-53	-3	-30
38B	-65	607	14	-13	129	-70	-875	-50	-17	-23	14602	4	-53	-3	66
38BC	-65	1201	27	-13	-103	-70	1012	-50	-17	-23	9779	7	-53	-3	-30
39Sap	-65	-363	214	-13	-103	134	2118	-50	-17	140	1074	5	-53	-3	-30
40Top	-65	-363	11	-13	-103	-70	912	-50	21	-23	6856	6	-53	-3	-30
40E	-65	-363	-9	-13	-103	-70	-875	61	-17	-23	7458	-3	-53	-3	-30
40B	-65	-363	11	-13	-103	-70	-875	-50	20	-23	11722	14	-53	-3	-30
41Top	-65	649	-9	31	-103	-70	-875	-50	23	-23	6198	-3	-53	-3	-30
41E	-65	-363	11	27	-103	-70	-875	-50	-17	-23	11099	6	-53	-3	-30
41B1	-65	1799	112	30	443	-70	22884	-50	-17	-23	7806	16	219	6	-30
41B2	-65	1894	65	19	349	85	23883	-50	43	-23	3187	12	211	6	-30
42Top	-65	-363	-9	82	-103	-70	-875	-50	18	72	13526	3	-53	-3	-30
42B	-65	1025	84	31	-103	-70	-875	-50	-17	-23	13812	9	297	-3	-30
43Top	-65	-363	-9	35	-103	-70	-875	-50	-17	-23	3092	-3	-53	-3	-30
43AE	-65	-363	-9	14	-103	-70	-875	-50	-17	28	3137	-3	93	-3	-30
43E	-65	-363	11	-13	-103	-70	-875	-50	-17	-23	7801	-3	-53	-3	-30
43G	68	-363	37	-13	-103	-70	-875	-50	-17	-23	10821	-3	-53	-3	-30
44Top	-65	-363	21	23	-103	83	-875	-50	-17	-23	4206	-3	-53	-3	-30
44A2	-65	-363	-9	20	-103	90	-875	54	26	-23	10167	6	-53	6	-30
44B	-65	-363	11	13	473	-70	-875	-50	25	37	27534	-3	60	3	-30
44C	-65	-363	17	-13	-103	-70	-875	-50	27	28	32646	-3	-53	-3	-30
44R	106	-363	27	13	118	72	-875	-50	23	27	22769	4	-53	-3	-30
45A	70	-363	18	32	103	78	1087	-50	27	25	2800	5	-53	-3	-30
45BA	134	-363	-9	22	-103	109	-875	-50	24	-23	1724	-3	55	-3	-30
45B	80	-363	13	21	-103	78	1353	-50	-17	-23	5013	10	-53	-3	-30
46A	-65	-363	10	20	-103	-70	-875	-50	-17	-23	1838	-3	-53	-3	-30
46B1	-65	-363	-9	28	-103	-70	-875	-50	-17	-23	5302	3	-53	-3	-30
46B2	-65	-363	-9	32	-103	-7	-12	-50	-17	-23	6784	-3	-53	-3	-30
46C	-65	-363	-9	-13	-103	-70	-875	-50	-17	-23	2971	-3	-53	-3	-30
47Top	-65	-363	-9	20	-103	-70	-875	-50	-17	-23	4529	-3	-53	-3	-30
47A1	-65	-363	-9	-13	-103	-70	-875	-50	-17	-23	10925	3	59	-3	-30
47B1	-65	-363	-9	-13	-103	-70	-875	-50	-17	-23	14042	-3	-53	-3	-30
47B2	-65	-363	-9	15	-103	-70	-875	-50	-17	-23	18529	-3	-53	-3	-30
47C	-65	656	-9	-13	-103	-70	-875	-50	-17	-23	4354	-3	-53	-3	68

**Table App-6:** The pH(KCl) values, the conductivities of the water-suspended soils in  $\mu\text{S cm}^{-1}$  [Cond.] and the proportions of gravel, sand, mud, LOP, silt and clay in weight percent of the total sample. The weight percentages of the particle size classes unified according to a Principal Component Analysis (section 2.8) are given on the right side of the table: CS = coarse sand, MS = medium sand, FS = fine sand, CST = coarse silt, F = fines and FC = fine clay. The range of particle sizes in the various classes is listed in Table 2.14.

Sample	Determined as outlined in section 2.7.							Based on results obtained with a settling column and a sedigraph (Table App-7)							
	pH	Cond.	Gravel	Sand	Mud	LOP	Sum	Silt	Clay	CS	MS	FS	CST	F	FC
1A	4.8	25	0.0	96.9	1.4	1.4	99.7	1.1	0.2	1.4	65.0	30.6	0.8	0.4	0.1
1E	5.0	51	0.0	98.1	1.6	0.3	100.0			1.2	59.1	37.8			
4A	7.3	210	1.9	85.1	1.7	11.3	100.0	1.6	0.4	0.6	34.4	49.8	1.0	0.8	0.2
5A	4.3	33	8.6	80.8	10.2	0.4	100.0	6.1	4.0	50.4	19.3	11.2	3.8	3.6	2.7
6AE	4.5	30	21.5	67.8	10.1	0.5	100.0	5.5	4.5	38.6	21.1	8.2	2.8	4.5	2.7
9A	4.8	116	7.4	84.6	7.8	0.3	100.0	5.1	2.6	45.9	25.5	13.2	3.0	2.9	1.8
10A	5.2	173	2.9	91.4	3.8	1.9	100.1	2.5	1.2	30.4	22.7	38.5	1.7	1.3	0.8
16A	5.4	42	0.1	98.1	1.3	0.6	100.1	1.1	0.1	1.3	74.0	22.8	0.7	0.6	0.0
16E	5.2	24	0.1	98.5	1.3	0.2	100.1			2.2	73.2	23.1			
17A	5.0	31	0.2	98.2	0.9	0.7	100.0			1.5	71.6	25.2			
18Top	5.0	22	0.1	98.7	0.7	0.5	100.0			3.8	73.1	21.7			
19A	4.1	71	0.2	98.1	0.9	0.9	100.1			2.8	72.6	22.7			
20Top	4.2	402	0.1	90.7	2.4	6.8	100.0			2.5	70.9	17.2			
21Top	4.9	47	0.1	98.3	1.0	0.6	100.0			5.5	78.7	14.1			
24Top	5.2	54	1.2	94.7	3.5	0.7	100.1	1.2	1.4	24.6	35.4	34.4	0.7	0.8	1.0
24A	4.6	56	2.8	91.0	6.0	0.3	100.1	4.7	2.0	31.3	29.6	29.4	3.8	1.5	1.5
24G	5.1	124	13.0	55.8	30.7	0.3	99.9	3.4	27.1	22.6	15.9	17.2	1.9	3.2	25.3
25Top	5.2	55	5.3	51.1	43.0	0.6	100.0	28.6	13.8	27.8	15.1	8.8	19.9	12.6	10.0
25A	4.9	32	6.1	86.6	6.7	0.6	100.0	4.8	1.7	43.8	24.1	18.8	3.2	2.3	1.1
25G	5.5	153	22.3	20.2	49.5	6.6	98.6	6.7	42.7	10.2	5.8	4.3	2.2	7.6	39.6
26AE	5.4	64	3.8	88.1	7.7	0.5	100.0	5.1	2.9	31.1	30.8	23.7	3.4	2.9	1.8
26B	5.7	218	6.0	59.1	26.8	8.1	99.9	3.2	23.5	19.3	23.7	16.1	1.8	1.8	23.1
28A	4.3	47	2.4	82.0	15.8	1.2	101.4	9.8	5.8	17.3	26.6	38.4	6.3	5.2	4.1
28E	4.2	27	76.4	19.0	4.4	0.2	100.0	2.4	2.0	4.2	6.9	8.0	1.5	1.6	1.3
28B	4.6	27	66.4	17.4	13.9	2.1	99.8	7.5	6.2	3.7	5.8	8.0	3.7	6.2	3.8
29Top	5.5	463	0.0	88.9	9.7	1.5	100.1	4.6	5.0	2.5	26.2	60.3	1.8	4.4	3.3
29E	5.5	174	0.3	92.2	7.0	0.5	100.0	3.2	3.7	2.3	24.2	65.9	1.5	3.1	2.3
29G	6.5	2000	0.1	83.7	15.9	0.3	100.0	4.0	12.8	2.5	21.1	59.2	2.6	3.9	10.3
30Top	5.0	74	5.6	74.8	17.5	2.1	100.0	11.2	6.5	31.6	16.6	26.4	7.0	6.3	4.4
30A	4.3	45	4.5	76.2	18.5	0.7	99.8	12.0	6.1	34.6	20.7	19.4	7.3	7.4	3.5
31Top	5.8	111	4.0	80.6	13.9	1.2	99.7	9.7	4.1	41.7	20.5	18.4	5.5	5.7	2.7
31AE	5.2	35	5.1	78.4	15.6	0.8	99.9	12.7	3.3	31.2	24.0	22.9	8.3	5.9	1.8
31B	4.9	610	51.3	33.0	14.9	0.6	99.8	9.9	4.8	12.5	8.6	12.1	4.9	6.4	3.5
32Top	5.2	105	5.4	87.2	6.5	0.9	99.9	3.3	0.6	53.6	19.0	17.2	1.8	2.1	0.0
32A	4.5	42	3.8	87.9	7.6	0.5	99.8	5.4	2.2	53.5	21.5	12.8	3.1	3.3	1.2
32GB	5.2	47	4.5	83.7	11.6	0.1	99.9	9.5	2.1	24.7	29.9	29.1	5.3	5.1	1.2
32G	4.9	130	0.6	38.5	58.7	2.4	100.1	17.5	41.0	13.0	18.4	7.3	4.9	22.6	31.0
33Top	4.8	273	4.5	89.7	4.8	1.0	100.0			65.3	15.8	8.5			
33AE	4.5	73	3.7	90.8	5.0	0.5	100.0	2.9	2.6	67.0	15.7	7.7	1.8	1.5	2.2
33G	4.7	521	5.4	46.9	46.7	0.9	99.9	2.6	44.0				1.1	5.4	40.1
34A	4.5	44	12.7	71.2	15.3	0.7	99.9	8.4	7.2	36.0	19.6	15.3	5.0	5.3	5.4
36Top	4.4	114	36.4	37.8	24.6	1.0	99.8			14.5	4.8	18.5			
36E	4.3	62	64.1	17.4	18.1	0.4	100.0	10.6	7.4	7.6	2.1	7.8	4.8	7.3	5.9
36B	4.0	101	0.1	13.2	85.2	1.6	100.1	19.1	65.9	2.5	0.9	10.1	5.8	16.7	62.4
37A	5.1	210	14.4	34.6	49.2	1.8	100.0	29.9	18.7	9.3	5.5	20.4	13.1	23.0	12.5
37B	5.7	281	24.5	26.6	47.8	1.1	100.0	26.0	21.6	7.7	4.5	14.6	10.1	22.6	14.9
38A	5.7	189	11.9	32.2	54.1	1.9	100.1	32.4	21.0	8.7	5.9	18.3	13.0	26.5	13.8
38B	6.5	687	12.0	20.4	66.6	1.2	100.2	18.1	48.3	8.1	4.2	8.3	6.0	21.6	38.8
38BC	7.2	1044	3.2	21.6	71.8	3.7	100.2	35.7	35.7	3.8	2.2	16.0	9.8	39.7	21.8
40Top	5.8	174	42.4	37.7	19.1	0.9	100.1			12.8	13.3	11.7			
40E	6.4	93	48.2	32.8	18.4	0.6	100.0			12.3	11.8	8.7			
40B	4.8	134	28.0	22.1	49.3	0.8	100.2	17.1	31.9	10.5	6.3	5.2	3.8	19.7	25.6
41Top	5.3	185	52.5	34.5	12.5	0.5	100.0			23.7	5.4	5.3			
41E	4.4	301	79.5	9.9	11.6	0.0	101.0			7.6	1.2	1.1			

continued ...

Sample	Determined as outlined in section 2.7.							Based on results obtained with a settling column and a sedigraph (Table App-7)							
	pH	Cond.	Gravel	Sand	Mud	LOP	Sum	Silt	Clay	CS	MS	FS	CST	F	FC
41B1	4.2	600	41.0	8.0	51.3	-0.1	100.2	5.4	45.7	5.5	1.3	1.4	0.8	8.7	41.6
41B2	4.2	783	7.4	12.9	80.2	-0.2	100.3	9.9	70.2	5.6	4.0	3.4	2.1	14.8	63.2
43Top	5.4	311	45.8	41.1	12.8	0.3	100.0			14.1	8.4	18.4			
43AE	5.2	456	50.0	38.8	11.1	0.1	100.0			11.7	12.2	14.7			
43E	6.1	354	81.1	13.0	6.2	0.0	100.4			4.2	2.0	6.9			
43G	6.8	1470	8.0	8.2	84.3	0.0	100.5	11.2	72.8	2.8	1.4	4.4	2.4	19.8	61.7
44Top	5.9	167	27.8	45.9	25.7	0.7	100.2			13.2	9.7	22.7			
44A2	5.7	47	58.9	25.0	16.0	0.2	100.1			9.0	4.3	11.4			
44B	5.9	101	2.7	19.3	78.0	0.4	100.3	14.6	63.4	2.4	3.4	13.2	3.9	21.5	52.7
44C	6.4	119	3.2	40.1	56.6	0.4	100.3	21.5	35.3	4.2	6.5	29.4	7.2	24.4	25.1
45A	4.9	291	0.4	76.4	22.4	0.9	100.1			9.3	19.7	46.8			
45BA	4.7	142	0.7	70.5	28.1	0.7	100.0	11.8	15.9	5.6	19.4	45.8	7.1	10.0	10.7
45B	5.4	256	1.3	38.0	59.7	1.1	100.1	16.1	43.3	5.8	12.2	20.4	4.6	17.3	37.5
46A	4.8	122	7.9	69.6	21.4	1.0	99.9			17.9	19.6	30.9			
46B1	4.9	127	21.4	52.2	25.9	0.6	100.1			16.4	16.3	19.4			
46B2	5.1	154	56.9	16.1	26.3	0.8	100.1	8.2	17.9	4.4	4.3	7.6	2.7	8.6	14.8
46C	5.3	91	2.8	35.6	60.6	1.3	100.2	18.4	42.1	8.8	11.9	14.9	4.7	18.1	37.7
47A1	5.6	59	5.4	67.6	26.5	0.6	100.1			18.9	25.5	23.0			
47B1	6.0	49	8.6	57.6	33.5	0.6	100.3	11.5	22.2	14.7	22.6	20.0	6.4	8.2	19.1
47B2	5.9	106	40.4	33.6	25.4	0.8	100.2			14.8	10.6	8.2			
47C	7.8	203	2.4	22.9	74.2	1.1	100.6	21.4	52.5	6.6	7.1	9.5	3.4	30.2	40.3
47A2	5.9	58	3.0	62.4	33.7	1.0	100.1	15.3	18.2	19.1	18.2	22.7	8.1	11.9	13.5

**Table App-7:** The proportions of individual phi units for the -2 mm sieved soil fraction as determined with the sedigraph and the settling column. The proportions are expressed in weight percent of the entire sample. Soil samples which have low totals have high proportions of gravel or organic matter.

phi units: Sample	>-1	>0	>1	>2	>3	>4.3	>5	>6	>7	>8	>9	>10	>11	<11	Total
1A	0.2	-0.1	1.2	65.0	28.9	1.7	0.4	0.4	0.1	0.1	0.1	0.1	0.0	0.1	98.3
1E	0.3	-0.1	0.9	59.1	35.4	2.4									98.1
4A	0.1	0.1	0.4	34.4	47.8	2.0	0.6	0.5	0.2	0.2	0.2	0.1	0.1	0.2	86.8
5A	0.2	10.4	39.8	19.3	7.0	4.2	1.5	2.3	1.0	0.6	0.7	0.7	0.6	2.7	91.0
6AE	0.5	7.2	30.9	21.1	4.7	3.5	1.0	1.8	1.1	0.8	0.9	0.9	0.9	2.7	77.9
9A	0.4	12.0	33.6	25.5	7.8	5.5	1.1	1.9	1.0	0.6	0.5	0.4	0.4	1.8	92.3
10A	0.2	6.3	23.9	22.7	32.6	5.9	0.8	0.9	0.3	0.3	0.3	0.2	0.2	0.8	95.3
16A	0.3	0.0	1.1	74.0	21.4	1.4	0.3	0.4	0.2	0.1	0.1	0.1	0.1	0.0	99.4
16E	0.3	0.8	1.1	73.2	21.8	1.4									98.5
17A	0.9	-0.4	1.0	71.6	23.6	1.5									98.2
18Top	0.4	-0.2	3.6	73.1	20.4	1.3									98.7
19A	0.6	0.5	1.7	72.6	21.1	1.6									98.1
20Top	0.7	-0.2	2.0	70.9	16.6	0.6									90.7
21Top	0.3	0.1	5.1	78.7	13.8	0.3									98.3
24Top	0.2	3.2	21.1	35.4	27.8	6.6	0.0	0.7	0.2	0.1	0.2	0.2	0.2	1.0	96.9
24A	0.7	7.1	23.4	29.6	21.8	7.6	2.4	1.4	0.3	0.2	0.3	0.3	0.3	1.5	97.0
24G	0.1	4.8	17.7	15.9	12.8	4.4	0.9	1.1	0.5	0.3	0.7	1.0	0.7	25.3	86.2
25Top	0.2	6.2	21.5	15.1	5.4	3.4	8.7	11.1	3.9	2.5	2.4	2.0	1.8	10.0	94.1
25A	1.9	11.3	30.6	24.1	12.8	6.1	1.5	1.7	0.7	0.5	0.4	0.4	0.3	1.1	93.3
25G	0.0	4.1	6.1	5.8	2.5	1.9	0.9	1.3	1.7	1.4	1.4	1.2	1.9	39.6	69.7
26AE	0.4	4.1	26.5	30.8	16.2	7.5	1.8	1.6	0.8	0.5	0.5	0.5	0.6	1.8	93.6
26B	0.1	2.9	16.3	23.7	12.3	3.7	0.7	1.1	0.7	0.5	0.2	0.1	0.2	23.1	85.8
28A	0.2	2.0	15.1	26.6	26.9	11.5	2.5	3.8	1.5	1.1	0.9	0.9	0.8	4.1	97.8
28E	0.2	0.3	3.7	6.9	6.0	2.0	0.6	0.9	0.4	0.3	0.3	0.3	0.4	1.3	23.4
28B	0.0	0.7	3.0	5.8	5.2	2.8	1.3	2.4	1.6	1.1	1.1	1.1	1.4	3.8	31.3
29Top	0.1	0.2	2.1	26.2	50.5	9.9	0.8	1.0	0.8	0.9	1.0	0.9	0.8	3.3	98.5
29E	0.3	0.0	2.0	24.2	51.3	14.6	0.7	0.8	0.6	0.6	0.6	0.7	0.7	2.3	99.2
29G	0.7	-0.4	2.2	21.1	50.2	9.0	1.5	1.1	0.5	0.3	0.6	1.0	1.5	10.3	99.6
30Top	0.3	5.7	25.6	16.6	16.2	10.2	2.9	4.1	1.8	1.2	1.2	1.2	0.9	4.4	92.3
30A	0.8	7.3	26.5	20.7	9.4	10.0	3.0	4.3	1.9	1.4	1.4	1.4	1.3	3.5	92.8

continued ...

Table App-7: Continued.

phi units: Sample	>-1	>0	>1	>2	>3	>4.3	>5	>6	>7	>8	>9	>10	>11	<11	Total
31Top	0.5	10.2	30.9	20.5	12.4	6.0	2.0	3.4	1.8	1.3	1.1	0.9	0.5	2.7	94.4
31AE	0.1	6.5	24.6	24.0	13.8	9.1	4.2	4.1	1.9	1.3	1.2	1.0	0.5	1.8	94.0
31B	0.1	3.4	9.0	8.6	7.4	4.7	1.5	3.4	2.3	1.5	1.3	0.9	0.5	3.5	47.9
32Top	1.0	14.0	38.6	19.0	10.5	6.7	0.6	1.2	0.6	0.5	0.5	0.4	0.2	0.0	93.7
32A	0.5	16.3	36.7	21.5	8.8	4.1	1.4	1.7	0.9	0.7	0.7	0.7	0.3	1.2	95.5
32GB	0.8	2.1	21.9	29.9	22.3	6.9	1.7	3.6	2.1	1.2	0.9	0.6	0.3	1.2	95.3
32G	0.7	1.3	11.0	18.4	5.2	2.1	1.2	3.7	4.5	3.9	4.2	4.1	5.9	31.0	97.1
33Top	1.7	22.1	41.4	15.8	6.6	1.9									89.7
33AE	0.1	19.1	47.8	15.7	4.9	2.7	1.1	0.7	0.4	0.3	0.3	0.3	0.2	2.2	95.8
33G							0.3	0.8	0.7	0.1	0.6	1.2	2.7	40.1	46.7
34A	0.2	9.2	26.7	19.6	8.1	7.2	2.2	2.8	1.4	1.0	1.0	1.0	0.9	5.4	86.5
36Top	0.2	5.3	9.0	4.8	10.0	8.5									37.8
36E	0.3	3.5	3.8	2.1	3.7	4.1	1.4	3.4	2.6	1.9	1.2	0.8	0.7	5.9	35.5
36B	1.6	0.2	0.7	0.9	4.0	6.1	0.9	4.9	5.5	4.9	2.9	2.1	1.4	62.4	98.4
37A	0.2	2.9	6.3	5.5	9.3	11.2	4.9	8.2	6.6	5.7	4.5	3.3	3.0	12.5	83.8
37B	0.2	1.9	5.5	4.5	7.3	7.4	3.2	6.9	5.7	5.3	4.9	3.7	3.1	14.9	74.4
38A	1.0	1.6	6.1	5.9	9.3	9.0	4.0	9.0	7.4	6.5	5.5	4.0	3.1	13.8	86.3
38B	1.1	2.0	4.9	4.2	3.9	4.4	2.3	3.7	3.5	3.9	4.7	4.8	4.7	38.8	87.0
38BC	1.1	0.6	2.1	2.2	8.4	7.6	3.4	6.4	7.6	8.2	10.1	8.6	5.3	21.8	93.3
40Top	0.3	3.3	9.1	13.3	7.7	4.0									37.7
40E	0.1	3.0	9.2	11.8	4.8	3.9									32.8
40B	0.5	1.5	8.5	6.3	2.3	2.9	0.8	3.0	4.1	4.6	4.7	3.9	2.5	25.6	70.9
41Top	0.1	10.1	13.6	5.4	2.9	2.4									34.5
41E	0.0	3.1	4.4	1.2	0.7	0.4									9.9
41B1	0.0	2.3	3.2	1.3	0.7	0.7	0.1	0.8	1.4	1.4	1.8	2.0	2.1	41.6	59.3
41B2	0.4	1.5	3.7	4.0	1.4	1.9	0.5	1.6	2.2	2.5	3.1	3.2	3.8	63.2	93.0
43Top	1.5	4.3	8.3	8.4	11.4	7.0									41.0
43AE	0.5	4.1	7.2	12.2	8.8	5.9									38.8
43E	0.5	2.0	1.8	2.0	4.0	2.9									13.0
43G	0.0	0.5	2.2	1.4	1.9	2.5	0.1	2.3	2.2	2.3	4.2	4.4	6.7	61.7	92.5
44Top	0.4	7.9	5.0	9.7	14.4	8.3									45.9
44A2	0.4	6.0	2.7	4.3	8.2	3.2									25.0
44B	0.2	1.1	1.2	3.4	9.0	4.3	0.9	3.1	3.3	3.6	3.8	3.9	6.9	52.7	97.2
44C	2.8	0.2	1.2	6.5	18.7	10.7	2.0	5.2	4.5	4.2	5.6	5.0	5.1	25.1	96.7
45A	2.7	0.5	6.1	19.7	33.6	13.2									76.4
45BA	0.4	0.2	5.1	19.4	32.8	12.9	3.0	4.1	1.7	1.2	1.8	2.4	2.9	10.7	98.6
45B	0.2	1.0	4.6	12.2	15.1	5.3	1.5	3.1	4.3	3.3	3.9	2.6	3.1	37.5	97.7
46A	3.4	1.4	13.1	19.6	23.4	7.5									68.4
46B1	1.6	2.1	12.6	16.3	15.3	4.1									52.2
46B2	0.9	0.6	2.9	4.3	5.2	2.3	0.7	2.0	2.0	1.8	1.8	1.5	1.6	14.8	42.4
46C	1.2	0.8	6.8	11.9	9.4	5.5	1.1	3.6	5.2	4.6	3.8	2.9	1.6	37.7	96.1
47A1	0.9	3.0	15.0	25.5	15.1	7.9									67.5
47B1	0.3	2.1	12.3	22.6	12.3	7.7	2.9	3.5	1.8	1.5	1.9	1.7	1.4	19.1	91.0
47B2	0.1	2.6	12.1	10.6	5.8	2.4									33.6
47C	0.1	1.1	5.4	7.1	7.5	2.0	0.7	2.7	5.3	5.8	6.8	5.7	6.5	40.3	97.1
47A2	4.4	1.6	13.2	18.2	16.6	6.0	3.2	4.9	2.8	2.1	2.3	2.4	2.3	13.5	93.5